UNIVERSITY OF CALIFORNIA,
IRVINE

Development of Late Transition Metal Insertion Polymerization Catalysts

DISSERTATION

submitted in partial satisfaction of the requirements
for the degree of

DOCTOR OF PHILOSOPHY

in Chemistry

by

Tobias Friedberger

Dissertation Committee:
Professor Zhibin Guan, Chair
Professor Andrew S. Borovik
Professor William J. Evans

2015

TABLE OF CONTENTS

Page

LIST OF FIGURES

LIST OF SCHEMES

LIST OF TABLES

ACKNOWLEDGMENTS

I would like to express my deep gratitude to my committee chair and advisor, Professor Zhibin Guan, who, through a combination of his neverending excitement about science, positive attitude, and high degree of granted freedom, facilitated this work and my growth as a scientist.

I would like to thank my committee members, Professor Andrew S. Borovik and Professor William J. Evans, for taking the time to provide advice and help on my thesis project, and their "my door is always open" mentality.

Professors Suzanne A. Blum, Vy M. Dong, and Alan F. Heyduk are thanked for their help and advice during the Advancement to Candidacy exams.

In addition, a thank you to Dr. Philip Dennison for his advice with NMR spectroscopy. I thank Dr. Joseph Ziller, Dr. Ryan Zarkesh, and Dr. Jordan Corbey for helping with the X-ray diffraction and solving structures. I would also like to thank Dr. John Greaves and Dr. Beniam Berhane for the MS assistance. Thanks to the Ruobing Zhao and Dr. Eduardo Baez for their help with high temperature GPC analysis.

Financial support was provided by NSF Grant CHE-1012422 and a University of California Regents' Dissertation Fellowship.

I would like to thank all past and present Guan lab members who provided a warm welcome, and a productive, supportive, and fun work environment: Guobin Sun, Sophia Liao, Tingbin Yu, Aaron Kushner, Jens Hentschel, Hiromitsu Urakami, Jane Bai, Adam Weisman, Bryan Le, Kanika Chawla, Yulin Chen, Yixuan Lu, Gregory Williams, Max Yen, Bahvin Joshi, Kevin Cheng, Hannah Little, Timothy Tiambeng, Hanxiang Zeng, Miguel Camacho Fernandez, Davoud Mozhdehi, Jason Lusk, Lalisa Stutts, Justin Crumrine, Mark Johnson, Olivia Cromwell, Thuy Lu, Juliet Kotyk, Jaeyoon Chung, Nathan Oldenhuis, Vanessa Arredondo, Jonathan Ruiz, Sergio Ayala, James Neal, Hongkai Zhao, Dongchu Yang, Alexander Eldredge, and Billy Ogden. A special thanks goes to my incredibly talented and helpful undergraduate students Hannah Nguyen and LeeAnne Wang.

Finally, a heartily thank you to all my friends and family for their support and love!

CURRICULUM VITAE

Tobias Friedberger

Education

2015 Ph.D. in Chemistry, University of California, Irvine

2010 Diplom in Chemistry, University of Konstanz, Germany

Awards and Honors

2015 Outstanding Upper Division Teaching Assistant Award, UC Irvine

2015 UC Regents' Dissertation Fellowship, UC Irvine

Publications

Jia, X.; Qin, C.; Friedberger, T.; Guan, Z.; Huang, Z. Efficient and Selective Degradation of Polyethylenes into Liquid Fuels and Waxes under Mild Conditions. *Manuscript under review.*

Friedberger, T.; Ziller, J. W.; Guan, Z.; Ruthenium(IV) Complexes for Ethylene Insertion Polymerization. *Organometallics*, **2014**, *33*, 1913 – 1916.

Friedberger, T.; Wucher, P.; Mecking, S.; Mechanistic Insights into Polar Monomer Insertion Polymerization from Acrylamides. *J. Am. Chem. Soc.* **2012**, *134*, 1010 – 1018.

Guironnet, D.; Friedberger, T.; Mecking, S.; Ethylene Polymerization in Supercritical Carbon Dioxide with Binuclear Nickel(II) Catalysts. *Dalton Trans.* **2009**, 8929 – 8934.

ABSTRACT OF THE DISSERTATION

Development of Late Transition Metal Insertion Polymerization Catalysts

By

Tobias Friedberger

Doctor of Philosophy in Chemistry

University of California, Irvine, 2015

Professor Zhibin Guan, Chair

Polyolefins are the largest volume commercially produced polymer, and find ubiquitous uses as plastics, elastomers, and fibers. They are produced from gaseous olefins such as ethylene and propylene through insertion polymerization facilitated by a transition metal catalyst. Despite tremendous academic and industrial efforts and successes in catalyst development over the past decades, the copolymerization of polar functional olefins with sufficiently high activities still remains a largely unsolved issue. Late transition metal catalysts were shown to be more suitable for this kind of polymerization reaction due to their generally lower oxophilic character. The main goal of this thesis was the development of novel late transition olefin polymerization catalysts based on ruthenium and palladium. Prior to this work, only few active olefin polymerization Ru-catalysts were reported.

Several series of complexes based on ruthenium were synthesized, characterized and investigated for olefin polymerization. Ru(II)-complexes of the type $RuCl_2$(*N,N,N*)L with facially coordinating nitrogen donor ligands (*N,N,N* = trispyridyl-, trispyrazoyl-, trisimidazoyl-methane derivatives) were found to be inactive towards ethylene polymerization. Employing bisanionic disulfonate phosphines as ligands gave Ru-complexes that produced linear, high-molecular weight

polyethylene in the presence of an aluminum-alkyl based cocatalyst. Increasing the electrophilicity of the complex, by decreasing the donor strength of the ligand and using higher oxidation state Ru(IV)-complexes, the polymerization activity could be increased, and one of the highest activities for any Ru-based catalyst was observed. Polar additives such as acetone fully inhibited even the most electron-rich catalysts and copolymerization reactions yielded no polymer.

In a different approach to solve the same problem, Pd-diimine complexes were modified with pendant olefin and boronate groups. Pd-diimine complexes can facilitate the copolymerization of ethylene with acrylates, and interactions of the pendant Lewis acid group with the functional, Lewis basic comonomer was anticipated to increase the efficiency of polar monomer incorporation. However, no effect of a pendant pinacol boronate was observed on the incorporation ratio of methyl acrylate in room temperature copolymerizations. The ability of the pendant olefin to coordinate to cationic Pd-species resulted in hemilabile effects. Increased catalyst stability at the cost of decreased activities was found in comparison with unfunctionalized ligands.

1 General Introduction to Olefin Polymerization and Late Transition Metal Catalysts

1.1 Insertion Polymerization

Polyolefins are the largest volume of synthetic polymeric materials including plastics, elastomers and fibers. Both nonpolar olefins, such as ethylene, propylene, styrene, or butadiene, and polar olefins, such as acrylates, vinyl acetate, vinyl halides or acrylonitrile, can be used as the monomers for making polyolefins. The polymerization method of choice depends on the monomer structure and its ability to stabilize reactive radical or ionic intermediates. Conjugation and charge delocalization of radicals, carbocations, and carbanions is possible through the functional group adjacent to the olefin. Polar α-olefins can hence be polymerized via ionic or radical chain-growth polymerization under mild conditions and, in the case of a living polymerization, with great control over the polymer structure. For unactivated nonpolar olefins, such as ethylene, which is lacking stabilizing interactions, radical polymerization requires harsh and energy-intensive conditions (typically >200 °C and 1500 bar). Due to degenerative chain transfer, for longer α-olefins such as propylene, radical polymerization is not productive for producing high molecular polymers.[1]

The seminal discovery of Ziegler, Natta, and coworkers[2] in the mid-1950s that heterogeneous mixtures of titanium salts and aluminum alkyls can act as catalysts to polymerize ethylene and propylene to semi-crystalline high molecular weight materials under mild conditions marked the birth of the transition metal-catalyzed olefin insertion polymerization field. It allowed the polymerization of propylene, which cannot be polymerized under radical conditions, and expanded the range of applications of polyolefins. The rapid commercialization following the discovery, and the continuing growth of the polyolefins industry underscore the importance of this technology. In 2008, the worldwide production of polyethylene was about 58 million metric tons,

with the majority being produced by Ziegler-Natta catalysts.[3] Intensive academic and industrial efforts, especially with the introduction of soluble single-site titanium and zirconium metallocenes catalysts, have resulted in fundamental mechanistic understanding of the underlying catalytic steps, and led to the development of different (co-)polymer products (Scheme 1.1), e.g. high density polyethylene (HDPE), linear low density polyethylene (LLDPE), and stereospecific polypropylene (iPP, sPP).

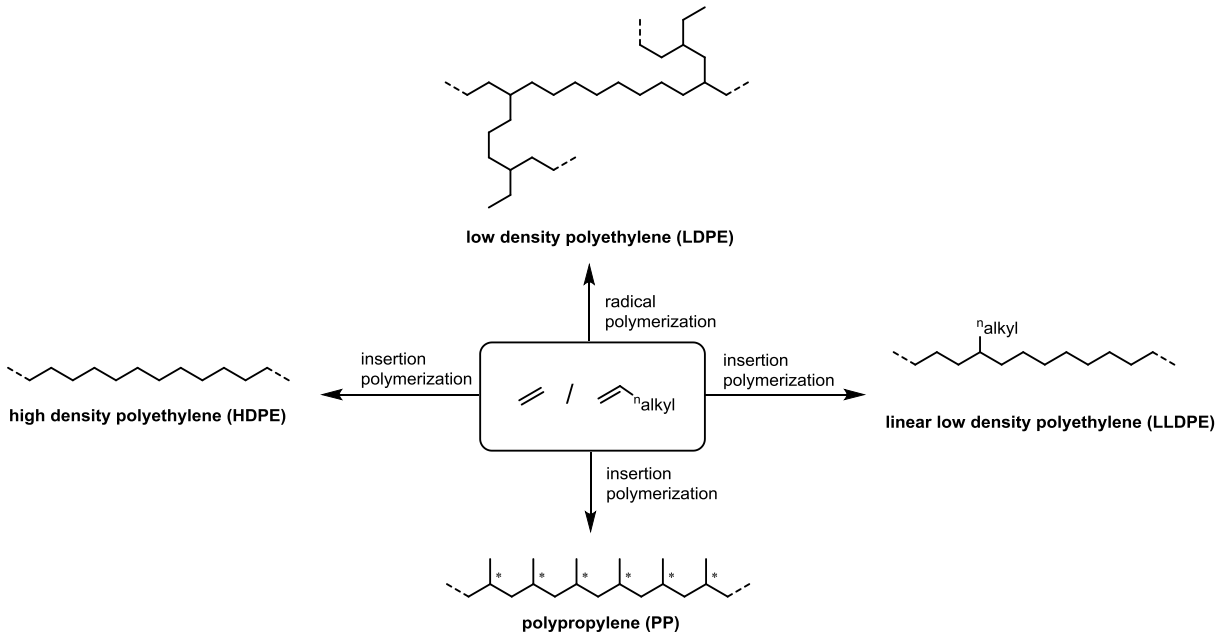

Scheme 1.1 Overview of different commercial polyolefins made from the same nonpolar olefins feedstock.

Most catalyst systems consist of a transition metal halide or pseudo-halide precatalyst and an aluminum alkyl cocatalyst. The cocatalyst is present in excess amounts, typically 100 – 10,000 equivalents per transition metal, which serves several functions. It activates the precatalyst, acts as a counterion to the cationic active metal-alkyl, and scavenges trace amounts of moisture and other possible contaminants. Activation occurs by double-alkylation of the transition metal and subsequent alkide abstraction forming a cationic metal-alkyl complex, which coordinates to the

olefin (Scheme 1.2). The nature of the cocatalyst is important as counterion effects often influence the polymerization activity and polymer properties.[4] The cationic alkyl ethylene complex is the active species that can undergo consecutive migratory insertion reactions of ethylene into the metal alkyl bond, leading to chain propagation. The underlying mechanism – first described by Cossee and Arlman,[5] and later refined by Brookhart and Green[6] – involves a 4-membered metallocyclic transition state, which results in a formal migration of the now extended alkyl group to the former coordination site of the olefin. Usually, this complex exhibits agostic interactions that stabilize the low valent intermediate, before coordinating another ethylene monomer, hence reforming another ethylene alkyl complex, which can undergo another migratory insertion. Several chain-transfer reactions are known and can lead to chain-termination:[7] (i) β-Hydride elimination results in olefin hydride complexes that can either reinsert the 1-olefin into the metal-hydride bond (at usually lower rates due to the increased steric bulk) or displace the 1-olefin with ethylene monomer. (ii) Chain transfer to monomer: A β-hydride of the growing polymer chain is transferred to an incoming olefin. This is the dominant chain termination mode under usual experimental conditions resulting in olefin terminated polymer chains. (iii) Chain-transfer to the cocatalyst exchanges the growing polymer chain with a short alkyl group of aluminum trialkyls. Methylaluminoxane (MAO), an ill-defined oligomer formed by partial hydrolysis of $AlMe_3$, has found wide-spread use as a cocatalyst for homogeneous catalyst systems.[8] Chain-transfer to aluminum can occur to MAO oligomers and to residual amounts of $AlMe_3$ in MAO[9], especially at lower olefin concentrations.[10] Other chain-transfer modes, such as β-methyl elimination, have been reported, but are limited to special cases.[11]

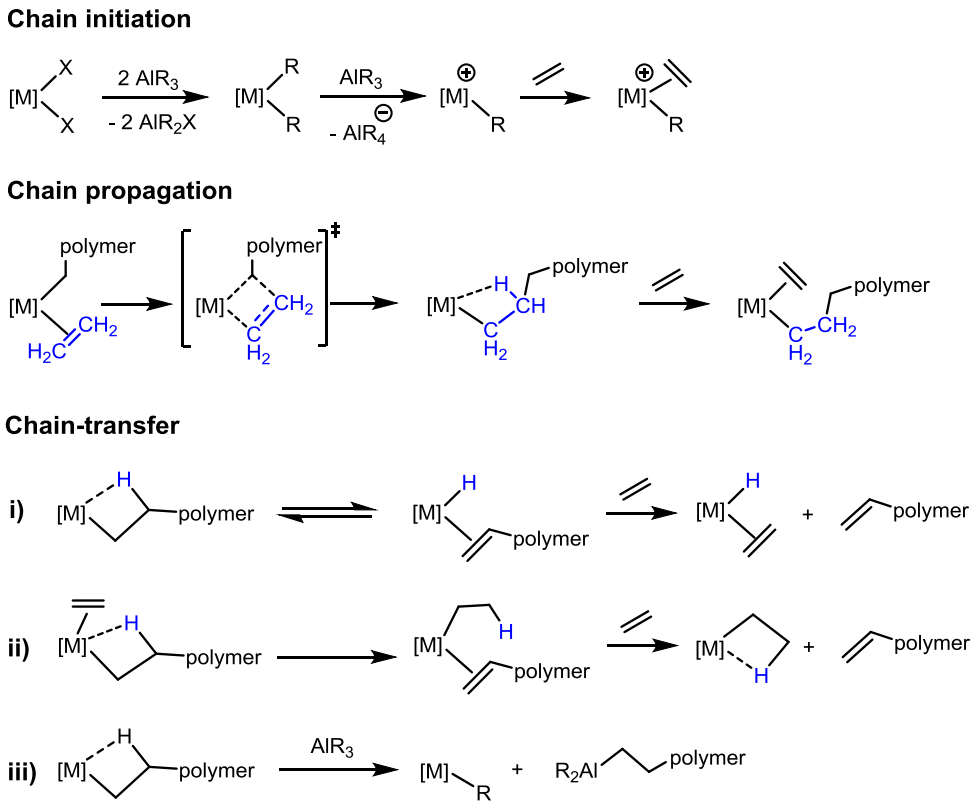

Scheme 1.2 Overview of elemental reactions involved in insertion polymerization. [M] indicates a metal center coordinated with the respective ligand. AlR_3 stands representatively for an aluminum based cocatalyst such as $AlMe_3$.

Despite their commercial success, early transition metal-based systems like the Ziegler-Natta, metallocene, or chromium-based catalysts, show some limitations in their monomer compatibility and therefore ground for further catalyst development. On the one hand, non-linear polymer architectures can only be obtained through copolymerization of ethylene with more expensive long-chain α-olefins. Such α-olefins are typically produced by ethylene tri-, and tetramerization and require a subsequent purification step. To this end, research towards one pot tandem ethylene trimerization – copolymerization systems are investigated.[12] On the other hand, the monomer scope of early transition metal catalysts is limited to nonpolar olefins. The highly electropositive nature of the metal centers generally prevents the (co-)polymerization of polar olefins due to the poisoning effect of irreversible heteroatom coordination to the metal center. Non-

polar polyolefin materials containing relatively small amounts of functional groups have enhanced material properties such as adhesion, dyeability, and gas permeability in comparison to unfunctionalized polyolefins. The current commercial method to obtain such materials is based on radical polymerization at high temperatures and extreme pressures (150 – 300 °C, 1500 – 7500 bar). It lacks tight control over polymer properties, yields branched, non-crystalline material, and requires high capital investment. Other synthetic methods that are investigated include the post-functionalization of polyethylene, or metathesis polymerization of functional monomers with subsequent hydrogenation. In addition, the use of protecting groups and remotely functionalized olefins provided successful strategies for the polar ethylene copolymerization with early transition catalysts.[13] However, from an industrial point of view, the insertion copolymerization of simple and readily available nonpolar and polar olefins represents the most cost and energy effective way to obtain such functional materials.

Note that the homopolymerization of certain polar monomers such as methacrylates is indeed possible with early transition metals (Scheme 1.3).[14] However, the chain-propagation proceeds via a coordination-addition mechanism found in group-transfer polymerizations, which excludes the possibility of forming copolymers with nonpolar monomers such as ethylene. The metal-enolate is not reactive enough for addition into coordinated ethylene, restricting cross-over from MMA to ethylene, hence only producing poly(MMA) even in the presence of ethylene.

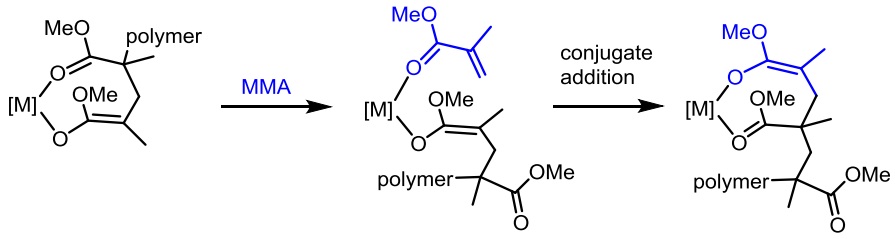

Scheme 1.3 Coordination - conjugate addition mechanism of methyl methacrylate (MMA) homopolymerization by strongly Lewis-acidic metal complexes.

1.2 Late Transition Metal Polymerization Catalysts

Late transition metals have intrinsically lower oxophilicity than their early transition metal counterparts, therefore, are promising candidates for functional group tolerant polymerization catalysts. However, their intrinsic propensity for β-hydride elimination, which is exploited in the Pd-catalyzed Heck-reaction, had been inhibitive to their development as polymerization catalysts. The high rates of chain termination with subsequent dissociation of the alkene outcompete the chain propagation, resulting in the formation of oligomeric products. An illustrative example is the Shell-Higher-Olefins-Process (SHOP), which demonstrates both functional group tolerance and high propensity for β-hydride elimination. Introduced by Shell in 1968, Ni-catalysts such as **1.1** and **1.2** with bidentate monoanionic ligands produce linear long-chain α-olefins in polar solvents (e.g. butanediol).[15] Over one million tons of these olefins are produced annually and are used as precursors for detergents and lubricants.[16] Under conditions in which the catalyst is only sparingly soluble, higher molecular weights could be obtained, albeit with low productivities. A Ni amino-bis(imino)phosphorane catalyst **1.3** was found to produce branched structures from ethylene, introducing the possibility to obtain non-linear polymer architectures from simple olefins.[17] The activities of these catalysts were generally inferior to early transition metal catalysts.

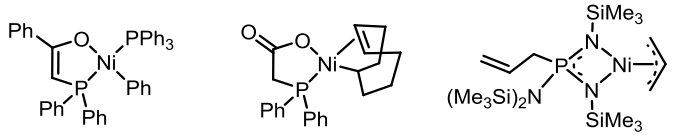

1.1 **1.2** **1.3**

Scheme 1.4 Examples of SHOP-type late transition metal olefin oligomerization catalysts.

1.3 α-Diimine Nickel and Palladium Complexes

The development of highly active late transition metal complexes for nonpolar olefin polymerization had not been realized until the mid-1990s. Brookhart and coworkers reported Pd and Ni α-diimine complexes that polymerize ethylene to high molecular weight products (Scheme 1.5, A).[18] The Ni catalysts exhibited activities on the order of Ziegler-Natta systems. The Pd analogues, while being two orders of magnitude less active, were able to tolerate polar groups and incorporate alkyl acrylates into polyethylenes.[19] The high activities were attributed to the neutral α-diimine ligand, and to the steric bulk of the ligand. The cationic complexes are more electrophilic than the neutral SHOP catalysts, and the sterics contribute to a higher ground state energy, therefore lowering the insertion barrier.[20] In addition, the steric bulk of the ligand also contributes strongly to the high molecular weight polymers. By blocking the axial positions, associative chain transfer following β-hydride elimination is disfavored.[18] A unique, highly branched polymer topology is observed for both homo- and copolymers obtained by Pd-diimines (Scheme 1.5, B). The mechanism in charge was termed "chain-walking" (Scheme 1.5, C):[20-21] Following a β-hydride elimination, the coordinated long-chain olefin can undergo a rotation around the metal-alkene bond, and reinsert into the Pd-H with opposite regiochemistry. Insertion of olefin monomer into this secondary carbon – metal bond results in methyl branches. Longer branches and branch-on-branches are obtained by subsequent β-hydride elimination, rotation, and reinsertion sequences. The ratio of the β-hydride elimination rate to the chain propagation rate determines the amount and length of branches. By adjusting the monomer concentration and the ligand sterics, different polyethylenes – from highly branched and amorphous to mostly linear and semi-crystalline – are produced. Even polyethylene dendrimers could be obtained by using subatmospheric ethylene pressures in a one-pot reaction.[22]

The acrylate units in ethylene – acrylate copolymers were exclusively incorporated into the chain-ends of the branched polyethylene backbone (Scheme 1.5, D). After insertion of functionalized olefin, the complex undergoes rapid rearrangements to form the most stable 6-membered chelate species. Further olefin insertion can occur after chelate-opening in the γ-position, explaining the exclusive end-chain enchainment of acrylate units. Elucidation of the detailed mechanistic characteristics was possible by low temperature NMR studies, making use of weakly coordinated cationic Pd-Me species and bulky non-coordinating counterions.[19] In addition to acrylates, vinyl ketones and vinyl silyl ethers were also incorporated into ethylene copolymers using Pd-diimines.

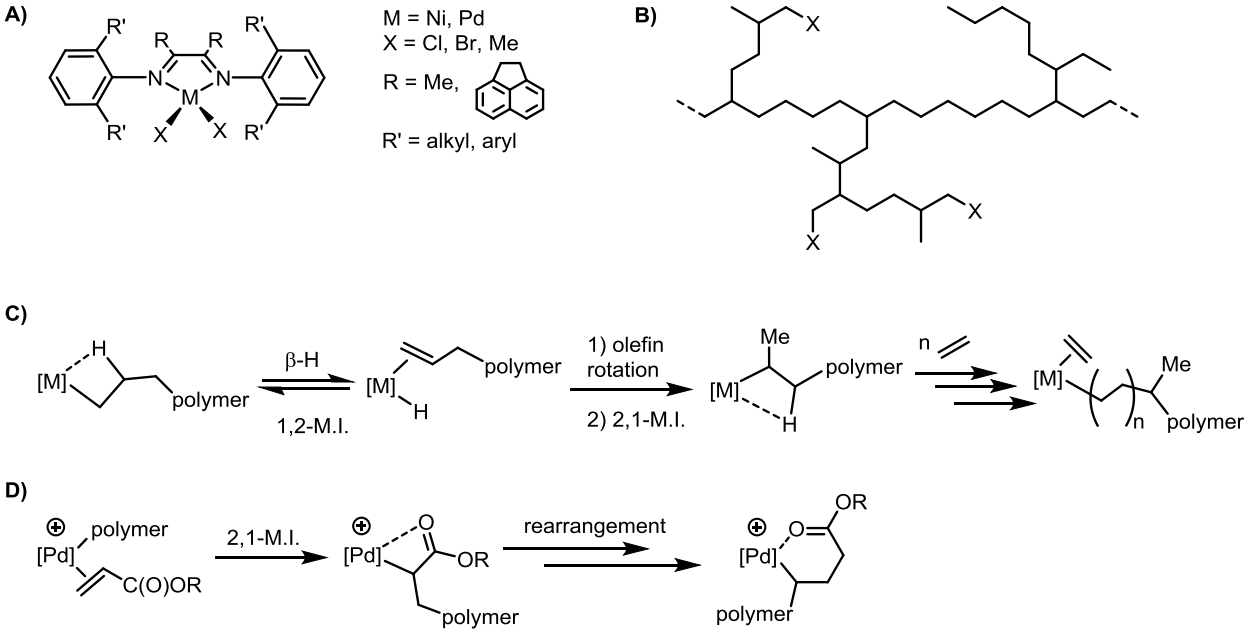

Scheme 1.5 A) General structure of diimine polymerization precatalysts. B) Highly branched structure of polymers obtained with Pd-diimines. In the case of copolymers of polar olefins, such as acrylates (X = COOR), vinyl ketones (X = C(O)R) and vinyl silyl ethers (X = $OSiR_3$), the functional group is found exclusively at chain-end positions. C) Elemental steps resulting in formal catalyst "chain-walking" – here the formation of a methyl branch. D) Chelate formation after acrylate insertion and subsequent rearrangements. ([M]: transition metal catalyst center, M.I.: migratory insertion, β-H: β-hydride elimination.)

1.4 Pyridine Diimine Iron and Cobalt Complexes

Highly active Fe and Co pyridine diimine (PDI) complexes (PDI)MX_2 (with X = Cl, Br) were discovered simultaneously by Brookhart, Gibson, and Bennett.[23] Activated with MAO or MMAO, the activities of Fe(PDI) catalysts compete with early metallocenes and are typically one order of magnitude lower for Co(PDI)s. A large number of PDIs is readily accessible by condensation of 2,6-diacyl pyridine with substituted anilines. Most of the complexes have a square pyramidal or trigonal bipyramidal geometry. The PDI chelates the metal meridionally, leaving the halides in a *cis* arrangement (Scheme 1.6). The steric parameters of the ligand greatly influence the polymer properties. Higher steric bulk in the ortho positions of the imine aryl groups leads to higher molecular weights. Similar to the case of diimine catalysts, the steric shielding of axial coordination sites is believed to suppress associative chain transfer processes.[24] Linear α-olefins with a Schulz-Flory distribution are produced with catalysts with only one "small" ortho aryl substituent, i.e. Me (precatalyst **1.5**).[25] The high activities are almost exclusively limited to ethylene as monomer. Propylene is polymerized isospecifically with significantly lower activities, reflecting the general inability to copolymerize ethylene with higher α-olefins.[26] Ethylene polymerization activities of Fe(PDI) catalysts were significantly diminished in the presence of polar monomers, and no incorporation was observed.[27]

The mechanism of activation and the nature of the propagating species have been investigated intensively, but are not as generally agreed upon as with the Pd-diimine systems. Difficulties arise due to facile redox events upon alkylation,[28] conflicting spectroscopic data on the oxidation state of the metal during polymerization[29] in combination with ligand non-innocence,[30] and the presence of several types of active species in the Fe case as indicated by broad bimodal molecular weight distributions.[23]

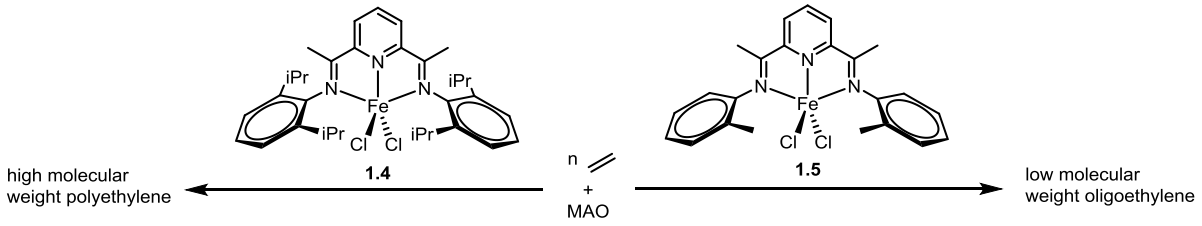

Scheme 1.6 Examples of "bulky" Fe(PDI) ethylene polymerization (**1.4**) and "open" oligomerization (**1.5**) precatalysts.

1.5 Phenoxyimine Nickel Complexes

Around the same time as the Fe/Co(PDI) systems were reported, another class of highly active late transition metal catalyst was developed by the groups of Grubbs[31] and DuPont.[32] The ligands are bidentate, monoanionic phenoxy-imines, and their Ni complexes show very high ethylene polymerization activities comparable to classical metallocenes. Phenoxyimine ligands are readily synthesized by condensation of salicylaldehyde with aniline derivatives of suitable substitution patterns. A typical Ni-phenoxyimine precatalyst of the formula (phenoxyimine)Ni(R)L, contains a methyl or phenyl R group, and an ancillary pyridine or phosphine L group. Addition of scavengers for L leads to more efficient activation and creates the neutral active species (phenoxyimine)Ni(R)(olefin). The polymerization activity and the polymer molecular weight correlate directly with the steric bulk of the aniline and the ortho-phenolate position, by blocking the axial positions. Large groups, such as 9-anthracenyl, in the ortho-phenolate position also result in faster phosphine dissociation in the precatalyst.[31] A significant effect of remote substituents on polymer weight and branching is observed.[33] The living polymerization of ethylene with a sterically demanding "sandwich" Ni- phenoxyimine catalyst to produce ultra-high molecular weight polyethylene (UHMWPE) was recently reported by Brookhart.[34]

Most remarkably, neutral Ni- phenoxyimine catalysts are very tolerant to functional groups and maintain polymerization activity in the presence of over 1500 equivalents of added polar additives such as ketones, esters, water, and tertiary amines.[35] Hydrolysis of Ni-alkyl bonds was found to be insignificant and substrate coordination outcompetes H_2O coordination.[36] This allows for the incorporation of polar monomers, with adequate spacers between the olefin and functional groups, into polyethylenes, and the emulsion polymerization of ethylene in water with certain Ni-phenoxyimines, creating polyethylene latexes.[37] The functional group tolerance has been attributed to the electroneutrality of the active catalytic species. A computational study suggested that Ni-olefin π-bonds are more stable than Ni-heteroatom σ-bonds, unlike any of the other classes of late transition metal catalysts.[20] Despite this functional group tolerance, incorporation of fundamental polar olefin such as acrylates, or acrylonitrile is not possible with Ni- phenoxyimine catalysts due to facile β-hydride elimination.[38] In contrast to diimine ligands, analogous Pd complexes are only marginally active.[39]

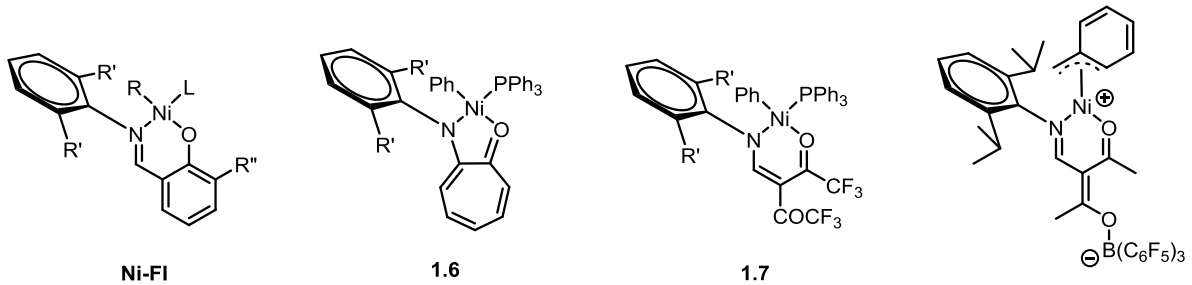

Scheme 1.7 Selection of monoanionic Ni catalysts based on the [NO] motif.

Structurally similar to phenoxyimines, anilinotropone-based neutral Ni catalysts **1.6** produce branched polyethylene with high activities. The degree of branching can be controlled over a wide range by changes in pressure and/or temperature.[40] Electron poor β–ketominato Ni complex **1.7** exhibit high activities and uniquely long catalyst lifetimes, showing no decrease in activity over the course of 5 hours at 35 ˚C.[41] Bazan and coworkers designed ketoaryliminato

ligands to study the Ni-catalyst activation by boranes. Addition of borane Lewis acid to neutral (NO)Ni(CH_2Ph)(PMe_3) resulted in the formation of zwitterionic complex **1.8** which showed increased activity in comparison with the neutral ketoaryliminato ligand due to the reduced electron density at the metal.[42]

1.6 Phosphine Sulfonate Palladium Complexes

The most recently developed class of uniquely active late transition metal catalysts is based on Pd and Ni complexes of bidentate phosphine sulfonate ligands. Initially reported in 2001 by Drent and Pugh[43] as an in-situ mixture of ortho-phosphinobenzenesulfonic acid and Pd(0), the incorporation of acrylates into the backbone of highly linear semicrystalline polyethylenes was observed for the first time. In contrast, Pd-diimines, the only other catalyst able of copolymerizing ethylene with acrylates, produced branched structures with the ester groups located at the chain ends. The groups of Nozaki, Rieger, and Jordan established well-defined mononuclear (PO)MR (PO = κ^2-*P*,*O*-ortho-phosphinobenzenesulfonate; M = Ni, Pd; R = alkyl group) complexes as the polymerization active species.[44] Numerous steric and electronic modifications of the phosphine substituents have been reported, but a comprehensive picture is still lacking. In general, more bulky substituents result in higher molecular weight via axial site blocking, but lead to diminished polar monomer incorporations.[45] Both Ni and Pd complexes are active ethylene polymerization catalysts, with activities of Ni ranging one order of magnitude higher than Pd. However, polar monomer incorporation was found to be exclusive for Pd complexes.

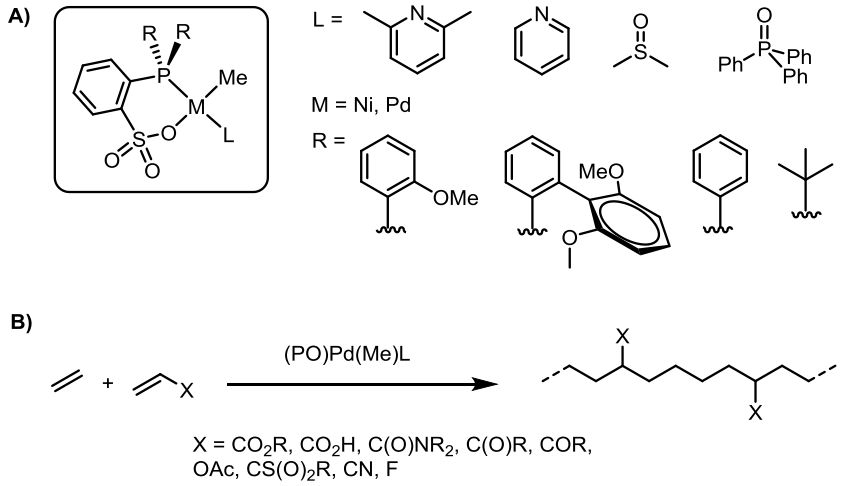

Scheme 1.8 A) Structure of well-defined phosphine sulfonate complexes with a selection of commonly used weakly coordinating ancillary ligands (L) and phosphine substituents (R). B) Copolymerization of ethylene with functional olefins to produce linear, in-chain functionalized polyethylene.

This class of Pd catalysts is able to incorporate a large variety of functionalized olefins into ethylene copolymers,[46] including previously unamenable monomers such as acrylonitrile,[47] acrylic acid,[48] vinyl acetate,[49] and vinyl halides.[50] Methyl acrylate shows incorporation ratios of over 50 mol% in ethylene copolymers,[51] and was also shown to be oligomerized in a coordination-insertion mechanism employing phosphine sulfonato Pd complexes.[52] In addition to olefinic monomers, these catalysts demonstrate unique copolymerization reactivities with carbon monoxide. Linear polyketones with up to 90 % ethylene content can be obtained,[44a,c,53] as well as alternating copolymers of CO and methyl acrylate[54] or vinyl acetate.[55] Among industrially relevant monomers, methyl methacrylate cannot be incorporated, due to the presence of the 1,2-disubstitution.[56]

This catalyst system has been extensively studied, both experimentally and theoretically.[57] The key features determining its unique properties are ascribed to the asymmetric nature of the phosphine sulfonato ligand: on the one hand, the weak σ–donor and weak π-donor/acceptor character of the hard oxygen atom, and on the other hand, the soft character of the phosphorous

with strong σ–donor and π-acceptor properties. This electronic arrangement results in a stabilized *cis*-coordination of the alkyl and phosphine groups in the isolated ground state complexes, as both groups exhibit a strong *trans*-influence. However, migratory insertion is more favorable from the less stable *cis*-π-complex. The π-back-donation from Pd to the π*-orbital of the olefin is enhanced by the lack of π-donor/acceptor character of the trans-SO_3 group, which leads to a shorter Pd-olefin bond, and an elongation of the olefin double bond, hence stabilizing the insertion transition state. In addition, the *trans*-influence of the phosphine further enhances the nucleophilicity of the alkyl ligand, which facilitates migratory insertion. The lower insertion energy of the *cis*-π-complex requires a preceding *cis*/*trans* isomerization, which has not been observed experimentally. Computational studies suggests a Berry's pseudorotation mechanism, involving a 5-coordinate transition state where the sulfonate coordinates in a κ^2-fashion.[58]

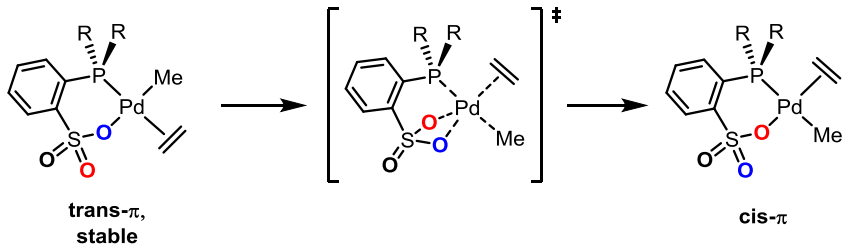

Scheme 1.9 Berry's pseudorotation mechanism responsible for cis/trans isomerization in phosphine sulfonate catalysts.[58]

The semicrystalline nature of the polyethylene originates from the suppressed β-hydride elimination. Under high ethylene pressures, the calculated elimination barrier is reasonably higher than the insertion barrier.[58] However, Pd-hydride formation through β-hydride elimination occurs under polymerization conditions. A polymerization in deuterated methanol gave deuterium incorporation into the polyethylene backbone by H/D exchange of the Pd-hydride intermediate.[59]

Recently, Nozaki and coworkers demonstrated the ethylene copolymerization with a range of functionalized olefins using a diphosphine monoxide Pd complex that forms a cationic catalyst.[60]

1.7 Ruthenium Complexes

Ruthenium complexes have shown great versatility as catalysts for various transformations, most notably for hydrogenation[61] and olefin metathesis reactions.[62] The high affinity for olefin binding combined with good functional group tolerance for Ru complexes[13] make them desirable for developing new olefin polymerization catalysts.

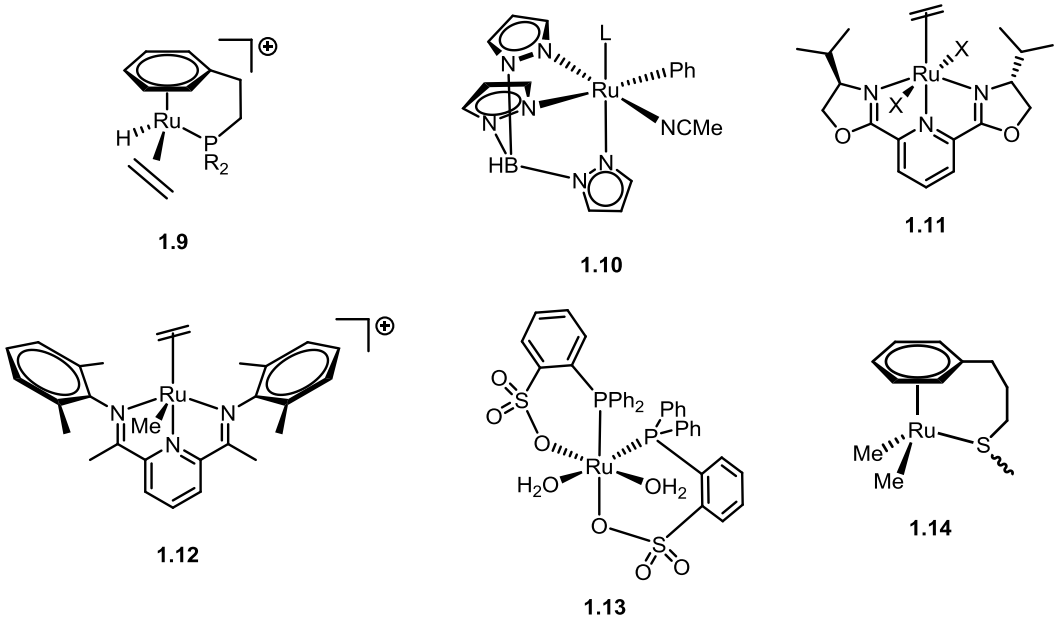

Scheme 1.10 Overview of Ru complexes investigated for ethylene polymerization.

Despite the high activities of Fe(PDI) catalysts for olefin polymerization,[23] very few Ru-based olefin insertion polymerization catalysts exist. Uses of Ru-hydrides (e.g. $(PPh_3)_3Ru(Cl)H$, $(PPh_3)_4RuH_2$) for butadiene and polar olefin polymerizations,[63] and direct and indirect demonstrations of up to two consecutive ethylene insertions into Ru-hydride, -aryl, and –alkyl bonds have been reported.[64] Faller and coworkers[64a] and Lee and coworkers[65] observed a single ethylene insertion into the Ru-hydrido and -phenyl bonds of tethered arene-phosphine complexes.

In each case, the insertion was followed by rapid reversible β-hydride elimination to yield stable hydrido olefin complex **1.9**. Two consecutive ethylene insertions into the Ru-phenyl bond of **1.10** were observed by Gunnoe and coworkers during the catalytic hydroarylation of ethylene with benzene, where higher ethylene pressures yielded significant amounts of *n*-butyl benzene.[64c] Facile β-hydride elimination (activation barrier calculated to 4.2 kcal/mol) and C-H activation of the olefinic substrate were identified as major obstacles for ethylene polymerization with **1.10**. Nevertheless, reducing the donor strength of ancillary ligand L by switching from PMe_3 to CO resulted in decreased activation barriers for ethylene insertion and slower ethylene C-H activation, facilitating two consecutive insertions. Nomura and coworkers first reported the synthesis of high molecular weight polyethylene with a Ru(pybox) complex **1.11**.[66] Brookhart and coworkers later showed that an analogous Ru(PDI) system was inactive for ethylene polymerization. Furthermore, the putative active species of this system, the $[Ru^{II}(PDI)Me(C_2H_4)]^+$ cation **1.12**, was thermally stable and did not undergo migratory insertion of the coordinated ethylene under high ethylene pressures.[67] The authors proposed that the meridional coordination geometry of the ligand results in distinctly different coordination sites for the coordinated ethylene and alkyl group (*cis* and *trans* to pyridine), which leads to high energetic barrier for alkyl migration. A computational study calculated the insertion barriers for this system to be >25 kcal mol^{-1}, which is conceivably too high for active ethylene polymerization.[68] More recently, the neutral Ru complex **1.13**, containing two ortho-phosphinobenzenesulfonate ligands was reported to exhibit relatively low activity towards ethylene polymerization.[69] Higher activities were achieved with oligomeric material of the formula "$Ru[PhP(2\text{-}SO_3\text{-}Ph)_2]$". No mechanistic detail was provided, and the obtained polyethylene was found to be chemically crosslinked.

Recently, a tethered thioether-arene complex **1.14** was reported by the Guan group to produce polyethylene upon activation with an acid cocatalyst in the absence of aluminum alkyls.[70] The consecutive migratory insertion of ethylene could be observed by variable-temperature NMR and mass spectroscopy, demonstrating the possibility of ethylene polymerization with Ru complexes. The absence of Al-cocatalysts allowed for the monitoring of ethylene insertion into the Ru-methyl bond by NMR spectroscopy. A migratory insertion barrier of 22.8 ± 0.1 kcal mol^{-1} was determined, consistent with the relatively low polymerization activity observed. In comparison, experimental insertion barriers for Ni-diimines are 13 – 14 kcal mol^{-1}, and Pd-diimines are 17 – 18 kcal mol^{-1} with much higher activity values.

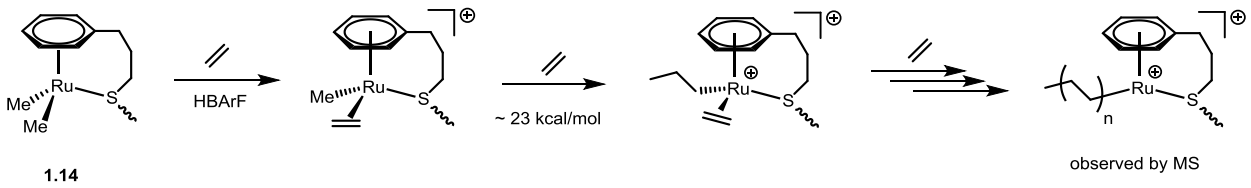

1.14

Scheme 1.11 Activation and observed chain-propagation with **1.14**.

1.8 Scope of Thesis

The main goal and driving force behind this thesis was the development of novel late transition catalysts capable of copolymerizing polar monomers with ethylene. Encouraged by the first direct demonstration of insertion polymerization by a Ru-complex developed by the Guan lab, and the known functional group tolerance of other Ru-complexes, my thesis research was mainly focused on developing new ruthenium complexes for olefin polymerization.. First, new active Ru-base ethylene polymerization complexes were developed, which were then investigated for their (co-)polymerization behavior. These efforts – exploring several different ligand frameworks - are presented in Chapters 2 - 4. A different approach based on the modification of Pd/Ni-diimine catalysts will be described in Chapter 5.

1.9 References

(1) Odian, G. *Principles of Polymerization*; John Wiley & Sons, Inc., 2004.

(2) a) Ziegler, K.; Holzkamp, E.; Breil, H.; Martin, H. *Angew. Chem.* **1955**, *67*, 541-547. b) Natta, G.; Pino, P.; Corradini, P.; Danusso, F.; Mantica, E.; Mazzanti, G.; Moraglio, G. *J. Am. Chem. Soc.* **1955**, *77*, 1708-1710.

(3) Hartwig, J. F. *Organotransition Metal Chemistry: From Bonding to Catalysis*, 2010.

(4) Chen, E. Y.-X.; Marks, T. J. *Chem. Rev.* **2000**, *100*, 1391-1434.

(5) a) Cossee, P. *J. Catal.* **1964**, *3*, 80-88. b) Arlman, E. J.; Cossee, P. *J. Catal.* **1964**, *3*, 99-104. c) Arlman, E. J. *J. Catal.* **1964**, *3*, 89-98.

(6) Brookhart, M.; Green, M. L. H. *J. Organomet. Chem.* **1983**, *250*, 395-408.

(7) Margl, P.; Deng, L.; Ziegler, T. *J. Am. Chem. Soc.* **1999**, *121*, 154-162.

(8) Zijlstra, H. S.; Harder, S. *Eur. J. Inorg. Chem.* **2015**, *2015*, 19-43.

(9) Resconi, L.; Bossi, S.; Abis, L. *Macromolecules* **1990**, *23*, 4489-4491.

(10) Naga, N.; Mizunuma, K. *Polymer* **1998**, *39*, 5059-5067.

(11) Resconi, L.; Piemontesi, F.; Camurati, I.; Balboni, D.; Sironi, A.; Moret, M.; Rychlicki, H.; Zeigler, R. *Organometallics* **1996**, *15*, 5046-5059.

(12) Liu, S.; Motta, A.; Delferro, M.; Marks, T. J. *J. Am. Chem. Soc.* **2013**, *135*, 8830-8833.

(13) Boffa, L. S.; Novak, B. M. *Chem. Rev.* **2000**, *100*, 1479-1494.

(14) Chen, E. Y. X. *Chem. Rev.* **2009**, *109*, 5157-5214.

(15) a) Keim, W.; Kowaldt, F. H.; Goddard, R.; Krüger, C. *Angew. Chem., Int. Ed.* **1978**, *17*, 466-467. b) Peuckert, M.; Keim, W. *Organometallics* **1983**, *2*, 594-597.

(16) Keim, W. *Angew. Chem., Int. Ed.* **2013**, *52*, 12492-12496.

(17) Keim, W.; Appel, R.; Storeck, A.; Krüger, C.; Goddard, R. *Angew. Chem., Int. Ed.* **1981**, *20*, 116-117.

(18) Johnson, L. K.; Killian, C. M.; Brookhart, M. *J. Am. Chem. Soc.* **1995**, *117*, 6414-6415.

(19) Johnson, L. K.; Mecking, S.; Brookhart, M. *J. Am. Chem. Soc.* **1996**, *118*, 267-268.

(20) Michalak, A.; Ziegler, T. *Organometallics* **2001**, *20*, 1521-1532.

(21) Guan, Z. *Chem. Eur. J.* **2002**, *8*, 3086-3092.

(22) Guan, Z.; Cotts, P. M.; McCord, E. F.; McLain, S. J. *Science* **1999**, *283*, 2059-2062.

(23) a) Small, B. L.; Brookhart, M.; Bennett, A. M. A. *J. Am. Chem. Soc.* **1998**, *120*, 4049-4050. b) Britovsek, G. J. P.; Gibson, V. C.; McTavish, S. J.; Solan, G. A.; White, A. J. P.; Williams, D. J.; Kimberley, B. S.; Maddox, P. J. *Chem. Commun.* **1998**, 849-850.

(24) Deng, L.; Margl, P.; Ziegler, T. *J. Am. Chem. Soc.* **1999**, *121*, 6479-6487.

(25) Britovsek, G. J. P.; Mastroianni, S.; Solan, G. A.; Baugh, S. P. D.; Redshaw, C.; Gibson, V. C.; White, A. J. P.; Williams, D. J.; Elsegood, M. R. J. *Chem. Eur. J.* **2000**, *6*, 2221-2231.

(26) a) Small, B. L.; Brookhart, M. *Macromolecules* **1999**, *32*, 2120-2130. b) Babik, S. T.; Fink, G. *J. Mol. Catal. A: Chem.* **2002**, *188*, 245-253.

(27) Kim, I.; Hwang, J.-M.; Lee, J. K.; Ha, C. S.; Woo, S. I. *Macromol. Rapid Commun.* **2003**, *24*, 508-511.

(28) Britovsek, G. J. P.; Clentsmith, G. K. B.; Gibson, V. C.; Goodgame, D. M. L.; McTavish, S. J.; Pankhurst, Q. A. *Catal. Commun.* **2002**, *3*, 207-211.

(29) Bryliakov, K. P.; Semikolenova, N. V.; Zudin, V. N.; Zakharov, V. A.; Talsi, E. P. *Catal. Commun.* **2004**, *5*, 45-48.

(30) Bryliakov, K. P.; Talsi, E. P.; Semikolenova, N. V.; Zakharov, V. A. *Organometallics* **2009**, *28*, 3225-3232.

(31) Wang, C.; Friedrich, S.; Younkin, T. R.; Li, R. T.; Grubbs, R. H.; Bansleben, D. A.; Day, M. W. *Organometallics* **1998**, *17*, 3149-3151.

(32) Bennett, A. M. A.; Coughlin, E. B.; Feldman, J.; Hauptman, E.; Ittel, S. D.; Johnson, L. K.; Parthasarathy, A.; Simpson, R. D.; Wang, L.; WO1998030609: 1998.

(33) a) Osichow, A.; Göttker-Schnetmann, I.; Mecking, S. *Organometallics* **2013**, *32*, 5239-5242. b) Weberski, M. P.; Chen, C.; Delferro, M.; Zuccaccia, C.; Macchioni, A.; Marks, T. J. *Organometallics* **2012**, *31*, 3773-3789. c) Wiedemann, T.; Voit, G.; Tchernook, A.; Roesle, P.; Göttker-Schnetmann, I.; Mecking, S. *J. Am. Chem. Soc.* **2014**, *136*, 2078-2085.

(34) Chen, Z.; Mesgar, M.; White, P. S.; Daugulis, O.; Brookhart, M. *ACS Catal.* **2015**, *5*, 631-636.

(35) Younkin, T. R.; Connor, E. F.; Henderson, J. I.; Friedrich, S. K.; Grubbs, R. H.; Bansleben, D. A. *Science* **2000**, *287*, 460-462.

(36) Berkefeld, A.; Mecking, S. *J. Am. Chem. Soc.* **2009**, *131*, 1565-1574.

(37) Bauers, F. M.; Mecking, S. *Angew. Chem., Int. Ed.* **2001**, *40*, 3020-3022.

(38) Waltman, A. W.; Younkin, T. R.; Grubbs, R. H. *Organometallics* **2004**, *23*, 5121-5123.

(39) Delferro, M.; McInnis, J. P.; Marks, T. J. *Organometallics* **2010**, *29*, 5040-5049.

(40) Hicks, F. A.; Brookhart, M. *Organometallics* **2001**, *20*, 3217-3219.

(41) Zhang, L.; Brookhart, M.; White, P. S. *Organometallics* **2006**, *25*, 1868-1874.

(42) Chen, Y.; Wu, G.; Bazan, G. C. *Angew. Chem.* **2005**, *117*, 1132-1136.

(43) Drent, E.; van Dijk, R.; van Ginkel, R.; van Oort, B.; Pugh, R. I. *Chem. Commun.* **2002**, 744-745.

(44) a) Hearley, A. K.; Nowack, R. J.; Rieger, B. *Organometallics* **2005**, *24*, 2755-2763. b) Kochi, T.; Yoshimura, K.; Nozaki, K. *Dalton Trans.* **2006**, 25-27. c) Newsham, D. K.;

Borkar, S.; Sen, A.; Conner, D. M.; Goodall, B. L. *Organometallics* **2007**, *26*, 3636-3638. d) Vela, J.; Lief, G. R.; Shen, Z.; Jordan, R. F. *Organometallics* **2007**, *26*, 6624-6635.

(45) Ota, Y.; Ito, S.; Kuroda, J.-i.; Okumura, Y.; Nozaki, K. *J. Am. Chem. Soc.* **2014**, *136*, 11898-11901.

(46) Nakamura, A.; Ito, S.; Nozaki, K. *Chem. Rev.* **2009**, *109*, 5215-5244.

(47) a) Nozaki, K.; Kusumoto, S.; Noda, S.; Kochi, T.; Chung, L. W.; Morokuma, K. *J. Am. Chem. Soc.* **2010**, *132*, 16030-16042. b) Kochi, T.; Noda, S.; Yoshimura, K.; Nozaki, K. *J. Am. Chem. Soc.* **2007**, *129*, 8948-8949.

(48) Rünzi, T.; Baier, M. C.; Negele, C.; Krumova, M.; Mecking, S. *Macromol. Rapid Commun.* **2015**, *36*, 165-173.

(49) Ito, S.; Munakata, K.; Nakamura, A.; Nozaki, K. *J. Am. Chem. Soc.* **2009**, *131*, 14606-14607.

(50) a) Shen, Z.; Jordan, R. F. *Macromolecules* **2010**, *43*, 8706-8708. b) Leicht, H.; Göttker-Schnetmann, I.; Mecking, S. *Angew. Chem., Int. Ed.* **2013**, *52*, 3963-3966.

(51) Guironnet, D.; Roesle, P.; Rünzi, T.; Göttker-Schnetmann, I.; Mecking, S. *J. Am. Chem. Soc.* **2008**, *131*, 422-423.

(52) Neuwald, B.; Caporaso, L.; Cavallo, L.; Mecking, S. *J. Am. Chem. Soc.* **2013**, *135*, 1026-1036.

(53) Drent, E.; van Dijk, R.; van Ginkel, R.; van Oort, B.; Pugh, R. I. *Chem. Commun.* **2002**, 964-965.

(54) a) Nakamura, A.; Munakata, K.; Ito, S.; Kochi, T.; Chung, L. W.; Morokuma, K.; Nozaki, K. *J. Am. Chem. Soc.* **2011**, *133*, 6761-6779. b) Nakamura, A.; Munakata, K.; Kochi, T.; Nozaki, K. *J. Am. Chem. Soc.* **2008**, *130*, 8128-8129.

(55) Kochi, T.; Nakamura, A.; Ida, H.; Nozaki, K. *J. Am. Chem. Soc.* **2007**, *129*, 7770-7771.

(56) Rünzi, T.; Guironnet, D.; Göttker-Schnetmann, I.; Mecking, S. *J. Am. Chem. Soc.* **2010**, *132*, 16623-16630.

(57) Nakamura, A.; Anselment, T. M. J.; Claverie, J.; Goodall, B.; Jordan, R. F.; Mecking, S.; Rieger, B.; Sen, A.; van Leeuwen, P. W. N. M.; Nozaki, K. *Acc. Chem. Res.* **2013**, *46*, 1438-1449.

(58) Noda, S.; Nakamura, A.; Kochi, T.; Chung, L. W.; Morokuma, K.; Nozaki, K. *J. Am. Chem. Soc.* **2009**, *131*, 14088-14100.

(59) Kanazawa, M.; Ito, S.; Nozaki, K. *Organometallics* **2011**, *30*, 6049-6052.

(60) Carrow, B. P.; Nozaki, K. *J. Am. Chem. Soc.* **2012**, *134*, 8802-8805.

(61) a) Noyori, R. *Angew. Chem., Int. Ed.* **2002**, *41*, 2008-2022. b) Warner, M. C.; Casey, C. P.; Baeckvall, J.-E. *Top. Organomet. Chem.* **2011**, *37*, 85-125.

(62) a) Vougioukalakis, G. C.; Grubbs, R. H. *Chem. Rev.* **2009**, *110*, 1746-1787. b) Trnka, T. M.; Grubbs, R. H. *Acc. Chem. Res.* **2000**, *34*, 18-29.

(63) a) James, B. R.; Markham, L. D. *J. Catal.* **1972**, *27*, 442-451. b) Komiya, S.; Yamamoto, A.; Ikeda, S. *Bull. Chem. Soc. Jpn.* **1975**, *48*, 101-107.

(64) a) Faller, J. W.; Chase, K. J. *Organometallics* **1995**, *14*, 1592-1600. b) Umezawa-Vizzini, K.; Lee, T. R. *Organometallics* **2004**, *23*, 1448-1452. c) Foley, N. A.; Lee, J. P.; Ke, Z.; Gunnoe, T. B.; Cundari, T. R. *Acc. Chem. Res.* **2009**, *42*, 585-597.

(65) Budagumpi, S.; Kim, K.-H.; Kim, I. *Coord. Chem. Rev.* **2011**, *255*, 2785-2809.

(66) Nomura, K.; Warit, S.; Imanishi, Y. *Macromolecules* **1999**, *32*, 4732-4734.

(67) Dias, E. L.; Brookhart, M.; White, P. S. *Organometallics* **2000**, *19*, 4995-5004.

(68) Heyndrickx, W.; Occhipinti, G.; Minenkov, Y.; Jensen, V. R. *J. Mol. Catal. A: Chem.* **2010**, *324*, 64-74.

(69) Piche, L.; Daigle, J.-C.; Claverie, J. P. *Chem. Commun.* **2011**, *47*, 7836-7838.

(70) Camacho-Fernandez, M. A.; Yen, M.; Ziller, J. W.; Guan, Z. *Chem. Sci.* **2013**, *4*, 2902-2906.

2 Tripodal Nitrogen-donor Ruthenium complexes

2.1 Introduction

The Cossee-Arlman mechanism of migratory insertion requires a *cis*-arrangement of the olefin substrate with the growing polymer coordination site. In the isolated [Ru(PDI)Me(C_2H_4)][BArF] (BArF = B(3,5-(CF_3)$_2$-C_6H_3)$_4$) complex (**1.12**) the methyl and ethylene groups are coordinated mutually *cis*, but are inactive towards insertion. This lack of reactivity can be ascribed to the nonequivalence of the two coordination sites for ethylene and the growing polymer chain, which was investigated computationally.[1] Two coordination isomers of the 5-coordinate square pyramidal complex **1.12** exist, with either the ethylene bound *trans* or *cis* to the PDI pyridine moiety (Scheme 2.1). Note that the olefin is oriented parallel to the PDI backbone and requires further rotation prior to insertion. The *trans*-π-complex is energetically favored over the *cis*-π-complex by 16.6 – 20.0 kcal mol^{-1} (depending on the level of theory), and the barrier for *cis*-*trans* isomerization is 25.1 – 29.8 kcal mol^{-1}, corroborating the experimentally determined presence of only the *trans*-π-complex even at elevated temperatures. The calculated migratory insertion barriers are prohibitively high (48.4 – 55.0 kcal mol^{-1}) for the more stable *trans*-π-complex, and for the *cis*-π-complex (22.7 – 28.4 kcal mol^{-1}). Analogous values were obtained for the structurally similar catalyst **1.11**. The formation of *cis* and *trans* isomers that result in very high insertion barriers is a direct consequence of the asymmetric nature of the PDI ligand. While electronic and steric modifications of the catalyst system, by virtue of the ligand, can be used to lower the insertion barriers, the use of symmetric ligands and coordination modes can circumvent the formation of *cis*- and *trans*-π-isomers.

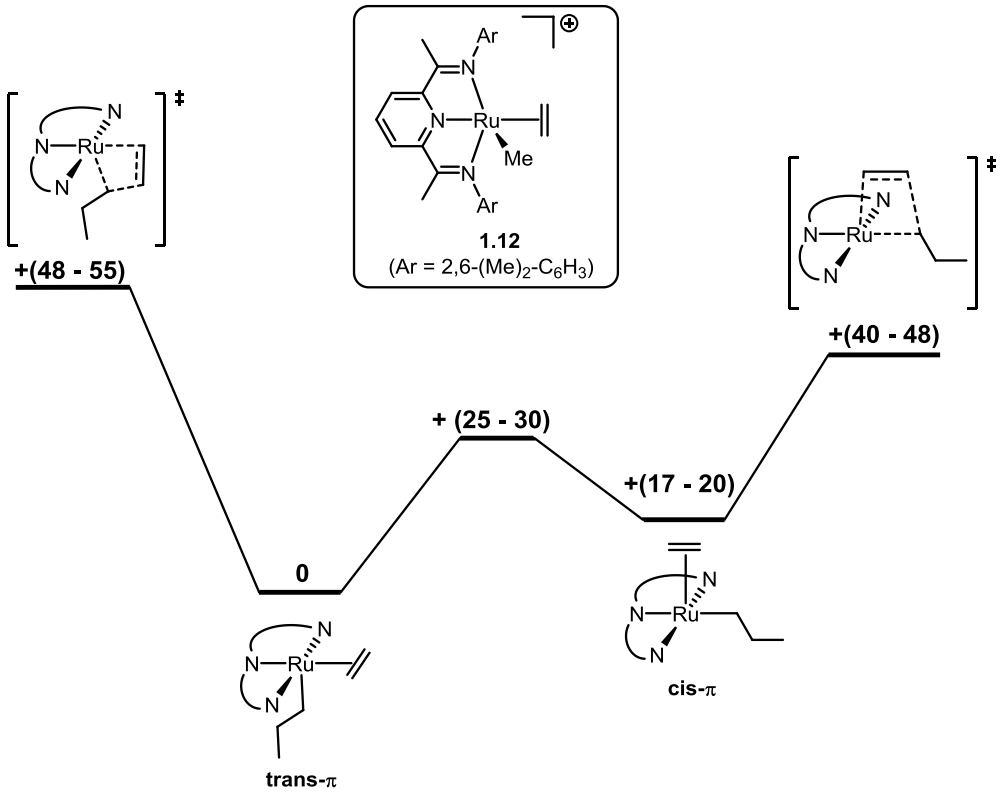

Scheme 2.1 Calculated energy profile for the *cis-trans* isomerization and insertion barriers (values are in kcal / mol).[1]

Tridentate ligands coordinate to octahedral complexes in a meridional (*mer*) or facial (*fac*) mode depending on the ligand structure and flexibility (Scheme 2.2). These modes are not mutually exclusive for a certain ligand and/or complex, and coordination isomerism can be observed. For the pincer-type PDI ligands, the rigid backbone favors exclusively meridional coordination. Facially chelating symmetric ligands (e.g. η^6-arenes) form octahedral complexes where the three other coordination sites are equivalent.

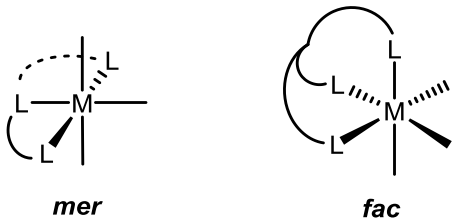

Scheme 2.2 Schematic depiction of meridional (*mer*) and facial (*fac*) coordination modes of tridentate ligands.

A few late transition metal insertion polymerization catalysts with nitrogen donor *fac*-ligands have been reported (Scheme 2.3). Iron and cobalt complexes of tris(2-pyridyl)amine or tris(2-pyridyl)phosphine (**2.1)** are active precursors for ethylene polymerization exhibiting moderate to high activities (up to 271 g(PE) mmol(**2.1**)$^{-1}$ h^{-1} bar^{-1}) at elevated temperatures up to 80 ˚C.[2] Catalysts based on Fe were only marginally more active than Co, and the effects of the bridgehead atom (*N* vs *P*) were negligible. Structural characterization of the complexes was not reported. A triazacyclononane Rh complex **2.2** produced polyethylene in a variety of solvents, including water, albeit at extremely low activity (circa one turnover number per day).[3]

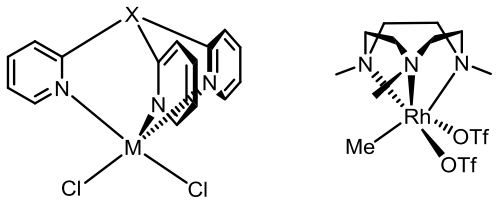

Scheme 2.3 Two examples of ethylene polymerization catalysts with facially coordinating tridentate ligands.

Based on these previous reports, investigation of Ru polymerization catalysts with the following properties seemed promising: 1) a neutral facially coordinating tridentate ligand with low donor strength; 2) relatively high electrophilicity at the metal center; and 3) an ancillary ligand

with donor strength comparable to ethylene. Pyridine, imidazole, or pyrazol based ligands were envisioned as suitable candidates. The corresponding tris(heteroaromatic)methane ligands adopt a facial coordination geometry,[4] and are chemically robust. They can also be modified at the pivotal sp^3-carbon to adjust solubility, and at the aromatic rings to alter their donor properties as well as sterics. These neutral ligands will result in cationic olefin alkyl intermediates after activation.

2.2 Synthesis of *fac*-Chelating Pyridine-Based Ligands

The tris(2-pyridyl)methane[5] framework and compound **2.3**[6] were prepared by following literature procedures. The synthesis (Scheme 2.4) consisted of an addition of 2-lithio pyridine to commercially available di(2-pyridyl)ketone to form tris(2-pyridyl)carbinol, followed by alkylation with benzyl bromide to afford ligand **2.3**. During the course of the study, it was found desirable to use ligands with purely hydrocarbon frameworks, to reduce potential side-reactions involving the ether functionality in compound **2.3**. Hence tris(2-pyridyl)carbinol was reduced in two steps via initial chlorination with thionyl chloride, and radical dehalogenation with tributyltin hydride to yield tris(2-pyridyl)methane.[5] Deprotonation of the bridgehead carbon with *n*-BuLi followed by treatment with benzyl bromide or methyl iodide gave the target ligands **2.4** and **2.5,** respectively. The α-picolyl variant was synthesized to modify the ligand sterics around the metal center. The unmodified tris(2-α-picolyl)methane (**2.6**) was provided by visiting scholar Dr. Kazuhito Hioki, and the backbone-benzylated derivative **2.7** was synthesized analogous to compound **2.4**. The structure of **2.3** – **2.7** was fully established by one- and two-dimensional ^{1}H and ^{13}C NMR and MS. Single crystals of X-ray quality were obtained via slow evaporation of an ether solution of ligand **2.5**. The molecular structure of **2.5** is given in Figure 2.1.

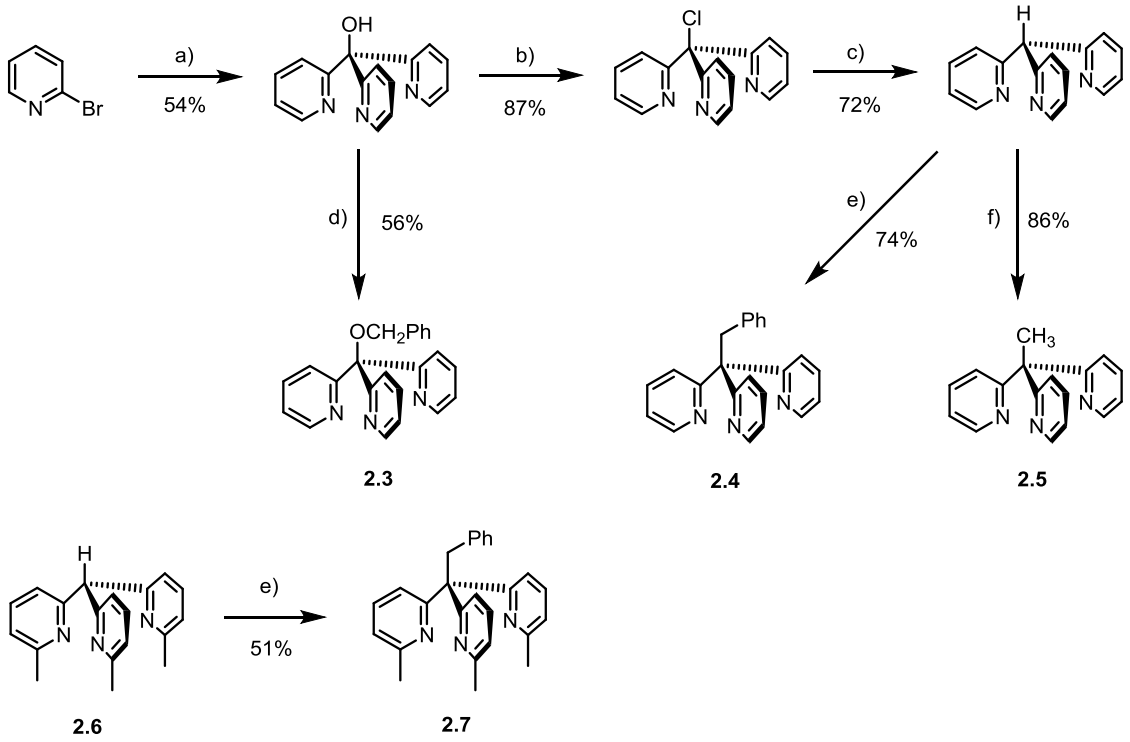

Scheme 2.4 Synthesis of tris(2-pyridyl)methane based ligands **2.3** – **2.7**. Reaction conditions: a) 1. *n*-BuLi, Et_2O, -78 °C 2. di(2-pyridyl)ketone, -78 °C to rt; b) 1. NaH, THF, rt 2. $SOCl_2$; c) $(n\text{-}Bu)_3SnH$, hν, THF; d) 1. NaH, THF 2. BnBr, 66 °C; e) 1. *n*-BuLi, THF, -78 °C 2. BnBr, -78 °C to rt; f) 1. *n*-BuLi, THF, -78 °C 2. MeI, -78 °C to rt.

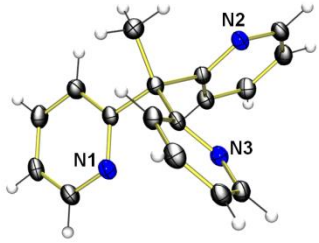

Figure 2.1 Single crystal X-ray structure of complex **2.5**.

2.3 Synthesis of *fac*-Chelating Imidazole-Based Ligand

Imidazoles are less Lewis basic heteroaromatic compounds compared to pyridine and can also be easily functionalized. In a tris(2-imidazoyl)methane system, the bite angle is not expected to be considerably different than with tris(2-pyridyl)methane, however, the hydrogen adjacent to the coordinating nitrogen would be pointing further away from the metal due to the 5-membered

ring. The tris(2-(*N*-methyl)imidazoyl)carbinol ligand was prepared according to a literature procedure[7] from *N*-methylimidazole and diethylcarbonate. The alcohol group was then methylated with methyl iodide to yield the desired ligand **2.8**.

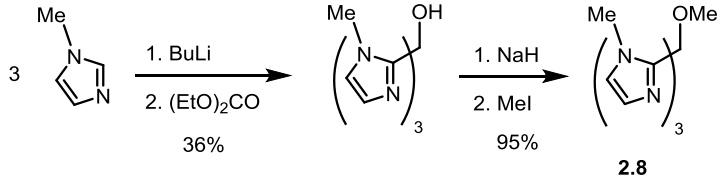

Scheme 2.5 Synthesis of tris(2-(*N*-methyl)imidazoyl) ligand **2.8**.

2.4 Synthesis of *fac*-Chelating Pyrazole-Based Ligands

The tris(1-pyrazolyl)methane compounds (**2.9** - **2.11**) were prepared by literature procedures published by Reger et al. in moderate to good yields (42 – 83 %).[8] The respective pyrazole was treated with excess Na_2CO_3 in water and then refluxed for several days after addition of chloroform and the phase transfer agent tetrabutylammonium bromide (TBAB) as depicted in Scheme 2.6. In all cases but **2.11**, the compounds were further purified by recrystallization.

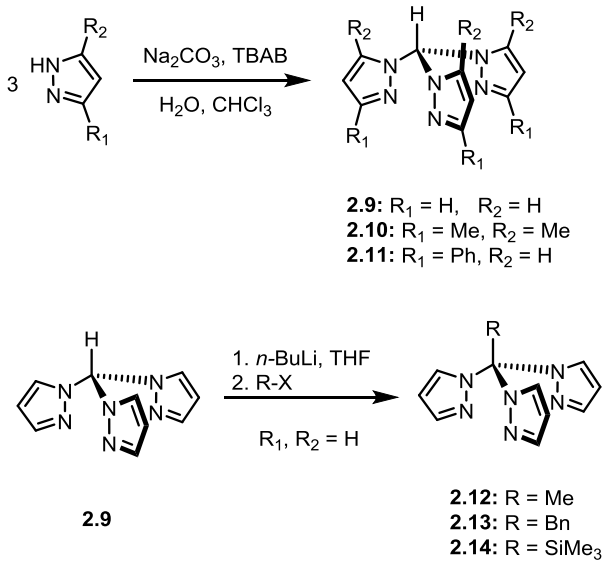

Scheme 2.6 Synthesis of tris(1-pyrazoyl)methane ligands **2.9** - **2.14**.

The substitution in the 3 position of the pyrazole (R_1) merely provides steric bulk and has little effect on the donor strength of the ligand: In complexes of the type $[(L)Mn(CO)_3][SO_3CF_3]$ with L = **2.9 – 2.11**, both carbonyl stretching frequencies show a maximum deviation of 7 cm^{-1} between the different complexes.[8a] To overcome solubility issues of the resulting complexes in common organic solvents (vide infra), the pivotal sp^3-carbon of ligand **2.9** was further functionalized with nonpolar groups. Deprotonation of the acidic backbone CH with *n*-butyl lithium at low temperatures and reaction with the respective electrophiles (methyl iodide, benzyl bromide, and trimethylsilyl chloride) afforded the functionalized ligands **2.12** – **2.14** in good yields (75 – 93 %).

2.5 Synthesis of Ru-Complexes

2.5.1 Trispyridine Complexes

The reaction of $RuCl_2(PPh_3)_3$ with ligands **2.3** or **2.5** yielded complexes of the type $RuCl_2(PPh_3)$(*fac*-trispyridine) in 84 – 94 % yield. Stirring a THF solution of the reactants for 2-3 days gave clean THF adducts of **2.15** and **2.16** as orange precipitates (Scheme 2.7). Removal of the product complex from the coordination equilibrium by precipitation seems to be the major driving force. Under the same conditions, the reaction with **2.4** reaches only about 40% conversion, determined by ^1H NMR of the crude reaction mixture, due to the fact that the resulting complex is soluble in THF.

In order to replace PPh_3 with weaker donor ligands that can be more readily displaced by olefins during the polymerization reaction, a procedure reported for the exchange of PPh_3 with pyridine in the analogous complex $RuCl_2(PPh_3)(N(2\text{-}pyr)_3)$) was used.[9] Complex **2.16** was treated with excess amounts of pyridine or acetonitrile in refluxing toluene for several hours to yield the

respective complexes **2.17** and **2.18** in 84 and 89% isolated yield. Under similar conditions, 2,6-lutidine was unable to replace PPh_3, likely due to the steric bulk of the additional methyl groups.

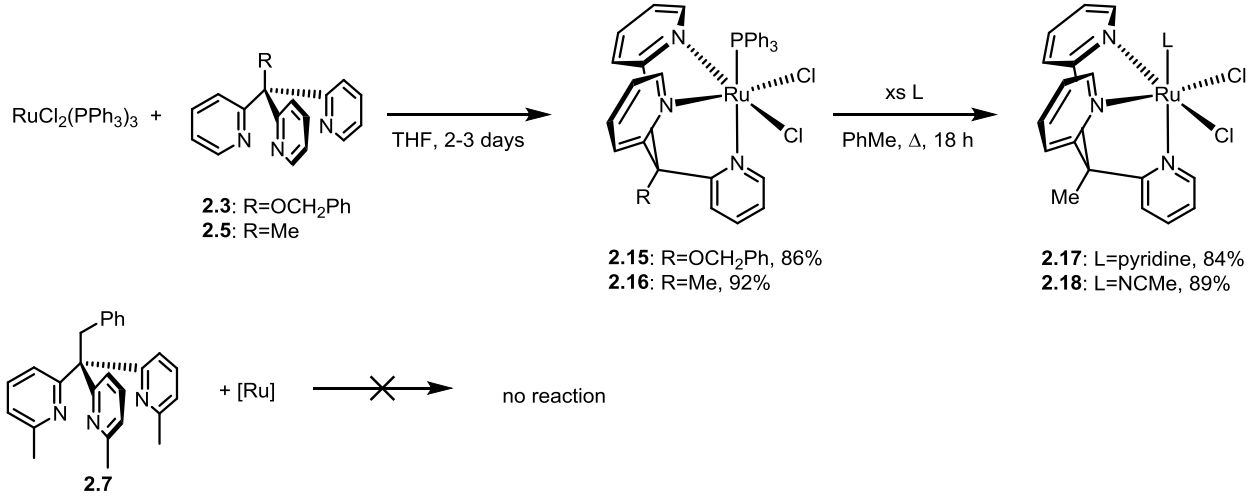

Scheme 2.7 Synthesis of complexes **2.15** – **2.18**.

Employing **2.7** in analogous reactions with $RuCl_2(PPh_3)_3$, $RuCl(H)(PPh_3)_3$, $RuCl_2(dmso)_4$ or $RuCl_3$ were unsuccessful. In each case, uncoordinated ligand could be retrieved while the ruthenium precursor decomposed. It can be assumed that the 6-methyl groups impose too large of a steric bulk for the formation of the complex.

Complexes **2.15** – **2.18** showed sufficient solubilities in chlorinated solvents and their diamagnetic nature allows for full NMR spectroscopic characterization (Scheme 2.8). Each complex shows two equivalent pyridyl moieties that are coordinated *trans* to the chlorides and the third nonequivalent pyridyl moiety coordinating trans to the ancillary *P*- or *N*-donor ligand. All proton resonances of the pyridine moiety *trans* to the ancillary ligand were downfield shifted. The CH protons adjacent to the pyridine nitrogen atom show significant downfield shifts with a 1:2 integral ratio. The overall resonance pattern is similar to $RuCl_2(PPh_3)(N(2\text{-pyr})_3)$), and strongly indicates the desired κ^3-*N* coordination of the tridentate ligand to the metal center.

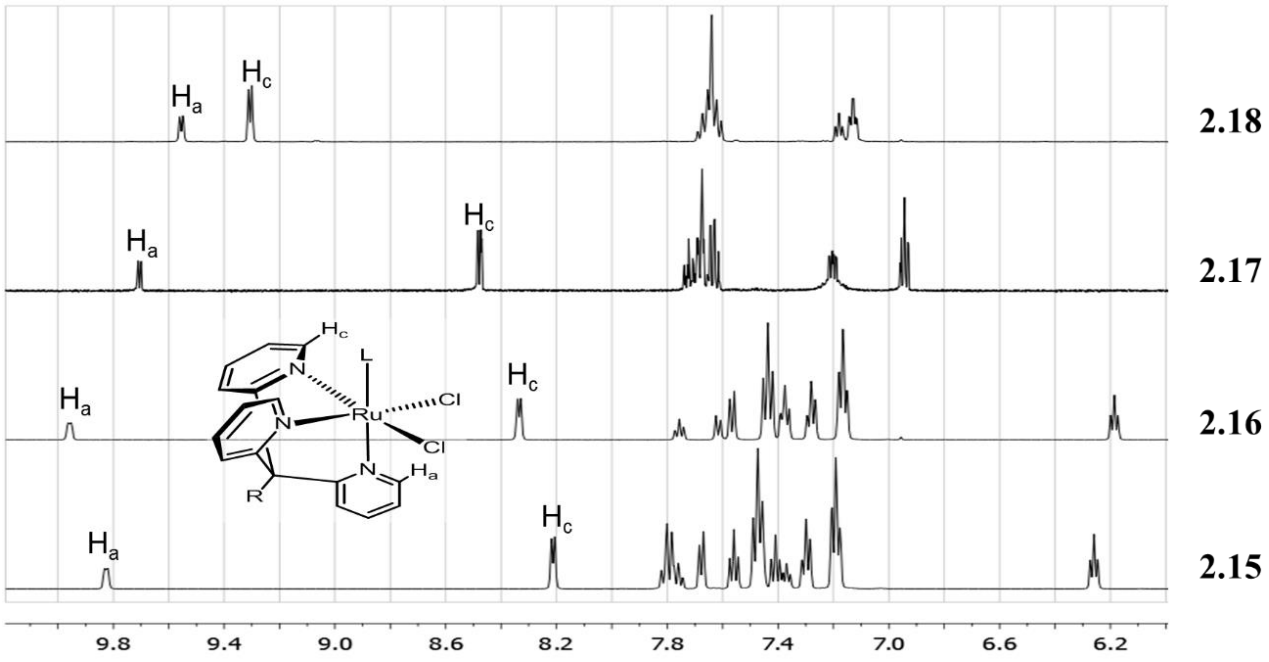

Scheme 2.8 Aromatic region of ^{1}H NMR of complexes **2.15** – **2.18** in CD_2Cl_2 at 298 K.

Comparing **2.16** to **2.18**, a downfield shift of the resonances was observed for the pyridines coordinated *trans* to chlorides, while the peaks for the pyridine *trans* to the ancillary ligand are moved upfield. The difference in chemical shift between the non-equivalent pyridyl moieties of the tripod ligand decreases, as the difference in steric bulk and *trans* effect between the ancillary and the chloride ligands becomes less pronounced. This is also reflected in the bond length and angle changes (Table 1).

The ^{1}H NMR of **2.17** showed temperature dependent features (Scheme 2.9) associated with the rotation of the ancillary pyridine around the Ru-N bond. At 25 °C, integration of all aromatic resonances resulted in 15 protons, where 17 are expected. The downfield region consists of two doublets at 8.48 and 9.71 ppm with an integral ratio of 2:1, corresponding to the H6 protons of the pyridine nitrogen atoms of the tripod ligand. The resonances of the same protons from the coordinated ancillary pyridine were expected to have similar chemical shift, but could not be

located. Cooling the sample to -80 °C lead to the appearance of an additional set of doublets at 9.77 ppm, which integrates for one proton. Another doublet, integrating for one proton, resonates at 6.73 ppm. These two signals were assigned as the protons adjacent to nitrogen in the ancillary pyridine by ^{1}H,^{1}H COSY NMR spectroscopy. The more shielded proton at 6.73 ppm most likely corresponds to the proton located between the two ligand pyridines, while the proton at 9.77 ppm is facing the chlorides, resulting in a similar chemical shift as H_a.

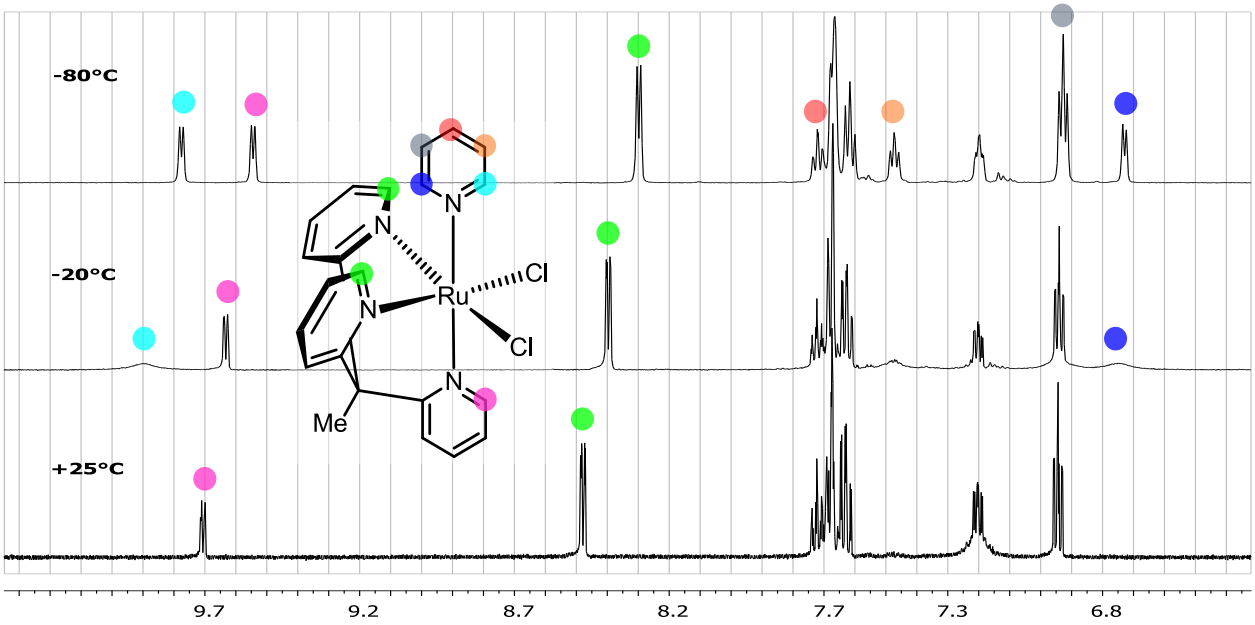

Scheme 2.9 ^{1}H NMR spectra of the aromatic region of complex **2.17** at 298 K, 253 K, and 193 K (bottom to top).

Such large differences in chemical shifts for the H2 vs. H6 protons of *N*-bonded non-rotating pyridines is in accordance with shielding of H2 resulting from its location between the pyridine moieties. Warming of the sample leads to broadening of the resonances above 0 °C, caused by rotation around the Ru-N bond. Coalescence of the H2 and H6 protons occurred around 313 K, from which a rotational barrier of 13 kcal mol^{-1} was calculated. Similar barriers have been found for other octahedral complexes.[10]

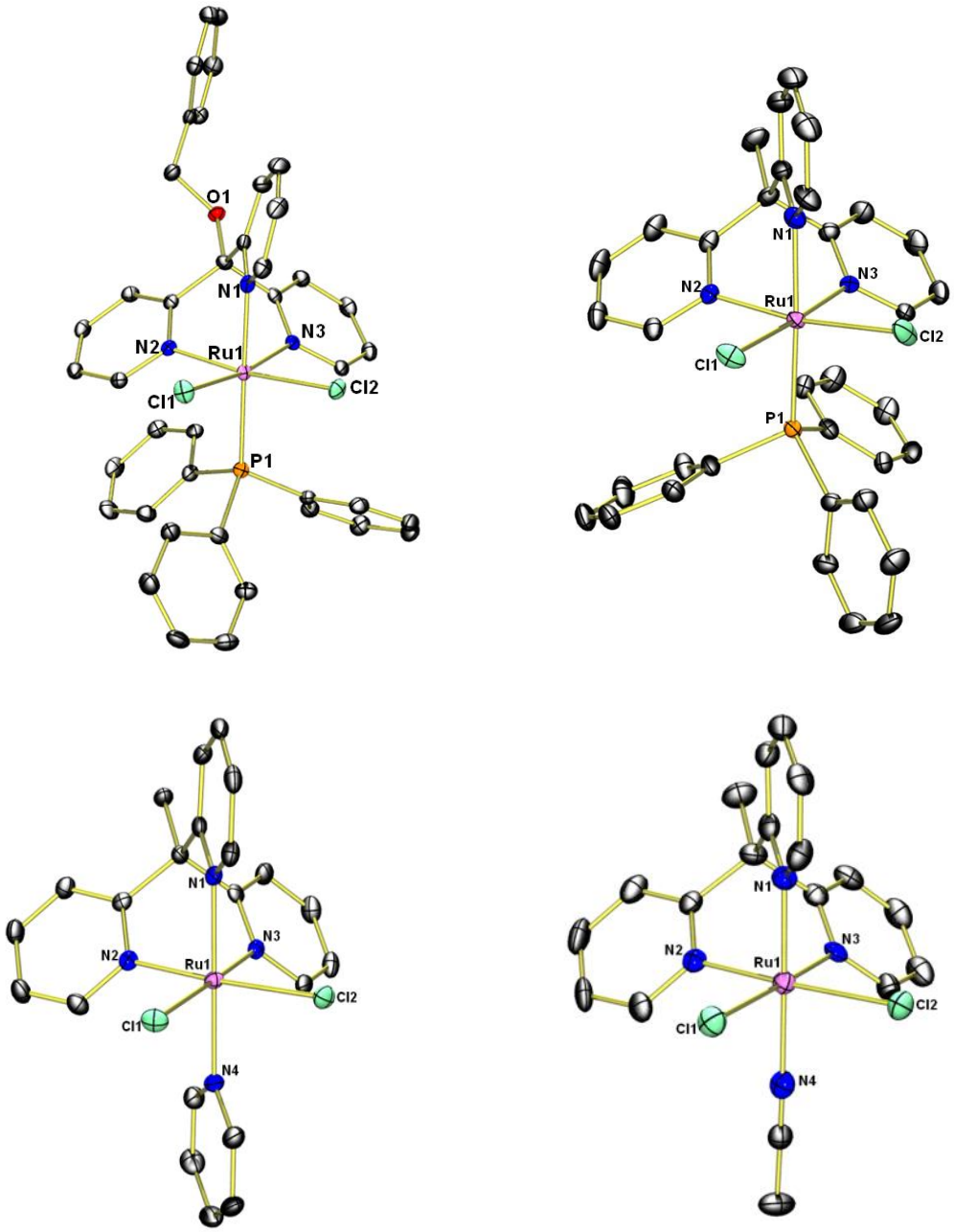

Figure 2.2 Molecular structures of complexes **2.15 - 2.18** (from top left to bottom right). Hydrogen atoms are omitted for clarity. See Table 1 for selected bond distanced and angles.

Red-orange single crystals of X-ray quality were obtained for **2.15** – **2.18** by slow diffusion of diethyl ether into a solution of the complex in dichloromethane. The molecular structures of

2.15 – **2.18** are shown in Figure 2.2 and important bond distances and angles are summarized in Table 1. Each complex shows a distorted octahedral coordination sphere around the ruthenium. The Ru-N bond lengths decrease from an average of 2.046 Å for Ru(1)-N(2/3) and 2.089 Å for Ru(1)-N(1) in **2.16** to 2.014 Å and 2.012 Å in **2.18** while the tripodal N-Ru-N angles increase and are almost uniform, between 87 and 88° in **2.18**. This is in agreement with the solution behavior mentioned above and demonstrates that the coordination sites become more similar by exchanging PPh_3 with acetonitrile. The acetonitrile in **2.18** is virtually linear with a torsion angle of 178.98°.

Table 1: Summary of important bond lengths (Å) and bond angles (°) of complexes **2.15** – **2.18**.

		2.15	**2.16**	**2.17**	**2.18**
Bond Lengths	Ru1-Cl1	2.4093(6)	2.4228(5)	2.4229(5)	2.4334(8)
	Ru1-Cl2	2.4185(6)	2.4368(6)	2.4269(5)	2.4338(8)
	Ru1-N1	2.0732(19)	2.0856(18)	2.0404(17)	2.012(2)
	Ru1-N2	2.0436(18)	2.0462(17)	2.0116(16)	2.023(3)
	Ru1-N3	2.0913(18)	2.0450(17)	2.0106(17)	2.005(3)
	Ru1-P1/Ru1-N4	2.3805(6)	2.3574(6)	2.0864(17)	2.051(3)
Bond Angles	Cl1-Ru1-Cl2	90.77(2)	89.86(2)	91.049(19)	90.64(3)
	N1-Ru1-N2	85.21(7)	83.41(7)	87.09(7)	87.27(11)
	N1-Ru1-N3	84.59(7)	83.87(7)	87.99(7)	87.56(10)
	N2-Ru1-N3	89.78(7)	90.94(7)	88.09(7)	87.64(10)

NMR spectroscopic studies of the insertion process can give valuable mechanistic information. However, observation of *in-situ* activated catalysts is often hampered due to excess amounts of cocatalyst, and overlap of metal-alkyl species and cocatalyst in the aliphatic region. To this end, cationic Ru-methyl (see Chapter 2.7) or Ru-hydride complexes are attractive precursors. The synthesis of Ru-hydride complexes from commercially available Ru-hydrides was investigated. Reaction of **2.5** with $Ru(Cl)H(PPh_3)_3$ in THF under reflux resulted in the formation

of a mixture of two products that precipitated (Scheme 2.10). The major product (3:2) was **2.16**, as confirmed by ^{1}H NMR. The second minor product was the dinuclear complex **2.19** with bridging hydrogen and chlorine atoms. The ^{1}H NMR resonance of the hydride at - 17.54 ppm shows a ddd splitting (with $^{2}J_{PH}$ values of 52.0, 16.4, and 10.9 Hz) from the three non-equivalent coordinated phosphines (Figure 2.3, right). Single crystals of both products could be obtained. The structure of **2.19** resembles the desired "RuCl(H)(PPh_3)(**2.5**)" unit, which underwent a C-H activation at the ortho position of the pyridine moiety trans to the phosphine (Figure 2.3, left).

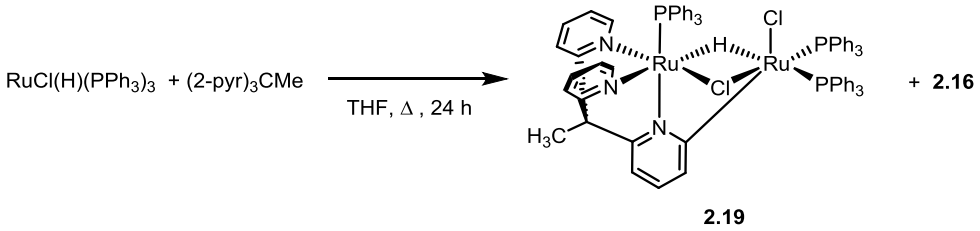

Scheme 2.10 CH activation of complex **2.5** with RuCl(H)(PPh_3)$_3$.

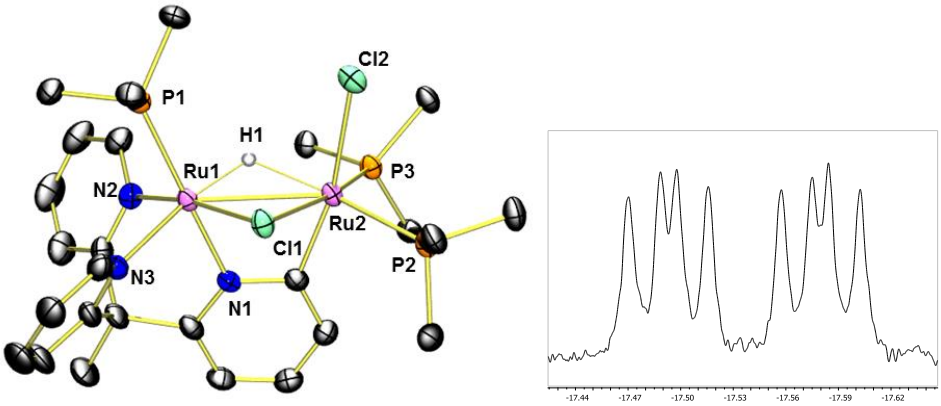

Figure 2.3 Left: Molecular structure of complex **2.19**. For visual clarity, C-bonded H-atoms, and one molecule of cocrystallized chloroform are omitted, and the phenyl groups of PPh_3 truncated. Important bond lengths (Å) and bond angles (°): Ru1-H1 1.62(3), Ru1-Cl1 2.3911(7), Ru2-H1 1.90(3), Ru2-Cl1 2.4458(7), Ru1-Ru2 2.8818(3), Ru2-C1 2.027(3), R2-Cl2 2.5434(7), H1-Ru1-Cl1 87.3(12), H1-Ru2-Cl1 80.2(10), Ru1-Cl1-Ru2 73.127(19), N1-Ru1-Ru2 110.33(18). Right: ^{1}H NMR resonance of the bridging hydride of **2.19** in $CDCl_3$ at 298 K.

2.5.2 Trisimidazole Complexes

Ruthenium(II) complexes of the tris(2-imidazoyl)methane framework are known. Elgafi *et al.* reported on ruthenium (and osmium) complexes of tris(2-(*N*-methyl)imidazoyl)methanol (Scheme 2.11, top). These cationic complexes **2.20** and **2.21** were obtained by treating the tripodal ligand with $RuCl_2(PPh_3)_4$ and $Ru(CO)Cl(H)(PPh_3)_3$, respectively. Analogous iron complexes are not known.

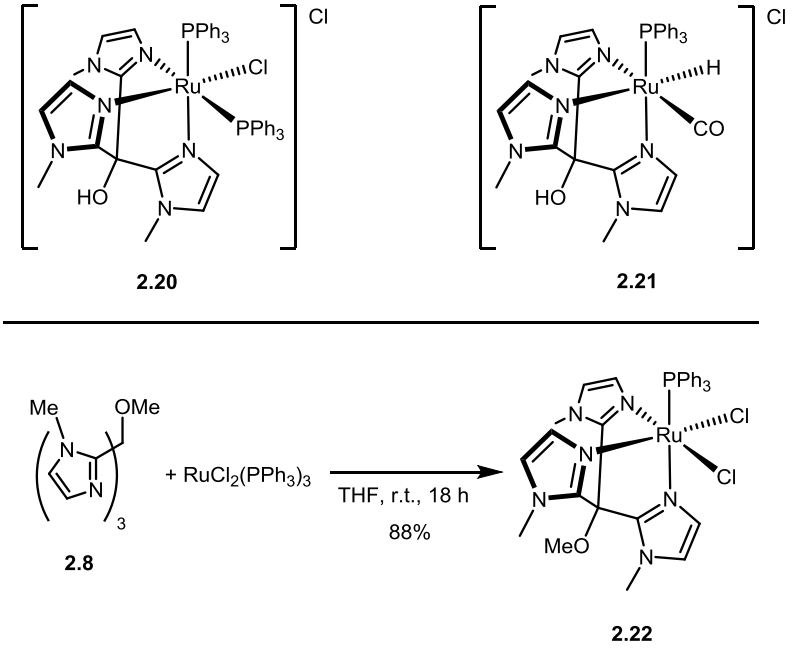

Scheme 2.11 Known tris(2-(*N*-methyl)imidazoyl)methanol Ru complexes (top). Synthesis of complex **2.22** (bottom).

Stirring a THF solution of ligand **2.8** and $RuCl_2(PPh_3)_3$ at room temperature results in the formation of neutral complex **2.22** as a pale yellow precipitate (Scheme 2.11, bottom). The complex was characterized by ^1H, ^{31}P NMR and ESI-MS. In analogy to the tris(2-pyridyl)methane ligands, the tris-imidazole complex adopts a similar structure.

2.5.3 Trispyrazole Complexes

Several ruthenium complexes containing ligand **2.9** have been reported using various Ru(II) and Ru(III) precursors.[11] Out of these complexes (κ^3-*N,N,N*-(HC(pz)$_3$))RuCl$_2$(dmso) and (κ^3-*N,N,N*-(HC(pz)$_3$))RuCl$_2$(pyridine) are structurally most similar to the target complex. Two chlorides are coordinated *cis* to the metal center, and can be activated with an appropriate cocatalyst. The other coordination site is occupied by a small monodentate ligand that can be replaced by ethylene under polymerization conditions.

The dmso coordinated complex **2.23** could be obtained following a literature procedure[11e] by reacting ligand **2.9** with RuCl$_2$(dmso)$_4$ in refluxing ethanol in 18 % yield. The resulting complex **2.23** showed limited solubility in organic solvents and was only observed to be soluble in water. Complexation of the methyl substituted ligand **2.12** to the ruthenium employing identical conditions resulted in hydrolysis of the ligand and the formation of undesired RuCl$_2$(dmso)$_2$(pzH)$_2$ (**2.24**) in 74 % yield. The product of trispyrazol decomposition has previously been reported by Alessio and coworkers as the main product of the reaction of **2.9** with RuCl$_2$(dmso)$_4$ in methanol (Scheme 2.12).[11e] The tris(2-pyrazoyl)methane ligand framework is prone to hydrolysis in protic reaction conditions, especially if the backbone is functionalized.

To avoid hydrolysis, it was found that the synthesis of **2.23** from **2.9** and RuCl$_2$(dmso)$_4$ can be carried out in dry toluene. After heating the reaction mixture to reflux for 2 days the complex could be obtained in approximately 90 % yield. The reaction is believed to proceed via the intermediate [RuCl(dmso)$_2$(HC(pz)$_3$)][Cl], which is insoluble in the reaction solvent. This results in prolonged reaction times. Extending this method to ligands with substituents in the 3-position was unsuccessful. No conversion was observed with ligands **2.10** and **2.11**, containing methyl and phenyl groups in the 3-position, after 2 and 5 days respectively. Both **2.10** and **2.11** were stable

under the reaction conditions and showed no hydrolytic decomposition. The higher steric bulk of the ligands may disfavor complexation.

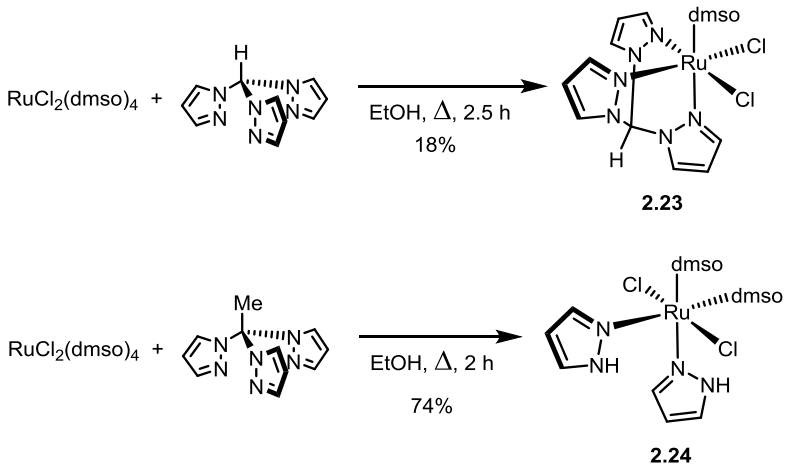

Scheme 2.12 Reactions of $RuCl_2(dmso)_4$ precursor with ligands **2.9** and **2.12** in protic solvents.

Complex $RuCl_2(dmso)(PhCH_2(pz)_3)$, the anticipated product from the reaction of **2.13** with $RuCl_2(dmso)_4$, was expected to be soluble in organic solvents. However, the reaction afforded complex **2.25** (Scheme 2.13), in which one pyrazole group was formally eliminated from **2.13** and the resulting bidentate ligand displaced two dmso ligands. Crystals suitable for X-ray crystallography were grown from a chloroform solution of complex **2.25** layered with diethyl ether (Figure 2.4). The octahedral complex exhibits a *cis* geometry of both chlorides and dmso groups respectively leading to both a chloride and a dmso in the *trans* position of the two pyrazole nitrogen atoms. The structure reveals that one of the dmso methyl groups is right above the centroids of a pyrazole moiety, experiencing a magnetic ring current giving rise to the upfield shifted ^{1}H NMR resonance at 2.28 ppm. An initial bidentate coordination of **2.13** to the metal would decrease the electron density of the pyrazole moieties and favor a (stepwise or concerted) intramolecular elimination reaction but a purely acid/base catalyzed stepwise reaction of either free or coordinated ligand cannot be ruled out.

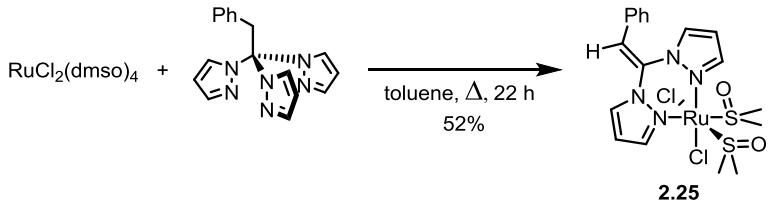

2.25

Scheme 2.13 Decomposition of ligand **2.13** during complexation reaction to form **2.25**.

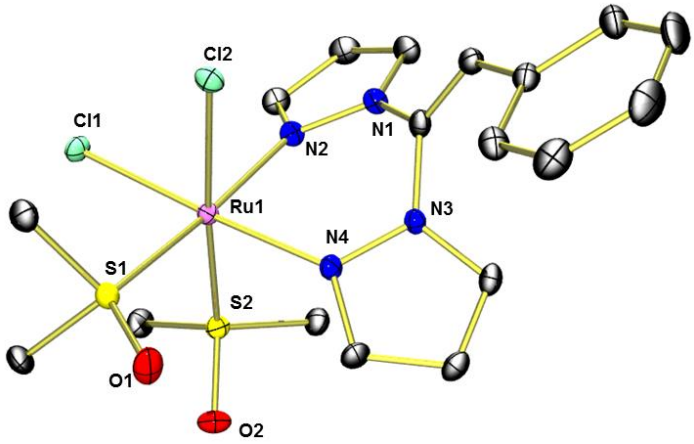

Figure 2.4 Molecular structure of **2.25**. Hydrogen atoms are omitted for clarity.

The cationic complex $[RuCl(PPh_3)_{2(}HC(pz)_3)]Cl$ was prepared from the commercial precursor $RuCl_2(PPh_3)_3$ and **2.9**.[11d] It was anticipated that the solubility of this complex in organic solvents could be increased by replacing the outer-sphere chloride with a 'greasier' non-coordinating anion such as tetraarylborate. However, extending the literature conditions to ligands **2.11**, **2.13** and **2.14** was unsuccessful. No complexation was observed by ^{1}H NMR after stirring for 24 h at room temperature or under reflux conditions. After 10 days standing at room temperature, a solution of $RuCl_2(PPh_3)_3$ and **2.9** in dry THF showed small amounts of yellow precipitate, which could be identified as $RuCl_2(PPh_3)[PhCH_2C(pz)_3]$ (**2.26**) (Scheme 2.14). The presence of only one PPh_3 unit per **2.9** was observed by ^{1}H NMR. The solubility of **2.26** was limited to water and dmso despite the modified backbone and the nonpolar phosphine ligand.

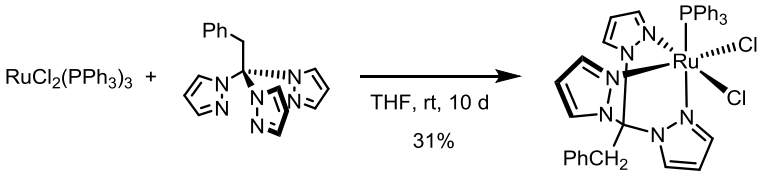

2.26

Scheme 2.14 Synthesis of complex **2.26**.

2.6 Ethylene Polymerization Attempts

To assess the activity towards olefin insertion, complexes **2.15** – **2.18**, **2.23**, and **2.26** were used as precursors in ethylene polymerization reactions. Different reaction conditions with varying temperatures (25 to 80 °C), pressures (up to 600 psi), times (up to 24 h), solvents (DCM, toluene) and cocatalysts (MAO, $AlMe_3$, $AlMe_2Cl$, and $AlMeCl_2$) were employed, but in no case was the production of more than trace amounts of solid polymer observed.

However, using methylaluminum dichloride as the activator resulted in the formation of a considerable amount of polymer when employed with **2.16**. A negative control run, without any ruthenium source, gave similar yields. Given also the similar polymer structures of the polymers obtained with neat $AlMeCl_2$ and **2.16**/$AlMeCl_2$**,** as indicated by similar melting points, it seems unlikely that a Ru species was involved in the polymerization. While $AlMeCl_2$ has been used successfully as cocatalyst for early and late TM precursors in ethylene polymerization, there is precedence for its neat polymerization ability in the presence of chlorinated activators like ethyl trichloroacetate or tosyl chloride.[12] The observed activity is comparable to the reported ones, however, here the initiation has to be attributed to the minimum amount (3-5 mL) of methylene chloride used to dissolve the Ru precursors.

The inactivity of **2.15** can be attributed to one or a combination of the following potential issues: A) the metal center is too electron rich due to the ancillary phosphine ligand; B) the ether

backbone undergoes some Lewis acid facilitated side reaction; or C) the employed activating conditions do not readily activate the dichloro precursor. A) and B) could be tested with complexes **2.17** – **2.18** having all-carbon backbones, and less strongly coordinating ancillary ligands, which also showed no increased activity. The activation issue C) is not easily assessed, but it was observed, that solutions of **2.15** – **2.18** change color from orange to light green when they are mixed with several hundred equivalents of MAO in the absence of ethylene. This indicates activation of the catalyst precursors to either the active species or an inactive side product.

2.7 Attempted Synthesis of Ru(II) Dimethyl Complexes

During further study of the reaction of ruthenium precursors with the aluminum cocatalyst, some stoichiometric reactions were investigated. Due to their superior stability, only the tris(2-pyridyl)methane based complexes **2.15** - **2.18** were considered. One major question to be answered is whether the activation of the dichloro precursors actually leads to the formation of Ru-methyl cations necessary for insertion. To this end, the direct methylation of **2.16** and **2.17** was attempted by reacting the dichloride complex with various transmetallation reagents (i.e. MeLi, MeMgBr, $SnMe_4$ and $AlMe_3$) in THF at low temperatures of typically -78 °C. The success rate of the respective alkylation reagent is quite unpredictable as noted in literature.[13] Under these conditions, the formation of a Ru-methyl species from **2.16** or **2.17** was not observed, and in most cases, the dichloride starting material could be recovered after warming to room temperature.

Several other reactions were observed. In the case of **2.16**/$AlMe_3$, ortho-metalation of one phenyl group of coordinated PPh_3 could be observed by ^1H NMR and mass spectrometry. Amongst other Ru-based examples,[14] Lee has shown ortho-metalation of $RuCl_2$(dppe) (dppe = 1,2-bis(diphenylphosphino)ethane) in the presence of $AlMe_3$.[15] This ortho-metalation requires the

prior abstraction of one chloride ligand. Complex **2.17** showed no reaction with $AlMe_3$ under identical conditions.

In further experiments, complex **2.18** reacted readily with excess amounts of MeLi and MeMgCl (3-5 equiv.) in methylene chloride at -78 and 0 °C respectively to form a dark orange compound within minutes. Detailed two-dimensional NMR ($^1H,^1H$ COSY and $^1H,^{13}C$ HSQC) experiments confirmed the addition of methide to the α-carbon of the coordinated acetonitrile (Scheme 2.15). It is believed that the anionic complex readily abstracts hydrogen/deuterium from trace sources of moisture or the solvent to form the observed imine complex **2.27.** The imine proton gives rise to a broad singlet at 10.9 ppm in the ^1H NMR spectrum. Such additions of lithium alkyls to the α-carbon of coordinated acetonitrile have precedence in literature, for example with a $W(PhCCPh)_3(MeCN)$ complex.[16]

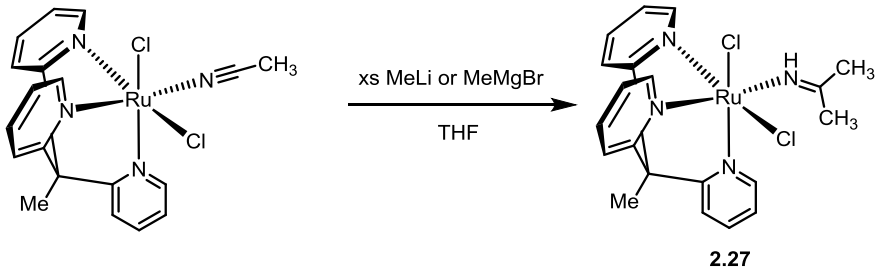

Scheme 2.15 Reduction of coordinated acetonitrile of complex **2.18** by metal methyls.

2.8 Conclusive Summary

The initial hypothesis of a more favorable energetic landscape for insertion polymerization with Ru-complexes, through the introduction of facially coordinating nitrogen-donor ligands could not be substantiated.

Several ligands based on the tris(2-pyridyl)methane, tris(2-imidazoyl)methane, and tris(1-pyrazoyl)methane framework were synthesized, as well as their corresponding Ru(II) complexes. The ligands based on pyrazol showed low hydrolytic stabilities in protic solvents

during complexation, but complexation of tris(2-pyridyl)methanes and tris(2-imidazoyl)methane gave the targeted $RuCl_2(PPh_3)$(fac-*N*,*N*,*N*) complexes. The coordinated PPh_3 could be replaced by pyridine or acetonitrile in the case of tris(2-pyridyl)methane ligands.

No activity in ethylene polymerization conditions was observed under a wide range of conditions with varying temperatures, solvents, and cocatalysts. A color change upon addition of cocatalyst to a solution of $RuCl_2L$(fac-*N*,*N*,*N*) (with fac-*N*,*N*,*N* = tris(2-pyridyl)methane, and L = MeCN, pyridine, or PPh_3) was observed, indicating activation of the dichloride precatalysts. However, several attempts at isolating Ru-alkyl species were unsuccessful.

Since the formation of catalytically active Ru-alkyl complexes could not be demonstrated, an insufficient activation cannot be ruled out as a cause for the catalyst inactivity. But the reasons could simply be a still prohibitively high barrier for migratory insertion as was observed for the Ru(PDI) complex.

2.9 Experimental Section

General considerations and materials

All solvents used were dried over alumina and all manipulations were done either in a glovebox or under nitrogen atmosphere utilizing standard Schlenk and cannula techniques, unless otherwise stated. NMR spectra were recorded on a Bruker AVANCE600 or DRX500 spectrometer at room temperature, unless otherwise noted, and referenced to solvent signals. All organic compounds were purchased from Sigma-Aldrich. $RuCl_2(PPh_3)_3$, and $RuCl_2(dmso)_4$ were obtained from Strem. Ligand precursors tris(2-pyridyl)methane[5], tris(N-methylimidazol-2-yl)methanol,[4c] and ligands **2.3**[6], **2.9 – 2.11**[8a,17], **2.12 - 2.14**[8b], were prepared according to literature procedures.

Syntheses

1,1,1-Tris(2-pyridyl)-2-phenylethane (**2.4**)

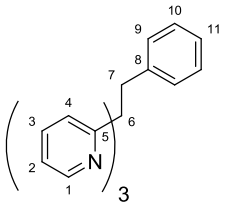

The crude tris(2-pyridyl)methane (347 mg, 1.0 equiv.) was dissolved in 20 mL of dry THF and 0.96 mL (1.1 equiv.) of a 1.6 M *n*-BuLi solution in hexanes was added dropwise at -78 °C, resulting in the precipitation of the a white solid. The solution was allowed to warm to room temperature and stirred for 3 h, after which it was cooled to -78 °C and 0.18 mL (1.1 equiv.) of benzyl bromide was added dropwise. The solution was stirred overnight at room temperature. The lightly turbid brown solution was quenched with 10 mL water and extracted with 3 x 20 mL dichloromethane. The combined organic extracts were dried with $MgSO_4$ and the solvent was evaporated under *vacuo*. The resulting reddish brown solid was purified by flash column chromatography (hexanes : ethyl acetate = 1 : 1) and recrystallized from hexanes to afford 350 mg

(74%) of off-white crystals as the title compound. ^{1}H NMR (500 MHz, acetone-d_6) δ 8.49 (dd, J = 4.8, 0.8 Hz, 3H, pyr), 7.56 (td, J = 8.0, 1.7 Hz, 3H, pyr), 7.29 (d, J = 8.1 Hz, 3H, pyr), 7.13 (dd, J = 7.4, 4.9 Hz, 3H, pyr), 6.94 (t, J = 7.3 Hz, 1H, Ph), 6.88 (t, J = 7.4 Hz, 2H, Ph), 6.71 (d, J = 7.4 Hz, 2H, Ph), 4.37 (s, 2H, CH_2). ^{13}C NMR (126 MHz, acetone-d_6) δ 165.3, 148.7, 140.4, 136.0, 131.8, 127.9, 126.2, 126.0, 121.9, 66.9, 44.3. ESI-MS: *m/z* 360.1480 ($C_{23}H_{19}N_3Na$, **2.4** + Na), calc. 360.1477.

1,1,1-Tris(2-pyridyl)ethane (**2.5**)

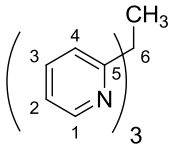

The tris(2-pyridyl)methane (1.04 g, 4.22 mmol, 1.0 equiv.) was dissolved in 100 mL of dry THF and 3.2 mL (1.1 equiv.) of a 1.6 M *n*-BuLi solution in hexanes was added dropwise at -78 °C resulting in the precipitation of the a white solid. The solution was stirred for 3 h at this temperature after which 0.3 mL (1.1 equiv.) of methyl iodide were added dropwise. The solution was allowed to warm up and stirred overnight at room temperature. The lightly turbid brown solution was quenched with 1 mL water and the solvent was removed briefly. Diluted $NaHCO_3$ (150 mL) was added and extracted with 5 x 75 mL dichloromethane until the extracts were colorless. The organic extracts were combined, dried with $MgSO_4$ and the solvent was evaporated under *vacuo*. The resulting red brown solid was purified by flash column chromatography (hexanes : ethyl acetate = 1 : 1) and recrystallized from diethyl ether to afford 950 mg (86%) of off-white crystals as the title compound. ^{1}H NMR (500 MHz, CD_2Cl_2) δ 8.53 (dd, $^{3}J_{HH}$ = 4.8 Hz, $^{4}J_{HH}$ = 0.8 Hz, 3H, 1-H), 7.58 (vtd, $^{3}J_{HH}$ = 8.0 Hz, J = 8.0, 1.8 Hz, 3H, 3-H), 7.14 (ddd, $^{3}J_{HH}$ = 7.4 Hz, $^{3}J_{HH}$ = 4.8 Hz, 0.9 Hz, 3H, 2-H), 7.09 (vd, J = 8.0 Hz, 3H, 4-H), 2.27 (s, 3H, C*H*$_3$). ^{13}C NMR (126 MHz, CD_2Cl_2) δ 166.5

(C5), 149.1 (C1), 136.3 (C3), 124.1 (C4), 121.7 (C2), 60.7 (C6), 27.6 (*C*H_3). ESI-MS: *m/z* 284.1167 ($C_{17}H_{15}N_3Na$, **2.5** + Na), calc. 284.1164.

1,1,1-Tris(2-methylpyridyl)-2-phenylethane (**2.7**)

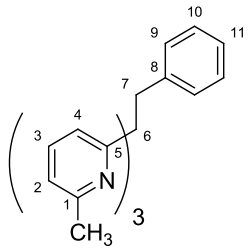

The tris(2-(2-methyl)pyridyl)methane (0.469 g, 1.62 mmol, 1.0 equiv.) was dissolved in 50 mL of dry THF and 1.22 mL (1.2 equiv.) of a 1.6 M *n*-BuLi solution in hexanes was added dropwise at -78 °C resulting in the precipitation of the a white solid. The solution was stirred for 3 h at this temperature after which 0.23 mL (1.1 equiv.) of benzyl bromide were added dropwise. The solution was allowed to warm to room temperature and stirred overnight. The lightly turbid brown solution was quenched with 1 mL water and the organic volatiles were removed. Diluted $NaHCO_3$ (50 mL) was added and extracted with 4 x 30 mL dichloromethane until the extracts were colorless. The organic extracts were combined, dried with $MgSO_4$ and the solvent was evaporated under *vacuo*. The resulting red brown solid was purified by flash column chromatography (hexanes : ethyl acetate = 1: 1) and recrystallized from diethyl ether to afford 312 mg (51%) of off-white crystals as the title compound. ^{1}H NMR (500 MHz, CD_2Cl_2) δ 7.38 (t, $^3J_{HH}$ = 7.8 Hz, 3H, 3-H), 6.98 (d, $^3J_{HH}$ = 7.8 Hz, 3H, 2-H), 6.95 (d, $^3J_{HH}$ = 7.5 Hz, 3H, 4-H), 6.94-6.96 (m, 1H, 11-H), 6.91 (vt, *J* = 7.1 Hz, 2H, 10-H), 6.75 (d, $^3J_{HH}$ = 7.1 Hz, 2H, 9-H), 4.28 (s, 2H, 7-H), 2.48 (s, 9H, C*H*$_3$). ^{13}C NMR (126 MHz, CD_2Cl_2) δ 164.41(C5), 157.13 (C1), 140.58 (C8), 135.91 (C3), 131.88 (C10), 127.25 (C9), 125.74 (C11), 122.64 (C2), 120.77 (C4), 66.27 (C6), 44.00 (C7), 24.78 (*C*H_3). ESI-MS: *m/z* 380.2135 ($C_{26}H_{26}N_3$, **2.7** + H), calc. 380.2127.

2,2',2''-(Methoxymethanetriyl)tris(1-methyl-1H-imidazole) (**2.8**)

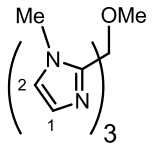

Sodium hydride (0.2 g as 60 % dispersion, 1.5 equiv.) in 50 mL dry THF were stirred at 0 °C for 20 minutes. To that suspension was added tris(2-(*N*-methyl)imidazyl)methanol (1.0 g, 3.3 mmol, 1.0 equiv.) dissolved in a mixture of 40 mL dry THF and 10 mL dry DMF. The reaction was stirred 15 min at room temperature and methyl iodide (0.31 mL, 1.5 equiv.) were added. The mixture was stirred overnight, and quenched with 1 mL and the solvent was removed. The residue was extracted with 3 x 50 mL dichloromethane from 50 mL water, dried with magnesium sulfate, and the solvent was removed. The pale yellow solid was recrystallized from toluene/ hexanes to yield 81% of pale yellow crystals. ^{1}H NMR (499 MHz, $CDCl_3$) δ 7.00 (d, J = 1.0 Hz, 3H), 6.90 (d, J = 1.0 Hz, 3H), 3.51 (s, 3H, O-CH_3), 3.46 (s, 9H, N-CH_3). ESI-MS: *m/z* 309.1432 ($C_{14}H_{18}N_6NaO$, **2.8**+Na), calc. 309.1440

$RuCl_2(PPh_3)[(2\text{-pyr})_3COCH_2Ph]$ (**2.15**)

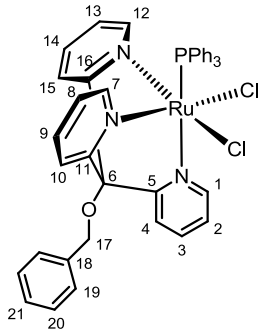

A solution of 100 mg (0.266 mmol, 1.0 equiv.) of **2.3** and 271 mg (1.0 equiv.) of $RuCl_2(PPh_3)_3$ in 10 mL dry THF was stirred under nitrogen for 2 days at room temperature. The mixture was cooled to -30 °C and the orange precipitate was filtrated and washed with 1 mL of

cold ether. The orange powder was dissolved in 2 mL dichloromethane and reprecipitated with ether to afford 193 mg (86 % isolated yield) pure THF free complex **2.15** after filtration and drying under *vacuo*. ^{1}H NMR (500 MHz, CD_2Cl_2) δ 9.83 (vd, *J* = 5.4 Hz, 1H, 1-H), 8.21 (vd, *J* = 5.8 Hz, 2H, 7-H and 12-H), 7.84 – 7.73 (m, 4H, 4-H, 10-H, 15-H, 3-H), 7.68 (vd, *J* = 7.5 Hz, 2H, 19-H), 7.56 (vt, *J* = 7.6 Hz, 2H, 20-H), 7.47 (vt, *J* = 8.3 Hz, 7H, 21-H and ortho PPh_3), 7.43 – 7.39 (m, 2H, 9-H and 14-H), 7.37 (vt, *J* = 6.5 Hz, 1H, 2-H), 7.30 (dd, *J* = 10.7, 4.0 Hz, 3H, para PPh_3), 7.20 (dd, *J* = 10.9, 4.3 Hz, 6H, meta PPh_3), 6.41 – 6.08 (m, 2H, 8-H and 13-H), 5.19 (s, 2H, 17-H). ^{13}C NMR (126 MHz, CD_2Cl_2) δ 161.47 and 161.45 (C7 and C12), 159.87 (C11 and C16), 158.45 (C1), 157.56 (C5), 137.94 (C18), 136.90 (C3), 135.70 (d, $^{2}J_{CP}$ = 9.1 Hz, ortho PPh_3), 134.91 (d, $^{1}J_{CP}$ = 35.9 Hz, ipso PPh_3), 134.67 (C14 and C9), 129.56 (C20) , 129.51 (d, $^{4}J_{CP}$ = 1.8 Hz, para PPh_3), 128.65 (C21), 127.99 (d, 3JCP = 8.7 Hz, meta PPh_3), 126.88 (C19), 123.75 (C2), 122.12 (C8 and C13), 121.38 (C10 and C15), 120.58 (C4), 89.58(C6), 68.73 (C17). ^{31}P NMR (162 MHz, CD_2Cl_2) δ 42.85. Anal. Calcd. For $C_{41}H_{34}Cl_2N_3OPRu$: C 62.52, H 4.35, N 5.33. Found: C 62.31, H 4.26, N 5.26.

$RuCl_2(PPh_3)[(2\text{-pyr})_3CCH_3]$ (**2.16**)

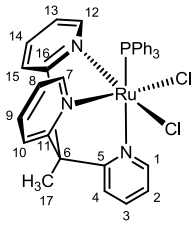

A solution of 137 mg (0.482 mmol, 1.0 equiv.) of **2.5** and 500 mg (1.0 equiv.) of $RuCl_2(PPh_3)_3$ in 20 mL dry THF was stirred under nitrogen for 3 days at room temperature. The mixture was cooled to -30 °C and the orange precipitate was filtrated and washed with 1 mL of cold THF. The orange powder was redispersed in 2 mL dichloromethane and reprecipitated with hexanes to afford 334 mg (92% isolated yield) pure THF free complex **2.16** after filtration and

drying under *vacuo*. ^{1}H NMR (500 MHz, CD_2Cl_2) δ 10.02 – 9.89 (m, 1H, 1-H), 8.33 (vd, *J* = 5.8 Hz, 2H, 11-H and 16-H), 7.76 (vt, *J* = 7.8 Hz, 1H, 3-H), 7.62 (vd, *J* = 8.1 Hz, 1H, 4-H), 7.57 (vd, *J* = 8.1 Hz, 2H, 8-H and 13-H), 7.44 (t, *J* = 8.3 Hz, 6H, ortho PPh_3), 7.41 – 7.33 (m, 3H, 2-H, 9-H and 14-H), 7.28 (t, $^{3}J_{HH}$ = 7.3 Hz, 3H, para PPh_3), 7.17 (vt, *J* = 8.3 Hz, 6H, meta PPh_3), 6.19 (vt, *J* = 6.6 Hz, 2H, 10-H and 15-H), 2.64 (s, 3H, 17-H). ^{13}C NMR (126 MHz, CD_2Cl_2) δ 161.60 (C11 and C16), 160.20 (C7 and C12), 158.64 (C1), 157.40 (C5), 136.69 (C3), 135.72 (d, $^{2}J_{CP}$ = 9.1 Hz, ortho PPh_3), 135.13 (d, $^{1}J_{CP}$ = 34.9 Hz, ipso PPh_3), 134.60 (C9 and C14), 129.39 (para PPh_3), 127.95 (d, $^{3}J_{CP}$ = 8.6 Hz, meta PPh_3), 123.52 (C2), 121.75 (C10 and C15), 120.79 (C8 and C13), 120.58 (C4), 56.04 (C6), 24.76 (C17). ^{31}P NMR (162 MHz, CD_2Cl_2) δ 44.19. Anal. Calcd. for **2.16**·CH_2Cl_2: C 55.40, H 4.13, N 5.38; Found: C 55.23, H 4.25, N 5.39.

$RuCl_2$(pyr)[(2-pyr)$_3$$CCH_3$] (**2.17**)

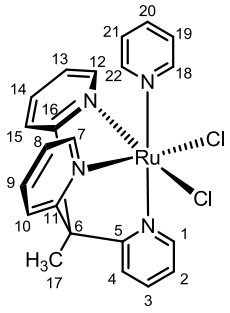

A 54 mg quantity of **2.16** (0.080 mmol) and 60 µL dry pyridine (10 equiv.) were dispersed in 5 mL dry toluene and heated to reflux for 20 hours. The suspension adopted a red-orange color. After cooling to room temperature the mixture was filtered and washed with 5 mL hexanes and dried under *vacuo* yielding 35 mg (84%) as a dark orange powder. Single crystals were obtained by slow diffusion of ether into a solution of complex **2.17** in methylene dichloride at room temperature. ^{1}H NMR (500 MHz, CD_2Cl_2, 193K) δ 9.78 (d, $^{3}J_{HH}$ = 5.8 Hz, 1H, 18-H), 9.54 (d, $^{3}J_{HH}$ = 5.1 Hz, 1H, 1-H), 8.30 (vd, *J* = 5.9 Hz, 2H, 7-H, 22-H), 7.75 – 7.69 (m, 1H, 20-H), 7.69 –

7.64 (m, 4H, 3-H, 4-H, 10-H, 15-H), 7.64 – 7.59 (m, 2H, 9-H, 14-H), 7.47 (vt, J = 6.7 Hz, 1H, 19-H), 7.24 – 7.16 (m, 1H, 2-H), 6.93 (m, 3H, 8-H, 13-H, 21-H), 6.73 (d, $^3J_{HH}$ = 5.7 Hz, 1H, 22-H), 2.67 (s, 3H, 17-H). Anal. Calcd. For $C_{22}H_{20}Cl_2N_4Ru$: C 51.57, H 3.93, N 10.93. Found: C 51.71, H 3.76, N 10.45.

$RuCl_2(NCMe)[(2\text{-}pyr)_3CCH_3]$ (**2.18**)

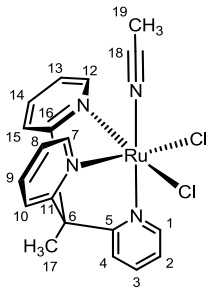

A 0.10 g quantity of **2.16**·THF (0.13 mmol) and 1 mL dry acetonitrile were dispersed in 5 mL dry toluene and heated to reflux for 6 hours. The suspension adopted a bright orange color. After cooling to room temperature the mixture was filtered and washed with 5 mL toluene, 5 mL pentane, and dried under *vacuo* yielding 61 mg (89%) **2.18**·0.5PhMe. Toluene free complex **2.18** is obtained by dissolving in methylene chloride and reprecipitation of the orange powder with pentane and drying under *vacuo*. ^{1}H NMR (500 MHz, CD_2Cl_2) δ 9.56 (vd, J = 5.7 Hz, 1H, 1-H), 9.31 (vd, J = 6.1 Hz, 2H, 11-H and 16-H), 7.71 – 7.59 (m, 6H, 3-H, 4-H, 8-H, 9-H, 13-H, 14-H), 7.18 (vt, J = 6.6 Hz, 1H, 2-H), 7.13 (td, $^3J_{HH}$ = 6.1 Hz, $^4J_{HH}$ = 2.5 Hz, 2H, 10-H and 15-H), 2.65 (s, 3H, 17-H), 2.54 (s, 3H, NC*CH*$_3$). ^{13}C NMR (126 MHz, CD_2Cl_2) δ 160.48 (C7 and C12), 159.58 (C1), 159.03 (C5), 158.90 (C11 and C16), 135.35 (C3), 134.64 (C9 and C14), 123.32 (C18), 123.19 (C10 and C15), 123.03 (C2), 121.44 (C8 and C13), 120.76 (C4), 56.03 (C6), 24.12 (C17), 5.18 (C19). ESI-MS: *m/z* 469.0722 ($C_{21}H_{24}ClN_4Ru$, **2.21**-Cl), calc. 469.0733.

$RuCl_2(PPh_3)[(2\text{-methylimidazoyl})_3COMe]$ (**2.22**)

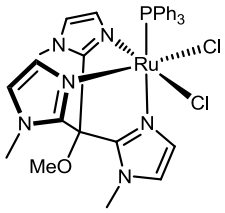

A solution of complex **2.8** (15 mg, 0.050 mmol, 1.0 equiv.) and $RuCl_2(PPh_3)_3$ (50 mg, 1.0 equiv.) in 5 mL dry THF was stirred at room temperature overnight, upon which a light yellow precipitate had formed. The solid was collected by filtration and washed with 2 x 10 mL dry ether and dried in *vacuo* to give 33 mg of the desired complex (88%). ^{1}H NMR (400 MHz, CD_3OD) δ 7.48 – 7.37 (m, J = 8.5 Hz, 3H), 7.37 – 7.25 (m, J = 14.3, 7.1 Hz, 2H), 7.12 (s, 1H), 6.94 (s, 1H), 6.81 (s, 1H), 6.38 (s, 1H), 6.17 (s, 1H), 4.13 (s, 1H), 4.08 (s, 1H), 4.04 (s, 1H), 4.01 (s, 1H). ^{31}P NMR (162 MHz, CD_3OD) δ 53.30 (s). ESI-MS: *m/z* 685.1171 ($C_{32}H_{33}ClN_6OPRu$, **2.22**-Cl), calc. 685.1185.

$RuCl_2(dmso)[HC(pz)_3]$ (**2.23**)

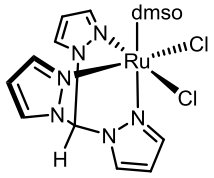

$RuCl_2(dmso)_4$ (0.10 g, 0.21 mmol, 1.0 equiv.) and **2.9** (44 mg, 0.21 mmol, 1.0 equiv.) were suspended in 10 mL dry toluene under a nitrogen atmosphere and refluxed for 1 day. The solution stayed virtually colorless and the precipitate turned a dull yellow color. The precipitate was filtered and washed with 10 mL diethyl ether. The mixture of desired product and proposed intermediate $[RuCl(dmso)_2(HC(pz)_3)]Cl$ was then resuspended in 10 mL dry toluene and heated to reflux for another day. After repeating the same workup the title compound was obtained as a dull yellow

powder in 89% yield. The spectroscopic data was in accordance with a sample of the title compound prepared by literature procedures.[11e]

$[RuCl_2(dmso)_2(pzH)_2]$ (**2.24**)

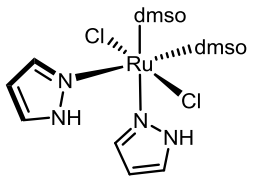

$RuCl_2(dmso)_4$ (0.13 g, 0.27 mmol, 1.0 equiv.) and **2.12** (62 mg, 0.27 mmol, 1.0 equiv.) were suspended in 5 mL ethanol and refluxed for 2 h. The mixture turned clear upon heating and the color turned an intense orange. The mixture was cooled to room temperature and stored at -30 °C overnight. The orange needles that formed were filtered and washed with 5 mL cold diethyl ether. Product yield: 93 mg (74%). The ^{1}NMR data was in accordance with a sample prepared by a literature procedure.[11e]

$RuCl_2(dmso)_2[PhC(H)=C(pz)_2]$ (**2.25**)

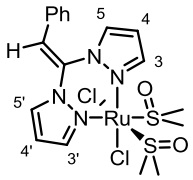

$RuCl_2(dmso)_4$ (0.10 mg, 0.21 mmol, 1.0 equiv.) and **2.13** (63 mg, 0.21 mmol, 1.0 equiv.) were suspended in 10 mL toluene and refluxed for 22 h. After cooling to room temperature the dark yellow precipitate was separated from the yellow solution by filtration and washed with 2 mL of cold diethyl ether and dried under *vacuo* overnight to result 61 mg of analytically pure title compound (52%). ^{1}H-NMR (CD_2Cl_2) δ: 8.48 (vd, J = 1.7 Hz, 1H, pz(1)-3/5), 8.42 (vd, J = 1.7 Hz, 1H, pz(2)-3/5), 8.19 (dd, $^3J_{HH}$ = 2.6 Hz, $^4J_{HH}$ = 0.7 Hz, 1H, pz(2)-3/5), 7.38 (dd, $^3J_{HH}$ = 2.6 Hz, $^4J_{HH}$ = 0.7 Hz, 1H, pz(1)-3/5), 7.31-7.34 (m, 3H, arom.), 7.12-7.15 (m, 2H, arom.), 6.94 (s, 1H,

=CH), 6.65 (vt, J = 2.6 Hz, 1H, pz(2)-4), 6.35 (vt, J = 2.6 Hz, 1H, pz(1)-4), 3.50 (s, 3H, dmso(1)), 3.49 (s, 3H, dmso(1)), 3.23 (s, 3H, dmso(2)), 2.23 (s, 3H, dmso(1)).

$RuCl_2(PPh_3)[PhCH_2C(pz)_3]$ (**2.26**)

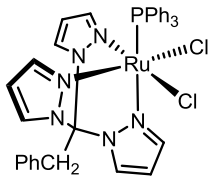

A solution of 126 mg $RuCl_2(PPh_3)_3$ and 40 mg (1 equiv.) of **2.13** was stirred at room temperature for 3 days. After that the stirring was stopped and the solution was let stand for 1 week upon which yellow precipitate formed. The solid was filtered off and washed with 3 mL of cold ether and dried under *vacuo* overnight. ^{1}H NMR (500 MHz, DMSO) δ 8.65 (s, 1H, pz(1)-3/5), 8.21 (s, 1H pz(1)-3/5), 7.92 (s, 2H, pz(2+3)-3/5), 7.69 (t, J = 8.3 Hz, 6H, PPh_3), 7.50 (t, J = 7.4 Hz, 2H, Bn arom.), 7.42 – 7.32 (m, 4H, PPh_3 and Bn arom.), 7.32 – 7.25 (m, 6H, PPh_3), 7.22 (br d, 2H, Bn arom.), 6.72 (s, 2H, pz(2+3)-3/5), 6.64 (s, 1H, pz(1)-4), 6.01 (dd, J = 3.0, 2.3 Hz, 2H, pz(2+3)-4), 5.54 (s, 2H, CH_2).

$RuCl_2(HN=C(CH_3))[(2\text{-}pyr)_3CCH_3]$ (**2.27**)[16a]

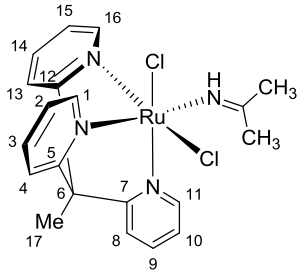

A NMR tube with rubber septa was charged with 8.0 mg (14 μmol) of **2.18** in 0.5 mL CD_2Cl_2. The orange suspension was cooled to -78°C and 0.03 mL of MeLi solution (1.6 M in diethyl ether, 3.5 equiv.) was added. The mixture was kept at that temperature for one hour during which it turned dark red and warmed to room temperature. The suspension was added to 5 mL dry

ether and the dark red precipitate separated. The title compound was extracted with 3 mL methylene chloride and dried *in vacuo*. ^{1}H NMR (600 MHz, CD_2Cl_2) δ 10.89 (s, N*H*, 1H), 9.62 (dd, $^{3}J_{HH}$ = 5.9 Hz, $^{4}J_{HH}$ = 1.1 Hz, 1H, 1-H), 9.04 (dd, $^{3}J_{HH}$ = 6.0 Hz, $^{4}J_{HH}$ = 0.7 Hz, 2H, 11-H, 16-H), 7.84 – 7.45 (m, 8H, 3-H, 4-H, 8-H, 9-H, 13-H, 14-H), 7.17 (ddd, $^{3}J_{HH}$ = 7.2 Hz, $^{3}J_{HH}$ = 5.9 Hz, $^{4}J_{HH}$ = 1.6 Hz, 1H, 2-H), 7.01 (ddd, $^{3}J_{HH}$ = 7.3 Hz, $^{3}J_{HH}$ = 6.0 Hz, $^{4}J_{HH}$ = 1.5 Hz, 2H, 10-H, 15-H), 2.66 (s, 3H, 17-H), 2.35 (s, 3H, C(CH_3)$_2$), 0.74 (s, 3H, C(CH_3)$_2$). ^{13}C NMR (126 MHz, CD_2Cl_2) δ 182.19 (=*C*(CH$_3$)$_2$), 160.91 (C12, C14), 159.56 (C1), 158.92 (C5), 158.84 (C11, C16), 134.79 (C3), 133.73 (C9, C14), 122.87 (C10, C15), 122.78 (C2), 121.36 (C8, C13), 120.93 (C4), 55.96 (C6), 30.89 (=C(*C*H$_3$)$_2$), 24.31 (C17), 22.96 (=C(*C*H$_3$)$_2$).

2.10 References

(1) Heyndrickx, W.; Occhipinti, G.; Minenkov, Y.; Jensen, V. R. *J. Mol. Catal. A: Chem.* **2010**, *324*, 64-74.

(2) Karam, A.; Tenia, R.; Martinez, M.; Lopez-Linares, F.; Albano, C.; Diaz-Barrios, A.; Sanchez, Y.; Catari, E.; Casas, E.; Pekerar, S.; Albornoz, A. *J. Mol. Catal. A: Chem.* **2007**, *265*, 127-132.

(3) a) Wang, L.; Flood, T. C. *J. Am. Chem. Soc.* **1992**, *114*, 3169-3170. b) Wang, L.; Lu, R. S.; Bau, R.; Flood, T. C. *J. Am. Chem. Soc.* **1993**, *115*, 6999-7000.

(4) a) White, D. L.; Faller, J. W. *Inorg. Chem.* **1982**, *21*, 3119-3122. b) Reger, D. L. *Comments on Inorganic Chemistry: A Journal of Critical Discussion of the Current Literature* **1999**, *21*, 1 - 28. c) Elgafi, S.; Field, L. D.; Messerle, B. A.; Buys, I. E.; Hambley, T. W. *J. Organomet. Chem.* **1997**, *538*, 119-128.

(5) Faller, J. W.; Ma, Y. *J. Am. Chem. Soc.* **1991**, *113*, 1579-1586.

(6) Levacher, V.; Adolfsson, H.; Moberg, C. *Acta Chem. Scand.* **1996**, *50*, 454-457.

(7) Sorrell, T. N.; Borovik, A. S. *J. Am. Chem. Soc.* **1986**, *108*, 2479-2481.

(8) a) Reger, D. L.; Grattan, T. C.; Brown, K. J.; Little, C. A.; Lamba, J. J. S.; Rheingold, A. L.; Sommer, R. D. *J. Organomet. Chem.* **2000**, *607*, 120-128. b) Reger, D. L.; Grattan, T. C. *Synthesis* **2003**, *2003*, 0350,0356.

(9) Mosny, K. K.; Gala, S. R.; Crabtree, R. H. *Transition Metal Chemistry* **1995**, *20*, 595-599.

(10) Delafuente, D. A.; Kosturko, G. W.; Graham, P. M.; Harman, W. H.; Myers, W. H.; Surendranath, Y.; Klet, R. C.; Welch, K. D.; Trindle, C. O.; Sabat, M.; Harman, W. D. *J. Am. Chem. Soc.* **2006**, *129*, 406-416.

(11) a) Llobet, A.; Doppelt, P.; Meyer, T. J. *Inorg. Chem.* **1988**, *27*, 514-520. b) Fajardo, M.; de la Hoz, A.; Diez-Barra, E.; Jalon, F. A.; Otero, A.; Rodriguez, A.; Tejeda, J.; Belletti, D.; Lanfranchi, M.; Pellinghelli, M. A. *J. Chem. Soc., Dalton Trans.* **1993**, 1935-1939. c) Bhambri, S.; Tocher, D. A. *Polyhedron* **1996**, *15*, 2763-2770. d) Field, L. D.; Messerle, B. A.; Soler, L.; Buys, I. E.; Hambley, T. W. *J. Chem. Soc., Dalton Trans.* **2001**, 1959-1965. e) Iengo, E.; Zangrando, E.; Baiutti, E.; Munini, F.; Alessio, E. *Eur. J. Inorg. Chem.* **2005**, *2005*, 1019-1031.

(12) Shaver, M. P.; Allan, L. E. N.; Gibson, V. C. *Organometallics* **2007**, *26*, 2252-2257.

(13) Tilley, T. D.; Grubbs, R. H.; Bercaw, J. E. *Organometallics* **1984**, *3*, 274-278.

(14) a) Cole-Hamilton, D. J.; Wilkinson, G. *J. Chem. Soc., Dalton Trans.* **1979**, 1283-1289. b) Bruce, M. I.; Cifuentes, M. P.; Humphrey, M. G.; Poczman, E.; Snow, M. R.; Tiekink, E. R. T. *J. Organomet. Chem.* **1988**, *338*, 237-248. c) Wilczynski, R.; Fordyce, W. A.; Halpern, J. *J. Am. Chem. Soc.* **1983**, *105*, 2066-2068.

(15) Umezawa-Vizzini, K.; Lee, T. R. *Organometallics* **2004**, *23*, 1448-1452.

(16) a) Yeh, W.-Y.; Ting, C.-S.; Peng, S.-M.; Lee, G.-H. *Organometallics* **1995**, *14*, 1417-1422. b) Kukushkin, V. Y.; Pombeiro, A. J. L. *Chem. Rev.* **2002**, *102*, 1771-1802.

(17) Desrochers, P. J.; Corken, A. L.; Tarkka, R. M.; Besel, B. M.; Mangum, E. E.; Linz, T. N. *Inorg. Chem.* **2009**, *48*, 3535-3541.

3 Disulfonate Phosphine Ruthenium(IV) Complexes

3.1 Introduction

Phosphine sulfonate palladium complexes are a unique class of insertion polymerization catalysts with the ability to incorporate virtually all mono-functionalized olefins into polyethylenes (see Chapter 1). Jordan and coworkers reported a similar disulfonate phosphine [OPO] palladium complex that demonstrated self-assembly and a solvent dependent polymerization activity.[1] The solid state structure of complex **3.1** was a cubic assembly of four **3.1** units, where the [OPO] ligand binds to each Pd as a κ^2-P,O chelator, and the four pendant SO_3Li groups are linked by Li-O bonds to form a central $Li_4S_4O_{12}$ cage (Scheme 3.1). This tetrametric assembly is stable in CD_2Cl_2 at - 10 ˚C and below, and reversible dissociation to monomeric species is observed at higher temperatures. Reaction of **3.1** with Krypt211 forms mononuclear **3.2**, in which the pendant sulfonate groups interacts weakly with the Pd (Pd-O distance: 3.08 Å, sum of van der Waals radii: 3.15 Å).

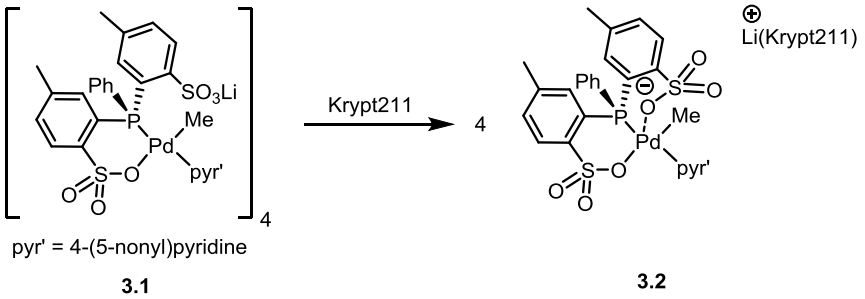

Scheme 3.1 Dissociation of tetrameric [OPO]Pd **3.1** complex facilitated by Krypt211.

In toluene at 80 ˚C, conditions favoring fragmentation, **3.1** behaves similar to phosphine sulfonate palladium catalysts, and produced linear, moderate molecular weight polyethylene (M_n = 8 kg mol^{-1}). However, in hexanes, high molecular weights (M_n = 1,000 kg mol^{-1}) and a broader

molecular weight distribution were observed while phosphine sulfonate palladium complexes behaved similar to toluene. **3.2** only produced ethylene oligomers in good yields. The pendant free $ArSO_3^-$ group strongly enhances chain-transfer. In contrast, the steric effects of the tetranuclear arrangement, where one axial face of the Pd center is blocked by $Li_4S_4O_{12}$ cage, likely disfavor associative chain-transfer.

The bis(phosphine sulfonate) ruthenium **1.13**,[2] and thioether tethered arene ruthenium **1.14**,[3] both show low activities in ethylene polymerization. Ru complexes with higher oxidation states should lead to an increase in the catalyst activity analogous to early TM. While both Ru(III) and Ru(IV) complexes are well-known in literature, Ru(IV) was chosen due to its diamagnetic nature, facilitating NMR spectroscopic characterization. To stabilize the higher charge of the Ru(IV) center, bisanionic bis(arenesulfonato)phosphines [OPO] ligands were chosen. The dianionic ligand was envisioned to chelate the Ru(IV) center, which upon activation, could afford a monocationic Ru^{IV}-alkyl complex as active catalytic species for olefin insertion polymerization.

3.2 Synthesis of OPO Ligands

The ligand **3.3** was synthesized following the literature procedure.[1] A series of novel Li_2(OPO) ligand variants **3.4 – 3.9** (Scheme 3.2) were synthesized by treating the respective phosphine dichloride with two equivalents ortho-lithioarenesulfonate. To tune the catalytic property of the Ru(IV) complexes, the substituent on the phosphine was systematically changed, including three phenyl variants with different electronic properties (**3.3 – 3.7)** and two alkyl substituents with different steric bulk (**3.8**, **3.9**). The structures of all the ligands were fully established by ^1H and ^{13}C NMR, ESI-MS, and elemental analysis. The solid-state structure of **3.6** was determined by X-ray diffraction analysis (see Appendix).

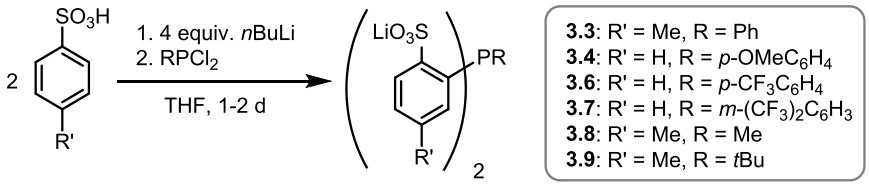

Scheme 3.2 Synthesis of Li_2(OPO) ligands **3.3 – 3.9**.

The electronic properties of phosphines can be compared by the ^{31}P NMR chemical shift if steric parameters of the compounds are similar. For the substituted triaryl phosphines **3.3** – **3.7.**, the chemical shift ranged from -13.06 to -15.60 ppm (Table 3.1). The electron donating group (*p*-(OMe)C_6H_4) caused the most upfield, while the most electron withdrawing group (*m*-$(CF_3)_2C_6H_3$) resulted in the most downfield shift for its ^{31}P resonance. Such a clear trend could not be observed for **3.8** and **3.9**, where the steric bulk of the substituents are very different.

Table 3.1 ^{31}P Chemical shifts of different [OPO] phosphines as lithium salts (in CD_3OD) and ruthenium complexes (in $CDCl_3$).

R	Ligand δ [ppm]	Complex δ [ppm]
Ph	-14.30	6.97
p-OMe	-15.69	6.69
p-CF_3	-13.89	8.32
m-$(CF_3)_2$	-13.06	9.81
Me	-31.83	-1.35
^{t}Bu	-7.64	6.34

3.3 Synthesis of Ru(IV) Complexes

Treating the Ru(IV) dimer [Ru(η^3:η^3-$C_{10}H_{16}$)(μ-Cl)Cl]$_2$ with **3.3 – 3.9** in the presence of $AgBF_4$ resulted in the formation of neutral Ru(η^3:η^3-$C_{10}H_{16}$)(OPO) complexes **3.10 – 3.15** in 55 – 73 % yield after purification (Scheme 3.3). All complexes were characterized by ^{1}H and ^{13}C NMR, ESI-MS, and elemental analysis (Figure 3.2 for a representative ^{1}H NMR of complex **3.14**). The ^{31}P NMR chemical shifts showed a similar trend based on the phosphine R substituents (Table

3.1), indicating that the electronic properties observed in the ligands were maintained in the complexes.

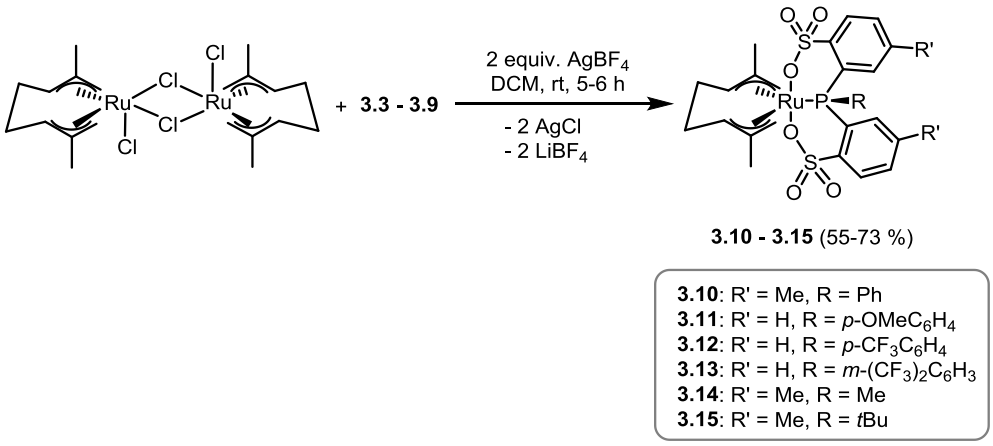

3.10 - 3.15 (55-73 %)

3.10: R' = Me, R = Ph
3.11: R' = H, R = *p*-$OMeC_6H_4$
3.12: R' = H, R = *p*-$CF_3C_6H_4$
3.13: R' = H, R = *m*-$(CF_3)_2C_6H_3$
3.14: R' = Me, R = Me
3.15: R' = Me, R = *t*Bu

Scheme 3.3 Synthesis of Ru(OPO) polymerization precursors **3.10 – 3.15.**

Single crystals of **3.13 – 3.15** were obtained, enabling the determination of their solid-state structure by X-ray diffraction analysis. The molecular geometries are depicted in Figure 3.1. All three complexes show a trigonal bipyramidal coordination of the Ru center. The sum of the bond angles of the phosphorous and the central allyl carbon atoms around the ruthenium center was 360.0° in all cases. The [OPO] fragment is coordinated meridionally with the phosphorus atom and the dienyl group occupying the equatorial, and the sulfonates the axial positions. The allyl methyl groups adopted an *anti*-configuration with respect to the equatorial plane. In **3.15** the Ru-P bond is elongated to 2.493 Å compared to 2.392 Å for **3.14**, and the Ru-P-C_{alkyl} angle widened from 123.8° to 131.4° due to the larger steric profile of the *tert*-butyl group. The same parameters are 2.371 Å and 125.83° for **3.13**.

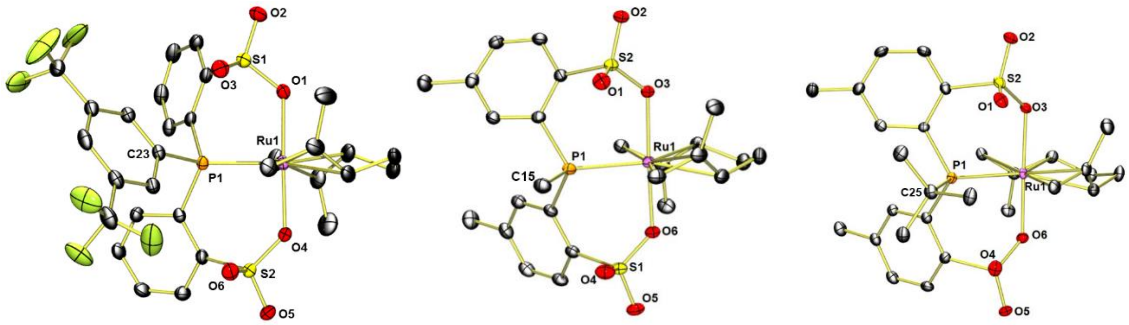

Figure 3.1 Ortep plots of **3.13 – 3.15** (left to right). Hydrogen atoms omitted for clarity. Selected bond distances (Å) and angles (˚) for **3.13**: Ru1-O4 2.089(2), Ru1-O1 2.104(2), Ru1-P1 2.3712(8); Ru1-P1-C23 125.83(10), O1-Ru1-P1 89.69(6), O4-Ru1-P1 91.55(6). Selected bond distances (Å) and angles (˚) for **3.14**: Ru1-O6 2.1132(11), Ru1-O3 2.0953(11), Ru1-P1 2.3919(4); Ru1-P1-C15 123.81(6), O3-Ru1-P1 93.05(3), O6-Ru1-P1 89.50(3). Selected bond distances (Å) and angles (˚) for **3.15**: Ru1-O6 2.1124(17), Ru1-O3 2.0998(17), Ru1-P1 2.4931(6); Ru1-P1-C25 131.42(8), O3-Ru1-P1 92.42(5), O6-Ru1-P1 89.43(5).

The solid-state structures agreed with the solution structures as determined by NMR spectroscopy. In all complexes, the allyl groups gave rise to non-equivalent NMR resonances. For example, in **3.14** the allyl methyl signals show a chemical shift of 1.42 and 2.24 ppm, respectively. Presumably, the ring current effect of the arylsulfonates experienced by the allyl group facing away from the phosphine alkyl moiety leads to an upfield shift of its resonance. A 1D NOE NMR experiment enabled the absolute assignment of the dienyl resonances for **3.14.** When the P-*Me* was irradiated, we only observed NOE enhancement for the terminal methylene protons of the downfield shifted allyl group.

3.4 Polymerization Studies

Complexes **3.10 – 3.15** were active for ethylene insertion polymerization when treated with $AlMe_3$-depleted methylaluminoxane (dMAO) in toluene at elevated temperatures (Table 3.2). Activation with normal MAO gave lower activity compared to dMAO while producing polymers with similar properties (run 9 vs. 11). This catalyst system showed relatively high thermal stability with optimal activities at polymerization temperature between 55 - 85 °C. The highest TOF

(1182 h^{-1}) was obtained with **3.12** (run 7), which, represents the most active Ru-based ethylene polymerization catalyst up to now. The activity is one order of magnitude higher than other previously reported Ru-based systems.[2-4]

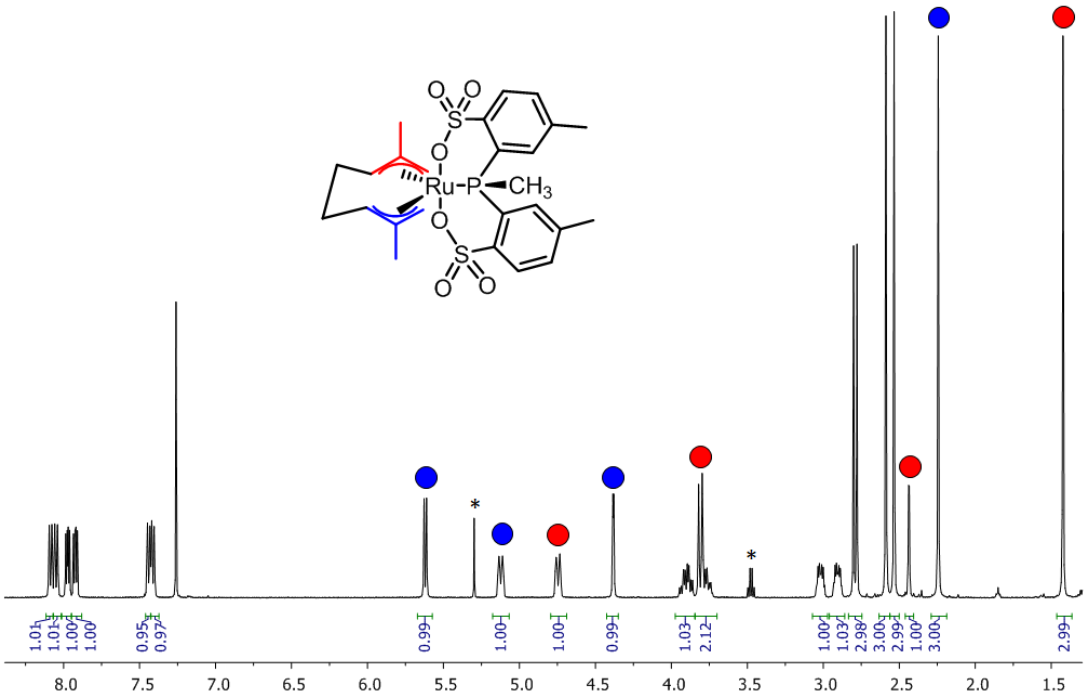

Figure 3.2 ^{1}H NMR of complex **3.14** in $CDCl_3$ at 298K. * = Residual ether solvent peaks.

A consistent trend was observed for the donor strength of [OPO] ligands on catalyst activity. Comparing **3.10 – 3.12** (runs 1, 3, 8) showed an increase in activity with decreasing donor strength of the ligand. Further decrease in donor strength led to a decreased activity (run 12 with **3.13**). A reduced catalyst stability is likely responsible for this observation. The most electron-rich **3.11** produced only trace amounts of polymer. However, it is difficult to directly compare the aryl-substituted and alkyl-substituted complexes, as the sterics for the two systems are significantly different. For example, alkyl-substituted **3.14** and **3.15**, containing electron-rich phosphines, gave

higher activities than **3.10** and **3.11**. The steric profile of **3.15** has pronounced influence on the polymer properties such as molecular weight (vide infra).

The effects of polymerization time (runs 6 – 9) and temperature (runs 4, 5, 9, 10) were investigated in more detail with the most productive **3.12**/dMAO system. In experiments with varying reaction time under otherwise identical conditions, the significantly higher productivity (TOF of 1182 h^{-1}) for the two-hour than one-hour polymerization (runs 6, 7) suggests a slow activation of **3.12**. The decrease in TOF for much longer time (runs 8, 9) was presumably due to catalyst deactivation with time. For temperature dependence, under otherwise identical conditions, the highest activity was observed at 85 °C. Presumably, initial increase of temperature (runs 4, 5, 9) accelerated the catalyst activation and increased the insertion rate until catalyst deactivation became more dominant at too high temperature (105 °C). The optimal temperature for maximal productivity is also ligand dependent; while **3.12** exhibited maximal productivity at 85 °C, **3.14** showed the highest productivity at 55 °C (runs 5 and 9 vs. 13 and 14).

The *cis* diallyl groups in **3.10 – 3.15** are ideally suited to be activated to form two active coordination sites in *cis* position. Nevertheless, numerous attempts of using solution NMR to elucidate the activation mechanism have proved to be elusive due to severe solubility issues encountered when species of **3.10 – 3.15** were activated by dMAO. On the other hand, small molecule activators, such as $AlMe_2Cl$, $Al(iBu)_3$, $B(C_6F_5)_3$ and $[Ph_3C][B(C_6F_5)_4]/Al(iBu)_3$, were ineffective for activating **3.10 – 3.15.**. Solution NMR experiments showed no reaction of **3.12** with excess $B(C_6F_5)_3$ or $[Ph_3C][B(C_6F_5)_4]$. This agrees with other reports of Ru(IV) allyl complexes that show no nucleophilic reactivity.[5] Regardless, based on control experiments (Table 3.2, runs

Table 3.2 Ethylene homopolymerization results.[a]

run	[Ru]	T [°C]	t [h]	yield [mg]	TOF[b]	T_m [°C][c]	X [%][d]	M_p [kg/mol] (M_w/M_n) [e]	N_{br}[g]
1	**3.10**	80	4	72	64	129	63	0.9, 257[f]	11
2	**3.11**	60	4	tr	N/A	n.d.	n.d.	n.d.	n.d.
3	**3.11**	80	4	tr	N/A	n.d.	n.d.	n.d.	n.d.
4	**3.12**	40	17	120	25	128	37	0.8, 28[f]	6
5	**3.12**	60	17	788	165	134	57	0.9, 289[f]	3
6	**3.12**	85	1	99	353	135	56	0.7, 179[f]	2
7	**3.12**	85	2	663	1182	133	62	0.7, 153[f]	5
8	**3.12**	85	4	835	744	135	59	214	1
9	**3.12**	85	17	934	196	133	60	1.1, 190[f]	5
10	**3.12**	105	17	115	24	128	49	0.8, 155[f]	11
11[h]	**3.12**	85	17	519	109	135	58	0.6, 174[f]	5
12	**3.13**	85	4	96	86	n.d.	n.d.	n.d.	n.d.
13	**3.14**	55	17	790	166	122	[i]	0.6, 250[f]	9
14	**3.14**	85	4	228	203	134	58	0.7, 219[f]	2
15	**3.15**	85	4	72	64	131	42	250	n.d.
16	**3.15**	95	4	201	179	129	37	250	12
Control runs									
17[j]	**3.15**	85	17	0	0	N/A	N/A	N/A	N/A
18	**3.6**	85	17	0	0	N/A	N/A	N/A	N/A
19	**3.6(H)**	85	17	0	0	N/A	N/A	N/A	N/A

a) Conditions: 10 μmol of catalyst, 1000 equiv. dMAO, 600 psi C_2H_4, 100 mL toluene. b) In units of (mol (C_2H_4) / ((mol [Ru]) x h). c) Determined by DSC. d) Crystallinity measured from DSC traces. A melting enthalpy of 293 J/g was used for 100 % crystalline PE.[6] e) Peak molecular weights determined by GPC in 1,2,4-trichlorobenzene at 140 °C vs. polyethylene standards. The high MW fraction is denoted with 1, the low MW fraction with 2. f) Bimodal molecular weight distribution g) Methyl branches per 1000 C. Determined by ^{1}H NMR in tetrachloroethane-*d*4 at 130 °C. h) MAO as cocatalyst (Al/Ru = 1000). i) Very broad melting endotherm makes hard to calculate the crystallinity. j) Without cocatalyst.

17 - 19), the observed activity was due to the Ru metal center involved in the catalytic process. Polymerization runs without Ru source or cocatalyst yielded no polymer under otherwise identical conditions. Similarly, when ligand salt **3.6** or protonated ligand **3.6(H)**[7] was employed with dMAO, no polymer was obtained. This also indicates that the observed polymerization activity was not due to Al/ligand complexes possibly present in the polymerization solution. However, it is possible that the Al cocatalysts undergo redox processes with transition metals, giving active species that differ in their oxidation state from the precatalyst.[8]

The molecular weight and distribution for the polyethylenes obtained in this study were characterized by gel permeation chromatography (GPC) using narrow polyethylene standards. Interestingly, most polymers show bimodal molecular weight distributions (MWD) with a low- (M_p = 0.6 – 1.1 kg mol^{-1}) and a high-molecular weight fraction (M_p = 28 – 289 kg mol^{-1}). The relatively narrow polydispersity index (M_w/M_n = 1.3 - 3.2) suggests that each active species acts as a single-site catalyst. One exception was **3.15**, which produced polymers with a very broad MWD (M_w/M_n = 26 – 28) and lower molecular weights (M_n = 20,000 g mol^{-1} for run 15). The molecular weight and the ratio of the two different mass fractions changed with polymerization temperature, time, cocatalyst loading, and precatalyst. The formation of two different types of polyethylene suggests the existence of two different catalytic species in the polymerization solution. This could potentially result from different catalyst activation pathways or complicated interactions of the active metal species with the aluminum cocatalyst (e.g., formation of different ion pairs or heterobimetallic species) which has been reported for other catalysts.[3,9] Chain transfer to dMAO is another potential pathway to give bimodal MWD which was investigated by varying the cocatalyst loading (Table 3.3).[10] The polymerization activity increased with increasing cocatalyst loading and leveled off at an Al/Ru ratio of ~1000. The polymer obtained with Al/Ru

= 500 was of low molecular weight (M_p = 1.3 kg mol^{-1}), while 2000 equivalents of dMAO gave mainly high molecular weight polymer (M_p = 404 kg mol^{-1}). This suggests that chain transfer to Al cocatalyst is unlikely to play a significant role, since it is expected that an increase in Al/Ru ratio leads to a decrease in MW.

Table 3.3 Ethylene homopolymerizations with different Ru/Al ratios.[a)]

run	[Ru]	solvent	Al/Ru	T [°C]	t [h]	yield [mg]	TOF[b]	M_p [kg/mol] (M_w/M_n) [c]
2.1	**3.12**	DCM	1000	40	4	tr	N/A	N/A
2.2	**3.12**	hex/tol[e]	1000	85	4	253	225	1.2 (35.7)
2.3	**3.12**	toluene	500	85	4	318	283	1.3 (15.7)
2.4	**3.12**	toluene	2000	85	4	765	682	403.6 / 0.8

a) Conditions: 10 μmol [Ru], cocatalyst dMAO, 600 psi C_2H_4, 100 mL total volume. b) In units of (mol (C_2H_4) / ((mol [Ru]) x h).c) Determined by GPC in 1,2,4-trichlorobenzene at 140 °C vs. polyethylene standards. Both peak molecular weight values (M_p) given for overlapping bimodal distributions. d) Methyl branches per 1000 C. Determined by ^{1}H NMR in tetrachloroethane-*d*4 at 130 °C. e) Hexanes : toluene = 1 :1 (v:v).

All polymers obtained were fully soluble in tetrachloroethane at elevated temperatures, allowing for high temperature NMR analysis on the polymers (Figure 3.3). The ^{1}H NMR spectra revealed that the polymers are highly linear with low degree of branching (<12 Me branches / 1000 carbons) and contain unsaturated end groups. The terminal olefinic group suggests that β-hydride elimination was a major mode of chain-transfer during the polymerization.

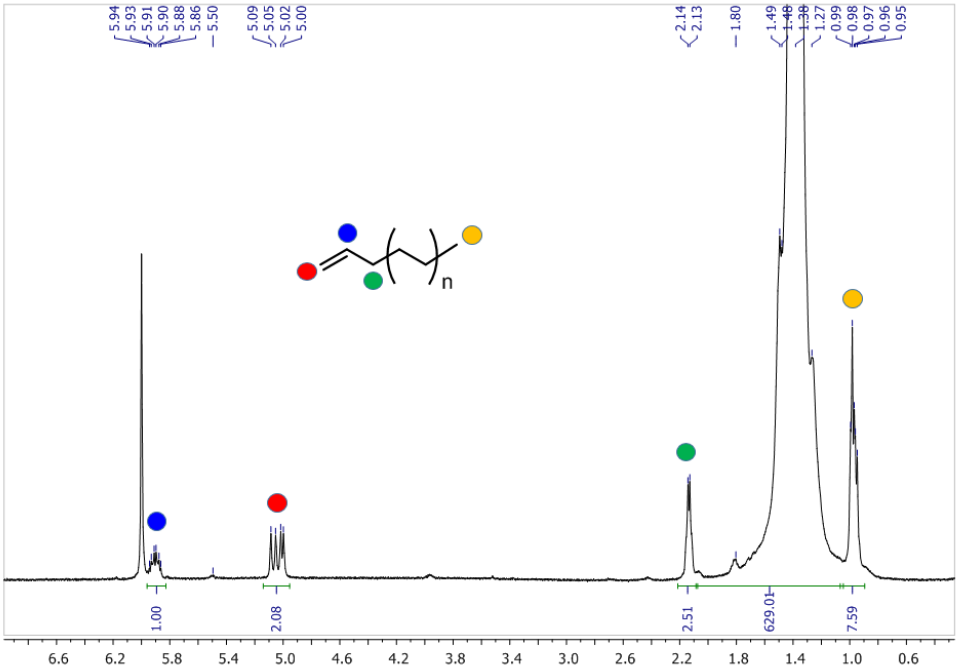

Figure 3.3 ^{1}H NMR of run 3 (**3.12**/dMAO) in $C_2D_2Cl_4$ at 403 K.

The melting temperature (T_m) and crystallinity of the polyethylenes were measured by differential scanning calorimetry (DSC). All the polymers were semicrystalline solids with relatively high T_m ranging from 129 – 135 °C (except for run 12 with 122 °C and a very broad melting transition). The polymer crystallinities range between 37% and 70 %. Some melting transitions were broad which is likely due to the two different polymer molecular weight fractions.

Copolymerizations were investigated with **3.12**/dMAO (Table 3.4). The catalyst activity decreased severely in the presence of α-olefins (i.e. 1-hexene) and trimethylsilyl vinyl ether. High temperature NMR of the polymers revealed no incorporation of the comonomers. The polymerization activity was fully suppressed by methyl- and tert-butyl acrylate and no polymer was obtained. It is known that the steric bulk of α-olefins slows down ethylene (co-) polymerization considerably. In addition, co-ordination of the functional groups (i.e. ether or ester) to the metal center can further decrease activity. The poisoning effect of functional groups on

3.12/dMAO was confirmed by an ethylene homopolymerization run in the presence of THF, which resulted in no polymer.

Table 3.4 Ethylene polymerizations with **3.12** in the presence of polar vinyl monomers and polar additives.[a]

run	comon.	conc. [M]	p [psi]	yield [mg]	activity[b]	α [%][c]
3.1	1-hexene	1.00	200	75	0.14[d]	0
3.2[e]	TMS-VE	0.10	200	tr	<0.2	0
3.3	MA	0.10	600	0	0	N/A
3.4	tBA	0.10	600	0	0	N/A
3.5	THF	0.12	600	0	0	N/A

a) Conditions: 10 μmol **3.12**, 1000 equiv. dMAO, 100 mL toluene, 85 °C, 4h. b) Unit: kg (polymer) x mol $[Ru]^{-1}$ x h^{-1} x bar^{-1}. c) Incorporation percentage of comonomer. d) T_m = 132.7 °C, M_n = 68 kg mol^{-1}, PDI = 3.06. e) 17h.

3.5 Conclusive Summary

In conclusion, several electronic and steric variants of the disulfonate phosphine ligand framework were synthesized, and their corresponding Ru(η^3:η^3-$C_{10}H_{16}$)(OPO) complexes obtained and characterized. These complexes are the first examples of Ru(IV) complexes that are active for ethylene insertion polymerization. Upon activation with dMAO, the polymerization activity for **3.12** is an order of magnitude higher than the most active Ru insertion polymerization catalyst reported previously. The polymerizations produce highly linear, semicrystalline polyethylenes with a bimodal molecular weight distribution. It was observed that the catalyst productivity increased with decreasing donor strength of the [OPO] ligand. Incorporation of α-olefins was unsuccessful, and the introduction of functional additives lead to deactivation of the catalyst.

3.6 Experimental Section

General considerations and materials

All reactions were carried out under nitrogen protection using standard Schlenk techniques or inside a Nitrogen glove box, unless stated otherwise. All solvents were dried and degassed (Argon) using the Grubbs/Dow method.[11] The following compounds were purchased and used without further purification: $PhPCl_2$, $MePCl_2$, $tBuPCl_2$, anhydrous $PhSO_3H$ (TCI America), and $[Ru(\eta^3:\eta^3\text{-}C_{10}H_{16})(\mu\text{-}Cl)Cl]_2$ (Strem). $AlMe_3$-depleted methylaluminoxane (dMAO) was obtained by removing all volatiles from an 11 wt% solution of MAO (Aldrich) *in vacuo* at 60 °C. Toluenesulfonic acid was dried azeotropically with a Dean-Stark apparatus using toluene. **3.3,** $(NEt_2)_2PCl$,[12] *p*-MeO-C_6H_4-PCl_2,[13] and *p*-CF_3-C_6H_4-PCl_2[14] were synthesized according to literature procedures. Deuterated solvents were purchased from Cambridge Isotope Laboratories and placed over activated 4Å molecular sieves. CD_2Cl_2 and $CDCl_3$ were dried over P_2O_5, vacuum transferred and deoxygenated by freeze-pump-thaw cycles. Ultrahigh purity grade ethylene gas (99.9%) was purchased from Praxair and used without further purification. ^1H NMR spectra were recorded using 500 MHz Bruker AVANCE and 600 MHz Bruker AVANCE spectrometers. 125 MHz ^{13}C NMR spectra were obtained using a cryoprobe. ^1H and ^{13}C spectra NMR were referenced to the residual solvent peaks. ^{19}F and ^{31}P NMR spectra were recorded using a 400 MHz Bruker DRX spectrometer and were referenced using the Ξ scale. Chemical shifts are reported in parts per million (ppm) on the δ scale. High resolution mass spectra (HRMS) were obtained by electrospray ionization (ESI) on a Waters Micromass LCT Premier (instrument variation $\sigma < 5$ ppm). Elemental analysis was performed by Atlantic Microlab, Inc. Molecular weights (M_n and M_w) and polydispersity indicies (M_w/M_n) were determined by high-temperature gel permeation chromatography (GPC), using a Waters Alliance GPCV 2000 GPC equipped with a Waters

differential refractive index (dRI) detector and in-line viscometer. The column set consisted of four Waters HT 6E and one Waters HT 2 and the samples were eluted at 140 °C with 1,2,4-trichlorobenzene containing 0.01 wt % di-tert-butyl-hydroxytoluene (BHT) at 1.0 mL/min. Data were calibrated using monomodal polyethylene standards (from Polymer Standards Service, Inc.). Polymers were placed in the 140 °C oven for at least 24 hours prior to sample analysis.

Ethylene Polymerization Procedure

Ethylene polymerizations were carried out in a stainless steel high-pressure reactor with glass liner (600 mL, Parr). The reactor was heated to 100 °C under vacuum overnight, backfilled with argon and cooled to the reaction temperature. After release of the pressure, a solution of the cocatalyst in the respective solvent (100 mL) was cannula transferred into the reactor and stirred under 600 psi of ethylene until it reached the reaction temperature. The pressure was slowly vented, the catalyst introduced as a solution or suspension in 5 mL toluene, and the vessel pressurized with ethylene. Prior to quenching the reaction with 100 mL methanolic HCl, the reactor was vented after the allotted reaction time, and the quenched mixture was poured into 200 mL methanol to precipitate the polymer. The polymer was collected by filtration, washed with methanol and acetone, and dried under reduced pressure over night.

Ligand synthesis

3,5-$(CF_3)_2C_6H_3$-PCl_2

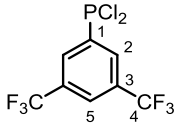

Dry *n*BuLi (3.0 mL 1.6 M solution in hexanes, 1.0 equiv.) was dissolved in 20 mL diethyl ether, cooled to -78 °C, and then l-bromo-3,5-bis(trifluoromethyl)benzene (1.4 g, 1.0 equiv.) was added and stirred for 20 minutes. To the light yellow suspension was then added 1.0 g $(NEt_2)_2PCl$ (4.8 mmol, 1.0 equiv.). The dark red-purple solution was stirred for 1 h, then HCl (23.7 mL 1.0 M

in diethyl ether, 5.0 equiv.) was added, allowed to warm to room temperature and stirred overnight. The white precipitate was separated by centrifugation and washed with ether. The solvent was removed from the combined organic phases yielding 0.71 g of the title compound as a colorless oil (2.3 mmol, 47%). The compound was used without further purification. ^{1}H NMR (400 MHz, $CDCl_3$) δ 8.33 (d, $^{3}J_{P,H}$ = 6.9 Hz, 2H, 2-H), 8.05 (s, 1H, 5-H). ^{13}C NMR (126 MHz, $CDCl_3$) δ 143.83 (d, $^{2}J_{P,C}$ = 57.9 Hz, C1), 132.71 (qd, J = 34.0, 6.5 Hz, C3), 130.71 – 130.13 (m, C2), 126.42 – 126.19 (m, C5), 122.90 (q, $^{1}J_{C,F}$ = 273.3 Hz, C4). ^{19}F NMR (376 MHz, $CDCl_3$) δ -63.02 (s). ^{31}P NMR (162 MHz, $CDCl_3$) δ 151.45 (s).

General procedure for [OPO] ligands: To a solution of anhydrous arenesulfonic acid (2.0 equiv.) in 50 mL dry THF was slowly added *n*-butyl lithium (4.0 equiv.) at 0 °C, resulting in a beige suspension. After stirring for two hours at room temperature, the light yellow suspension was cannula transferred into a solution of the respective phosphine dichloride (1.0 equiv.) in 50 mL dry diethyl ether at -78 °C. After warming to room temperature the clear solution was stirred for 2 - 4 days upon which a white precipitate formed. The product was collected by filtration, washed with dry THF and dry diethyl ether and dried under vacuum.

p-(4-OMe-C_6H_4)P(2-SO_3Li-C_6H_4)$_2$ (**3.4**)

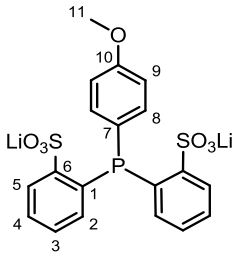

The above procedure with 0.90 g (5.7 mmol) anhydrous benzenesulfonic acid, 7.1 mL *n*-butyl lithium (1.6 M in hexanes, 11 mmol) and 0.60 mL PCl_2(4-OMe-C_6H_4) (2.8 mmol) yielded 1.07 g white solid (68%). The title compound contained 1.2 equivalents of THF, as established by

^{1}H NMR. ^{1}H NMR (400 MHz, CD_3OD) δ 8.04 (dd, J = 6.8, 4.0 Hz, 2H, 5-H), 7.38 (td, J = 7.7, 0.9 Hz, 2H, 4-H), 7.29 (td, J = 7.5, 0.9 Hz, 2H, 3-H), 7.04 (dd, J = 8.1, 7.1 Hz, 2H, 8-H), 6.94 (dd, J = 7.6, 2.1 Hz, 2H, 2-H), 6.84 (d, J = 8.1 Hz, 2H, 9-H), 3.77 (s, 3H, 11-H). ^{13}C NMR (126 MHz, CD_3OD) δ 161.36 (s), 149.45 (d, J = 25.9 Hz), 137.90 (d, J = 26.4 Hz), 136.73 (s), 136.37 (d, J = 22.4 Hz), 131.00 (s), 130.37 (d, J = 11.3 Hz), 129.29 (s), 128.88 (d, J = 4.0 Hz), 114.85 (d, J = 7.5 Hz), 55.59 (s, C11). ^{31}P {^{1}H} NMR (162 MHz, CD_3OD) δ -15.49 (s). HRMS(ESI) m/z calcd for $C_{19}H_{15}Li_2O_7PS_2$ $(M - Li)^-$ 457.0157, found 457.0178.

p-(4-CF_3-C_6H_4)P(2-SO_3Li-C_6H_4)$_2$ (**3.6**)

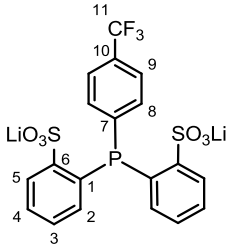

The above procedure with 0.71 g (4.5 mmol) anhydrous benzenesulfonic acid, 5.6 mL *n*-butyl lithium (1.6 M in hexanes, 8.9 mmol) and 0.55 g PCl_2(4-CF_3-C_6H_4) (2.2 mmol) yielded 0.67 g white solid (60%). The title compound contained 0.8 equivalents of THF, as established by ^{1}H NMR. X-ray quality crystals were obtained by dissolving **3.6** in a minimal amount of methanol and letting diethyl ether diffuse into the solution at room temperature. ^{1}H NMR (500 MHz, CD_3OD) δ 8.12 – 7.97 (m, 2H, 5-H), 7.52 (d, $^{3}J_{H,H}$ = 7.9 Hz, 2H, 8-H), 7.44 (td, $^{3}J_{H,H}$ = 7.6, $^{5}J_{P,H}$ = 0.8 Hz, 2H, 4-H), 7.32 (td, $^{3}J_{H,H}$ = 7.6, $^{4}J_{P,H}$ = 1.0 Hz, 2H, 3-H), 7.28 (vt, J = 7.1 Hz, 2H, 9-H), 6.92 (dd, $^{3}J_{H,H}$ = 7.5, $^{3}J_{P,H}$ = 2.3 Hz, 2H, 2-H). ^{31}P NMR (162 MHz, CD_3OD) δ -13.89 (s). ^{19}F NMR (376 MHz, CD_3OD) δ -64.10 (s). ^{13}C NMR (126 MHz, $CDCl_3$) δ 150.23 (d, J = 26.8 Hz), 147.00 (d, J = 18.9 Hz), 136.93 (s), 136.43 (d, J = 27.0 Hz), 135.13 (d, J = 20.8 Hz), 131.27 (s), 130.66 (d, J = 32.2 Hz), 129.83 (s), 129.01 (d, J = 4.3 Hz), 126.92 (s), 125.52 (s). HRMS(ESI) m/z

calcd for $C_{19}H_{12}F_3Li_2O_6PS_2$ $(M - Li)^-$ 494.9926, found 494.9940. Anal C 49.19, H 3.96, S 10.15 % calc for $C_{25}H_{24}Li_2O_{7.5}PS_2$ (**3.6**·1.5 THF), found C 49.86, H 3.79, S 10.63 %.

$(3,5\text{-}(CF_3)_2C_6H_3)P(2\text{-}SO_3Li\text{-}C_6H_4)_2$ (**3.7**)

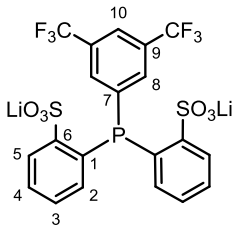

The above procedure with 0.71 g (4.5 mmol) anhydrous benzenesulfonic acid, 5.6 mL *n*-butyl lithium (1.6 M in hexanes, 8.9 mmol) and 0.71 g 3,5-$(CF_3)_2C_6H_3$-PCl_2 (2.3 mmol) yielded 0.16 g white solid (12%) after stirring for 7 days. The title compound contained 0.7 equivalents of THF, as established by ^{1}H NMR. ^{1}H NMR (400 MHz, CD_3OD) δ 8.11 (ddd, J = 7.8, 4.1, 1.2 Hz, 2H), 7.81 (s, 1H), 7.64 (d, J = 5.4 Hz, 2H), 7.48 (td, J = 7.6, 1.3 Hz, 2H), 7.37 (td, J = 7.5, 1.4 Hz, 2H). ^{19}F NMR (376 MHz, CD3OD) δ -64.41 (s). ^{31}P NMR (162 MHz, CD_3OD) δ -13.06 (s). HRMS(ESI) m/z calcd for $C_{20}H_{11}F_6Li_2O_6PS_2$ $(M - Li)^-$ 562.9799, found 562.9792.

$MeP(2\text{-}SO_3Li\text{-}C_6H_4)_2$ (**3.8**)

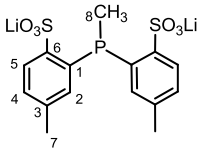

The above procedure with 2.10 g (12.2 mmol) anhydrous toluenesulfonic acid, 15.3 mL *n*-butyl lithium (1.6 M in hexanes, 24.4 mmol) and 0.55 mL PCl_2Me (6.1 mmol) yielded 1.94 g white solid (68%). The title compound contained one equivalent of THF, as established by ^{1}H NMR. ^{1}H NMR (500 MHz, D_2O) δ 7.85 (dd, $^3J_{HH}$ = 8.0 Hz, $^5J_{HH}$ = 3.9 Hz, 2H, 5-H), 7.28 (d, $^3J_{HH}$ = 8.0 Hz, 2H, 4-H), 7.10 (s, 2H, 2-H), 2.23 (s, 6H, 7-H), 1.66 (d, $^2J_{PH}$ = 6.1 Hz, 3H, 8-H). ^{13}C NMR (126 MHz, D_2O) δ 143.89 (d, $^2J_{PC}$ = 23.9 Hz, C6), 142.75 (s, C3), 138.87 (d, $^1J_{PC}$ = 27.4 Hz, C1), 134.64

(s, C2), 130.05 (s, C2), 128.59 (d, $^{4}J_{PC}$ = 3.6 Hz, C4), 21.16 (s, C7), 13.23 (d, $^{1}J_{PC}$ = 15.0 Hz, C8). ^{31}P {^{1}H} NMR (162 MHz, D_2O) δ -28.53. HRMS(ESI) m/z calcd for $C_{15}H_{15}Li_2O_6PS_2$ (M - Li)$^-$ 393.0208, found 393.0201. Anal C 44.89, H 5.35, S 13.61 % calc for $C_{19}H_{27}Li_2O_9PS_2$ (**3.8**·1THF·$2H_2O$), found C 45.27, H 4.61, S 13.82 %.

^{t}BuP(2-SO_3Li-C_6H_4)$_2$ (**3.9**)

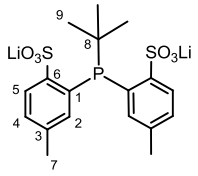

The above procedure with 0.54 g (3.1 mmol) anhydrous toluenesulfonic acid, 3.9 mL *n*-butyl lithium (1.6 M in hexanes, 6.3 mmol) and 0.25 g $PCl_2{}^{t}$Bu (1.6 mmol) yielded 0.36 g white solid (47%). The title compound contained 0.4 equivalents of THF, as established by ^{1}H NMR. ^{1}H NMR (400 MHz, CD_3OD) δ 7.99 (dd, $^{3}J_{H,H}$ = 8.0 Hz, $^{4}J_{P,H}$ = 4.2 Hz, 2H, 5-H), 7.70 (s, 2H, 2-H), 7.22 (d, $^{3}J_{H,H}$ = 8.0 Hz, 1H, 4-H), 2.35 (s, 6H, 7-H), 1.27 (d, $^{3}J_{P,H}$ = 12.6 Hz, 9H, 9-H). ^{31}P {^{1}H} NMR (162 MHz, CD_3OD) δ -7.64 (s). ^{13}C NMR (126 MHz, CD_3OD) δ 148.42 (d, $^{2}J_{P,C}$ = 26.4 Hz, C6), 140.23 (s, C3), 137.54 (s, C2), 135.24 (d, $^{1}J_{P,C}$ = 31.1 Hz, C1), 130.16 (d, $^{3}J_{P,C}$ = 5.1 Hz, C5), 130.11 (s, C4), 32.76 (d, $^{1}J_{P,C}$ = 17.9 Hz, C8), 30.53 (d, $^{2}J_{P,C}$ = 15.7 Hz, C9), 21.25 (s, C7). Anal C 44.82, H 5.80, S 12.21 %, calcd for $C_{19.6}H_{30.2}Li_2O_{9.4}PS_2$ (**1e**·0.4THF·$3H_2O$), found C 44.70, H 5.39, S 12.22 %.

Complex synthesis

General procedure: A suspension of [Ru(η^3:η^3-$C_{10}H_{16}$)(μ-Cl)Cl]$_2$ (1.0 equiv.) and Li_2[OPO] (2.0 equiv.) in 20 mL dry dichloromethane was stirred at room temperature for 30 minutes and then $AgBF_4$ (4.0 equiv.) was added portion wise. The resulting mixture was stirred for 5 - 6 h in dark, after which the off-white precipitate was removed by centrifugation and washed

with 5 mL dichloromethane. The combined yellow organic phases were evaporated *in vacuo,* redissolved in a small amount of dichloromethane or toluene and filtered through a short plug of Celite to remove residual inorganic salts. The product was then precipitated with pentane or hexanes, collected by filtration, washed with pentane and dried *in vacuo*.

$[Ru(\eta^3:\eta^3\text{-}C_{10}H_{16})^{Ph}(OPO)]$ (**3.10**)

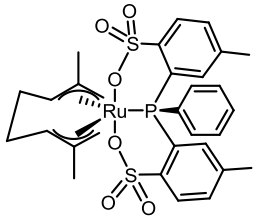

The above procedure with 75 mg $[\{Ru(\eta^3:\eta^3\text{-}C_{10}H_{16})(\mu\text{-}Cl)Cl\}_2]$ (2.4 mmol [Ru]), 141 mg **3.3**·1.8THF (2.43 mmol) and 95 mg $AgBF_4$ (4.9 mmol) yielded 92 mg yellow powder (69%) as the title compound. ^{1}H NMR (400 MHz, $CDCl_3$) δ 8.09 (dd, *J* = 7.4, 5.7 Hz, 1H), 7.96 (dd, *J* = 7.8, 5.0 Hz, 1H), 7.81 – 7.60 (m, 4H), 7.55 – 7.29 (m, 5H), 5.24 (d, *J* = 9.3 Hz, 1H), 5.10 (d, *J* = 11.5 Hz, 1H), 4.82 (d, *J* = 11.8 Hz, 1H), 4.48 (s, 1H), 4.04 (d, *J* = 10.8 Hz, 1H), 3.96 – 3.66 (m, 3H), 3.06 – 2.96 (m, *J* = 12.3, 6.0 Hz, 1H), 2.95 – 2.83 (m, 1H), 2.46 (d, *J* = 3.4 Hz, 6H), 2.19 (s, 3H), 2.08 (s, 1H), 1.66 (s, 3H). ^{13}C NMR (126 MHz, $CDCl_3$) δ 143.30 (d, *J* = 13.7 Hz), 142.64 (d, *J* = 13.5 Hz), 140.53 (d, *J* = 5.8 Hz), 140.16 (d, *J* = 5.8 Hz), 135.59 (s), 134.59 (s), 134.23 (s), 134.01 (d, *J* = 33.9 Hz), 132.55 (d, *J* = 1.7 Hz), 132.17 (d, *J* = 1.7 Hz), 131.59 (s), 130.87 (d, *J* = 43.6 Hz), 130.36 (d, *J* = 2.9 Hz), 130.05 (d, *J* = 8.4 Hz), 129.82 (d, *J* = 8.4 Hz), 129.45 (d, *J* = 44.0 Hz), 129.18 (s), 128.37 (s), 128.15 (d, *J* = 12.0 Hz), 125.44 (s), 118.18 (d, *J* = 8.2 Hz), 113.66 (d, *J* = 7.7 Hz), 72.26 (s), 72.23 (s), 37.52 (s), 37.35 (s), 21.82 (s), 21.66 (s), 19.97 (s), 19.18 (s). ^{31}P NMR (162 MHz, $CDCl_3$) δ 6.97 (s). Anal C 54.82, H 5.20, S 8.56 % calcd for $C_{34.2}H_{38.6}Cl_{0.2}O_6PRuS_2$ (**3.10**·0.5toluene·0.1dichloromethane·0.1hexane), found C 54.31, H 5.18, S 8.45 %.

[Ru(η^3:η^3-$C_{10}H_{16}$)^{OMe}(OPO)] (**3.11**)

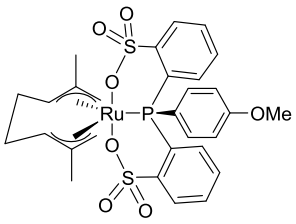

The above procedure with 60 mg [{Ru(η^3:η^3-$C_{10}H_{16}$)(μ-Cl)Cl}$_2$] (2.0 mmol [Ru]), 107 mg **3.4**·1.2 THF (1.95 mmol) and 71 mg $AgBF_4$ (3.6 mmol) yielded 85 mg light yellow powder (63%) as the title complex. ^{1}H NMR (400 MHz, $CDCl_3$) δ 8.24 – 8.17 (m, 1H), 8.12 – 8.05 (m, 1H), 7.99 – 7.87 (m, 2H), 7.70 – 7.57 (m, 7H), 6.85 (d, *J* = 7.6 Hz, 2H), 5.26 (d, *J* = 9.5 Hz, 1H), 5.10 (d, *J* = 11.1 Hz, 1H), 4.83 (d, *J* = 11.1 Hz, 1H), 4.50 – 4.46 (m, 1H), 4.00 (d, *J* = 10.2 Hz, 1H), 3.96 – 3.81 (m, 1H), 3.78 (s, 3H), 3.08 – 2.96 (m, 1H), 2.96 – 2.85 (m, 1H), 2.21 (s, 3H), 2.21 (s, 3H), 2.07 (s, 1H), 1.65 (s, 3H). ^{31}P NMR (162 MHz, $CDCl_3$) δ 6.69 (s). ^{13}C NMR (126 MHz, $CDCl_3$) δ 161.18 (d, J = 2.8 Hz), 145.80 (d, J = 13.7 Hz), 145.22 (d, J = 13.6 Hz), 135.83 (d, J = 12.1 Hz), 134.84 (s), 133.31 (s), 131.91 (d, J = 1.7 Hz), 131.75 (s), 131.68 (d, J = 1.9 Hz), 131.55 (d, J = 0.7 Hz), 131.40 (s), 130.29 (s), 130.25 (s), 129.99 (d, J = 5.9 Hz), 129.94 (s), 129.83 (d, J = 7.9 Hz), 129.64 (d, J = 8.0 Hz), 128.17 (s), 124.79 (s), 124.31 (s), 118.18 (d, J = 8.2 Hz), 113.87 (d, J = 13.1 Hz), 113.74 (d, J = 7.8 Hz), 72.18 (d, J = 4.5 Hz), 72.11 (d, J = 3.6 Hz), 55.33 (s), 37.53 (s, J = 19.7 Hz), 37.37 (s), 19.93 (s), 19.19 (s). Anal C 51.64, H 4.92, S 9.04 % calc for $C_{30.5}H_{34.6}O_7PRuS_2$ (**3.11**·0.3pentane), found C 51.94, H 4.92, S 8.69 %.

[Ru(η^3:η^3-$C_{10}H_{16}$)^{CF3}(OPO)] (**3.12**)

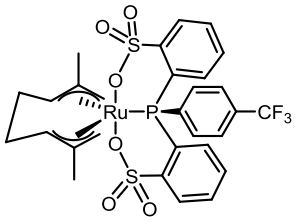

The above procedure with 75 mg [{Ru(η^3:η^3-$C_{10}H_{16}$)(μ-Cl)Cl}$_2$] (2.4 mmol [Ru]), 136 mg **3.6**·0.8 THF (2.43 mmol) and 95 mg $AgBF_4$ (4.9 mmol) yielded 128 mg yellow powder (72%) as the title complex. ^{1}H NMR (500 MHz, $CDCl_3$) δ 8.26 – 8.16 (m, 1H), 8.14 – 8.06 (m, 1H), 8.01 – 7.92 (m, 1H), 7.88 (t, *J* = 9.1 Hz, 3H), 7.75 – 7.62 (m, 4H), 7.57 (d, *J* = 7.2 Hz, 2H), 5.23 (d, *J* = 9.3 Hz, 1H), 5.15 (d, *J* = 11.7 Hz, 1H), 4.86 (d, *J* = 11.7 Hz, 1H), 4.50 (d, *J* = 2.6 Hz, 1H), 4.06 (d, *J* = 11.1 Hz, 1H), 2.20 (s, 3H), 2.00 (d, *J* = 2.4 Hz, 1H), 1.66 (s, 3H). ^{13}C NMR (126 MHz, $CDCl_3$) δ 145.91 (d, *J* = 14.1 Hz), 145.07 (d, *J* = 13.9 Hz), 139.21 (s), 135.04 (s), 134.34 (d, *J* = 10.9 Hz), 133.13 (s), 132.39 (s), 132.10 (s), 131.86 (s), 130.52 (d, *J* = 5.9 Hz), 130.37 (s), 130.15 (d, *J* = 5.7 Hz), 129.98 (d, *J* = 7.8 Hz), 129.76 (d, *J* = 8.0 Hz), 129.09 (d, *J* = 4.1 Hz), 128.71 (s), 128.27 (d, *J* = 5.1 Hz), 125.36 (s), 125.04 – 124.62 (m), 118.81 (d, *J* = 8.4 Hz), 114.15 (d, *J* = 7.7 Hz), 72.38 (d, *J* = 3.4 Hz), 71.95 (d, *J* = 4.6 Hz), 37.49 (s, *J* = 22.5 Hz), 37.31 (s), 19.89 (s), 19.12 (s). ^{19}F NMR (376 MHz, $CDCl_3$) δ -63.13 (s). ^{31}P {^{1}H} NMR (162 MHz, $CDCl_3$) δ 8.32 (s). Anal C 48.00, H 3.89 % calcd for $C_{29}H_{28}F_3O_6PRuS_2$, found C 47.55, H 4.05 %.

[Ru(η^3:η^3-$C_{10}H_{16}$)$^{3,5(CF3)}$(OPO)] (**3.13**)

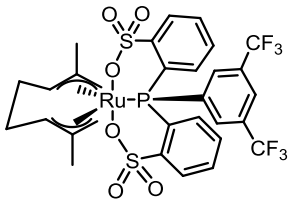

The above procedure with 50 mg [Ru(η^3:η^3-$C_{10}H_{16}$)(μ-Cl)Cl]$_2$ (1.0 equiv.), 93 mg **3.7**·0.7 THF (1.6 mmol, 2.0 equiv.) and 63 mg $AgBF_4$ (3.2 mmol) yielded 110 mg yellow powder (78%) as the title complex. ^{1}H NMR (500 MHz, $CDCl_3$) δ 8.28 (d, *J* = 11.8 Hz, 2H), 8.26 – 8.22 (m, 1H), 8.14 – 8.10 (m, 1H), 8.01 – 7.96 (m, 1H), 7.95 – 7.87 (m, 2H), 7.77 – 7.67 (m, 4H), 5.17 (dt, *J* = 7.0, 3.7 Hz, 1H), 5.12 (d, *J* = 8.8 Hz, 1H), 4.90 – 4.84 (m, 1H), 4.50 (d, *J* = 2.8 Hz, 1H), 4.07 (d, *J* = 11.5 Hz, 1H), 3.93 (ddd, *J* = 17.4, 12.7, 5.5 Hz, 1H), 3.81 (ddd, *J* = 25.4, 12.5, 5.3 Hz, 1H), 3.08 – 3.00 (m, 1H), 2.97 – 2.89 (m, *J* = 9.3, 4.6 Hz, 1H), 2.21 (s, 3H), 2.00 (d, *J* = 2.6 Hz,

1H), 1.64 (s, 3H). ^{19}F NMR (376 MHz, $CDCl_3$) δ -62.88 (s). ^{31}P NMR (162 MHz, $CDCl_3$) δ 9.81 (s). HRMS(ESI) m/z calcd for $C_{32}H_{39}F_6NaO_6PRuS_2$ (**3.13** + Na)$^+$ 853.0771, found 853.0789.

[Ru(η^3:η^3-$C_{10}H_{16}$)^{Me}(OPO)] (**3.14**)

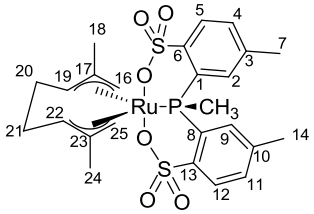

The above procedure with 75 mg [Ru(η^3:η^3-$C_{10}H_{16}$)(μ-Cl)Cl]$_2$ (2.4 mmol [Ru]), 122 mg **3.8**·1.8THF (2.43 mmol) and 95 mg $AgBF_4$ (4.9 mmol) yielded 109 mg yellow powder (72%) as the title compound. X-ray quality single crystals were grown by slow diffusion of diethyl ether into a saturated dichloromethane solution at room temperature. ^{1}H NMR (500 MHz, $CDCl_3$) δ 8.09 (d, $^3J_{H,P}$ = 8.6 Hz, 1H, 2-H), 8.05 (d, $^3J_{H,P}$ = 9.2 Hz, 1H, 9-H), 7.97 (dd, $^3J_{H,H}$ = 8.0 Hz, $^4J_{H,P}$ = 4.9 Hz, 1H, 12-H), 7.92 (dd, $^3J_{H,H}$ = 8.0 Hz, $^4J_{H,P}$ = 4.8 Hz, 1H, 5-H), 7.44 (d, $^3J_{H,H}$ = 8.0 Hz, 1H, 4-H), 7.41 (d, $^3J_{H,H}$ = 8.0 Hz, 1H, 11-H), 5.62 (d, J = 8.2 Hz, 1H, 25-H$_a$), 5.12 (d, J = 11.5 Hz, 1H, 22-H), 4.75 (d, J = 11.5 Hz, 1H, 19-H), 4.38 (d, J = 2.9 Hz, 1H, 25-H$_b$), 3.90 (ddd, J = 24.9, 12.5, 5.3 Hz, 1H, 21-H), 3.84 – 3.72 (m, 2H, 16-H$_a$ and 20-H), 3.07 – 2.97 (m, 1H, 21-H), 2.96 – 2.85 (m, 1H, 20-H), 2.79 (d, $^1J_{H,P}$ = 11.2 Hz, 3H, 15-H), 2.59 (s, 3H, 7-H), 2.53 (s, 3H, 14-H), 2.44 (d, J = 2.3 Hz, 1H, 16-H$_b$), 2.24 (s, 3H, 24-H), 1.42 (s, 3H, 18-H). ^{13}C NMR (126 MHz, $CDCl_3$) δ 143.74 (d, $^2J_{C,P}$ = 14.0 Hz, C13), 142.19 (d, $^2J_{C,P}$ = 12.4 Hz, C6), 140.53 (d, $^3J_{C,P}$ = 6.1 Hz, C3), 140.05 (d, $^3J_{C,P}$ = 5.8 Hz, C10), 134.97 (s, C2), 133.00 (d, $^1J_{C,P}$ = 42.5 Hz, C8), 132.49 (d, $^4J_{C,P}$ = 2.2 Hz, C4), 131.57 (d, $^4J_{C,P}$ = 2.0 Hz, C11), 131.36 (s, C9), 130.29 – 129.83 (m, C1 and C12), 129.71 (d, $^3J_{C,P}$ = 8.9 Hz, C5), 128.53 (s, C17), 127.63 (s, C23), 118.40 (d, $^2J_{C,P}$ = 7.9 Hz, C22), 113.52 (d, $^2J_{C,P}$ = 7.6 Hz, C19), 74.95 (d, $^2J_{C,P}$ = 4.2 Hz, C16), 67.66 (d, $^2J_{C,P}$ = 4.7 Hz, C25), 37.69 (s, C20), 37.31 (s, C21), 21.95 (s, C14), 21.66 (s, C7), 19.27 (s, C18 or C24), 19.23 (s, C18 or

C24), 18.67 (d, $^{1}J_{C,P}$ = 32.2 Hz, C15 (P-Me)). ^{31}P {^{1}H} NMR (162 MHz, $CDCl_3$) δ -1.35 (s). HRMS(ESI) m/z calcd for $C_{25}H_{31}O_6PRuS_2$ $(M + Na)^+$ 647.0241, found 647.0267. Anal C 48.48, H 5.24, S 9.92 % calcd for $C_{26.1}H_{33.6}Cl_{0.2}O_6PRuS_2$ (**3.14**·0.2pentane·0.1dichloromethane), found C 48.38, H 5.01, S 9.71 %.

[Ru(η^3:η^3-$C_{10}H_{16}$)^{tBu}(OPO)] (**3.15**)

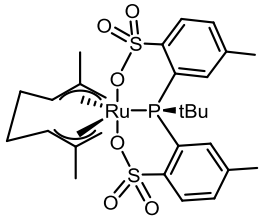

The above procedure with 75 mg [Ru(η^3:η^3-$C_{10}H_{16}$)(μ-Cl)Cl]$_2$ (2.4 mmol [Ru]), 115 mg **3.9**·0.4 THF (2.43 mmol) and 95 mg $AgBF_4$ (4.9 mmol) yielded 89 mg light yellow powder (55%) as the title complex. X-ray quality single crystals were obtained by slow diffusion of diethyl ether into a saturated solution of **3.15** in dichloromethane at room temperature. ^{1}H NMR (400 MHz, $CDCl_3$) δ 8.49 (d, *J* = 7.3 Hz, 1H), 8.23 (d, *J* = 6.8 Hz, 1H), 8.01 (dd, *J* = 8.0, 4.6 Hz, 1H), 7.89 (dd, *J* = 7.9, 4.4 Hz, 1H), 7.38 (d, *J* = 8.1 Hz, 2H), 6.56 (d, *J* = 6.3 Hz, 1H), 5.30 (s, 1H), 5.19 – 5.05 (m, *J* = 11.2 Hz, 1H), 4.62 – 4.53 (m, *J* = 11.6 Hz, 1H), 4.45 (d, *J* = 2.4 Hz, 1H), 4.15 (d, *J* = 10.2 Hz, 1H), 3.76 – 3.64 (m, *J* = 12.6, 5.2 Hz, 1H), 3.63 – 3.43 (m, 1H), 2.95 – 2.83 (m, *J* = 12.2, 5.2 Hz, 1H), 2.82 – 2.70 (m, *J* = 12.5, 4.7 Hz, 1H), 2.61 (s, 3H), 2.57 (s, 3H), 2.48 (d, *J* = 2.2 Hz, 1H), 2.20 (s, 3H), 1.51 (d, *J* = 16.8 Hz, 9H), 1.29 (s, 3H). ^{13}C NMR (126 MHz, $CDCl_3$) δ 143.25 (d, *J* = 13.9 Hz), 141.89 (d, *J* = 13.7 Hz), 139.74 (d, *J* = 4.3 Hz), 138.18 (d, *J* = 4.3 Hz), 136.54 (d, *J* = 2.3 Hz), 134.54 (d, *J* = 24.5 Hz), 131.95 (s), 131.78 (d, *J* = 1.8 Hz), 131.72 (s), 131.51 (d, *J* = 2.0 Hz), 130.96 (d, *J* = 1.7 Hz), 130.31 (d, *J* = 7.3 Hz), 129.74 (d, *J* = 8.1 Hz), 128.17 (s), 126.36 (s), 119.81 (d, *J* = 8.7 Hz), 108.27 (d, *J* = 7.5 Hz), 82.08 (d, *J* = 2.7 Hz), 67.32 (d, *J* = 4.4 Hz), 46.62 (d, *J* = 14.3 Hz), 36.91 (s), 35.96 (s), 33.63 (d, *J* = 3.5 Hz), 21.94 (d, *J* = 35.1 Hz), 19.30 (s),

18.22 (s). ^{31}P NMR (162 MHz, $CDCl_3$) δ 6.34 (s). HRMS(ESI) m/z calcd for $C_{28}H_{37}O_6PRuS_2$ (M + Na)$^+$ 689.0710, found 689.0717. Anal C 48.69, H 5.52, S 8.96 % calcd for $C_{29}H_{39.2}ClO_6PRuS_2$ (**3.15**·0.1pentane·0.5dichloromethane), found C 48.15, H 5.60, S 8.13 %.

3.7 References

(1) Shen, Z.; Jordan, R. F. *J. Am. Chem. Soc.* **2009**, *132*, 52-53.

(2) Piche, L.; Daigle, J.-C.; Claverie, J. P. *Chem. Commun.* **2011**, *47*, 7836-7838.

(3) Camacho-Fernandez, M. A.; Yen, M.; Ziller, J. W.; Guan, Z. *Chem. Sci.* **2013**, *4*, 2902-2906.

(4) Nomura, K.; Warit, S.; Imanishi, Y. *Macromolecules* **1999**, *32*, 4732-4734.

(5) Renaud, J.-L.; Demerseman, B.; Mbaye, M. D.; Bruneau, C. *Curr. Org. Chem.* **2006**, *10*, 115-133.

(6) TN 48, "Polymer Heats of Fusion", TA Instruments, New Castle, DE

(7) See Chapter 4 for synthesis.

(8) Britovsek, G. J. P.; Clentsmith, G. K. B.; Gibson, V. C.; Goodgame, D. M. L.; McTavish, S. J.; Pankhurst, Q. A. *Catal. Commun.* **2002**, *3*, 207-211.

(9) a) Corker, J. M.; Evans, J. *J. Chem. Soc., Chem. Commun.* **1991**, 1104-1106. b) Fernando de Souza, R.; Simon, L. C.; Alves, M. d. C. M. *J. Catal.* **2003**, *214*, 165-168. c) Bryliakov, K. P.; Talsi, E. P.; Semikolenova, N. V.; Zakharov, V. A. *Organometallics* **2009**, *28*, 3225-3232.

(10) Small, B. L.; Brookhart, M.; Bennett, A. M. A. *J. Am. Chem. Soc.* **1998**, *120*, 4049-4050.

(11) Pangborn, A. B.; Giardello, M. A.; Grubbs, R. H.; Rosen, R. K.; Timmers, F. J. *Organometallics* **1996**, *15*, 1518-1520.

(12) Magnelli, D. D.; Tesi, G.; Lowe, J. U.; McQuistion, W. E. *Inorg. Chem.* **1966**, *5*, 457-461.

(13) Miles, J. A.; Beeny, M. T.; Ratts, K. W. *J. Org. Chem.* **1975**, *40*, 343-347.

(14) Clark, T. J.; Rodezno, J. M.; Clendenning, S. B.; Aouba, S.; Brodersen, P. M.; Lough, A. J.; Ruda, H. E.; Manners, I. *Chem. Eur. J.* **2005**, *11*, 4526-4534.

4 Modifications of Disulfonate Phosphine Ruthenium Polymerization Catalysts

4.1 Disulfonate Phosphine Ruthenium(II) Complexes

4.1.1 Introduction

In Chapter 3, it was found that Ru(IV) complexes of disulfonato phosphine ligands [OPO] act as ethylene polymerization catalysts when activated with dMAO. Decreasing the ligand electron donation leads to increased activities, as the metal centers are more electron deficient. However, the increased electrophilicity also strengthens heteroatom coordination of functionalized olefins. For Ru(IV)(OPO) catalysts **3.10** – **3.15**, the addition of several hundred equivalents of polar comonomers, such as methyl acrylate or vinyl acetate, or tetrahydrofuran to a polymerization reaction resulted in complete deactivation and no (co-)polymer was obtained.

Reducing the ruthenium oxidation state would lower the electrophilicity of the resulting complex and increase the likelihood of polar monomer incorporation. However, it can be anticipated that these lower oxidation state catalysts would also show decreased activity in comparison with their Ru(IV) analogues. This inverse correlation between activity and functional group incorporation is a known common dilemma in the olefin insertion polymerization field. Solely considering ligand electronic effects, striking a compromise between activity and the degree of functionalization is inevitable.[1] In the first part of this chapter, Ru(II)(OPO) complexes were synthesized and investigated for their polymerization behavior.

Prior to this work, ruthenium(II) complexes of tridentate disulfonato phosphines were not known, but a few examples of Ru(II) complexes with ortho-phosphinobenzenesulfonate (PO) ligands have been reported by the groups of Claverie[2] and Bruneau.[3]

4.1.2 Disulfonate Phosphine Ruthenium(II) Complex Synthesis

Stirring a methanol suspension of $RuCl_2(PPh_3)_3$ with ligand salt $Li_2^{Ph}[OPO]$ (**3.3)** at room temperature resulted in the formation of a light brown material, that is readily soluble in chlorinated solvents but insoluble in the reaction solvent (Scheme 4.1). The material was identified as a formally 6-coordinate complex **4.1** by ^{1}H, ^{31}P, ^{13}C NMR, ESI-MS, elemental analysis, and X-ray diffraction analysis (Figure 4.1). The proton NMR spectrum shows only aromatic signals between 6.5 and 8.1 ppm. The resonances for the two sulfonate aryl moieties are identical, suggesting equivalence of the two groups in solution. The ratio of triphenylphosphine to the disulfonate phosphine ligand is 2:1 based on integrational values. The $^{31}P\{^{1}H\}$ spectrum consists of three distinct doublets of doublets at 59.78, 24.46, and 12.96 ppm, in equal integrated ratios. The most downfield shifted signal shows two small coupling constants indicative of a *cis* arrangement ($^{2}J_{PP,cis}$ = 28 and 30 Hz) and the other two signals show a large *trans* coupling constant ($^{2}J_{PP,trans}$ = 297 Hz) in addition to a *cis* coupling. This indicates a *mer*-arrangement of three phosphorus atoms around the metal center, with the middle phosphorus having the most downfield shifted resonance. The crystal structure of complex **4.1** (Figure 4.1, left) confirms the assignments and reveals a 6-coordinate Ru(II) complex, where the [OPO]-ligand is coordinated in a *mer* fashion and one sulfonate group binds κ^2-*O*. The interaction of the second sulfonate oxygen was weaker (Ru1-O2 2.398 Å vs. Ru1-O1 2.144), and gave rise to an increased bond distance of 1.474 Å between S1 and O2 (for comparison: nonbonding S1–O1 1.491 Å, bonding S1–O3 1.435 Å). A similar coordination of sulfonate phosphines to ruthenium carbene complexes was reported,[2b] as well as κ^2 coordination of sulfonate to transition metals with equal oxygen-metal bond lengths.[4]

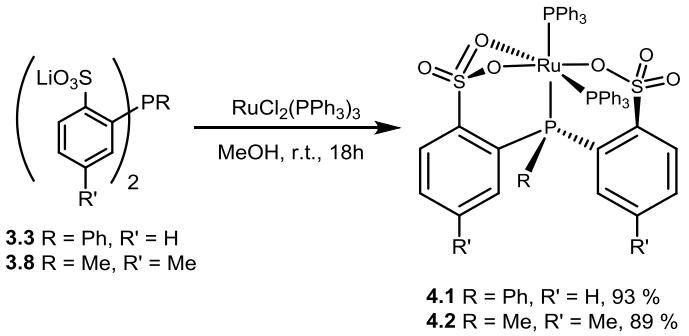

3.3 R = Ph, R' = H
3.8 R = Me, R' = Me

4.1 R = Ph, R' = H, 93 %
4.2 R = Me, R' = Me, 89 %

Scheme 4.1 Synthesis of Ru(II) complex **4.1** from the ligand salt **3.3**.

Complex **4.2** was obtained in 89 % isolated yield from ligand **3.8** using the same reaction conditions as with **4.1** as shown in Scheme 4.1. Complex **4.2** showed similar structural features, as determined by ^{1}H and ^{31}P NMR spectroscopy, and X-ray diffraction analysis (Figure 4.1, right). Both aryl sulfonate moieties are magnetically equivalent at room temperature, and the solid state structure featured one κ^2-sulfonate coordination. The aryl-methyl groups in **4.2** allow for the analysis of the temperature dependent dynamicity of the [OPO] coordination via ^{1}H and ^{31}P NMR spectroscopy (Figure 4.2). The aryl-methyl groups (R') gave rise to a slightly broadened singlet resonance at 2.40 ppm at 298 K. Two sharp, isolated singlet resonances at 2.15 and 2.56 ppm were observed at 198 K, which coalesce at around 248 K. This is in accordance with a fluxional κ^2-sulfonate interaction in the solution phase, where an equilibrium between different sulfonate oxygen coordination isomers exists at higher temperatures. The activation energy barrier $\Delta G^{\ddagger}$ for this $\kappa^2 - \kappa^1$ isomerization process was calculated to be 11.4 kcal mol^{-1}. Across the temperature range 198 – 313 K, three ^{31}P resonances were observed (Figure 4.3). They only shifted slightly (less than 5 ppm), maintained their splitting patterns, and showed virtually no line broadening. Based on the ^{31}P NMR spectra, the coordination geometry around the ruthenium center was maintained in solution.

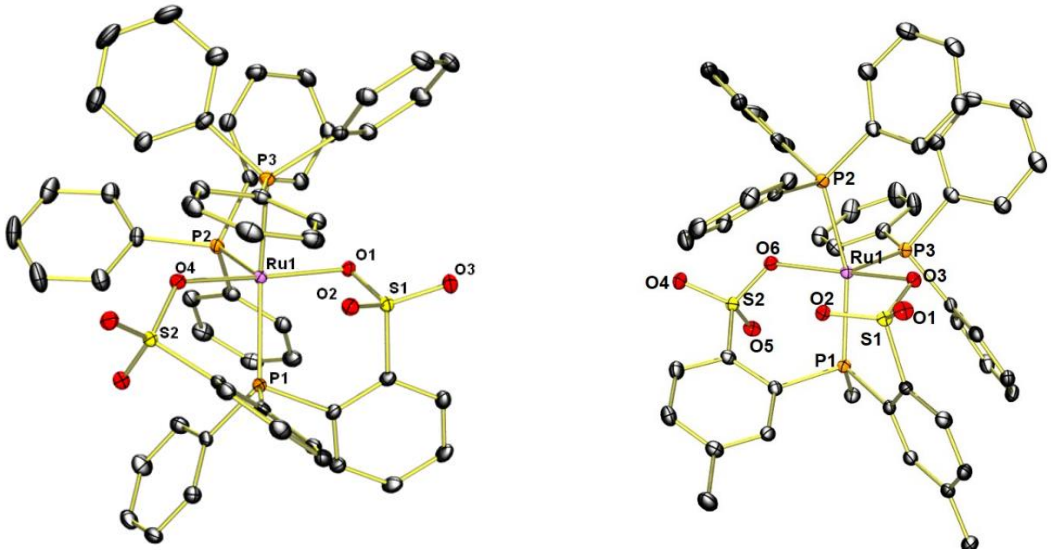

Figure 4.1 Solid state structures of **4.1** (left) and **4.2** (right). Hydrogen atoms omitted for clarity. Selected bond distances (Å) and angles (˚): **4.1**: Ru1-O1 2.1444(11), Ru1-O2 2.3979(12), Ru1-O4 2.1170(12), Ru1-P1 2.3738(4), Ru1-P2 2.2570(4), Ru1-P3 2.3970(5), S1-O1 1.4996(12), S1-O2 1.4744(12), S2-O4 1.5014(12), O4-Ru1-O1 169.76(5), O4-Ru1-P2 98.40(3), O1-Ru1-P2 90.43(3), P2-Ru1-P1 104.015(16), O1-Ru1-O2 62.75(4). **4.2**: Ru1-O6 2.1217(13), Ru1-O3 2.1321(13), Ru1-O2 2.3686(13), Ru1-P3 2.2506(5), Ru1-P1 2.3492(5), Ru1-P2 2.4306(5), S1-O1 1.4294(14), S1-O2 1.4714(14), S1-O3 1.5043(14), O6-Ru1-O3 165.20(5), O6-Ru1-P3 102.82(4), O3-Ru1-P3 91.04(4), O6-Ru1-P1 89.48(4), O3-Ru1-P1 93.91(4), O3-Ru1-O2 63.57(5).

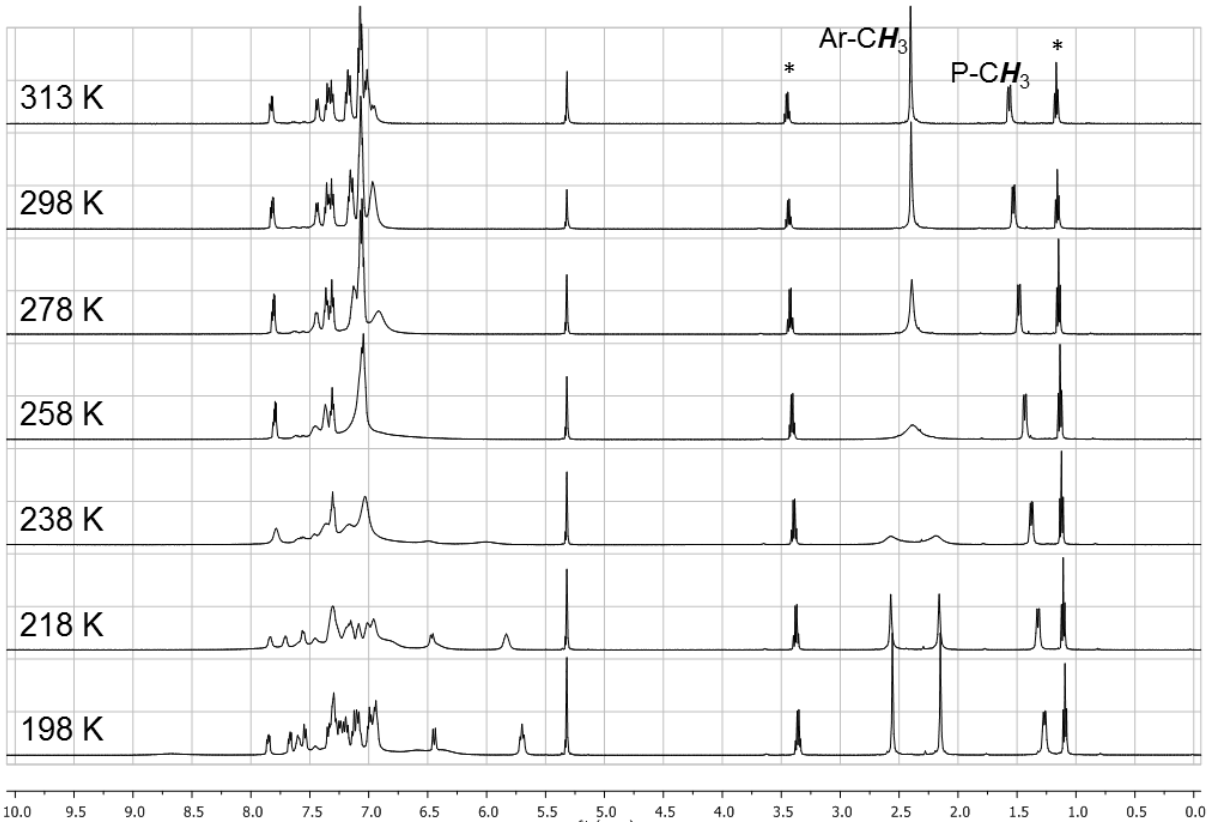

Figure 4.2 ^{1}H NMR of complex **4.2** in CD_2Cl_2 at 198, 258, and 298 K. Residual diethyl ether peaks: *.

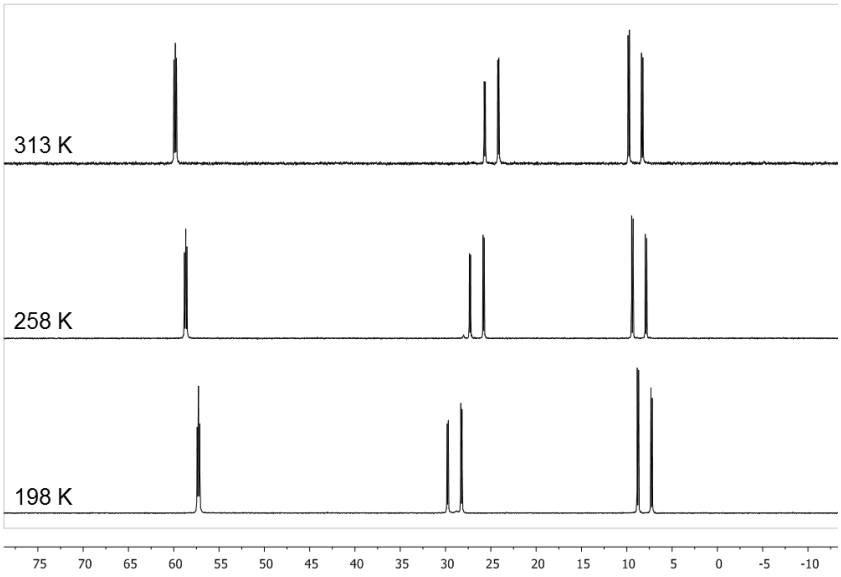

Figure 4.3 ^{31}P NMR of complex **4.2** in CD_2Cl_2 at 198, 258, and 298 K.

The facile κ^2- κ^1 sulfonate isomerization in complexes **4.1** and **4.2** gave rise to the question of ligand association and substitution reactions. Favorable ethylene coordination is essential for polymer formation. Treatment of complex **4.1** with excess acetonitrile (MeCN) in chloroform-*d* (Scheme 4.2) lead to the immediate appearance of a singlet phosphorus signal at -5.45 ppm, corresponding to uncoordinated PPh_3, and the appearance of two sets of two doublets with *cis* coupling constants at 59.63 and 50.95, and 44.25 and 39.27 ppm, indicating the formation of two species. The starting complex was consumed completely over the course of 2 days at room temperature, and yellow crystals of X-ray quality formed. The crystals corresponded to the more downfield shifted set of ^{31}P resonances, and the structure of the resulting MeCN coordinated complex **4.3** is depicted in Figure 4.4. The complex is a true 5-coordinate compound with square pyramidal geometry, in which one MeCN has formally substituted the *trans* PPh_3. The [OPO]-ligand underwent structural rearrangement, and is coordinated in a facial geometry in **4.3**, with the phosphorus occupying the apical position of the pyramid. The *trans* position is vacant, and no κ^2-coordination of a sulfonate group or CH agostic bonds from the PPh_3 is observed.

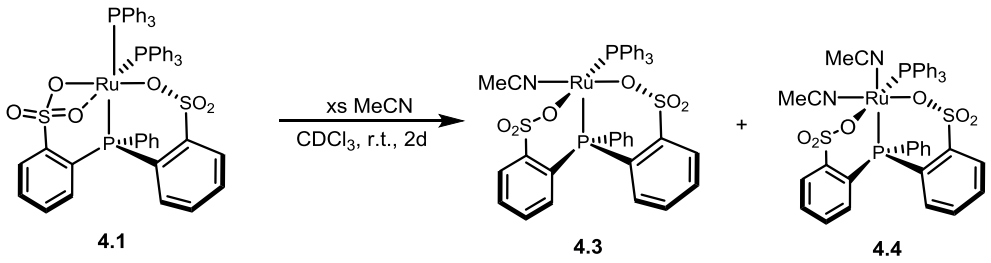

4.1 **4.3** **4.4**

Scheme 4.2 Room temperature synthesis of complexes **4.3** and **4.4**.

Layering of the remaining reaction solution with diethyl ether resulted in the formation of pale yellow single crystals of **4.4** at room temperature. This species, which corresponds to the more upfield set of ^{31}P doublets, turned out to be the 6-coordinated complex **4.4**, in which an additional MeCN binds to the vacant coordination site *trans* to the [OPO] phosphorus. The structure (Figure

4.4) is otherwise similar to **4.3**. The poor quality of the X-ray diffraction data of both complexes **4.3** and **4.4** does not allow for a detailed comparison. When a suspension of **4.1** in toluene with a large excess of MeCN was heated for three hours, a mixture was obtained (**4.3** : **4.4** = 1 : 1.6), but if heating is prolonged (1-2 days), **4.3** disappears completely in favor for **4.4** and another unidentified minor species with one *trans* coupling in the ^{31}P NMR.

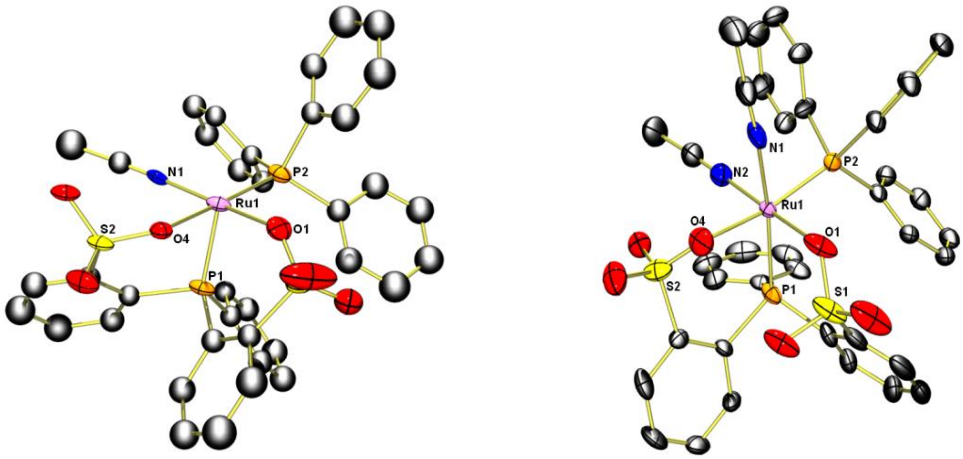

Figure 4.4: Solid state structure of **4.3** (left) and **4.4** (right). Hydrogen atoms and solvent molecules omitted for clarity.

The coordination behavior of dimethyl sulfoxide (dmso) to **4.1** was observed in a similar way. However, only 30 % conversion of **4.1** was observed via ^{31}P NMR with excess dmso, and no products were isolated. In the presence of ethylene at room temperature, **4.1** was stable towards ligand displacement.

The coordination of ethylene to 5-coordinate **4.3** was investigated briefly. In an NMR tube, **4.3** was suspended in CD_2Cl_2 and 22 equivalents of C_2H_4 were introduced. No changes were observed after 1 hour at room temperature. Heating the sealed tube for 17 h resulted in color change to an orange suspension. The starting complex was completely converted, and several new ^{31}P resonances appeared between 14 – 30 ppm. The resonances of bound ethylene could not be definitively assigned. After removal of the solvent, pure complex **4.3** was recovered, as evidenced

by ^{1}H and ^{31}P NMR. This indicates that ethylene coordination is possible, although weak and fully reversible.

Heating a suspension of **4.1** in toluene without additional ligands resulted in the formation of yellow material, which was insoluble in common organic solvents (Scheme 4.3). Analysis of the reaction solution after separation of the solid precipitate showed only presence of PPh_3. Elemental analysis of the dried yellow solid agrees with the composition "$Ru^{Ph}(OPO)(PPh_3)$", in which each metal center has lost one PPh_3 molecule. Consequent inter- and possibly intramolecular coordination of sulfonate moieties to the vacant site(s) results in oligomeric material **4.5** that is insoluble in the reaction solvent. Such bridging behavior of the sulfonate groups has already been reported with other phosphine sulfonato complexes.[2a,5]

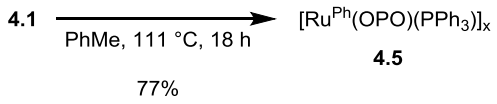

Scheme 4.3 Formation of oligomeric **4.5** from **4.1**.

When the other ^{R}[OPO] ligand variants **3.4** – **3.7**, and **3.9** were subjected to complexation conditions that were successful in synthesis of **4.1** and **4.2**, the reaction with $RuCl_2(PPh_3)_3$ in methanol at room temperature, the desired complexes were not obtained. The presumed driving force of this reaction, product precipitation, did not occur with these ligand variants, and the insoluble ruthenium starting material stayed undissolved. Raising the reaction temperature had no effect on the outcome of the reaction. A solvent screen using polar aprotic (dmf, thf, acetonitrile, acetone), polar protic (H_2O, ethanol, butanol), nonpolar solvents (dichloromethane, toluene, diethylether), or mixed systems, did not lead to formation of product complexes, determined by ^{1}H, ^{31}P NMR and ESI-MS of reaction aliquots and crude reaction mixtures. Complexation of **3.3**

to different ruthenium precursors (i.e. $[Ru(cod)Cl_2]_x$, $RuCl_2(PhCN)_4$, $RuH_2(CO)(PPh_3)_3$, $RuBr_2(PPh_3)_4$) was attempted, but the desired coordination product was never isolated.

A successful route was found in the reaction of half an equivalent $[RuCl_2(p\text{-cymene})]_2$ with $Li_2^{Ph}(OPO)^{Me}$ (**4.6**) ligand salt in the presence of 2 molecules of $AgBF_4$, which afforded $Ru^{Ph}(OPO)^{Me}(p\text{-cymene})$ (**4.7**) in excellent isolated yield (Scheme 4.4). The *p*-cymene could be replaced by two molecules of acetonitrile to afford $Ru^{Ph}(OPO)(MeCN)_2$ (**4.8**). Free residual MeCN (0.75 equivalent) was observed by ^1H NMR. At room temperature, one set of resonances was observed for the sulfonate-aryl moieties, and the magnetically equivalent bound acetonitrile molecules resonated at 2.31 ppm in the ^1H NMR spectrum. ^1H NMR spectra were not recorded at different temperatures, but it can be assumed that a dynamic behavior similar to **4.2** was present.

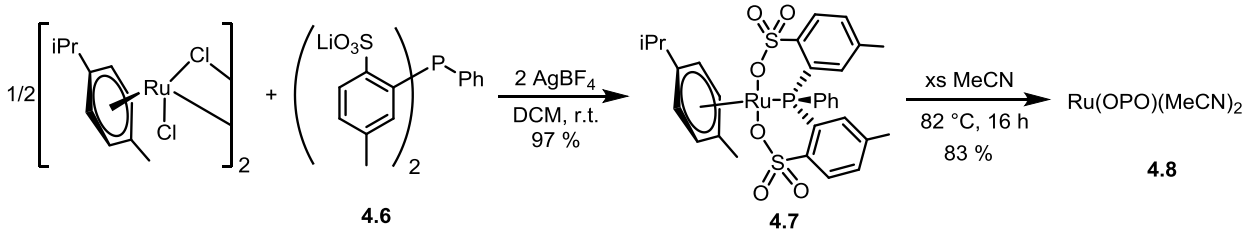

Scheme 4.4 Synthesis of Ru(II)(OPO) complexes **4.7** and **4.8** via silver salt metathesis.

The sulfonic acid variants of the [OPO] ligands were successfully prepared. Stirring an aqueous solution of the ligand salts with acidic cation exchange resin (Amberlite® IR120 H) for two hours resulted in the formation of the free acid of the ligands **4.9** – **4.11** (Scheme 4.5).

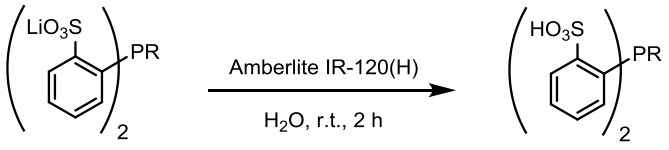

4.9: R = p-CF_3-C_6H_4, 78%
4.10: R = Ph, 72%
4.11: R = p-MeO-C_6H_4, 52%

Scheme 4.5 Protonation of [OPO] ligand salts to obtain ligand acids **4.9** – **4.11**.

A clean reaction of the acid ligand **4.10** with $Ru(cod)(\eta^3\text{-}C_4H_7)_2$ occurred in dichloromethane, as observed by the quantitative formation of isobutene in ^1H NMR spectroscopy. However, the isolated material with the tentative formula $[Ru^{Ph}(OPO)(cod)]$ precipitated from polar solvents like methanol within several minutes. Likely, the coordinative unsaturation and the lability of the cod ligand lead to cluster formation by bridging sulfonates. In order to stabilize mononuclear complexes, cod was replaced by PPh_3. The cod was replaced first with 2 PPh_3 molecules,[6] and the resulting $Ru(PPh_3)_2(\eta^3\text{-}C_4H_7)_2$ readily reacted with **4.10** (Scheme 4.6). Quantitative conversion was observed by ^1H NMR with **4.9** – **4.11**, but surprisingly, the expected complexes **4.12** – **4.14** could not be isolated. Removal of the reaction solvent at 0 ˚C, or precipitation from the reaction mixture with pentane resulted in mixtures of unidentified compounds.

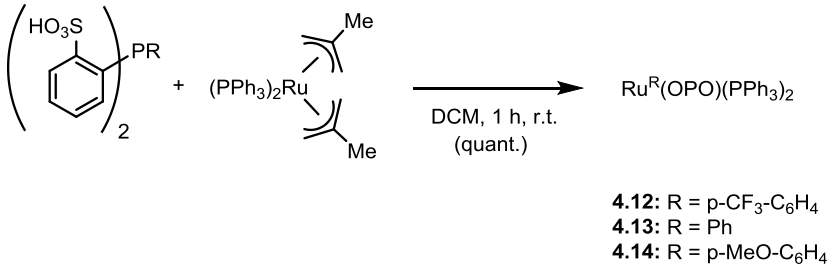

Scheme 4.6 In-situ formation of $Ru^R(OPO)(PPh_3)_2$ complexes **4.12** – **4.14**.

4.1.3 Ethylene Polymerizations And Polymer Characterization

Ethylene polymerizations were carried out in a high pressure Parr reactor and the results are summarized in Table 4.1. By comparing runs 3, 5, and 7, $AlMe_3$–depleted methylaluminoxane (dMAO) appears to be the best activator/cocatalyst for these complexes. Employing regular MAO resulted in virtually no activity (runs 1 and 2). Compared to Ru(IV)(OPO) complexes **3.10** – **3.15** (Chapter 3), the deactivating effect of $AlMe_3$ on the complexes was much more pronounced with **4.1**. It can be speculated that the Lewis acid forms adducts with the sulfonate oxygens, which could

lead to catalyst deactivation/decomposition. Coordination of Lewis acids to the sulfonate oxygen has been reported for the case of sulfonate phosphine palladium complexes.[7] Formation of heterobimetallic Ru-Al species with bridging methyl groups also seems plausible.

The maximum activity with **4.1** was achieved at polymerization temperatures of 60 °C. This activity is similar to the reported **1.13**/dMAO system. A direct comparison is not possible, as no reaction times were reported.[2a] Increase or decrease of the temperature by 20 °C resulted in a decrease of activity by more than a factor of 2. The catalyst seems to decompose thermally at temperatures above 60 °C (runs 6 – 8). In contrast, **4.5** shows higher activities at 40 °C than 60 °C (run 10 vs. 11). In order to obtain the active species, one ligand has to dissociate from the precursor. The weaker coordinating MeCN in **4.5** requires lower temperatures to dissociate than the PPh_3 in **4.1,** which results in the higher observed activities at lower temperatures. However, the highest activity of **4.3** is lower than that of **4.1**. Complex **4.5**, containing no 'additional' ligands, shows the lowest activity. This seems to contradict the behavior of **4.1** and **4.3**, but can possibly be attributed to its initial insolubility, and hence incomplete activation. Precatalyst **4.2** produced polyethylene with activities similar to **4.1** (run 7 vs. 9).

Table 4.1 Ethylene polymerizations.[a]

run	cat.	cocat.	Al/Ru	solvent	T [°C]	t [h]	yield [mg]	TOF [b]	$M_n(1)$[c] [g/mol] (PDI)	$M_n(2)$[c] [g/mol] (PDI)	T_m[d] [°C]
1	**4.1**	MAO	1600	PhMe	60	24	60	9	n.d.	n.d.	123.0
2	**4.1**	MAO	1600	PhMe	60	7	31	16	n.d.	n.d.	128.2
3	**4.1**	$AlMe_2Cl$	1000	DCM	30	6	tr	<5	-	-	-
4	**4.1**	$AlMe_2Cl$	2000	PhMe	60	6	tr	<5	-	-	-
5	**4.1**	MAO	1000	PhMe	60	6	tr	<5	-	-	-
6	**4.1**	dMAO	1000	PhMe	40	6	88	52	1,012 (1.62)	57,774 (2.00)	127.8
7	**4.1**	dMAO	1000	PhMe	60	6	178	106	996 (1.62)	54,571 (1.92)	126.5
8	**4.1**	dMAO	1000	PhMe	80	6	62	37	914 (1.76)	90,125 (2.00)	123.7
9	**4.2**	dMAO	1000	PhMe	60	6	154	92	910 (1.75)	70,640 (2.01)	125.7
10	**4.3**	dMAO	1000	PhMe	40	6	113	67	1,067 (1.83)	67,634 (2.12)	127.4
11	**4.3**	dMAO	1000	PhMe	60	6	48	29	1,066 (2.13)	265,036 (3.30)	126.7
12	**4.5**	MAO	1000	PhMe	60	6	tr	<5	-	-	-
13	**4.5**	dMAO	1000	PhMe	60	6	38	23	1,054 (1.51)	64,474 (3.96)	126.5
14[e]	-	dMAO	1000	PhMe	60	6	0	0	-	-	-

a) Reaction conditions: 100 mL solvent, 600 psi ethylene, 10 µmol [Ru]. b) Turnover frequency in mol(PE) $mol(Ru)^{-1}$ h^{-1}. c) Determined by GPC. d) Determined by DSC. e) Blank run without [Ru]. tr) Trace amounts (< 10 mg).

The polymers were obtained as white powder and characterized by high temperature gel permeation chromatography (HT-GPC), differential scanning calorimetry (DSC) and high temperature ^{1}H NMR. All analyzed samples had melting temperatures in the range of 123 – 128 °C, indicating semicrystalline, highly linear polymers. The molecular weight distribution, determined

by HT-GPC, shows bimodal behavior for all analyzed polymers, hinting at the presence of two different active species. The low molecular weight fraction has a constant number-averaged molecular weight ($M_n(1)$) around 1 kg mol^{-1} for all samples. The high molecular weight fractions have $M_n(2)$ = 50 – 70 kg mol^{-1}, except for runs 8 and 11, where higher M_ns of 90 and 265 kg mol^{-1} were obtained during the high temperature runs with **4.3** and **4.5** respectively. The average M_n of the entire bimodal distribution is 2 - 3 kg mol^{-1} for all samples. This value is in good agreement with the molecular weight determined by ^{1}H NMR (e.g. 2.7 kg mol^{-1} for run 7).[8] End group analysis by ^{1}H NMR shows mainly terminal olefins as the unsaturated chain end, indicating β-H elimination as a main chain-termination reaction. Internal olefin was also observed in a small amount (< 10%), which is assumed to originate from isomerized terminal olefins. The polymer is mostly linear with a low number of methyl branches (e.g. 7 branches per 1000 C atoms for run 7 by ^{1}H NMR[8]). The similarity of the obtained polymers indicates identical active species for all catalyst precursors.

Polar additives lead to complete deactivation of the catalyst system **4.1**/MAO and **4.2**/MAO. When as low as 100 equivalents of either polymerizable (methyl acrylate or vinyl acetate) and saturated (tetrahydrofurane or acetone) additives were present under optimized reaction conditions, no polymer was obtained.

Polymerizations with in-situ formed precatalysts **4.12** – **4.14** were performed in dichloromethane with $AlMe_2Cl$ cocatalyst. Only complex **4.12**, with the least electron donating [OPO] ligand, produced significant amounts of solid polyethylene. This is in line with the ligand effects in Ru(IV)(OPO) catalysts (see Chapter 3).

Table 4.2 Ethylene Polymerization with in-situ formed $Ru(PPh_3)_2{}^R(OPO)$.[a]

Run	Cat.	T [°C]	t [h]	Yield [mg]	TOF
1	**4.12**	30	2	57	102
2	**4.13**	30	2	tr	<5
3	**4.14**	30	2	tr	<5

a) Conditions: 10 µmol $Ru(PPh_3)_2(\eta^3\text{-}C_4H_7)_2$ and 10 µmol $H_2{}^R(OPO)$ premixed in 5 mL DCM and stirred for 5 minutes before injection. Total volume: 100 mL DCM, 1000 equiv. $AlMe_2Cl$, 600 psi ethylene.

4.2 Disulfonate Thioether Ruthenium complexes

4.2.1 Introduction

The $Ru^{IV}(\eta^3{:}\eta^3\text{-}C_{10}H_{16})(OPO)$ (OPO = bis(2-sulfonato arene)phosphine) complexes **3.10 - 3.15** reported in Chapter 3 (Scheme 4.7), exhibited one of the highest activities for the insertion polymerization of ethylene amongst ruthenium catalysts.[9] The activity could be modulated by electronic perturbation of the phosphine substituents, and increased with decreasing donor strengths of the [OPO] ligand. Further reduction in electron density on the metal center is hence desirable in order to achieve increased turnover frequencies.

It has been shown that in arene-tethered Ru(II) complexes, by changing the tether heteroatom from phosphorus to sulfur, an increase in polymerization activity can be obtained. While the phosphorus tethered complex **1.9** is unable to facilitate two consecutive ethylene insertions,[10] the sulfur analogue **1.14** produces solid polyethylene once activated.[11] Sulfur, a weaker σ-donor and π-acceptor than phosphorus,[12] renders the metal center more electrophilic, facilitating olefin binding and lowering the insertion barrier.

Applying this strategy to the Ru(IV)(OPO) catalysts, bis(2-sulfonato arene)sulfides **[OSO]$^{2-}$** and their corresponding ruthenium complexes were prepared and will be described in this part of the chapter.

To date, there are no reports on bis(2-sulfonate arene)sulfides or metal complexes thereof, or on the analogous bidentate 2-sulfonato arene sulfides. The coordination of structurally similar 2-mercaptoethanesulfonate, coenzyme M, to transition metals has been studied.[13] The only structurally characterized complex, Ni(cyclam)(*S*$CH_2CH_2SO_2$*O*) **4.15**, contains a thiolate, in contrast to the desired neutral arylthioether functionality.[13b]

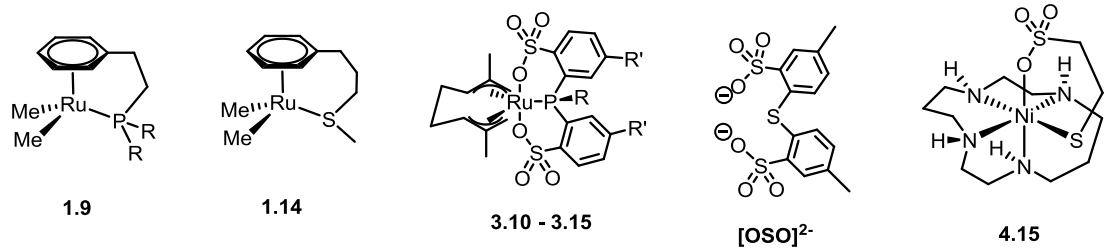

Scheme 4.7 Selected Ru complexes investigated in the context of olefin polymerization and the target ligand structure **[OSO]$^{2-}$**.

4.2.2 Disulfonate Thioether Ligand And Ruthenium Complex Synthesis

The synthesis of **4.16** was achieved by double sulfonation of di(*p*-tolyl)sulfide with 2.5 equivalents chlorosulfuric acid. Deprotonation of the sulfonic acid groups with potassium tert-butoxide resulted in **4.17** which was used for subsequent complexation reactions to Ru(II) and Ru(IV) precursors (Scheme 4.8).

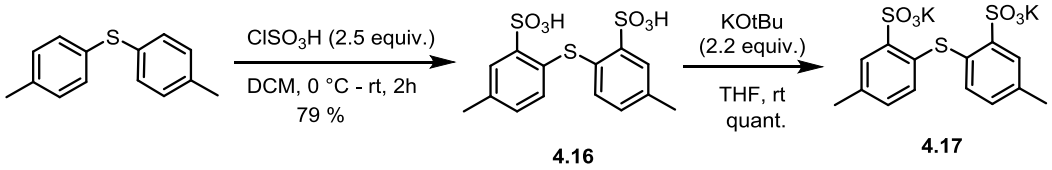

Scheme 4.8 Synthesis of bis(2-sulfonato arene)sulfide ligands **4.16** and **4.17**.

The reaction of 0.5 equivalents of dimeric $[Ru(\eta^3:\eta^3\text{-}C_{10}H_{16})Cl_2]_2$ with **4.17** in the presence of $AgBF_4$ gave $Ru(\eta^3:\eta^3\text{-}C_{10}H_{16})(OSO)$ (OSO = κ^3-*O*,*S*,*O*-(2-*O*SO_2-(4-CH_3)-C_6H_3)$_2$*S*) (**4.18**), which was isolated in 68 % yield (Scheme 4.9, top). Employing a similar silver salt metathesis approach, Ru(*p*-cymene)(OSO) (**4.19**) was obtained from $[Ru(p\text{-cymene})Cl_2]_2$, **4.17**, and $AgBF_4$ in 75 % yield after purification.

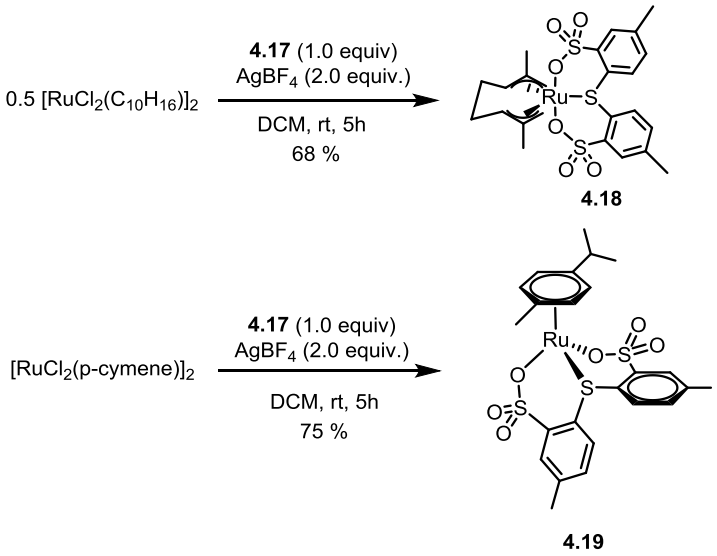

Scheme 4.9 Synthesis of bis(2-sulfonato arene)sulfide ruthenium complexes **4.18** and **4.19**.

The structure of complex **4.18** closely resembled complex **3.10**, as was revealed by X-Ray diffraction analysis (Figure 4.5). The complex geometry was distorted trigonal pyramid (τ parameter for five-coordinated complexes[14]: 0.78), with the sulfonate groups occupying both axial sites. The [OSO] ligand binds meridionally to the ruthenium forming two 6-membered chelates that both adopt boat conformations. The *anti*-configuration of the allyl-methyl groups with respect to the equatorial coordination plane of the complex in the starting material is maintained in **4.18**. The Ru(1)-S(1) distance in **4.18** is 2.455 Å, which is 0.043 Å longer than the respective Ru-P bond in **3.10**. A similar trend, denoting a weaker donation, was observed between **1.14** (Ru-S = 2.319

Å) and **1.9** (Ru-P = 2.307 (R = Cy) or 2.263 (R = Ph). The other metric parameters of **4.18** compare closely with **3.10**.

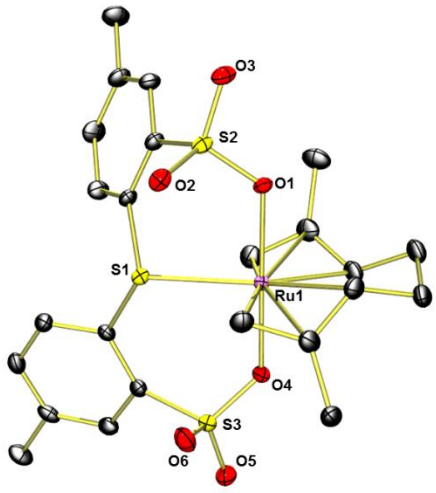

Figure 4.5. Ortep plot of **4.18** drawn at 50% probability. Hydrogen atoms omitted for clarity. Selected bond distances (Å) and angles (˚): Ru1-O4 2.0924(24), Ru1-O1 2.1088(14), Ru1-S1 2.4545(6), Ru1-C8 2.241(2), Ru1-C3 2.246(2), Ru1-C1 2.276(2), Ru1-C6 2.283(2), Ru1-C7 2.285(2), Ru1-C2 2.297(2), C2-Ru1-S1 113.47(6), C7-Ru1-S1 115.36(6), C7-Ru1-C2 131.14(8), O1-Ru1-S1 88.03(4), O4-Ru1-S1 92.42(4), O4-Ru1-O1 178.06(9), C11-S1-C18 104.43(10).

Complex **4.18** showed dynamic behavior in solution. Due to the second lone pair on the thioether sulfur, the two possible coordination modes lead to two enantiomers. At room temperature, the ^{1}H NMR features broad, unresolved signals for the bis(π-allyl) fragments. The inversion around the sulfur atom exchanges the environment of the [OSO] aryl rings with respect to the allyl-methyl groups. Increasing the temperature of a solution of **4.18** in $C_2D_2Cl_4$ to 358 K results in an exchange rate faster than the "NMR timescale" and a total of ten ^{1}H NMR resonances are observed (Scheme 4.10). At the low temperature limit (173 K, in CD_2Cl_2), each group of protons gives rise to an individual resonance, resembling the solid-state structure. For example, the allyl-C*H*$_3$ groups give rise to two singlets at 2.12 and 1.40 ppm (2.15 ppm at 385K), with the signal at 1.40 ppm corresponding to the methyl group *syn* to the [OSO] aryl groups, and the tolyl-

C*H₃* groups to two singlets at 2.34 and 2.38 ppm (2.48 ppm at 385 K). Note that different solvents were used for the low- and high-temperature limit spectra. An activation energy barrier $\Delta G^{\ddagger}$ = 10.0 kcal mol^{-1} for the inversion was estimated for a coalescence temperature T_c = 228 K. Unlike configurationally stable sulfoxides, typical metal-thioether inversion barriers are in the range of 10 – 15 kcal/mol[15], and for **1.14** it was 14.4 kcal mol^{-1}.[11]

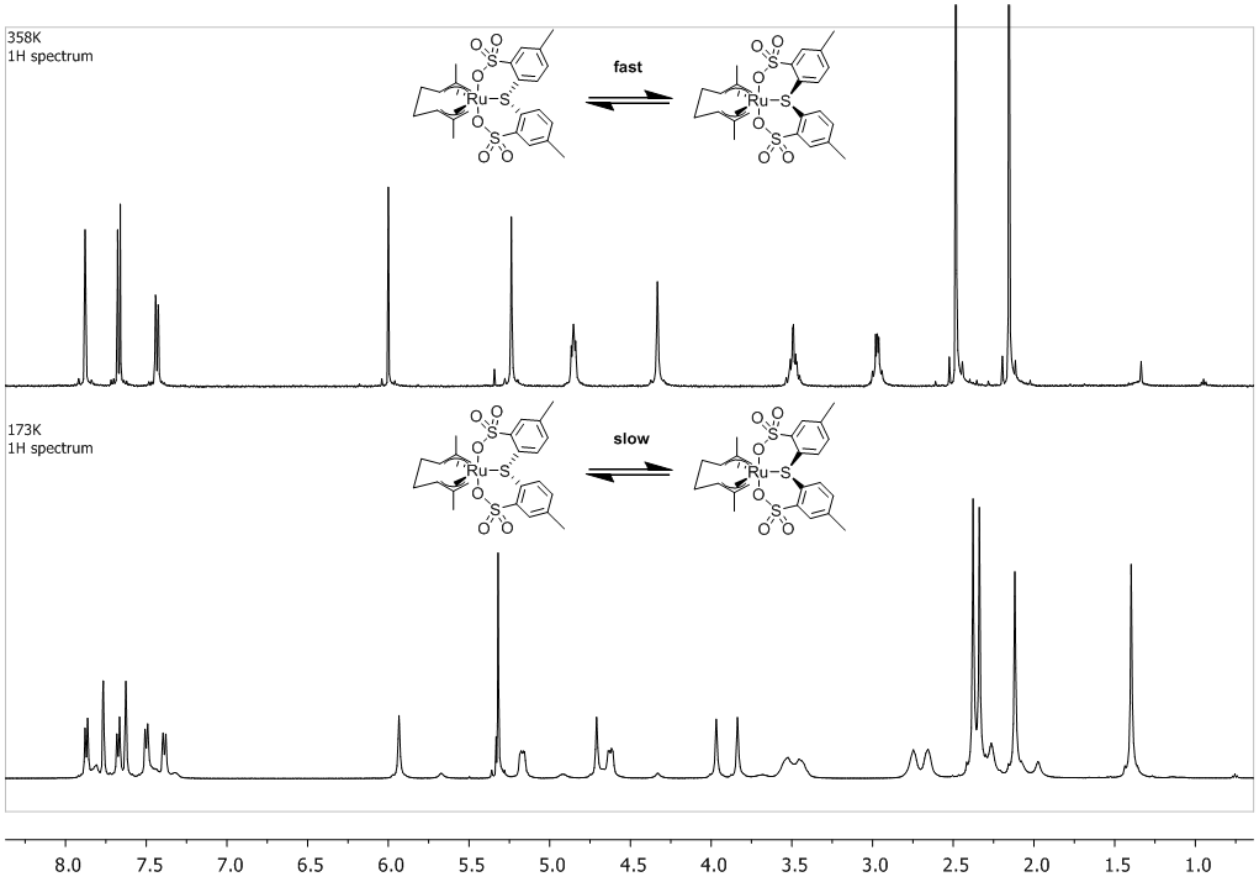

Scheme 4.10. ^{1}H NMR of **4.18**: in $C_2D_2Cl_4$ at 385 K (top), and in CD_2Cl_2 at 173 K (bottom).

For complex **4.19**, an X-ray diffraction dataset of sufficient quality could not be obtained, prohibiting the discussion of metric parameters of the solid state structure. A low quality solution of the structure is given in Figure 4.6 as a guide to the eye. In the octahedral complex, the [OSO] fragment was bound in a facial fashion, in contrast to **4.18**. One [OSO] aryl moiety was oriented

parallel to the *p*-cymene and created a 6-membered chelate with a half-chair conformation, while the second one was positioned almost perpendicular to the *p*-cymene plane with a boat conformation of the 6-membered chelate. Similar to **4.17**, inversion around the thioether sulfur results in two enantiomers, and raising the temperature leads to equivalent arenesulfonate resonances in the ^{1}H NMR. At low temperatures of 193 K, the frozen dynamics gives rise to single resonances, and e.g. H-23 showed an upfield shift to 6.42 ppm due to ringcurrent of the other arenesulfonate moiety in the ^{1}H NMR spectrum (vs. 7.84 ppm for H-16). The inversion activation energy barrier was estimated to 11.6 kcal mol^{-1} via coalescence in CD_2Cl_2.

Attempts to replace the *p*-cymene group with monodentate ligands (e.g. acetonitrile) as demonstrated by Jiang et al. with Ru(*p*-cymene)Cl(PO) (PO = κ^2-*P*,*O*-(2-*O*-SO_2-C_6H_4-*P*Ph_2)) were unsuccessful.[3c]

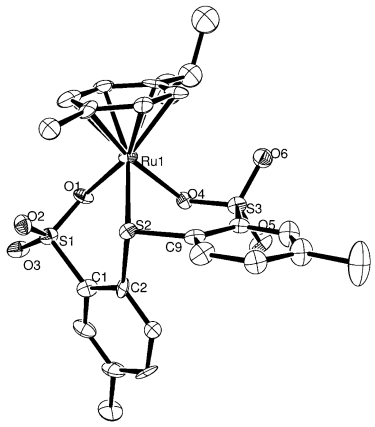

Figure 4.6. Ortep plot of **4.19**. Hydrogen atoms and one cocrystallized chloroform molecule are omitted for clarity. Bond distances and lengths are not given due to the low quality of the dataset.

Surprisingly, complexes **4.18** and **4.19** were completely inactive for ethylene polymerization under the optimized conditions for their [OPO] counterparts, and under a variety of different conditions of varying cocatalyst, solvent, and temperature. No solid polymer, nor low

molecular weight oligomer oils or waxes were obtained in either case. The reasons for the Ru(OSO) complexes' inability to polymerize ethylene can only be speculated, and no further mechanistic studies were conducted.

4.3 Conclusive Summary

Ruthenium(II) complexes $Ru^{R}(OPO)(PPh_3)_2$ (R = Ph (**4.1**), Me (**4.2**)) were synthesized and characterized by spectroscopic and X-ray diffraction methods. They are octahedral complexes with one κ^2-, and one κ^1-coordinated sulfonate group, which isomerize at room temperature. Small molecules such as dmso and ethylene coordinate weakly to the complexes. One bound PPh_3 ligand is displaced in the presence of acetonitrile to form square-pyramidal $Ru^{Ph}(OPO)(PPh_3)(MeCN)$ (**4.3**) and octahedral $Ru^{Ph}(OPO)(PPh_3)(MeCN)_2$ (**4.3**), which can be separated by recrystallization. This displacement is accompanied by a rearrangement of the [OPO]-ligand from a *fac*- to a *mer*-coordination mode with two κ^1-coordinated sulfonates. For [OPO]-ligands with other phosphine substituents R, defined Ru(II) complexes could not be isolated. However, reaction of sulfonic acid ligands $H_2{}^{R}(OPO)$ with $Ru(\eta^3\text{-}C_4H_7)_2(PPh_3)_2$ gave in-situ $Ru^{R}(OPO)(PPh_3)_2$ complexes, which were used for ethylene polymerization. $Ru^{R}(OPO)(PPh_3)_2$ (R = Ph, Me) are active ethylene polymerization catalysts, and produce highly linear, bimodal polymer when activated with 1000 equivalents dMAO. The activities are on the same order of magnitude to the Ru(IV)(OPO) system with the same substitution patterns. The reduction in electrophilicity by the lower oxidation state in Ru(II) complexes had no effect on the functional group tolerance in comparison with the analogous Ru(IV). The polymerization is inhibited completely by 100 equivalents polar additives.

Formally replacing the phosphine in the [OPO]-ligands with sulfur lead to the disulfonato thioether ligand (**4.16** and **4.17**). A Ru(IV) complex, $Ru(\eta^3\text{:}\eta^3\text{-}C_{10}H_{16})(OSO)$ (**4.18**) and a Ru(II) complex, Ru(*p*-cymene)(OSO) (**4.19**), were synthesized. The geometric parameters of these

complexes were similar to their [OPO] analogues, where the [OSO]-ligand coordinates facially in **4.18**, and meridionally in **4.19**. Energy barriers for inversion around the coordinated thioether sulfur were estimated to 10.0 (**4.18**) and 11.6 kcal mol^{-1} (**4.19**) by VT-^{1}H NMR. Surprisingly, these complexes were not active as ethylene polymerization catalysts. The reasons therefore are likely related to the activation step. The [OSO]-ligand is sterically less strained than the [OPO] analogue, and the formation of stable complexes through κ^2-chelation of both sulfonate groups after activation are also possible.

4.4 Experimental Section

The following compounds were purchased and used without further purification: $RuCl_2(PPh_3)_3$, Ru(cod)(η^3-$C_4H_7)_2$, [Ru(*p*-cymene)$Cl_2]_2$, [Ru(η^3:η^3-$C_{10}H_{16}$)$Cl_2]_2$, and $RuH_2(CO)(PPh_3)_3$ (Strem), $PhPCl_2$, $MePCl_2$, and $PhSO_3H$ (TCI America). $RuCl_2(PhCN)_4$,[16] Ru(η^3-$C_4H_7)_2(PPh_3)_2$,[6] $RuBr_2(PPh_3)_4$,[17] and di(*p*-tolyl)sulfide[18] were synthesized according to literature procedures.

Ethylene polymerization

Ethylene polymerizations were carried out in a stainless steel high pressure reactor with glass liner (600mL, Parr). The reactor was heated to 100 °C *in vacuo* overnight, backfilled with argon and cooled to the reaction temperature. After release of the pressure, a solution of the cocatalyst in the respective solvent (100 mL) was cannula transferred into the reactor and stirred under 100 psi of ethylene until it reached the desired reaction temperature. The pressure was slowly vented and the catalyst was introduced as a solution or suspension in 5 mL of the same solvent, and the vessel pressurized with 600 psi ethylene. Prior to quenching the reaction with 100 mL methanolic HCl, the reactor was vented after the allotted reaction time, and the quenched mixture

was poured into 250 mL methanol to precipitate the polymer. The polymer was collected by filtration, washed with methanol and acetone, and dried under reduced pressure over night.

Syntheses

$Ru^{Ph}(OPO)(PPh_3)_2$ (**4.1**)

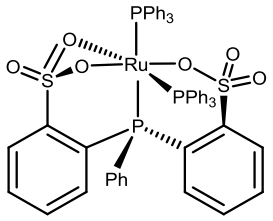

A suspension of $RuCl_2(PPh_3)_3$ (0.50 g, 0.52 mmol) and **3.3**·1.8THF (0.30 g, 0.54 mmol, 1.05 equiv.) in 20 mL dry methanol was stirred at room temperature in a nitrogen atmosphere for 2 days. The resulting light brown precipitate was filtered off, washed with 2 x 5 mL dry methanol and 5 mL diethyl ether, and dried *in vacuo* overnight. 0.51 g (0.49 mmol) of the title compound were obtained in 93% yield. ^{1}H NMR (500 MHz, CD_2Cl_2) δ 7.99 (dd, J = 6.8, 4.2 Hz, 2H), 7.65 (t, J = 7.6 Hz, 2H), 7.52 (t, J = 7.6 Hz, 2H), 7.40 – 7.28 (m, 4H), 7.24 (t, J = 6.9 Hz, 4H), 7.15 – 7.04 (m, 17H), 7.04 – 6.88 (m, 10H), 6.63 (dd, J = 10.5, 8.3 Hz, 2H). ^{31}P{^{1}H} NMR (162 MHz, $CDCl_3$) δ 59.78 (dd, $^2J_{PP,cis}$ = 30.4, $^2J_{PP,cis}$ = 28.0 Hz), 24.46 (dd, $^2J_{PP,trans}$ = 297.4, $^2J_{PP,cis}$ = 28.0 Hz), 12.96 (dd, $^2J_{PP,trans}$ = 297.4, $^2J_{PP,cis}$ = 30.4 Hz). ^{13}C NMR (126 MHz, $CDCl_3$) δ 144.52 (d, J = 13.1 Hz), 136.04 (s), 135.79 (s), 135.70 (s), 135.66 (s), 135.54 (d, J = 9.7 Hz), 134.59 (s), 134.42 (d, J = 9.7 Hz), 132.32 (d, J = 5.5 Hz), 132.18 (s), 131.87 (s), 131.55 (br s), 131.48 (s), 131.19 (s), 130.64 (d, J = 2.1 Hz), 130.42 (d, J = 2.2 Hz), 130.25 (s), 129.95 (s), 128.87 (d, J = 6.7 Hz), 128.44 (d, J = 10.2 Hz), 128.21 (d, J = 9.2 Hz), 128.04 (d, J = 10.2 Hz), 127.92 (s). Calc. for $C_{54}H_{43}O_6P_3RuS_2$: C 62.00, H 4.14, S 6.13; Found C 61.76, H 4.18, S 5.96.

$Ru^{Me}(OPO)^{Me}(PPh_3)_2$ (**4.2**)

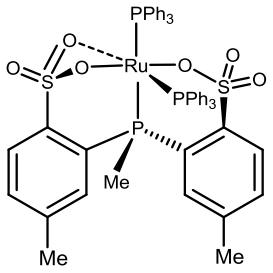

A suspension of $RuCl_2(PPh_3)_3$ (0.50 g, 0.52 mmol) and **3.8**·1.8THF (0.28 g, 0.56 mmol, 1.08 equiv.) in 20 mL dry methanol was stirred at room temperature in a nitrogen atmosphere for 2 days. The resulting light brown precipitate was filtered off, washed with 3 mL dry methanol and 10 mL ether, and dried *in vacuo* overnight. 0.45 g (0.46 mmol) of the title compound were obtained in 89% yield. ^{1}H NMR (400 MHz, $CDCl_3$) δ 7.88 (dd, J = 7.8, 4.2 Hz, 2H), 7.37 (d, J = 8.1 Hz, 2H), 7.35 – 7.28 (m, 8H), 7.21 – 7.10 (m, 6H), 7.04 (t, J = 6.5 Hz, 18H), 6.88 (d, J = 8.8 Hz, 2H), 2.38 (s, 6H), 1.57 (d, J = 9.6 Hz, 3H). ^{31}P NMR (162 MHz, $CDCl_3$) δ 60.56 (dd, J = 32.1, 25.5 Hz), 25.06 (dd, J = 300.9, 25.5 Hz), 8.99 (dd, J = 300.9, 32.2 Hz). Calc. for $C_{52}H_{48}O_6P_3RuS_2$: C 60.81, H 4.71, S 6.24; Found C 60.37, H 4.89, S 5.65.

$Ru^{Ph}(OPO)(PPh_3)(MeCN)$ (**4.3**) and $Ru^{Ph}(OPO)(PPh_3)(MeCN)_2$ (**4.4**)

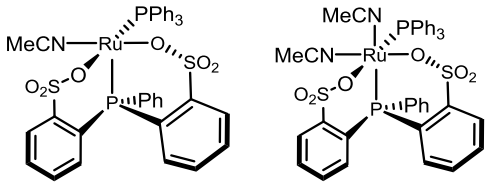

A toluene suspension (15 mL) of **4.1** (85 mg, 81 μmol) and 0.3 mL MeCN was stirred at 110 °C for 4h. After cooling, the yellow solid was filtered, and washed with 10 mL toluene and 10 mL pentane. It was then dissolved in 4 mL DCM and yellow crystals of **4.3** formed overnight upon standing. The solution was filtered, washed with 5 mL diethyl ether and dried *in vacuo* to yield 35 mg (42 μmol, 52%) of **4.3**. Diethyl ether was slowly diffused into the remaining DCM solution

and yellow single crystals of **4.4** formed upon standing overnight at room temperature. After washing with 5 mL pentane and drying *in vacuo*, 28 mg (32 μmol, 40%) of **4.4** was obtained. **4.3**: ^{1}H NMR (400 MHz, $CDCl_3$) δ 8.26 (dd, J = 7.5, 4.6 Hz, 1H), 7.65 (t, J = 9.2 Hz, 6H), 7.58 (t, J = 7.4 Hz, 1H), 7.47 (dd, J = 7.5, 3.2 Hz, 1H), 7.38 (t, J = 7.5 Hz, 1H), 7.30 (t, J = 7.5 Hz, 1H), 7.24 – 6.93 (m, 16H), 6.93 – 6.84 (m, 1H), 1.72 (s, 3H). ^{31}P{^{1}H} NMR (162 MHz, $CDCl_3$) δ 59.63 (d, $^{2}J_{PP,cis}$ = 36.0 Hz), 50.89 (d, $^{2}J_{PP,cis}$ = 36.0 Hz). Calc. for $C_{38}H_{31}NO_6P_2RuS_2$: C 55.34, H 3.79, N 1.70, S 7.78; Found C 55.27, H 3.77, N 1.60, S 7.86. **4.4**: ^{1}H NMR (500 MHz, CD_2Cl_2) δ 8.15 (dd, J = 7.6, 4.4 Hz, 1H), 8.06 (dd, J = 7.4, 4.3 Hz, 1H), 7.82 – 7.71 (m, 1H), 7.68 – 7.52 (m, 3H), 7.49 – 7.08 (m, 18H), 7.09 – 7.02 (m, 2H), 6.82 (vt, J = 10.3 Hz, 2H), 2.20 (s, 3H), 1.55 (s, 3H). ^{31}P{^{1}H} NMR (162 MHz, CD_2Cl_2) δ 43.91 (d, $^{2}J_{PP,cis}$ = 31.1 Hz), 38.60 (d, $^{2}J_{PP,cis}$ = 31.1 Hz).

$Ru^{Ph}(OPO)(PPh_3)$ (**4.5**)

A suspension of **4.1** (50 mg, 50 μmol) in 5 mL toluene was stirred at 110°C for 24 hours. The yellow-orange precipitate was filtered and washed twice with 5 mL diethyl ether and dried *in vacuo* to yield 29 mg (0.037 mmol, 77%) of the title compound. Calc. for $C_{36}H_{28}O_6P_2RuS_2$: C 55.17, H 3.60, S 8.18; Found C 55.49, H 3.52, S 8.09.

$Ru(\eta^6$-p-cymene$)^{Ph}(OPO)^{Me}$ (**4.7**)

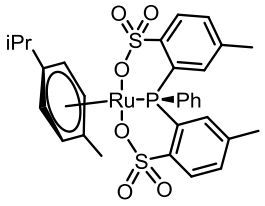

A suspension of $[Ru(\eta^6$-*p-cymene*$)Cl_2]_2$ (24 mg, 0.78 mmol [Ru]) and **4.6** (45 mg, 1.0 equiv.) in 10 mL dry dichloromethane was stirred at room temperature and $AgBF_4$ (29 mg, 2.0 equiv.) added under exclusion of light. The resulting mixture was stirred for 28 h and the off white precipitate was removed by centrifugation and washed with 5 mL dichloromethane. The orange

organic phases were evaporated in vacuo and the product was precipitated with 20 mL pentane from a 2 mL dichloromethane solution as a yellow-orange powder (52 mg, 97%). ^{1}H NMR (400 MHz, $CDCl_3$) δ 8.13 – 7.95 (m, 1H), 7.66 – 7.49 (m, 3H), 7.42 (d, *J* = 8.4 Hz, 1H), 6.96 (d, *J* = 11.0 Hz, 1H), 5.71 (d, *J* = 5.5 Hz, 1H), 5.65 (d, *J* = 5.0 Hz, 1H), 3.21 – 3.06 (m, 1H), 2.26 (s, 6H), 1.51 (s, 3H), 1.30 (d, *J* = 6.7 Hz, 6H). ^{31}P NMR (162 MHz, $CDCl_3$) δ 12.15 (s). Calc. for $C_{30}H_{31}O_6PRuS_2$: C 52.70, H 4.57, S 9.38; Found C 53.19, H 4.47, S 9.09.

$Ru(MeCN)_2^{Ph}(OPO)^{Me}$ (**4.8**)

A bright orange solution of **4.7** (50 mg, 0.073 mmol) was dissolved in 5 mL dry acetonitrile and heated to 80 °C for 24 h. The yellow solution was filtered through a plug of Celite to remove some off-white solids and concentrated *in vacuo*. Addition of dry ether afforded the title compound as a light yellow solid precipitate, which was washed with 5 mL ether and dried *in vacuo* (43 mg, 83%). Free residual acetonitrile (0.75 equiv.) was determined by ^{1}H NMR and elemental analysis. ^{1}H NMR (400 MHz, CD_3OD) δ 7.97 (dd, *J* = 8.0, 4.3 Hz, 2H), 7.64 – 7.43 (m, 5H), 7.33 (dd, *J* = 11.7, 7.3 Hz, 2H), 7.08 (d, *J* = 10.9 Hz, 2H), 2.31 (s, 6H), 2.09 (s, 6H). ^{31}P NMR (162 MHz, $CDCl_3$) δ 62.81 (s). Calc. for $C_{25.5}H_{25.25}N_{2.75}O_6PRuS_2$ (**4.8** + 0.75 MeCN): C 46.27, H 4.57, S 9.68, N 5.82; Found C 46.50, H 4.27, S 9.87, N 5.48.

para-Trifluoromethanephenylphosphine bis(2-benzenesulfonic acid) (**4.9**)

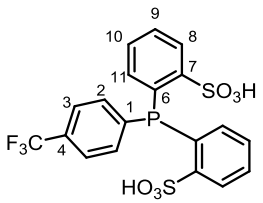

A solution of **3.6** (0.15 g, 2.9 mmol) in 20 mL H_2O was stirred for 3 hours in the presence of 300 mg ion exchange resin (Amberlite IR-120(H)). The resin was filtered off, washed with 2 x 5 ml H_2O and the solvent was removed *in vacuo* and lyophilized. The title compound was obtained

as light pink colored powder (0.11 g, 78%). ^{1}H NMR (400 MHz, DMSO) δ 7.91 (dd, *J* = 7.2, 3.6 Hz, 2H), 7.60 (d, *J* = 8.0 Hz, 2H), 7.41 (t, *J* = 7.6 Hz, 2H), 7.27 (t, *J* = 7.5 Hz, 2H), 7.20 (t, *J* = 7.2 Hz, 2H), 6.72 (dd, *J* = 7.3, 4.0 Hz, 2H), 6.50 (s, 2H). ^{19}F NMR (376 MHz, DMSO) δ -60.94 (s). ^{31}P {^{1}H} NMR (162 MHz, DMSO) δ -10.66 (s). ^{1}H NMR (400 MHz, CD_3OD) δ 8.17 (dd, *J* = 7.3, 5.3 Hz, 2H), 7.78 (dd, *J* = 12.8, 6.9 Hz, 2H), 7.64 (dd, *J* = 11.7, 8.3 Hz, 2H), 7.54 (t, *J* = 7.7 Hz, 2H), 7.12 (dd, *J* = 11.1, 7.9 Hz, 2H). ^{19}F NMR (376 MHz, CD_3OD) δ -64.75 (s). ^{31}P {^{1}H} NMR (162 MHz, CD_3OD) δ -0.30 (s).

Phenylphosphine bis(2-benzenesulfonic acid) (**4.10**)

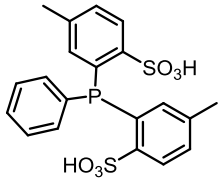

A solution of **3.3** (0.40 g, 6.9 mmol) in 20 mL H_2O was stirred for 2 hours in the presence of 1g ion exchange resin (Amberlite IR-120(H)). The resin was filtered off, washed with 2 x 10 ml H_2O and the solvent removed *in vacuo* and lyophilized. The title compound was obtained as light pink colored powder (0.295 g, 95%). ^{1}H NMR (400 MHz, DMSO) δ 7.88 (dd, *J* = 7.9, 5.0 Hz, 2H), 7.63 (t, *J* = 7.4 Hz, 1H), 7.60 – 7.49 (m, 4H), 7.35 (dd, *J* = 13.7, 7.4 Hz, 2H), 6.76 (d, *J* = 12.8 Hz, 2H), 5.51 (s, 2H), 2.21 (s, 6H, 10-H). ^{31}P {^{1}H} NMR (162 MHz, DMSO) δ 1.82 (s).

para-Methoxyphenylphosphine bis(2-benzenesulfonic acid) (**4.11**)

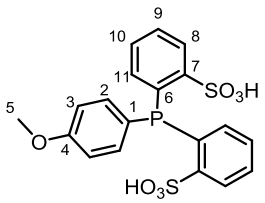

A solution of **3.4** (0.45 g, 7.7 mmol) in 20 mL H_2O was stirred for 2 hours in the presence of 1g ion exchange resin (Amberlite IR-120(H)). The resin was filtered off, washed with 2 x 10

ml H_2O and the solvent removed *in vacuo* and lyophilized. The title compound was obtained as light pink colored powder (0.18 g, 52%). ^{1}H NMR (600 MHz, DMSO) δ 8.05 – 7.93 (m, 2H, 8-H), 7.76 (t, *J* = 7.6 Hz, 2H, 9-H), 7.52 (t, *J* = 7.6 Hz, 2H, 10-H), 7.29 (dd, *J* = 13.2, 8.8 Hz, 2H, 2-H), 7.10 (dd, *J* = 8.8, 2.0 Hz, 2H, 3-H), 6.98 (dd, *J* = 13.0, 7.8 Hz, 2H, 11-H), 5.66 (s, 2H, SO_3H), 3.82 (s, 3H, 5-H). ^{13}C NMR (126 MHz, $CDCl_3$) δ 162.39 (s, C4), 151.68 (d, $J_{C,P}$ = 10.4 Hz), 134.88 (d, $J_{C,P}$ = 9.5 Hz), 134.45 (d, $J_{C,P}$ = 13.5 Hz), 133.42 (s), 129.69 (d, $J_{C,P}$ = 10.7 Hz), 128.17 (d, $J_{C,P}$ = 8.3 Hz), 127.64 (s), 125.49 (s), 114.96 (d, $J_{C,P}$ = 13.7 Hz), 55.49 (s, C5). ^{31}P {^{1}H} NMR (162 MHz, DMSO) δ 2.23 (s).

6,6'-Thiobis(3-methylbenzenesulfonic acid) (**4.16**)

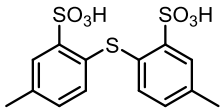

A three-neck round bottom flask with nitrogen inlet, and reflux condenser with tubing connecting to $NaOH_{(aq)}$ was charged with a solution of di-p-tolylsulfide (1.0 g, 4.7 mmol) in 40 mL dry dichloromethane. At 0 °C, 0.65 ml chlorosulfuric acid (2.1 equiv.) were added dropwise with a glass pipette, leading to an immediate change to a green color. Over the course of 10 minutes the color changed to a light blue and a white precipitate formed. The reaction was warmed to room temperature and stirred for two hours. The white precipitate was separated by centrifugation and washed with 2 x 20 mL dry dichloromethane and dried *in vacuo*. The white powder (1.38 g, 79%) titrated as 2.3 molar against NaOH. ^{1}H NMR (500 MHz, DMSO-d_6, δ) 10.46 (s, 2H), 7.64 (s, 2H), 6.97 (d, $^3J_{HH}$ = 8.0 Hz, 2H), 6.92 (d, $^3J_{HH}$ = 8.0 Hz, 2H), 2.25 (s, 6H). ^{13}C NMR (126 MHz, DMSO-d_6, δ) 146.96 (s), 134.71 (s), 133.59 (s), 133.28 (s), 129.99 (s), 127.93 (s), 20.58 (s). HRMS(ESI) m/z calcd for $C_{14}H_{12}O_6S_3Na$ $[M-2H+Na]^-$ 394.9694, found 394.9684.

Potassium 6,6'-thiobis(3-methylbenzenesulfonate) (**4.17**)

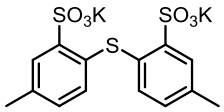

To a solution of KO*t*Bu (66 mg, 2.2 equiv) in 10 mL dry THF was slowly added a solution of **4.16** (0.10 g, 0.27 mmol) in dry THF and stirred for 18 h. The white precipitate was separated by centrifugation, washed with 2 x 5 mL THF and 5 mL Et_2O, and dried *in vacuo*. The white solid was used without further purification.

$Ru(\eta^3:\eta^3\text{-}C_{10}H_{16})(OSO)$ (**4.18**)

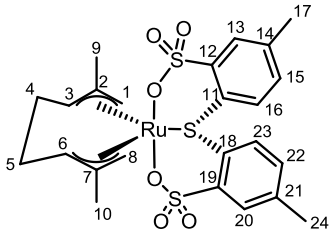

A suspension of $[Ru(\eta^3:\eta^3\text{-}C_{10}H_{16})Cl_2]_2$ (40.7 mg, 1.0 equiv.) and **4.17** (60.0 mg, 2.0 equiv.) in 20 mL dry dichloromethane was stirred at room temperature for 10 minutes and then $AgBF_4$ (51.8 mg, 4.0 equiv.) was added portion wise. The resulting mixture was stirred for 6 h in the dark, after which the off-white precipitate was removed by centrifugation and washed with 5 mL dichloromethane. The combined yellow organic phases were evaporated *in vacuo,* redissolved in a small amount of dichloromethane filtered through a short plug of Celite to remove residual inorganic salts. The product was then precipitated with pentane, collected by filtration, washed with pentane and dried *in vacuo* to yield 55 mg yellow powder (68%). ^{1}H NMR (499 MHz, CD_2Cl_2, 173 K, δ) 7.87 (d, J = 8.1 Hz, 1H, H-23 or H-16), 7.77 (s, 1H, H-20 or H-13), 7.67 (d, J = 8.3 Hz, 1H, H-16 or H-23), 7.63 (s, 1H, H-13 or H-20), 7.50 (d, J = 8.1 Hz, 1H, H-22 or H-15), 7.39 (d, J = 8.3 Hz, 1H, H-15 or H-22), 5.93 (s, 1H, H_a-8), 5.22 – 5.13 (m, 1H, H-6), 4.71 (s, 1H, H_b-8), 4.66

– 4.59 (m, 1H, H-3), 3.97 (s, 1H, H_b-1), 3.84 (s, 1H, H_a-1), 3.60 – 3.38 (m, 2H, H_b-5 and H_b-4 or H_a-5 and H_a-4), 2.75 (br s, 1H, H_a-5 or H_b-5), 2.66 (br s, 1H, H_a-4 or H_b-4), 2.38 (s, 3H, H-24 or H-17), 2.34 (s, 3H, H-17 or H-24), 2.12 (s, 3H, H-10), 1.40 (s, 3H, H-9). ^{13}C NMR (126 MHz, CD_2Cl_2, 173 K, δ) 142.0, 141.4, 139.3, 136.7, 135.6, 132.4, 132.2, 130.9, 130.8, 130.3, 129.3, 129.1, 123.3, 119.3, 109.8, 105.3, 87.4, 76.6, 36.4, 36.0, 20.9, 20.4, 19.1, 18.7. ^{1}H NMR (499 MHz, $C_2D_2Cl_4$, 358 K, δ) 7.88 (d, J = 1.1 Hz, 2H, H-13 and H-20), 7.67 (d, J = 8.1 Hz, 2H, H-16 and H-23), 7.48 – 7.34 (m, 2H, H-15 and H-22), 5.24 (s, 2H, H-1b and H-8b or H-1a and H-8a), 4.92 – 4.77 (m, 2H, H-3 and H-6), 4.33 (s, 2H, H-1a and H-8a or H-1b and H-8b), 3.63 – 3.37 (m, 2H, H_a-4 and H_a-5 or H_b-4 and H_b-5), 3.12 – 2.84 (m, 2H, H_b-4 and H_b-5 or H_a-4 and H_a-5), 2.48 (s, 6H, H-17 and H-24), 2.15 (s, 6H, H-9 and H-10). ^{13}C NMR (126 MHz, $C_2D_2Cl_4$, 358 K, δ) 141.8, 141.3, 131.8, 131.1, 130.8, 130.7, 126.0, 109.6, 82.1, 36.2, 21.2, 18.8. Anal C 47.28, H 4.63, S 15.77 for $C_{24}H_{40}O_6RuS_3$, found C 47.00, H 4.79, S 15.34.

Labeling of bis-π-allyl fragment:

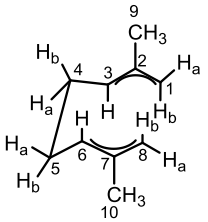

Ru(*p*-cymene)(OSO) (**4.19**)

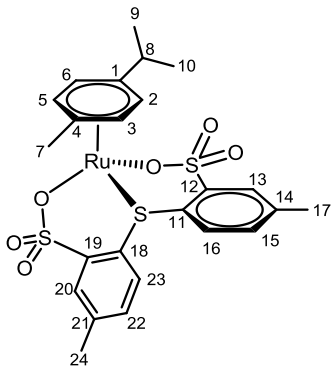

A suspension of $[RuCl_2(p\text{-cymene})]_2$ (68 mg, 0.11 mmol, 1.0 equiv.) and **4.17** (100 mg, 2.0 equiv.) in 20 mL dry dichloromethane was stirred at room temperature for 10 minutes and then $AgBF_4$ (86 mg, 4.0 equiv.) was added portion wise. The resulting mixture was stirred for 4 h in the dark, after which the off-white precipitate was removed by centrifugation and washed with 5 mL dichloromethane. The combined yellow organic phases were evaporated *in vacuo,* redissolved in a small amount of dichloromethane, and filtered through a short plug of Celite to remove residual inorganic salts. The product was then precipitated with 20 mL pentane, collected by filtration, washed with pentane (2 x 5 mL) and dried *in vacuo* to yield 51 mg yellow powder (75%). ^{1}H NMR (499 MHz, CD_2Cl_2, 193K, δ) 7.95 (s, 1H, H-13), 7.84 (d, $^3J_{HH}$ = 7.9 Hz, 1H, H-16), 7.56 (s, 1H, H-20), 7.44 (d, $^3J_{HH}$ = 7.9 Hz, 1H, H-15), 7.04 (d, $^3J_{HH}$ = 8.3 Hz, 1H, H-22), 6.42 (d, $^3J_{HH}$ = 8.3 Hz, 1H, H-23), 5.73 (vt, 2H, H-2 and H-6), 5.60 (d, $^3J_{HH}$ = 5.9 Hz, 1H, H-3 or 5), 5.03 (d, $^3J_{HH}$ = 5.9 Hz, 1H, H-5 or 3), 3.17 – 2.99 (m, 1H, H-8), 2.47 (s, 3H, H-17), 2.19 (s, 3H, H-24), 2.06 (s, 3H, H-7), 1.27 (d, $^3J_{HH}$ = 6.3 Hz, 6H, H-9 and H-10). ^{13}C NMR (126 MHz, CD_2Cl_2, 193K, δ) 146.1, 143.6, 139.9, 138.9, 135.4, 133.0, 132.4, 132.3, 129.5, 128.3, 126.5, 121.4, 109.4, 96.5, 85.0, 83.0, 80.9, 79.9, 31.0, 22.1, 21.9, 21.8, 21.1, 18.5. ^{1}H NMR (499 MHz, $C_2D_2Cl_4$, 363K, δ) 7.92 (s, 2H, H-13 and H-20), 7.27 (d, $^3J_{HH}$ = 7.0 Hz, 2H, H-15 and H-22), 7.10 (d, $^3J_{HH}$ = 7.0 Hz,

2H, H-16 and H-23), 5.84 (d, $^{3}J_{HH}$ = 5.5 Hz, 2H, H-3 and H-5), 5.45 (d, $^{3}J_{HH}$ = 5.5 Hz, 2H, H-2 and H-6), 3.29 – 3.02 (m, 1H, H-8), 2.45 (s, 6H, H-17 and H-24), 2.22 (s, 3H, H-7), 1.43 (d, $^{3}J_{HH}$ = 6.8 Hz, 6H, H-9 and H-10). ^{13}C NMR (126 MHz, $C_2D_2Cl_4$, 363K, δ) 143.0, 142.3, 131.7, 131.5, 130.9, 124.1, 108.6, 97.9, 83.6, 81.2, 30.7, 21.9, 20.9, 17.6. Anal calc C 48.22, H 4.69, S 15.44 % for $C_{25}H_{29}O_6RuS_3$, found C 46.74, H 4.61, S 15.07 %.

Determination of inversion activation energy barriers via coalescence

The activation energy barrier was calculated using the equation:

$\Delta G^{\ddagger} = \frac{4.575 \cdot 10^{-3} kcal}{mol} \left[9.972 + log\left(\frac{T_c}{\Delta\nu}\right)\right] T_c$, where T_c is the coalescence temperature in K, and Δν is the separation in Hz of the two exchanging resonances in question at non-exchanging temperature.[19] In all cases, the methyl resonances or the [OPO] or [OSO] backbone were used. **4.2**: T_c = 248 K, and Δν = 205 Hz (at 198 K): $\Delta G^{\ddagger}$ = 11.4 kcal mol^{-1}. **4.18**: T_c = 198 K, and Δν = 19.2 Hz (at 183 K): $\Delta G^{\ddagger}$ = 10.0 kcal mol^{-1}. **4.19**: T_c = 248 K, and Δν = 144.5 Hz (at 183 K): $\Delta G^{\ddagger}$ = 11.6 kcal mol^{-1}.

4.5 References

(1) Heyndrickx, W.; Occhipinti, G.; Bultinck, P.; Jensen, V. R. *Organometallics* **2012**, *31*, 6022-6031.

(2) a) Piche, L.; Daigle, J.-C.; Claverie, J. P. *Chem. Commun.* **2011**, *47*, 7836-7838. b) Bashir, O.; Piche, L.; Claverie, J. P. *Organometallics* **2014**, *33*, 3695-3701.

(3) a) Sundararaju, B.; Tang, Z.; Achard, M.; Sharma, G. V. M.; Toupet, L.; Bruneau, C. *Adv. Synth. Catal.* **2010**, *352*, 3141-3146. b) Sundararaju, B.; Achard, M.; Sharma, G. V. M.; Bruneau, C. *J. Am. Chem. Soc.* **2011**, *133*, 10340-10343. c) Jiang, F.; Yuan, K.; Achard, M.; Bruneau, C. *Chemistry* **2013**, *19*, 10343-10352. d) Sahli, Z.; Sundararaju, B.; Achard, M.; Bruneau, C. *Org. Lett.* **2011**, *13*, 3964-3967.

(4) Werner, H.; Bosch, M.; E. Schneider, M.; Hahn, C.; Kukla, F.; Manger, M.; Windmuller, B.; Weberndorfer, B.; Laubender, M. *J. Chem. Soc., Dalton Trans.* **1998**, 3549-3558.

(5) Vela, J.; Lief, G. R.; Shen, Z.; Jordan, R. F. *Organometallics* **2007**, *26*, 6624-6635.

(6) Powell, J.; Shaw, B. L. *J. Chem. Soc. A* **1968**, *0*, 159-161.

(7) Cai, Z.; Shen, Z.; Zhou, X.; Jordan, R. F. *ACS Catal.* **2012**, *2*, 1187-1195.

(8) Daugulis, O.; Brookhart, M.; White, P. S. *Organometallics* **2002**, *21*, 5935-5943.

(9) Friedberger, T.; Ziller, J. W.; Guan, Z. *Organometallics* **2014**, *33*, 1913-1916.

(10) Umezawa-Vizzini, K.; Lee, T. R. *Organometallics* **2003**, *22*, 3066-3076.

(11) Camacho-Fernandez, M. A.; Yen, M.; Ziller, J. W.; Guan, Z. *Chem. Sci.* **2013**, *4*, 2902-2906.

(12) Kraatz, H. B.; Jacobsen, H.; Ziegler, T.; Boorman, P. M. *Organometallics* **1993**, *12*, 76-80.

(13) a) Srogl, J.; Liu, W.; Marshall, D.; Liebeskind, L. S. *J. Am. Chem. Soc.* **1999**, *121*, 9449-9450. b) Nishigaki, J.-i.; Matsumoto, T.; Tatsumi, K. *Inorg. Chem.* **2012**, *51*, 3690-3697.

(14) Addison, A. W.; Rao, T. N.; Reedijk, J.; van Rijn, J.; Verschoor, G. C. *J. Chem. Soc., Dalton Trans.* **1984**, 1349-1356.

(15) Masdeu-Bultó, A. M.; Diéguez, M.; Martin, E.; Gómez, M. *Coord. Chem. Rev.* **2003**, *242*, 159-201.

(16) Duff, C. M.; Heath, G. A. *J. Chem. Soc., Dalton Trans.* **1991**, 2401-2411.

(17) Stephenson, T. A.; Wilkinson, G. *J. Inorg. Nucl. Chem.* **1966**, *28*, 945-956.

(18) Cheng, C.; Stock, L. M. *J. Org. Chem.* **1991**, *56*, 2436-2443.

(19) Sanstrom, J. *Dynamic NMR Spectroscopy*; Academic Press: London, 1982.

5 α-Diimine Palladium and Nickel Complexes with Pendant Functional Groups

5.1 Introduction

Several obstacles towards the practical insertion copolymerization of fundamental polar vinyl monomers have been identified, which mainly originate from the Lewis basic nature of the polar functional group.[1] The coordination equilibrium between heteroatom σ- and olefin π-coordination decreases catalyst productivity, with the reversibility of this deactivation depending on the strength of the σ-coordination. Similarly, chelation of inserted polar monomer leads to catalyst inhibition as well. In general, activities of insertion copolymerization reactions are orders of magnitude lower than of ethylene homopolymerization by the same catalyst system, due to σ-coordination of the comonomer. Disfavoring the metal-functional group interaction is crucial to increase copolymerization productivities. In addition, higher activities indirectly enable higher functional group incorporation ratios because higher polar monomer feed ratios are possible. One strategy is to decrease the metal electrophilicity through ligand electronic effects, which decreases the strength of the functional group coordination.

An underexplored strategy consists of employing bifunctional ligands which reversibly interact with the functional groups of the polar monomer. Jordan and coworkers recently introduced amide-functionalized α-diimine Pd complexes that exhibited H-bonding to coordinated small molecules (Scheme 5.1).[2] Both H-bond acceptors (acetate in complex **5.1**), and H-bond donors (pyrazole in complex **5.2**) can bind to the bifunctional complex. This interaction results in a circa 120 times stronger pyrazole coordination in complex **5.2** than in the non-amide-functionalized complex, as determined by ligand exchange experiments with acetonitrile. The polymerization behavior of these complexes was not reported.

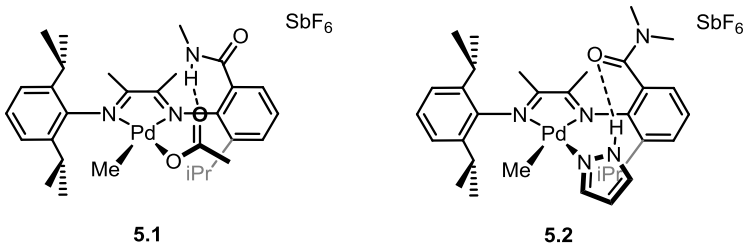

Scheme 5.1 Amide-functionalized α-diimine Pd complexes with H-bonds to metal coordinated substrates.

A different functional group capable of interacting with the Lewis basic functional groups are Lewis acids (LAs). Tethered to the ligand framework they can interact with the functional group and shift the pre-insertion equilibrium to favor π- over σ-coordination of polar monomer, as well as the chelate-opening equilibrium after polar monomer insertion (Scheme 5.2). In addition to the increase of copolymerization activity, the local concentration of polar monomer (coordinated to the tethered LA) can also increase its incorporation ratio. Depending on the nature of the Lewis acid, a wide range of acidities can be accessed, with interaction forces much greater the H-bonds being possible. Boronic esters in particular have been used widely in organic chemistry and their Lewis acidity is highly tunable through variations of the diol moiety.

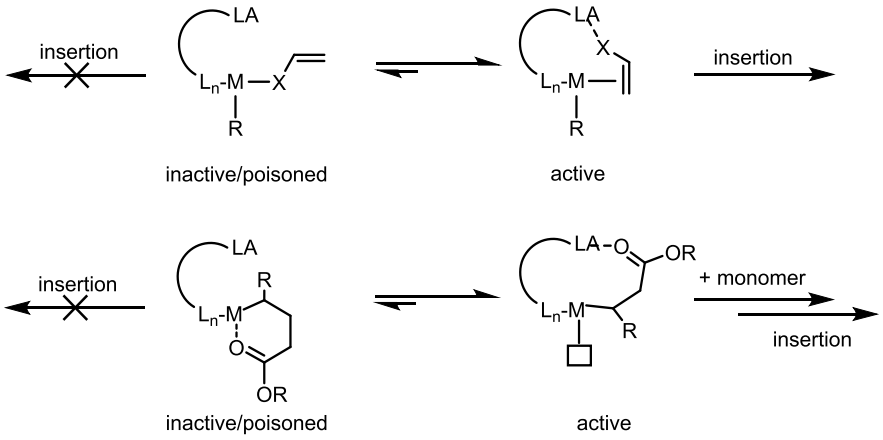

Scheme 5.2 Hypothesized beneficial interactions of pendant Lewis Acid catalysts with polar monomers. L_n = ligand framework. LA = Lewis acid. X = functional group / heteroatom. R = alkyl / polymeryl group. □ = vacant coordination site.

Several examples of pendant boron-containing metal complexes are known where the Lewis acid plays a functional role (Scheme 5.3). Pinacol boronate tethered Fe(PDI) complex **5.3**, prepared by Gilbertson and coworkers, was employed for electrochemical reduction where the Lewis acid affected the reduction potential.[3] The direct interaction of the CO ligands with the boronate secondary coordination sphere have not been studied. A V(terpyridine) complex modified with a Lewis acidic boronate and a Lewis base, activated hydrazine in an unusual way to yield η^2-coordinated substrate exhibiting a N-B interaction (complex **5.4**).[4] A η^1-coordinated hydrazine was observed with unmodified analogue. Complex **5.5**, reported by the Emslie group, shows a partially zwitterionic character, due to the enone activation of a dibenzylideneacetone by a Pd center and pendant triarylborane.[5]

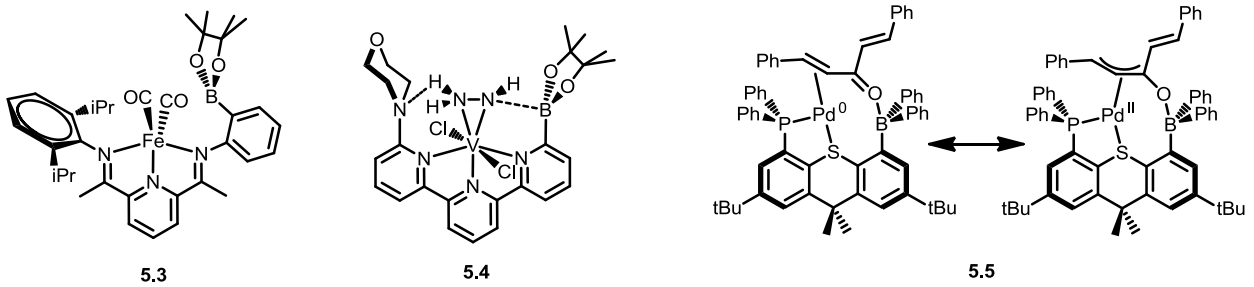

Scheme 5.3 Pendant boronic ester and borane complexes reported prior to this work.

The aim of this project was to synthesize pendant borane/boronate ligand complexes to study the effects of the pendant groups on copolymerizations with polar monomers. The focus was set on the Pd(α-diimine) complexes, as successful copolymerization had already been demonstrated, allowing for the facile establishment of pendant borane effects through comparison.

5.2 Ligand and Complex Synthesis

Different synthetic strategies to obtain the pendant boron Lewis acid ligands and complexes were explored, including condensation of ortho-boronate anilines, boronate

esterification of pendant alcohol α-diimine ligands prior and after complexation, and the reaction of pendant alkene α-diimine ligands and complexes through hydroboration and olefin metathesis.

5.2.1 Direct Condensation of Boronate Anilines

Commercially available *o*-aminophenylboronic acid pinacol ester was subjected to various condensation conditions with butadione and acenaphthoquinone to obtain the desired α-diimines. These conditions are standard protocols used by various research groups, i.e. azeotropic water removal with toluene and catalytic amounts of toluenesulfonic acid, or heating a methanol solution of butadione with formic acid catalyst (Scheme 5.4). In no case was the isolation of the desired α-diimine ligand successful. The reasons therefore were deboration in the presence of strong acids such as toluenesulfonic acid, low conversions with other methods, and decomposition on silica.

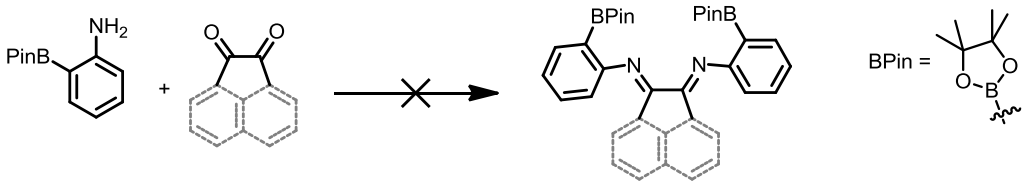

Scheme 5.4 Attempted synthesis of pendant boronate α-diimine. Conditions: 2.5 equivalents aniline per diimine A) Acenaphthoquinone, toluene (dry), molecular sieves, sealed vessel, 130 °C, 5 d. B) Butadione, benzene, cat. AcOH, Dean-Stark water removal, 80 °C, 5 d. C) Butanedione, methanol, cat. formic acid, 65 °C, 18 h. D) Acenaphthoquinone, toluene, cat. TsOH, Dean-Stark water removal, 110 °C, 3 d.

5.2.2 Esterification of Pendant Alcohol α-Diimines

Installation of the boron-based Lewis acid through reaction with alcohol groups was investigated next. Alcohols can be used to form B-O bonds through a variety of reactions including transesterification with boric esters $B(OR)_3$, or substitution of boranes with hydrogen formation.

Protection of the pendant alcohol group was necessary. Condensation reactions of butadione with 2-hydroxy aniline or 2-amino benzylalcohol resulted in the formation of heterocyclic oxazine derivatives **5.6** and **5.7** through addition of the alcohol into the imine carbon

(Scheme 5.5). In both cases, the typical C=N stretching band around 1630 cm^{-1}, and imine ^{13}C NMR resonances around 170 ppm were both absent. The previously reported oxazoline formation from 2-hydroxy aniline, instead of oxazine **5.6**, was shown to be incorrect by an X-ray diffraction analysis of 5.6 (see Figure 5.1).

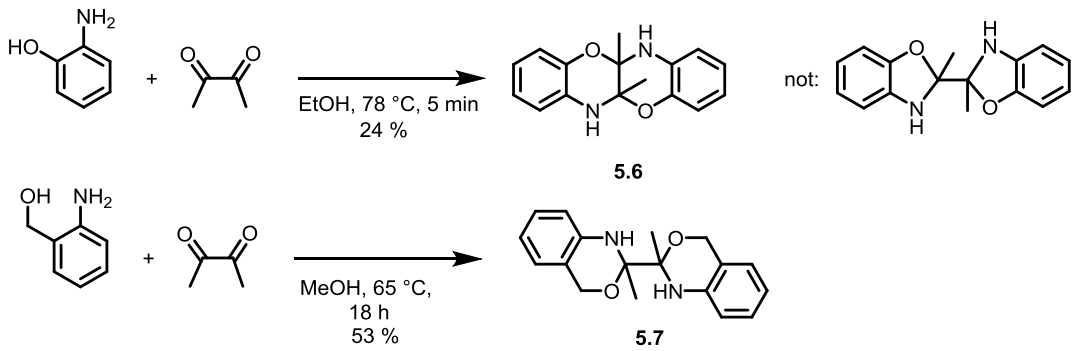

Scheme 5.5 Attempted synthesis of pendant alcohol diimine ligands with unprotected alcohols.

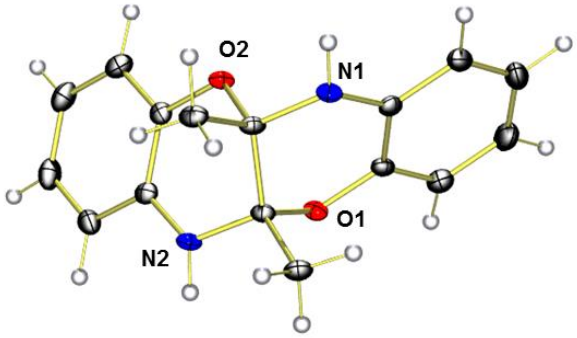

Figure 5.1 Ortep plot of fused bisoxazoline **5.6**.

Using tert-butyl diphenyl silyl (TBDPS) ether protected 2-amino benzylalcohol, α-diimines of butadione (**5.8**) and acenaphthoquinone (**5.9**) were obtained employing established condensation reactions in methanol (Scheme 5.6). The PdMeCl-complex **5.10** and the $PdCl_2$-complex **5.11** were formed by reacting **5.9** and **5.8**, respectively, with the corresponding Pd-precursors in dichloromethane at room temperature. These complexes were fully characterized by NMR spectroscopy and elemental analysis.

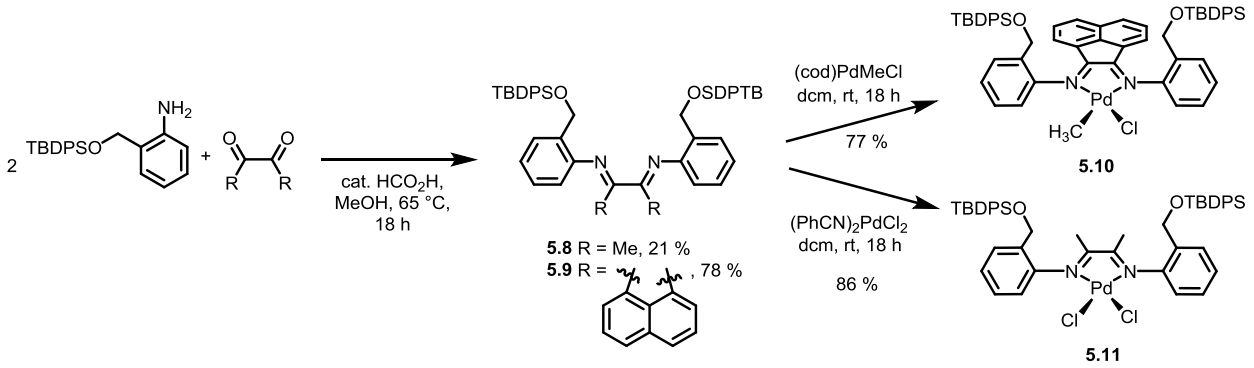

Scheme 5.6 Synthesis of pendant silylether α-diimines **5.8** and **5.9** and their Pd complexes.

Attempts to deprotect the alcohol and obtain pendant alcohol Pd-diimine complexes were unsuccessful (Scheme 5.7). Treatment of **5.8** and **5.9** with $(n\text{-Bu})_4NF$ (TBAF) resulted in the formation of complex product mixtures, which could not be separated, but did not contain the desired free alcohol product. Lowering the reaction temperature to 0 ˚C, reducing the equivalents of TBAF, or employing different TBAF grades with varying levels of water did not improve the reaction outcome. The decomposition pathway could not be established with certainty, but it was observed that treatment of TBDPS-protected ligand **5.9** under the same conditions lead to formation of the oxazine derivative **5.12** in 80% isolated yield, which requires successful silylether deprotection. However, it was also observed that unmodified complex **5.13** decomposed to a mixture of unidentified compounds under the deprotection conditions.

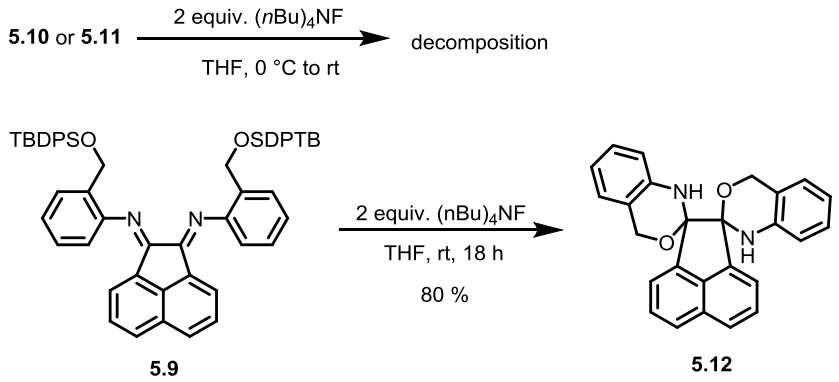

Scheme 5.7 Silylether deprotection with TBAF.

The pendant (silylether protected) alcohol strategy proved to be unsuitable for the installation of boron-based Lewis acids.

5.2.3 Pendant Alkene α-Diimines

Pendant α-alkene groups allow for the installation of boron-based Lewis acids through hydroboration with boranes such as catecholborane, pinacolborane, or 9-BBN, or cross-metathesis with vinyl boronic esters. An initial proof-of-concept experiment was conducted to assess the stability of (α-diimine)PdMeCl complexes towards borohydrides. An equimolar mixture of styrene, 9-BBN and the isopropyl substituted complex **5.13** were dissolved in deuterated tetrahydrofuran and monitored via ^{1}H NMR at room temperature (Scheme 5.8). After three hours, 70% of styrene had reacted to the hydroboration product **5.14**. The Pd-complex remained mostly unreacted, but small amounts (ca. 5%) of methane were observed. Transmetallation of the hydride can lead to a (α-diimine)PdMeH complex, that can release methane via reductive elimination. Overall, this NMR experiment suggested that hydroboration outcompetes undesired side-/ decomposition-reactions of the Pd-complex.

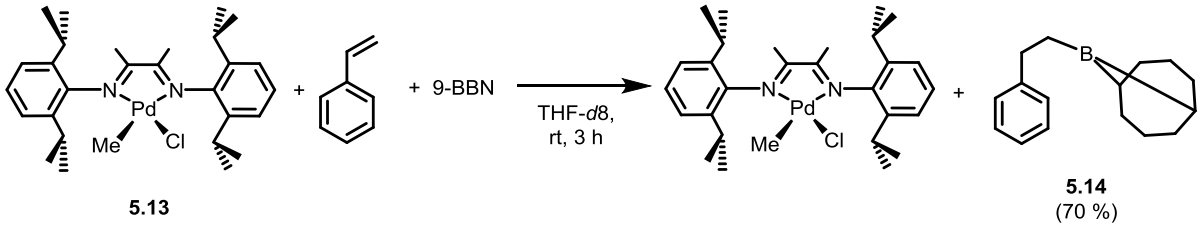

5.13 **5.14** (70 %)

Scheme 5.8 Proof-of-concept ^{1}H NMR experiment to assess the stability of PdMeCl complex **5.13** towards borohydrides, here 9-BBN.

The synthesis of pendant α-alkene α-diimine ligand and complexes was hence pursued. Initial attempts to form an α-diimine from butadione and 2-aminostyrene under acid catalysis and water removal conditions gave crude reaction mixtures with no olefin groups as determined by ^{1}H NMR. Likely a quinoline derivative was formed. Similar reaction outcomes have been reported previously.[6] Switching to a metal promoted, basic route provided successful access to the desired ligands. The respective 2-substituted anilines were reacted first with $AlMe_3$ to form Al-amides that undergo subsequent α-diimine formation when treated with keto-imine **5.15** (Scheme 5.9). Asymmetric α-diimines **5.16 - 5.18** were obtained from 2-ethyl-, 2-vinyl-, 2-allyl-aniline in moderate to good isolated yields (45 – 69%). The acenaphthoquinone backbone was chosen due to the silica stability of the final ligands which facilitated their purification by flash chromatography and crystallization.

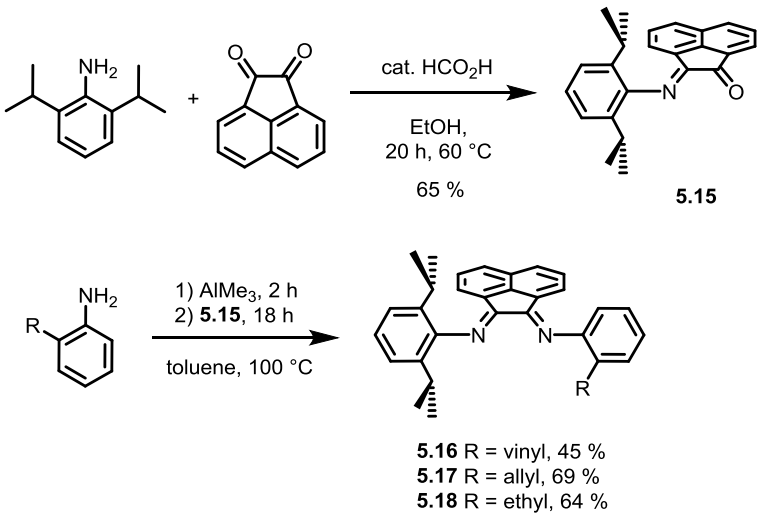

Scheme 5.9 Synthesis of the pendant alkene and ethyl α-diimine ligands **5.16 - 5.18**.

Palladium and nickel complexes **5.19** – **5.26** of the pendant alkene diimine ligands **5.16 - 5.18** were obtained by reactions with (cod)Pd(Me)Cl, $(MeCN)_2PdCl_2$, and $(dme)NiBr_2$ precursors in dichloromethane (Scheme 5.10). PdMeCl complexes **5.21** – **5.23** existed as a mixture of *anti* and *syn* isomers with respect to the relative orientation of the Pd-Me and the pendant R moieties in ratios of 1.3-1.8 to 1 as determined by ^{1}H NMR. The excess of the *anti*-isomer is reflecting the *trans*-orientation of the strong Pd-Me donor and the weaker imine.[7] The identity of (α-diimine)$PdCl_2$ complexes **5.19** and **5.20** was established by NMR and elemental analysis, and for (α-diimine)$NiBr_2$ complexes **5.24** – **5.26** with elemental analysis. A crystal structure of complex **5.22** could be obtained, and shows the typical square-pyramidal coordination with the imine aryls perpendicular to the coordination plane. It also showed no interaction of the pendant alkene with the axial Pd coordination site (Figure 5.2). A common way to purify (α-diimine)PdMeCl complexes besides crystallization is silica flash chromatography, as these complexes are stable in air for prolonged times. When subjecting a crude reaction mixture of **5.22** to silica chromatography, pure orange-red complex **5.22** was obtained in 50% yield, in addition to

another dark redbrown Pd-species **5.27** in 17% yield (Scheme 5.11). This side product was identified as the 2,1-insertion product of the pendant allyl group into the Pd-Me bond by NMR, EA, and X-ray crystallography (Figure 5.3). The complexation of the ligand **5.17** with (cod)PdMeCl in CD_2Cl_2 by ^1H NMR at room temperature showed no formation of the insertion product after 3h. Interactions with the SiO_2 seem to promote transient chloride abstraction, after which the pendant alkene coordinates and inserts in a 2,1-fashion, yielding the observed complex after chloride re-coordination (Scheme 5.11).

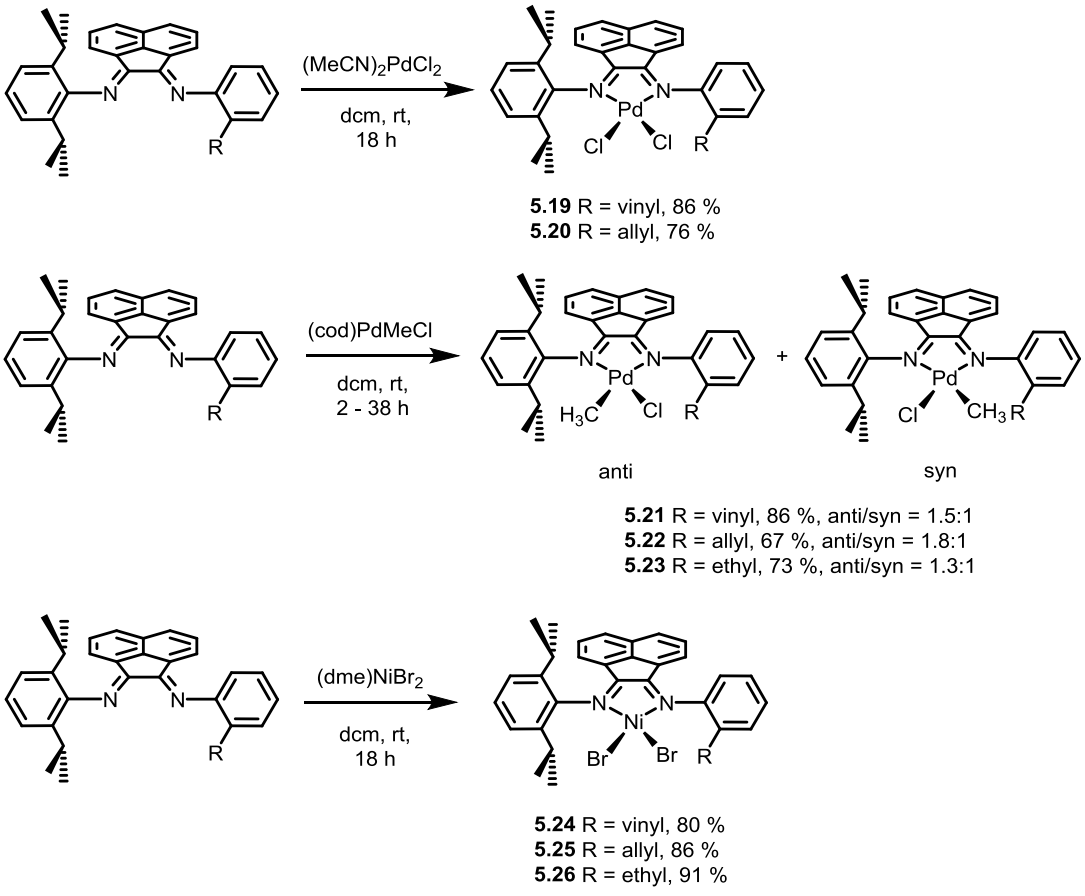

Scheme 5.10 Synthesis of pendant alkene α-diimine Pd and Ni complexes.

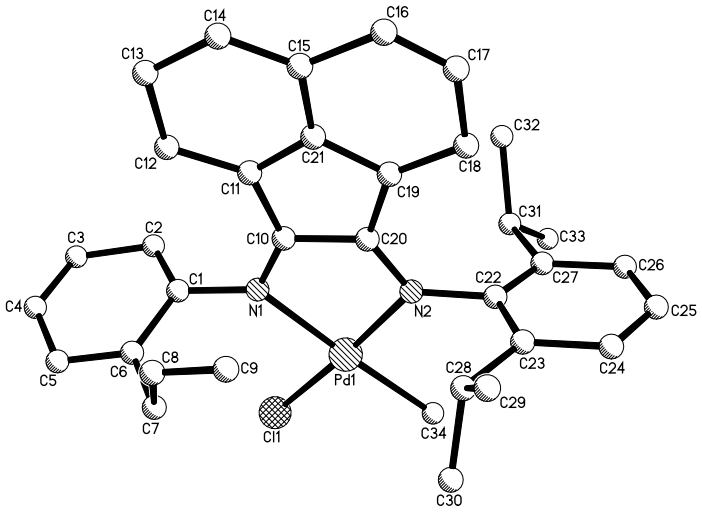

Figure 5.2 Molecular structure of pendant allyl Pd-complex **5.22**. All hydrogen atoms omitted for clarity.

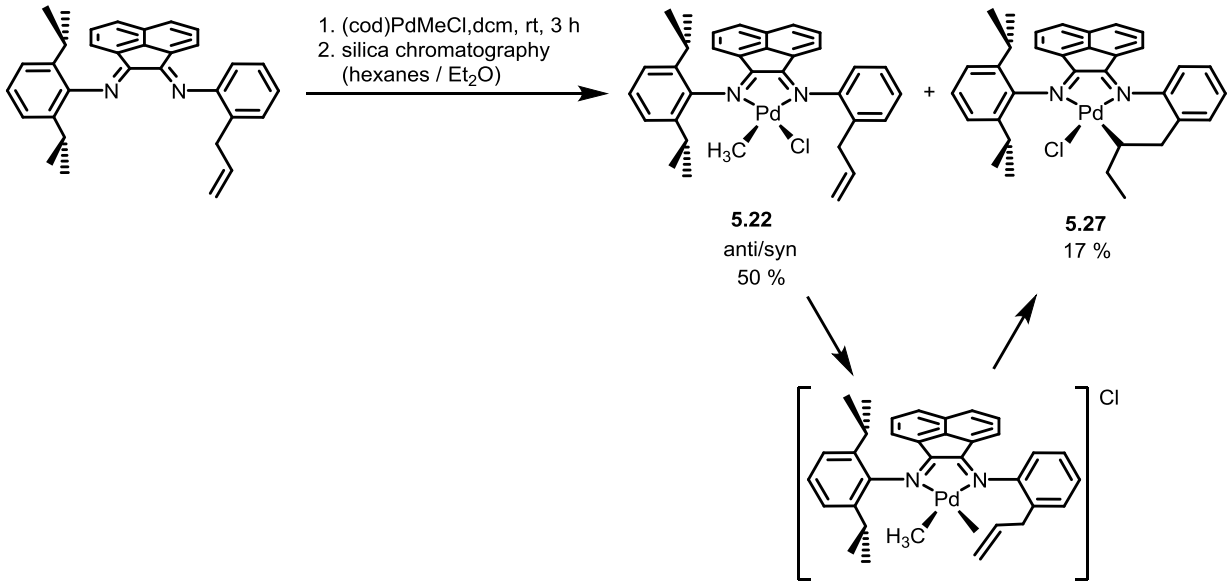

Scheme 5.11 Synthesis of complexes **5.27** via SiO_2 chromatographic purification, and proposed intermediate.

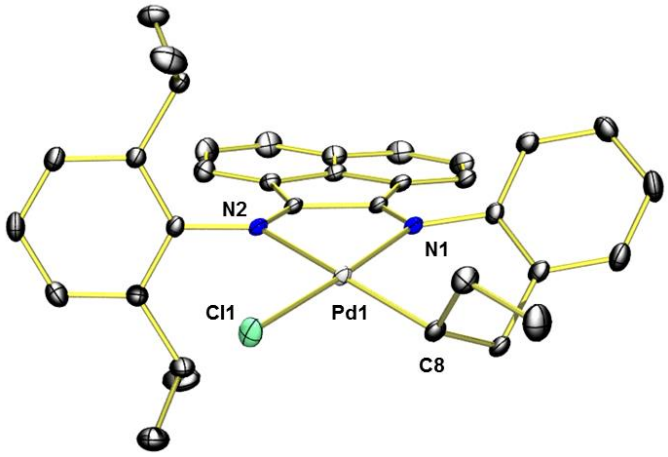

Figure 5.3 Molecular structure of complex **5.27**. All hydrogen atoms and one molecule cocrystallized dichloromethane omitted for clarity.

With the pendant alkene complexes in hand both hydroboration and cross-metathesis were explored as routes to install the boron Lewis acid. In general, the hydroboration with boranes such as 9-BBN proceeds at room temperature, but with boronic esters such as pinacol- and catecholborane (PinBH and CatBH) elevated temperatures, or transition metal catalysts[8] are required for appreciable reaction conversions. For complex **5.21**, hydroboration attempts were unsuccessful (Scheme 5.12). Reaction with equimolar amounts of 9-BBN lead to rapid decomposition as indicated by methane and Pd-black formation, which was also observed with less hydridic PinBH and CatBH in the presence of catalysts (10% $(PPh_3)_3RhCl$, or 5% $^{tBu}(PNN)FeCl_2$ / 10% $NaBEt_3H$). Contrary to the proof-of-concept reaction (Scheme 5.8), hydroboration does not outcompete the decomposition in the case of the vinyl complex **5.21**. The decrease in rate likely results from the steric crowding in the ortho-position of the styrene group. In case of $PdCl_2$ complex **5.19** and $NiBr_2$ complex **5.24**, no appreciable decomposition nor hydroboration was observed supporting the detrimental effect of the steric bulk ortho to the vinyl

group. Hydroboration of the pendant vinyl ligand **5.16**, expected to be less sterically crowded prior to complexation, did not proceed, presumably due to strong B-N interactions.

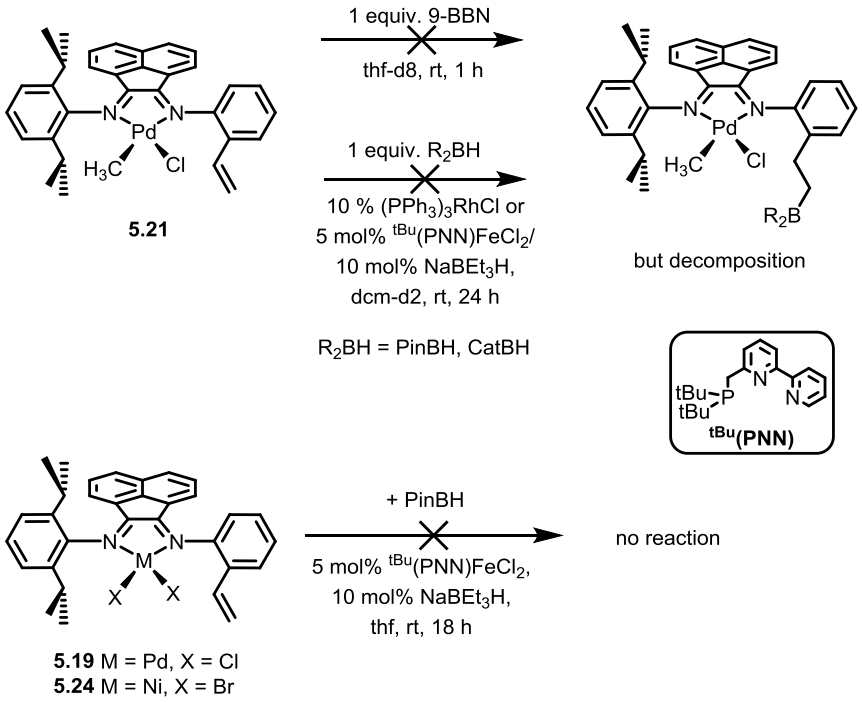

Scheme 5.12 Hydroboration attempts of pendant vinyl diimine complexes.

Similarly, the cross-metathesis of vinyl ligand with vinyl boronic acid pinacol ester (vinylBPin) employing Grubbs 2nd generation Ru-catalyst resulted in no formation of the desired product. Coordination of the bidentate α-diimine to the Ru can lead to catalyst deactivation. The analogous cross-metathesis with pendant vinyl complex **5.21** was very sluggish. Prolonged heating of a reaction mixture resulted in approximately 5% NMR yield. Again, the large steric bulk inhibits the reactivity of the vinyl group, which has previously been identified as an issue for cross-metathesis of styrene derivatives.[9]

For the complexes featuring the pendant allyl group, the issues associated with the steric bulk were expected to be less pronounced. Indeed, the cross-metathesis reaction of pendant allyl Pd-complexes **5.20** and **5.22** with vinylBPin yielded the desired pendant boronate complexes **5.28**

and **5.29** (Scheme 5.13). For the PdMeCl complex **5.29**, metathesis catalyst was added in portionwise in 1 hour intervals to obtain complete conversion. The reaction progress was monitored by ESI-MS, and complete disappearance of the starting alkene was observed in the ^{1}H NMR of the crude mixture. Residual Ru-catalyst was removed in an unoptimized procedure, stirring with 10 equivalents of PPh_3PO overnight with subsequent silica flash chromatography. In both cases, only the trans-alkene metathesis product was produced.

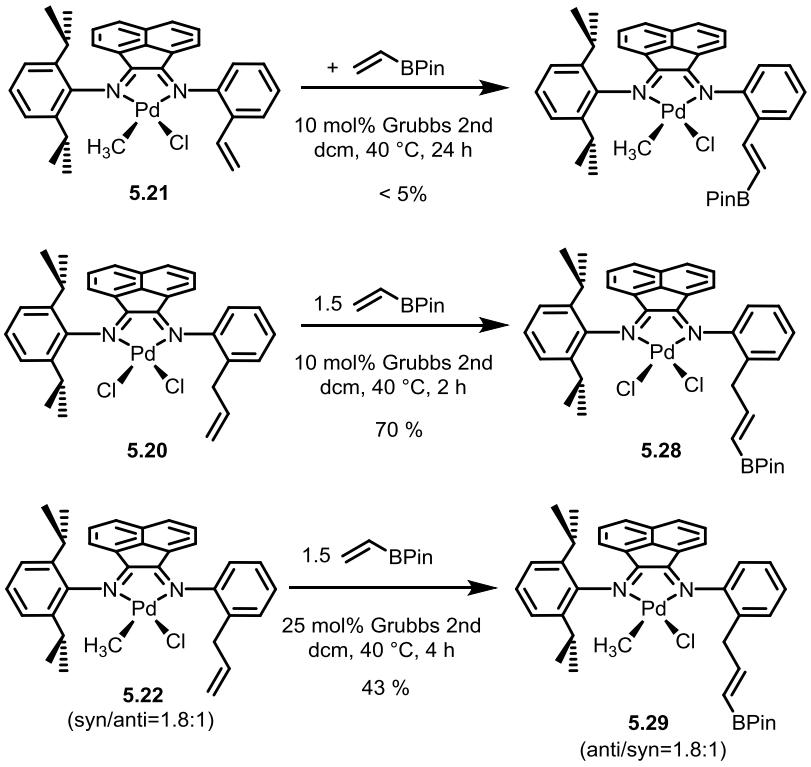

Scheme 5.13 Cross-metathesis of pendant alkene Pd-complexes with vinylBPin.

5.3 Polymerization Studies

5.3.1 Ethylene Homo- And Copolymerizations with Pd-complexes

(α-Diimine)PdMeCl complexes can be activated via chloride abstraction with sodium tetrakis[3,5-bis(trifluoromethyl)phenyl]borate (NaBArF). Treatment of complexes **5.21** – **5.23** with 2 equivalents NaBArF gave active ethylene polymerization catalysts (Table 5.1). Monoethyl

substituted complex **5.23** gave highly branched, low molecular weight polyethylene oils with 100 branches per 1000 carbon atoms and 1,300 g mol^{-1} number-averaged molecular weight (M_n, determined by GPC) under atmospheric ethylene pressure and room temperature (run 1.1). The low molecular weights are a direct result of the low steric bulk of the asymmetric ligand, facilitating associative chain-transfer. Pendant allyl complex **5.22** behaved similarly under the same reaction conditions, and produced polyethylene having 83 methyl branches per 1000 carbons, and M_n = 900 g mol^{-1} at slightly higher productivities (40 vs 31 h^{-1} TOF). It was also found that the inserted pendant allyl complex **5.27** is an active polymerization precursor. With slightly lower yields, polyethylene of similar composition as obtained in run 1.2 was produced. The active species for polymerization must therefore be very similar. In contrast, pendant vinyl complex **5.21** only produced 10% of the polyethylene yield under the same conditions (run 1.3), indicating possible inhibiting effects from coordination of the pendant vinyl group. The molecular weight distribution of the polymer was broader than that of pendant allyl complex while retaining the same number of branches.

In order to analyze effects of the pendant olefin groups on catalyst lifetime and thermal stability, shorter 6 hours runs were conducted at room temperature and 35 ˚C. The runs at room temperature (run 1.5 – 1.7) yielded polymers with virtually identical properties as the polymers from the 24 hour runs. The productivity of pendant ethyl complex **5.23** was almost unaltered (run 1.1 vs 1.5), but decreased by 75% for pendant allyl complex **5.22**, and circa 50% for complex **5.21**. Increasing the reaction temperatures to 35 ˚C resulted in an increased polymer yield with pendant allyl (~630%, run 1.6 vs 1.9) and vinyl (300%, run 1.7 vs 1.10) complexes, but decreased yield (~25%) for complex **5.23**.

Table 5.1 Ethylene homopolymerizations with Pd-complexes.[a]

Run	Precat.	T [°C]	t [h]	Yield [mg]	TOF [h^{-1}]	N_{br}[b]	M_n[c] [g/mol]	M_w/M_n[c]
1.1	**5.23**	22	24	211	31	100	1,278	1.59
1.2	**5.22**	22	24	271	40	83	910	2.03
1.3	**5.21**	22	24	21	3	94	917	4.40
1.4	**5.27**	22	24	212	32	82	912	1.87
1.5	**5.23**	22	6	202	120	99	1,428	1.57
1.6	**5.22**	22	6	63	38	86	827	1.88
1.7	**5.21**	22	6	9	5	104	897	4.66
1.8	**5.23**	35	6	154	92	127	578	1.72
1.9	**5.22**	35	6	402	239	96	1,151	1.96
1.10	**5.21**	35	6	25	15	176	447	7.37

a) Polymerization conditions: 10 µmol [Pd], 40 mL DCM, 2 equiv. NaBArF, 1 atm. b) Determined by ^{1}H NMR at 25 °C in $CDCl_3$. c) Determined by GPC in THF vs PS standards.

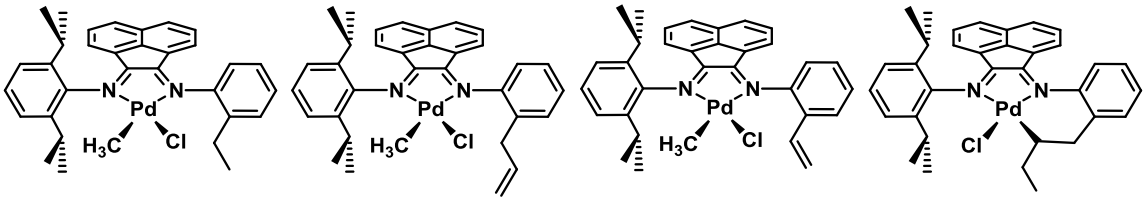

5.23 **5.22** **5.21** **5.27**

Interaction of the pendant olefin groups with the cationic active complex leads to prolonged catalyst lifetimes and increased thermal stability, compared with saturated ligand substitutions. Complex **5.22** showed quasi living character at room temperature with no decrease in activity after 24 h. However, this stabilization comes at the expense of catalyst activity at shorter polymerization runs. The pendant olefin is competing with ethylene for coordination to the catalyst, which slows

down the rate of polymerization. Stabilization of reactive 14-electron active Pd-species after insertion by transient interactions with hemilabile ligand groups has previously been reported.[10] These interactions altered not only the activity but also the polymer structure. It is assumed that the coordination of pendant vinyl group is stronger than the allyl olefin due to a favorable ring-size. Additionally, the formation of **5.27** demonstrates that the insertion of the pendant alkene is possible once coordinated, whereas a similar product was not observed in the case of **5.21**. The virtually identical polymerization properties of **5.22** and **5.27** suggest that ethylene insertion into the Pd-C bond of a secondary carbon is possible and happens during ethylene polymerization with **5.22**. Due to the high rate of chain-transfer the growing pendant ligand group is expected to be released by β-H elimination, after which recoordination and insertion is entropically more disfavored. This is supported by an ESI-chromatograph taken after quenching of run 1.2, which showed a series of molecular ions for $[M_{ligand}+(28)_n]^+$ and $[M_{ligand}+14+(28)_n]^+$ (n = 1, 2, 3, 4, …), resulting from consecutive ethylene insertions after insertion of the pendant allyl group into a Pd-H and Pd-Me species, respectively (Scheme 5.14). Such ligand non-innocence has been reported for pendant-olefin Fe(DPI) complexes.[11]

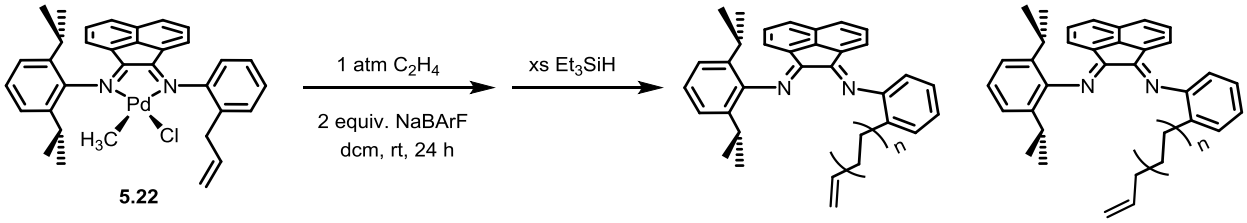

Scheme 5.14 Non-innocence of pendant allyl ligand during ethylene polymerization, as detected by ESI-MS. Note that branching is possible, but cannot be detected by this MS technique.

Treatment of complex **5.21** with one equivalent NaBArF gave the cationic pendant vinyl coordinated complex **5.30** (Scheme 5.15), which was stable at room temperature for over one day under inert conditions. Insertion was not detected by ^{1}H NMR at elevated temperatures up to 80 ˚C,

where the complex decomposed within 1 hour. Addition of several equivalents ethylene gas to **5.30** resulted in rapid formation of oligoethylenes.

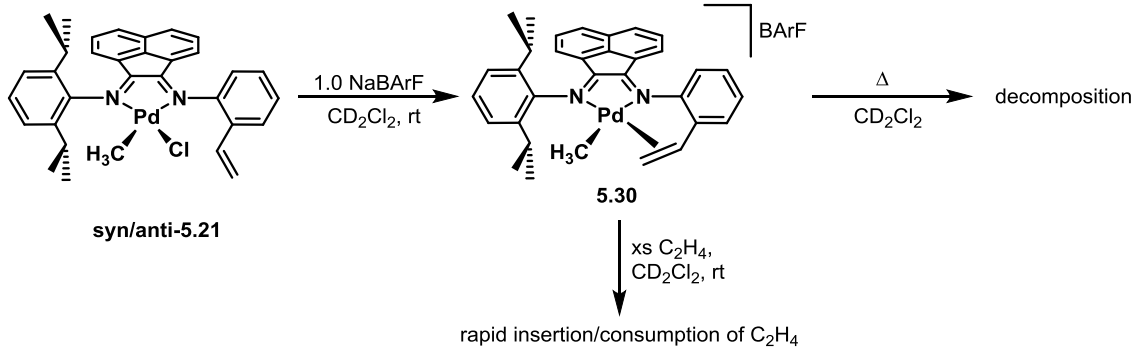

Scheme 5.15 Formation of cationic pendant vinyl coordinated complex **5.30**.

In copolymerization reactions with methyl acrylate (MA) and vinyl acetate (VA), no effect of the functional groups, including the pendant boronate of complex **5.29**, on the incorporation ratio of the polar monomer could be detected (Table 5.2). In all cases (runs 2.1 – 2.4 and runs 2.5 – 2.8), the MA incorporation was ~2%, while VA was not incorporated into the polyethylene. The presence of the polar comonomer lead to decreased activities, but the number of branches and the molecular weight and distribution were similar to ethylene homopolymerizations for complexes **5.22**, **5.23**, and **5.29**. Surprisingly, complex **5.21** produced polymers with a circa 50% increased number of branches, even in the case of VA, which was not incorporated.

Table 5.2 Copolymerization reactions with Pd-complexes.[a]

Run	Precat.	n [µmol]	Comon./ Conc. [M]	TOF [h^{-1}]	yield [mg]	N_{br}[b]	M_n[c] [g/mol]	M_w/M_n[c]	χ[d] [%]
2.1	**5.23**	10	MA / 0.28	17	112	93	1,219	1.73	2.5
2.2	**5.21**	10	MA / 0.28	1	10	143	527	3.51	2.1
2.3	**5.22**	7	MA / 0.28	5	23	100	879	1.64	2.2
2.4	**5.29**	10	MA / 0.28	3	19	111	808	1.66	1.9
2.5	**5.23**	10	VA / 0.27	10	64	101	1,400	1.48	0
2.6	**5.21**	7	VA / 0.27	1	<5	150	814	2.93	0
2.7	**5.22**	10	VA / 0.27	4	27	89	870	1.62	0
2.8	**5.29**	10	VA / 0.27	1	9	103	891	1.64	0

a) Polymerization conditions: 10 µmol [Pd], 40 mL DCM, 2 equiv. NaBArF, room temperature, 1 atm. b) Determined by ^{1}H NMR at 25 °C in $CDCl_3$. c) Determined by GPC in THF vs PS standards. d) Molar incorporation ratio of polar monomer. Determined ^{1}H NMR at 25 °C in $CDCl_3$.

Several reasons for the unaltered incorporation ratios with pendant Lewis acid complex **5.29** are plausible. The remote position of the boronate makes coordination to the polar monomer groups unfavorable. In addition, the Lewis acidity of the boronate is presumably several orders of magnitude lower than that of a cationic Pd center. More insights can be obtained by employing polar monomers with longer spacers between the olefin and polar group to achieve favorable bidentate binding to the metal and the Lewis acid. In addition, lower polymerization temperatures might result in a better differentiation of the Lewis acidities of the boronate and Pd-center. Finally, the installation of more Lewis acidic groups likely has the greatest beneficial effect.

5.3.2 Ethylene Homopolymerizations with Ni-Complexes

The $NiBr_2$-complexes can be activated with MAO. They are typically orders of magnitude more active than their Pd-analogues, but do not incorporate polar monomers. Complexes **5.24** –

5.26 produced semicrystalline polyethylene with activities of up to 2.6 x 10^3 h^{-1} after 15 min at 0 °C, which is comparable to previous reports with similar ligand frameworks.[12] In a 5 minute run (run 3.1 – 3.3), pendant allyl complex **5.25** produced the most polyethylene, while pendant vinyl complex **5.24** was ~50% less active. This result is similar to properties of the analogous Pd-complexes. The pendant olefin groups led to a reduced number of branches compared with ethyl complex **5.26** (run 3.2, 3.3 vs 3.1). The decreased number of branches resulted in the expect increase in melting temperature (118 vs 124 °C). The hemilabile effects of the pendant olefins are also observed in the Ni-complexes.

Table 5.3 Ethylene homopolymerizations with Ni-complexes.[a]

Run	Precat.	time [min]	yield [mg]	TOF [10^3 h^{-1}]	T_m [°C][b]	N_{br}[c]
3.1	**5.26**	5	204	17.5	118	31
3.2	**5.25**	5	260	22.3	124	12
3.3	**5.24**	5	141	12.1	124	13

a) Polymerization conditions: 5 µmol [Ni], 50 mL toluene, 150 equiv. MAO, 0 °C, 1 atm. b) Determined by DSC. c) Number of branches. Determined by ^{1}H NMR at 130 °C in $C_2D_2Cl_4$.

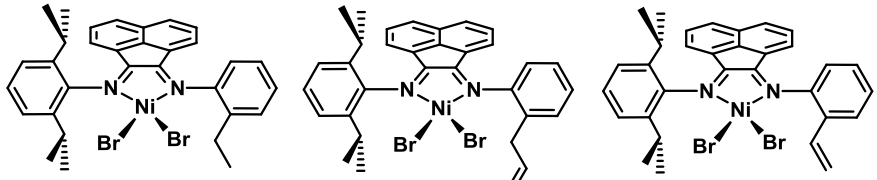

5.26 **5.25** **5.24**

5.4 Conclusive Summary and Outlook

(α-Diimine)Pd- and Ni-complexes with pendant α-alkene (vinyl, and allyl) and boronate groups were synthesized and characterized. No effect of the Lewis acid group on the incorporation ratio in copolymerizations with MA and VA was observed. Potential future improvements are the use of polar monomers with longer spacers between the olefin and polar group to achieve favorable

bidentate binding to the metal and the Lewis acid. In addition, lower polymerization temperatures might result in a better differentiation of the Lewis acidities of the boronate and Pd-center, and the installation of more Lewis acidic groups would likely have the greatest beneficial effect on the incorporation ratio. To this end, cross-metathesis with more Lewis acidic vinylboronates (i.e. vinylBCat), and hydroboration of the pendant allyl group seems most promising due to the decreased steric bulk around the olefin as compared with the pendant vinyl complex. The use of recently developed, more active and functional group tolerant hydroboration catalysts such as (^{tBu}PNN)CoCl[8b] provides additional options.

During the course of the study, hemilability and non-innocence of the pendant olefin ligands were determined, which led to prolonged, living catalyst lifetimes and increased thermal stability of the pendant allyl complex. These pendant olefins can be further functionalized to install different kinds of reactivities, e.g. H-bonding motifs.

5.5 Experimental Section

Materials

The following compounds were purchased and used without further purification: $(cod)PdCl_2$, $(PhCN)_2PdCl_2$, $(MeCN)_2PdCl_2$, $(dme)NiBr_2$, $SnMe_4$ (Strem), vinylboronicacid pinacol ester, methyl acrylate, vinyl acetate, trimethylaluminum (2.0 M in hexanes), methaylaluminoxane (10% in toluene) and triethylsilane (Sigma Aldrich). 2-Amino-styrene,[13] 2-(tert-butyldiphenylsilanyloxymethyl)-phenylamine,[14] (2E)-2-[(2,6-diisopropylphenyl)-imino]acenaphthylen-1(2H)-one (**5.15**),[15] 2-allylaniline,[16] (cod)Pd(Me)Cl,[17] and NaBArF[18] were prepared following literature procedures.

Polymerization procedures

All polymerizations were carried out in 100 mL glass flasks connected to a double Schlenk line connected to an ethylene gas tank. After flame-drying the flasks under vacuum, they were backfilled with ethylene and the bulk solvent was introduced by cannula transfer.

Pd-catalyzed polymerizations

A solution of the precatalyst in minimal amounts (~2 mL) of dichloromethane were introduced by syringe transfer and stirred for 10 minutes before addition of the activator via syringe to commence the polymerization run. In case of ethylene homopolymerizations, the NaBArF was added as a slurry in ~3 mL dichloromethane, and for copolymerizations as a clear solution in the polar monomer. For the run at 35 ˚C, the order of addition was inverted, and the precatalyst solution added last to prevent thermal decomposition. After the allotted reaction times, the reaction was quenched by addition of 0.5 mL Et_3SiH. All volatiles were removed with a rotary evaporator, filtered through a short-plug of silica and alumina, and washed with hexanes. After removal of the hexanes, the polymer samples were dried in a tared vial under a mild vacuum at 70 ˚C over night.

Ni-catalyzed polymerizations

A solution of the precatalyst in minimal amounts (~2 mL) of toluene were introduced via syringe transfer and stirred for 10 minutes at 0 ˚C. Addition of the MAO solution via syringe commenced the polymerization run. After the allotted reaction times, the reaction was quenched by addition of 5 mL methanol. The quenched mixture was poured into 200 mL acidic methanol to precipitate the polymer. The polymer was collected by filtration, washed with copious amounts of methanol and acetone, and dried in a tared vial under a mild vacuum at 70 ˚C over night.

Syntheses of Ligands and Complexes

5a,11a-Dimethyl-5a,6,11a,12-tetrahydrobenzo[b]benzo[5,6][1,4]oxazino[2,3-e][1,4]oxazine (**5.6**)

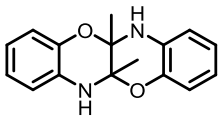

A suspension of 6.5 g 2-aminophenol (0.060 mol) in 25 mL ethanol was heated to reflux and 2.6 mL diacetyl (0.030 mol) were added. The mixture was refluxed until all reagents were dissolved (5 minutes) and cooled to room temperature overnight. The light precipitate was filtered off the dark black solution, washed with cold ethanol, recrystallized from ethanol and dried. The colorless plates had X-ray quality (1.95 g, two crystallization batches, 24%). ^{1}H NMR (500 MHz, DMSO-d6, δ) 7.20 (s, 2H, N*H*), 6.78 – 6.69 (m, 2H, arom.), 6.68 (t, J = 5.9 Hz, 2H, arom.), 6.63 – 6.52 (m, 4H, arom), 1.42 (s, 6H, CH_3). ^{13}C NMR (126 MHz, DMSO-d6, δ) 141.07, 129.07, 120.14, 118.57, 115.58, 113.77, 81.52, 20.75. HRMS(ESI) m/z calcd for $C_{16}H_{16}O_2N_2Na$ $[M+Na]^+$ 291.1110, found 291.1125. EA: calcd for $C_{16}H_{16}O_2N_2$: C 71.62, H 6.01, N 10.44; found C 71.65, H 6.00, N 10.36.

2,2'-Dimethyl-1,1',4,4'-tetrahydro-2H,2'H-2,2'-bibenzo[d][1,3]oxazine (**5.7**)

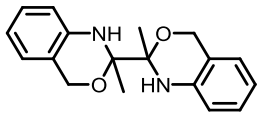

A solution of 2-amino benzylalcohol (0.50 g, 4.1 mmol, 3 equiv.), 2,3-butadione (115 mg) and 1 drop of 97% formic acid in 10 mL methanol were stirred overnight at 65 ˚C. The white precipitate was separated by filtration, washed with 2 x 2 mL cold methanol and dried *in vacuo* to give 0.43 g of the title product as a white powder (53%). ^{1}H NMR (500 MHz, $CDCl_3$, δ) 7.08 (t, *J* = 7.6 Hz, 2H), 6.95 (d, *J* = 7.4 Hz, 2H), 6.72 (t, *J* = 7.4 Hz, 2H), 6.61 (d, *J* = 8.0 Hz, 2H), 4.92 (d, *J* = 14.4 Hz, 2H), 4.77 (d, *J* = 14.4 Hz, 2H), 4.43 (s, 2H), 1.47 (s, 6H). ^{13}C NMR (126 MHz, $CDCl_3$, δ) 141.19, 127.91, 124.64, 119.82, 117.80, 115.16, 87.40, 62.21, 18.20.

N,N'-(Butane-2,3-diylidene)bis(2-(((tert-butyldiphenylsilyl)oxy)methyl)aniline) (**5.8**)

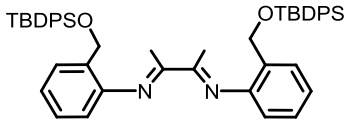

A solution of crude 2-(tert-butyldiphenylsilanyloxymethyl)phenylamine (0.5 g), 2,3-butadione (33 mg, 0.38 mmol) and 1 drop of 97% formic acid in 2 mL methanol were stirred overnight. The white precipitate was separated by centrifugation and washed with 2 mL methanol and dried *in vacuo* to give 62 mg of the desired product as a white powder (21%). ^{1}H NMR (500 MHz, $CDCl_3$) δ 7.70 – 7.65 (m, *J* = 8.0, 1.4 Hz, 8H), 7.64 (d, *J* = 7.4 Hz, 2H), 7.41 – 7.36 (m, 4H), 7.36 – 7.29 (m, *J* = 11.2, 4.4 Hz, 8H), 7.29 – 7.22 (m, 2H), 7.20 – 7.14 (m, *J* = 7.5, 0.9 Hz, 2H), 6.58 – 6.50 (m, *J* = 7.1 Hz, 2H), 4.56 (s, 4H), 1.93 (s, 6H), 1.03 (s, 18H). ^{13}C NMR (126 MHz, $CDCl_3$) δ 168.02, 147.71, 135.78, 135.66, 133.63, 130.69, 129.93, 129.79, 127.89, 127.82, 127.52, 127.44, 124.26, 117.68, 62.32, 26.95, 26.88, 19.39, 15.66. HRMS(ESI) m/z calcd for $C_{50}H_{56}N_2NaO_2Si_2$ $[M+Na]^+$ 795.3778, found 759.3765.

(1E,2E)-N^1,N^2-bis(2-(((tert-butyldiphenylsilyl)oxy)methyl)phenyl)acenaphthylene-1,2-diimine (**5.9**)

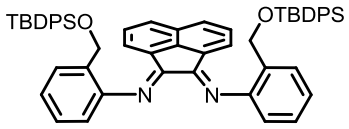

Acenaphthoquinone (0.10 g, 0.55 mmol), 2-(tert-butyldiphenylsilanyloxymethyl)-phenylamine (0.4 g, 2.0 equiv.), and 1 drop of formic acid was heated in 3 mL degassed methanol to 70 ˚C for 20 h. The thick orange suspension was filtered through a Buchner filter. The solid product was washed with 10 mL cold methanol and dried *in vacuo* to give 375 mg (78%). ^{1}H NMR (500 MHz, $CDCl_3$, δ) 7.85 (d, *J* = 8.2 Hz, 2H), 7.70 (d, *J* = 7.5 Hz, 2H), 7.53 (d, *J* = 6.9 Hz, 8H), 7.39 – 7.22 (m, 12H), 7.17 (t, *J* = 7.4 Hz, 8H), 6.84 (d, *J* = 7.5 Hz, 2H), 6.73 (d, *J* = 7.2 Hz, 2H), 4.72 (s, 4H), 0.78 (s, 18H). ^{13}C NMR (126 MHz, $CDCl_3$, δ) 161.6, 149.8, 141.7, 135.6, 133.5, 131.2, 129.6, 129.6, 129.1, 128.8, 128.3, 128.2, 127.9, 127.7, 124.5, 124.0, 117.5, 62.8, 26.6, 19.2. HRMS(ESI) m/z calcd for $C_{58}H_{56}N_2NaO_2Si_2$ $[M+Na]^+$ 891.3778, found 891.3801.

(^{TBDPSO}ArBIAN)PdMeCl (**5.10**)

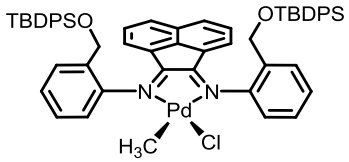

A dichloromethane solution (5 mL) of **5.9** (0.16 g, 0.19 mmol) and (cod)PdMeCl (50 mg, 1.0 equiv.) was stirred at room temperature overnight. The dark red-purple solution was purified on a silica column with dcm as the eluent. After removal of the solvent, the complex was precipitated from a minimal amount of dcm with diethylether, filtered and dried *in vacuo* overnight to yield 151 mg (77%). ^{1}H NMR (500 MHz, CD_2Cl_2, δ) 8.05 (d, *J* = 8.3 Hz, 1H), 8.01 (d, *J* = 8.3 Hz, 1H), 7.77 – 7.70 (m, 3H), 7.67 (d, *J* = 6.8 Hz, 2H), 7.63 – 7.54 (m, 5H), 7.54 – 7.50 (m, 2H),

7.48 – 7.15 (m, 17H), 7.04 – 6.95 (m, 2H), 6.84 (d, J = 7.3 Hz, 1H), 6.51 (d, J = 7.3 Hz, 1H), 5.46 (d, J = 12.1 Hz, 1H), 5.03 (d, J = 12.7 Hz, 1H), 4.79 (d, J = 6.3 Hz, 1H), 4.76 (d, J = 6.9 Hz, 1H), 0.68 (s, 9H), 0.66 (s, 3H), 0.62 (s, 9H). ^{13}C NMR (126 MHz, CD_2Cl_2, δ) 173.5, 168.3, 145.9, 145.3, 145.1, 136.1, 136.1, 136.1, 136.0, 133.8, 133.7, 133.3, 133.3, 132.9, 132.8, 131.8, 131.6, 131.2, 130.3, 130.2, 130.2, 130.1, 130.1, 129.6, 129.3, 129.2, 129.0, 128.4, 128.3, 128.2, 128.1, 127.7, 127.5, 126.8, 125.9, 125.8, 121.8, 120.7, 64.5, 63.1, 26.7, 26.7, 19.2, 1.8. EA: calcd for $C_{59}H_{59}ClN_2O_2PdSi_2$: C 69.06, H 5.80, N 2.73; found C 68.95, H 5.99, N 2.82.

(^{TBDPSO}ArBIAN)$PdCl_2$ (**5.11**)

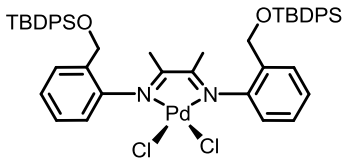

A dichloromethane solution (5 mL) of **5.8** (50 mg, 0.064 mmol) and $(PhCN)_2PdCl_2$ (24.8 mg, 1.0 equiv.) was stirred at room temperature overnight. The yellow orange solution was evaporated and the residue washed twice with 5 mL diethylether, and dried *in vacuo* overnight to yield 53 mg (86%). ^{1}H NMR (600 MHz, $CDCl_3$, δ) 7.84 – 7.78 (m, 8H), 7.49 – 7.45 (m, 6H), 7.45 – 7.42 (m, 6H), 7.40 – 7.34 (m, 6H), 6.75 – 6.70 (m, 2H), 5.43 (d, J = 12.3 Hz, 2H), 4.77 (d, J = 12.4 Hz, 2H), 1.77 (s, 6H), 1.09 (s, 18H). EA: calcd for $C_{58}H_{56}Cl_2N_2O_2PdSi_2$: C 66.56, H 5.39, N 2.68; found C 66.14, H 5.06, N 3.07.

1,1'',4,4''-tetrahydrodispiro[benzo[d][1,3]oxazine-2,1'-acenaphthylene-2',2''-benzo[d][1,3]oxazine] (**5.12**)

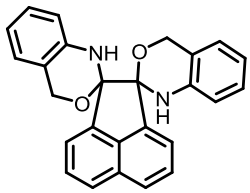

α-Diimine **5.9** (0.20 g, 0.23 mmol) was dissolved in 5 mL dry THF under N_2 and cooled to 0 ˚C. TBAF (0.51 mL of 1.0 M solution in THF, 2.2 equiv.) was added, and the solution was left stirring overnight at room temperature. After 18 h, the brown-red solution was evaporated, the residue dissolved in 20 mL EtOAc, washed with 2 x 5 mL H_2O, dried over MgSO4 and the volatiles removed. The yellow residue was washed with hexanes to remove *t*Bu(Ph)$_2$SiF, dried *in vacuo* overnight to yield 72 mg of the desired product in 80% yield. ^{1}H NMR (600 MHz, $CDCl_3$, δ) 7.80 (d, *J* = 8.2 Hz, 2H), 7.48 (dd, *J* = 8.2, 7.0 Hz, 2H), 7.31 (d, *J* = 6.9 Hz, 2H), 7.14 (t, *J* = 7.7 Hz, 2H), 6.99 (d, *J* = 7.5 Hz, 2H), 6.78 (dd, *J* = 14.1, 7.6 Hz, 4H), 5.52 (s, 2H, N*H*), 4.95 (d, *J* = 14.7 Hz, 2H, O-C*H*$_2$), 4.82 (d, *J* = 14.8 Hz, 2H, O-C*H*$_2$). HRMS(ESI) m/z calcd for $C_{26}H_{20}N_2NaO_2$ $[M+Na]^+$ 415.1422, found 415.1410.

(1E,2E)-N^1-(2,6-Diisopropylphenyl)-N2-(2-vinylphenyl)acenaphthylene-1,2-diimine (**5.16**)

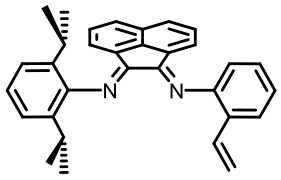

Trimethylaluminum (0.35 mL of 2.0 M solution in hexanes, 0.71 mmol) was added to a solution of 2,6-diisopropyl-aniline (0.133 mL, 1.0 equiv.) in 20 mL toluene and heated to reflux for 2 h. After cooling to room temperature, a solution of **5.15** (0.20 g, 1.0 equiv.) in 20 mL toluene was added and the mixture heated to reflux for 16 h. At room temperature, 10 mL $NaOH_{(aq)}$ (1.0 M) was added slowly and the phases were separated. The aqueous layer was extracted with 2 x 10 mL EtOAc, and the organic phases were combined, dried with $MgSO_4$ and evaporated to dryness. Silica column chromatography provided insufficient separation. Recrystallization from EtOH gave the desired product as orange microcrystals in 44% yield. ^{1}H NMR (600 MHz, $CDCl_3$, δ) 7.87 (t,

J = 8.7 Hz, 2H), 7.66 (d, J = 7.7 Hz, 1H), 7.47 – 7.33 (m, 4H), 7.31 – 7.19 (m, 4H), 7.07 (d, J = 7.7 Hz, 1H), 6.88 – 6.76 (m, 2H), 6.62 (d, J = 7.2 Hz, 1H), 5.72 (d, J = 17.6 Hz, 1H), 5.14 (d, J = 11.2 Hz, 1H), 3.10 – 2.88 (m, 2H), 1.24 (d, J = 6.8 Hz, 6H), 0.97 (d, J = 6.8 Hz, 6H). HRMS(ESI) m/z calcd for $C_{32}H_{30}N_2Na$ $[M+Na]^+$ 465.2307, found 465.2310.

(1E,2E)-N1-(2-Allylphenyl)-N2-(2,6-diisopropylphenyl)acenaphthylene-1,2-diimine (**5.17**)

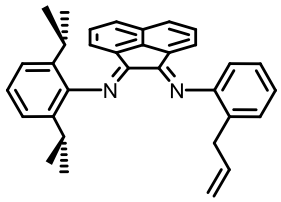

Trimethylaluminum (1.9 mL of 2.0 M solution in hexanes, 1.0 equiv.) was added to a solution of 2-allylaniline (0.51 g, 1.0 equiv.) in 125 mL dry toluene and heated to reflux for 2 h. After cooling to room temperature, a solution of **5.15** (1.3 g, 3.8 mmol) in 20 mL toluene was added and the mixture heated to reflux for 16 h. At room temperature, 50 mL $NaOH_{(aq)}$ (1.0 M) was added slowly and the phases were separated. The aqueous layer was extracted with 2 x 50 mL EtOAc, and the organic phases were combined, dried with $MgSO_4$ and evaporated to dryness. The residue was dissolved in 50 mL diethylether and stored at -30 ˚C overnight. The precipitated dark-red material was filtered, washed with minimal amounts of cold hexanes. The mother liquor was concentrated and cooled to -30 ˚C again to produce a 2nd batch of precipitate. In total, 1.3 g were isolated (69% yield). ^{1}H NMR (500 MHz, $CDCl_3$, δ) 7.88 (dd, J = 7.8, 6.8 Hz, 2H), 7.40 – 7.30 (m, 4H), 7.29 – 7.21 (m, 4H), 7.05 (d, J = 7.6 Hz, 1H), 6.81 (d, J = 7.2 Hz, 1H), 6.60 (d, J = 7.2 Hz, 1H), 5.77 (ddt, J = 16.8, 9.9, 6.8 Hz, 1H), 4.95 (dd, J = 17.0, 1.4 Hz, 1H), 4.75 (d, J = 9.9 Hz, 1H), 3.39 (d, J = 6.8 Hz, 2H), 3.06 – 2.96 (m, 2H), 1.23 (d, J = 6.8 Hz, 6H), 0.95 (d, J = 6.9 Hz, 6H). ^{13}C NMR (126 MHz, $CDCl_3$, δ) 161.47, 160.81, 150.48, 147.44, 141.20, 136.92, 135.64,

131.23, 130.21, 129.51, 129.38, 128.99, 128.95, 128.68, 127.96, 127.91, 127.36, 124.66, 124.47, 123.70, 123.66, 123.54, 117.93, 115.64, 36.64, 28.58, 23.69, 23.48. HRMS(ESI) m/z calcd for $C_{33}H_{32}N_2Na$ $[M+Na]^+$ 479.2463, found 479.2481.

(1E,2E)-N1-(2,6-Diisopropylphenyl)-N2-(2-ethylphenyl)acenaphthylene-1,2-diimine (**5.18**)

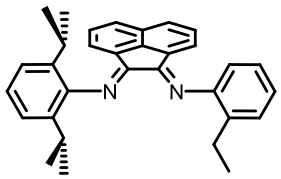

Ligand **5.18** was obtained in 64% yield after recrystallization from hexanes/toluene following the same procedure as for **5.17**. ^{1}H NMR (499 MHz, $CDCl_3$) δ 7.93 (dd, *J* = 8.1, 6.2 Hz, 2H), 7.48 – 7.22 (m, 8H), 7.08 (d, *J* = 7.6 Hz, 1H), 6.86 (d, *J* = 7.2 Hz, 1H), 6.67 (d, *J* = 7.2 Hz, 1H), 3.13 – 3.00 (m, 2H), 2.64 (q, *J* = 7.5 Hz, 2H), 1.28 (d, *J* = 6.8 Hz, 6H), 1.16 (t, *J* = 7.5 Hz, 3H), 1.02 (d, *J* = 6.9 Hz, 6H). HRMS(ESI) m/z calcd for $C_{33}H_{33}N_2Na$ $[M+Na]^+$ 467.2463, found 467.2450.

(^{vinyl}ArBIAN)$PdCl_2$ (**5.19**)

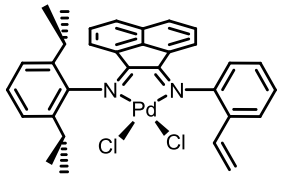

α-Diimine **5.16** (25 mg, 5.6 x 10^{-5} mol) and $(PhCN)_2PdCl_2$ (22 mg, 1.0 equiv.) were suspended in 3 mL dcm and stirred at room temperature overnight. The dark yellow-brown solution was evaporated to dryness and to the residue was added 5 mL diethyl ether and the mixture was stirred for 2 h. After decanting the solvent, the dark brown precipitate was dried *in vacuo* overnight yielding ca. 30 mg (ca. 86%). ^{1}H NMR (600 MHz, $CDCl_3$, δ) 8.12 (t, *J* = 8.9 Hz, 2H),

7.71 (d, *J* = 7.5 Hz, 1H), 7.58 – 7.46 (m, 5H), 7.41 (d, *J* = 7.4 Hz, 1H), 7.36 (t, *J* = 6.9 Hz, 2H), 7.18 (dd, *J* = 17.5, 11.0 Hz, 1H), 6.66 (d, *J* = 7.3 Hz, 1H), 6.50 (d, *J* = 7.3 Hz, 1H), 5.84 (d, *J* = 17.4 Hz, 1H), 5.38 (d, *J* = 11.1 Hz, 1H), 3.55 – 3.44 (m, 2H), 1.53 (d, *J* = 6.7 Hz, 3H), 1.48 (d, *J* = 6.7 Hz, 3H), 0.98 (d, *J* = 6.9 Hz, 3H), 0.96 (d, *J* = 6.9 Hz, 3H). Insufficient elemental analysis: calcd for $C_{32}H_{30}Cl_2N_2Pd$: C 62.00, H 4.88, N 4.52; found C 57.14, H 4.71, N 4.19.

(^{allyl}ArBIAN)$PdCl_2$ (**5.20**)

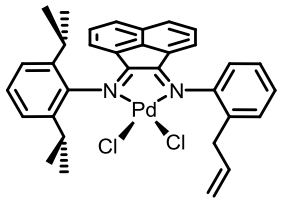

α-Diimine **5.17** (0.25 g, 0.55 mmol) and $(MeCN)_2PdCl_2$ (142 mg, 1.0 equiv.) were suspended in 12 mL dcm and stirred at room temperature overnight. The dark red-orange solution was filtered through a short plug of Celite, washed with dcm, and evaporated to dryness. The residue was washed with 5 mL diethyl ether and 2 x 5 mL pentane, and the orange solid was dried *in vacuo* overnight yielding 263 mg (76%). ^{1}H NMR (500 MHz, $CDCl_3$) δ 8.15 (d, *J* = 8.3 Hz, 2H), 7.60 – 7.45 (m, 6H), 7.43 – 7.33 (m, 3H), 6.68 (d, *J* = 7.3 Hz, 1H), 6.47 (d, *J* = 7.3 Hz, 1H), 5.83 – 5.70 (m, 1H), 5.15 (d, *J* = 17.0 Hz, 1H), 4.71 (d, *J* = 9.9 Hz, 1H), 4.09 (dd, *J* = 15.6, 8.4 Hz, 1H), 3.67 – 3.57 (m, 1H), 3.52 – 3.41 (m, 2H), 1.49 (d, *J* = 6.8 Hz, 3H), 1.45 (d, *J* = 6.7 Hz, 3H), 0.98 (d, *J* = 6.9 Hz, 3H), 0.93 (d, *J* = 6.9 Hz, 3H). ^{13}C NMR (126 MHz, $CDCl_3$) δ 177.02, 176.17, 147.76, 144.77, 141.18, 140.89, 140.53, 137.00, 133.24, 133.12, 133.00, 131.86, 131.56, 129.74, 129.65, 129.60, 128.23, 126.70, 126.52, 125.43, 125.18, 124.94, 124.82, 122.66, 116.65, 38.19, 29.86, 29.76, 24.44, 24.21, 24.16, 23.86. EA: calcd for $C_{33}H_{32}Cl_2N_2Pd$: C 62.52, H 5.09, N 4.42; found C 62.04, H 5.11, N 4.32.

(^{vinyl}ArBIAN)PdMeCl (**5.21**)

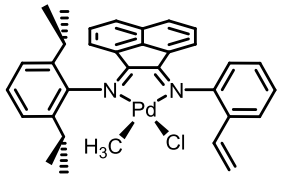

α-Diimine **5.16** (64 mg, 0.014 mmol) and (cod)PdMeCl (38 mg, 1.0 equiv.) were dissolved in 5 mL dichloromethane and stirred at room temperature overnight. The dark red solution was filtered through a short-plug of Celite and precipitated from 20 mL pentane. The orange solid was isolated by centrifugation, washed with another 10 mL pentane and dried *in vacuo* overnight yielding 75 mg (86%). The complex exists as a 1.5:1 mixture of **anti-5.21** to **syn-5.21**, as determined by ^{1}H NMR, which hampered full assignments of resonances. ^{1}H NMR (500 MHz, $CDCl_3$, δ) 8.07 (ddd, *J* = 14.3, 8.1, 4.2 Hz, 1H), 7.82 (d, *J* = 7.6 Hz, 1H), 7.78 (d, *J* = 7.7 Hz, 1H), 7.59 – 7.39 (m, 3H), 7.36 (t, *J* = 6.4 Hz, 1H), 7.30 – 7.26 (m, 1H), 7.13 (dd, *J* = 17.5, 11.1 Hz, 1H), 7.02 (dd, *J* = 17.5, 11.2 Hz, 1H), 6.85 (d, *J* = 7.3 Hz, 1H), 6.65 (d, *J* = 7.2 Hz, 1H), 6.55 (d, *J* = 7.3 Hz, 1H), 6.45 (d, *J* = 7.3 Hz, 1H), 5.87 (d, *J* = 17.5 Hz, 1H), 5.82 (d, *J* = 17.5 Hz, 1H), 5.34 (d, *J* = 7.1 Hz, 1H), 5.28 (d, *J* = 11.1 Hz, 1H), 3.45 – 3.21 (m, 1H), 1.45 (d, *J* = 6.8 Hz, 1H), 1.41 (d, *J* = 6.8 Hz, 1H), 1.39 (d, *J* = 6.8 Hz, 1H), 1.35 (d, *J* = 6.8 Hz, 1H), 0.98 (d, *J* = 6.9 Hz, 1H), 0.96 (d, *J* = 6.9 Hz, 1H), 0.94 – 0.85 (m, 2H), 0.74 (s, 1H), 0.72 (s, 1H). ^{13}C NMR (126 MHz, $CDCl_3$) δ 173.17, 172.77, 168.77, 168.03, 144.93, 144.87, 144.68, 144.27, 142.70, 141.71, 140.19, 139.94, 139.26, 138.86, 132.91, 131.88, 131.83, 131.81, 131.50, 131.47, 131.41, 130.37, 130.07, 129.74, 129.44, 129.36, 129.29, 129.13, 128.82, 128.48, 127.83, 127.75, 127.61, 127.55, 127.47, 127.03, 126.90, 126.71, 125.62, 125.48, 125.40, 125.26, 125.14, 125.11, 124.34, 124.27, 122.44, 121.52, 118.01, 116.74, 29.51, 29.43, 29.13, 28.98, 24.72, 24.40, 24.22, 24.17, 24.04, 23.90, 23.69,

23.66, 22.89, 14.38, 2.88, 2.16, 1.31. EA: calcd for $C_{33}H_{33}ClN_2Pd$: C 66.11, H 5.55, N 4.67; found C 65.17, H 5.69, N 4.63.

(^{allyl}ArBIAN)PdMeCl (**5.22**)

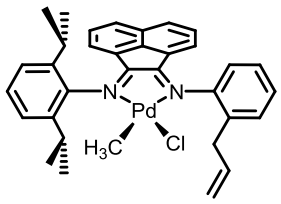

α-Diimine **5.17** (543 mg, 1.25 mmol) and (cod)PdMeCl (300 mg, 1.0 equiv.) were dissolved in 10 mL dichloromethane and stirred at room temperature overnight. One gram of silica was added, the solvent removed, and the mixture separated by flash chromatography (hexanes / 50-100% diethylether). The first, dark redbrown fraction contained complex **5.27** (120, 17%), and the second fraction the title compound (348 mg, 50%), which exists as a 1.8:1 mixture of **anti-5.22** to **syn-5.22**, as determined by ^{1}H NMR, which hampered full assignments of resonances. Alternative synthesis of **5.22**: After the full reaction time, the solution is filtered through a short-plug of Celite, and the volatiles removed. The residue is washed with little diethylether, and pentane, to give the pendant allyl complex in 67% yield. ^{1}H NMR (500 MHz, $CDCl_3$) δ 8.14 (d, *J* = 8.3 Hz, 3H), 8.10 (dd, *J* = 8.3, 4.1 Hz, 3H), 7.59 – 7.44 (m, 21H), 7.41 (t, *J* = 7.2 Hz, 2H), 7.30 (dd, *J* = 11.2, 7.7 Hz, 3H), 6.96 (d, *J* = 7.3 Hz, 2H), 6.68 (d, *J* = 7.3 Hz, 1H), 6.60 (d, *J* = 7.4 Hz, 1H), 6.47 (d, *J* = 7.3 Hz, 2H), 5.88 – 5.70 (m, 3H), 5.07 (d, *J* = 17.0 Hz, 3H), 4.74 (d, *J* = 10.0 Hz, 1H), 4.71 (d, *J* = 9.9 Hz, 2H), 4.17 (d, *J* = 8.3 Hz, 1H), 4.14 (d, *J* = 7.9 Hz, 1H), 3.81 (d, *J* = 8.1 Hz, 1H), 3.60 (td, *J* = 15.1, 5.1 Hz, 3H), 3.49 – 3.28 (m, 6H), 1.49 (d, *J* = 6.8 Hz, 3H), 1.46 (d, *J* = 6.8 Hz, 3H), 1.43 (d, *J* = 6.8 Hz, 6H), 1.39 (d, *J* = 6.8 Hz, 6H), 1.02 (d, *J* = 6.9 Hz, 3H), 1.00 – 0.96 (m, 8H), 0.95 – 0.89 (m, 9H), 0.77 (s, 6H), 0.73 (s, 3H). ^{13}C NMR (126 MHz, $CDCl_3$) δ 172.73, 172.16, 168.26, 167.18, 145.35, 144.84, 144.27, 144.20, 142.15, 141.19, 139.70, 139.34,

138.71, 138.35, 136.99, 135.96, 131.87, 131.51, 131.33, 131.28, 131.26, 131.10, 130.97, 130.86, 130.76, 130.72, 128.78, 128.71, 128.68, 128.26, 127.96, 127.95, 127.44, 127.26, 127.19, 127.05, 126.35, 126.31, 125.03, 124.99, 124.67, 124.60, 124.55, 123.81, 123.71, 121.73, 120.45, 116.28, 115.27, 37.56, 36.50, 34.13, 28.91, 28.85, 28.71, 28.51, 28.40, 24.20, 23.90, 23.72, 23.65, 23.51, 23.36, 23.25, 23.08, 22.34, 13.83, 2.31, 1.57, 0.76, -0.41. EA: calcd for $C_{34}H_{35}ClN_2Pd$: C 66.56, H 5.75, N 4.57; found C 67.26, H 6.31, N 4.32.

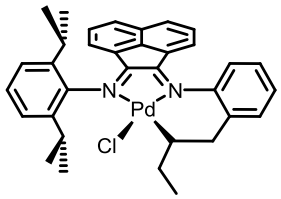

5.27

^{1}H NMR (600 MHz, $CDCl_3$) δ 8.20 (d, *J* = 7.4 Hz, 1H), 8.12 (d, *J* = 8.2 Hz, 1H), 8.02 (d, *J* = 8.2 Hz, 1H), 7.86 (d, *J* = 7.5 Hz, 1H), 7.58 (d, *J* = 7.8 Hz, 1H), 7.50 (d, *J* = 7.0 Hz, 1H), 7.45 – 7.32 (m, 4H), 7.31 (s, 1H), 7.29 (s, 1H), 7.26 (s, 1H), 6.59 (d, *J* = 7.2 Hz, 1H), 3.75 (s, 1H), 3.36 (s, 1H), 3.31 – 3.23 (m, 1H), 3.22 – 3.12 (m, 1H), 1.95 (d, *J* = 11.5 Hz, 1H), 1.52 (s, 1H), 1.45 (d, *J* = 6.7 Hz, 3H), 1.40 (d, *J* = 6.8 Hz, 3H), 1.32 – 1.28 (m, 1H), 1.03 (d, *J* = 6.9 Hz, 3H), 0.89 (t, *J* = 7.0 Hz, 3H), 0.81 (d, *J* = 6.9 Hz, 3H). ^{13}C NMR (126 MHz, $CDCl_3$) δ 143.93, 142.69, 141.72, 140.70, 138.72, 137.89, 132.50, 131.56, 131.05, 130.53, 129.89, 128.73, 128.31, 127.80, 127.19, 126.89, 126.61, 124.85, 124.12, 123.79, 122.46, 53.58, 48.11, 36.98, 31.74, 28.95, 28.90, 27.37, 24.54, 24.07, 23.86, 23.85, 22.81, 12.46. EA: calcd for $C_{34}H_{35}ClN_2Pd$: C 66.56, H 5.75, N 4.57; found C 65.45, H 6.34, N 4.00.

(^{ethyl}ArBIAN)PdMeCl (**5.23**)

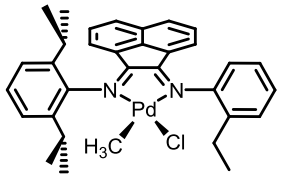

α-Diimine **5.18** (0.10 g, 0.22 mmol) and (cod)PdMeCl (60 mg, 1.0 equiv.) were dissolved in 10 mL dichloromethane and stirred at room temperature overnight. One gram of silica was added, the solvent removed, and the mixture separated by flash chromatography (hexanes / 50-100% diethylether). The title orange compound (99 mg, 73%) exists as a 1.3:1 mixture of **anti-5.23** to **syn-5.23**, as determined by ^{1}H NMR, which hampered full assignments of resonances. ^{1}H NMR (600 MHz, CD_2Cl_2) δ 8.09 (d, *J* = 8.4 Hz, 2H), 8.07 – 8.03 (m, 2H), 7.54 – 7.33 (m, 15H), 7.26 – 7.19 (m, 2H), 6.89 (d, *J* = 7.3 Hz, 1H), 6.65 (d, *J* = 7.3 Hz, 1H), 6.58 (d, *J* = 7.3 Hz, 1H), 6.45 (d, *J* = 7.3 Hz, 1H), 3.46 – 3.33 (m, 3H), 3.28 (dt, *J* = 13.5, 6.7 Hz, 1H), 3.02 (dq, *J* = 15.0, 7.4 Hz, 1H), 2.90 – 2.73 (m, 3H), 1.44 (d, *J* = 6.8 Hz, 2H), 1.42 (d, *J* = 6.7 Hz, 2H), 1.39 (d, *J* = 6.8 Hz, 3H), 1.35 (d, *J* = 6.8 Hz, 3H), 1.19 – 1.14 (m, 6H), 0.99 (d, *J* = 6.9 Hz, 2H), 0.94 (t, *J* = 7.5 Hz, 6H), 0.87 (d, *J* = 6.9 Hz, 3H), 0.72 (s, 3H), 0.68 (s, 2H). EA: calcd for $C_{33}H_{35}ClN_2Pd$: C 65.89, H 5.87, N 4.66; found C 65.90, H 5.97, N 4.60.

(^{vinyl}ArBIAN)$NiBr_2$ (**5.24**)

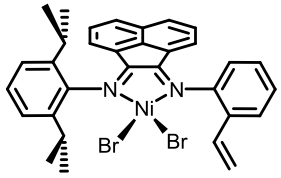

α-Diimine **5.16** (25 mg, 5.6 x 10^{-5} mol) and (dme)$NiBr_2$ (17.4 mg, 1.0 equiv.) were suspended in 3 mL dcm and stirred at room temperature overnight. The dark red solution was filtered through a short-plug of Celite, washed with 2 mL dcm, and evaporated to dryness. The

residue was added 5 mL diethyl ether and the mixture was stirred for 2 h. After decanting the solvent, the dark redbrown solid was dried *in vacuo* overnight yielding ca. 30 mg (ca. 80%). EA: calcd for $C_{32}H_{30}Br_2N_2Ni$: C 58.14, H 4.57, N 4.24; found C 58.90, H 5.01, N 4.14.

(^{allyl}ArBIAN)$NiBr_2$ (**5.25**)

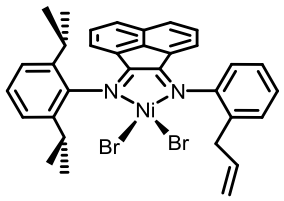

Following the above procedure, α-diimine **5.17** (150 mg) and (dme)$NiBr_2$ (101 mg, 1.0 equiv.) yielded 191 mg of the title compound as an orange-brown solid (86%). EA: calcd for $C_{33}H_{32}Br_2N_2Ni$: C 58.71, H 4.78, N 4.15; found C 58.38, H 5.03, N 4.10.

(^{ethyl}ArBIAN)$NiBr_2$ (**5.26**)

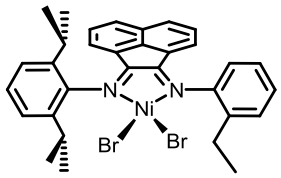

Following the above procedure, α-diimine **5.18** (0.20 mg, 0.42 mmol) and (dme)$NiBr_2$ (110 mg, 1.0 equiv.) yielded 136 mg of the title compound as an orange-brown solid (91%). EA: calcd for $C_{32}H_{32}Br_2N_2Ni$: C 57.96, H 4.86, N 4.22; found C 57.87, H 5.07, N 4.20.

(^{BPin}ArBIAN)$PdCl_2$ (**5.28**)

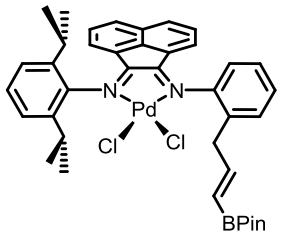

Complex **5.20** (0.10 g, 0.16 mmol) were dissolved in 10 mL dcm and vinylBPin (27 µL, 1.5 equiv.) and Grubbs 2nd generation Ru-catalyst (14 mg, 10mol%) were added and the mixture heated to reflux under a stream of dry nitrogen for 2 hours. Afterwards the reaction was cooled to room temperature, 45 mg Ph_3PO added, and stirred overnight. The volatiles were removed, the residue dissolved in diethylether and filtered through a short-plug of Celite, to give off-yellow powder as the title compound (70%). ^{1}H NMR (600 MHz, $CDCl_3$) δ 8.07 (dd, *J* = 8.2, 4.6 Hz, 2H), 7.58 – 7.41 (m, 6H), 7.36 (d, *J* = 7.9 Hz, 2H), 7.34 (d, *J* = 7.2 Hz, 1H), 6.76 (d, *J* = 7.3 Hz, 1H), 6.50 (d, *J* = 7.3 Hz, 1H), 6.46 (ddd, *J* = 17.9, 8.5, 4.1 Hz, 1H), 5.38 (d, *J* = 18.2 Hz, 1H), 4.54 (dd, *J* = 16.0, 8.4 Hz, 1H), 3.67 (vd, *J* = 15.7 Hz, 1H), 3.59 – 3.51 (m, 1H), 3.46 – 3.40 (m, 1H), 1.57 (d, *J* = 6.8 Hz, 3H), 1.47 (d, *J* = 6.7 Hz, 3H), 1.02 (d, *J* = 6.8 Hz, 3H), 0.96 (d, *J* = 6.9 Hz, 3H), 0.75 (s, 6H), 0.68 (s, 6H). EA: calcd for $C_{39}H_{43}BCl_2N_2O_2Pd$: C 61.64, H 5.70, N 3.69; found C 61.0, H 6.04, N 3.46.

(^{BPin}ArBIAN)PdMeCl (**5.29**)

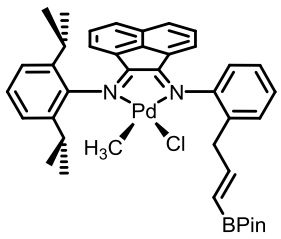

Complex 5.22 (0.17 g, 2.7 mmol) were dissolved in 15 mL dcm and vinylBPin (46 µL, 1.5 equiv.) and Grubbs 2nd generation Ru-catalyst (23 mg, 10mol%) were added and the mixture heated to reflux under a stream of dry nitrogen. The reaction progress was monitored by ESI-MS, and another portion of the Ru-catalyst (10 mol%) was added twice in one hour intervals. After 3 hours the reaction was cooled to room temperature, 250 mg Ph3PO added, and stirred overnight. The mixture was purified by silica flash chromatography (hexanes / 50-100 % diethylether) to

yield the title compound as a dark red brittle foam (86 mg, 43%). The compound exists as a 1.8:1 mixture of **anti-5.29** to **syn-5.29**, as determined by ^{1}H NMR, which hampered full assignments of resonances. ^{1}H NMR (600 MHz, CD_2Cl_2) δ 8.05 (d, *J* = 8.3 Hz, 2H), 8.01 (t, *J* = 7.8 Hz, 2H), 7.55 – 7.33 (m, 9H), 7.26 (d, *J* = 7.2 Hz, 1H), 7.24 – 7.22 (m, 1H), 6.94 (d, *J* = 7.3 Hz, 1H), 6.63 (d, *J* = 7.3 Hz, 1H), 6.58 (d, *J* = 7.4 Hz, 1H), 6.45 (d, *J* = 7.3 Hz, 1H), 6.41 (dd, *J* = 8.5, 4.2 Hz, 1H), 6.38 (dd, *J* = 8.4, 4.2 Hz, 1H), 6.30 (ddd, *J* = 17.6, 8.5, 4.4 Hz, 1H), 5.26 (d, *J* = 17.8 Hz, 2H), 4.41 (dd, *J* = 15.5, 8.6 Hz, 1H), 4.06 (d, *J* = 8.9 Hz, 1H), 3.60 – 3.51 (m, 2H), 3.46 – 3.31 (m, 3H), 3.27 – 3.19 (m, 1H), 1.49 (d, *J* = 6.8 Hz, 2H), 1.45 – 1.39 (m, 6H), 1.35 (d, *J* = 6.8 Hz, 3H), 1.20 (s, 3H), 1.03 (d, *J* = 6.9 Hz, 2H), 0.97 (d, *J* = 6.9 Hz, 3H), 0.95 (d, *J* = 6.9 Hz, 2H), 0.92 (d, *J* = 6.8 Hz, 3H), 0.88 (t, *J* = 7.2 Hz, 3H), 0.77 (s, 3H), 0.73 (s, 9H), 0.70 (s, 3H), 0.66 (s, 2H), 0.65 (s, 5H). ^{13}C NMR (126 MHz, $CDCl_3$) δ 173.27, 168.78, 167.91, 151.96, 150.92, 146.04, 145.58, 144.84, 144.77, 142.72, 141.80, 140.24, 140.03, 139.34, 139.00, 132.14, 132.03, 131.83, 131.68, 131.52, 131.26, 131.12, 129.36, 129.34, 129.24, 129.14, 128.75, 128.65, 128.57, 128.01, 127.92, 127.68, 127.63, 126.97, 126.93, 125.82, 125.79, 125.39, 125.07, 125.02, 124.30, 124.16, 122.30, 120.85, 82.98, 82.84, 40.31, 39.53, 30.62, 29.48, 29.33, 29.04, 28.99, 25.18, 24.84, 24.70, 24.60, 24.54, 24.42, 24.26, 24.09, 23.78, 23.73, 23.65, 22.89, 14.38, 3.06, 2.03, 0.13. ^{11}B NMR (160 MHz, CD_2Cl_2) δ 29.13 (broad). EA: calcd for $C_{40}H_{46}BClN_2O_2Pd$: C 64.97, H 6.27, N 3.79; found C 65.10, H 6.56, N 3.68.

5.6 References

(1) Carrow, B. P.; Nozaki, K. *Macromolecules* **2014**, *47*, 2541-2555.

(2) Zhai, F.; Jordan, R. F. *Organometallics* **2014**, *33*, 7176-7192.

(3) Thammavongsy, Z.; LeDoux, M. E.; Breuhaus-Alvarez, A. G.; Seda, T.; Zakharov, L. N.; Gilbertson, J. D. *Eur. J. Inorg. Chem.* **2013**, *2013*, 4008-4015.

(4) Tutusaus, O.; Ni, C.; Szymczak, N. K. *J. Am. Chem. Soc.* **2013**, *135*, 3403-3406.

(5) Emslie, D. J. H.; Blackwell, J. M.; Britten, J. F.; Harrington, L. E. *Organometallics* **2006**, *25*, 2412-2414.

(6) Zhang, X.; Xu, X.; Yu, L.; Zhao, Q. *Tetrahedron Lett.* **2014**, *55*, 2280-2282.

(7) Amoroso, F.; Zangrando, E.; Carfagna, C.; Muller, C.; Vogt, D.; Hagar, M.; Ragaini, F.; Milani, B. *Dalton Trans.* **2013**, *42*, 14583-14602.

(8) a) Zhang, L.; Peng, D.; Leng, X.; Huang, Z. *Angew. Chem., Int. Ed.* **2013**, *52*, 3676-3680. b) Zhang, L.; Zuo, Z.; Leng, X.; Huang, Z. *Angew. Chem., Int. Ed.* **2014**, *53*, 2696-2700. c) Pereira, S.; Srebnik, M. *Tetrahedron Lett.* **1996**, *37*, 3283-3286.

(9) Chatterjee, A. K.; Choi, T.-L.; Sanders, D. P.; Grubbs, R. H. *J. Am. Chem. Soc.* **2003**, *125*, 11360-11370.

(10) a) Leung, D. H.; Ziller, J. W.; Guan, Z. *J. Am. Chem. Soc.* **2008**, *130*, 7538-7539. b) Popeney, C. S.; Rheingold, A. L.; Guan, Z. *Organometallics* **2009**, *28*, 4452-4463. c) Popeney, C. S.; Levins, C. M.; Guan, Z. *Organometallics* **2011**, *30*, 2432-2452.

(11) Wallenhorst, C.; Kehr, G.; Frohlich, R.; Erker, G. *Organometallics* **2008**, *27*, 6557-6564.

(12) Johnson, L. K.; Killian, C. M.; Brookhart, M. *J. Am. Chem. Soc.* **1995**, *117*, 6414-6415.

(13) Chen, Y.-Y.; Zhang, X.-J.; Yuan, H.-M.; Wei, W.-T.; Yan, M. *Chem. Commun.* **2013**, *49*, 10974-10976.

(14) Yu, C.; Liu, B.; Hu, L. *J. Org. Chem.* **2001**, *66*, 919-924.

(15) Schmiege, B. M.; Carney, M. J.; Small, B. L.; Gerlach, D. L.; Halfen, J. A. *Dalton Trans.* **2007**, 2547-2562.

(16) Muñiz, K.; Hövelmann, C. H.; Streuff, J. *J. Am. Chem. Soc.* **2008**, *130*, 763-773.

(17) Salo, E. V.; Guan, Z. *Organometallics* **2003**, *22*, 5033-5046.

(18) Yakelis, N. A.; Bergman, R. G. *Organometallics* **2005**, *24*, 3579-3581.

APPENDIX

X-ray Data Collection, Structure Solution and Refinements

and

NMR Spectra of Previously Unreported Molecules

X-ray Data Collection, Structure Solution and Refinement for complex 2.5

A colorless crystal of approximate dimensions 0.215 x 0.223 x 0.275 mm was mounted on a glass fiber and transferred to a Bruker SMART APEX II diffractometer. The APEX2[1] program package was used to determine the unit-cell parameters and for data collection (30 sec/frame scan time for a sphere of diffraction data). The raw frame data was processed using SAINT[2] and SADABS[3] to yield the reflection data file. Subsequent calculations were carried out using the SHELXTL[4] program. The diffraction symmetry was 2/*m* and the systematic absences were consistent with the monoclinic space group $P2_1/c$ that was later determined to be correct.

The structure was solved by direct methods and refined on F^2 by full-matrix least-squares techniques. The analytical scattering factors[5] for neutral atoms were used throughout the analysis. Hydrogen atoms were included using a riding model.

At convergence, wR2 = 0.1175 and Goof = 1.046 for 182 variables refined against 2683 data (0.80Å), R1 = 0.0427 for those 2192 data with $I > 2.0\sigma(I)$.

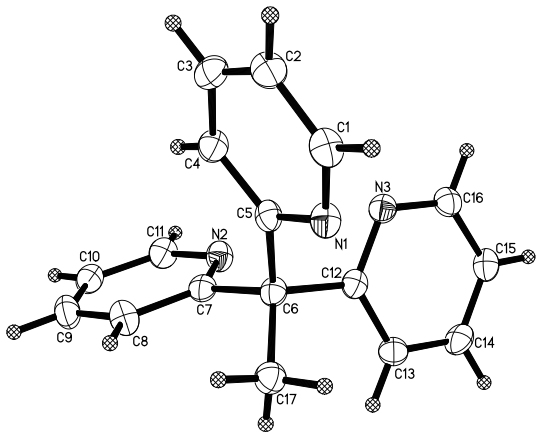

Table 1 Crystal data and structure refinement for **2.5**.

Identification code	zg42 (Tobias Friedberger)	
Empirical formula	$C_{17}H_{15}N_3$	
Formula weight	261.32	
Temperature	143(2) K	
Wavelength	0.71073 Å	
Crystal system	Monoclinic	
Space group	$P2_1/c$	
Unit cell dimensions	a = 9.2508(16) Å	α= 90°.
	b = 9.0173(15) Å	β= 95.439(2)°.
	c = 15.778(3) Å	γ = 90°.
Volume	1310.3(4) $Å^3$	
Z	4	
Density (calculated)	1.325 Mg/m^3	
Absorption coefficient	0.080 mm^{-1}	
F(000)	552	
Crystal color	colorless	
Crystal size	0.275 x 0.223 x 0.215 mm^3	
Theta range for data collection	2.211 to 26.372°	

Index ranges	$-11 \le h \le 11$, $-11 \le k \le 11$, $-19 \le l \le 19$
Reflections collected	13440
Independent reflections	2683 [R(int) = 0.0535]
Completeness to theta = 25.500°	100.0 %
Absorption correction	Numerical
Max. and min. transmission	1.0000 and 0.6604
Refinement method	Full-matrix least-squares on F^2
Data / restraints / parameters	2683 / 0 / 182
Goodness-of-fit on F^2	1.046
Final R indices [I>2sigma(I) = 2192 data]	R1 = 0.0427, wR2 = 0.1100
R indices (all data, 0.80Å)	R1 = 0.0542, wR2 = 0.1175
Largest diff. peak and hole	0.331 and -0.201 e.Å^{-3}

Table 2. Atomic coordinates (x 10^4) and equivalent isotropic displacement parameters (Å^{2}x 10^3) for **2.5**. U(eq) is defined as one third of the trace of the orthogonalized U^{ij} tensor.

	x	y	z	U(eq)
N(1)	8270(1)	-378(1)	1542(1)	23(1)
N(2)	6772(1)	3803(1)	46(1)	25(1)
N(3)	6082(1)	2302(1)	1727(1)	22(1)
C(1)	7882(2)	-1812(2)	1491(1)	26(1)
C(2)	7049(2)	-2433(2)	810(1)	28(1)
C(3)	6575(2)	-1517(2)	138(1)	28(1)
C(4)	6966(2)	-29(2)	175(1)	24(1)
C(5)	7813(2)	502(2)	884(1)	21(1)
C(6)	8283(2)	2132(2)	987(1)	21(1)
C(7)	7982(2)	2983(2)	145(1)	21(1)
C(8)	8927(2)	2876(2)	-487(1)	28(1)
C(9)	8613(2)	3643(2)	-1242(1)	29(1)
C(10)	7370(2)	4485(2)	-1352(1)	27(1)
C(11)	6483(2)	4534(2)	-697(1)	27(1)
C(12)	7415(2)	2842(2)	1666(1)	20(1)
C(13)	7982(2)	3998(2)	2181(1)	24(1)
C(14)	7136(2)	4614(2)	2767(1)	27(1)
C(15)	5756(2)	4078(2)	2832(1)	25(1)
C(16)	5286(2)	2914(2)	2301(1)	24(1)
C(17)	9923(2)	2158(2)	1274(1)	26(1)

Table 3 Bond lengths [Å] and angles [°] for **2.5**.

N(1)-C(1)	1.342(2)
N(1)-C(5)	1.3424(18)
N(2)-C(7)	1.3387(19)
N(2)-C(11)	1.3487(18)
N(3)-C(12)	1.3382(18)
N(3)-C(16)	1.3396(19)
C(1)-C(2)	1.380(2)
C(2)-C(3)	1.383(2)
C(3)-C(4)	1.389(2)
C(4)-C(5)	1.389(2)
C(5)-C(6)	1.5372(19)
C(6)-C(7)	1.5376(19)

C(6)-C(12)	1.5379(19)
C(6)-C(17)	1.541(2)
C(7)-C(8)	1.390(2)
C(8)-C(9)	1.384(2)
C(9)-C(10)	1.375(2)
C(10)-C(11)	1.379(2)
C(12)-C(13)	1.3928(19)
C(13)-C(14)	1.384(2)
C(14)-C(15)	1.378(2)
C(15)-C(16)	1.387(2)

C(1)-N(1)-C(5)	117.45(12)
C(7)-N(2)-C(11)	117.80(12)
C(12)-N(3)-C(16)	117.90(13)
N(1)-C(1)-C(2)	124.29(14)
C(1)-C(2)-C(3)	117.90(14)
C(2)-C(3)-C(4)	118.83(14)
C(3)-C(4)-C(5)	119.44(14)
N(1)-C(5)-C(4)	122.09(13)
N(1)-C(5)-C(6)	114.72(12)
C(4)-C(5)-C(6)	123.18(12)
C(5)-C(6)-C(7)	111.07(11)
C(5)-C(6)-C(12)	108.12(11)
C(7)-C(6)-C(12)	109.28(11)
C(5)-C(6)-C(17)	107.86(11)
C(7)-C(6)-C(17)	109.78(11)
C(12)-C(6)-C(17)	110.72(11)
N(2)-C(7)-C(8)	122.04(13)
N(2)-C(7)-C(6)	117.26(12)
C(8)-C(7)-C(6)	120.69(13)
C(9)-C(8)-C(7)	119.15(14)
C(10)-C(9)-C(8)	119.30(14)
C(9)-C(10)-C(11)	118.24(14)
N(2)-C(11)-C(10)	123.47(14)
N(3)-C(12)-C(13)	121.98(13)
N(3)-C(12)-C(6)	116.35(12)
C(13)-C(12)-C(6)	121.67(13)
C(14)-C(13)-C(12)	118.97(14)
C(15)-C(14)-C(13)	119.69(14)
C(14)-C(15)-C(16)	117.47(13)
N(3)-C(16)-C(15)	123.98(14)

Table 4 Anisotropic displacement parameters ($Å^2 x\ 10^3$) for **2.5**. The anisotropic displacement factor exponent takes the form: $-2\pi^2[\ h^2\ a^{*2}U^{11} + ...\ + 2\ h\ k\ a^*\ b^*\ U^{12}\ ]$

	U^{11}	U^{22}	U^{33}	U^{23}	U^{13}	U^{12}
N(1)	29(1)	20(1)	22(1)	1(1)	4(1)	3(1)
N(2)	30(1)	22(1)	22(1)	2(1)	4(1)	2(1)
N(3)	27(1)	18(1)	22(1)	0(1)	2(1)	-1(1)
C(1)	31(1)	20(1)	27(1)	4(1)	6(1)	5(1)
C(2)	35(1)	17(1)	33(1)	-2(1)	9(1)	0(1)
C(3)	34(1)	24(1)	27(1)	-6(1)	3(1)	-2(1)

C(4)	30(1)	21(1)	22(1)	1(1)	3(1)	0(1)
C(5)	25(1)	18(1)	20(1)	-1(1)	6(1)	2(1)
C(6)	25(1)	18(1)	19(1)	-1(1)	3(1)	0(1)
C(7)	26(1)	15(1)	22(1)	-1(1)	3(1)	-2(1)
C(8)	31(1)	26(1)	28(1)	3(1)	8(1)	3(1)
C(9)	38(1)	27(1)	24(1)	0(1)	12(1)	-4(1)
C(10)	38(1)	20(1)	21(1)	2(1)	2(1)	-5(1)
C(11)	34(1)	22(1)	25(1)	3(1)	2(1)	2(1)
C(12)	26(1)	16(1)	18(1)	2(1)	2(1)	1(1)
C(13)	28(1)	20(1)	25(1)	-1(1)	3(1)	-3(1)
C(14)	37(1)	19(1)	24(1)	-4(1)	0(1)	-2(1)
C(15)	34(1)	19(1)	22(1)	0(1)	6(1)	4(1)
C(16)	28(1)	20(1)	25(1)	1(1)	6(1)	-1(1)
C(17)	27(1)	26(1)	25(1)	-1(1)	3(1)	0(1)

Table 5 Hydrogen coordinates (x 10^4) and isotropic displacement parameters ($Å^2$x 10^3)for **2.5**.

	x	y	z	U(eq)
H(1A)	8202	-2440	1955	31
H(2A)	6809	-3458	804	33
H(3A)	5992	-1898	-341	34
H(4A)	6657	619	-281	29
H(8A)	9778	2284	-401	33
H(9A)	9249	3588	-1679	35
H(10A)	7129	5018	-1865	32
H(11A)	5623	5114	-773	32
H(13A)	8936	4358	2130	29
H(14A)	7505	5403	3124	32
H(15A)	5150	4491	3224	30
H(16A)	4342	2526	2348	29
H(17A)	10277	3182	1270	39
H(17B)	10441	1558	882	39
H(17C)	10093	1751	1850	39

X-ray Data Collection, Structure Solution and Refinement for complex 2.15

An orange crystal of approximate dimensions 0.277 x 0.076 x 0.065 mm was mounted on a glass fiber and transferred to a Bruker SMART APEX II diffractometer. The APEX2[1] program package was used to determine the unit-cell parameters and for data collection (30 sec/frame scan time for a sphere of diffraction data). The raw frame data was processed using SAINT[2] and SADABS[3] to yield the reflection data file. Subsequent calculations were carried out using the SHELXTL[4] program. There were no systematic absences nor any diffraction symmetry other than the Friedel condition. The centrosymmetric triclinic space group $P\bar{1}$ was assigned and later determined to be correct.

The structure was solved by direct methods and refined on F^2 by full-matrix least-squares techniques. The analytical scattering factors[5] for neutral atoms were used throughout the analysis. Hydrogen atoms were included using a riding model.

At convergence, wR2 = 0.0704 and Goof = 1.031 for 442 variables refined against 7671 data (0.75 Å), R1 = 0.0305 for those 6392 data with $I > 2.0\sigma(I)$.

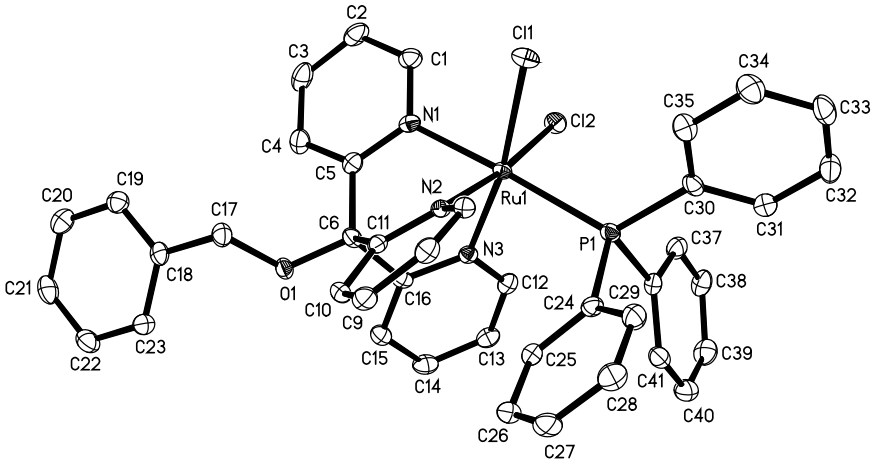

Table 6 Crystal data and structure refinement for **2.15**

Identification code	zg37 (Tobias Friedberger)	
Empirical formula	$C_{41}H_{34}Cl_2N_3OPRu$	
Formula weight	787.65	
Temperature	143(2) K	
Wavelength	0.71073 Å	
Crystal system	Triclinic	
Space group	$P\bar{1}$	
Unit cell dimensions	a = 9.2383(6) Å	α= 92.0729(8)°.
	b = 12.9817(9) Å	β= 100.8971(8)°.
	c = 14.9981(10) Å	γ = 107.3651(8)°.
Volume	1677.52(19) $Å^3$	
Z	2	
Density (calculated)	1.559 Mg/m^3	
Absorption coefficient	0.714 mm^{-1}	
F(000)	804	
Crystal color	orange	
Crystal size	0.277 x 0.076 x 0.065 mm^3	
Theta range for data collection	1.389 to 28.404°	
Index ranges	$-12 \le h \le 12$, $-17 \le k \le 17$, $-19 \le l \le 20$	
Reflections collected	19390	
Independent reflections	7671 [R(int) = 0.0302]	
Completeness to theta = 25.500°	99.8 %	
Absorption correction	Numerical	
Max. and min. transmission	1.0000 and 0.8495	
Refinement method	Full-matrix least-squares on F^2	
Data / restraints / parameters	7671 / 0 / 442	
Goodness-of-fit on F^2	1.031	
Final R indices [I>2sigma(I) = 6392 data]	R1 = 0.0305, wR2 = 0.0663	

R indices (all data, 0.75 Å)	R1 = 0.0419, wR2 = 0.0704
Largest diff. peak and hole	0.789 and -0.969 e.Å^{-3}

Table 7. Atomic coordinates (x 10^4) and equivalent isotropic displacement parameters (Å^{2}x 10^3) for **2.15**. U(eq) is defined as one third of the trace of the orthogonalized U^{ij} tensor.

	x	y	z	U(eq)
Ru(1)	8835(1)	8715(1)	7542(1)	12(1)
Cl(1)	9988(1)	7825(1)	8729(1)	20(1)
Cl(2)	11148(1)	9139(1)	6915(1)	18(1)
P(1)	7537(1)	7134(1)	6505(1)	14(1)
O(1)	6716(2)	11287(1)	8199(1)	16(1)
N(1)	9891(2)	10129(2)	8411(1)	14(1)
N(2)	7018(2)	8536(1)	8179(1)	13(1)
N(3)	7987(2)	9713(1)	6662(1)	13(1)
C(1)	11401(3)	10402(2)	8832(2)	19(1)
C(2)	12196(3)	11426(2)	9258(2)	24(1)
C(3)	11450(3)	12205(2)	9218(2)	26(1)
C(4)	9895(3)	11915(2)	8803(2)	20(1)
C(5)	9116(3)	10846(2)	8447(2)	15(1)
C(6)	7378(2)	10473(2)	8000(2)	15(1)
C(7)	6261(2)	7581(2)	8460(2)	15(1)
C(8)	4851(3)	7397(2)	8711(2)	18(1)
C(9)	4144(3)	8200(2)	8637(2)	18(1)
C(10)	4955(2)	9200(2)	8409(2)	16(1)
C(11)	6437(2)	9363(2)	8238(1)	13(1)
C(12)	8108(3)	9735(2)	5780(2)	16(1)
C(13)	7456(3)	10333(2)	5179(2)	18(1)
C(14)	6657(3)	10965(2)	5494(2)	21(1)
C(15)	6599(3)	11010(2)	6410(2)	17(1)
C(16)	7288(2)	10395(2)	6974(2)	13(1)
C(17)	6729(3)	11563(2)	9153(2)	18(1)
C(18)	6677(3)	12711(2)	9233(2)	16(1)
C(19)	7798(3)	13510(2)	9852(2)	19(1)
C(20)	7688(3)	14555(2)	9933(2)	23(1)
C(21)	6462(3)	14800(2)	9399(2)	24(1)
C(22)	5354(3)	14017(2)	8776(2)	23(1)
C(23)	5455(3)	12974(2)	8694(2)	19(1)
C(24)	5450(2)	6679(2)	6500(2)	16(1)
C(25)	4668(3)	7453(2)	6411(2)	16(1)
C(26)	3117(3)	7189(2)	6466(2)	19(1)
C(27)	2327(3)	6141(2)	6614(2)	23(1)
C(28)	3072(3)	5360(2)	6684(2)	23(1)
C(29)	4625(3)	5621(2)	6626(2)	20(1)
C(30)	8024(2)	5858(2)	6623(2)	16(1)
C(31)	8006(3)	5190(2)	5872(2)	21(1)
C(32)	8321(3)	4214(2)	5992(2)	26(1)
C(33)	8635(3)	3892(2)	6854(2)	24(1)
C(34)	8627(3)	4535(2)	7600(2)	25(1)
C(35)	8332(3)	5517(2)	7487(2)	21(1)
C(36)	7516(3)	7261(2)	5283(2)	15(1)
C(37)	8930(3)	7535(2)	4990(2)	20(1)
C(38)	8968(3)	7707(2)	4089(2)	22(1)

C(39)	7617(3)	7607(2)	3459(2)	24(1)
C(40)	6206(3)	7295(2)	3732(2)	23(1)
C(41)	6160(3)	7127(2)	4638(2)	19(1)

Table 8 Bond lengths [Å] and angles [°] for **2.15**.

Ru(1)-N(2)	2.0436(18)
Ru(1)-N(1)	2.0732(19)
Ru(1)-N(3)	2.0913(18)
Ru(1)-P(1)	2.3805(6)
Ru(1)-Cl(1)	2.4093(6)
Ru(1)-Cl(2)	2.4185(6)
P(1)-C(24)	1.839(2)
P(1)-C(36)	1.842(2)
P(1)-C(30)	1.847(2)
O(1)-C(6)	1.418(3)
O(1)-C(17)	1.459(3)
N(1)-C(5)	1.339(3)
N(1)-C(1)	1.351(3)
N(2)-C(11)	1.343(3)
N(2)-C(7)	1.355(3)
N(3)-C(12)	1.350(3)
N(3)-C(16)	1.358(3)
C(1)-C(2)	1.375(3)
C(2)-C(3)	1.381(4)
C(3)-C(4)	1.384(3)
C(4)-C(5)	1.390(3)
C(5)-C(6)	1.538(3)
C(6)-C(16)	1.523(3)
C(6)-C(11)	1.538(3)
C(7)-C(8)	1.379(3)
C(8)-C(9)	1.384(3)
C(9)-C(10)	1.383(3)
C(10)-C(11)	1.397(3)
C(12)-C(13)	1.379(3)
C(13)-C(14)	1.381(3)
C(14)-C(15)	1.386(3)
C(15)-C(16)	1.382(3)
C(17)-C(18)	1.507(3)
C(18)-C(19)	1.391(3)
C(18)-C(23)	1.397(3)
C(19)-C(20)	1.393(3)
C(20)-C(21)	1.385(3)
C(21)-C(22)	1.379(4)
C(22)-C(23)	1.387(3)
C(24)-C(29)	1.397(3)
C(24)-C(25)	1.398(3)
C(25)-C(26)	1.390(3)
C(26)-C(27)	1.388(3)
C(27)-C(28)	1.381(3)
C(28)-C(29)	1.393(3)
C(30)-C(35)	1.391(3)
C(30)-C(31)	1.391(3)
C(31)-C(32)	1.393(3)

C(32)-C(33)	1.377(4)
C(33)-C(34)	1.375(3)
C(34)-C(35)	1.391(3)
C(36)-C(41)	1.391(3)
C(36)-C(37)	1.407(3)
C(37)-C(38)	1.382(3)
C(38)-C(39)	1.385(3)
C(39)-C(40)	1.389(3)
C(40)-C(41)	1.390(3)

N(2)-Ru(1)-N(1)	85.21(7)
N(2)-Ru(1)-N(3)	89.78(7)
N(1)-Ru(1)-N(3)	84.59(7)
N(2)-Ru(1)-P(1)	93.84(5)
N(1)-Ru(1)-P(1)	177.18(5)
N(3)-Ru(1)-P(1)	92.76(5)
N(2)-Ru(1)-Cl(1)	88.78(5)
N(1)-Ru(1)-Cl(1)	86.12(5)
N(3)-Ru(1)-Cl(1)	170.69(5)
P(1)-Ru(1)-Cl(1)	96.52(2)
N(2)-Ru(1)-Cl(2)	172.71(5)
N(1)-Ru(1)-Cl(2)	87.49(5)
N(3)-Ru(1)-Cl(2)	89.50(5)
P(1)-Ru(1)-Cl(2)	93.45(2)
Cl(1)-Ru(1)-Cl(2)	90.77(2)
C(24)-P(1)-C(36)	101.23(10)
C(24)-P(1)-C(30)	101.83(10)
C(36)-P(1)-C(30)	100.05(10)
C(24)-P(1)-Ru(1)	110.63(7)
C(36)-P(1)-Ru(1)	117.62(7)
C(30)-P(1)-Ru(1)	122.46(8)
C(6)-O(1)-C(17)	117.81(16)
C(5)-N(1)-C(1)	119.7(2)
C(5)-N(1)-Ru(1)	118.42(15)
C(1)-N(1)-Ru(1)	121.13(16)
C(11)-N(2)-C(7)	117.93(18)
C(11)-N(2)-Ru(1)	118.82(14)
C(7)-N(2)-Ru(1)	122.87(14)
C(12)-N(3)-C(16)	116.61(19)
C(12)-N(3)-Ru(1)	123.37(15)
C(16)-N(3)-Ru(1)	120.02(14)
N(1)-C(1)-C(2)	121.6(2)
C(1)-C(2)-C(3)	119.0(2)
C(2)-C(3)-C(4)	119.0(2)
C(3)-C(4)-C(5)	119.4(2)
N(1)-C(5)-C(4)	120.5(2)
N(1)-C(5)-C(6)	117.61(19)
C(4)-C(5)-C(6)	121.6(2)
O(1)-C(6)-C(16)	106.71(17)
O(1)-C(6)-C(11)	110.97(17)
C(16)-C(6)-C(11)	107.83(18)
O(1)-C(6)-C(5)	109.61(17)
C(16)-C(6)-C(5)	106.00(17)
C(11)-C(6)-C(5)	115.25(18)
N(2)-C(7)-C(8)	122.6(2)

C(7)-C(8)-C(9)	118.9(2)
C(10)-C(9)-C(8)	118.5(2)
C(9)-C(10)-C(11)	119.5(2)
N(2)-C(11)-C(10)	121.3(2)
N(2)-C(11)-C(6)	117.73(18)
C(10)-C(11)-C(6)	120.62(19)
N(3)-C(12)-C(13)	123.7(2)
C(12)-C(13)-C(14)	118.8(2)
C(13)-C(14)-C(15)	118.6(2)
C(16)-C(15)-C(14)	119.4(2)
N(3)-C(16)-C(15)	122.6(2)
N(3)-C(16)-C(6)	115.28(18)
C(15)-C(16)-C(6)	122.1(2)
O(1)-C(17)-C(18)	106.91(18)
C(19)-C(18)-C(23)	119.1(2)
C(19)-C(18)-C(17)	121.4(2)
C(23)-C(18)-C(17)	119.4(2)
C(18)-C(19)-C(20)	120.1(2)
C(21)-C(20)-C(19)	120.1(2)
C(22)-C(21)-C(20)	120.3(2)
C(21)-C(22)-C(23)	119.9(2)
C(22)-C(23)-C(18)	120.5(2)
C(29)-C(24)-C(25)	118.4(2)
C(29)-C(24)-P(1)	123.73(17)
C(25)-C(24)-P(1)	117.79(17)
C(26)-C(25)-C(24)	121.2(2)
C(27)-C(26)-C(25)	119.6(2)
C(28)-C(27)-C(26)	120.0(2)
C(27)-C(28)-C(29)	120.6(2)
C(28)-C(29)-C(24)	120.3(2)
C(35)-C(30)-C(31)	118.5(2)
C(35)-C(30)-P(1)	119.17(18)
C(31)-C(30)-P(1)	122.26(18)
C(30)-C(31)-C(32)	120.3(2)
C(33)-C(32)-C(31)	120.5(2)
C(34)-C(33)-C(32)	119.8(2)
C(33)-C(34)-C(35)	120.1(2)
C(30)-C(35)-C(34)	120.9(2)
C(41)-C(36)-C(37)	118.2(2)
C(41)-C(36)-P(1)	122.79(17)
C(37)-C(36)-P(1)	118.95(17)
C(38)-C(37)-C(36)	120.5(2)
C(37)-C(38)-C(39)	120.7(2)
C(38)-C(39)-C(40)	119.4(2)
C(39)-C(40)-C(41)	120.2(2)
C(40)-C(41)-C(36)	120.9(2)

Table 9 Anisotropic displacement parameters ($Å^2 x\ 10^3$) for **2.15**. The anisotropic displacement factor exponent takes the form: $-2\pi^2[\ h^2\ a^{*2}U^{11} + ...\ + 2\ h\ k\ a^*\ b^*\ U^{12}\ ]$

	U^{11}	U^{22}	U^{33}	U^{23}	U^{13}	U^{12}
Ru(1)	9(1)	13(1)	13(1)	2(1)	2(1)	4(1)
Cl(1)	16(1)	23(1)	22(1)	7(1)	2(1)	9(1)

Cl(2)	12(1)	24(1)	20(1)	1(1)	6(1)	5(1)
P(1)	11(1)	14(1)	16(1)	1(1)	3(1)	4(1)
O(1)	19(1)	16(1)	15(1)	1(1)	4(1)	9(1)
N(1)	11(1)	18(1)	12(1)	2(1)	2(1)	3(1)
N(2)	11(1)	15(1)	11(1)	1(1)	1(1)	5(1)
N(3)	10(1)	12(1)	14(1)	1(1)	2(1)	2(1)
C(1)	14(1)	25(1)	18(1)	1(1)	3(1)	5(1)
C(2)	13(1)	31(1)	21(1)	-6(1)	1(1)	0(1)
C(3)	23(1)	21(1)	27(1)	-9(1)	6(1)	-2(1)
C(4)	19(1)	18(1)	23(1)	-2(1)	7(1)	4(1)
C(5)	16(1)	16(1)	13(1)	2(1)	5(1)	4(1)
C(6)	14(1)	13(1)	18(1)	2(1)	3(1)	6(1)
C(7)	15(1)	15(1)	14(1)	1(1)	2(1)	6(1)
C(8)	17(1)	17(1)	16(1)	1(1)	4(1)	2(1)
C(9)	12(1)	23(1)	18(1)	-1(1)	4(1)	3(1)
C(10)	13(1)	17(1)	18(1)	0(1)	3(1)	7(1)
C(11)	13(1)	16(1)	11(1)	0(1)	1(1)	4(1)
C(12)	14(1)	14(1)	16(1)	0(1)	4(1)	0(1)
C(13)	18(1)	20(1)	15(1)	3(1)	3(1)	2(1)
C(14)	20(1)	21(1)	19(1)	7(1)	0(1)	6(1)
C(15)	17(1)	16(1)	20(1)	3(1)	4(1)	6(1)
C(16)	9(1)	13(1)	17(1)	2(1)	2(1)	1(1)
C(17)	21(1)	18(1)	16(1)	2(1)	6(1)	8(1)
C(18)	19(1)	18(1)	14(1)	3(1)	9(1)	7(1)
C(19)	19(1)	22(1)	17(1)	3(1)	4(1)	6(1)
C(20)	26(1)	19(1)	20(1)	-1(1)	3(1)	3(1)
C(21)	32(1)	18(1)	29(1)	4(1)	11(1)	13(1)
C(22)	24(1)	26(1)	24(1)	6(1)	5(1)	14(1)
C(23)	17(1)	22(1)	17(1)	0(1)	2(1)	6(1)
C(24)	11(1)	18(1)	16(1)	-1(1)	2(1)	3(1)
C(25)	16(1)	16(1)	15(1)	-1(1)	2(1)	4(1)
C(26)	16(1)	23(1)	19(1)	0(1)	1(1)	9(1)
C(27)	11(1)	30(1)	25(1)	-1(1)	4(1)	3(1)
C(28)	16(1)	18(1)	30(1)	1(1)	5(1)	-1(1)
C(29)	18(1)	18(1)	24(1)	-1(1)	4(1)	5(1)
C(30)	11(1)	15(1)	24(1)	1(1)	4(1)	5(1)
C(31)	20(1)	20(1)	22(1)	-1(1)	0(1)	8(1)
C(32)	26(1)	20(1)	29(1)	-6(1)	4(1)	9(1)
C(33)	23(1)	14(1)	35(2)	2(1)	7(1)	7(1)
C(34)	29(1)	23(1)	26(1)	8(1)	8(1)	10(1)
C(35)	22(1)	20(1)	23(1)	2(1)	8(1)	8(1)
C(36)	17(1)	13(1)	15(1)	-1(1)	4(1)	4(1)
C(37)	17(1)	18(1)	22(1)	-3(1)	3(1)	3(1)
C(38)	21(1)	19(1)	23(1)	-3(1)	9(1)	1(1)
C(39)	32(1)	26(1)	17(1)	3(1)	6(1)	9(1)
C(40)	23(1)	27(1)	20(1)	2(1)	2(1)	11(1)
C(41)	18(1)	19(1)	21(1)	2(1)	4(1)	8(1)

Table 10 Hydrogen coordinates (x 10^4) and isotropic displacement parameters ($Å^2$x 10^3) for **2.15**.

	x	y	z	U(eq)
H(1A)	11927	9875	8833	23

H(2A)	13243	11594	9576	28
H(3A)	11996	12930	9472	31
H(4A)	9365	12441	8761	24
H(7A)	6720	7015	8486	18
H(8A)	4373	6729	8932	21
H(9A)	3124	8068	8740	22
H(10A)	4507	9772	8368	19
H(12A)	8674	9314	5561	19
H(13A)	7555	10310	4560	22
H(14A)	6158	11362	5090	25
H(15A)	6089	11460	6648	21
H(17A)	7682	11506	9551	21
H(17B)	5819	11063	9337	21
H(19A)	8640	13343	10219	23
H(20A)	8455	15099	10356	28
H(21A)	6383	15511	9461	29
H(22A)	4523	14191	8405	28
H(23A)	4688	12435	8266	22
H(25A)	5208	8172	6313	19
H(26A)	2601	7723	6401	23
H(27A)	1274	5960	6668	27
H(28A)	2520	4640	6773	28
H(29A)	5125	5077	6673	24
H(31A)	7777	5400	5274	25
H(32A)	8320	3766	5477	31
H(33A)	8857	3228	6932	28
H(34A)	8823	4308	8194	30
H(35A)	8340	5961	8007	25
H(37A)	9866	7602	5414	24
H(38A)	9932	7896	3901	26
H(39A)	7654	7750	2846	29
H(40A)	5270	7196	3299	27
H(41A)	5190	6918	4818	22

X-ray Data Collection, Structure Solution and Refinement for complex 2.16.

An orange crystal of approximate dimensions 0.071 x 0.188 x 0.193 mm was mounted on a glass fiber and transferred to a Bruker SMART APEX II diffractometer. The APEX2[1] program package was used to determine the unit-cell parameters and for data collection (30 sec/frame scan time for a sphere of diffraction data). The raw frame data was processed using SAINT[2] and SADABS[3] to yield the reflection data file. Subsequent calculations were carried out using the SHELXTL[4] program. The diffraction symmetry was 2/*m* and the systematic absences were consistent with the monoclinic space group $P2_1/c$ that was later determined to be correct.

The structure was solved by direct methods and refined on F^2 by full-matrix least-squares techniques. The analytical scattering factors[5] for neutral atoms were used throughout the analysis. Hydrogen atoms were included using a riding model. There was a mixture of approximately 35% $CDCl_3$ and 65% CH_2Cl_2 solvent present. The solvents were disordered and included using partial site-occupancy-factors. The mass contribution from deuterium was not included.

At convergence, wR2 = 0.0733 and Goof = 1.028 for 443 variables refined against 7857 data (0.75Å), R1 = 0.0289 for those 6680 data with I > 2.0σ(I).

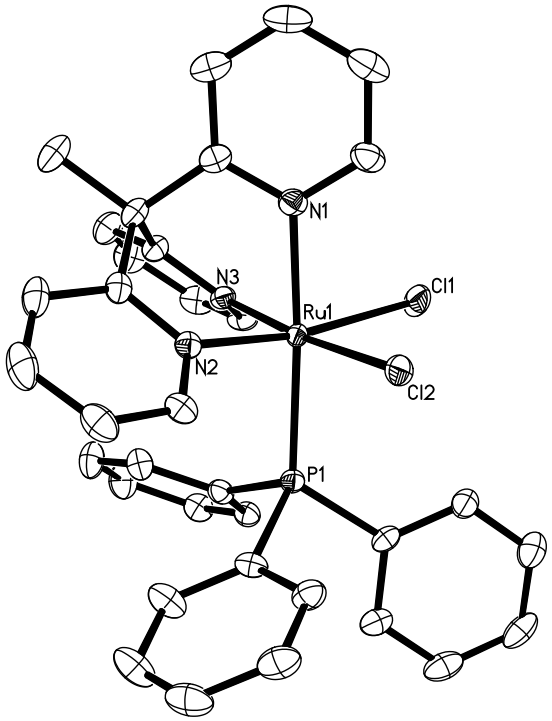

Figure 1 The thermal ellipsoid plot of **2.16** shown at the 50% probability level. Hydrogen atoms, and cocrystallized solvent are omitted for clarity.

Table 11 Crystal data and structure refinement for **2.16**.

Identification code	zg41	
Empirical formula	$C_{35}\ H_{30}\ Cl_2\ N_3\ P\ Ru \bullet (CH_2Cl_2)_{0.65} \bullet (CDCl_3)_{0.35}$	
Formula weight	792.54	
Temperature	143(2) K	
Wavelength	0.71073 Å	
Crystal system	Monoclinic	
Space group	$P2_1/c$	
Unit cell dimensions	a = 17.7137(10) Å	α= 90°.
	b = 10.7907(6) Å	β= 92.5214(7)°.
	c = 17.3209(10) Å	γ = 90°.
Volume	3307.6(3) $Å^3$	
Z	4	
Density (calculated)	1.592 Mg/m^3	
Absorption coefficient	0.906 mm^{-1}	
F(000)	1606	
Crystal color	orange	
Crystal size	0.193 x 0.188 x 0.071 mm^3	
Theta range for data collection	2.211 to 28.291°	
Index ranges	$-23 \le h \le 23$, $-14 \le k \le 14$, $-22 \le l \le 22$	

Reflections collected	37564
Independent reflections	7857 [R(int) = 0.0297]
Completeness to theta = 25.500°	99.9 %
Absorption correction	Numerical
Max. and min. transmission	1.0000 and 0.8633
Refinement method	Full-matrix least-squares on F^2
Data / restraints / parameters	7857 / 0 / 443
Goodness-of-fit on F^2	1.028
Final R indices [I>2sigma(I) = 6680 data]	R1 = 0.0289, wR2 = 0.0692
R indices (all data, 0.75Å)	R1 = 0.0377, wR2 = 0.0733
Largest diff. peak and hole	0.880 and -0.767 e.$Å^{-3}$

Table 12. Atomic coordinates (x 10^4) and equivalent isotropic displacement parameters ($Å^2$x 10^3) for **2.16**. U(eq) is defined as one third of the trace of the orthogonalized U^{ij} tensor.

	x	y	z	U(eq)
Ru(1)	-3151(1)	5961(1)	3615(1)	14(1)
Cl(1)	-3262(1)	8209(1)	3532(1)	30(1)
Cl(2)	-2748(1)	6140(1)	4965(1)	24(1)
P(1)	-1879(1)	5863(1)	3272(1)	15(1)
N(1)	-4284(1)	5928(2)	3894(1)	19(1)
N(2)	-3236(1)	4079(2)	3726(1)	16(1)
N(3)	-3584(1)	5874(2)	2502(1)	16(1)
C(1)	-4544(1)	6709(2)	4430(1)	26(1)
C(2)	-5288(1)	6707(3)	4635(1)	32(1)
C(3)	-5784(1)	5878(3)	4283(2)	34(1)
C(4)	-5521(1)	5080(2)	3728(2)	30(1)
C(5)	-4765(1)	5114(2)	3542(1)	21(1)
C(6)	-4432(1)	4235(2)	2940(1)	20(1)
C(7)	-3808(1)	3459(2)	3348(1)	18(1)
C(8)	-3839(2)	2173(2)	3375(1)	27(1)
C(9)	-3305(2)	1501(2)	3812(2)	33(1)
C(10)	-2762(1)	2150(2)	4238(1)	27(1)
C(11)	-2748(1)	3423(2)	4186(1)	20(1)
C(12)	-4122(1)	5038(2)	2296(1)	19(1)
C(13)	-4399(1)	4946(2)	1532(1)	27(1)
C(14)	-4131(2)	5733(2)	975(1)	30(1)
C(15)	-3604(1)	6623(2)	1194(1)	27(1)
C(16)	-3351(1)	6667(2)	1956(1)	20(1)
C(17)	-5053(1)	3379(2)	2604(1)	31(1)
C(18)	-1202(1)	7126(2)	3466(1)	18(1)
C(19)	-1395(1)	8200(2)	3846(1)	22(1)
C(20)	-855(1)	9124(2)	3991(1)	30(1)
C(21)	-122(1)	8967(2)	3769(1)	30(1)
C(22)	78(1)	7890(2)	3407(1)	29(1)
C(23)	-453(1)	6975(2)	3249(1)	24(1)
C(24)	-1294(1)	4589(2)	3694(1)	19(1)
C(25)	-1039(1)	4705(2)	4464(1)	24(1)
C(26)	-623(1)	3758(2)	4818(2)	30(1)
C(27)	-449(1)	2700(2)	4415(2)	33(1)
C(28)	-689(2)	2586(2)	3651(2)	34(1)
C(29)	-1112(1)	3531(2)	3291(1)	28(1)
C(30)	-1825(1)	5594(2)	2230(1)	18(1)

C(31)	-1514(1)	6452(2)	1732(1)	20(1)
C(32)	-1598(1)	6307(2)	939(1)	23(1)
C(33)	-1984(2)	5288(2)	631(1)	30(1)
C(34)	-2279(2)	4409(2)	1119(1)	30(1)
C(35)	-2205(1)	4567(2)	1912(1)	22(1)
C(36)	-1863(5)	11(8)	1554(6)	35(2)
Cl(3)	-1985(1)	1631(2)	1332(2)	54(1)
Cl(4)	-2404(2)	-365(2)	2305(2)	54(1)
Cl(5)	-934(7)	-310(7)	1752(5)	34(1)
C(37)	-2036(2)	-272(4)	1872(2)	26(1)
Cl(6)	-2425(1)	1228(1)	1929(1)	58(1)
Cl(7)	-1072(4)	-246(5)	1779(4)	59(2)

Table 13. Bond lengths [Å] and angles [°] for **2.16**.

Ru(1)-N(3)	2.0450(17)
Ru(1)-N(2)	2.0462(17)
Ru(1)-N(1)	2.0856(18)
Ru(1)-P(1)	2.3574(6)
Ru(1)-Cl(2)	2.4228(5)
Ru(1)-Cl(1)	2.4368(6)
P(1)-C(30)	1.836(2)
P(1)-C(18)	1.837(2)
P(1)-C(24)	1.852(2)
N(1)-C(1)	1.349(3)
N(1)-C(5)	1.351(3)
N(2)-C(11)	1.351(3)
N(2)-C(7)	1.358(3)
N(3)-C(12)	1.350(3)
N(3)-C(16)	1.353(3)
C(1)-C(2)	1.380(3)
C(2)-C(3)	1.377(4)
C(3)-C(4)	1.386(4)
C(4)-C(5)	1.391(3)
C(5)-C(6)	1.546(3)
C(6)-C(17)	1.531(3)
C(6)-C(12)	1.534(3)
C(6)-C(7)	1.535(3)
C(7)-C(8)	1.390(3)
C(8)-C(9)	1.389(4)
C(9)-C(10)	1.378(4)
C(10)-C(11)	1.377(3)
C(12)-C(13)	1.394(3)
C(13)-C(14)	1.385(3)
C(14)-C(15)	1.381(4)
C(15)-C(16)	1.375(3)
C(18)-C(19)	1.383(3)
C(18)-C(23)	1.403(3)
C(19)-C(20)	1.398(3)
C(20)-C(21)	1.381(4)
C(21)-C(22)	1.375(4)
C(22)-C(23)	1.383(3)
C(24)-C(29)	1.384(3)
C(24)-C(25)	1.395(3)

C(25)-C(26)	1.386(3)
C(26)-C(27)	1.380(4)
C(27)-C(28)	1.377(4)
C(28)-C(29)	1.397(3)
C(30)-C(31)	1.395(3)
C(30)-C(35)	1.397(3)
C(31)-C(32)	1.383(3)
C(32)-C(33)	1.389(3)
C(33)-C(34)	1.387(3)
C(34)-C(35)	1.383(3)
C(36)-Cl(5)	1.701(14)
C(36)-Cl(4)	1.699(10)
C(36)-Cl(3)	1.801(10)
C(37)-Cl(7)	1.723(8)
C(37)-Cl(6)	1.763(4)

N(3)-Ru(1)-N(2)	90.94(7)
N(3)-Ru(1)-N(1)	83.87(7)
N(2)-Ru(1)-N(1)	83.41(7)
N(3)-Ru(1)-P(1)	94.77(5)
N(2)-Ru(1)-P(1)	93.10(5)
N(1)-Ru(1)-P(1)	176.23(5)
N(3)-Ru(1)-Cl(2)	174.83(5)
N(2)-Ru(1)-Cl(2)	90.47(5)
N(1)-Ru(1)-Cl(2)	91.35(5)
P(1)-Ru(1)-Cl(2)	90.112(19)
N(3)-Ru(1)-Cl(1)	87.96(5)
N(2)-Ru(1)-Cl(1)	170.81(5)
N(1)-Ru(1)-Cl(1)	87.39(5)
P(1)-Ru(1)-Cl(1)	96.08(2)
Cl(2)-Ru(1)-Cl(1)	89.86(2)
C(30)-P(1)-C(18)	103.57(10)
C(30)-P(1)-C(24)	102.64(10)
C(18)-P(1)-C(24)	97.41(10)
C(30)-P(1)-Ru(1)	110.26(7)
C(18)-P(1)-Ru(1)	122.98(7)
C(24)-P(1)-Ru(1)	117.31(7)
C(1)-N(1)-C(5)	119.26(19)
C(1)-N(1)-Ru(1)	120.65(15)
C(5)-N(1)-Ru(1)	120.09(14)
C(11)-N(2)-C(7)	118.06(18)
C(11)-N(2)-Ru(1)	121.86(14)
C(7)-N(2)-Ru(1)	120.05(14)
C(12)-N(3)-C(16)	118.05(18)
C(12)-N(3)-Ru(1)	120.79(14)
C(16)-N(3)-Ru(1)	121.14(14)
N(1)-C(1)-C(2)	122.3(2)
C(3)-C(2)-C(1)	119.1(2)
C(2)-C(3)-C(4)	118.9(2)
C(3)-C(4)-C(5)	120.1(2)
N(1)-C(5)-C(4)	120.5(2)
N(1)-C(5)-C(6)	116.84(18)
C(4)-C(5)-C(6)	122.7(2)
C(17)-C(6)-C(12)	109.79(18)
C(17)-C(6)-C(7)	109.66(18)

C(12)-C(6)-C(7)	111.73(17)
C(17)-C(6)-C(5)	109.75(19)
C(12)-C(6)-C(5)	107.68(17)
C(7)-C(6)-C(5)	108.18(17)
N(2)-C(7)-C(8)	120.4(2)
N(2)-C(7)-C(6)	117.41(18)
C(8)-C(7)-C(6)	122.1(2)
C(9)-C(8)-C(7)	120.8(2)
C(10)-C(9)-C(8)	117.9(2)
C(11)-C(10)-C(9)	119.1(2)
N(2)-C(11)-C(10)	123.3(2)
N(3)-C(12)-C(13)	120.9(2)
N(3)-C(12)-C(6)	117.15(18)
C(13)-C(12)-C(6)	121.87(19)
C(14)-C(13)-C(12)	120.0(2)
C(15)-C(14)-C(13)	118.9(2)
C(16)-C(15)-C(14)	118.3(2)
N(3)-C(16)-C(15)	123.6(2)
C(19)-C(18)-C(23)	118.8(2)
C(19)-C(18)-P(1)	122.32(16)
C(23)-C(18)-P(1)	118.82(17)
C(18)-C(19)-C(20)	120.1(2)
C(21)-C(20)-C(19)	120.5(2)
C(22)-C(21)-C(20)	119.7(2)
C(21)-C(22)-C(23)	120.5(2)
C(22)-C(23)-C(18)	120.5(2)
C(29)-C(24)-C(25)	119.0(2)
C(29)-C(24)-P(1)	123.44(17)
C(25)-C(24)-P(1)	117.58(17)
C(26)-C(25)-C(24)	120.0(2)
C(27)-C(26)-C(25)	120.9(2)
C(28)-C(27)-C(26)	119.5(2)
C(27)-C(28)-C(29)	120.0(2)
C(24)-C(29)-C(28)	120.6(2)
C(31)-C(30)-C(35)	118.6(2)
C(31)-C(30)-P(1)	122.85(16)
C(35)-C(30)-P(1)	117.92(16)
C(32)-C(31)-C(30)	120.7(2)
C(31)-C(32)-C(33)	120.0(2)
C(34)-C(33)-C(32)	120.0(2)
C(35)-C(34)-C(33)	119.9(2)
C(34)-C(35)-C(30)	120.8(2)
Cl(5)-C(36)-Cl(4)	111.7(7)
Cl(5)-C(36)-Cl(3)	110.3(6)
Cl(4)-C(36)-Cl(3)	109.2(5)
Cl(7)-C(37)-Cl(6)	112.4(3)

Table 14 Anisotropic displacement parameters ($Å^2 x\ 10^3$) for **2.16**. The anisotropic displacement factor exponent takes the form: $-2\pi^2[\ h^2\ a^{*2}U^{11} + ... + 2\ h\ k\ a^*\ b^*\ U^{12}\ ]$

	U^{11}	U^{22}	U^{33}	U^{23}	U^{13}	U^{12}
Ru(1)	13(1)	12(1)	16(1)	-2(1)	-2(1)	0(1)

Cl(1)	25(1)	13(1)	51(1)	-5(1)	-14(1)	2(1)
Cl(2)	22(1)	30(1)	18(1)	-9(1)	-4(1)	4(1)
P(1)	14(1)	15(1)	16(1)	0(1)	-1(1)	1(1)
N(1)	17(1)	22(1)	17(1)	0(1)	-2(1)	2(1)
N(2)	17(1)	17(1)	14(1)	0(1)	3(1)	-1(1)
N(3)	13(1)	16(1)	18(1)	1(1)	-1(1)	0(1)
C(1)	22(1)	32(1)	23(1)	-3(1)	-1(1)	7(1)
C(2)	30(1)	41(2)	26(1)	1(1)	6(1)	14(1)
C(3)	20(1)	47(2)	36(1)	11(1)	10(1)	4(1)
C(4)	20(1)	36(1)	33(1)	7(1)	1(1)	-4(1)
C(5)	19(1)	24(1)	19(1)	4(1)	-1(1)	-1(1)
C(6)	20(1)	21(1)	19(1)	0(1)	-1(1)	-7(1)
C(7)	23(1)	18(1)	14(1)	-1(1)	4(1)	-3(1)
C(8)	36(1)	18(1)	28(1)	-3(1)	4(1)	-8(1)
C(9)	50(2)	14(1)	35(1)	3(1)	10(1)	-1(1)
C(10)	34(1)	21(1)	27(1)	6(1)	7(1)	7(1)
C(11)	22(1)	21(1)	17(1)	3(1)	4(1)	3(1)
C(12)	18(1)	20(1)	18(1)	0(1)	0(1)	-2(1)
C(13)	27(1)	30(1)	22(1)	-2(1)	-6(1)	-4(1)
C(14)	35(1)	38(1)	17(1)	2(1)	-4(1)	2(1)
C(15)	26(1)	31(1)	23(1)	11(1)	4(1)	4(1)
C(16)	14(1)	20(1)	26(1)	6(1)	1(1)	3(1)
C(17)	29(1)	32(1)	30(1)	-1(1)	-3(1)	-15(1)
C(18)	16(1)	22(1)	16(1)	2(1)	-3(1)	-4(1)
C(19)	22(1)	23(1)	22(1)	-2(1)	0(1)	-3(1)
C(20)	32(1)	26(1)	32(1)	-4(1)	0(1)	-9(1)
C(21)	27(1)	38(1)	25(1)	6(1)	-4(1)	-18(1)
C(22)	20(1)	45(2)	23(1)	9(1)	1(1)	-7(1)
C(23)	18(1)	31(1)	22(1)	2(1)	-1(1)	-2(1)
C(24)	16(1)	21(1)	21(1)	4(1)	2(1)	4(1)
C(25)	21(1)	25(1)	25(1)	3(1)	-4(1)	0(1)
C(26)	25(1)	34(1)	28(1)	10(1)	-6(1)	1(1)
C(27)	28(1)	33(1)	39(1)	16(1)	1(1)	10(1)
C(28)	42(2)	28(1)	34(1)	6(1)	9(1)	17(1)
C(29)	33(1)	29(1)	23(1)	4(1)	6(1)	12(1)
C(30)	18(1)	20(1)	17(1)	-1(1)	0(1)	4(1)
C(31)	19(1)	18(1)	21(1)	1(1)	0(1)	2(1)
C(32)	25(1)	24(1)	21(1)	3(1)	4(1)	1(1)
C(33)	39(1)	32(1)	17(1)	-5(1)	3(1)	-1(1)
C(34)	38(1)	26(1)	24(1)	-8(1)	2(1)	-6(1)
C(35)	27(1)	19(1)	20(1)	0(1)	3(1)	0(1)
C(36)	33(5)	40(5)	33(5)	-11(4)	12(4)	-5(4)
Cl(3)	57(1)	38(1)	66(2)	2(1)	-7(1)	4(1)
Cl(4)	57(1)	46(1)	57(1)	3(1)	0(1)	-2(1)
Cl(5)	30(3)	21(2)	50(2)	8(1)	-8(2)	-4(1)
C(37)	28(2)	34(2)	15(2)	3(2)	14(2)	-11(2)
Cl(6)	77(1)	30(1)	67(1)	-9(1)	-1(1)	12(1)
Cl(7)	39(2)	53(2)	84(2)	23(1)	-9(1)	-15(2)

Table 15 Hydrogen coordinates (x 10^4) and isotropic displacement parameters ($Å^2$x 10^3) for **2.16**.

	x	y	z	U(eq)
H(1A)	-4203	7280	4675	31
H(2A)	-5456	7269	5013	39
H(3A)	-6298	5854	4418	41
H(4A)	-5857	4509	3475	36
H(8A)	-4230	1748	3090	33
H(9A)	-3315	620	3817	39
H(10A)	-2402	1725	4562	33
H(11A)	-2377	3862	4490	24
H(13A)	-4771	4342	1393	32
H(14A)	-4307	5662	451	36
H(15A)	-3420	7191	827	32
H(16A)	-2994	7288	2107	24
H(17A)	-4842	2838	2213	46
H(17B)	-5462	3878	2366	46
H(17C)	-5251	2871	3018	46
H(19A)	-1896	8309	4009	26
H(20A)	-993	9866	4245	36
H(21A)	243	9600	3866	36
H(22A)	585	7773	3263	35
H(23A)	-310	6238	2993	29
H(25A)	-1150	5433	4747	29
H(26A)	-456	3839	5344	35
H(27A)	-166	2054	4663	40
H(28A)	-566	1864	3369	41
H(29A)	-1277	3447	2764	34
H(31A)	-1241	7142	1939	23
H(32A)	-1392	6905	605	28
H(33A)	-2046	5193	87	36
H(34A)	-2531	3700	910	35
H(35A)	-2416	3971	2243	26
H(36A)	-2039	-485	1093	42
H(37A)	-2152	-741	2344	31
H(37B)	-2276	-711	1423	31

X-ray Data Collection, Structure Solution and Refinement for complex 2.17.

An orange crystal of approximate dimensions 0.061 x 0.073 x 0.272 mm was mounted on a glass fiber and transferred to a Bruker SMART APEX II diffractometer. The APEX2[1] program package was used to determine the unit-cell parameters and for data collection (60 sec/frame scan time for a sphere of diffraction data). The raw frame data was processed using SAINT[2] and SADABS[3] to yield the reflection data file. Subsequent calculations were carried out using the SHELXTL[4] program. The diffraction symmetry was 2/*m* and the systematic absences were consistent with the monoclinic space group $P2_1/c$ that was later determined to be correct.

The structure was solved by direct methods and refined on F^2 by full-matrix least-squares techniques. The analytical scattering factors[5] for neutral atoms were used throughout the analysis. Hydrogen atoms were included using a riding model.

At convergence, wR2 = 0.0624 and Goof = 1.024 for 263 variables refined against 4896 data (0.75Å), R1 = 0.0251 for those 4276 data with $I > 2.0\sigma(I)$.

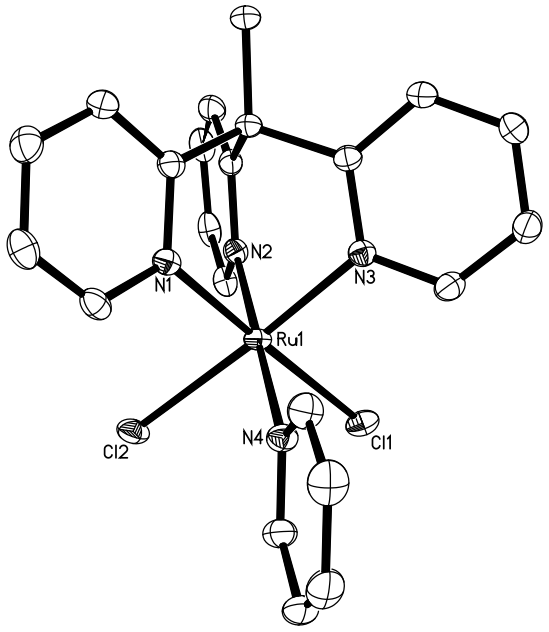

Table 16 Crystal data and structure refinement for **2.17**

Identification code	zg44 (Tobias Friedberger)	
Empirical formula	C_{22} H_{20} Cl_2 N_4 Ru	
Formula weight	512.39	
Temperature	143(2) K	
Wavelength	0.71073 Å	
Crystal system	Monoclinic	
Space group	$P2_1/c$	
Unit cell dimensions	a = 11.8393(7) Å	α= 90°.
	b = 9.9946(6) Å	β= 93.4481(7)°.
	c = 17.4877(10) Å	γ = 90°.
Volume	2065.6(2) $Å^3$	
Z	4	
Density (calculated)	1.648 Mg/m^3	
Absorption coefficient	1.034 mm^{-1}	
F(000)	1032	
Crystal color	orange	
Crystal size	0.272 x 0.073 x 0.061 mm^3	
Theta range for data collection	1.723 to 28.281°	
Index ranges	$-15 \le h \le 15$, $-13 \le k \le 12$, $-23 \le l \le 23$	
Reflections collected	23396	
Independent reflections	4896 [R(int) = 0.0269]	

Completeness to theta = 25.500°	100.0 %
Absorption correction	Numerical
Max. and min. transmission	1.0000 and 0.8644
Refinement method	Full-matrix least-squares on F^2
Data / restraints / parameters	4896 / 0 / 263
Goodness-of-fit on F^2	1.024
Final R indices [I>2sigma(I) = 4276 data]	R1 = 0.0251, wR2 = 0.0595
R indices (all data, 0.75Å)	R1 = 0.0321, wR2 = 0.0624
Largest diff. peak and hole	0.547 and -0.372 e.Å^{-3}

Table 17. Atomic coordinates (x 10^4) and equivalent isotropic displacement parameters (Å^{2}x 10^3) for **2.17**. U(eq) is defined as one third of the trace of the orthogonalized U^{ij} tensor.

	x	y	z	U(eq)
Ru(1)	2357(1)	1070(1)	1364(1)	13(1)
Cl(1)	1746(1)	1588(1)	50(1)	20(1)
Cl(2)	2752(1)	3412(1)	1630(1)	20(1)
N(1)	2851(1)	584(2)	2449(1)	15(1)
N(2)	3992(1)	805(2)	1089(1)	15(1)
N(3)	2128(1)	-893(2)	1152(1)	15(1)
N(4)	686(1)	1331(2)	1653(1)	17(1)
C(1)	2479(2)	1276(2)	3053(1)	19(1)
C(2)	2815(2)	978(2)	3801(1)	22(1)
C(3)	3575(2)	-50(2)	3944(1)	24(1)
C(4)	3961(2)	-767(2)	3332(1)	20(1)
C(5)	3580(2)	-451(2)	2587(1)	16(1)
C(6)	3968(2)	-1216(2)	1887(1)	15(1)
C(7)	4604(2)	-235(2)	1390(1)	16(1)
C(8)	5736(2)	-386(2)	1243(1)	21(1)
C(9)	6242(2)	509(2)	762(1)	24(1)
C(10)	5601(2)	1539(2)	443(1)	22(1)
C(11)	4489(2)	1666(2)	621(1)	19(1)
C(12)	2933(2)	-1784(2)	1411(1)	15(1)
C(13)	2814(2)	-3136(2)	1239(1)	18(1)
C(14)	1864(2)	-3593(2)	815(1)	22(1)
C(15)	1041(2)	-2686(2)	573(1)	22(1)
C(16)	1202(2)	-1355(2)	745(1)	19(1)
C(17)	4749(2)	-2375(2)	2152(1)	20(1)
C(18)	151(2)	417(2)	2068(1)	22(1)
C(19)	-961(2)	549(3)	2247(1)	28(1)
C(20)	-1560(2)	1671(3)	1988(1)	29(1)
C(21)	-1031(2)	2605(2)	1567(1)	26(1)
C(22)	94(2)	2415(2)	1409(1)	21(1)

Table 18 Bond lengths [Å] and angles [°] for **2.17**.

Ru(1)-N(1)	2.0106(17)
Ru(1)-N(3)	2.0116(16)
Ru(1)-N(2)	2.0404(17)
Ru(1)-N(4)	2.0864(17)
Ru(1)-Cl(1)	2.4229(5)
Ru(1)-Cl(2)	2.4269(5)

N(1)-C(1)	1.358(3)
N(1)-C(5)	1.359(3)
N(2)-C(11)	1.347(3)
N(2)-C(7)	1.355(3)
N(3)-C(16)	1.352(3)
N(3)-C(12)	1.362(3)
N(4)-C(22)	1.346(3)
N(4)-C(18)	1.349(3)
C(1)-C(2)	1.377(3)
C(2)-C(3)	1.379(3)
C(3)-C(4)	1.389(3)
C(4)-C(5)	1.388(3)
C(5)-C(6)	1.538(3)
C(6)-C(17)	1.537(3)
C(6)-C(7)	1.537(3)
C(6)-C(12)	1.546(3)
C(7)-C(8)	1.389(3)
C(8)-C(9)	1.387(3)
C(9)-C(10)	1.377(3)
C(10)-C(11)	1.377(3)
C(12)-C(13)	1.390(3)
C(13)-C(14)	1.387(3)
C(14)-C(15)	1.378(3)
C(15)-C(16)	1.375(3)
C(18)-C(19)	1.378(3)
C(19)-C(20)	1.389(4)
C(20)-C(21)	1.364(4)
C(21)-C(22)	1.390(3)

N(1)-Ru(1)-N(3)	88.09(7)
N(1)-Ru(1)-N(2)	87.99(7)
N(3)-Ru(1)-N(2)	87.09(7)
N(1)-Ru(1)-N(4)	91.64(7)
N(3)-Ru(1)-N(4)	92.73(7)
N(2)-Ru(1)-N(4)	179.59(7)
N(1)-Ru(1)-Cl(1)	178.33(5)
N(3)-Ru(1)-Cl(1)	90.26(5)
N(2)-Ru(1)-Cl(1)	92.13(5)
N(4)-Ru(1)-Cl(1)	88.23(5)
N(1)-Ru(1)-Cl(2)	90.62(5)
N(3)-Ru(1)-Cl(2)	176.62(5)
N(2)-Ru(1)-Cl(2)	89.75(5)
N(4)-Ru(1)-Cl(2)	90.42(5)
Cl(1)-Ru(1)-Cl(2)	91.049(19)
C(1)-N(1)-C(5)	118.74(18)
C(1)-N(1)-Ru(1)	121.43(14)
C(5)-N(1)-Ru(1)	119.83(13)
C(11)-N(2)-C(7)	118.94(17)
C(11)-N(2)-Ru(1)	121.03(14)
C(7)-N(2)-Ru(1)	120.02(13)
C(16)-N(3)-C(12)	118.73(17)
C(16)-N(3)-Ru(1)	121.73(14)
C(12)-N(3)-Ru(1)	119.52(14)
C(22)-N(4)-C(18)	117.59(18)
C(22)-N(4)-Ru(1)	120.52(14)

C(18)-N(4)-Ru(1)	121.87(14)
N(1)-C(1)-C(2)	122.8(2)
C(1)-C(2)-C(3)	118.7(2)
C(2)-C(3)-C(4)	119.1(2)
C(5)-C(4)-C(3)	120.2(2)
N(1)-C(5)-C(4)	120.47(18)
N(1)-C(5)-C(6)	116.94(17)
C(4)-C(5)-C(6)	122.58(18)
C(17)-C(6)-C(7)	110.18(17)
C(17)-C(6)-C(5)	109.73(17)
C(7)-C(6)-C(5)	108.25(16)
C(17)-C(6)-C(12)	109.18(16)
C(7)-C(6)-C(12)	109.19(16)
C(5)-C(6)-C(12)	110.29(16)
N(2)-C(7)-C(8)	120.71(19)
N(2)-C(7)-C(6)	116.15(17)
C(8)-C(7)-C(6)	123.14(18)
C(9)-C(8)-C(7)	119.9(2)
C(10)-C(9)-C(8)	118.70(19)
C(9)-C(10)-C(11)	119.3(2)
N(2)-C(11)-C(10)	122.4(2)
N(3)-C(12)-C(13)	120.27(18)
N(3)-C(12)-C(6)	117.03(17)
C(13)-C(12)-C(6)	122.70(17)
C(14)-C(13)-C(12)	120.29(19)
C(15)-C(14)-C(13)	118.9(2)
C(16)-C(15)-C(14)	118.9(2)
N(3)-C(16)-C(15)	122.89(19)
N(4)-C(18)-C(19)	122.9(2)
C(18)-C(19)-C(20)	118.6(2)
C(21)-C(20)-C(19)	119.2(2)
C(20)-C(21)-C(22)	119.4(2)
N(4)-C(22)-C(21)	122.3(2)

Table 19 Anisotropic displacement parameters ($Å^2 x\ 10^3$) for **2.17**. The anisotropic displacement factor exponent takes the form: $-2\pi 2[\ h^2\ a^*2U^{11} + ...\ + 2\ h\ k\ a^*\ b^*\ U^{12}\ ]$

	U^{11}	U^{22}	U^{33}	U^{23}	U^{13}	U^{12}
Ru(1)	11(1)	12(1)	17(1)	2(1)	2(1)	2(1)
Cl(1)	18(1)	23(1)	19(1)	6(1)	0(1)	3(1)
Cl(2)	19(1)	12(1)	30(1)	1(1)	1(1)	1(1)
N(1)	13(1)	13(1)	18(1)	0(1)	2(1)	-1(1)
N(2)	15(1)	15(1)	14(1)	-1(1)	2(1)	0(1)
N(3)	15(1)	14(1)	16(1)	2(1)	2(1)	-1(1)
N(4)	14(1)	18(1)	20(1)	0(1)	2(1)	2(1)
C(1)	16(1)	15(1)	26(1)	-4(1)	4(1)	-2(1)
C(2)	26(1)	21(1)	20(1)	-4(1)	7(1)	-4(1)
C(3)	31(1)	22(1)	18(1)	2(1)	-1(1)	-3(1)
C(4)	23(1)	16(1)	22(1)	1(1)	-2(1)	1(1)
C(5)	14(1)	13(1)	20(1)	1(1)	0(1)	-2(1)
C(6)	14(1)	14(1)	18(1)	-1(1)	-1(1)	3(1)
C(7)	16(1)	16(1)	15(1)	-3(1)	0(1)	0(1)

C(8)	16(1)	21(1)	25(1)	-6(1)	1(1)	3(1)
C(9)	15(1)	28(1)	28(1)	-11(1)	6(1)	-3(1)
C(10)	22(1)	23(1)	20(1)	-7(1)	6(1)	-9(1)
C(11)	22(1)	18(1)	17(1)	-3(1)	2(1)	-3(1)
C(12)	14(1)	16(1)	15(1)	1(1)	2(1)	1(1)
C(13)	19(1)	16(1)	20(1)	2(1)	0(1)	2(1)
C(14)	24(1)	16(1)	26(1)	-1(1)	-3(1)	-2(1)
C(15)	22(1)	21(1)	23(1)	1(1)	-5(1)	-3(1)
C(16)	16(1)	20(1)	21(1)	3(1)	-1(1)	0(1)
C(17)	18(1)	17(1)	24(1)	-1(1)	-4(1)	5(1)
C(18)	20(1)	23(1)	24(1)	1(1)	3(1)	-2(1)
C(19)	23(1)	34(1)	27(1)	-1(1)	8(1)	-5(1)
C(20)	14(1)	43(1)	31(1)	-12(1)	4(1)	3(1)
C(21)	20(1)	30(1)	28(1)	-7(1)	-2(1)	9(1)
C(22)	19(1)	21(1)	24(1)	1(1)	0(1)	4(1)

Table 20 Hydrogen coordinates (x 10^4) and isotropic displacement parameters ($Å^2$x 10^3)for **2.17**.

	x	y	z	U(eq)
H(1)	1966	1995	2955	23
H(2)	2528	1472	4211	27
H(3)	3831	-265	4455	29
H(4)	4487	-1476	3423	24
H(8)	6165	-1101	1470	25
H(9)	7015	413	655	28
H(10)	5923	2155	105	26
H(11)	4055	2388	405	22
H(13)	3387	-3750	1412	22
H(14)	1781	-4516	695	27
H(15)	375	-2976	291	27
H(16)	637	-732	571	23
H(17A)	4336	-2991	2470	30
H(17B)	5409	-2019	2451	30
H(17C)	5000	-2854	1704	30
H(18)	559	-353	2245	27
H(19)	-1311	-114	2543	34
H(20)	-2328	1787	2102	35
H(21)	-1428	3378	1383	31
H(22)	458	3074	1119	26

X-ray Data Collection, Structure Solution and Refinement for complex 2.18

An orange crystal of approximate dimensions 0.16 x 0.19 x 0.23 mm was mounted on a glass fiber and transferred to a Bruker SMART APEX II diffractometer. The APEX2[1] program package was used to determine the unit-cell parameters and for data collection (25 sec/frame scan time for a sphere of diffraction data). The raw frame data was processed using SAINT[2] and SADABS[3] to yield the reflection data file. Subsequent calculations were carried out using the SHELXTL[4]

program. The diffraction symmetry was *mmm* and the systematic absences were consistent with the orthorhombic space group $P2_12_12_1$ that was later determined to be correct.

The structure was solved by direct methods and refined on F^2 by full-matrix least-squares techniques. The analytical scattering factors[5] for neutral atoms were used throughout the analysis. Hydrogen atoms were included using a riding model.

At convergence, wR2 = 0.0901 and Goof = 1.041 for 238 variables refined against 5404 data (0.78Å), R1 = 0.0348 for those 5097 data with $I > 2.0\sigma(I)$. The absolute structure could not be assigned by inversion of the model or by refinement of the Flack parameter[6]. There were several high residuals present in the final difference-Fourier map. It was not possible to determine the nature of the residuals although it is probable that methanol solvent was present. The SQUEEZE routine in the PLATON[7] program package was used to account for the electrons in the solvent accessible voids.

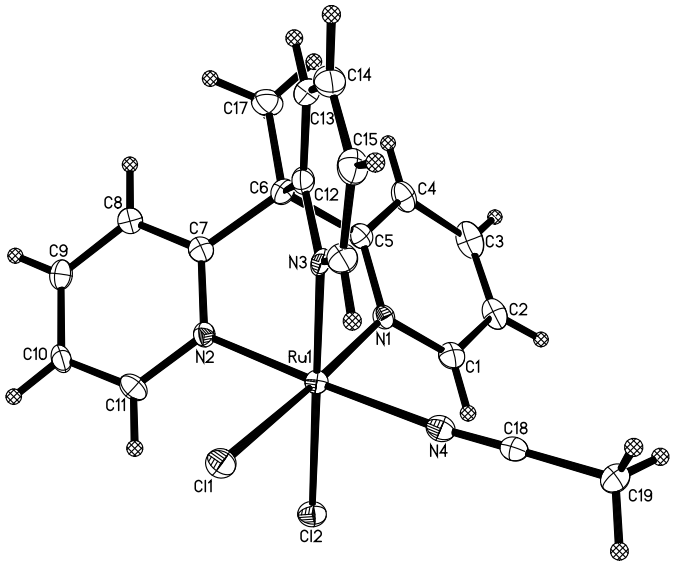

Table 21 Crystal data and structure refinement for **2.18**

Identification code	zg45 (Tobias Friedberger)	
Empirical formula	$C_{19}\ H_{18}\ Cl_2\ N_4\ Ru$	
Formula weight	474.34	
Temperature	143(2) K	
Wavelength	0.71073 Å	
Crystal system	Orthorhombic	
Space group	$P2_12_12_1$	
Unit cell dimensions	a = 7.9709(11) Å	α= 90°.
	b = 13.9446(19) Å	β= 90°.
	c = 22.098(3) Å	γ = 90°.
Volume	2456.2(6) $Å^3$	
Z	4	
Density (calculated)	1.283 Mg/m^3	
Absorption coefficient	0.864 mm^{-1}	
F(000)	952	

Crystal color	orange
Crystal size	0.23 x 0.19 x 0.16 mm^3
Theta range for data collection	1.73 to 27.10°
Index ranges	$-10 \leq h \leq 10$, $-17 \leq k \leq 17$, $-28 \leq l \leq 28$
Reflections collected	27108
Independent reflections	5404 [R(int) = 0.0519]
Completeness to theta = 27.10°	99.9 %
Absorption correction	Numerical
Max. and min. transmission	0.8713 and 0.8287
Refinement method	Full-matrix least-squares on F^2
Data / restraints / parameters	5404 / 0 / 238
Goodness-of-fit on F^2	1.041
Final R indices [I>2sigma(I) = 5097 data]	R1 = 0.0348, wR2 = 0.0891
R indices (all data, 0.78 Å)	R1 = 0.0367, wR2 = 0.0901
Absolute structure parameter	0.57(4)
Largest diff. peak and hole	2.063 and -0.413 e.$Å^{-3}$

Table 22. Atomic coordinates (x 10^4) and equivalent isotropic displacement parameters ($Å^2$x 10^3) for **2.18**. U(eq) is defined as one third of the trace of the orthogonalized U^{ij} tensor.

	x	y	z	U(eq)
Ru(1)	4978(1)	7652(1)	3418(1)	20(1)
Cl(1)	3643(1)	8847(1)	4060(1)	29(1)
Cl(2)	3659(1)	6368(1)	3991(1)	28(1)
N(1)	6055(3)	6694(2)	2851(1)	21(1)
N(2)	3043(3)	7705(2)	2834(1)	22(1)
N(3)	6064(3)	8690(2)	2927(1)	22(1)
N(4)	7012(3)	7596(2)	3986(1)	25(1)
C(1)	6856(4)	5912(2)	3079(2)	28(1)
C(2)	7670(5)	5269(2)	2701(2)	30(1)
C(3)	7592(6)	5377(3)	2102(2)	40(1)
C(4)	6800(4)	6202(3)	1852(2)	32(1)
C(5)	6046(4)	6847(2)	2248(1)	23(1)
C(6)	5165(4)	7763(2)	2021(1)	27(1)
C(7)	3324(4)	7751(2)	2225(1)	24(1)
C(8)	2008(4)	7767(2)	1819(1)	25(1)
C(9)	363(4)	7742(3)	2028(2)	29(1)
C(10)	79(4)	7715(2)	2647(1)	27(1)
C(11)	1435(4)	7686(3)	3029(1)	27(1)
C(12)	6049(4)	8646(2)	2309(1)	24(1)
C(13)	6820(5)	9358(3)	1969(2)	31(1)
C(14)	7597(5)	10092(3)	2243(2)	36(1)
C(15)	7680(5)	10157(3)	2876(2)	35(1)
C(16)	6820(4)	9434(2)	3192(2)	28(1)
C(17)	5262(5)	7819(3)	1330(2)	37(1)
C(18)	8189(4)	7568(2)	4262(1)	24(1)
C(19)	9738(4)	7515(3)	4632(2)	37(1)

Table 23 Bond lengths [Å] and angles [°] for **2.18**.

Ru(1)-N(3)	2.005(3)
Ru(1)-N(2)	2.012(2)

Ru(1)-N(1)	2.023(3)
Ru(1)-N(4)	2.051(3)
Ru(1)-Cl(2)	2.4334(8)
Ru(1)-Cl(1)	2.4338(8)
N(1)-C(5)	1.351(4)
N(1)-C(1)	1.360(4)
N(2)-C(11)	1.352(4)
N(2)-C(7)	1.367(4)
N(3)-C(16)	1.334(4)
N(3)-C(12)	1.367(4)
N(4)-C(18)	1.120(4)
C(1)-C(2)	1.386(5)
C(2)-C(3)	1.334(7)
C(3)-C(4)	1.424(6)
C(4)-C(5)	1.392(5)
C(5)-C(6)	1.541(4)
C(6)-C(17)	1.532(4)
C(6)-C(7)	1.535(4)
C(6)-C(12)	1.554(5)
C(7)-C(8)	1.380(4)
C(8)-C(9)	1.391(4)
C(9)-C(10)	1.388(5)
C(10)-C(11)	1.372(5)
C(12)-C(13)	1.388(5)
C(13)-C(14)	1.341(6)
C(14)-C(15)	1.404(7)
C(15)-C(16)	1.406(5)
C(18)-C(19)	1.483(4)

N(3)-Ru(1)-N(2)	87.56(10)
N(3)-Ru(1)-N(1)	87.64(10)
N(2)-Ru(1)-N(1)	87.27(11)
N(3)-Ru(1)-N(4)	91.00(10)
N(2)-Ru(1)-N(4)	177.84(9)
N(1)-Ru(1)-N(4)	91.06(10)
N(3)-Ru(1)-Cl(2)	178.57(8)
N(2)-Ru(1)-Cl(2)	91.69(8)
N(1)-Ru(1)-Cl(2)	91.11(8)
N(4)-Ru(1)-Cl(2)	89.71(7)
N(3)-Ru(1)-Cl(1)	90.59(8)
N(2)-Ru(1)-Cl(1)	90.77(8)
N(1)-Ru(1)-Cl(1)	177.41(8)
N(4)-Ru(1)-Cl(1)	90.86(8)
Cl(2)-Ru(1)-Cl(1)	90.64(3)
C(5)-N(1)-C(1)	119.6(3)
C(5)-N(1)-Ru(1)	120.3(2)
C(1)-N(1)-Ru(1)	120.0(2)
C(11)-N(2)-C(7)	118.0(3)
C(11)-N(2)-Ru(1)	121.5(2)
C(7)-N(2)-Ru(1)	120.5(2)
C(16)-N(3)-C(12)	118.6(3)
C(16)-N(3)-Ru(1)	121.2(2)
C(12)-N(3)-Ru(1)	120.3(2)
C(18)-N(4)-Ru(1)	175.2(2)
N(1)-C(1)-C(2)	121.1(3)

C(3)-C(2)-C(1)	120.1(4)
C(2)-C(3)-C(4)	119.9(4)
C(5)-C(4)-C(3)	118.0(3)
N(1)-C(5)-C(4)	121.1(3)
N(1)-C(5)-C(6)	117.0(3)
C(4)-C(5)-C(6)	121.9(3)
C(17)-C(6)-C(7)	109.9(3)
C(17)-C(6)-C(5)	110.0(3)
C(7)-C(6)-C(5)	109.4(3)
C(17)-C(6)-C(12)	110.2(3)
C(7)-C(6)-C(12)	108.8(3)
C(5)-C(6)-C(12)	108.5(2)
N(2)-C(7)-C(8)	121.1(3)
N(2)-C(7)-C(6)	116.4(3)
C(8)-C(7)-C(6)	122.4(3)
C(7)-C(8)-C(9)	120.0(3)
C(10)-C(9)-C(8)	118.8(3)
C(11)-C(10)-C(9)	118.6(3)
N(2)-C(11)-C(10)	123.5(3)
N(3)-C(12)-C(13)	120.3(3)
N(3)-C(12)-C(6)	116.6(3)
C(13)-C(12)-C(6)	123.1(3)
C(14)-C(13)-C(12)	120.5(4)
C(13)-C(14)-C(15)	121.3(4)
C(14)-C(15)-C(16)	115.3(4)
N(3)-C(16)-C(15)	124.0(3)
N(4)-C(18)-C(19)	179.0(4)

Table 24 Anisotropic displacement parameters ($Å^2 x\ 10^3$) for **2.18**. The anisotropic displacement factor exponent takes the form: $-2\pi 2[\ h^2\ a^*2U11 + ...\ + 2\ h\ k\ a^*\ b^*\ U12\ ]$

	U^{11}	U^{22}	U^{33}	U^{23}	U^{13}	U^{12}
Ru(1)	20(1)	19(1)	21(1)	0(1)	0(1)	0(1)
Cl(1)	33(1)	28(1)	25(1)	-5(1)	1(1)	3(1)
Cl(2)	30(1)	26(1)	28(1)	2(1)	2(1)	-5(1)
N(1)	18(1)	22(1)	24(1)	-1(1)	0(1)	-2(1)
N(2)	17(1)	23(1)	25(1)	0(1)	-2(1)	0(1)
N(3)	18(1)	22(1)	25(1)	4(1)	-5(1)	5(1)
N(4)	26(1)	22(1)	28(1)	1(1)	3(1)	-5(1)
C(1)	26(2)	20(2)	37(2)	3(1)	2(1)	-5(1)
C(2)	25(2)	13(2)	51(2)	-3(1)	5(2)	-1(1)
C(3)	33(2)	28(2)	58(3)	-21(2)	2(2)	2(2)
C(4)	23(2)	38(2)	36(2)	-13(2)	0(1)	-2(1)
C(5)	21(2)	24(2)	24(1)	-4(1)	-2(1)	-3(1)
C(6)	24(2)	33(2)	23(1)	2(1)	-4(1)	2(2)
C(7)	24(2)	17(1)	30(2)	-1(1)	1(1)	-3(1)
C(8)	26(2)	23(2)	27(1)	-3(1)	-1(1)	-1(1)
C(9)	23(2)	28(2)	35(2)	-2(1)	-7(1)	1(1)
C(10)	18(1)	26(1)	36(2)	0(1)	4(1)	5(2)
C(11)	26(2)	27(1)	28(2)	-8(1)	6(1)	-2(1)
C(12)	18(2)	26(2)	29(2)	2(1)	-2(1)	1(1)
C(13)	27(2)	36(2)	30(2)	10(1)	0(1)	5(1)

C(14)	30(2)	30(2)	48(2)	12(2)	5(2)	-1(2)
C(15)	26(2)	28(2)	51(2)	8(2)	-3(2)	-4(2)
C(16)	30(2)	21(2)	34(2)	3(1)	2(1)	-1(1)
C(17)	35(2)	52(2)	25(2)	0(1)	0(1)	-5(2)
C(18)	25(2)	24(2)	22(1)	0(1)	4(1)	0(1)
C(19)	30(2)	57(2)	23(2)	2(1)	-3(1)	4(2)

Table 25 Hydrogen coordinates (x 10^4) and isotropic displacement parameters ($Å^2$x 10^3)for **2.18**.

	x	y	z	U(eq)
H(1A)	6856	5804	3503	33
H(2A)	8286	4750	2870	36
H(3A)	8064	4905	1843	48
H(4A)	6786	6308	1427	39
H(8A)	2226	7795	1396	30
H(9A)	-551	7742	1751	35
H(10A)	-1031	7717	2804	32
H(11A)	1235	7651	3452	33
H(13A)	6797	9324	1540	37
H(14A)	8102	10579	2003	43
H(15A)	8275	10654	3076	42
H(16A)	6774	9477	3621	34
H(17A)	4909	7205	1156	56
H(17B)	6418	7958	1208	56
H(17C)	4521	8330	1185	56
H(19A)	10337	8128	4609	56
H(19B)	10459	7001	4477	56
H(19C)	9441	7381	5054	56

X-ray Data Collection, Structure Solution and Refinement for complex 2.19.

A red crystal of approximate dimensions 0.044 x 0.490 x 0.535 mm was mounted on a glass fiber and transferred to a Bruker SMART APEX II diffractometer. The APEX2[1] program package was used to determine the unit-cell parameters and for data collection (45 sec/frame scan time for a hemisphere of diffraction data). The raw frame data was processed using SAINT[2] and SADABS[3] to yield the reflection data file. Subsequent calculations were carried out using the SHELXTL[4] program. The diffraction symmetry was *mmm* and the systematic absences were consistent with the orthorhombic space group *Pbca* that was later determined to be correct.

The structure was solved by direct methods and refined on F^2 by full-matrix least-squares techniques. The analytical scattering factors[5] for neutral atoms were used throughout the analysis. The hydride atom was located from a difference-Fourier map and refined (x,y,z and fixed U_{iso}). The remaining hydrogen atoms were included using a riding model.

At convergence, wR2 = 0.0797 and Goof = 1.041 for 734 variables refined against 12933 data (0.80Å), R1 = 0.0322 for those 10097 data with $I > 2.0\sigma(I)$.

There were several high residuals present in the final difference-Fourier map. It was not possible to determine the nature of the residuals although it was probable that dichloromethane solvent was present. The SQUEEZE[6a] routine in the PLATON[6b] program package was used to account for the electrons in the solvent accessible voids.

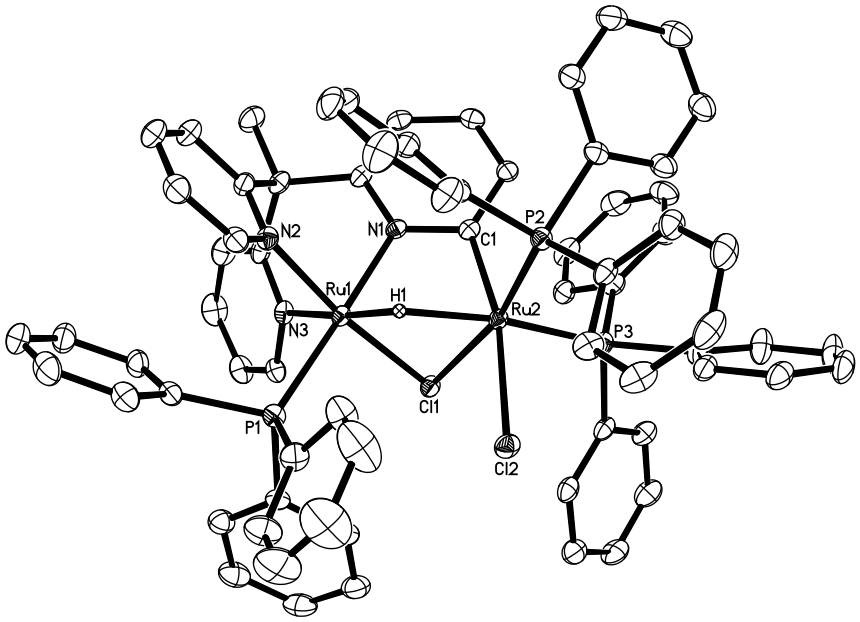

Table 26 Crystal data and structure refinement for **2.19**.

Identification code	zg43 (Tobias Friedberger)	
Empirical formula	$C_{71}\ H_{60}\ Cl_2\ N_3\ P_3\ Ru_2$	
Formula weight	1321.17	
Temperature	198(2) K	
Wavelength	0.71073 Å	
Crystal system	Orthorhombic	
Space group	*Pbca*	
Unit cell dimensions	a = 22.8329(18) Å	α= 90°.
	b = 20.5412(16) Å	β= 90°.
	c = 26.924(2) Å	γ = 90°.
Volume	12627.7(17) Å^3	
Z	8	
Density (calculated)	1.390 Mg/m^3	
Absorption coefficient	0.683 mm^{-1}	
F(000)	5392	
Crystal color	red	
Crystal size	0.535 x 0.490 x 0.044 mm^3	
Theta range for data collection	1.756 to 26.398°	
Index ranges	$-27 \le h \le 28$, $-25 \le k \le 25$, $-33 \le l \le 33$	
Reflections collected	99293	
Independent reflections	12933 [R(int) = 0.0583]	
Completeness to theta = 25.500°	100.0 %	
Absorption correction	Numerical	
Max. and min. transmission	0.9719 and 0.7540	
Refinement method	Full-matrix least-squares on F^2	
Data / restraints / parameters	12933 / 0 / 734	

Goodness-of-fit on F^2	1.041
Final R indices [I>2sigma(I) = 10097 data]	R1 = 0.0322, wR2 = 0.0727
R indices (all data, 0.80Å)	R1 = 0.0501, wR2 = 0.0797
Largest diff. peak and hole	1.167 and -0.383 e.Å^{-3}

Table 27 Atomic coordinates (x 10^4) and equivalent isotropic displacement parameters (Å^{2}x 10^3) for **2.19**. U(eq) is defined as one third of the trace of the orthogonalized U^{ij} tensor.

	x	y	z	U(eq)
Ru(1)	1228(1)	2147(1)	1270(1)	21(1)
Ru(2)	1781(1)	3203(1)	744(1)	21(1)
Cl(1)	2250(1)	2232(1)	1087(1)	26(1)
Cl(2)	2223(1)	3802(1)	1481(1)	32(1)
P(1)	1306(1)	2248(1)	2130(1)	27(1)
P(2)	1151(1)	4013(1)	487(1)	25(1)
P(3)	2611(1)	3370(1)	259(1)	26(1)
N(1)	1118(1)	2090(1)	520(1)	22(1)
N(2)	341(1)	2025(1)	1309(1)	27(1)
N(3)	1311(1)	1136(1)	1247(1)	26(1)
C(1)	1382(1)	2584(1)	266(1)	23(1)
C(2)	1306(1)	2573(1)	-251(1)	27(1)
C(3)	975(1)	2098(1)	-476(1)	30(1)
C(4)	701(1)	1619(1)	-197(1)	31(1)
C(5)	774(1)	1629(1)	313(1)	27(1)
C(6)	471(1)	1156(1)	676(1)	31(1)
C(7)	82(1)	1548(1)	1034(1)	30(1)
C(8)	-513(1)	1419(2)	1082(1)	43(1)
C(9)	-852(1)	1769(2)	1405(1)	51(1)
C(10)	-597(1)	2262(2)	1679(1)	44(1)
C(11)	-7(1)	2379(2)	1614(1)	33(1)
C(12)	931(1)	779(1)	977(1)	30(1)
C(13)	977(2)	101(1)	976(1)	44(1)
C(14)	1422(2)	-201(2)	1228(1)	48(1)
C(15)	1831(2)	172(1)	1475(1)	39(1)
C(16)	1763(1)	832(1)	1475(1)	29(1)
C(17)	98(2)	676(2)	371(1)	44(1)
C(18)	1992(1)	1936(1)	2396(1)	29(1)
C(19)	2042(1)	1349(2)	2650(1)	40(1)
C(20)	2597(2)	1098(2)	2763(1)	49(1)
C(21)	3094(2)	1431(2)	2628(1)	51(1)
C(22)	3049(2)	2024(2)	2390(1)	47(1)
C(23)	2502(1)	2273(2)	2272(1)	39(1)
C(24)	1254(1)	3048(1)	2438(1)	37(1)
C(25)	1415(2)	3122(2)	2932(1)	52(1)
C(26)	1362(2)	3720(2)	3166(2)	75(1)
C(27)	1146(3)	4243(2)	2905(2)	93(2)
C(28)	990(2)	4180(2)	2415(2)	82(2)
C(29)	1042(2)	3580(2)	2179(1)	50(1)
C(30)	721(1)	1783(1)	2455(1)	30(1)
C(31)	321(1)	2070(2)	2779(1)	40(1)
C(32)	-156(2)	1716(2)	2958(1)	50(1)
C(33)	-243(2)	1080(2)	2822(1)	50(1)
C(34)	154(2)	788(2)	2508(1)	47(1)

C(35)	624(1)	1138(2)	2322(1)	37(1)
C(36)	400(1)	3898(1)	726(1)	27(1)
C(37)	113(1)	4357(2)	1011(1)	45(1)
C(38)	-462(2)	4256(2)	1167(2)	56(1)
C(39)	-761(1)	3711(2)	1027(1)	46(1)
C(40)	-484(1)	3251(2)	742(1)	40(1)
C(41)	94(1)	3338(1)	600(1)	33(1)
C(42)	1004(1)	4075(1)	-187(1)	28(1)
C(43)	1472(1)	4212(2)	-502(1)	36(1)
C(44)	1402(2)	4213(2)	-1014(1)	44(1)
C(45)	869(2)	4077(2)	-1222(1)	49(1)
C(46)	394(2)	3966(2)	-915(1)	47(1)
C(47)	461(1)	3970(2)	-404(1)	38(1)
C(48)	1257(1)	4884(1)	642(1)	29(1)
C(49)	1435(1)	5054(1)	1116(1)	36(1)
C(50)	1518(1)	5701(2)	1247(1)	44(1)
C(51)	1414(1)	6187(2)	898(2)	48(1)
C(52)	1221(2)	6025(2)	431(1)	46(1)
C(53)	1141(1)	5379(1)	301(1)	37(1)
C(54)	2846(1)	4192(1)	67(1)	32(1)
C(55)	3235(2)	4321(2)	-322(1)	49(1)
C(56)	3387(2)	4956(2)	-439(2)	59(1)
C(57)	3156(1)	5465(2)	-173(2)	50(1)
C(58)	2789(1)	5349(2)	219(1)	42(1)
C(59)	2637(1)	4711(1)	342(1)	35(1)
C(60)	3326(1)	3106(1)	527(1)	29(1)
C(61)	3424(1)	3091(1)	1035(1)	33(1)
C(62)	3973(1)	2939(1)	1225(1)	40(1)
C(63)	4431(1)	2788(2)	911(1)	44(1)
C(64)	4337(1)	2788(2)	406(1)	45(1)
C(65)	3794(1)	2950(2)	217(1)	38(1)
C(66)	2642(1)	2875(1)	-312(1)	30(1)
C(67)	2569(1)	3108(2)	-792(1)	39(1)
C(68)	2573(2)	2689(2)	-1190(1)	48(1)
C(69)	2645(2)	2031(2)	-1122(1)	50(1)
C(70)	2712(1)	1788(2)	-645(1)	46(1)
C(71)	2706(1)	2203(1)	-243(1)	34(1)

Table 28 Bond lengths [Å] and angles [°] for **2.19**.

Ru(1)-H(1)	1.62(3)
Ru(1)-N(1)	2.037(2)
Ru(1)-N(2)	2.046(2)
Ru(1)-N(3)	2.086(2)
Ru(1)-P(1)	2.3326(8)
Ru(1)-Cl(1)	2.3911(7)
Ru(1)-Ru(2)	2.8818(3)
Ru(2)-H(1)	1.90(3)
Ru(2)-C(1)	2.027(3)
Ru(2)-P(2)	2.3059(7)
Ru(2)-P(3)	2.3261(8)
Ru(2)-Cl(1)	2.4458(7)
Ru(2)-Cl(2)	2.5434(7)
P(1)-C(18)	1.838(3)

P(1)-C(24)	1.843(3)
P(1)-C(30)	1.860(3)
P(2)-C(36)	1.847(3)
P(2)-C(42)	1.849(3)
P(2)-C(48)	1.853(3)
P(3)-C(66)	1.845(3)
P(3)-C(54)	1.846(3)
P(3)-C(60)	1.866(3)
N(1)-C(5)	1.351(3)
N(1)-C(1)	1.364(3)
N(2)-C(11)	1.354(4)
N(2)-C(7)	1.362(4)
N(3)-C(12)	1.349(4)
N(3)-C(16)	1.353(3)
C(1)-C(2)	1.404(4)
C(2)-C(3)	1.373(4)
C(3)-C(4)	1.387(4)
C(4)-C(5)	1.383(4)
C(5)-C(6)	1.543(4)
C(6)-C(12)	1.537(4)
C(6)-C(7)	1.538(4)
C(6)-C(17)	1.540(4)
C(7)-C(8)	1.391(4)
C(8)-C(9)	1.369(5)
C(9)-C(10)	1.380(5)
C(10)-C(11)	1.379(4)
C(12)-C(13)	1.398(4)
C(13)-C(14)	1.370(5)
C(14)-C(15)	1.379(5)
C(15)-C(16)	1.365(4)
C(18)-C(19)	1.391(4)
C(18)-C(23)	1.395(4)
C(19)-C(20)	1.401(4)
C(20)-C(21)	1.375(5)
C(21)-C(22)	1.380(5)
C(22)-C(23)	1.387(5)
C(24)-C(29)	1.384(5)
C(24)-C(25)	1.389(5)
C(25)-C(26)	1.385(5)
C(26)-C(27)	1.376(6)
C(27)-C(28)	1.372(6)
C(28)-C(29)	1.393(5)
C(30)-C(35)	1.389(4)
C(30)-C(31)	1.395(4)
C(31)-C(32)	1.395(5)
C(32)-C(33)	1.371(5)
C(33)-C(34)	1.377(5)
C(34)-C(35)	1.386(4)
C(36)-C(37)	1.381(4)
C(36)-C(41)	1.389(4)
C(37)-C(38)	1.395(5)
C(38)-C(39)	1.364(5)
C(39)-C(40)	1.373(5)
C(40)-C(41)	1.386(4)
C(42)-C(47)	1.387(4)

C(42)-C(43)	1.391(4)
C(43)-C(44)	1.388(4)
C(44)-C(45)	1.368(5)
C(45)-C(46)	1.384(5)
C(46)-C(47)	1.384(4)
C(48)-C(49)	1.386(4)
C(48)-C(53)	1.395(4)
C(49)-C(50)	1.388(4)
C(50)-C(51)	1.391(5)
C(51)-C(52)	1.375(5)
C(52)-C(53)	1.383(4)
C(54)-C(59)	1.383(4)
C(54)-C(55)	1.398(4)
C(55)-C(56)	1.387(5)
C(56)-C(57)	1.371(5)
C(57)-C(58)	1.368(5)
C(58)-C(59)	1.395(4)
C(60)-C(61)	1.387(4)
C(60)-C(65)	1.394(4)
C(61)-C(62)	1.390(4)
C(62)-C(63)	1.381(5)
C(63)-C(64)	1.378(5)
C(64)-C(65)	1.381(4)
C(66)-C(67)	1.388(4)
C(66)-C(71)	1.400(4)
C(67)-C(68)	1.375(5)
C(68)-C(69)	1.374(5)
C(69)-C(70)	1.388(5)
C(70)-C(71)	1.378(4)

H(1)-Ru(1)-N(1)	85.6(12)
H(1)-Ru(1)-N(2)	94.3(12)
N(1)-Ru(1)-N(2)	85.49(9)
H(1)-Ru(1)-N(3)	170.8(12)
N(1)-Ru(1)-N(3)	85.73(9)
N(2)-Ru(1)-N(3)	88.24(9)
H(1)-Ru(1)-P(1)	92.4(12)
N(1)-Ru(1)-P(1)	176.67(6)
N(2)-Ru(1)-P(1)	91.96(7)
N(3)-Ru(1)-P(1)	96.35(6)
H(1)-Ru(1)-Cl(1)	87.3(12)
N(1)-Ru(1)-Cl(1)	85.49(6)
N(2)-Ru(1)-Cl(1)	170.68(7)
N(3)-Ru(1)-Cl(1)	88.74(6)
P(1)-Ru(1)-Cl(1)	97.14(3)
H(1)-Ru(1)-Ru(2)	38.3(12)
N(1)-Ru(1)-Ru(2)	67.13(6)
N(2)-Ru(1)-Ru(2)	123.51(6)
N(3)-Ru(1)-Ru(2)	134.09(6)
P(1)-Ru(1)-Ru(2)	112.783(19)
Cl(1)-Ru(1)-Ru(2)	54.310(16)
H(1)-Ru(2)-C(1)	84.2(10)
H(1)-Ru(2)-P(2)	87.8(10)
C(1)-Ru(2)-P(2)	88.94(7)
H(1)-Ru(2)-P(3)	168.7(10)

C(1)-Ru(2)-P(3)	95.82(8)
P(2)-Ru(2)-P(3)	103.49(3)
H(1)-Ru(2)-Cl(1)	80.2(10)
C(1)-Ru(2)-Cl(1)	85.61(7)
P(2)-Ru(2)-Cl(1)	167.21(2)
P(3)-Ru(2)-Cl(1)	88.59(2)
H(1)-Ru(2)-Cl(2)	85.9(10)
C(1)-Ru(2)-Cl(2)	167.86(8)
P(2)-Ru(2)-Cl(2)	97.67(3)
P(3)-Ru(2)-Cl(2)	92.54(3)
Cl(1)-Ru(2)-Cl(2)	85.81(2)
H(1)-Ru(2)-Ru(1)	32.0(10)
C(1)-Ru(2)-Ru(1)	69.01(8)
P(2)-Ru(2)-Ru(1)	114.65(2)
P(3)-Ru(2)-Ru(1)	138.001(19)
Cl(1)-Ru(2)-Ru(1)	52.562(16)
Cl(2)-Ru(2)-Ru(1)	98.913(19)
Ru(1)-Cl(1)-Ru(2)	73.127(19)
C(18)-P(1)-C(24)	100.97(14)
C(18)-P(1)-C(30)	104.42(13)
C(24)-P(1)-C(30)	101.57(14)
C(18)-P(1)-Ru(1)	114.88(9)
C(24)-P(1)-Ru(1)	121.40(11)
C(30)-P(1)-Ru(1)	111.50(9)
C(36)-P(2)-C(42)	100.59(13)
C(36)-P(2)-C(48)	99.52(12)
C(42)-P(2)-C(48)	100.22(13)
C(36)-P(2)-Ru(2)	112.49(9)
C(42)-P(2)-Ru(2)	117.25(9)
C(48)-P(2)-Ru(2)	123.17(9)
C(66)-P(3)-C(54)	105.08(14)
C(66)-P(3)-C(60)	97.40(13)
C(54)-P(3)-C(60)	96.89(12)
C(66)-P(3)-Ru(2)	114.71(9)
C(54)-P(3)-Ru(2)	121.92(10)
C(60)-P(3)-Ru(2)	116.87(10)
C(5)-N(1)-C(1)	124.8(2)
C(5)-N(1)-Ru(1)	121.46(18)
C(1)-N(1)-Ru(1)	113.52(17)
C(11)-N(2)-C(7)	117.5(2)
C(11)-N(2)-Ru(1)	123.2(2)
C(7)-N(2)-Ru(1)	119.30(18)
C(12)-N(3)-C(16)	119.0(2)
C(12)-N(3)-Ru(1)	119.85(18)
C(16)-N(3)-Ru(1)	120.99(18)
N(1)-C(1)-C(2)	115.5(2)
N(1)-C(1)-Ru(2)	110.33(18)
C(2)-C(1)-Ru(2)	134.1(2)
C(3)-C(2)-C(1)	121.2(3)
C(2)-C(3)-C(4)	120.8(3)
C(5)-C(4)-C(3)	118.2(3)
N(1)-C(5)-C(4)	119.4(3)
N(1)-C(5)-C(6)	116.1(2)
C(4)-C(5)-C(6)	124.5(2)
C(12)-C(6)-C(7)	109.1(2)

C(12)-C(6)-C(17)	109.6(2)
C(7)-C(6)-C(17)	110.5(2)
C(12)-C(6)-C(5)	110.2(2)
C(7)-C(6)-C(5)	109.2(2)
C(17)-C(6)-C(5)	108.3(2)
N(2)-C(7)-C(8)	120.7(3)
N(2)-C(7)-C(6)	117.8(2)
C(8)-C(7)-C(6)	121.5(3)
C(9)-C(8)-C(7)	120.7(3)
C(8)-C(9)-C(10)	119.1(3)
C(11)-C(10)-C(9)	118.2(3)
N(2)-C(11)-C(10)	123.8(3)
N(3)-C(12)-C(13)	119.6(3)
N(3)-C(12)-C(6)	116.8(2)
C(13)-C(12)-C(6)	123.6(3)
C(14)-C(13)-C(12)	120.5(3)
C(13)-C(14)-C(15)	119.2(3)
C(16)-C(15)-C(14)	118.4(3)
N(3)-C(16)-C(15)	123.0(3)
C(19)-C(18)-C(23)	118.6(3)
C(19)-C(18)-P(1)	124.4(2)
C(23)-C(18)-P(1)	116.4(2)
C(18)-C(19)-C(20)	120.1(3)
C(21)-C(20)-C(19)	120.3(3)
C(20)-C(21)-C(22)	120.1(3)
C(21)-C(22)-C(23)	119.9(3)
C(22)-C(23)-C(18)	120.9(3)
C(29)-C(24)-C(25)	119.2(3)
C(29)-C(24)-P(1)	120.0(2)
C(25)-C(24)-P(1)	120.8(3)
C(26)-C(25)-C(24)	120.6(4)
C(27)-C(26)-C(25)	119.6(4)
C(28)-C(27)-C(26)	120.6(4)
C(27)-C(28)-C(29)	120.0(4)
C(24)-C(29)-C(28)	120.0(4)
C(35)-C(30)-C(31)	117.3(3)
C(35)-C(30)-P(1)	119.0(2)
C(31)-C(30)-P(1)	123.2(2)
C(32)-C(31)-C(30)	120.4(3)
C(33)-C(32)-C(31)	121.2(3)
C(32)-C(33)-C(34)	118.9(3)
C(33)-C(34)-C(35)	120.3(3)
C(34)-C(35)-C(30)	121.8(3)
C(37)-C(36)-C(41)	117.6(3)
C(37)-C(36)-P(2)	123.2(2)
C(41)-C(36)-P(2)	119.1(2)
C(36)-C(37)-C(38)	120.8(3)
C(39)-C(38)-C(37)	120.7(3)
C(38)-C(39)-C(40)	119.2(3)
C(39)-C(40)-C(41)	120.3(3)
C(40)-C(41)-C(36)	121.2(3)
C(47)-C(42)-C(43)	117.4(3)
C(47)-C(42)-P(2)	124.3(2)
C(43)-C(42)-P(2)	118.2(2)
C(44)-C(43)-C(42)	121.2(3)

C(45)-C(44)-C(43)	120.5(3)
C(44)-C(45)-C(46)	119.2(3)
C(47)-C(46)-C(45)	120.4(3)
C(46)-C(47)-C(42)	121.2(3)
C(49)-C(48)-C(53)	118.6(3)
C(49)-C(48)-P(2)	119.3(2)
C(53)-C(48)-P(2)	122.1(2)
C(48)-C(49)-C(50)	121.0(3)
C(49)-C(50)-C(51)	119.6(3)
C(52)-C(51)-C(50)	119.9(3)
C(51)-C(52)-C(53)	120.4(3)
C(52)-C(53)-C(48)	120.6(3)
C(59)-C(54)-C(55)	118.4(3)
C(59)-C(54)-P(3)	117.1(2)
C(55)-C(54)-P(3)	124.5(2)
C(56)-C(55)-C(54)	120.3(3)
C(57)-C(56)-C(55)	120.3(3)
C(58)-C(57)-C(56)	120.3(3)
C(57)-C(58)-C(59)	119.9(3)
C(54)-C(59)-C(58)	120.7(3)
C(61)-C(60)-C(65)	117.6(3)
C(61)-C(60)-P(3)	122.0(2)
C(65)-C(60)-P(3)	120.3(2)
C(60)-C(61)-C(62)	120.9(3)
C(63)-C(62)-C(61)	120.6(3)
C(64)-C(63)-C(62)	119.1(3)
C(63)-C(64)-C(65)	120.3(3)
C(64)-C(65)-C(60)	121.5(3)
C(67)-C(66)-C(71)	118.5(3)
C(67)-C(66)-P(3)	125.5(2)
C(71)-C(66)-P(3)	115.8(2)
C(68)-C(67)-C(66)	120.6(3)
C(69)-C(68)-C(67)	120.8(3)
C(68)-C(69)-C(70)	119.4(3)
C(71)-C(70)-C(69)	120.2(3)
C(70)-C(71)-C(66)	120.4(3)

Table 29 Anisotropic displacement parameters ($Å^2 x\ 10^3$) for **2.19**. The anisotropic displacement factor exponent takes the form: $-2\pi^2[\ h^2\ a^{*2}U^{11} + ...\ + 2\ h\ k\ a^*\ b^*\ U^{12}\ ]$

	U^{11}	U^{22}	U^{33}	U^{23}	U^{13}	U^{12}
Ru(1)	20(1)	16(1)	26(1)	-1(1)	1(1)	0(1)
Ru(2)	21(1)	17(1)	26(1)	1(1)	-1(1)	-1(1)
Cl(1)	21(1)	22(1)	34(1)	4(1)	0(1)	0(1)
Cl(2)	35(1)	24(1)	37(1)	-3(1)	-5(1)	-3(1)
P(1)	30(1)	22(1)	28(1)	-1(1)	0(1)	2(1)
P(2)	25(1)	20(1)	29(1)	2(1)	0(1)	1(1)
P(3)	23(1)	22(1)	33(1)	4(1)	2(1)	-1(1)
N(1)	21(1)	20(1)	26(1)	-3(1)	-1(1)	0(1)
N(2)	24(1)	27(1)	31(1)	2(1)	2(1)	2(1)
N(3)	27(1)	20(1)	30(1)	0(1)	6(1)	2(1)
C(1)	19(1)	21(1)	28(1)	-2(1)	1(1)	4(1)

C(2)	22(1)	31(1)	28(2)	2(1)	1(1)	3(1)
C(3)	30(2)	34(2)	27(2)	-2(1)	-3(1)	7(1)
C(4)	28(2)	32(2)	33(2)	-8(1)	-6(1)	-2(1)
C(5)	21(1)	21(1)	39(2)	-3(1)	1(1)	1(1)
C(6)	30(2)	24(1)	38(2)	-4(1)	-1(1)	-8(1)
C(7)	26(2)	30(2)	35(2)	4(1)	0(1)	-4(1)
C(8)	28(2)	54(2)	48(2)	4(2)	0(2)	-10(2)
C(9)	24(2)	76(3)	52(2)	11(2)	5(2)	-6(2)
C(10)	31(2)	62(2)	39(2)	9(2)	9(1)	14(2)
C(11)	30(2)	38(2)	31(2)	3(1)	3(1)	7(1)
C(12)	31(2)	21(1)	37(2)	-2(1)	7(1)	-3(1)
C(13)	53(2)	22(2)	57(2)	-5(1)	4(2)	-7(1)
C(14)	66(2)	18(1)	59(2)	1(1)	10(2)	7(2)
C(15)	48(2)	27(2)	43(2)	5(1)	6(2)	10(1)
C(16)	32(2)	27(1)	28(2)	3(1)	6(1)	5(1)
C(17)	47(2)	38(2)	48(2)	-7(2)	-4(2)	-17(2)
C(18)	31(2)	31(2)	26(2)	-4(1)	-4(1)	1(1)
C(19)	42(2)	37(2)	40(2)	2(1)	-6(2)	0(1)
C(20)	58(2)	42(2)	48(2)	5(2)	-15(2)	11(2)
C(21)	40(2)	68(2)	46(2)	-6(2)	-15(2)	12(2)
C(22)	34(2)	66(2)	42(2)	-3(2)	-6(2)	-4(2)
C(23)	42(2)	43(2)	33(2)	-1(1)	-6(1)	-6(1)
C(24)	48(2)	29(2)	36(2)	-11(1)	2(2)	-3(1)
C(25)	65(2)	46(2)	45(2)	-13(2)	-8(2)	8(2)
C(26)	109(4)	60(3)	57(3)	-30(2)	-11(3)	5(3)
C(27)	160(5)	43(2)	77(3)	-27(2)	3(3)	15(3)
C(28)	150(5)	33(2)	62(3)	-5(2)	15(3)	26(2)
C(29)	77(3)	30(2)	43(2)	-4(2)	9(2)	7(2)
C(30)	31(2)	33(2)	27(2)	3(1)	1(1)	4(1)
C(31)	44(2)	40(2)	36(2)	2(1)	4(2)	8(2)
C(32)	40(2)	66(2)	42(2)	6(2)	14(2)	15(2)
C(33)	35(2)	67(2)	49(2)	7(2)	9(2)	-10(2)
C(34)	48(2)	51(2)	43(2)	0(2)	7(2)	-17(2)
C(35)	38(2)	41(2)	32(2)	-2(1)	9(1)	-5(1)
C(36)	26(1)	26(1)	31(2)	6(1)	-1(1)	3(1)
C(37)	39(2)	36(2)	60(2)	-9(2)	8(2)	-2(1)
C(38)	42(2)	50(2)	75(3)	-10(2)	20(2)	7(2)
C(39)	26(2)	51(2)	60(2)	9(2)	9(2)	-1(2)
C(40)	32(2)	40(2)	48(2)	7(2)	-5(2)	-3(1)
C(41)	30(2)	30(2)	39(2)	4(1)	-1(1)	2(1)
C(42)	33(2)	22(1)	30(2)	1(1)	-3(1)	6(1)
C(43)	32(2)	42(2)	34(2)	5(1)	-2(1)	7(1)
C(44)	40(2)	55(2)	37(2)	9(2)	7(2)	7(2)
C(45)	53(2)	61(2)	32(2)	2(2)	-4(2)	7(2)
C(46)	41(2)	63(2)	38(2)	3(2)	-9(2)	-1(2)
C(47)	34(2)	45(2)	34(2)	6(1)	-2(1)	1(1)
C(48)	24(1)	19(1)	43(2)	-1(1)	2(1)	0(1)
C(49)	33(2)	32(2)	44(2)	-4(1)	-1(1)	6(1)
C(50)	35(2)	39(2)	58(2)	-17(2)	-3(2)	4(1)
C(51)	37(2)	21(2)	86(3)	-8(2)	5(2)	-1(1)
C(52)	45(2)	24(2)	69(2)	8(2)	2(2)	1(1)
C(53)	35(2)	26(2)	49(2)	6(1)	0(1)	2(1)
C(54)	23(2)	25(1)	48(2)	9(1)	2(1)	0(1)
C(55)	41(2)	38(2)	67(2)	10(2)	20(2)	2(2)
C(56)	48(2)	50(2)	79(3)	24(2)	20(2)	-8(2)

C(57)	38(2)	31(2)	83(3)	22(2)	-4(2)	-6(1)
C(58)	35(2)	28(2)	62(2)	3(2)	-8(2)	-2(1)
C(59)	29(2)	29(2)	46(2)	5(1)	-3(1)	-3(1)
C(60)	23(2)	21(1)	44(2)	0(1)	0(1)	-3(1)
C(61)	30(2)	22(1)	47(2)	3(1)	1(1)	-2(1)
C(62)	37(2)	33(2)	48(2)	4(1)	-5(2)	0(1)
C(63)	25(2)	42(2)	67(2)	3(2)	-8(2)	4(1)
C(64)	28(2)	46(2)	62(2)	-7(2)	4(2)	2(1)
C(65)	28(2)	40(2)	47(2)	-2(2)	1(1)	-2(1)
C(66)	19(1)	34(2)	35(2)	-1(1)	4(1)	0(1)
C(67)	29(2)	49(2)	40(2)	7(2)	3(1)	5(1)
C(68)	42(2)	74(3)	29(2)	0(2)	2(1)	6(2)
C(69)	44(2)	65(2)	42(2)	-20(2)	3(2)	-3(2)
C(70)	38(2)	41(2)	58(2)	-10(2)	7(2)	-5(2)
C(71)	29(2)	37(2)	35(2)	-1(1)	6(1)	-1(1)

Table 30 Hydrogen coordinates (x 10^4) and isotropic displacement parameters (Å^{2}x 10^3) for **2.19**.

	x	y	z	U(eq)
H(1)	1191(15)	2930(17)	1193(13)	60
H(2A)	1485	2899	-449	32
H(3A)	934	2098	-827	36
H(4A)	469	1294	-352	37
H(8A)	-687	1084	888	52
H(9A)	-1257	1675	1441	61
H(10A)	-821	2513	1906	52
H(11A)	165	2728	1793	39
H(13A)	698	-153	800	52
H(14A)	1448	-663	1233	57
H(15A)	2153	-25	1640	47
H(16A)	2046	1090	1643	35
H(17A)	353	422	151	67
H(17B)	-187	918	171	67
H(17C)	-110	381	597	67
H(19A)	1701	1118	2747	48
H(20A)	2630	695	2934	59
H(21A)	3469	1253	2698	61
H(22A)	3392	2262	2308	57
H(23A)	2474	2679	2104	47
H(25A)	1562	2759	3112	62
H(26A)	1475	3768	3503	90
H(27A)	1104	4652	3066	112
H(28A)	847	4546	2237	98
H(29A)	932	3536	1840	60
H(31A)	374	2510	2879	48
H(32A)	-425	1918	3178	59
H(33A)	-572	845	2942	60
H(34A)	105	344	2418	57
H(35A)	887	932	2099	45
H(37A)	311	4746	1103	54
H(38A)	-648	4570	1372	67
H(39A)	-1157	3651	1127	55

H(40A)	-690	2871	642	48
H(41A)	285	3008	413	40
H(43A)	1845	4305	-364	43
H(44A)	1727	4309	-1222	53
H(45A)	826	4059	-1572	59
H(46A)	19	3887	-1055	57
H(47A)	130	3898	-198	45
H(49A)	1502	4722	1356	43
H(50A)	1645	5811	1572	53
H(51A)	1476	6631	983	57
H(52A)	1142	6358	195	55
H(53A)	1006	5272	-22	44
H(55A)	3397	3970	-507	58
H(56A)	3651	5040	-704	71
H(57A)	3252	5900	-262	60
H(58A)	2638	5702	407	50
H(59A)	2387	4633	617	42
H(61A)	3112	3187	1257	39
H(62A)	4034	2938	1574	47
H(63A)	4807	2686	1042	53
H(64A)	4646	2675	186	54
H(65A)	3738	2957	-133	46
H(67A)	2517	3561	-846	47
H(68A)	2525	2856	-1517	58
H(69A)	2649	1745	-1399	60
H(70A)	2762	1333	-595	55
H(71A)	2745	2033	84	41

X-ray Data Collection, Structure Solution and Refinement for complex 2.25.

A yellow crystal of approximate dimensions 0.130 x 0.104 x 0.098 mm was mounted on a glass fiber and transferred to a Bruker SMART APEX II diffractometer. The APEX2[1] program package was used to determine the unit-cell parameters and for data collection (40 sec/frame scan time for a sphere of diffraction data). The raw frame data was processed using SAINT[2] and SADABS[3] to yield the reflection data file. Subsequent calculations were carried out using the SHELXTL[4] program. There were no systematic absences nor any diffraction symmetry other than the Friedel condition. The centrosymmetric triclinic space group $P\bar{1}$ was assigned and later determined to be correct.

The structure was solved by direct methods and refined on F^2 by full-matrix least-squares techniques. The analytical scattering factors[5] for neutral atoms were used throughout the analysis. There were two molecules in the asymmetric unit. There was one cocrystallized $CHCl_3$ molecule of solvation present per formula unit. Hydrogen atoms were included using a riding model. At convergence, wR2 = 0.0636 and Goof = 1.018 for 603 variables refined against 12755 data (0.73 Å), R1 = 0.0285 for those 10693 data with $I > 2.0\sigma(I)$.

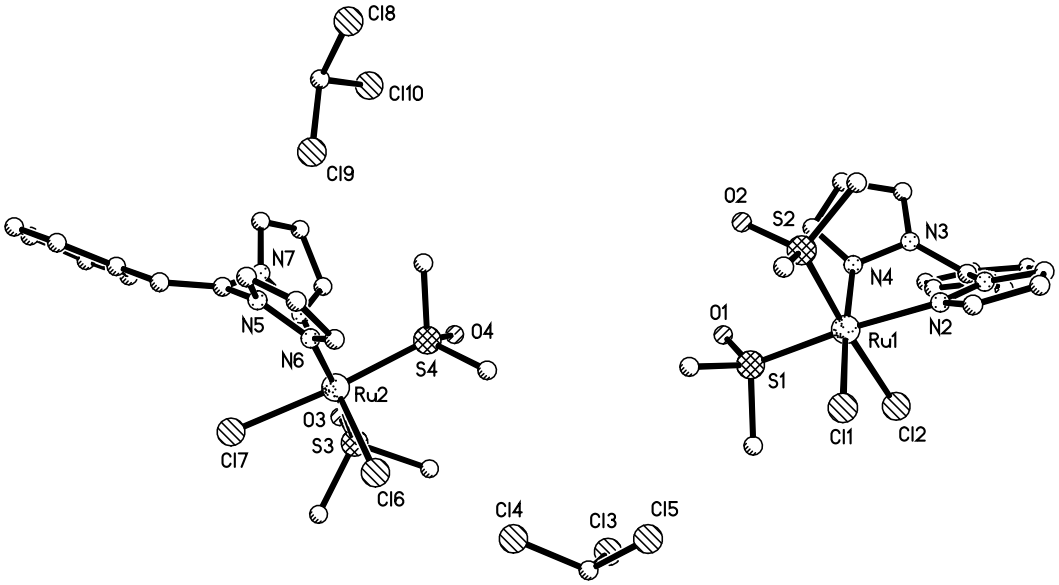

Table 31 Crystal data and structure refinement for **2.25**.

Identification code	zg36 (Tobias Friedberger)	
Empirical formula	$C_{19}H_{25}Cl_5N_4O_2RuS_2$	
Formula weight	683.87	
Temperature	88(2) K	
Wavelength	0.71073 Å	
Crystal system	Triclinic	
Space group	$P\bar{1}$	
Unit cell dimensions	a = 8.2971(10) Å	α= 84.9753(14)°.
	b = 15.3869(18) Å	β= 88.2322(14)°.
	c = 21.072(3) Å	γ = 81.2577(13)°.
Volume	2648.3(5) Å^3	
Z	4	
Density (calculated)	1.715 Mg/m^3	
Absorption coefficient	1.280 mm^{-1}	
F(000)	1376	
Crystal color	yellow	
Crystal size	0.130 x 0.104 x 0.098 mm^3	
Theta range for data collection	1.722 to 28.916°	
Index ranges	$-11 \le h \le 10$, $-20 \le k \le 20$, $-28 \le l \le 28$	
Reflections collected	32252	
Independent reflections	12755 [R(int) = 0.0302]	
Completeness to theta = 25.500°	99.8 %	
Absorption correction	Numerical	
Max. and min. transmission	0.9746 and 0.9074	
Refinement method	Full-matrix least-squares on F^2	
Data / restraints / parameters	12755 / 0 / 603	
Goodness-of-fit on F^2	1.018	
Final R indices [I>2sigma(I) = 10693 data]	R1 = 0.0285, wR2 = 0.0602	

R indices (all data, 0.73 Å)	R1 = 0.0383, wR2 = 0.0636
Largest diff. peak and hole	0.951 and -0.816 e.Å^{-3}

Table 32 Atomic coordinates (x 10^4) and equivalent isotropic displacement parameters (Å^{2}x 10^3) for **2.25**. U(eq) is defined as one third of the trace of the orthogonalized U^{ij} tensor.

	x	y	z	U(eq)
Ru(1)	18751(1)	2360(1)	8673(1)	11(1)
Cl(1)	19364(1)	3526(1)	9272(1)	15(1)
Cl(2)	17536(1)	1697(1)	9628(1)	15(1)
Cl(3)	11268(1)	5310(1)	9229(1)	31(1)
Cl(4)	12021(1)	6924(1)	8553(1)	26(1)
Cl(5)	14506(1)	5777(1)	9292(1)	25(1)
S(1)	16293(1)	3173(1)	8438(1)	15(1)
S(2)	19930(1)	2868(1)	7779(1)	14(1)
O(1)	15181(2)	2820(1)	8023(1)	26(1)
O(2)	18880(2)	3064(1)	7208(1)	19(1)
N(1)	21191(2)	691(1)	9054(1)	14(1)
N(2)	20962(2)	1589(1)	8966(1)	14(1)
N(3)	19232(2)	486(1)	8304(1)	12(1)
N(4)	18339(2)	1308(1)	8176(1)	13(1)
C(1)	19947(3)	203(1)	8905(1)	14(1)
C(2)	19621(3)	-501(2)	9266(1)	15(1)
C(3)	18374(3)	-1053(2)	9153(1)	16(1)
C(4)	16879(3)	-710(2)	8871(1)	18(1)
C(5)	15743(3)	-1260(2)	8778(1)	24(1)
C(6)	16076(3)	-2154(2)	8978(1)	27(1)
C(7)	17522(3)	-2492(2)	9275(1)	27(1)
C(8)	18672(3)	-1947(2)	9367(1)	20(1)
C(9)	22697(3)	379(2)	9286(1)	18(1)
C(10)	23472(3)	1090(2)	9345(1)	20(1)
C(11)	22352(3)	1826(2)	9144(1)	16(1)
C(12)	19102(3)	-38(2)	7826(1)	15(1)
C(13)	18119(3)	450(2)	7377(1)	16(1)
C(14)	17662(3)	1279(2)	7613(1)	15(1)
C(15)	15159(3)	3453(2)	9144(1)	18(1)
C(16)	16440(3)	4274(2)	8109(1)	21(1)
C(17)	20900(3)	3825(2)	7832(1)	20(1)
C(18)	21643(3)	2112(2)	7535(1)	18(1)
C(19)	12394(3)	6196(2)	9241(1)	21(1)
Ru(2)	9796(1)	7541(1)	6238(1)	10(1)
Cl(6)	10680(1)	7964(1)	7225(1)	14(1)
Cl(7)	8138(1)	8986(1)	6027(1)	13(1)
Cl(8)	16111(1)	6231(1)	3390(1)	32(1)
Cl(9)	13796(1)	7129(1)	4225(1)	44(1)
Cl(10)	13296(1)	5432(1)	3805(1)	34(1)
S(3)	7618(1)	7069(1)	6771(1)	14(1)
S(4)	11344(1)	6210(1)	6353(1)	14(1)
O(3)	6426(2)	6697(1)	6407(1)	20(1)
O(4)	10505(2)	5423(1)	6414(1)	20(1)
N(5)	11590(2)	8497(1)	5157(1)	12(1)
N(6)	11719(2)	8089(1)	5760(1)	12(1)
N(7)	9694(2)	7632(1)	4800(1)	12(1)
N(8)	9161(2)	7216(1)	5352(1)	13(1)

C(20)	10205(3)	8477(1)	4778(1)	12(1)
C(21)	9610(3)	9180(2)	4397(1)	13(1)
C(22)	8267(3)	9306(2)	3941(1)	14(1)
C(23)	8318(3)	9977(1)	3451(1)	13(1)
C(24)	7117(3)	10153(2)	2995(1)	16(1)
C(25)	5822(3)	9676(2)	3030(1)	18(1)
C(26)	5728(3)	9030(2)	3528(1)	18(1)
C(27)	6936(3)	8841(2)	3982(1)	15(1)
C(28)	12945(3)	8873(2)	4991(1)	16(1)
C(29)	13981(3)	8695(2)	5495(1)	17(1)
C(30)	13173(3)	8211(2)	5958(1)	15(1)
C(31)	9617(3)	7143(2)	4299(1)	16(1)
C(32)	9005(3)	6398(2)	4524(1)	20(1)
C(33)	8721(3)	6474(2)	5176(1)	18(1)
C(34)	8172(3)	6302(2)	7445(1)	21(1)
C(35)	6489(3)	7927(2)	7194(1)	19(1)
C(36)	12776(3)	6064(2)	6985(1)	22(1)
C(37)	12759(3)	6056(2)	5697(1)	22(1)
C(38)	14045(3)	6432(2)	3601(1)	23(1)

Table 33. Bond lengths [Å] and angles [°] for **2.25**.

Ru(1)-N(4)	2.0792(18)
Ru(1)-N(2)	2.1056(19)
Ru(1)-S(2)	2.2314(6)
Ru(1)-S(1)	2.2695(6)
Ru(1)-Cl(1)	2.4048(6)
Ru(1)-Cl(2)	2.4362(6)
Cl(3)-C(19)	1.768(3)
Cl(4)-C(19)	1.758(2)
Cl(5)-C(19)	1.776(3)
S(1)-O(1)	1.4822(17)
S(1)-C(15)	1.784(2)
S(1)-C(16)	1.793(2)
S(2)-O(2)	1.4894(16)
S(2)-C(18)	1.787(2)
S(2)-C(17)	1.795(2)
N(1)-C(9)	1.359(3)
N(1)-N(2)	1.362(3)
N(1)-C(1)	1.423(3)
N(2)-C(11)	1.335(3)
N(3)-C(12)	1.360(3)
N(3)-N(4)	1.374(2)
N(3)-C(1)	1.421(3)
N(4)-C(14)	1.334(3)
C(1)-C(2)	1.325(3)
C(2)-C(3)	1.473(3)
C(3)-C(8)	1.397(3)
C(3)-C(4)	1.400(3)
C(4)-C(5)	1.388(3)
C(5)-C(6)	1.392(4)
C(6)-C(7)	1.379(4)
C(7)-C(8)	1.391(3)
C(9)-C(10)	1.366(3)

C(10)-C(11)	1.396(3)
C(12)-C(13)	1.364(3)
C(13)-C(14)	1.404(3)
Ru(2)-N(8)	2.0775(18)
Ru(2)-N(6)	2.1056(18)
Ru(2)-S(4)	2.2431(6)
Ru(2)-S(3)	2.2762(6)
Ru(2)-Cl(6)	2.4016(6)
Ru(2)-Cl(7)	2.4442(6)
Cl(8)-C(38)	1.745(3)
Cl(9)-C(38)	1.756(3)
Cl(10)-C(38)	1.761(3)
S(3)-O(3)	1.4802(17)
S(3)-C(35)	1.787(2)
S(3)-C(34)	1.791(2)
S(4)-O(4)	1.4811(17)
S(4)-C(36)	1.788(2)
S(4)-C(37)	1.793(2)
N(5)-C(28)	1.364(3)
N(5)-N(6)	1.367(2)
N(5)-C(20)	1.425(3)
N(6)-C(30)	1.333(3)
N(7)-C(31)	1.357(3)
N(7)-N(8)	1.373(2)
N(7)-C(20)	1.423(3)
N(8)-C(33)	1.336(3)
C(20)-C(21)	1.329(3)
C(21)-C(22)	1.474(3)
C(22)-C(23)	1.399(3)
C(22)-C(27)	1.401(3)
C(23)-C(24)	1.386(3)
C(24)-C(25)	1.387(3)
C(25)-C(26)	1.391(3)
C(26)-C(27)	1.388(3)
C(28)-C(29)	1.369(3)
C(29)-C(30)	1.393(3)
C(31)-C(32)	1.366(3)
C(32)-C(33)	1.400(3)

N(4)-Ru(1)-N(2)	87.22(7)
N(4)-Ru(1)-S(2)	86.60(5)
N(2)-Ru(1)-S(2)	91.28(5)
N(4)-Ru(1)-S(1)	94.20(5)
N(2)-Ru(1)-S(1)	175.45(5)
S(2)-Ru(1)-S(1)	93.11(2)
N(4)-Ru(1)-Cl(1)	176.78(5)
N(2)-Ru(1)-Cl(1)	89.56(5)
S(2)-Ru(1)-Cl(1)	93.71(2)
S(1)-Ru(1)-Cl(1)	88.99(2)
N(4)-Ru(1)-Cl(2)	89.91(5)
N(2)-Ru(1)-Cl(2)	86.29(5)
S(2)-Ru(1)-Cl(2)	175.84(2)
S(1)-Ru(1)-Cl(2)	89.39(2)
Cl(1)-Ru(1)-Cl(2)	89.65(2)
O(1)-S(1)-C(15)	106.93(11)

O(1)-S(1)-C(16)	106.54(11)
C(15)-S(1)-C(16)	97.72(11)
O(1)-S(1)-Ru(1)	118.87(7)
C(15)-S(1)-Ru(1)	111.32(8)
C(16)-S(1)-Ru(1)	113.21(9)
O(2)-S(2)-C(18)	104.80(11)
O(2)-S(2)-C(17)	105.92(11)
C(18)-S(2)-C(17)	99.61(12)
O(2)-S(2)-Ru(1)	116.34(7)
C(18)-S(2)-Ru(1)	112.14(8)
C(17)-S(2)-Ru(1)	116.17(8)
C(9)-N(1)-N(2)	110.83(18)
C(9)-N(1)-C(1)	128.24(19)
N(2)-N(1)-C(1)	120.93(18)
C(11)-N(2)-N(1)	105.22(18)
C(11)-N(2)-Ru(1)	130.67(16)
N(1)-N(2)-Ru(1)	123.98(14)
C(12)-N(3)-N(4)	110.87(18)
C(12)-N(3)-C(1)	125.73(19)
N(4)-N(3)-C(1)	122.61(18)
C(14)-N(4)-N(3)	105.15(18)
C(14)-N(4)-Ru(1)	131.78(15)
N(3)-N(4)-Ru(1)	120.38(13)
C(2)-C(1)-N(3)	123.9(2)
C(2)-C(1)-N(1)	122.5(2)
N(3)-C(1)-N(1)	113.29(19)
C(1)-C(2)-C(3)	126.7(2)
C(8)-C(3)-C(4)	119.1(2)
C(8)-C(3)-C(2)	118.1(2)
C(4)-C(3)-C(2)	122.7(2)
C(5)-C(4)-C(3)	120.4(2)
C(4)-C(5)-C(6)	119.8(2)
C(7)-C(6)-C(5)	120.2(2)
C(6)-C(7)-C(8)	120.3(2)
C(7)-C(8)-C(3)	120.1(2)
N(1)-C(9)-C(10)	107.4(2)
C(9)-C(10)-C(11)	105.3(2)
N(2)-C(11)-C(10)	111.2(2)
N(3)-C(12)-C(13)	107.3(2)
C(12)-C(13)-C(14)	105.8(2)
N(4)-C(14)-C(13)	110.9(2)
Cl(4)-C(19)-Cl(3)	110.38(13)
Cl(4)-C(19)-Cl(5)	110.21(13)
Cl(3)-C(19)-Cl(5)	109.51(13)
N(8)-Ru(2)-N(6)	86.59(7)
N(8)-Ru(2)-S(4)	87.47(5)
N(6)-Ru(2)-S(4)	90.98(5)
N(8)-Ru(2)-S(3)	95.26(5)
N(6)-Ru(2)-S(3)	175.02(5)
S(4)-Ru(2)-S(3)	93.72(2)
N(8)-Ru(2)-Cl(6)	175.98(5)
N(6)-Ru(2)-Cl(6)	89.40(5)
S(4)-Ru(2)-Cl(6)	92.75(2)
S(3)-Ru(2)-Cl(6)	88.73(2)
N(8)-Ru(2)-Cl(7)	88.73(5)

N(6)-Ru(2)-Cl(7)	86.84(5)
S(4)-Ru(2)-Cl(7)	175.72(2)
S(3)-Ru(2)-Cl(7)	88.58(2)
Cl(6)-Ru(2)-Cl(7)	90.912(19)
O(3)-S(3)-C(35)	106.87(11)
O(3)-S(3)-C(34)	107.02(11)
C(35)-S(3)-C(34)	97.50(12)
O(3)-S(3)-Ru(2)	118.51(7)
C(35)-S(3)-Ru(2)	111.20(8)
C(34)-S(3)-Ru(2)	113.52(9)
O(4)-S(4)-C(36)	106.28(11)
O(4)-S(4)-C(37)	105.78(11)
C(36)-S(4)-C(37)	98.58(12)
O(4)-S(4)-Ru(2)	117.77(7)
C(36)-S(4)-Ru(2)	115.31(9)
C(37)-S(4)-Ru(2)	111.05(8)
C(28)-N(5)-N(6)	110.70(18)
C(28)-N(5)-C(20)	127.86(19)
N(6)-N(5)-C(20)	121.41(17)
C(30)-N(6)-N(5)	105.12(18)
C(30)-N(6)-Ru(2)	131.52(15)
N(5)-N(6)-Ru(2)	123.03(13)
C(31)-N(7)-N(8)	110.91(18)
C(31)-N(7)-C(20)	126.54(19)
N(8)-N(7)-C(20)	122.53(17)
C(33)-N(8)-N(7)	104.88(18)
C(33)-N(8)-Ru(2)	130.55(16)
N(7)-N(8)-Ru(2)	121.12(13)
C(21)-C(20)-N(7)	125.5(2)
C(21)-C(20)-N(5)	120.25(19)
N(7)-C(20)-N(5)	113.86(18)
C(20)-C(21)-C(22)	130.5(2)
C(23)-C(22)-C(27)	118.8(2)
C(23)-C(22)-C(21)	116.0(2)
C(27)-C(22)-C(21)	125.1(2)
C(24)-C(23)-C(22)	120.9(2)
C(23)-C(24)-C(25)	120.0(2)
C(24)-C(25)-C(26)	119.6(2)
C(27)-C(26)-C(25)	120.8(2)
C(26)-C(27)-C(22)	119.8(2)
N(5)-C(28)-C(29)	107.3(2)
C(28)-C(29)-C(30)	105.4(2)
N(6)-C(30)-C(29)	111.5(2)
N(7)-C(31)-C(32)	107.5(2)
C(31)-C(32)-C(33)	105.4(2)
N(8)-C(33)-C(32)	111.3(2)
Cl(8)-C(38)-Cl(9)	108.78(14)
Cl(8)-C(38)-Cl(10)	110.45(14)
Cl(9)-C(38)-Cl(10)	112.29(15)

Table 34 Anisotropic displacement parameters ($Å^2 x\ 10^3$) for **2.25**. The anisotropic displacement factor exponent takes the form: $-2\pi^2[\ h^2\ a^{*2}U^{11} + ...\ + 2\ h\ k\ a^*\ b^*\ U^{12}\ ]$

	U^{11}	U^{22}	U^{33}	U^{23}	U^{13}	U^{12}
Ru(1)	11(1)	10(1)	11(1)	-1(1)	-2(1)	-3(1)
Cl(1)	19(1)	14(1)	14(1)	-3(1)	-1(1)	-6(1)
Cl(2)	13(1)	15(1)	15(1)	2(1)	0(1)	-3(1)
Cl(3)	36(1)	28(1)	33(1)	-6(1)	5(1)	-15(1)
Cl(4)	34(1)	26(1)	16(1)	2(1)	-2(1)	0(1)
Cl(5)	30(1)	17(1)	27(1)	-1(1)	-5(1)	-2(1)
S(1)	16(1)	13(1)	17(1)	-2(1)	-4(1)	0(1)
S(2)	15(1)	13(1)	13(1)	-1(1)	0(1)	-4(1)
O(1)	21(1)	23(1)	34(1)	-13(1)	-15(1)	2(1)
O(2)	20(1)	24(1)	13(1)	1(1)	-4(1)	-4(1)
N(1)	12(1)	13(1)	16(1)	0(1)	-1(1)	-2(1)
N(2)	14(1)	14(1)	15(1)	-1(1)	1(1)	-4(1)
N(3)	11(1)	10(1)	15(1)	-2(1)	-1(1)	-2(1)
N(4)	14(1)	10(1)	14(1)	-2(1)	-2(1)	-3(1)
C(1)	11(1)	12(1)	18(1)	-4(1)	-1(1)	0(1)
C(2)	14(1)	15(1)	15(1)	-2(1)	-1(1)	0(1)
C(3)	17(1)	15(1)	15(1)	-2(1)	4(1)	-4(1)
C(4)	17(1)	17(1)	20(1)	-1(1)	5(1)	-4(1)
C(5)	19(1)	30(1)	26(1)	-8(1)	4(1)	-8(1)
C(6)	29(1)	25(1)	32(2)	-9(1)	5(1)	-17(1)
C(7)	38(2)	13(1)	31(2)	-1(1)	7(1)	-8(1)
C(8)	22(1)	16(1)	22(1)	-2(1)	4(1)	-2(1)
C(9)	13(1)	19(1)	21(1)	-1(1)	-2(1)	2(1)
C(10)	12(1)	26(1)	21(1)	-2(1)	-3(1)	-4(1)
C(11)	13(1)	19(1)	18(1)	-2(1)	0(1)	-6(1)
C(12)	14(1)	14(1)	19(1)	-5(1)	4(1)	-4(1)
C(13)	13(1)	20(1)	16(1)	-7(1)	1(1)	-5(1)
C(14)	15(1)	18(1)	14(1)	-4(1)	-2(1)	-6(1)
C(15)	14(1)	17(1)	21(1)	-1(1)	1(1)	-1(1)
C(16)	27(1)	14(1)	19(1)	2(1)	-1(1)	1(1)
C(17)	24(1)	16(1)	20(1)	-1(1)	3(1)	-9(1)
C(18)	18(1)	18(1)	17(1)	-4(1)	3(1)	-2(1)
C(19)	29(1)	18(1)	15(1)	1(1)	1(1)	-6(1)
Ru(2)	11(1)	9(1)	11(1)	-1(1)	-1(1)	-2(1)
Cl(6)	18(1)	12(1)	12(1)	-1(1)	-2(1)	-2(1)
Cl(7)	13(1)	11(1)	15(1)	0(1)	-1(1)	-1(1)
Cl(8)	27(1)	30(1)	41(1)	-6(1)	11(1)	-7(1)
Cl(9)	55(1)	29(1)	50(1)	-16(1)	32(1)	-18(1)
Cl(10)	30(1)	21(1)	51(1)	2(1)	1(1)	-11(1)
S(3)	14(1)	12(1)	15(1)	0(1)	1(1)	-4(1)
S(4)	16(1)	11(1)	14(1)	-1(1)	0(1)	0(1)
O(3)	17(1)	21(1)	24(1)	-4(1)	0(1)	-9(1)
O(4)	24(1)	13(1)	23(1)	-1(1)	0(1)	-4(1)
N(5)	13(1)	13(1)	11(1)	1(1)	-1(1)	-3(1)
N(6)	13(1)	11(1)	12(1)	0(1)	-1(1)	-2(1)
N(7)	14(1)	11(1)	12(1)	-1(1)	-1(1)	-4(1)
N(8)	14(1)	12(1)	12(1)	0(1)	0(1)	-2(1)
C(20)	13(1)	13(1)	11(1)	-1(1)	1(1)	-4(1)
C(21)	15(1)	13(1)	13(1)	-3(1)	2(1)	-4(1)
C(22)	13(1)	13(1)	14(1)	-3(1)	2(1)	-1(1)
C(23)	14(1)	12(1)	15(1)	-1(1)	1(1)	-2(1)
C(24)	16(1)	15(1)	16(1)	1(1)	-1(1)	-1(1)
C(25)	13(1)	20(1)	19(1)	-1(1)	-4(1)	-1(1)

C(26)	14(1)	18(1)	23(1)	-2(1)	1(1)	-5(1)
C(27)	16(1)	15(1)	16(1)	-1(1)	2(1)	-4(1)
C(28)	16(1)	14(1)	18(1)	-2(1)	4(1)	-4(1)
C(29)	14(1)	19(1)	20(1)	-5(1)	1(1)	-6(1)
C(30)	13(1)	16(1)	17(1)	-1(1)	-4(1)	0(1)
C(31)	20(1)	16(1)	13(1)	-3(1)	-3(1)	-1(1)
C(32)	24(1)	17(1)	19(1)	-6(1)	-5(1)	-7(1)
C(33)	21(1)	13(1)	22(1)	0(1)	-4(1)	-7(1)
C(34)	24(1)	18(1)	19(1)	6(1)	3(1)	-3(1)
C(35)	17(1)	19(1)	20(1)	-3(1)	4(1)	-2(1)
C(36)	22(1)	19(1)	25(1)	1(1)	-7(1)	2(1)
C(37)	26(1)	18(1)	22(1)	-2(1)	5(1)	2(1)
C(38)	15(1)	17(1)	35(2)	1(1)	-4(1)	-2(1)

Table 35 Hydrogen coordinates (x 10^4) and isotropic displacement parameters (Å^{2}x 10^3) for **2.25**

	x	y	z	U(eq)
H(2A)	20259	-666	9636	18
H(4A)	16642	-98	8743	22
H(5A)	14740	-1027	8578	29
H(6A)	15305	-2532	8910	33
H(7A)	17734	-3101	9417	32
H(8A)	19661	-2183	9576	24
H(9A)	23132	-223	9389	22
H(10A)	24546	1084	9492	23
H(11A)	22552	2418	9134	19
H(12A)	19604	-633	7808	18
H(13A)	17809	267	6986	19
H(14A)	16964	1756	7401	18
H(15A)	14135	3832	9027	27
H(15B)	15800	3767	9404	27
H(15C)	14920	2913	9386	27
H(16A)	15345	4614	8067	31
H(16B)	16978	4253	7689	31
H(16C)	17079	4556	8392	31
H(17A)	21138	4077	7402	29
H(17B)	21919	3656	8065	29
H(17C)	20172	4264	8057	29
H(18A)	22077	2342	7127	27
H(18B)	21301	1539	7487	27
H(18C)	22490	2040	7858	27
H(19A)	12049	6523	9624	25
H(21A)	10137	9682	4423	16
H(23A)	9187	10316	3430	16
H(24A)	7182	10600	2658	19
H(25A)	5003	9791	2715	21
H(26A)	4826	8715	3559	22
H(27A)	6861	8397	4320	18
H(28A)	13136	9198	4599	19
H(29A)	15028	8866	5523	21
H(30A)	13604	7994	6364	18
H(31A)	9932	7292	3871	19

H(32A)	8812	5927	4287	23
H(33A)	8272	6053	5457	22
H(34A)	7186	6189	7687	31
H(34B)	8890	6549	7719	31
H(34C)	8743	5747	7299	31
H(35A)	5602	7696	7441	28
H(35B)	6030	8414	6891	28
H(35C)	7213	8141	7484	28
H(36A)	13428	5476	6986	34
H(36B)	12188	6120	7393	34
H(36C)	13496	6514	6922	34
H(37A)	13343	5451	5736	34
H(37B)	13542	6473	5700	34
H(37C)	12165	6160	5296	34
H(38A)	13432	6744	3225	27

X-ray Data Collection, Structure Solution and Refinement for complex 3.6

A colorless crystal of approximate dimensions 0.288 x 0.237 x 0.156 mm was mounted on a glass fiber and transferred to a Bruker SMART APEX II diffractometer. The APEX2[1] program package was used to determine the unit-cell parameters and for data collection (20 sec/frame scan time for a sphere of diffraction data). The raw frame data was processed using SAINT[2] and SADABS[3] to yield the reflection data file. Subsequent calculations were carried out using the SHELXTL[4] program. There were no systematic absences nor any diffraction symmetry other than the Friedel condition. The centrosymmetric triclinic space group $P\bar{1}$ was assigned and later determined to be correct. The structure was solved by direct methods and refined on F^2 by full-matrix least-squares techniques. The analytical scattering factors[5] for neutral atoms were used throughout the analysis. H7, H8, and H9 were located from a difference-Fourier map and refined (x,y,z and U_{iso}). H7 was refined with a fixed d(O-H) = 0.80(2)Å. All other hydrogen atoms were included using a riding model. The molecule forms and extended structure. At convergence, wR2 = 0.0849 and Goof = 1.047 for 370 variables refined against 5564 data (0.79 Å), R1 = 0.0321 for those 4961 data with $I > 2.0\sigma(I)$.

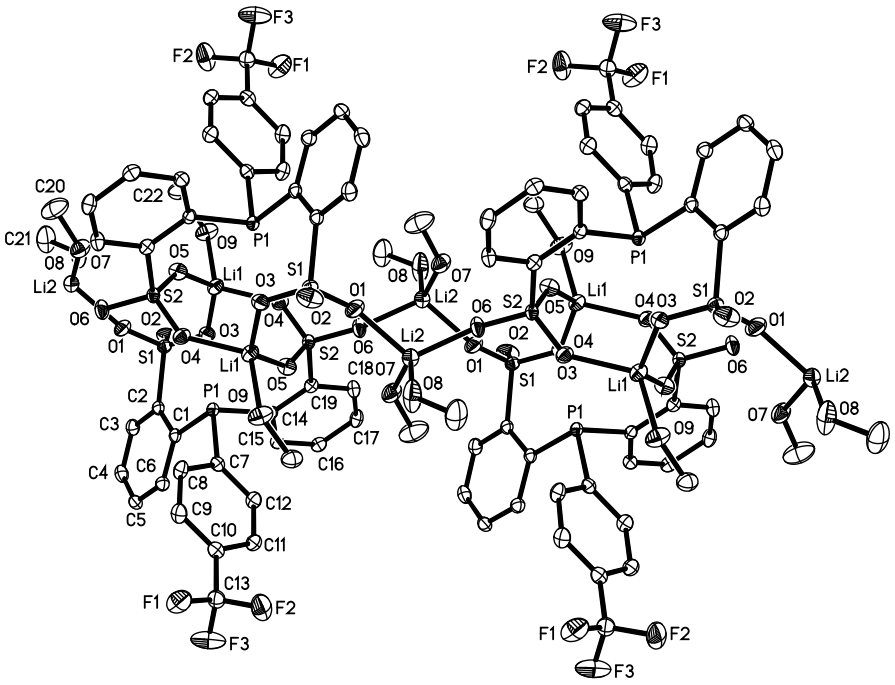

Figure 2 The thermal ellipsoid plot of **3.6** shown at the 50% probability level. Hydrogen atoms are omitted for clarity.

Table 36 Crystal data and structure refinement for **3.6**.

Empirical formula	$C_{22}\ H_{24}\ F_3\ Li_2\ O_9\ P\ S_2$	
Formula weight	598.38	
Temperature	143(2) K	
Wavelength	0.71073 Å	
Crystal system	Triclinic	
Space group	$P\bar{1}$	
Unit cell dimensions	a = 10.1347(8) Å	α = 104.7052(8)°.
	b = 10.8117(8) Å	β = 91.9422(9)°.
	c = 13.1228(10) Å	γ = 109.1931(8)°.
Volume	1302.62(17) Å^3	
Z	2	
Density (calculated)	1.526 Mg/m^3	
Absorption coefficient	0.337 mm-1	
F(000)	616	
Crystal color	colorless	
Crystal size	0.288 x 0.237 x 0.156 mm^3	
Theta range for data collection	1.618 to 26.860°	
Index ranges	$-12 \le h \le 12$, $-13 \le k \le 13$, $-16 \le l \le 16$	
Reflections collected	14701	
Independent reflections	5564 [R(int) = 0.0180]	
Completeness to theta = 25.242°	99.7 %	
Absorption correction	Numerical	
Max. and min. transmission	0.9995 and 0.9189	
Refinement method	Full-matrix least-squares on F^2	

Data / restraints / parameters	5564 / 1 / 370
Goodness-of-fit on F^2	1.047
Final R indices [I>2sigma(I) = 4961 data]	R1 = 0.0321, wR2 = 0.0818
R indices (all data, 0.79 Å)	R1 = 0.0368, wR2 = 0.0849
Largest diff. peak and hole	0.459 and -0.353 e.Å-3

Table 37 Atomic coordinates (x 10^4) and equivalent isotropic displacement parameters (Å^{2}x 10^3) for **3.6**. U(eq) is defined as one third of the trace of the orthogonalized U^{ij} tensor.

	x	y	z	U(eq)
S(1)	-8807(1)	-7765(1)	6215(1)	16(1)
S(2)	-3501(1)	-5961(1)	5616(1)	14(1)
P(1)	-5765(1)	-5130(1)	7196(1)	13(1)
F(1)	-2659(1)	1431(1)	10154(1)	40(1)
F(2)	-979(1)	709(1)	10370(1)	47(1)
F(3)	-2632(2)	413(1)	11340(1)	47(1)
O(1)	-9563(1)	-7117(1)	5698(1)	30(1)
O(2)	-9620(1)	-9148(1)	6201(1)	29(1)
O(3)	-7454(1)	-7660(1)	5833(1)	22(1)
O(4)	-4735(1)	-6753(1)	4846(1)	20(1)
O(5)	-3249(1)	-4505(1)	5959(1)	21(1)
O(6)	-2243(1)	-6226(1)	5278(1)	22(1)
O(7)	-10061(1)	-6354(1)	3728(1)	27(1)
O(8)	-12110(2)	-9120(2)	4223(2)	43(1)
C(1)	-7232(2)	-5633(2)	7993(1)	14(1)
C(2)	-8452(2)	-6784(2)	7573(1)	15(1)
C(3)	-9526(2)	-7177(2)	8183(1)	19(1)
C(4)	-9440(2)	-6416(2)	9224(1)	21(1)
C(5)	-8272(2)	-5251(2)	9647(1)	19(1)
C(6)	-7185(2)	-4877(2)	9043(1)	17(1)
C(7)	-4660(2)	-3503(2)	8143(1)	15(1)
C(8)	-4918(2)	-2338(2)	8065(1)	19(1)
C(9)	-4192(2)	-1071(2)	8781(1)	21(1)
C(10)	-3175(2)	-956(2)	9566(1)	18(1)
C(11)	-2875(2)	-2100(2)	9640(1)	19(1)
C(12)	-3616(2)	-3360(2)	8934(1)	18(1)
C(13)	-2365(2)	390(2)	10348(1)	22(1)
C(14)	-4805(2)	-6251(2)	7427(1)	14(1)
C(15)	-5036(2)	-6830(2)	8273(1)	16(1)
C(16)	-4325(2)	-7668(2)	8463(1)	17(1)
C(17)	-3356(2)	-7945(2)	7807(1)	20(1)
C(18)	-3100(2)	-7383(2)	6962(1)	18(1)
C(19)	-3820(2)	-6552(2)	6769(1)	14(1)
C(20)	-10498(3)	-6094(2)	2799(2)	45(1)
C(21)	-13555(2)	-9798(2)	4004(2)	46(1)
O(9)	-7985(1)	-8720(1)	3530(1)	28(1)
C(22)	-8777(2)	-8755(2)	2600(1)	26(1)
Li(1)	-6731(3)	-7039(3)	4590(2)	19(1)
Li(2)	-11048(3)	-7236(3)	4699(2)	21(1)

Table 38 Bond lengths [Å] and angles [°] for **3.6**.

S(1)-O(2)	1.4459(13)
S(1)-O(1)	1.4474(13)
S(1)-O(3)	1.4559(12)
S(1)-C(2)	1.7821(16)
S(2)-O(4)	1.4456(12)
S(2)-O(5)	1.4542(12)
S(2)-O(6)	1.4561(12)
S(2)-C(19)	1.7853(16)
P(1)-C(7)	1.8423(16)
P(1)-C(14)	1.8577(15)
P(1)-C(1)	1.8617(16)
F(1)-C(13)	1.335(2)
F(2)-C(13)	1.329(2)
F(3)-C(13)	1.334(2)
O(1)-Li(2)	1.911(3)
O(3)-Li(1)	1.991(3)
O(4)-Li(1)	1.947(3)
O(5)-Li(1)#1	1.984(3)
O(6)-Li(2)#2	1.935(3)
O(7)-C(20)	1.407(2)
O(7)-Li(2)	1.900(3)
O(8)-C(21)	1.387(2)
O(8)-Li(2)	1.888(3)
C(1)-C(6)	1.402(2)
C(1)-C(2)	1.405(2)
C(2)-C(3)	1.391(2)
C(3)-C(4)	1.387(2)
C(4)-C(5)	1.384(2)
C(5)-C(6)	1.391(2)
C(7)-C(8)	1.395(2)
C(7)-C(12)	1.398(2)
C(8)-C(9)	1.392(2)
C(9)-C(10)	1.385(2)
C(10)-C(11)	1.392(2)
C(10)-C(13)	1.497(2)
C(11)-C(12)	1.385(2)
C(14)-C(15)	1.399(2)
C(14)-C(19)	1.406(2)
C(15)-C(16)	1.390(2)
C(16)-C(17)	1.384(2)
C(17)-C(18)	1.388(2)
C(18)-C(19)	1.392(2)
O(9)-C(22)	1.423(2)
O(9)-Li(1)	1.983(3)
Li(1)-O(5)#1	1.984(3)
Li(2)-O(6)#3	1.935(3)
O(2)-S(1)-O(1)	114.39(8)
O(2)-S(1)-O(3)	111.96(8)
O(1)-S(1)-O(3)	112.10(8)
O(2)-S(1)-C(2)	106.21(7)
O(1)-S(1)-C(2)	104.33(7)
O(3)-S(1)-C(2)	107.09(7)

O(4)-S(2)-O(5)	114.55(7)
O(4)-S(2)-O(6)	112.47(7)
O(5)-S(2)-O(6)	111.21(7)
O(4)-S(2)-C(19)	106.05(7)
O(5)-S(2)-C(19)	106.25(7)
O(6)-S(2)-C(19)	105.55(7)
C(7)-P(1)-C(14)	99.85(7)
C(7)-P(1)-C(1)	98.95(7)
C(14)-P(1)-C(1)	99.04(7)
S(1)-O(1)-Li(2)	150.50(13)
S(1)-O(3)-Li(1)	128.04(11)
S(2)-O(4)-Li(1)	141.46(11)
S(2)-O(5)-Li(1)#1	141.98(11)
S(2)-O(6)-Li(2)#2	159.44(12)
C(20)-O(7)-Li(2)	133.28(16)
C(21)-O(8)-Li(2)	130.54(16)
C(6)-C(1)-C(2)	116.41(14)
C(6)-C(1)-P(1)	121.79(12)
C(2)-C(1)-P(1)	121.80(12)
C(3)-C(2)-C(1)	121.49(14)
C(3)-C(2)-S(1)	114.97(12)
C(1)-C(2)-S(1)	123.37(12)
C(4)-C(3)-C(2)	120.67(15)
C(5)-C(4)-C(3)	119.07(15)
C(4)-C(5)-C(6)	120.12(15)
C(5)-C(6)-C(1)	122.18(15)
C(8)-C(7)-C(12)	118.42(14)
C(8)-C(7)-P(1)	116.44(12)
C(12)-C(7)-P(1)	125.13(12)
C(9)-C(8)-C(7)	120.83(15)
C(10)-C(9)-C(8)	119.77(15)
C(9)-C(10)-C(11)	120.27(15)
C(9)-C(10)-C(13)	121.42(15)
C(11)-C(10)-C(13)	118.31(15)
C(12)-C(11)-C(10)	119.59(15)
C(11)-C(12)-C(7)	121.08(15)
F(2)-C(13)-F(3)	106.09(15)
F(2)-C(13)-F(1)	106.27(14)
F(3)-C(13)-F(1)	105.60(14)
F(2)-C(13)-C(10)	112.75(14)
F(3)-C(13)-C(10)	112.32(14)
F(1)-C(13)-C(10)	113.22(14)
C(15)-C(14)-C(19)	117.18(14)
C(15)-C(14)-P(1)	120.83(12)
C(19)-C(14)-P(1)	121.99(11)
C(16)-C(15)-C(14)	121.78(15)
C(17)-C(16)-C(15)	120.01(15)
C(16)-C(17)-C(18)	119.63(15)
C(17)-C(18)-C(19)	120.26(15)
C(18)-C(19)-C(14)	121.14(14)
C(18)-C(19)-S(2)	117.02(12)
C(14)-C(19)-S(2)	121.77(12)
C(22)-O(9)-Li(1)	125.10(14)
O(4)-Li(1)-O(9)	119.26(15)
O(4)-Li(1)-O(5)#1	103.64(13)

O(9)-Li(1)-O(5)#1	106.21(13)
O(4)-Li(1)-O(3)	101.79(13)
O(9)-Li(1)-O(3)	94.12(12)
O(5)#1-Li(1)-O(3)	133.46(16)
O(8)-Li(2)-O(7)	119.14(17)
O(8)-Li(2)-O(1)	103.94(15)
O(7)-Li(2)-O(1)	102.90(14)
O(8)-Li(2)-O(6)#3	110.06(15)
O(7)-Li(2)-O(6)#3	106.19(14)
O(1)-Li(2)-O(6)#3	114.77(15)

Symmetry transformations used to generate equivalent atoms: #1 -x-1,-y-1,-z+1 #2 x+1,y,z #3 x-1,y,z

Table 39 Anisotropic displacement parameters ($Å^2 x\ 10^3$) for **3.6**. The anisotropic displacement factor exponent takes the form: $-2\pi^2[\ h^2\ a^{*2}U^{11} + ...\ + 2\ h\ k\ a^*\ b^*\ U^{12}\ ]$

	U^{11}	U^{22}	U^{33}	U^{23}	U^{13}	U^{12}
S(1)	15(1)	15(1)	16(1)	2(1)	0(1)	4(1)
S(2)	12(1)	15(1)	16(1)	6(1)	3(1)	5(1)
P(1)	13(1)	14(1)	14(1)	5(1)	2(1)	6(1)
F(1)	50(1)	16(1)	47(1)	1(1)	-16(1)	11(1)
F(2)	20(1)	30(1)	70(1)	-12(1)	-1(1)	3(1)
F(3)	70(1)	31(1)	23(1)	1(1)	5(1)	-1(1)
O(1)	34(1)	35(1)	23(1)	3(1)	-7(1)	20(1)
O(2)	33(1)	17(1)	26(1)	1(1)	6(1)	-2(1)
O(3)	19(1)	26(1)	18(1)	2(1)	3(1)	7(1)
O(4)	16(1)	24(1)	18(1)	6(1)	1(1)	4(1)
O(5)	27(1)	16(1)	21(1)	8(1)	5(1)	7(1)
O(6)	18(1)	30(1)	26(1)	14(1)	10(1)	13(1)
O(7)	19(1)	35(1)	26(1)	13(1)	1(1)	3(1)
O(8)	22(1)	18(1)	83(1)	3(1)	0(1)	7(1)
C(1)	14(1)	15(1)	16(1)	6(1)	2(1)	7(1)
C(2)	15(1)	15(1)	16(1)	4(1)	1(1)	7(1)
C(3)	15(1)	18(1)	24(1)	6(1)	3(1)	6(1)
C(4)	19(1)	24(1)	24(1)	10(1)	9(1)	11(1)
C(5)	22(1)	22(1)	16(1)	4(1)	4(1)	12(1)
C(6)	17(1)	17(1)	18(1)	4(1)	1(1)	7(1)
C(7)	14(1)	14(1)	17(1)	5(1)	4(1)	4(1)
C(8)	16(1)	18(1)	26(1)	9(1)	0(1)	6(1)
C(9)	20(1)	14(1)	30(1)	8(1)	3(1)	6(1)
C(10)	17(1)	15(1)	19(1)	6(1)	5(1)	4(1)
C(11)	19(1)	20(1)	19(1)	7(1)	1(1)	7(1)
C(12)	20(1)	15(1)	21(1)	7(1)	2(1)	6(1)
C(13)	21(1)	18(1)	25(1)	4(1)	2(1)	6(1)
C(14)	12(1)	12(1)	16(1)	3(1)	-1(1)	4(1)
C(15)	17(1)	16(1)	16(1)	4(1)	3(1)	6(1)
C(16)	19(1)	15(1)	18(1)	7(1)	1(1)	4(1)
C(17)	17(1)	18(1)	28(1)	10(1)	1(1)	8(1)
C(18)	15(1)	20(1)	24(1)	9(1)	6(1)	8(1)
C(19)	13(1)	13(1)	16(1)	6(1)	1(1)	3(1)
C(20)	64(2)	32(1)	36(1)	12(1)	-15(1)	14(1)
C(21)	25(1)	25(1)	74(2)	-2(1)	-6(1)	4(1)

O(9)	27(1)	24(1)	24(1)	10(1)	-2(1)	-3(1)
C(22)	26(1)	27(1)	21(1)	7(1)	3(1)	5(1)
Li(1)	19(1)	17(1)	20(1)	7(1)	0(1)	4(1)
Li(2)	19(1)	20(1)	23(1)	6(1)	3(1)	8(1)

Table 40 Hydrogen coordinates (x 10^4) and isotropic displacement parameters ($Å^2$x 10^3) for **3.6**.

	x	y	z	U(eq)
H(7)	-9320(20)	-5830(30)	3970(20)	67(10)
H(8)	-11740(30)	-9630(30)	4150(20)	41(7)
H(3A)	-10327	-7974	7884	23
H(4A)	-10172	-6691	9640	25
H(5A)	-8213	-4705	10352	23
H(6A)	-6385	-4083	9352	21
H(8A)	-5598	-2410	7516	23
H(9A)	-4393	-289	8731	25
H(11A)	-2166	-2017	10172	22
H(12A)	-3413	-4140	8987	22
H(15A)	-5696	-6646	8731	19
H(16A)	-4505	-8050	9043	21
H(17A)	-2868	-8517	7935	24
H(18A)	-2430	-7566	6513	22
H(20A)	-9945	-6350	2237	68
H(20B)	-10353	-5120	2944	68
H(20C)	-11499	-6630	2569	68
H(21A)	-13794	-10369	3266	69
H(21B)	-14034	-9130	4110	69
H(21C)	-13859	-10374	4482	69
H(9)	-8460(30)	-9290(30)	3730(20)	44(7)
H(22C)	-8863	-9579	2036	36(6)
H(22B)	-8295	-7947	2367	39(6)
H(22A)	-9717	-8762	2758	41(6)

X-ray Data Collection, Structure Solution and Refinement for complex 3.13.

A yellow crystal of approximate dimensions 0.209 x 0.165 x 0.150 mm was mounted on a glass fiber and transferred to a Bruker SMART APEX II diffractometer. The APEX2 program package was used to determine the unit-cell parameters and for data collection (25 sec/frame scan time for a sphere of diffraction data). The raw frame data was processed using SAINT and SADABS to yield the reflection data file. Subsequent calculations were carried out using the SHELXTL program. The diffraction symmetry was 2/*m* and the systematic absences were

consistent with the monoclinic space group $P2_1/c$ that was later determined to be correct. The structure was solved by direct methods and refined on F^2 by full-matrix least-squares techniques. The analytical scattering factors for neutral atoms were used throughout the analysis. Hydrogen atoms were included using a riding model. At convergence, wR2 = 0.1005 and Goof = 1.014 for 417 variables refined against 6752 data (0.78 Å), R1 = 0.0379 for those 5613 data with $I > 2.0\sigma(I)$.

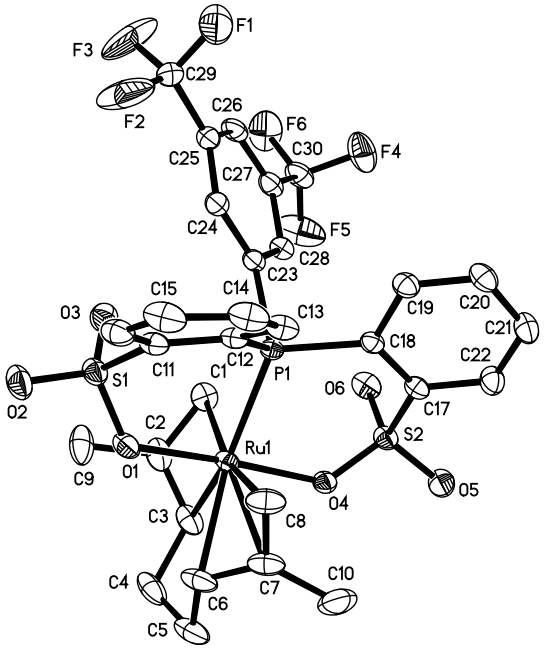

Figure 3 The thermal ellipsoid plot of **3.13** shown at the 50% probability level. Hydrogen atoms are omitted for clarity.

Table 41 Crystal data and structure refinement for **3.13**.

Empirical formula	$C_{30}\ H_{27}\ F_6\ O_6\ P\ Ru\ S_2$	
Formula weight	793.67	
Temperature	143(2) K	
Wavelength	0.71073 Å	
Crystal system	Monoclinic	
Space group	$P2_1/c$	
Unit cell dimensions	a = 16.5644(9) Å	α = 90°.
	b = 11.5626(6) Å	β = 105.5543(7)°.
	c = 16.6110(9) Å	γ = 90°.
Volume	3064.9(3) $Å^3$	
Z	4	
Density (calculated)	1.720 Mg/m^3	
Absorption coefficient	0.780 mm^{-1}	

F(000)	1600
Crystal color	yellow
Crystal size	0.209 x 0.165 x 0.150 mm^3
Theta range for data collection	1.276 to 27.103°
Index ranges	$-21 \leq h \leq 21$, $-14 \leq k \leq 14$, $-21 \leq l \leq 21$
Reflections collected	34518
Independent reflections	6752 [R(int) = 0.0350]
Completeness to theta = 25.242°	99.9 %
Absorption correction	Numerical
Max. and min. transmission	0.9428 and 0.8672
Refinement method	Full-matrix least-squares on F^2
Data / restraints / parameters	6752 / 0 / 417
Goodness-of-fit on F^2	1.014
Final R indices [I>2sigma(I) = 5613 data]	R1 = 0.0379, wR2 = 0.0943
R indices (all data, 0.78 Å)	R1 = 0.0487, wR2 = 0.1005
Largest diff. peak and hole	2.294 and -0.693 e.$Å^{-3}$

Table 42 Atomic coordinates (x 10^4) and equivalent isotropic displacement parameters ($Å^2$x 10^3) for **3.13**. U(eq) is defined as one third of the trace of the orthogonalized U^{ij} tensor.

	x	y	z	U(eq)
Ru(1)	3733(1)	4949(1)	2216(1)	18(1)
S(1)	2663(1)	2903(1)	1105(1)	24(1)
S(2)	3528(1)	7118(1)	3428(1)	22(1)
P(1)	2458(1)	4648(1)	2577(1)	16(1)
F(1)	-1185(2)	3664(3)	1382(2)	68(1)
F(2)	-401(2)	2732(2)	828(3)	96(1)
F(3)	-1179(2)	4010(3)	159(2)	86(1)
F(4)	-16(2)	8305(2)	1904(2)	47(1)
F(5)	904(2)	8495(2)	1234(2)	58(1)
F(6)	-368(2)	8100(2)	586(1)	50(1)
O(1)	3504(1)	3448(2)	1474(1)	25(1)
O(2)	2761(2)	1930(2)	604(2)	34(1)
O(3)	2035(1)	3738(2)	713(1)	28(1)
O(4)	4030(1)	6370(2)	3018(1)	21(1)
O(5)	4096(1)	7793(2)	4062(2)	30(1)
O(6)	2896(1)	7758(2)	2828(2)	28(1)
C(1)	2980(2)	6156(3)	1280(2)	25(1)
C(2)	3664(2)	5808(3)	972(2)	29(1)
C(3)	4464(2)	6024(3)	1490(2)	28(1)
C(4)	5269(2)	5537(3)	1371(3)	39(1)
C(5)	5721(2)	5028(3)	2207(3)	38(1)
C(6)	5072(2)	4272(3)	2440(3)	34(1)
C(7)	4878(2)	4297(3)	3212(2)	32(1)
C(8)	4149(2)	3689(3)	3251(2)	33(1)
C(9)	3522(3)	5118(3)	178(2)	40(1)
C(10)	5344(2)	5046(4)	3929(3)	44(1)
C(11)	2386(2)	2358(3)	1999(2)	22(1)
C(12)	2344(2)	3076(3)	2672(2)	19(1)
C(13)	2262(2)	2539(3)	3401(2)	24(1)
C(14)	2163(2)	1350(3)	3428(2)	30(1)
C(15)	2150(2)	669(3)	2747(2)	32(1)

C(16)	2277(2)	1164(3)	2034(2)	28(1)
C(17)	2938(2)	6234(3)	3946(2)	20(1)
C(18)	2412(2)	5321(3)	3563(2)	18(1)
C(19)	1791(2)	4960(3)	3931(2)	23(1)
C(20)	1734(2)	5401(3)	4688(2)	26(1)
C(21)	2298(2)	6232(3)	5090(2)	28(1)
C(22)	2880(2)	6662(3)	4713(2)	26(1)
C(23)	1412(2)	5083(3)	1950(2)	18(1)
C(24)	781(2)	4275(3)	1635(2)	20(1)
C(25)	-13(2)	4641(3)	1196(2)	22(1)
C(26)	-190(2)	5804(3)	1053(2)	26(1)
C(27)	430(2)	6608(3)	1383(2)	24(1)
C(28)	1230(2)	6258(3)	1842(2)	21(1)
C(29)	-689(2)	3754(3)	897(2)	28(1)
C(30)	244(2)	7875(3)	1272(2)	30(1)

Table 43 Bond lengths [Å] and angles [°] for **3.13**.

Ru(1)-O(4)	2.089(2)
Ru(1)-O(1)	2.104(2)
Ru(1)-C(1)	2.209(3)
Ru(1)-C(8)	2.217(3)
Ru(1)-C(2)	2.268(3)
Ru(1)-C(7)	2.284(3)
Ru(1)-C(6)	2.287(3)
Ru(1)-C(3)	2.291(3)
Ru(1)-P(1)	2.3712(8)
S(1)-O(2)	1.435(2)
S(1)-O(3)	1.439(2)
S(1)-O(1)	1.503(2)
S(1)-C(11)	1.783(3)
S(2)-O(5)	1.438(2)
S(2)-O(6)	1.442(2)
S(2)-O(4)	1.485(2)
S(2)-C(17)	1.786(3)
P(1)-C(18)	1.833(3)
P(1)-C(23)	1.837(3)
P(1)-C(12)	1.839(3)
F(1)-C(29)	1.302(4)
F(2)-C(29)	1.291(4)
F(3)-C(29)	1.310(4)
F(4)-C(30)	1.332(4)
F(5)-C(30)	1.323(4)
F(6)-C(30)	1.332(4)
C(1)-C(2)	1.421(5)
C(2)-C(3)	1.395(5)
C(2)-C(9)	1.505(5)
C(3)-C(4)	1.508(5)
C(4)-C(5)	1.510(6)
C(5)-C(6)	1.514(5)
C(6)-C(7)	1.404(5)
C(7)-C(8)	1.414(5)
C(7)-C(10)	1.507(5)
C(11)-C(16)	1.395(4)

C(11)-C(12)	1.409(4)
C(12)-C(13)	1.399(4)
C(13)-C(14)	1.388(5)
C(14)-C(15)	1.374(5)
C(15)-C(16)	1.381(5)
C(17)-C(22)	1.394(4)
C(17)-C(18)	1.408(4)
C(18)-C(19)	1.394(4)
C(19)-C(20)	1.383(5)
C(20)-C(21)	1.381(5)
C(21)-C(22)	1.376(5)
C(23)-C(28)	1.393(4)
C(23)-C(24)	1.394(4)
C(24)-C(25)	1.388(4)
C(25)-C(26)	1.383(5)
C(25)-C(29)	1.501(5)
C(26)-C(27)	1.386(5)
C(27)-C(28)	1.399(4)
C(27)-C(30)	1.498(5)

O(4)-Ru(1)-O(1)	175.70(9)
O(4)-Ru(1)-C(1)	86.77(11)
O(1)-Ru(1)-C(1)	97.45(11)
O(4)-Ru(1)-C(8)	92.97(12)
O(1)-Ru(1)-C(8)	83.20(12)
C(1)-Ru(1)-C(8)	163.73(12)
O(4)-Ru(1)-C(2)	100.53(10)
O(1)-Ru(1)-C(2)	82.52(10)
C(1)-Ru(1)-C(2)	36.97(12)
C(8)-Ru(1)-C(2)	157.42(13)
O(4)-Ru(1)-C(7)	77.90(11)
O(1)-Ru(1)-C(7)	97.83(11)
C(1)-Ru(1)-C(7)	156.99(13)
C(8)-Ru(1)-C(7)	36.59(12)
C(2)-Ru(1)-C(7)	129.32(13)
O(4)-Ru(1)-C(6)	96.56(11)
O(1)-Ru(1)-C(6)	80.03(11)
C(1)-Ru(1)-C(6)	132.12(13)
C(8)-Ru(1)-C(6)	64.09(13)
C(2)-Ru(1)-C(6)	96.19(14)
C(7)-Ru(1)-C(6)	35.77(14)
O(4)-Ru(1)-C(3)	80.93(10)
O(1)-Ru(1)-C(3)	100.16(10)
C(1)-Ru(1)-C(3)	64.21(12)
C(8)-Ru(1)-C(3)	131.82(13)
C(2)-Ru(1)-C(3)	35.64(13)
C(7)-Ru(1)-C(3)	96.15(13)
C(6)-Ru(1)-C(3)	69.21(13)
O(4)-Ru(1)-P(1)	91.55(6)
O(1)-Ru(1)-P(1)	89.69(6)
C(1)-Ru(1)-P(1)	84.11(8)
C(8)-Ru(1)-P(1)	79.64(9)
C(2)-Ru(1)-P(1)	117.62(9)
C(7)-Ru(1)-P(1)	113.05(9)
C(6)-Ru(1)-P(1)	143.11(10)

C(3)-Ru(1)-P(1)	147.67(9)
O(2)-S(1)-O(3)	116.38(15)
O(2)-S(1)-O(1)	109.13(14)
O(3)-S(1)-O(1)	112.45(13)
O(2)-S(1)-C(11)	107.49(15)
O(3)-S(1)-C(11)	107.32(14)
O(1)-S(1)-C(11)	103.08(14)
O(5)-S(2)-O(6)	116.02(15)
O(5)-S(2)-O(4)	108.37(13)
O(6)-S(2)-O(4)	111.94(13)
O(5)-S(2)-C(17)	107.01(14)
O(6)-S(2)-C(17)	103.69(14)
O(4)-S(2)-C(17)	109.48(13)
C(18)-P(1)-C(23)	97.59(13)
C(18)-P(1)-C(12)	108.26(14)
C(23)-P(1)-C(12)	102.45(13)
C(18)-P(1)-Ru(1)	114.65(10)
C(23)-P(1)-Ru(1)	125.83(10)
C(12)-P(1)-Ru(1)	106.61(9)
S(1)-O(1)-Ru(1)	125.91(13)
S(2)-O(4)-Ru(1)	133.30(13)
C(2)-C(1)-Ru(1)	73.75(19)
C(3)-C(2)-C(1)	116.4(3)
C(3)-C(2)-C(9)	122.3(3)
C(1)-C(2)-C(9)	121.0(3)
C(3)-C(2)-Ru(1)	73.07(19)
C(1)-C(2)-Ru(1)	69.28(18)
C(9)-C(2)-Ru(1)	121.6(2)
C(2)-C(3)-C(4)	125.4(3)
C(2)-C(3)-Ru(1)	71.29(18)
C(4)-C(3)-Ru(1)	118.5(2)
C(3)-C(4)-C(5)	105.3(3)
C(4)-C(5)-C(6)	104.4(3)
C(7)-C(6)-C(5)	125.0(3)
C(7)-C(6)-Ru(1)	72.01(18)
C(5)-C(6)-Ru(1)	119.0(2)
C(6)-C(7)-C(8)	116.0(3)
C(6)-C(7)-C(10)	122.7(3)
C(8)-C(7)-C(10)	120.8(4)
C(6)-C(7)-Ru(1)	72.2(2)
C(8)-C(7)-Ru(1)	69.12(18)
C(10)-C(7)-Ru(1)	122.2(2)
C(7)-C(8)-Ru(1)	74.3(2)
C(16)-C(11)-C(12)	121.0(3)
C(16)-C(11)-S(1)	116.7(3)
C(12)-C(11)-S(1)	122.1(2)
C(13)-C(12)-C(11)	117.5(3)
C(13)-C(12)-P(1)	123.3(2)
C(11)-C(12)-P(1)	119.1(2)
C(14)-C(13)-C(12)	120.5(3)
C(15)-C(14)-C(13)	121.1(3)
C(14)-C(15)-C(16)	119.7(3)
C(15)-C(16)-C(11)	119.8(3)
C(22)-C(17)-C(18)	119.5(3)
C(22)-C(17)-S(2)	114.7(2)

C(18)-C(17)-S(2)	124.3(2)
C(19)-C(18)-C(17)	117.8(3)
C(19)-C(18)-P(1)	118.5(2)
C(17)-C(18)-P(1)	123.6(2)
C(20)-C(19)-C(18)	121.8(3)
C(21)-C(20)-C(19)	119.6(3)
C(22)-C(21)-C(20)	119.8(3)
C(21)-C(22)-C(17)	121.1(3)
C(28)-C(23)-C(24)	119.4(3)
C(28)-C(23)-P(1)	118.6(2)
C(24)-C(23)-P(1)	121.9(2)
C(25)-C(24)-C(23)	120.1(3)
C(26)-C(25)-C(24)	121.0(3)
C(26)-C(25)-C(29)	120.1(3)
C(24)-C(25)-C(29)	118.9(3)
C(25)-C(26)-C(27)	118.9(3)
C(26)-C(27)-C(28)	121.0(3)
C(26)-C(27)-C(30)	120.1(3)
C(28)-C(27)-C(30)	119.0(3)
C(23)-C(28)-C(27)	119.6(3)
F(2)-C(29)-F(1)	107.0(4)
F(2)-C(29)-F(3)	105.9(3)
F(1)-C(29)-F(3)	105.2(3)
F(2)-C(29)-C(25)	113.2(3)
F(1)-C(29)-C(25)	112.9(3)
F(3)-C(29)-C(25)	112.1(3)
F(5)-C(30)-F(6)	107.6(3)
F(5)-C(30)-F(4)	106.3(3)
F(6)-C(30)-F(4)	105.6(3)
F(5)-C(30)-C(27)	113.0(3)
F(6)-C(30)-C(27)	112.4(3)
F(4)-C(30)-C(27)	111.5(3)

Table 44 Anisotropic displacement parameters ($Å^2 x\ 10^3$) for **3.13**. The anisotropic displacement factor exponent takes the form: $-2\pi^2[\ h^2\ a^{*2}U^{11} + ...\ + 2\ h\ k\ a^*\ b^*\ U^{12}\ ]$

	U^{11}	U^{22}	U^{33}	U^{23}	U^{13}	U^{12}
Ru(1)	16(1)	17(1)	24(1)	0(1)	9(1)	0(1)
S(1)	25(1)	21(1)	30(1)	-5(1)	13(1)	-3(1)
S(2)	21(1)	19(1)	27(1)	-2(1)	11(1)	-5(1)
P(1)	15(1)	15(1)	19(1)	2(1)	5(1)	1(1)
F(1)	72(2)	85(2)	64(2)	-36(2)	47(2)	-53(2)
F(2)	28(1)	50(2)	191(4)	-62(2)	-4(2)	-3(1)
F(3)	66(2)	126(3)	42(2)	21(2)	-26(1)	-55(2)
F(4)	65(2)	38(1)	45(1)	-1(1)	23(1)	21(1)
F(5)	44(1)	28(1)	110(2)	22(1)	34(2)	12(1)
F(6)	62(2)	42(1)	40(1)	9(1)	1(1)	29(1)
O(1)	23(1)	21(1)	36(1)	-5(1)	15(1)	-2(1)
O(2)	40(1)	27(1)	42(1)	-13(1)	22(1)	-6(1)
O(3)	29(1)	28(1)	26(1)	1(1)	8(1)	-1(1)
O(4)	18(1)	21(1)	25(1)	-4(1)	8(1)	-4(1)
O(5)	29(1)	29(1)	36(1)	-11(1)	14(1)	-12(1)

O(6)	29(1)	20(1)	37(1)	2(1)	14(1)	0(1)
C(1)	32(2)	22(2)	24(2)	7(1)	11(1)	-1(1)
C(2)	43(2)	21(2)	28(2)	3(1)	19(2)	-4(1)
C(3)	35(2)	20(2)	38(2)	-2(1)	24(2)	-7(1)
C(4)	38(2)	29(2)	63(3)	-17(2)	37(2)	-13(2)
C(5)	23(2)	26(2)	72(3)	-13(2)	24(2)	-3(1)
C(6)	19(2)	22(2)	63(2)	-5(2)	15(2)	3(1)
C(7)	18(2)	29(2)	45(2)	8(2)	5(2)	7(1)
C(8)	22(2)	29(2)	44(2)	14(2)	4(2)	10(1)
C(9)	62(3)	37(2)	30(2)	-8(2)	28(2)	-17(2)
C(10)	24(2)	57(3)	43(2)	4(2)	-4(2)	4(2)
C(11)	16(1)	18(2)	32(2)	1(1)	7(1)	0(1)
C(12)	13(1)	16(1)	28(2)	1(1)	6(1)	1(1)
C(13)	19(2)	25(2)	30(2)	7(1)	8(1)	2(1)
C(14)	24(2)	26(2)	43(2)	13(2)	11(2)	4(1)
C(15)	26(2)	15(2)	57(2)	8(2)	16(2)	2(1)
C(16)	21(2)	21(2)	45(2)	-3(1)	11(2)	0(1)
C(17)	19(1)	20(2)	24(2)	1(1)	10(1)	0(1)
C(18)	16(1)	19(1)	19(1)	2(1)	5(1)	3(1)
C(19)	22(2)	21(2)	27(2)	0(1)	10(1)	-2(1)
C(20)	28(2)	24(2)	31(2)	2(1)	16(1)	-1(1)
C(21)	33(2)	26(2)	26(2)	-5(1)	14(1)	0(1)
C(22)	30(2)	25(2)	26(2)	-5(1)	11(1)	-5(1)
C(23)	17(1)	21(2)	18(1)	2(1)	7(1)	2(1)
C(24)	20(1)	21(2)	20(2)	1(1)	6(1)	2(1)
C(25)	18(1)	30(2)	20(2)	-2(1)	6(1)	1(1)
C(26)	18(2)	38(2)	22(2)	4(1)	6(1)	10(1)
C(27)	23(2)	26(2)	24(2)	3(1)	10(1)	7(1)
C(28)	19(1)	22(2)	22(2)	1(1)	8(1)	1(1)
C(29)	18(2)	36(2)	29(2)	-7(1)	3(1)	1(1)
C(30)	27(2)	33(2)	32(2)	7(2)	12(1)	13(1)

Table 45 Hydrogen coordinates (x 10^4) and isotropic displacement parameters (Å^{2}x 10^3) for **3.13**.

	x	y	z	U(eq)
H(1A)	2420	5878	964	30
H(1B)	2980	6974	1456	30
H(3A)	4530	6846	1684	34
H(4A)	5608	6155	1209	47
H(4B)	5151	4934	932	47
H(5A)	5917	5644	2628	46
H(5B)	6210	4564	2162	46
H(6A)	5083	3463	2228	41
H(8A)	3949	3830	3752	39
H(8B)	4125	2864	3087	39
H(9A)	3683	5583	-248	60
H(9B)	2929	4909	-21	60
H(9C)	3863	4413	286	60
H(10A)	5834	4626	4263	66
H(10B)	4973	5240	4280	66
H(10C)	5527	5757	3711	66
H(13A)	2274	2993	3881	29

H(14A)	2104	1000	3926	36
H(15A)	2055	-140	2766	38
H(16A)	2290	694	1569	34
H(19A)	1397	4395	3655	27
H(20A)	1309	5134	4929	31
H(21A)	2284	6505	5625	33
H(22A)	3248	7261	4980	32
H(24A)	895	3473	1721	24
H(26A)	-729	6047	734	31
H(28A)	1646	6818	2077	25

X-ray Data Collection, Structure Solution and Refinement for complex 3.14.

A bronze crystal of approximate dimensions 0.376 x 0.300 x 0.242 mm was mounted on a glass fiber and transferred to a Bruker SMART APEX II diffractometer. The APEX2 program package was used to determine the unit-cell parameters and for data collection (15 sec/frame scan time for a sphere of diffraction data). The raw frame data was processed using SAINT and SADABS to yield the reflection data file. Subsequent calculations were carried out using the SHELXTL program. The diffraction symmetry was *mmm* and the systematic absences were consistent with the orthorhombic space group *Pbca* that was later determined to be correct. The structure was solved by direct methods and refined on F^2 by full-matrix least-squares techniques. The analytical scattering factors for neutral atoms were used throughout the analysis. Hydrogen atoms were located from a difference-Fourier map and refined (x,y,z and U_{iso}). At convergence, wR2 = 0.0573 and Goof = 1.052 for 440 variables refined against 6136 data (0.75 Å), R1 = 0.0220 for those 5610 data with $I > 2.0\sigma(I)$.

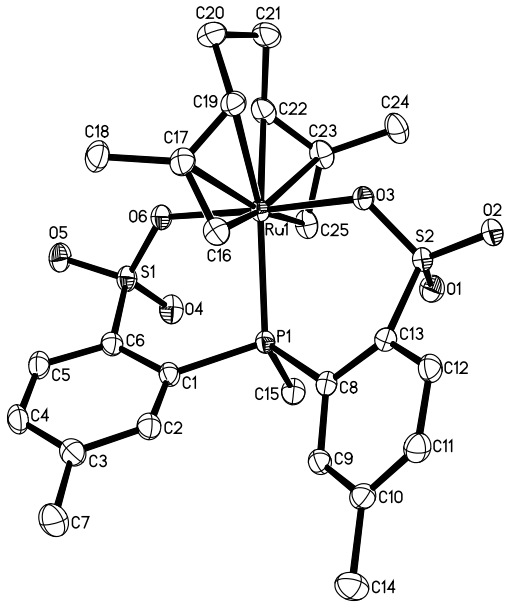

Figure 4 The thermal ellipsoid plot of **3.14** shown at the 50% probability level. Hydrogen atoms are omitted for clarity.

Table 46 Crystal data and structure refinement for **3.14**.

Empirical Formula	$C_{25}\ H_{31}\ O_6\ P\ Ru\ S_2$
Formula weight	623.66
Temperature	143(2) K
Wavelength	0.71073 Å
Crystal system	Orthorhombic
Space group	*Pbca*
Unit cell dimensions	a = 12.9654(7) Å α = 90°. b = 17.2909(10) Å β = 90°. c = 22.5692(13) Å γ = 90°.
Volume	5059.6(5) $Å^3$
Z	8
Density (calculated)	1.637 Mg/m^3
Absorption coefficient	0.888 mm^{-1}
F(000)	2560
Crystal color	bronze
Crystal size	0.376 x 0.300 x 0.242 mm^3
Theta range for data collection	1.805 to 28.304°
Index ranges	$-16 \le h \le 17$, $-22 \le k \le 22$, $-29 \le l \le 30$
Reflections collected	55722
Independent reflections	6136 [R(int) = 0.0239]
Completeness to theta = 25.500°	100.0 %
Absorption correction	Numerical
Max. and min. transmission	0.8934 and 0.7777
Refinement method	Full-matrix least-squares on F^2
Data / restraints / parameters	6136 / 0 / 440
Goodness-of-fit on F^2	1.052

Final R indices [I>2sigma(I) = 5610 data]	R1 = 0.0220, wR2 = 0.0555
R indices (all data, 0.75 Å)	R1 = 0.0253, wR2 = 0.0573
Largest diff. peak and hole	0.599 and -0.386 e.Å^{-3}

Table 47 Atomic coordinates (x 10^4) and equivalent isotropic displacement parameters (Å^{2}x 10^3) for **3.14**. U(eq) is defined as one third of the trace of the orthogonalized U^{ij} tensor.

	x	y	z	U(eq)
Ru(1)	8540(1)	2018(1)	3846(1)	15(1)
P(1)	10243(1)	1798(1)	4218(1)	16(1)
S(1)	9125(1)	3312(1)	4859(1)	20(1)
S(2)	9296(1)	369(1)	3402(1)	18(1)
O(1)	9279(1)	104(1)	4008(1)	24(1)
O(2)	9112(1)	-207(1)	2954(1)	24(1)
O(3)	8583(1)	1040(1)	3299(1)	18(1)
O(4)	9209(1)	2764(1)	5340(1)	25(1)
O(5)	8804(1)	4078(1)	5028(1)	26(1)
O(6)	8438(1)	3025(1)	4374(1)	20(1)
C(1)	10866(1)	2761(1)	4248(1)	18(1)
C(2)	11791(1)	2924(1)	3962(1)	21(1)
C(3)	12263(1)	3650(1)	3974(1)	23(1)
C(4)	11754(1)	4250(1)	4256(1)	24(1)
C(5)	10801(1)	4123(1)	4518(1)	23(1)
C(6)	10359(1)	3390(1)	4524(1)	18(1)
C(7)	13315(2)	3746(1)	3701(1)	31(1)
C(8)	11034(1)	1200(1)	3724(1)	17(1)
C(9)	12113(1)	1203(1)	3752(1)	19(1)
C(10)	12716(1)	837(1)	3323(1)	21(1)
C(11)	12226(1)	446(1)	2863(1)	22(1)
C(12)	11163(1)	364(1)	2865(1)	21(1)
C(13)	10572(1)	717(1)	3299(1)	18(1)
C(14)	13874(1)	877(1)	3358(1)	28(1)
C(15)	10515(1)	1354(1)	4932(1)	23(1)
C(16)	9477(1)	2508(1)	3110(1)	20(1)
C(17)	8535(1)	2917(1)	3115(1)	22(1)
C(18)	8503(2)	3768(1)	3252(1)	28(1)
C(19)	7638(1)	2473(1)	3050(1)	22(1)
C(20)	6545(1)	2757(1)	3146(1)	30(1)
C(21)	6055(1)	2155(1)	3546(1)	30(1)
C(22)	6812(1)	2057(1)	4053(1)	24(1)
C(23)	7208(1)	1352(1)	4261(1)	24(1)
C(24)	6832(2)	587(1)	4026(1)	28(1)
C(25)	8050(1)	1400(1)	4654(1)	23(1)

Table 48 Bond lengths [Å] and angles [°] for **3.14**.

Ru(1)-O(3)	2.0953(11)
Ru(1)-O(6)	2.1132(11)
Ru(1)-C(25)	2.2064(16)
Ru(1)-C(16)	2.2262(16)
Ru(1)-C(17)	2.2674(16)

Ru(1)-C(23)	2.2770(16)
Ru(1)-C(19)	2.2845(16)
Ru(1)-C(22)	2.2891(17)
Ru(1)-P(1)	2.3919(4)
P(1)-C(15)	1.8199(17)
P(1)-C(8)	1.8328(16)
P(1)-C(1)	1.8525(16)
S(1)-O(5)	1.4409(12)
S(1)-O(4)	1.4458(12)
S(1)-O(6)	1.4955(12)
S(1)-C(6)	1.7744(17)
S(2)-O(2)	1.4387(12)
S(2)-O(1)	1.4429(12)
S(2)-O(3)	1.5012(11)
S(2)-C(13)	1.7764(16)
C(1)-C(2)	1.391(2)
C(1)-C(6)	1.415(2)
C(2)-C(3)	1.397(2)
C(3)-C(4)	1.385(2)
C(3)-C(7)	1.506(3)
C(4)-C(5)	1.386(3)
C(5)-C(6)	1.391(2)
C(8)-C(9)	1.400(2)
C(8)-C(13)	1.405(2)
C(9)-C(10)	1.396(2)
C(10)-C(11)	1.392(2)
C(10)-C(14)	1.504(2)
C(11)-C(12)	1.386(2)
C(12)-C(13)	1.386(2)
C(16)-C(17)	1.411(2)
C(17)-C(19)	1.401(2)
C(17)-C(18)	1.504(2)
C(19)-C(20)	1.515(2)
C(20)-C(21)	1.518(3)
C(21)-C(22)	1.517(3)
C(22)-C(23)	1.404(2)
C(23)-C(25)	1.408(2)
C(23)-C(24)	1.507(2)

O(3)-Ru(1)-O(6)	177.31(4)
O(3)-Ru(1)-C(25)	95.94(5)
O(6)-Ru(1)-C(25)	85.13(6)
O(3)-Ru(1)-C(16)	81.52(5)
O(6)-Ru(1)-C(16)	98.15(5)
C(25)-Ru(1)-C(16)	163.38(6)
O(3)-Ru(1)-C(17)	97.14(5)
O(6)-Ru(1)-C(17)	81.13(5)
C(25)-Ru(1)-C(17)	158.86(6)
C(16)-Ru(1)-C(17)	36.60(6)
O(3)-Ru(1)-C(23)	81.62(5)
O(6)-Ru(1)-C(23)	97.89(5)
C(25)-Ru(1)-C(23)	36.58(6)
C(16)-Ru(1)-C(23)	155.96(6)
C(17)-Ru(1)-C(23)	130.09(6)
O(3)-Ru(1)-C(19)	80.08(5)

O(6)-Ru(1)-C(19)	97.37(5)
C(25)-Ru(1)-C(19)	132.03(6)
C(16)-Ru(1)-C(19)	63.95(6)
C(17)-Ru(1)-C(19)	35.86(6)
C(23)-Ru(1)-C(19)	96.29(6)
O(3)-Ru(1)-C(22)	99.79(5)
O(6)-Ru(1)-C(22)	78.45(5)
C(25)-Ru(1)-C(22)	64.17(7)
C(16)-Ru(1)-C(22)	132.44(6)
C(17)-Ru(1)-C(22)	97.19(6)
C(23)-Ru(1)-C(22)	35.82(6)
C(19)-Ru(1)-C(22)	69.45(6)
O(3)-Ru(1)-P(1)	93.05(3)
O(6)-Ru(1)-P(1)	89.50(3)
C(25)-Ru(1)-P(1)	84.22(5)
C(16)-Ru(1)-P(1)	79.54(4)
C(17)-Ru(1)-P(1)	111.52(4)
C(23)-Ru(1)-P(1)	118.38(5)
C(19)-Ru(1)-P(1)	143.42(4)
C(22)-Ru(1)-P(1)	146.79(5)
C(15)-P(1)-C(8)	101.06(8)
C(15)-P(1)-C(1)	105.16(8)
C(8)-P(1)-C(1)	106.62(7)
C(15)-P(1)-Ru(1)	123.81(6)
C(8)-P(1)-Ru(1)	113.17(5)
C(1)-P(1)-Ru(1)	105.79(5)
O(5)-S(1)-O(4)	115.18(7)
O(5)-S(1)-O(6)	109.11(7)
O(4)-S(1)-O(6)	112.14(7)
O(5)-S(1)-C(6)	107.67(8)
O(4)-S(1)-C(6)	107.59(7)
O(6)-S(1)-C(6)	104.49(7)
O(2)-S(2)-O(1)	116.35(7)
O(2)-S(2)-O(3)	108.93(7)
O(1)-S(2)-O(3)	112.45(7)
O(2)-S(2)-C(13)	107.32(7)
O(1)-S(2)-C(13)	104.19(7)
O(3)-S(2)-C(13)	106.97(7)
S(2)-O(3)-Ru(1)	123.32(6)
S(1)-O(6)-Ru(1)	130.46(7)
C(2)-C(1)-C(6)	116.69(14)
C(2)-C(1)-P(1)	122.70(12)
C(6)-C(1)-P(1)	120.35(12)
C(1)-C(2)-C(3)	123.40(16)
C(4)-C(3)-C(2)	118.26(16)
C(4)-C(3)-C(7)	122.49(16)
C(2)-C(3)-C(7)	119.21(16)
C(3)-C(4)-C(5)	120.10(15)
C(4)-C(5)-C(6)	121.09(16)
C(5)-C(6)-C(1)	120.28(15)
C(5)-C(6)-S(1)	116.45(12)
C(1)-C(6)-S(1)	123.20(12)
C(9)-C(8)-C(13)	117.26(14)
C(9)-C(8)-P(1)	121.96(12)
C(13)-C(8)-P(1)	120.78(12)

C(10)-C(9)-C(8)	121.82(15)
C(11)-C(10)-C(9)	118.70(15)
C(11)-C(10)-C(14)	121.17(15)
C(9)-C(10)-C(14)	120.13(15)
C(12)-C(11)-C(10)	120.22(15)
C(11)-C(12)-C(13)	120.33(15)
C(12)-C(13)-C(8)	120.66(14)
C(12)-C(13)-S(2)	117.22(12)
C(8)-C(13)-S(2)	120.60(12)
C(17)-C(16)-Ru(1)	73.29(9)
C(19)-C(17)-C(16)	116.29(15)
C(19)-C(17)-C(18)	122.34(16)
C(16)-C(17)-C(18)	121.02(16)
C(19)-C(17)-Ru(1)	72.74(9)
C(16)-C(17)-Ru(1)	70.11(9)
C(18)-C(17)-Ru(1)	121.37(12)
C(17)-C(19)-C(20)	125.70(16)
C(17)-C(19)-Ru(1)	71.41(9)
C(20)-C(19)-Ru(1)	118.56(12)
C(19)-C(20)-C(21)	104.72(15)
C(22)-C(21)-C(20)	104.78(15)
C(23)-C(22)-C(21)	125.90(16)
C(23)-C(22)-Ru(1)	71.62(10)
C(21)-C(22)-Ru(1)	118.87(12)
C(22)-C(23)-C(25)	116.29(16)
C(22)-C(23)-C(24)	121.69(16)
C(25)-C(23)-C(24)	121.67(16)
C(22)-C(23)-Ru(1)	72.56(10)
C(25)-C(23)-Ru(1)	68.98(9)
C(24)-C(23)-Ru(1)	122.94(12)
C(23)-C(25)-Ru(1)	74.44(10)

Table 49 Anisotropic displacement parameters ($Å^2 x\ 10^3$) for **3.14**. The anisotropic displacement factor exponent takes the form: $-2\pi^2[\ h^2 a^{*2} U^{11} + ... + 2\ h\ k\ a^*\ b^*\ U^{12}\ ]$

	U^{11}	U^{22}	U^{33}	U^{23}	U^{13}	U^{12}
Ru(1)	16(1)	13(1)	15(1)	-1(1)	1(1)	0(1)
P(1)	18(1)	13(1)	15(1)	-1(1)	0(1)	0(1)
S(1)	25(1)	16(1)	18(1)	-4(1)	1(1)	0(1)
S(2)	19(1)	14(1)	21(1)	-2(1)	-1(1)	0(1)
O(1)	26(1)	20(1)	25(1)	4(1)	0(1)	-1(1)
O(2)	24(1)	18(1)	30(1)	-8(1)	-4(1)	0(1)
O(3)	19(1)	16(1)	19(1)	-4(1)	-1(1)	1(1)
O(4)	35(1)	23(1)	18(1)	-1(1)	2(1)	-1(1)
O(5)	32(1)	19(1)	27(1)	-8(1)	2(1)	2(1)
O(6)	22(1)	16(1)	21(1)	-4(1)	0(1)	1(1)
C(1)	22(1)	15(1)	17(1)	-1(1)	-4(1)	-2(1)
C(2)	24(1)	18(1)	20(1)	1(1)	-2(1)	-1(1)
C(3)	26(1)	23(1)	21(1)	6(1)	-5(1)	-5(1)
C(4)	31(1)	16(1)	26(1)	4(1)	-6(1)	-6(1)
C(5)	31(1)	15(1)	22(1)	-1(1)	-5(1)	-1(1)
C(6)	22(1)	17(1)	16(1)	0(1)	-3(1)	-1(1)

C(7)	29(1)	28(1)	38(1)	8(1)	2(1)	-7(1)
C(8)	20(1)	14(1)	17(1)	-1(1)	0(1)	1(1)
C(9)	21(1)	17(1)	19(1)	-1(1)	-3(1)	-1(1)
C(10)	19(1)	19(1)	24(1)	2(1)	1(1)	1(1)
C(11)	23(1)	21(1)	22(1)	-2(1)	4(1)	2(1)
C(12)	25(1)	18(1)	20(1)	-3(1)	-2(1)	0(1)
C(13)	18(1)	15(1)	20(1)	-1(1)	-2(1)	1(1)
C(14)	20(1)	34(1)	28(1)	-3(1)	2(1)	-2(1)
C(15)	29(1)	21(1)	18(1)	0(1)	-2(1)	0(1)
C(16)	23(1)	21(1)	16(1)	2(1)	1(1)	-2(1)
C(17)	29(1)	20(1)	17(1)	3(1)	-3(1)	0(1)
C(18)	37(1)	18(1)	29(1)	4(1)	-5(1)	0(1)
C(19)	24(1)	20(1)	21(1)	0(1)	-4(1)	2(1)
C(20)	25(1)	28(1)	36(1)	-3(1)	-7(1)	6(1)
C(21)	18(1)	31(1)	40(1)	-7(1)	-1(1)	1(1)
C(22)	19(1)	25(1)	29(1)	-7(1)	6(1)	-3(1)
C(23)	23(1)	24(1)	25(1)	-2(1)	9(1)	-6(1)
C(24)	26(1)	24(1)	34(1)	-4(1)	6(1)	-9(1)
C(25)	28(1)	21(1)	21(1)	-1(1)	7(1)	-4(1)

Table 50 Hydrogen coordinates (x 10^4) and isotropic displacement parameters ($Å^2$x 10^3) for **3.14**.

	x	y	z	U(eq)
H(2A)	12118(15)	2559(12)	3750(8)	20(5)
H(4A)	12083(16)	4739(13)	4293(9)	30(5)
H(5A)	10448(16)	4531(12)	4690(9)	23(5)
H(7A)	13610(20)	4235(18)	3793(12)	55(8)
H(7B)	13280(20)	3716(15)	3287(13)	53(7)
H(7C)	13780(20)	3328(19)	3826(12)	61(8)
H(9A)	12424(15)	1429(12)	4067(9)	20(5)
H(11A)	12610(15)	219(11)	2574(9)	24(5)
H(12A)	10819(15)	79(12)	2580(9)	24(5)
H(14A)	14170(20)	392(16)	3275(11)	52(7)
H(14B)	14096(19)	973(14)	3726(12)	41(6)
H(14C)	14110(20)	1228(17)	3101(13)	68(9)
H(15A)	11221(16)	1337(11)	4992(8)	19(5)
H(15B)	10268(17)	817(13)	4920(10)	34(6)
H(15C)	10217(17)	1627(13)	5231(10)	33(6)
H(16A)	10090(14)	2814(10)	3178(8)	14(4)
H(16B)	9542(14)	2078(10)	2874(8)	13(4)
H(18A)	8324(18)	4018(15)	2913(12)	45(7)
H(18B)	9164(18)	3923(13)	3373(10)	37(6)
H(18C)	7990(19)	3896(14)	3538(11)	42(6)
H(19A)	7677(15)	2029(11)	2856(9)	21(5)
H(20A)	6536(15)	3238(13)	3331(9)	27(5)
H(20B)	6199(18)	2780(13)	2787(11)	38(6)
H(21A)	5974(18)	1665(14)	3330(10)	35(6)
H(21B)	5424(19)	2321(14)	3707(11)	41(6)
H(22A)	6884(15)	2478(12)	4296(9)	23(5)
H(24A)	6148(18)	518(13)	4187(10)	34(6)
H(24B)	7257(18)	200(14)	4162(10)	36(6)

H(24C)	6781(18)	566(13)	3597(11)	36(6)
H(25A)	8397(15)	937(12)	4745(9)	24(5)
H(25B)	8082(17)	1802(13)	4923(9)	28(5)

X-ray Data Collection, Structure Solution and Refinement for complex 3.15.

A yellow crystal of approximate dimensions 0.287 x 0.168 x 0.056 mm was mounted on a glass fiber and transferred to a Bruker SMART APEX II diffractometer. The APEX2 program package was used to determine the unit-cell parameters and for data collection (120 sec/frame scan time for a sphere of diffraction data). The raw frame data was processed using SAINT and SADABS to yield the reflection data file. Subsequent calculations were carried out using the SHELXTL program. The diffraction symmetry was 2/*m* and the systematic absences were consistent with the monoclinic space group $P2_1/c$ that was later determined to be correct. The structure was solved by direct methods and refined on F^2 by full-matrix least-squares techniques. The analytical scattering factors for neutral atoms were used throughout the analysis. Hydrogen atoms were included using a riding model. There was one molecule of dichloromethane present per formula unit. At convergence, wR2 = 0.0811 and Goof = 1.006 for 377 variables refined against 6862 data (0.78 Å), R1 = 0.0312 for those 5619 data with $I > 2.0\sigma(I)$.

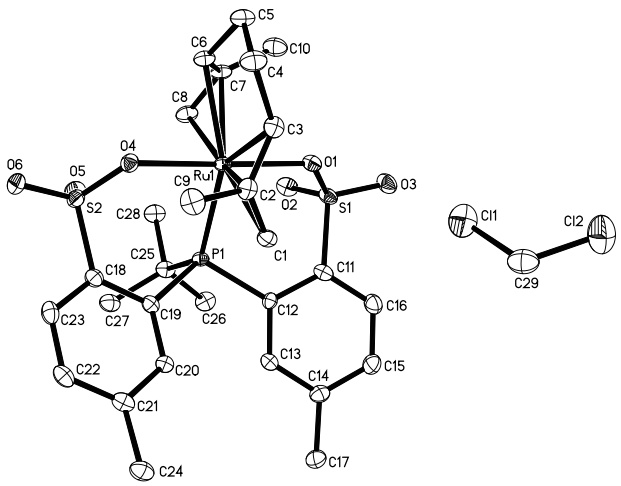

Figure 5 The thermal ellipsoid plot of **3.15** shown at the 50% probability level. Hydrogen atoms are omitted for clarity.

Table 51 Crystal data and structure refinement for **3.15**.

Empirical formula	C_{29} H_{39} Cl_2 O_6 P Ru S_2	
Formula weight	750.66	
Temperature	83(2) K	
Wavelength	0.71073 Å	
Crystal system	Monoclinic	
Space group	$P2_1/c$	
Unit cell dimensions	a = 14.7647(9) Å	α = 90°.
	b = 13.6816(8) Å	β = 106.5907(7)°.
	c = 16.0357(10) Å	γ = 90°.
Volume	3104.4(3) $Å^3$	
Z	4	
Density (calculated)	1.606 Mg/m^3	
Absorption coefficient	0.905 mm^{-1}	
F(000)	1544	
Crystal color	yellow	
Crystal size	0.287 x 0.168 x 0.056 mm^3	
Theta range for data collection	1.993 to 27.128°	
Index ranges	$-18 \le h \le 18$, $-17 \le k \le 17$, $-20 \le l \le 20$	
Reflections collected	34708	
Independent reflections	6862 [R(int) = 0.0503]	
Completeness to theta = 25.242°	99.9 %	
Absorption correction	Numerical	
Max. and min. transmission	1.0000 and 0.7673	
Refinement method	Full-matrix least-squares on F^2	
Data / restraints / parameters	6862 / 0 / 377	
Goodness-of-fit on F^2	1.006	
Final R indices [I>2sigma(I) = 5619 data]	R1 = 0.0312, wR2 = 0.0751	
R indices (all data, 0.78 Å)	R1 = 0.0443, wR2 = 0.0811	

Largest diff. peak and hole	0.872 and -0.825 e.Å^{-3}

Table 52 Atomic coordinates (x 10^4) and equivalent isotropic displacement parameters (Å^{2}x 10^3) for **3.15**. U(eq) is defined as one third of the trace of the orthogonalized U^{ij} tensor.

	x	y	z	U(eq)
Ru(1)	2595(1)	207(1)	2249(1)	12(1)
P(1)	3031(1)	1931(1)	2039(1)	12(1)
S(1)	726(1)	1486(1)	1619(1)	17(1)
S(2)	4769(1)	352(1)	2175(1)	16(1)
O(1)	1174(1)	576(1)	2082(1)	16(1)
O(2)	939(1)	1621(1)	800(1)	21(1)
O(3)	-260(1)	1490(1)	1578(1)	23(1)
O(4)	4017(1)	-210(1)	2435(1)	16(1)
O(5)	4448(1)	685(1)	1286(1)	20(1)
O(6)	5634(1)	-203(1)	2402(1)	22(1)
C(1)	2705(2)	896(2)	3542(2)	16(1)
C(2)	2978(2)	-84(2)	3703(2)	16(1)
C(3)	2301(2)	-785(2)	3288(2)	18(1)
C(4)	2475(2)	-1877(2)	3276(2)	23(1)
C(5)	2086(2)	-2173(2)	2323(2)	21(1)
C(6)	2470(2)	-1417(2)	1827(2)	17(1)
C(7)	1927(2)	-840(2)	1137(2)	18(1)
C(8)	2403(2)	-81(2)	846(2)	19(1)
C(9)	3975(2)	-331(2)	4215(2)	23(1)
C(10)	874(2)	-948(2)	773(2)	24(1)
C(11)	1264(2)	2507(2)	2264(2)	16(1)
C(12)	2214(2)	2753(2)	2390(2)	13(1)
C(13)	2500(2)	3685(2)	2730(2)	14(1)
C(14)	1903(2)	4327(2)	2992(2)	18(1)
C(15)	975(2)	4042(2)	2891(2)	23(1)
C(16)	656(2)	3145(2)	2512(2)	22(1)
C(17)	2268(2)	5308(2)	3374(2)	23(1)
C(18)	4954(2)	1394(2)	2855(2)	16(1)
C(19)	4218(2)	2052(2)	2869(2)	14(1)
C(20)	4425(2)	2720(2)	3554(2)	14(1)
C(21)	5326(2)	2813(2)	4156(2)	17(1)
C(22)	6038(2)	2196(2)	4075(2)	19(1)
C(23)	5851(2)	1477(2)	3442(2)	18(1)
C(24)	5492(2)	3573(2)	4858(2)	21(1)
C(25)	3162(2)	2621(2)	1009(2)	17(1)
C(26)	2520(2)	3530(2)	820(2)	20(1)
C(27)	4185(2)	2961(2)	1159(2)	21(1)
C(28)	2862(2)	1982(2)	188(2)	20(1)
C(29)	-192(2)	1342(2)	4871(2)	32(1)
Cl(1)	0(1)	1077(1)	3862(1)	42(1)
Cl(2)	-1394(1)	1188(1)	4827(1)	50(1)

Table 53 Bond lengths [Å] and angles [°] for **3.15**.

Ru(1)-O(1)	2.0998(17)

Ru(1)-O(4)	2.1124(17)
Ru(1)-C(8)	2.221(2)
Ru(1)-C(1)	2.241(2)
Ru(1)-C(2)	2.272(2)
Ru(1)-C(7)	2.280(2)
Ru(1)-C(3)	2.285(2)
Ru(1)-C(6)	2.314(2)
Ru(1)-P(1)	2.4931(6)
P(1)-C(12)	1.851(2)
P(1)-C(19)	1.882(2)
P(1)-C(25)	1.959(2)
S(1)-O(3)	1.4390(19)
S(1)-O(2)	1.4466(19)
S(1)-O(1)	1.5027(18)
S(1)-C(11)	1.785(3)
S(2)-O(6)	1.4401(19)
S(2)-O(5)	1.4418(18)
S(2)-O(4)	1.5040(17)
S(2)-C(18)	1.769(3)
C(1)-C(2)	1.403(3)
C(2)-C(3)	1.407(4)
C(2)-C(9)	1.506(4)
C(3)-C(4)	1.518(3)
C(4)-C(5)	1.526(4)
C(5)-C(6)	1.511(3)
C(6)-C(7)	1.408(4)
C(7)-C(8)	1.407(4)
C(7)-C(10)	1.504(4)
C(11)-C(16)	1.388(4)
C(11)-C(12)	1.401(3)
C(12)-C(13)	1.403(3)
C(13)-C(14)	1.392(3)
C(14)-C(15)	1.389(4)
C(14)-C(17)	1.509(3)
C(15)-C(16)	1.391(4)
C(18)-C(23)	1.394(3)
C(18)-C(19)	1.415(3)
C(19)-C(20)	1.395(3)
C(20)-C(21)	1.408(3)
C(21)-C(22)	1.384(4)
C(21)-C(24)	1.501(3)
C(22)-C(23)	1.382(4)
C(25)-C(27)	1.532(3)
C(25)-C(28)	1.536(3)
C(25)-C(26)	1.541(3)
C(29)-Cl(1)	1.759(3)
C(29)-Cl(2)	1.769(3)

O(1)-Ru(1)-O(4)	178.08(6)
O(1)-Ru(1)-C(8)	94.59(9)
O(4)-Ru(1)-C(8)	85.95(8)
O(1)-Ru(1)-C(1)	79.76(8)
O(4)-Ru(1)-C(1)	100.15(8)
C(8)-Ru(1)-C(1)	165.09(9)
O(1)-Ru(1)-C(2)	96.84(8)

O(4)-Ru(1)-C(2)	82.07(8)
C(8)-Ru(1)-C(2)	158.57(9)
C(1)-Ru(1)-C(2)	36.23(9)
O(1)-Ru(1)-C(7)	81.85(8)
O(4)-Ru(1)-C(7)	97.56(8)
C(8)-Ru(1)-C(7)	36.39(9)
C(1)-Ru(1)-C(7)	152.71(9)
C(2)-Ru(1)-C(7)	128.14(9)
O(1)-Ru(1)-C(3)	81.05(8)
O(4)-Ru(1)-C(3)	97.18(8)
C(8)-Ru(1)-C(3)	129.64(9)
C(1)-Ru(1)-C(3)	63.50(9)
C(2)-Ru(1)-C(3)	35.96(9)
C(7)-Ru(1)-C(3)	93.88(9)
O(1)-Ru(1)-C(6)	101.57(8)
O(4)-Ru(1)-C(6)	77.01(8)
C(8)-Ru(1)-C(6)	63.69(9)
C(1)-Ru(1)-C(6)	130.81(9)
C(2)-Ru(1)-C(6)	96.19(9)
C(7)-Ru(1)-C(6)	35.67(9)
C(3)-Ru(1)-C(6)	68.16(9)
O(1)-Ru(1)-P(1)	92.42(5)
O(4)-Ru(1)-P(1)	89.43(5)
C(8)-Ru(1)-P(1)	89.65(7)
C(1)-Ru(1)-P(1)	76.90(6)
C(2)-Ru(1)-P(1)	107.85(7)
C(7)-Ru(1)-P(1)	124.01(7)
C(3)-Ru(1)-P(1)	140.40(7)
C(6)-Ru(1)-P(1)	150.53(6)
C(12)-P(1)-C(19)	106.71(11)
C(12)-P(1)-C(25)	101.14(11)
C(19)-P(1)-C(25)	104.91(11)
C(12)-P(1)-Ru(1)	108.57(8)
C(19)-P(1)-Ru(1)	102.23(8)
C(25)-P(1)-Ru(1)	131.42(8)
O(3)-S(1)-O(2)	115.91(11)
O(3)-S(1)-O(1)	108.86(10)
O(2)-S(1)-O(1)	112.10(10)
O(3)-S(1)-C(11)	107.46(12)
O(2)-S(1)-C(11)	104.47(11)
O(1)-S(1)-C(11)	107.55(11)
O(6)-S(2)-O(5)	115.72(11)
O(6)-S(2)-O(4)	109.37(10)
O(5)-S(2)-O(4)	112.11(10)
O(6)-S(2)-C(18)	107.40(12)
O(5)-S(2)-C(18)	107.70(11)
O(4)-S(2)-C(18)	103.73(11)
S(1)-O(1)-Ru(1)	123.03(10)
S(2)-O(4)-Ru(1)	127.24(10)
C(2)-C(1)-Ru(1)	73.08(14)
C(1)-C(2)-C(3)	115.9(2)
C(1)-C(2)-C(9)	119.9(2)
C(3)-C(2)-C(9)	123.8(2)
C(1)-C(2)-Ru(1)	70.70(13)
C(3)-C(2)-Ru(1)	72.52(14)

C(9)-C(2)-Ru(1)	121.11(17)
C(2)-C(3)-C(4)	125.2(2)
C(2)-C(3)-Ru(1)	71.52(14)
C(4)-C(3)-Ru(1)	120.43(17)
C(3)-C(4)-C(5)	104.9(2)
C(6)-C(5)-C(4)	104.8(2)
C(7)-C(6)-C(5)	125.6(2)
C(7)-C(6)-Ru(1)	70.85(14)
C(5)-C(6)-Ru(1)	120.89(17)
C(8)-C(7)-C(6)	116.6(2)
C(8)-C(7)-C(10)	120.2(2)
C(6)-C(7)-C(10)	122.9(2)
C(8)-C(7)-Ru(1)	69.53(14)
C(6)-C(7)-Ru(1)	73.48(14)
C(10)-C(7)-Ru(1)	122.25(17)
C(7)-C(8)-Ru(1)	74.08(14)
C(16)-C(11)-C(12)	120.8(2)
C(16)-C(11)-S(1)	116.14(19)
C(12)-C(11)-S(1)	122.20(19)
C(11)-C(12)-C(13)	116.9(2)
C(11)-C(12)-P(1)	121.57(18)
C(13)-C(12)-P(1)	121.37(18)
C(14)-C(13)-C(12)	123.0(2)
C(15)-C(14)-C(13)	118.4(2)
C(15)-C(14)-C(17)	121.5(2)
C(13)-C(14)-C(17)	120.1(2)
C(14)-C(15)-C(16)	119.9(2)
C(11)-C(16)-C(15)	120.9(2)
C(23)-C(18)-C(19)	121.5(2)
C(23)-C(18)-S(2)	115.60(19)
C(19)-C(18)-S(2)	122.56(19)
C(20)-C(19)-C(18)	115.6(2)
C(20)-C(19)-P(1)	124.44(18)
C(18)-C(19)-P(1)	119.79(18)
C(19)-C(20)-C(21)	123.4(2)
C(22)-C(21)-C(20)	118.4(2)
C(22)-C(21)-C(24)	121.8(2)
C(20)-C(21)-C(24)	119.8(2)
C(23)-C(22)-C(21)	120.3(2)
C(22)-C(23)-C(18)	120.4(2)
C(27)-C(25)-C(28)	109.7(2)
C(27)-C(25)-C(26)	108.0(2)
C(28)-C(25)-C(26)	106.3(2)
C(27)-C(25)-P(1)	110.17(17)
C(28)-C(25)-P(1)	111.97(16)
C(26)-C(25)-P(1)	110.54(17)
Cl(1)-C(29)-Cl(2)	111.20(17)

Table 54 Anisotropic displacement parameters ($Å^2 x\ 10^3$) for **3.15**. The anisotropic displacement factor exponent takes the form: $-2\pi^2[\ h^2\ a^{*2}U^{11} + ...\ + 2\ h\ k\ a^*\ b^*\ U^{12}\ ]$

	U^{11}	U^{22}	U^{33}	U^{23}	U^{13}	U^{12}

Ru(1)	14(1)	11(1)	10(1)	-1(1)	1(1)	-1(1)
P(1)	14(1)	12(1)	11(1)	-1(1)	2(1)	-1(1)
S(1)	13(1)	15(1)	19(1)	1(1)	-1(1)	-2(1)
S(2)	17(1)	14(1)	18(1)	0(1)	7(1)	1(1)
O(1)	15(1)	15(1)	17(1)	0(1)	2(1)	-2(1)
O(2)	21(1)	21(1)	16(1)	3(1)	0(1)	-1(1)
O(3)	14(1)	22(1)	30(1)	1(1)	1(1)	-1(1)
O(4)	16(1)	14(1)	17(1)	1(1)	5(1)	2(1)
O(5)	26(1)	18(1)	17(1)	0(1)	8(1)	0(1)
O(6)	18(1)	18(1)	30(1)	-2(1)	9(1)	3(1)
C(1)	20(1)	18(1)	11(1)	-2(1)	6(1)	-4(1)
C(2)	20(1)	21(1)	9(1)	2(1)	5(1)	1(1)
C(3)	22(1)	18(1)	16(1)	3(1)	8(1)	0(1)
C(4)	31(2)	17(1)	19(1)	2(1)	5(1)	0(1)
C(5)	28(1)	14(1)	20(1)	-1(1)	6(1)	-3(1)
C(6)	23(1)	13(1)	15(1)	-4(1)	5(1)	-1(1)
C(7)	22(1)	15(1)	14(1)	-6(1)	3(1)	-3(1)
C(8)	27(1)	18(1)	12(1)	-4(1)	4(1)	-1(1)
C(9)	22(1)	28(2)	15(1)	6(1)	1(1)	2(1)
C(10)	26(1)	21(1)	21(1)	-3(1)	-1(1)	-4(1)
C(11)	16(1)	15(1)	16(1)	1(1)	1(1)	-2(1)
C(12)	12(1)	13(1)	13(1)	1(1)	4(1)	2(1)
C(13)	15(1)	14(1)	13(1)	3(1)	2(1)	-1(1)
C(14)	23(1)	13(1)	18(1)	2(1)	6(1)	1(1)
C(15)	21(1)	18(1)	31(2)	-1(1)	10(1)	3(1)
C(16)	16(1)	20(1)	30(2)	1(1)	7(1)	0(1)
C(17)	25(1)	16(1)	29(2)	-3(1)	10(1)	0(1)
C(18)	16(1)	15(1)	17(1)	1(1)	6(1)	-2(1)
C(19)	14(1)	16(1)	12(1)	2(1)	4(1)	-2(1)
C(20)	15(1)	14(1)	13(1)	1(1)	3(1)	0(1)
C(21)	19(1)	18(1)	13(1)	2(1)	1(1)	-4(1)
C(22)	15(1)	22(1)	18(1)	3(1)	1(1)	-4(1)
C(23)	14(1)	19(1)	22(1)	6(1)	6(1)	2(1)
C(24)	22(1)	23(1)	16(1)	-1(1)	2(1)	-5(1)
C(25)	21(1)	15(1)	13(1)	2(1)	5(1)	-2(1)
C(26)	26(1)	18(1)	16(1)	5(1)	6(1)	2(1)
C(27)	26(1)	19(1)	18(1)	1(1)	9(1)	-5(1)
C(28)	28(1)	19(1)	12(1)	2(1)	5(1)	-2(1)
C(29)	34(2)	28(2)	30(2)	-1(1)	0(1)	1(1)
Cl(1)	43(1)	45(1)	41(1)	8(1)	15(1)	7(1)
Cl(2)	37(1)	68(1)	48(1)	4(1)	16(1)	4(1)

Table 55 Hydrogen coordinates (x 10^4) and isotropic displacement parameters ($Å^2$x 10^3) for **3.15**.

	x	y	z	U(eq)
H(1A)	3211	1390	3746	19
H(1B)	2102	1086	3651	19
H(3A)	1670	-641	3376	22
H(4A)	2141	-2228	3641	27
H(4B)	3159	-2024	3494	27
H(5A)	2305	-2836	2225	25
H(5B)	1386	-2165	2141	25

H(6A)	3063	-1651	1707	21
H(8A)	2001	389	433	23
H(8B)	2978	-271	685	23
H(9A)	3994	-483	4817	34
H(9B)	4388	228	4208	34
H(9C)	4192	-900	3953	34
H(10A)	733	-1420	293	36
H(10B)	595	-314	559	36
H(10C)	607	-1181	1231	36
H(13A)	3130	3886	2783	17
H(15A)	559	4459	3081	27
H(16A)	13	2966	2421	26
H(17A)	1760	5793	3202	35
H(17B)	2796	5509	3157	35
H(17C)	2483	5259	4010	35
H(20A)	3933	3135	3618	17
H(22A)	6659	2266	4455	23
H(23A)	6337	1038	3407	22
H(24A)	6086	3433	5305	31
H(24B)	4969	3565	5121	31
H(24C)	5530	4220	4606	31
H(26A)	2519	3808	257	30
H(26B)	2758	4017	1279	30
H(26C)	1875	3343	806	30
H(27A)	4240	3314	644	31
H(27B)	4605	2391	1262	31
H(27C)	4364	3394	1666	31
H(28A)	2987	2333	-301	30
H(28B)	2186	1836	52	30
H(28C)	3223	1371	290	30
H(29A)	2	2024	5038	39
H(29B)	203	904	5322	39

X-ray Data Collection, Structure Solution and Refinement for complex 4.1

An orange crystal of approximate dimensions 0.038 x 0.140 x 0.219 mm was mounted on a glass fiber and transferred to a Bruker SMART APEX II diffractometer. The APEX2[1] program package was used to determine the unit-cell parameters and for data collection (90 sec/frame scan time for a sphere of diffraction data). The raw frame data was processed using SAINT[2] and SADABS[3] to yield the reflection data file. Subsequent calculations were carried out using the SHELXTL[4] program. There were no systematic absences nor any diffraction symmetry other than the Friedel condition. The centrosymmetric triclinic space group $P\bar{1}$ was assigned and later determined to be correct.

The structure was solved by direct methods and refined on F^2 by full-matrix least-squares techniques. The analytical scattering factors[5] for neutral atoms were used throughout the analysis. Hydrogen atoms were located from a difference-Fourier map and refined (x,y,z and U_{iso}).

At convergence, wR2 = 0.0662 and Goof = 1.019 for 767 variables refined against 11126 data (0.75Å), R1 = 0.0263 for those 9713 data with $I > 2.0\sigma(I)$.

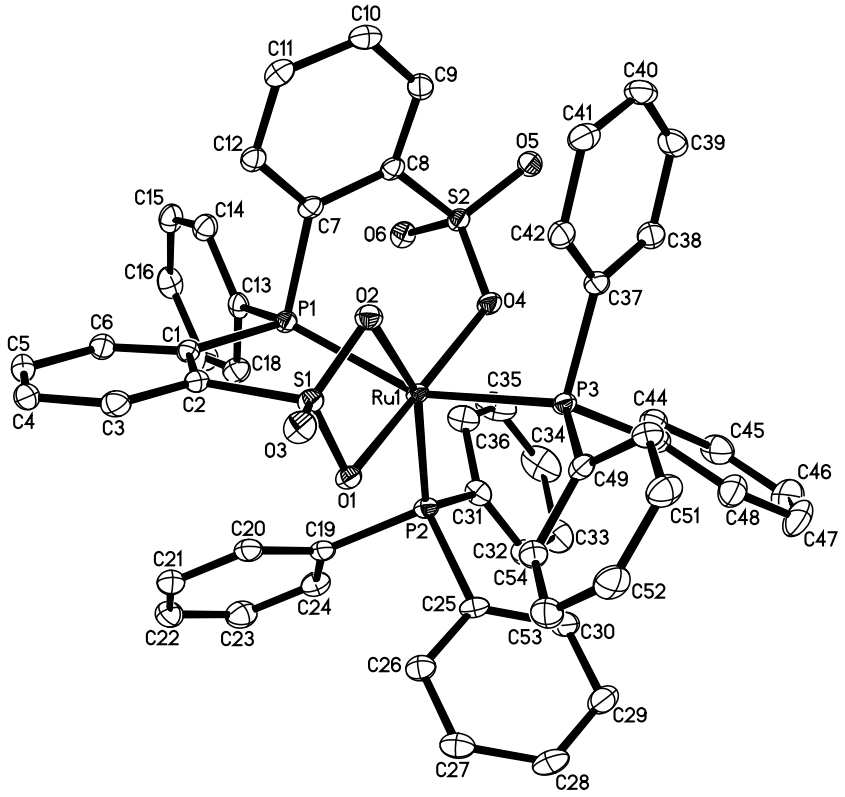

Table 56 Crystal data and structure refinement for **4.1**

Identification code	zg50 (Tobias Friedberger)	
Empirical formula	$C_{54}\ H_{43}\ O_6\ P_3\ Ru\ S_2$	
Formula weight	1045.98	
Temperature	88(2) K	
Wavelength	0.71073 Å	
Crystal system	Triclinic	
Space group	$P\bar{1}$	
Unit cell dimensions	a = 11.9850(4) Å	α= 89.6707(4)°.
	b = 12.8570(5) Å	β= 89.2580(4)°.
	c = 16.4659(6) Å	γ = 67.0350(4)°.
Volume	2335.96(15) $Å^3$	
Z	2	
Density (calculated)	1.487 Mg/m^3	
Absorption coefficient	0.580 mm^{-1}	
F(000)	1072	
Crystal color	orange	
Crystal size	0.219 x 0.140 x 0.038 mm^3	
Theta range for data collection	1.846 to 28.308°	
Index ranges	$-15 \le h \le 15$, $-17 \le k \le 17$, $-21 \le l \le 21$	
Reflections collected	28461	
Independent reflections	11126 [R(int) = 0.0199]	
Completeness to theta = 25.500°	99.8 %	
Absorption correction	Numerical	
Max. and min. transmission	1.0000 and 0.8993	

Refinement method	Full-matrix least-squares on F^2
Data / restraints / parameters	11126 / 0 / 767
Goodness-of-fit on F^2	1.019
Final R indices [I>2sigma(I) = 9713 data]	R1 = 0.0263, wR2 = 0.0632
R indices (all data, 0.75 Å)	R1 = 0.0330, wR2 = 0.0662
Largest diff. peak and hole	0.883 and -0.408 e.Å^{-3}

Table 57. Atomic coordinates (x 10^4) and equivalent isotropic displacement parameters (Å^{2}x 10^3) for **4.1**. U(eq) is defined as one third of the trace of the orthogonalized U^{ij} tensor.

	x	y	z	U(eq)
Ru(1)	2104(1)	2174(1)	2778(1)	10(1)
S(1)	2998(1)	2066(1)	4345(1)	13(1)
S(2)	-721(1)	2790(1)	2336(1)	13(1)
P(1)	1368(1)	906(1)	3421(1)	12(1)
P(2)	3284(1)	1152(1)	1752(1)	13(1)
P(3)	2094(1)	3996(1)	2451(1)	12(1)
O(1)	3653(1)	1712(1)	3548(1)	13(1)
O(2)	1761(1)	2860(1)	4147(1)	15(1)
O(3)	3632(1)	2450(1)	4927(1)	18(1)
O(4)	455(1)	2900(1)	2140(1)	14(1)
O(5)	-1722(1)	3754(1)	2030(1)	18(1)
O(6)	-689(1)	1694(1)	2107(1)	17(1)
C(1)	2264(2)	262(1)	4318(1)	13(1)
C(2)	2911(2)	804(1)	4732(1)	13(1)
C(3)	3567(2)	329(2)	5428(1)	17(1)
C(4)	3608(2)	-708(2)	5714(1)	19(1)
C(5)	3001(2)	-1260(2)	5307(1)	19(1)
C(6)	2336(2)	-782(2)	4614(1)	16(1)
C(7)	-21(2)	1954(1)	3886(1)	13(1)
C(8)	-838(2)	2832(1)	3415(1)	13(1)
C(9)	-1768(2)	3735(2)	3776(1)	16(1)
C(10)	-1924(2)	3771(2)	4617(1)	18(1)
C(11)	-1158(2)	2892(2)	5085(1)	16(1)
C(12)	-211(2)	1996(2)	4725(1)	15(1)
C(13)	891(2)	-198(1)	3061(1)	14(1)
C(14)	-152(2)	-287(2)	3386(1)	18(1)
C(15)	-502(2)	-1141(2)	3129(1)	20(1)
C(16)	172(2)	-1902(2)	2546(1)	22(1)
C(17)	1199(2)	-1810(2)	2213(1)	24(1)
C(18)	1562(2)	-964(2)	2469(1)	19(1)
C(19)	4049(2)	-372(2)	1965(1)	15(1)
C(20)	4388(2)	-756(2)	2756(1)	17(1)
C(21)	4964(2)	-1907(2)	2919(1)	21(1)
C(22)	5220(2)	-2689(2)	2295(1)	24(1)
C(23)	4897(2)	-2318(2)	1505(1)	24(1)
C(24)	4314(2)	-1172(2)	1337(1)	19(1)
C(25)	4610(2)	1509(2)	1564(1)	15(1)
C(26)	5651(2)	999(2)	2032(1)	17(1)
C(27)	6630(2)	1318(2)	1952(1)	20(1)
C(28)	6594(2)	2150(2)	1399(1)	22(1)
C(29)	5568(2)	2658(2)	930(1)	23(1)
C(30)	4582(2)	2349(2)	1010(1)	18(1)

C(31)	2618(2)	1137(2)	765(1)	16(1)
C(32)	3206(2)	1119(2)	22(1)	21(1)
C(33)	2641(2)	1075(2)	-701(1)	29(1)
C(34)	1504(2)	1020(2)	-686(1)	35(1)
C(35)	925(2)	1026(2)	46(1)	31(1)
C(36)	1480(2)	1080(2)	772(1)	22(1)
C(37)	620(2)	5007(1)	2825(1)	14(1)
C(38)	-354(2)	5487(2)	2298(1)	17(1)
C(39)	-1480(2)	6221(2)	2591(1)	19(1)
C(40)	-1652(2)	6478(2)	3409(1)	21(1)
C(41)	-694(2)	6002(2)	3944(1)	19(1)
C(42)	434(2)	5269(2)	3655(1)	16(1)
C(43)	2101(2)	4417(2)	1389(1)	16(1)
C(44)	1537(2)	3993(2)	812(1)	18(1)
C(45)	1563(2)	4268(2)	-6(1)	26(1)
C(46)	2132(2)	4969(2)	-254(1)	32(1)
C(47)	2684(2)	5396(2)	314(1)	32(1)
C(48)	2674(2)	5122(2)	1134(1)	24(1)
C(49)	3186(2)	4458(2)	2932(1)	14(1)
C(50)	2878(2)	5570(2)	3185(1)	18(1)
C(51)	3741(2)	5899(2)	3534(1)	22(1)
C(52)	4922(2)	5121(2)	3626(1)	22(1)
C(53)	5243(2)	4022(2)	3352(1)	22(1)
C(54)	4382(2)	3685(2)	3012(1)	17(1)

Table 58 Bond lengths [Å] and angles [°] for **4.1**.

Ru(1)-O(4)	2.1170(12)
Ru(1)-O(1)	2.1444(11)
Ru(1)-P(2)	2.2570(4)
Ru(1)-P(1)	2.3738(4)
Ru(1)-P(3)	2.3970(5)
Ru(1)-O(2)	2.3979(12)
Ru(1)-S(1)	2.7901(4)
S(1)-O(3)	1.4325(12)
S(1)-O(2)	1.4744(12)
S(1)-O(1)	1.4996(12)
S(1)-C(2)	1.7803(17)
S(2)-O(5)	1.4412(12)
S(2)-O(6)	1.4463(13)
S(2)-O(4)	1.5014(12)
S(2)-C(8)	1.7792(17)
P(1)-C(13)	1.8289(17)
P(1)-C(1)	1.8325(17)
P(1)-C(7)	1.8438(17)
P(2)-C(31)	1.8224(18)
P(2)-C(25)	1.8401(17)
P(2)-C(19)	1.8441(18)
P(3)-C(49)	1.8247(17)
P(3)-C(43)	1.8284(17)
P(3)-C(37)	1.8382(17)
C(1)-C(6)	1.396(2)
C(1)-C(2)	1.412(2)
C(2)-C(3)	1.395(2)

C(3)-C(4)	1.394(3)
C(4)-C(5)	1.379(3)
C(5)-C(6)	1.395(2)
C(7)-C(12)	1.395(2)
C(7)-C(8)	1.408(2)
C(8)-C(9)	1.387(2)
C(9)-C(10)	1.393(3)
C(10)-C(11)	1.384(3)
C(11)-C(12)	1.393(2)
C(13)-C(18)	1.393(3)
C(13)-C(14)	1.398(2)
C(14)-C(15)	1.389(3)
C(15)-C(16)	1.381(3)
C(16)-C(17)	1.387(3)
C(17)-C(18)	1.390(3)
C(19)-C(20)	1.398(2)
C(19)-C(24)	1.404(2)
C(20)-C(21)	1.394(3)
C(21)-C(22)	1.386(3)
C(22)-C(23)	1.390(3)
C(23)-C(24)	1.391(3)
C(25)-C(26)	1.400(2)
C(25)-C(30)	1.400(2)
C(26)-C(27)	1.392(2)
C(27)-C(28)	1.388(3)
C(28)-C(29)	1.388(3)
C(29)-C(30)	1.392(3)
C(31)-C(36)	1.395(3)
C(31)-C(32)	1.400(3)
C(32)-C(33)	1.389(3)
C(33)-C(34)	1.392(3)
C(34)-C(35)	1.381(3)
C(35)-C(36)	1.390(3)
C(37)-C(38)	1.398(2)
C(37)-C(42)	1.404(2)
C(38)-C(39)	1.393(3)
C(39)-C(40)	1.382(3)
C(40)-C(41)	1.393(3)
C(41)-C(42)	1.392(2)
C(43)-C(48)	1.394(3)
C(43)-C(44)	1.402(3)
C(44)-C(45)	1.393(3)
C(45)-C(46)	1.382(3)
C(46)-C(47)	1.385(3)
C(47)-C(48)	1.394(3)
C(49)-C(50)	1.395(2)
C(49)-C(54)	1.397(2)
C(50)-C(51)	1.391(3)
C(51)-C(52)	1.388(3)
C(52)-C(53)	1.388(3)
C(53)-C(54)	1.390(2)

O(4)-Ru(1)-O(1)	169.76(5)
O(4)-Ru(1)-P(2)	98.40(3)
O(1)-Ru(1)-P(2)	90.43(3)

O(4)-Ru(1)-P(1)	89.45(3)
O(1)-Ru(1)-P(1)	93.45(3)
P(2)-Ru(1)-P(1)	104.015(16)
O(4)-Ru(1)-P(3)	79.10(3)
O(1)-Ru(1)-P(3)	94.36(3)
P(2)-Ru(1)-P(3)	99.747(16)
P(1)-Ru(1)-P(3)	154.897(16)
O(4)-Ru(1)-O(2)	108.46(4)
O(1)-Ru(1)-O(2)	62.75(4)
P(2)-Ru(1)-O(2)	153.12(3)
P(1)-Ru(1)-O(2)	77.59(3)
P(3)-Ru(1)-O(2)	84.90(3)
O(4)-Ru(1)-S(1)	140.02(3)
O(1)-Ru(1)-S(1)	32.12(3)
P(2)-Ru(1)-S(1)	121.416(15)
P(1)-Ru(1)-S(1)	78.327(14)
P(3)-Ru(1)-S(1)	96.151(14)
O(2)-Ru(1)-S(1)	31.89(3)
O(3)-S(1)-O(2)	116.26(8)
O(3)-S(1)-O(1)	114.22(7)
O(2)-S(1)-O(1)	105.97(7)
O(3)-S(1)-C(2)	107.61(8)
O(2)-S(1)-C(2)	108.14(7)
O(1)-S(1)-C(2)	103.80(7)
O(3)-S(1)-Ru(1)	149.08(6)
O(2)-S(1)-Ru(1)	59.23(5)
O(1)-S(1)-Ru(1)	49.50(4)
C(2)-S(1)-Ru(1)	102.36(6)
O(5)-S(2)-O(6)	116.08(8)
O(5)-S(2)-O(4)	110.14(7)
O(6)-S(2)-O(4)	111.57(7)
O(5)-S(2)-C(8)	107.43(8)
O(6)-S(2)-C(8)	105.54(8)
O(4)-S(2)-C(8)	105.34(7)
C(13)-P(1)-C(1)	102.93(8)
C(13)-P(1)-C(7)	103.69(8)
C(1)-P(1)-C(7)	101.69(8)
C(13)-P(1)-Ru(1)	134.43(6)
C(1)-P(1)-Ru(1)	110.85(6)
C(7)-P(1)-Ru(1)	98.52(5)
C(31)-P(2)-C(25)	106.71(8)
C(31)-P(2)-C(19)	101.41(8)
C(25)-P(2)-C(19)	100.08(8)
C(31)-P(2)-Ru(1)	119.69(6)
C(25)-P(2)-Ru(1)	112.12(6)
C(19)-P(2)-Ru(1)	114.57(6)
C(49)-P(3)-C(43)	104.04(8)
C(49)-P(3)-C(37)	103.75(8)
C(43)-P(3)-C(37)	102.54(8)
C(49)-P(3)-Ru(1)	119.32(6)
C(43)-P(3)-Ru(1)	119.95(6)
C(37)-P(3)-Ru(1)	104.85(5)
S(1)-O(1)-Ru(1)	98.38(6)
S(1)-O(2)-Ru(1)	88.87(6)
S(2)-O(4)-Ru(1)	127.27(7)

C(6)-C(1)-C(2)	117.73(15)
C(6)-C(1)-P(1)	121.32(13)
C(2)-C(1)-P(1)	120.95(12)
C(3)-C(2)-C(1)	120.99(16)
C(3)-C(2)-S(1)	117.81(13)
C(1)-C(2)-S(1)	121.07(12)
C(4)-C(3)-C(2)	119.83(17)
C(5)-C(4)-C(3)	119.86(17)
C(4)-C(5)-C(6)	120.44(17)
C(5)-C(6)-C(1)	121.13(17)
C(12)-C(7)-C(8)	117.78(16)
C(12)-C(7)-P(1)	121.20(13)
C(8)-C(7)-P(1)	120.44(12)
C(9)-C(8)-C(7)	121.11(16)
C(9)-C(8)-S(2)	118.38(13)
C(7)-C(8)-S(2)	120.49(13)
C(8)-C(9)-C(10)	120.09(17)
C(11)-C(10)-C(9)	119.45(17)
C(10)-C(11)-C(12)	120.48(16)
C(11)-C(12)-C(7)	121.01(16)
C(18)-C(13)-C(14)	119.25(16)
C(18)-C(13)-P(1)	120.73(13)
C(14)-C(13)-P(1)	120.02(14)
C(15)-C(14)-C(13)	120.27(17)
C(16)-C(15)-C(14)	120.20(17)
C(15)-C(16)-C(17)	119.85(17)
C(16)-C(17)-C(18)	120.42(18)
C(17)-C(18)-C(13)	120.00(17)
C(20)-C(19)-C(24)	118.52(17)
C(20)-C(19)-P(2)	120.53(13)
C(24)-C(19)-P(2)	120.94(14)
C(21)-C(20)-C(19)	120.70(17)
C(22)-C(21)-C(20)	120.26(18)
C(21)-C(22)-C(23)	119.63(18)
C(22)-C(23)-C(24)	120.48(18)
C(23)-C(24)-C(19)	120.41(18)
C(26)-C(25)-C(30)	118.22(16)
C(26)-C(25)-P(2)	119.62(13)
C(30)-C(25)-P(2)	121.95(13)
C(27)-C(26)-C(25)	121.07(17)
C(28)-C(27)-C(26)	120.24(17)
C(29)-C(28)-C(27)	119.18(17)
C(28)-C(29)-C(30)	120.91(18)
C(29)-C(30)-C(25)	120.38(17)
C(36)-C(31)-C(32)	119.37(17)
C(36)-C(31)-P(2)	116.55(14)
C(32)-C(31)-P(2)	123.99(14)
C(33)-C(32)-C(31)	120.02(18)
C(32)-C(33)-C(34)	120.0(2)
C(35)-C(34)-C(33)	120.23(19)
C(34)-C(35)-C(36)	120.1(2)
C(35)-C(36)-C(31)	120.26(19)
C(38)-C(37)-C(42)	118.63(16)
C(38)-C(37)-P(3)	120.84(13)
C(42)-C(37)-P(3)	120.45(13)

C(39)-C(38)-C(37)	120.53(17)
C(40)-C(39)-C(38)	120.35(17)
C(39)-C(40)-C(41)	119.94(17)
C(42)-C(41)-C(40)	120.00(17)
C(41)-C(42)-C(37)	120.55(17)
C(48)-C(43)-C(44)	119.16(16)
C(48)-C(43)-P(3)	122.06(14)
C(44)-C(43)-P(3)	118.76(13)
C(45)-C(44)-C(43)	120.06(18)
C(46)-C(45)-C(44)	120.4(2)
C(45)-C(46)-C(47)	119.80(19)
C(46)-C(47)-C(48)	120.5(2)
C(43)-C(48)-C(47)	120.09(19)
C(50)-C(49)-C(54)	119.04(16)
C(50)-C(49)-P(3)	122.06(13)
C(54)-C(49)-P(3)	118.82(13)
C(51)-C(50)-C(49)	120.53(17)
C(52)-C(51)-C(50)	120.07(18)
C(53)-C(52)-C(51)	119.67(17)
C(52)-C(53)-C(54)	120.51(18)
C(53)-C(54)-C(49)	120.14(17)

Table 59 Anisotropic displacement parameters ($Å^2 x\ 10^3$) for **4.1**. The anisotropic displacement factor exponent takes the form: $-2\pi^2[\ h^2\ a^{*2}U^{11} + ...\ + 2\ h\ k\ a^*\ b^*\ U^{12}\ ]$

	U^{11}	U^{22}	U^{33}	U^{23}	U^{13}	U^{12}
Ru(1)	9(1)	14(1)	10(1)	1(1)	0(1)	-5(1)
S(1)	12(1)	17(1)	11(1)	0(1)	-1(1)	-7(1)
S(2)	10(1)	18(1)	12(1)	3(1)	-2(1)	-7(1)
P(1)	10(1)	14(1)	11(1)	2(1)	-1(1)	-6(1)
P(2)	10(1)	17(1)	12(1)	0(1)	0(1)	-6(1)
P(3)	10(1)	15(1)	12(1)	2(1)	0(1)	-5(1)
O(1)	11(1)	19(1)	10(1)	1(1)	-1(1)	-7(1)
O(2)	13(1)	16(1)	15(1)	0(1)	0(1)	-6(1)
O(3)	19(1)	24(1)	14(1)	-1(1)	-3(1)	-11(1)
O(4)	11(1)	20(1)	14(1)	3(1)	-1(1)	-7(1)
O(5)	12(1)	22(1)	18(1)	7(1)	-4(1)	-6(1)
O(6)	17(1)	20(1)	16(1)	1(1)	-2(1)	-10(1)
C(1)	11(1)	17(1)	12(1)	2(1)	0(1)	-4(1)
C(2)	11(1)	16(1)	13(1)	2(1)	1(1)	-4(1)
C(3)	13(1)	24(1)	15(1)	1(1)	-2(1)	-7(1)
C(4)	13(1)	25(1)	15(1)	6(1)	-2(1)	-5(1)
C(5)	16(1)	19(1)	21(1)	8(1)	-1(1)	-6(1)
C(6)	14(1)	18(1)	16(1)	3(1)	-1(1)	-7(1)
C(7)	10(1)	16(1)	15(1)	0(1)	0(1)	-8(1)
C(8)	11(1)	18(1)	13(1)	2(1)	-1(1)	-8(1)
C(9)	12(1)	17(1)	20(1)	3(1)	-2(1)	-7(1)
C(10)	14(1)	21(1)	21(1)	-3(1)	3(1)	-7(1)
C(11)	17(1)	22(1)	14(1)	-1(1)	1(1)	-11(1)
C(12)	12(1)	18(1)	15(1)	3(1)	-1(1)	-8(1)
C(13)	14(1)	15(1)	15(1)	4(1)	-5(1)	-7(1)
C(14)	18(1)	20(1)	17(1)	2(1)	-1(1)	-9(1)

C(15)	19(1)	22(1)	24(1)	7(1)	-5(1)	-13(1)
C(16)	24(1)	17(1)	28(1)	3(1)	-8(1)	-12(1)
C(17)	24(1)	20(1)	27(1)	-6(1)	1(1)	-9(1)
C(18)	17(1)	21(1)	22(1)	0(1)	0(1)	-9(1)
C(19)	10(1)	17(1)	19(1)	1(1)	1(1)	-6(1)
C(20)	12(1)	21(1)	19(1)	-1(1)	1(1)	-7(1)
C(21)	15(1)	25(1)	24(1)	5(1)	-1(1)	-8(1)
C(22)	18(1)	17(1)	34(1)	3(1)	2(1)	-6(1)
C(23)	23(1)	21(1)	27(1)	-5(1)	6(1)	-9(1)
C(24)	19(1)	23(1)	17(1)	-3(1)	3(1)	-9(1)
C(25)	12(1)	20(1)	14(1)	-4(1)	3(1)	-7(1)
C(26)	16(1)	20(1)	14(1)	-3(1)	1(1)	-7(1)
C(27)	14(1)	25(1)	21(1)	-4(1)	-1(1)	-7(1)
C(28)	17(1)	32(1)	23(1)	-2(1)	2(1)	-15(1)
C(29)	20(1)	29(1)	22(1)	4(1)	2(1)	-13(1)
C(30)	14(1)	22(1)	16(1)	0(1)	1(1)	-6(1)
C(31)	16(1)	17(1)	14(1)	-2(1)	-3(1)	-5(1)
C(32)	19(1)	22(1)	18(1)	-2(1)	1(1)	-6(1)
C(33)	34(1)	32(1)	15(1)	-4(1)	-1(1)	-6(1)
C(34)	34(1)	43(1)	23(1)	-8(1)	-13(1)	-7(1)
C(35)	20(1)	39(1)	31(1)	-11(1)	-6(1)	-9(1)
C(36)	19(1)	24(1)	22(1)	-5(1)	-1(1)	-8(1)
C(37)	12(1)	14(1)	19(1)	1(1)	1(1)	-6(1)
C(38)	15(1)	18(1)	19(1)	1(1)	-1(1)	-7(1)
C(39)	13(1)	18(1)	27(1)	2(1)	-3(1)	-6(1)
C(40)	12(1)	18(1)	32(1)	-2(1)	5(1)	-6(1)
C(41)	19(1)	20(1)	21(1)	-3(1)	5(1)	-10(1)
C(42)	15(1)	16(1)	18(1)	1(1)	-1(1)	-8(1)
C(43)	13(1)	18(1)	13(1)	4(1)	2(1)	-3(1)
C(44)	14(1)	22(1)	16(1)	3(1)	0(1)	-4(1)
C(45)	20(1)	34(1)	17(1)	4(1)	-4(1)	-4(1)
C(46)	31(1)	43(1)	18(1)	14(1)	0(1)	-9(1)
C(47)	35(1)	38(1)	28(1)	13(1)	4(1)	-18(1)
C(48)	24(1)	26(1)	23(1)	6(1)	0(1)	-11(1)
C(49)	14(1)	19(1)	13(1)	2(1)	0(1)	-9(1)
C(50)	13(1)	19(1)	21(1)	1(1)	2(1)	-7(1)
C(51)	21(1)	22(1)	26(1)	-4(1)	4(1)	-13(1)
C(52)	19(1)	26(1)	25(1)	0(1)	-3(1)	-15(1)
C(53)	15(1)	22(1)	29(1)	5(1)	-4(1)	-8(1)
C(54)	14(1)	17(1)	19(1)	2(1)	-1(1)	-7(1)

Table 60 Hydrogen coordinates (x 10^4) and isotropic displacement parameters ($Å^2$x 10^3)for **4.1**.

	x	y	z	U(eq)
H(3)	3943(19)	726(18)	5683(13)	20(5)
H(4)	4064(19)	-1009(18)	6176(13)	21(5)
H(5)	3030(20)	-1956(19)	5464(13)	22(6)
H(6)	1940(19)	-1189(18)	4341(13)	19(5)
H(9)	-2283(19)	4311(18)	3442(13)	17(5)
H(10)	-2525(19)	4346(18)	4857(13)	17(5)
H(11)	-1260(18)	2901(17)	5646(13)	14(5)

H(12)	287(18)	1438(17)	5052(12)	12(5)
H(14)	-620(19)	256(18)	3766(13)	20(5)
H(15)	-1220(20)	-1202(19)	3359(14)	28(6)
H(16)	-50(20)	-2450(19)	2378(13)	24(6)
H(17)	1660(20)	-2309(19)	1805(13)	23(6)
H(18)	2220(20)	-919(18)	2253(13)	21(5)
H(20)	4220(19)	-216(18)	3172(13)	18(5)
H(21)	5170(20)	-2133(19)	3437(14)	26(6)
H(22)	5590(20)	-3450(20)	2390(14)	26(6)
H(23)	5053(19)	-2864(18)	1082(13)	19(5)
H(24)	4083(19)	-950(17)	837(13)	18(5)
H(26)	5676(19)	452(19)	2393(14)	22(6)
H(27)	7340(20)	945(19)	2275(14)	26(6)
H(28)	7240(20)	2358(19)	1350(13)	25(6)
H(29)	5520(20)	3220(20)	566(14)	26(6)
H(30)	3912(19)	2695(17)	687(13)	16(5)
H(32)	3970(20)	1137(17)	3(12)	17(5)
H(33)	3060(20)	1090(20)	-1210(16)	38(7)
H(34)	1120(20)	960(20)	-1160(16)	40(7)
H(35)	120(20)	1000(20)	52(15)	37(7)
H(36)	1070(20)	1097(19)	1259(14)	24(6)
H(38)	-239(19)	5296(18)	1718(13)	20(5)
H(39)	-2100(20)	6552(18)	2225(13)	23(6)
H(40)	-2370(20)	6948(19)	3596(13)	26(6)
H(41)	-794(18)	6171(17)	4497(13)	16(5)
H(42)	1076(19)	4927(18)	4016(13)	20(5)
H(44)	1123(19)	3526(18)	974(13)	18(5)
H(45)	1210(20)	3950(20)	-392(15)	34(7)
H(46)	2150(20)	5150(20)	-799(16)	42(7)
H(47)	3060(20)	5870(20)	180(15)	34(7)
H(48)	3066(19)	5402(17)	1536(13)	18(5)
H(50)	2078(19)	6122(17)	3136(12)	15(5)
H(51)	3500(20)	6660(20)	3699(14)	27(6)
H(52)	5500(20)	5350(20)	3876(15)	37(7)
H(53)	6010(20)	3539(18)	3407(13)	20(5)
H(54)	4613(18)	2920(18)	2832(12)	15(5)

X-ray Data Collection, Structure Solution and Refinement for complex 4.2.

A red crystal of approximate dimensions 0.092 x 0.126 x 0.249 mm was mounted on a glass fiber and transferred to a Bruker SMART APEX II diffractometer. The APEX2[1] program package was used to determine the unit-cell parameters and for data collection (25 sec/frame scan time for a sphere of diffraction data). The raw frame data was processed using SAINT[2] and SADABS[3] to yield the reflection data file. Subsequent calculations were carried out using the SHELXTL[4] program. The diffraction symmetry was 2/*m* and the systematic absences were consistent with the monoclinic space groups *Cc* and *C*2/*c*. It was later determined that space group *C*2/*c* was correct.

The structure was solved by direct methods and refined on F^2 by full-matrix least-squares techniques. The analytical scattering factors[5] for neutral atoms were used throughout the analysis.

Hydrogen atoms were included using a riding model. There were several high residuals present in the final difference-Fourier map. It was not possible to determine the nature of the residuals although it is probable that pentane or diethyl ether solvent was present. The SQUEEZE routine in the PLATON[6] program package was used to account for the electrons in the solvent accessible voids.

At convergence, wR2 = 0.0780 and Goof = 1.032 for 571 variables refined against 10388 data (0.78 Å), R1 = 0.0298 for those 8938 data with $I > 2.0\sigma(I)$.

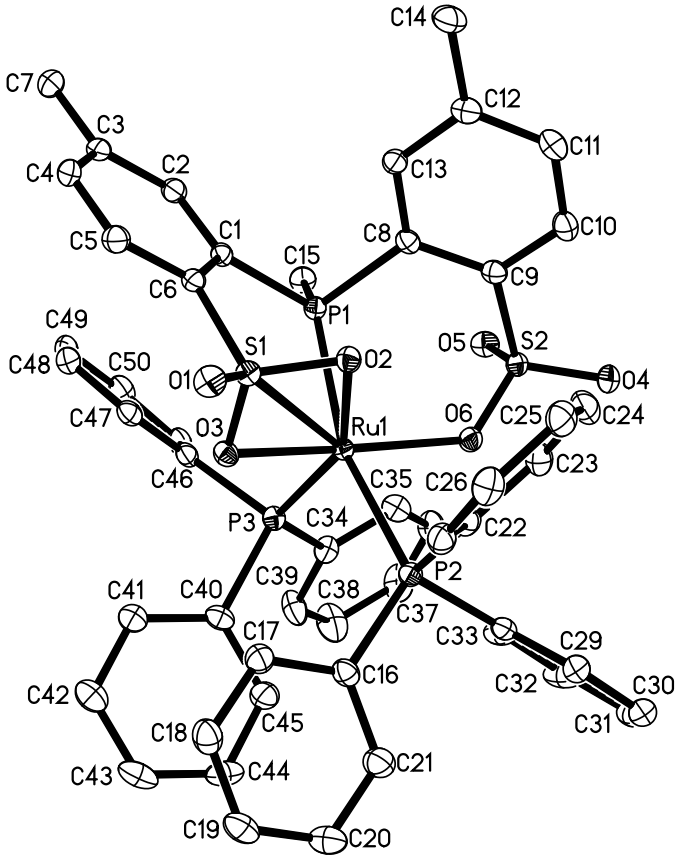

Table 61 Crystal data and structure refinement for **4.2**

Identification code	zg61 (Tobias Friedberger)	
Empirical formula	C_{51} H_{45} O_6 P_3 Ru S_2	
Formula weight	1011.97	
Temperature	83(2) K	
Wavelength	0.71073 Å	
Crystal system	Monoclinic	
Space group	*C* 2/*c*	
Unit cell dimensions	a = 45.4953(16) Å	α= 90°.
	b = 11.6401(4) Å	β= 107.4923(4)°.
	c = 18.6910(7) Å	γ = 90°.
Volume	9440.5(6) Å^3	
Z	8	
Density (calculated)	1.424 Mg/m^3	

Absorption coefficient	0.571 mm^{-1}
F(000)	4160
Crystal color	red
Crystal size	0.249 x 0.126 x 0.092 mm^3
Theta range for data collection	1.811 to 27.102°
Index ranges	$-58 \leq h \leq 58$, $-14 \leq k \leq 14$, $-23 \leq l \leq 23$
Reflections collected	53342
Independent reflections	10388 [R(int) = 0.0369]
Completeness to theta = 25.500°	99.9 %
Absorption correction	Numerical
Refinement method	Full-matrix least-squares on F^2
Data / restraints / parameters	10388 / 0 / 571
Goodness-of-fit on F^2	1.032
Final R indices [I>2sigma(I) = 8938 data]	R1 = 0.0298, wR2 = 0.0752
R indices (all data, 0.78 Å)	R1 = 0.0368, wR2 = 0.0780
Largest diff. peak and hole	0.922 and -0.523 e.$Å^{-3}$

Table 62. Atomic coordinates (x 10^4) and equivalent isotropic displacement parameters ($Å^2$x 10^3) for **4.2**. U(eq) is defined as one third of the trace of the orthogonalized U^{ij} tensor.

	x	y	z	U(eq)
Ru(1)	1132(1)	6808(1)	1530(1)	11(1)
S(1)	959(1)	6072(1)	2750(1)	13(1)
S(2)	686(1)	8369(1)	158(1)	14(1)
P(1)	668(1)	5836(1)	957(1)	12(1)
P(2)	1490(1)	8284(1)	2186(1)	13(1)
P(3)	1438(1)	5723(1)	1056(1)	13(1)
O(1)	1017(1)	6067(1)	3545(1)	18(1)
O(2)	834(1)	7140(1)	2354(1)	15(1)
O(3)	1240(1)	5783(1)	2520(1)	14(1)
O(4)	660(1)	9574(1)	-26(1)	20(1)
O(5)	630(1)	7597(1)	-479(1)	18(1)
O(6)	991(1)	8140(1)	724(1)	15(1)
C(1)	572(1)	4804(2)	1591(1)	13(1)
C(2)	386(1)	3852(2)	1327(1)	16(1)
C(3)	320(1)	3048(2)	1814(1)	17(1)
C(4)	442(1)	3221(2)	2583(1)	17(1)
C(5)	630(1)	4161(2)	2864(1)	17(1)
C(6)	695(1)	4948(2)	2369(1)	14(1)
C(7)	121(1)	2023(2)	1491(1)	20(1)
C(8)	369(1)	6941(2)	873(1)	14(1)
C(9)	398(1)	8045(2)	596(1)	14(1)
C(10)	194(1)	8908(2)	625(1)	19(1)
C(11)	-48(1)	8695(2)	917(1)	21(1)
C(12)	-88(1)	7613(2)	1186(1)	18(1)
C(13)	124(1)	6753(2)	1164(1)	15(1)
C(14)	-347(1)	7366(2)	1509(1)	24(1)
C(15)	560(1)	5101(2)	54(1)	17(1)
C(16)	1852(1)	7993(2)	2924(1)	16(1)
C(17)	1864(1)	7126(2)	3449(1)	19(1)
C(18)	2138(1)	6916(2)	4014(1)	23(1)
C(19)	2401(1)	7532(2)	4053(1)	23(1)
C(20)	2393(1)	8384(2)	3534(1)	25(1)

C(21)	2119(1)	8621(2)	2974(1)	22(1)
C(22)	1266(1)	9138(2)	2664(1)	15(1)
C(23)	1006(1)	9705(2)	2211(1)	19(1)
C(24)	811(1)	10291(2)	2528(1)	22(1)
C(25)	872(1)	10323(2)	3299(1)	22(1)
C(26)	1130(1)	9776(2)	3753(1)	22(1)
C(27)	1328(1)	9183(2)	3440(1)	19(1)
C(28)	1603(1)	9371(2)	1610(1)	18(1)
C(29)	1667(1)	10498(2)	1864(1)	24(1)
C(30)	1768(1)	11298(2)	1432(2)	33(1)
C(31)	1802(1)	10974(2)	748(2)	35(1)
C(32)	1738(1)	9862(2)	491(1)	34(1)
C(33)	1637(1)	9065(2)	920(1)	24(1)
C(34)	1519(1)	6071(2)	178(1)	17(1)
C(35)	1307(1)	6740(2)	-356(1)	20(1)
C(36)	1351(1)	6975(2)	-1044(1)	24(1)
C(37)	1602(1)	6535(2)	-1215(1)	29(1)
C(38)	1813(1)	5861(2)	-697(1)	33(1)
C(39)	1773(1)	5627(2)	-2(1)	26(1)
C(40)	1827(1)	5523(2)	1718(1)	16(1)
C(41)	1894(1)	4600(2)	2217(1)	19(1)
C(42)	2183(1)	4495(2)	2746(1)	23(1)
C(43)	2411(1)	5305(2)	2776(1)	26(1)
C(44)	2348(1)	6207(2)	2276(1)	26(1)
C(45)	2058(1)	6325(2)	1751(1)	22(1)
C(46)	1293(1)	4241(2)	889(1)	16(1)
C(47)	1191(1)	3674(2)	1432(1)	17(1)
C(48)	1059(1)	2587(2)	1292(1)	20(1)
C(49)	1022(1)	2054(2)	606(1)	23(1)
C(50)	1123(1)	2608(2)	68(1)	22(1)
C(51)	1260(1)	3687(2)	206(1)	19(1)

Table 63 Bond lengths [Å] and angles [°] for **4.2**

Ru(1)-O(6)	2.1217(13)
Ru(1)-O(3)	2.1321(13)
Ru(1)-P(3)	2.2506(5)
Ru(1)-P(1)	2.3492(5)
Ru(1)-O(2)	2.3686(13)
Ru(1)-P(2)	2.4306(5)
Ru(1)-S(1)	2.7620(5)
S(1)-O(1)	1.4294(14)
S(1)-O(2)	1.4714(14)
S(1)-O(3)	1.5043(14)
S(1)-C(6)	1.7748(19)
S(2)-O(4)	1.4412(14)
S(2)-O(5)	1.4514(14)
S(2)-O(6)	1.4942(14)
S(2)-C(9)	1.781(2)
P(1)-C(15)	1.8239(19)
P(1)-C(1)	1.8286(19)
P(1)-C(8)	1.8437(19)
P(2)-C(28)	1.834(2)
P(2)-C(22)	1.835(2)

P(2)-C(16)	1.837(2)
P(3)-C(34)	1.831(2)
P(3)-C(46)	1.840(2)
P(3)-C(40)	1.841(2)
C(1)-C(2)	1.394(3)
C(1)-C(6)	1.403(3)
C(2)-C(3)	1.399(3)
C(3)-C(4)	1.391(3)
C(3)-C(7)	1.508(3)
C(4)-C(5)	1.390(3)
C(5)-C(6)	1.394(3)
C(8)-C(13)	1.396(3)
C(8)-C(9)	1.407(3)
C(9)-C(10)	1.380(3)
C(10)-C(11)	1.391(3)
C(11)-C(12)	1.388(3)
C(12)-C(13)	1.400(3)
C(12)-C(14)	1.504(3)
C(16)-C(21)	1.393(3)
C(16)-C(17)	1.397(3)
C(17)-C(18)	1.393(3)
C(18)-C(19)	1.378(3)
C(19)-C(20)	1.380(3)
C(20)-C(21)	1.393(3)
C(22)-C(27)	1.392(3)
C(22)-C(23)	1.397(3)
C(23)-C(24)	1.387(3)
C(24)-C(25)	1.383(3)
C(25)-C(26)	1.381(3)
C(26)-C(27)	1.396(3)
C(28)-C(33)	1.390(3)
C(28)-C(29)	1.396(3)
C(29)-C(30)	1.397(3)
C(30)-C(31)	1.388(4)
C(31)-C(32)	1.381(4)
C(32)-C(33)	1.391(3)
C(34)-C(39)	1.396(3)
C(34)-C(35)	1.398(3)
C(35)-C(36)	1.387(3)
C(36)-C(37)	1.376(3)
C(37)-C(38)	1.383(3)
C(38)-C(39)	1.391(3)
C(40)-C(41)	1.395(3)
C(40)-C(45)	1.396(3)
C(41)-C(42)	1.393(3)
C(42)-C(43)	1.389(3)
C(43)-C(44)	1.378(3)
C(44)-C(45)	1.394(3)
C(46)-C(51)	1.397(3)
C(46)-C(47)	1.400(3)
C(47)-C(48)	1.392(3)
C(48)-C(49)	1.387(3)
C(49)-C(50)	1.384(3)
C(50)-C(51)	1.392(3)

O(6)-Ru(1)-O(3)	165.20(5)
O(6)-Ru(1)-P(3)	102.82(4)
O(3)-Ru(1)-P(3)	91.04(4)
O(6)-Ru(1)-P(1)	89.48(4)
O(3)-Ru(1)-P(1)	93.91(4)
P(3)-Ru(1)-P(1)	97.393(18)
O(6)-Ru(1)-O(2)	103.45(5)
O(3)-Ru(1)-O(2)	63.57(5)
P(3)-Ru(1)-O(2)	152.91(4)
P(1)-Ru(1)-O(2)	76.38(3)
O(6)-Ru(1)-P(2)	81.66(4)
O(3)-Ru(1)-P(2)	90.66(4)
P(3)-Ru(1)-P(2)	101.246(18)
P(1)-Ru(1)-P(2)	160.720(18)
O(2)-Ru(1)-P(2)	89.01(3)
O(6)-Ru(1)-S(1)	135.45(4)
O(3)-Ru(1)-S(1)	32.69(4)
P(3)-Ru(1)-S(1)	120.930(17)
P(1)-Ru(1)-S(1)	77.728(16)
O(2)-Ru(1)-S(1)	32.18(3)
P(2)-Ru(1)-S(1)	96.640(16)
O(1)-S(1)-O(2)	116.64(8)
O(1)-S(1)-O(3)	112.88(8)
O(2)-S(1)-O(3)	106.17(8)
O(1)-S(1)-C(6)	107.76(9)
O(2)-S(1)-C(6)	107.97(8)
O(3)-S(1)-C(6)	104.70(8)
O(1)-S(1)-Ru(1)	148.25(6)
O(2)-S(1)-Ru(1)	59.02(5)
O(3)-S(1)-Ru(1)	49.96(5)
C(6)-S(1)-Ru(1)	102.97(6)
O(4)-S(2)-O(5)	115.16(9)
O(4)-S(2)-O(6)	109.51(8)
O(5)-S(2)-O(6)	111.60(8)
O(4)-S(2)-C(9)	107.30(9)
O(5)-S(2)-C(9)	105.92(9)
O(6)-S(2)-C(9)	106.89(8)
C(15)-P(1)-C(1)	103.99(9)
C(15)-P(1)-C(8)	105.21(9)
C(1)-P(1)-C(8)	101.57(9)
C(15)-P(1)-Ru(1)	126.99(7)
C(1)-P(1)-Ru(1)	112.16(6)
C(8)-P(1)-Ru(1)	103.97(6)
C(28)-P(2)-C(22)	101.93(9)
C(28)-P(2)-C(16)	102.70(9)
C(22)-P(2)-C(16)	103.82(9)
C(28)-P(2)-Ru(1)	117.08(7)
C(22)-P(2)-Ru(1)	104.13(6)
C(16)-P(2)-Ru(1)	124.30(7)
C(34)-P(3)-C(46)	102.36(9)
C(34)-P(3)-C(40)	102.70(9)
C(46)-P(3)-C(40)	102.67(9)
C(34)-P(3)-Ru(1)	122.86(7)
C(46)-P(3)-Ru(1)	111.04(7)
C(40)-P(3)-Ru(1)	112.93(6)

S(1)-O(2)-Ru(1)	88.79(6)
S(1)-O(3)-Ru(1)	97.34(7)
S(2)-O(6)-Ru(1)	130.58(8)
C(2)-C(1)-C(6)	118.15(17)
C(2)-C(1)-P(1)	122.11(15)
C(6)-C(1)-P(1)	119.73(14)
C(1)-C(2)-C(3)	121.90(18)
C(4)-C(3)-C(2)	118.50(18)
C(4)-C(3)-C(7)	122.28(18)
C(2)-C(3)-C(7)	119.22(18)
C(5)-C(4)-C(3)	120.98(18)
C(4)-C(5)-C(6)	119.68(18)
C(5)-C(6)-C(1)	120.80(18)
C(5)-C(6)-S(1)	118.14(15)
C(1)-C(6)-S(1)	120.89(14)
C(13)-C(8)-C(9)	117.48(17)
C(13)-C(8)-P(1)	120.79(15)
C(9)-C(8)-P(1)	121.31(15)
C(10)-C(9)-C(8)	120.70(18)
C(10)-C(9)-S(2)	117.47(15)
C(8)-C(9)-S(2)	121.77(15)
C(9)-C(10)-C(11)	120.6(2)
C(12)-C(11)-C(10)	120.52(19)
C(11)-C(12)-C(13)	118.17(18)
C(11)-C(12)-C(14)	121.45(19)
C(13)-C(12)-C(14)	120.36(19)
C(8)-C(13)-C(12)	122.54(18)
C(21)-C(16)-C(17)	118.93(19)
C(21)-C(16)-P(2)	121.36(16)
C(17)-C(16)-P(2)	119.70(15)
C(18)-C(17)-C(16)	119.66(19)
C(19)-C(18)-C(17)	121.0(2)
C(18)-C(19)-C(20)	119.8(2)
C(19)-C(20)-C(21)	120.0(2)
C(16)-C(21)-C(20)	120.6(2)
C(27)-C(22)-C(23)	118.87(18)
C(27)-C(22)-P(2)	124.00(15)
C(23)-C(22)-P(2)	116.96(15)
C(24)-C(23)-C(22)	120.52(19)
C(25)-C(24)-C(23)	120.4(2)
C(26)-C(25)-C(24)	119.65(19)
C(25)-C(26)-C(27)	120.48(19)
C(22)-C(27)-C(26)	120.11(19)
C(33)-C(28)-C(29)	119.2(2)
C(33)-C(28)-P(2)	119.79(17)
C(29)-C(28)-P(2)	121.01(17)
C(28)-C(29)-C(30)	120.0(2)
C(31)-C(30)-C(29)	120.0(2)
C(32)-C(31)-C(30)	120.2(2)
C(31)-C(32)-C(33)	119.9(2)
C(28)-C(33)-C(32)	120.7(2)
C(39)-C(34)-C(35)	118.45(19)
C(39)-C(34)-P(3)	122.52(16)
C(35)-C(34)-P(3)	118.86(15)
C(36)-C(35)-C(34)	120.8(2)

C(37)-C(36)-C(35)	120.3(2)
C(36)-C(37)-C(38)	119.8(2)
C(37)-C(38)-C(39)	120.5(2)
C(38)-C(39)-C(34)	120.2(2)
C(41)-C(40)-C(45)	118.35(19)
C(41)-C(40)-P(3)	121.27(16)
C(45)-C(40)-P(3)	120.33(16)
C(42)-C(41)-C(40)	120.8(2)
C(43)-C(42)-C(41)	120.2(2)
C(44)-C(43)-C(42)	119.4(2)
C(43)-C(44)-C(45)	120.7(2)
C(44)-C(45)-C(40)	120.5(2)
C(51)-C(46)-C(47)	118.49(19)
C(51)-C(46)-P(3)	121.44(16)
C(47)-C(46)-P(3)	119.90(15)
C(48)-C(47)-C(46)	120.62(19)
C(49)-C(48)-C(47)	120.4(2)
C(50)-C(49)-C(48)	119.2(2)
C(49)-C(50)-C(51)	120.9(2)
C(50)-C(51)-C(46)	120.3(2)

Table 64 Anisotropic displacement parameters ($Å^2 x\ 10^3$) for **4.2**. The anisotropic displacement factor exponent takes the form: $-2\pi^2[\ h^2\ a^{*2}U^{11} + ...\ + 2\ h\ k\ a^*\ b^*\ U^{12}\ ]$

	U^{11}	U^{22}	U^{33}	U^{23}	U^{13}	U^{12}
Ru(1)	11(1)	11(1)	11(1)	0(1)	3(1)	0(1)
S(1)	14(1)	14(1)	11(1)	-1(1)	4(1)	-1(1)
S(2)	14(1)	14(1)	14(1)	2(1)	3(1)	0(1)
P(1)	13(1)	12(1)	11(1)	0(1)	3(1)	0(1)
P(2)	13(1)	13(1)	13(1)	1(1)	2(1)	0(1)
P(3)	15(1)	13(1)	13(1)	0(1)	5(1)	1(1)
O(1)	21(1)	22(1)	12(1)	-2(1)	4(1)	-2(1)
O(2)	15(1)	13(1)	16(1)	0(1)	4(1)	0(1)
O(3)	14(1)	16(1)	12(1)	1(1)	3(1)	1(1)
O(4)	20(1)	15(1)	23(1)	7(1)	6(1)	1(1)
O(5)	17(1)	22(1)	13(1)	-1(1)	3(1)	-1(1)
O(6)	15(1)	14(1)	14(1)	2(1)	2(1)	-1(1)
C(1)	13(1)	12(1)	15(1)	2(1)	5(1)	2(1)
C(2)	14(1)	15(1)	17(1)	-1(1)	4(1)	1(1)
C(3)	12(1)	14(1)	24(1)	2(1)	6(1)	1(1)
C(4)	17(1)	16(1)	20(1)	6(1)	6(1)	1(1)
C(5)	16(1)	20(1)	15(1)	2(1)	4(1)	0(1)
C(6)	12(1)	12(1)	17(1)	0(1)	4(1)	1(1)
C(7)	19(1)	16(1)	24(1)	1(1)	5(1)	-2(1)
C(8)	13(1)	14(1)	12(1)	-2(1)	2(1)	1(1)
C(9)	13(1)	18(1)	12(1)	1(1)	3(1)	0(1)
C(10)	19(1)	18(1)	19(1)	3(1)	4(1)	3(1)
C(11)	19(1)	21(1)	22(1)	0(1)	6(1)	6(1)
C(12)	15(1)	22(1)	18(1)	0(1)	5(1)	0(1)
C(13)	14(1)	15(1)	15(1)	2(1)	2(1)	-1(1)
C(14)	17(1)	28(1)	29(1)	3(1)	10(1)	3(1)
C(15)	18(1)	17(1)	14(1)	-2(1)	2(1)	-1(1)

C(16)	16(1)	17(1)	14(1)	-2(1)	1(1)	2(1)
C(17)	19(1)	17(1)	20(1)	-1(1)	3(1)	-1(1)
C(18)	26(1)	20(1)	18(1)	1(1)	2(1)	2(1)
C(19)	18(1)	29(1)	18(1)	-3(1)	0(1)	4(1)
C(20)	17(1)	32(1)	23(1)	-1(1)	3(1)	-3(1)
C(21)	19(1)	26(1)	22(1)	4(1)	5(1)	0(1)
C(22)	16(1)	10(1)	18(1)	-2(1)	5(1)	-3(1)
C(23)	24(1)	16(1)	18(1)	-1(1)	5(1)	1(1)
C(24)	20(1)	19(1)	25(1)	1(1)	4(1)	6(1)
C(25)	25(1)	16(1)	26(1)	-3(1)	12(1)	2(1)
C(26)	29(1)	18(1)	18(1)	-2(1)	7(1)	-1(1)
C(27)	20(1)	16(1)	19(1)	0(1)	2(1)	-1(1)
C(28)	11(1)	19(1)	22(1)	6(1)	1(1)	0(1)
C(29)	17(1)	18(1)	36(1)	4(1)	7(1)	1(1)
C(30)	18(1)	22(1)	57(2)	12(1)	6(1)	-1(1)
C(31)	17(1)	41(2)	44(2)	25(1)	4(1)	-3(1)
C(32)	20(1)	55(2)	25(1)	14(1)	3(1)	-9(1)
C(33)	17(1)	34(1)	20(1)	5(1)	2(1)	-5(1)
C(34)	21(1)	15(1)	17(1)	-1(1)	9(1)	0(1)
C(35)	20(1)	23(1)	16(1)	-3(1)	6(1)	2(1)
C(36)	30(1)	23(1)	18(1)	1(1)	7(1)	3(1)
C(37)	44(1)	29(1)	21(1)	3(1)	19(1)	6(1)
C(38)	40(1)	37(1)	33(1)	7(1)	24(1)	15(1)
C(39)	30(1)	26(1)	25(1)	8(1)	14(1)	12(1)
C(40)	14(1)	21(1)	15(1)	-3(1)	5(1)	3(1)
C(41)	18(1)	21(1)	18(1)	-1(1)	6(1)	1(1)
C(42)	22(1)	28(1)	18(1)	-1(1)	6(1)	6(1)
C(43)	15(1)	37(1)	23(1)	-8(1)	2(1)	6(1)
C(44)	17(1)	29(1)	33(1)	-11(1)	10(1)	-5(1)
C(45)	18(1)	20(1)	29(1)	-1(1)	9(1)	1(1)
C(46)	14(1)	13(1)	17(1)	0(1)	2(1)	3(1)
C(47)	15(1)	16(1)	19(1)	-1(1)	5(1)	4(1)
C(48)	18(1)	17(1)	26(1)	4(1)	7(1)	2(1)
C(49)	23(1)	12(1)	30(1)	0(1)	1(1)	1(1)
C(50)	25(1)	18(1)	20(1)	-4(1)	0(1)	4(1)
C(51)	22(1)	18(1)	15(1)	1(1)	2(1)	4(1)

Table 65 Hydrogen coordinates (x 10^4) and isotropic displacement parameters ($Å^2$x 10^{3})for **4.2**.

	x	y	z	U(eq)
H(2A)	300	3745	801	19
H(4A)	398	2689	2921	21
H(5A)	713	4267	3390	20
H(7A)	105	1523	1900	30
H(7B)	214	1595	1163	30
H(7C)	-85	2285	1202	30
H(10A)	219	9653	445	23
H(11A)	-187	9296	933	25
H(13A)	101	6013	1354	18
H(14A)	-462	8074	1519	36
H(14B)	-262	7070	2021	36

H(14C)	-485	6792	1198	36
H(15A)	337	4989	-121	25
H(15B)	664	4352	109	25
H(15C)	623	5566	-312	25
H(17A)	1686	6681	3420	23
H(18A)	2144	6341	4379	27
H(19A)	2588	7370	4436	27
H(20A)	2574	8809	3559	30
H(21A)	2113	9216	2623	27
H(23A)	962	9689	1681	23
H(24A)	634	10673	2214	27
H(25A)	736	10719	3514	26
H(26A)	1173	9802	4282	26
H(27A)	1505	8809	3756	23
H(29A)	1642	10722	2331	29
H(30A)	1812	12064	1607	40
H(31A)	1871	11518	454	42
H(32A)	1762	9642	23	41
H(33A)	1590	8303	739	29
H(35A)	1131	7036	-247	24
H(36A)	1207	7441	-1399	28
H(37A)	1631	6694	-1688	35
H(38A)	1986	5556	-816	40
H(39A)	1918	5163	350	31
H(41A)	1740	4036	2196	23
H(42A)	2224	3867	3086	28
H(43A)	2607	5237	3139	31
H(44A)	2505	6755	2289	31
H(45A)	2019	6955	1412	27
H(47A)	1213	4035	1901	20
H(48A)	994	2207	1668	24
H(49A)	928	1318	507	28
H(50A)	1098	2246	-403	27
H(51A)	1331	4049	-166	23

X-ray Data Collection, Structure Solution and Refinement for complex 4.18

A yellow crystal of approximate dimensions 0.073 x 0.167 x 0.168 mm was mounted on a glass fiber and transferred to a Bruker SMART APEX II diffractometer. The APEX2[1] program package was used to determine the unit-cell parameters and for data collection (60 sec/frame scan time for a sphere of diffraction data). The raw frame data was processed using SAINT[2] and SADABS[3] to yield the reflection data file. Subsequent calculations were carried out using the SHELXTL[4] program. The diffraction symmetry was 2/*m* and the systematic absences were consistent with the monoclinic space group $P2_1/c$ that was later determined to be correct.

The structure was solved by direct methods and refined on F^2 by full-matrix least-squares techniques. The analytical scattering factors[5] for neutral atoms were used throughout the analysis. Hydrogen atoms were located from a difference-Fourier map and refined (x,y,z and U_{iso}).

At convergence, wR2 = 0.0697 and Goof = 0.98 for 419 variables refined against 6016 data (0.75Å), R1 = 0.0288 for those 4997 data with I > 2.0σ(I).

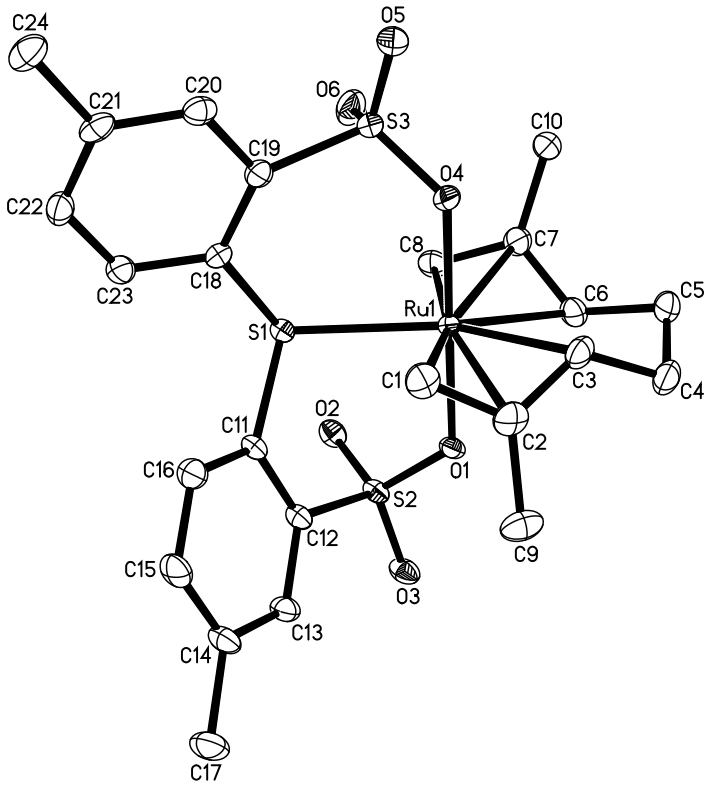

Table 66 Crystal data and structure refinement for **4.18**

Identification code	zg77 (Tobias Friedberger)	
Empirical formula	C_{24} H_{28} O_6 Ru S_3	
Formula weight	609.71	
Temperature	88(2) K	
Wavelength	0.71073 Å	
Crystal system	Monoclinic	
Space group	$P2_1/c$	
Unit cell dimensions	a = 8.2195(14) Å	α= 90°.
	b = 18.517(3) Å	β= 92.489(2)°.
	c = 16.114(3) Å	γ = 90°.
Volume	2450.3(7) Å^3	
Z	4	
Density (calculated)	1.653 Mg/m^3	
Absorption coefficient	0.934 mm^{-1}	
F(000)	1248	
Crystal color	yellow	
Crystal size	0.168 x 0.167 x 0.073 mm^3	
Theta range for data collection	1.676 to 28.346°	
Index ranges	$-10 \le h \le 10$, $-24 \le k \le 24$, $-21 \le l \le 21$	
Reflections collected	29640	
Independent reflections	6016 [R(int) = 0.0487]	

Completeness to theta = 25.500°	100.0 %
Absorption correction	Numerical
Max. and min. transmission	0.9570 and 0.8569
Refinement method	Full-matrix least-squares on F^2
Data / restraints / parameters	6016 / 0 / 419
Goodness-of-fit on F^2	0.982
Final R indices [I>2sigma(I) = 4997 data]	R1 = 0.0288, wR2 = 0.0667
R indices (all data, 0.75Å)	R1 = 0.0385, wR2 = 0.0697
Largest diff. peak and hole	1.067 and -0.696 e.Å^{-3}

Table 67. Atomic coordinates (x 10^4) and equivalent isotropic displacement parameters (Å^{2}x 10^3) for **4.18**. U(eq) is defined as one third of the trace of the orthogonalized U^{ij} tensor.

	x	y	z	U(eq)
Ru(1)	6377(1)	5532(1)	7192(1)	12(1)
S(1)	5185(1)	4926(1)	8376(1)	14(1)
S(2)	7211(1)	6312(1)	8953(1)	15(1)
S(3)	5013(1)	3999(1)	6551(1)	21(1)
O(1)	7276(2)	6330(1)	8026(1)	15(1)
O(2)	7936(2)	5663(1)	9304(1)	18(1)
O(3)	7827(2)	6983(1)	9290(1)	20(1)
O(4)	5424(2)	4765(1)	6350(1)	20(1)
O(5)	4376(2)	3653(1)	5811(1)	33(1)
O(6)	6337(2)	3636(1)	6992(1)	29(1)
C(1)	3798(3)	5953(1)	6951(2)	23(1)
C(2)	4850(3)	6485(1)	6683(1)	22(1)
C(3)	5987(3)	6275(1)	6100(1)	21(1)
C(4)	7413(3)	6723(1)	5837(2)	24(1)
C(5)	8811(3)	6189(1)	5820(2)	26(1)
C(6)	8817(3)	5826(1)	6657(2)	21(1)
C(7)	8822(3)	5082(1)	6810(2)	21(1)
C(8)	8538(3)	4872(1)	7622(2)	21(1)
C(9)	4890(4)	7218(1)	7097(2)	28(1)
C(10)	8954(3)	4546(1)	6104(2)	25(1)
C(11)	4148(3)	5664(1)	8876(1)	16(1)
C(12)	5105(3)	6264(1)	9132(1)	16(1)
C(13)	4381(3)	6866(1)	9478(1)	18(1)
C(14)	2722(3)	6892(1)	9595(1)	21(1)
C(15)	1798(3)	6294(1)	9356(2)	24(1)
C(16)	2489(3)	5694(1)	8993(1)	20(1)
C(17)	1955(3)	7550(2)	9963(2)	28(1)
C(18)	3587(3)	4305(1)	8076(1)	15(1)
C(19)	3427(3)	3988(1)	7280(1)	17(1)
C(20)	2180(3)	3497(1)	7113(1)	19(1)
C(21)	1099(3)	3287(1)	7716(2)	19(1)
C(22)	1351(3)	3568(1)	8509(2)	21(1)
C(23)	2579(3)	4067(1)	8693(1)	19(1)
C(24)	-224(3)	2747(1)	7509(2)	25(1)

Table 68 Bond lengths [Å] and angles [°] for **4.18**.

Ru(1)-O(4)	2.0924(15)
Ru(1)-O(1)	2.1088(14)

Ru(1)-C(8)	2.241(2)
Ru(1)-C(3)	2.246(2)
Ru(1)-C(1)	2.276(2)
Ru(1)-C(6)	2.283(2)
Ru(1)-C(7)	2.285(2)
Ru(1)-C(2)	2.297(2)
Ru(1)-S(1)	2.4545(6)
S(1)-C(18)	1.795(2)
S(1)-C(11)	1.817(2)
S(2)-O(3)	1.4397(16)
S(2)-O(2)	1.4458(15)
S(2)-O(1)	1.4987(15)
S(2)-C(12)	1.769(2)
S(3)-O(5)	1.4327(17)
S(3)-O(6)	1.4395(19)
S(3)-O(4)	1.4969(16)
S(3)-C(19)	1.792(2)
C(1)-C(2)	1.391(3)
C(2)-C(3)	1.410(3)
C(2)-C(9)	1.511(3)
C(3)-C(4)	1.511(3)
C(4)-C(5)	1.517(4)
C(5)-C(6)	1.507(3)
C(6)-C(7)	1.400(3)
C(7)-C(8)	1.395(3)
C(7)-C(10)	1.517(3)
C(11)-C(16)	1.386(3)
C(11)-C(12)	1.413(3)
C(12)-C(13)	1.392(3)
C(13)-C(14)	1.385(3)
C(14)-C(15)	1.387(3)
C(14)-C(17)	1.507(3)
C(15)-C(16)	1.388(3)
C(18)-C(23)	1.393(3)
C(18)-C(19)	1.412(3)
C(19)-C(20)	1.388(3)
C(20)-C(21)	1.399(3)
C(21)-C(22)	1.387(3)
C(21)-C(24)	1.504(3)
C(22)-C(23)	1.390(3)

O(4)-Ru(1)-O(1)	178.06(6)
O(4)-Ru(1)-C(8)	95.73(8)
O(1)-Ru(1)-C(8)	86.20(8)
O(4)-Ru(1)-C(3)	82.60(8)
O(1)-Ru(1)-C(3)	96.00(7)
C(8)-Ru(1)-C(3)	131.37(9)
O(4)-Ru(1)-C(1)	78.60(8)
O(1)-Ru(1)-C(1)	99.58(8)
C(8)-Ru(1)-C(1)	163.61(9)
C(3)-Ru(1)-C(1)	63.66(9)
O(4)-Ru(1)-C(6)	103.18(7)
O(1)-Ru(1)-C(6)	77.53(7)
C(8)-Ru(1)-C(6)	63.23(9)
C(3)-Ru(1)-C(6)	69.87(9)

C(1)-Ru(1)-C(6)	132.90(9)
O(4)-Ru(1)-C(7)	83.50(7)
O(1)-Ru(1)-C(7)	98.02(7)
C(8)-Ru(1)-C(7)	35.90(8)
C(3)-Ru(1)-C(7)	96.29(9)
C(1)-Ru(1)-C(7)	154.50(9)
C(6)-Ru(1)-C(7)	35.71(8)
O(4)-Ru(1)-C(2)	96.14(7)
O(1)-Ru(1)-C(2)	81.95(7)
C(8)-Ru(1)-C(2)	160.61(9)
C(3)-Ru(1)-C(2)	36.14(8)
C(1)-Ru(1)-C(2)	35.42(8)
C(6)-Ru(1)-C(2)	99.06(9)
C(7)-Ru(1)-C(2)	131.14(8)
O(4)-Ru(1)-S(1)	92.43(4)
O(1)-Ru(1)-S(1)	88.03(4)
C(8)-Ru(1)-S(1)	81.25(6)
C(3)-Ru(1)-S(1)	147.26(7)
C(1)-Ru(1)-S(1)	83.62(6)
C(6)-Ru(1)-S(1)	142.15(6)
C(7)-Ru(1)-S(1)	115.36(6)
C(2)-Ru(1)-S(1)	113.47(6)
C(18)-S(1)-C(11)	104.43(10)
C(18)-S(1)-Ru(1)	113.31(7)
C(11)-S(1)-Ru(1)	102.20(7)
O(3)-S(2)-O(2)	115.96(10)
O(3)-S(2)-O(1)	109.27(9)
O(2)-S(2)-O(1)	112.08(9)
O(3)-S(2)-C(12)	108.21(9)
O(2)-S(2)-C(12)	106.56(10)
O(1)-S(2)-C(12)	103.96(9)
O(5)-S(3)-O(6)	116.30(11)
O(5)-S(3)-O(4)	108.73(10)
O(6)-S(3)-O(4)	112.10(10)
O(5)-S(3)-C(19)	106.88(11)
O(6)-S(3)-C(19)	103.16(10)
O(4)-S(3)-C(19)	109.25(9)
S(2)-O(1)-Ru(1)	126.40(9)
S(3)-O(4)-Ru(1)	125.78(9)
C(2)-C(1)-Ru(1)	73.09(14)
C(1)-C(2)-C(3)	116.7(2)
C(1)-C(2)-C(9)	120.0(2)
C(3)-C(2)-C(9)	122.7(2)
C(1)-C(2)-Ru(1)	71.49(13)
C(3)-C(2)-Ru(1)	69.96(13)
C(9)-C(2)-Ru(1)	122.09(17)
C(2)-C(3)-C(4)	125.4(2)
C(2)-C(3)-Ru(1)	73.90(13)
C(4)-C(3)-Ru(1)	118.03(16)
C(3)-C(4)-C(5)	104.15(19)
C(6)-C(5)-C(4)	104.3(2)
C(7)-C(6)-C(5)	126.6(2)
C(7)-C(6)-Ru(1)	72.22(13)
C(5)-C(6)-Ru(1)	118.38(17)
C(8)-C(7)-C(6)	116.1(2)

C(8)-C(7)-C(10)	122.8(2)
C(6)-C(7)-C(10)	120.8(2)
C(8)-C(7)-Ru(1)	70.35(13)
C(6)-C(7)-Ru(1)	72.08(13)
C(10)-C(7)-Ru(1)	122.23(17)
C(7)-C(8)-Ru(1)	73.75(14)
C(16)-C(11)-C(12)	117.84(19)
C(16)-C(11)-S(1)	125.00(17)
C(12)-C(11)-S(1)	117.10(16)
C(13)-C(12)-C(11)	120.3(2)
C(13)-C(12)-S(2)	117.64(17)
C(11)-C(12)-S(2)	121.85(16)
C(14)-C(13)-C(12)	121.5(2)
C(13)-C(14)-C(15)	117.7(2)
C(13)-C(14)-C(17)	120.8(2)
C(15)-C(14)-C(17)	121.5(2)
C(14)-C(15)-C(16)	121.8(2)
C(11)-C(16)-C(15)	120.8(2)
C(23)-C(18)-C(19)	118.8(2)
C(23)-C(18)-S(1)	117.52(17)
C(19)-C(18)-S(1)	123.29(17)
C(20)-C(19)-C(18)	119.2(2)
C(20)-C(19)-S(3)	115.63(17)
C(18)-C(19)-S(3)	123.29(17)
C(19)-C(20)-C(21)	122.2(2)
C(22)-C(21)-C(20)	117.5(2)
C(22)-C(21)-C(24)	122.0(2)
C(20)-C(21)-C(24)	120.4(2)
C(21)-C(22)-C(23)	121.5(2)
C(22)-C(23)-C(18)	120.5(2)

Table 69 Anisotropic displacement parameters ($Å^2 x\ 10^3$) for **4.18**. The anisotropic displacement factor exponent takes the form: $-2\pi^2[\ h^2\ a^{*2}U^{11} + ...\ + 2\ h\ k\ a^*\ b^*\ U^{12}\ ]$

	U^{11}	U^{22}	U^{33}	U^{23}	U^{13}	U^{12}
Ru(1)	17(1)	10(1)	11(1)	0(1)	2(1)	0(1)
S(1)	16(1)	14(1)	13(1)	-1(1)	3(1)	1(1)
S(2)	12(1)	19(1)	14(1)	-4(1)	2(1)	1(1)
S(3)	32(1)	14(1)	18(1)	-3(1)	9(1)	-5(1)
O(1)	16(1)	14(1)	14(1)	-4(1)	3(1)	1(1)
O(2)	15(1)	22(1)	16(1)	0(1)	1(1)	3(1)
O(3)	17(1)	24(1)	20(1)	-9(1)	2(1)	-3(1)
O(4)	31(1)	13(1)	14(1)	-1(1)	3(1)	-5(1)
O(5)	53(1)	26(1)	21(1)	-9(1)	12(1)	-18(1)
O(6)	31(1)	18(1)	40(1)	7(1)	16(1)	5(1)
C(1)	22(1)	23(1)	23(1)	3(1)	-1(1)	4(1)
C(2)	26(1)	20(1)	21(1)	5(1)	-6(1)	6(1)
C(3)	28(1)	16(1)	19(1)	5(1)	-2(1)	-2(1)
C(4)	33(2)	19(1)	21(1)	5(1)	0(1)	-6(1)
C(5)	33(2)	22(1)	23(1)	-1(1)	9(1)	-10(1)
C(6)	19(1)	23(1)	22(1)	-2(1)	7(1)	-2(1)
C(7)	18(1)	19(1)	27(1)	-1(1)	7(1)	0(1)
C(8)	21(1)	19(1)	24(1)	0(1)	5(1)	7(1)

C(9)	32(2)	18(1)	33(2)	-1(1)	-6(1)	6(1)
C(10)	30(1)	19(1)	27(1)	-2(1)	13(1)	-1(1)
C(11)	16(1)	16(1)	14(1)	-2(1)	5(1)	2(1)
C(12)	15(1)	18(1)	15(1)	-2(1)	3(1)	2(1)
C(13)	19(1)	18(1)	19(1)	-6(1)	3(1)	-1(1)
C(14)	19(1)	23(1)	21(1)	-6(1)	6(1)	4(1)
C(15)	14(1)	28(1)	29(1)	-4(1)	8(1)	1(1)
C(16)	15(1)	21(1)	23(1)	-4(1)	2(1)	-4(1)
C(17)	24(2)	24(1)	37(2)	-9(1)	8(1)	4(1)
C(18)	18(1)	11(1)	17(1)	0(1)	2(1)	-1(1)
C(19)	22(1)	13(1)	16(1)	2(1)	2(1)	2(1)
C(20)	24(1)	15(1)	18(1)	0(1)	-2(1)	2(1)
C(21)	17(1)	12(1)	29(1)	1(1)	-2(1)	1(1)
C(22)	21(1)	18(1)	24(1)	5(1)	6(1)	1(1)
C(23)	25(1)	17(1)	16(1)	0(1)	2(1)	0(1)
C(24)	19(1)	19(1)	37(2)	-1(1)	0(1)	-3(1)

Table 70 Hydrogen coordinates (x 10^4) and isotropic displacement parameters ($Å^2$x 10^{3})for **4.18**.

	x	y	z	U(eq)
H(1A)	3480(30)	5553(12)	6576(16)	22(7)
H(1B)	3160(30)	6057(14)	7446(17)	32(7)
H(3A)	5630(30)	5884(14)	5712(15)	23(6)
H(4A)	7730(30)	7140(12)	6260(14)	19(6)
H(4B)	7090(30)	6931(14)	5321(17)	35(8)
H(5A)	8670(30)	5845(13)	5358(15)	17(6)
H(5B)	9890(30)	6419(15)	5749(16)	35(8)
H(6A)	9180(30)	6149(13)	7109(16)	22(7)
H(8A)	8980(30)	5184(13)	8103(15)	19(6)
H(8B)	8180(30)	4377(13)	7693(15)	22(7)
H(9A)	5990(40)	7368(17)	7260(19)	49(9)
H(9B)	4220(30)	7241(14)	7612(17)	36(8)
H(9C)	4540(40)	7583(18)	6720(20)	57(10)
H(10A)	8750(30)	4063(16)	6286(17)	38(8)
H(10B)	10100(40)	4572(15)	5928(18)	40(8)
H(10C)	8240(30)	4647(13)	5600(15)	18(6)
H(13A)	4990(30)	7235(13)	9607(15)	23(7)
H(15A)	710(30)	6276(13)	9447(15)	24(7)
H(16A)	1820(30)	5325(14)	8820(15)	22(7)
H(17A)	2360(40)	7947(18)	9770(20)	60(11)
H(17B)	2100(30)	7503(15)	10579(19)	37(8)
H(17C)	860(40)	7567(15)	9833(17)	36(8)
H(20A)	2170(30)	3289(13)	6612(15)	20(6)
H(22A)	680(30)	3406(12)	8928(14)	11(6)
H(23A)	2640(30)	4258(12)	9250(15)	17(6)
H(24A)	-550(30)	2500(15)	7992(17)	32(7)
H(24B)	40(30)	2416(17)	7080(18)	44(9)
H(24C)	-1130(40)	2975(16)	7300(18)	42(8)

Table 71 Torsion angles [°] for **4.18.**

O(3)-S(2)-O(1)-Ru(1)	-175.17(10)
O(2)-S(2)-O(1)-Ru(1)	54.86(13)
C(12)-S(2)-O(1)-Ru(1)	-59.83(12)
O(5)-S(3)-O(4)-Ru(1)	179.36(11)
O(6)-S(3)-O(4)-Ru(1)	-50.66(14)
C(19)-S(3)-O(4)-Ru(1)	63.05(14)
Ru(1)-C(1)-C(2)-C(3)	55.01(19)
Ru(1)-C(1)-C(2)-C(9)	-117.0(2)
C(1)-C(2)-C(3)-C(4)	-169.0(2)
C(9)-C(2)-C(3)-C(4)	2.7(4)
Ru(1)-C(2)-C(3)-C(4)	-113.3(2)
C(1)-C(2)-C(3)-Ru(1)	-55.79(19)
C(9)-C(2)-C(3)-Ru(1)	116.0(2)
C(2)-C(3)-C(4)-C(5)	136.8(2)
Ru(1)-C(3)-C(4)-C(5)	47.1(2)
C(3)-C(4)-C(5)-C(6)	-51.6(2)
C(4)-C(5)-C(6)-C(7)	128.8(2)
C(4)-C(5)-C(6)-Ru(1)	40.6(2)
C(5)-C(6)-C(7)-C(8)	-169.1(2)
Ru(1)-C(6)-C(7)-C(8)	-56.51(19)
C(5)-C(6)-C(7)-C(10)	4.8(4)
Ru(1)-C(6)-C(7)-C(10)	117.4(2)
C(5)-C(6)-C(7)-Ru(1)	-112.6(2)
C(6)-C(7)-C(8)-Ru(1)	57.42(19)
C(10)-C(7)-C(8)-Ru(1)	-116.3(2)
C(18)-S(1)-C(11)-C(16)	1.3(2)
Ru(1)-S(1)-C(11)-C(16)	119.56(19)
C(18)-S(1)-C(11)-C(12)	-175.98(17)
Ru(1)-S(1)-C(11)-C(12)	-57.71(17)
C(16)-C(11)-C(12)-C(13)	-1.0(3)
S(1)-C(11)-C(12)-C(13)	176.47(17)
C(16)-C(11)-C(12)-S(2)	-175.86(17)
S(1)-C(11)-C(12)-S(2)	1.6(3)
O(3)-S(2)-C(12)-C(13)	5.4(2)
O(2)-S(2)-C(12)-C(13)	130.71(18)
O(1)-S(2)-C(12)-C(13)	-110.73(18)
O(3)-S(2)-C(12)-C(11)	-179.65(17)
O(2)-S(2)-C(12)-C(11)	-54.3(2)
O(1)-S(2)-C(12)-C(11)	64.26(19)
C(11)-C(12)-C(13)-C(14)	1.2(3)
S(2)-C(12)-C(13)-C(14)	176.26(18)
C(12)-C(13)-C(14)-C(15)	0.0(4)
C(12)-C(13)-C(14)-C(17)	-179.5(2)
C(13)-C(14)-C(15)-C(16)	-1.5(4)
C(17)-C(14)-C(15)-C(16)	178.1(2)
C(12)-C(11)-C(16)-C(15)	-0.4(3)
S(1)-C(11)-C(16)-C(15)	-177.64(19)
C(14)-C(15)-C(16)-C(11)	1.7(4)
C(11)-S(1)-C(18)-C(23)	-54.61(19)
Ru(1)-S(1)-C(18)-C(23)	-165.01(15)
C(11)-S(1)-C(18)-C(19)	132.98(19)
Ru(1)-S(1)-C(18)-C(19)	22.6(2)
C(23)-C(18)-C(19)-C(20)	5.7(3)

S(1)-C(18)-C(19)-C(20)	178.05(16)
C(23)-C(18)-C(19)-S(3)	-157.88(17)
S(1)-C(18)-C(19)-S(3)	14.4(3)
O(5)-S(3)-C(19)-C(20)	18.1(2)
O(6)-S(3)-C(19)-C(20)	-105.01(18)
O(4)-S(3)-C(19)-C(20)	135.59(17)
O(5)-S(3)-C(19)-C(18)	-177.74(18)
O(6)-S(3)-C(19)-C(18)	59.1(2)
O(4)-S(3)-C(19)-C(18)	-60.3(2)
C(18)-C(19)-C(20)-C(21)	-2.0(3)
S(3)-C(19)-C(20)-C(21)	162.87(17)
C(19)-C(20)-C(21)-C(22)	-2.5(3)
C(19)-C(20)-C(21)-C(24)	-179.3(2)
C(20)-C(21)-C(22)-C(23)	3.2(3)
C(24)-C(21)-C(22)-C(23)	180.0(2)
C(21)-C(22)-C(23)-C(18)	0.6(3)
C(19)-C(18)-C(23)-C(22)	-5.1(3)
S(1)-C(18)-C(23)-C(22)	-177.88(18)

X-ray Data Collection, Structure Solution and Refinement for complex 5.6.

A colorless crystal of approximate dimensions 0.056 x 0.288 x 0.477 mm was mounted on a glass fiber and transferred to a Bruker SMART APEX II diffractometer. The APEX2[1] program package and the CELL_NOW[2] program were used to determine the unit-cell parameters. Data was collected using a 45 sec/frame scan time for a sphere of diffraction data. The raw frame data was processed using SAINT[3] and TWINABS[4] to yield the reflection data file (HKLF 4/5 format)[4]. Subsequent calculations were carried out using the SHELXTL[5] program. The diffraction symmetry was 2/*m* and the systematic absences were consistent with the monoclinic space group $P2_1/c$ that was later determined to be correct.

The structure was solved by direct methods and refined on F^2 by full-matrix least-squares techniques. The analytical scattering factors[6] for neutral atoms were used throughout the analysis. Hydrogen atoms were located from a difference-Fourier map and refined (x,y,z and U_{iso}).

At convergence, wR2 = 0.1019 and Goof = 1.025 for 246 variables refined against 3214 data (0.75Å), R1 = 0.0384 for those 2501 with $I > 2.0\sigma(I)$. The structure was refined as a two-component twin, BASF[5] = 0.43.

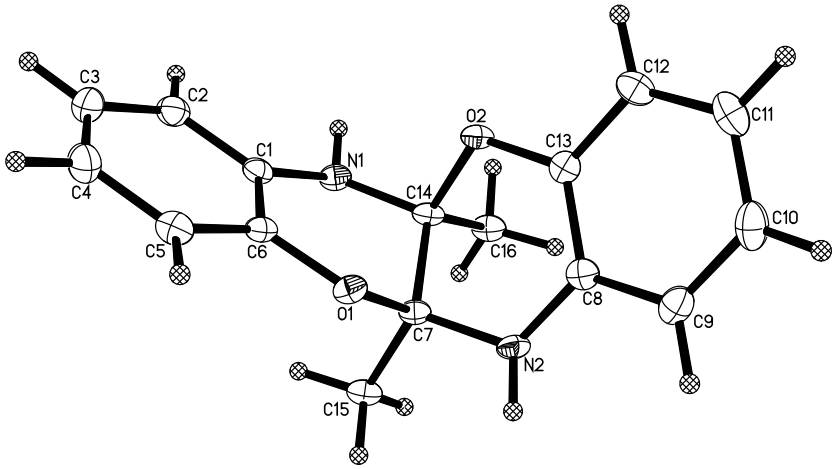

Table 72 Crystal data and structure refinement for **5.6**.

Identification code	zg83 (Tobias Friedberger)	
Empirical formula	$C_{16}\ H_{16}\ N_2\ O_2$	
Formula weight	268.31	
Temperature	133(2) K	
Wavelength	0.71073 Å	
Crystal system	Monoclinic	
Space group	$P2_1/c$	
Unit cell dimensions	a = 10.9889(9) Å	α= 90°.
	b = 11.1558(9) Å	β= 105.5621(11)°.
	c = 11.4943(9) Å	γ = 90°.
Volume	1357.43(19) $Å^3$	
Z	4	
Density (calculated)	1.313 Mg/m^3	
Absorption coefficient	0.088 mm^{-1}	
F(000)	568	
Crystal color	colorless	
Crystal size	0.477 x 0.288 x 0.056 mm^3	
Theta range for data collection	1.924 to 28.274°	
Index ranges	$-14 \le h \le 13,\ 0 \le k \le 14,\ 0 \le l \le 15$	
Reflections collected	3214	
Independent reflections	3214 [R(int) = ?]	
Completeness to theta = 25.500°	100.0 %	
Absorption correction	Semi-empirical from equivalents	
Max. and min. transmission	0.8621 and 0.7926	
Refinement method	Full-matrix least-squares on F^2	
Data / restraints / parameters	3214 / 0 / 246	
Goodness-of-fit on F^2	1.025	
Final R indices [I>2sigma(I) = 2501 data]	R1 = 0.0384, wR2 = 0.0925	
R indices (all data, 0.75Å)	R1 = 0.0541, wR2 = 0.1019	
Largest diff. peak and hole	0.334 and -0.289 $e.Å^{-3}$	

Table 73 Atomic coordinates (x 10^4) and equivalent isotropic displacement parameters ($Å^2$x 10^3) for **5.6**. U(eq) is defined as one third of the trace of the orthogonalized U^{ij} tensor.

	x	y	z	U(eq)
O(2)	798(1)	3516(1)	724(1)	15(1)
O(1)	-756(1)	1487(1)	333(1)	15(1)
N(1)	-1099(1)	3751(1)	-762(1)	16(1)
N(2)	1129(1)	1249(1)	-198(1)	16(1)
C(1)	-1965(1)	3318(1)	-169(2)	15(1)
C(2)	-3011(1)	3989(1)	-84(2)	20(1)
C(3)	-3867(2)	3524(2)	489(2)	24(1)
C(4)	-3701(2)	2379(2)	979(3)	25(1)
C(5)	-2666(2)	1702(1)	900(2)	20(1)
C(6)	-1806(1)	2167(2)	336(2)	15(1)
C(7)	-77(2)	1812(1)	-564(1)	14(1)
C(8)	2002(1)	1680(1)	840(2)	16(1)
C(9)	3042(1)	1002(1)	1459(2)	20(1)
C(10)	3899(2)	1462(2)	2473(2)	24(1)
C(11)	3748(2)	2613(2)	2878(3)	24(1)
C(12)	2718(2)	3297(1)	2264(2)	20(1)
C(13)	1850(1)	2832(2)	1259(2)	15(1)
C(14)	103(2)	3190(1)	-523(1)	14(1)
C(15)	-813(2)	1347(1)	-1788(1)	18(1)
C(16)	834(2)	3649(1)	-1377(2)	18(1)

Table 74 Bond lengths [Å] and angles [°] for **5.6**.

O(2)-C(13)	1.3842(19)
O(2)-C(14)	1.4769(17)
O(1)-C(6)	1.3810(19)
O(1)-C(7)	1.4718(17)
N(1)-C(1)	1.397(2)
N(1)-C(14)	1.420(2)
N(2)-C(8)	1.399(2)
N(2)-C(7)	1.424(2)
C(1)-C(2)	1.397(2)
C(1)-C(6)	1.401(2)
C(2)-C(3)	1.385(2)
C(3)-C(4)	1.388(3)
C(4)-C(5)	1.388(3)
C(5)-C(6)	1.383(2)
C(7)-C(15)	1.513(2)
C(7)-C(14)	1.5496(15)
C(8)-C(9)	1.396(2)
C(8)-C(13)	1.398(2)
C(9)-C(10)	1.385(2)
C(10)-C(11)	1.390(3)
C(11)-C(12)	1.390(3)
C(12)-C(13)	1.386(2)
C(14)-C(16)	1.514(2)
C(13)-O(2)-C(14)	116.66(12)

C(6)-O(1)-C(7)	116.57(12)
C(1)-N(1)-C(14)	118.24(13)
C(8)-N(2)-C(7)	118.12(13)
C(2)-C(1)-N(1)	122.04(15)
C(2)-C(1)-C(6)	118.38(15)
N(1)-C(1)-C(6)	119.56(13)
C(3)-C(2)-C(1)	120.62(16)
C(2)-C(3)-C(4)	120.35(18)
C(3)-C(4)-C(5)	119.7(2)
C(6)-C(5)-C(4)	120.08(18)
O(1)-C(6)-C(5)	118.09(15)
O(1)-C(6)-C(1)	120.95(14)
C(5)-C(6)-C(1)	120.89(15)
N(2)-C(7)-O(1)	106.92(11)
N(2)-C(7)-C(15)	110.32(12)
O(1)-C(7)-C(15)	108.78(13)
N(2)-C(7)-C(14)	109.09(11)
O(1)-C(7)-C(14)	107.87(10)
C(15)-C(7)-C(14)	113.61(11)
C(9)-C(8)-C(13)	118.62(15)
C(9)-C(8)-N(2)	121.92(15)
C(13)-C(8)-N(2)	119.44(14)
C(10)-C(9)-C(8)	120.48(16)
C(9)-C(10)-C(11)	120.55(18)
C(12)-C(11)-C(10)	119.4(2)
C(13)-C(12)-C(11)	120.13(18)
O(2)-C(13)-C(12)	118.05(16)
O(2)-C(13)-C(8)	121.04(14)
C(12)-C(13)-C(8)	120.81(15)
N(1)-C(14)-O(2)	106.94(11)
N(1)-C(14)-C(16)	110.68(12)
O(2)-C(14)-C(16)	108.62(13)
N(1)-C(14)-C(7)	109.10(11)
O(2)-C(14)-C(7)	107.59(10)
C(16)-C(14)-C(7)	113.65(12)

Table 75 Anisotropic displacement parameters ($Å^2 x\ 10^3$) for **5.6**. The anisotropic displacement factor exponent takes the form: $-2\pi^2[\ h^2\ a^{*2}U^{11} + ...\ + 2\ h\ k\ a^*\ b^*\ U^{12}\ ]$

	U^{11}	U^{22}	U^{33}	U^{23}	U^{13}	U^{12}
O(2)	20(1)	11(1)	12(1)	-2(1)	3(1)	1(1)
O(1)	20(1)	12(1)	15(1)	2(1)	7(1)	1(1)
N(1)	20(1)	10(1)	17(1)	2(1)	5(1)	1(1)
N(2)	20(1)	10(1)	18(1)	-1(1)	5(1)	2(1)
C(1)	16(1)	14(1)	13(1)	-2(1)	1(1)	-1(1)
C(2)	20(1)	17(1)	22(1)	-2(1)	2(1)	1(1)
C(3)	18(1)	27(1)	27(1)	-6(1)	5(1)	2(1)
C(4)	21(1)	29(1)	28(1)	-3(1)	10(1)	-6(1)
C(5)	23(1)	18(1)	18(1)	-1(1)	5(1)	-3(1)
C(6)	18(1)	13(1)	13(1)	-2(1)	3(1)	0(1)
C(7)	19(1)	10(1)	12(1)	1(1)	5(1)	0(1)
C(8)	18(1)	14(1)	16(1)	2(1)	7(1)	-2(1)

C(9)	20(1)	17(1)	26(1)	4(1)	10(1)	2(1)
C(10)	17(1)	27(1)	27(1)	10(1)	3(1)	1(1)
C(11)	21(1)	29(1)	19(1)	3(1)	1(1)	-6(1)
C(12)	24(1)	18(1)	18(1)	0(1)	4(1)	-5(1)
C(13)	17(1)	14(1)	15(1)	4(1)	6(1)	-1(1)
C(14)	20(1)	11(1)	10(1)	-1(1)	2(1)	0(1)
C(15)	24(1)	14(1)	14(1)	-2(1)	5(1)	-2(1)
C(16)	25(1)	13(1)	16(1)	1(1)	9(1)	-2(1)

Table 76 Hydrogen coordinates (x 10^4) and isotropic displacement parameters ($Å^2$x 10^3)for **5.6.**.

	x	y	z	U(eq)
H(1A)	-1081(17)	4559(19)	-850(17)	28(5)
H(2A)	1095(17)	460(18)	-290(16)	23(5)
H(2)	-3091(16)	4804(18)	-424(17)	27(5)
H(3)	-4588(18)	4011(17)	543(18)	27(5)
H(4)	-4323(18)	2046(19)	1362(19)	29(5)
H(5)	-2496(17)	901(17)	1256(17)	24(5)
H(9)	3142(16)	199(17)	1173(16)	26(5)
H(10)	4590(20)	960(18)	2880(19)	32(5)
H(11)	4344(18)	2900(20)	3610(20)	32(5)
H(12)	2576(17)	4100(18)	2542(17)	26(5)
H(15A)	-1673(18)	1687(17)	-2018(18)	25(5)
H(15B)	-868(16)	461(17)	-1720(16)	22(4)
H(15C)	-367(16)	1527(16)	-2397(16)	25(5)
H(16A)	391(15)	3452(15)	-2204(16)	19(5)
H(16B)	915(17)	4537(18)	-1294(17)	24(5)
H(16C)	1704(17)	3312(16)	-1144(17)	21(5)

Table 77 Torsion angles [°] for **5.6**.

C(14)-N(1)-C(1)-C(2)	162.31(13)
C(14)-N(1)-C(1)-C(6)	-19.1(2)
N(1)-C(1)-C(2)-C(3)	178.70(15)
C(6)-C(1)-C(2)-C(3)	0.1(2)
C(1)-C(2)-C(3)-C(4)	-0.5(3)
C(2)-C(3)-C(4)-C(5)	0.5(4)
C(3)-C(4)-C(5)-C(6)	0.0(4)
C(7)-O(1)-C(6)-C(5)	161.79(14)
C(7)-O(1)-C(6)-C(1)	-21.1(2)
C(4)-C(5)-C(6)-O(1)	176.71(19)
C(4)-C(5)-C(6)-C(1)	-0.4(3)
C(2)-C(1)-C(6)-O(1)	-176.66(14)
N(1)-C(1)-C(6)-O(1)	4.7(2)
C(2)-C(1)-C(6)-C(5)	0.4(2)
N(1)-C(1)-C(6)-C(5)	-178.28(14)
C(8)-N(2)-C(7)-O(1)	-69.88(16)
C(8)-N(2)-C(7)-C(15)	171.99(13)
C(8)-N(2)-C(7)-C(14)	46.53(17)
C(6)-O(1)-C(7)-N(2)	164.01(12)

C(6)-O(1)-C(7)-C(15)	-76.86(15)
C(6)-O(1)-C(7)-C(14)	46.79(15)
C(7)-N(2)-C(8)-C(9)	161.56(14)
C(7)-N(2)-C(8)-C(13)	-20.0(2)
C(13)-C(8)-C(9)-C(10)	0.5(2)
N(2)-C(8)-C(9)-C(10)	178.98(15)
C(8)-C(9)-C(10)-C(11)	-1.0(3)
C(9)-C(10)-C(11)-C(12)	0.8(3)
C(10)-C(11)-C(12)-C(13)	0.1(3)
C(14)-O(2)-C(13)-C(12)	162.16(14)
C(14)-O(2)-C(13)-C(8)	-21.3(2)
C(11)-C(12)-C(13)-O(2)	175.95(18)
C(11)-C(12)-C(13)-C(8)	-0.6(3)
C(9)-C(8)-C(13)-O(2)	-176.13(14)
N(2)-C(8)-C(13)-O(2)	5.4(2)
C(9)-C(8)-C(13)-C(12)	0.3(2)
N(2)-C(8)-C(13)-C(12)	-178.20(15)
C(1)-N(1)-C(14)-O(2)	-70.35(16)
C(1)-N(1)-C(14)-C(16)	171.50(13)
C(1)-N(1)-C(14)-C(7)	45.75(17)
C(13)-O(2)-C(14)-N(1)	163.80(12)
C(13)-O(2)-C(14)-C(16)	-76.72(15)
C(13)-O(2)-C(14)-C(7)	46.71(16)
N(2)-C(7)-C(14)-N(1)	-173.81(9)
O(1)-C(7)-C(14)-N(1)	-58.01(15)
C(15)-C(7)-C(14)-N(1)	62.66(16)
N(2)-C(7)-C(14)-O(2)	-58.13(14)
O(1)-C(7)-C(14)-O(2)	57.67(12)
C(15)-C(7)-C(14)-O(2)	178.34(14)
N(2)-C(7)-C(14)-C(16)	62.17(16)
O(1)-C(7)-C(14)-C(16)	177.97(14)
C(15)-C(7)-C(14)-C(16)	-61.36(14)

Table 78 Hydrogen bonds for **5.6** [Å and °].

D-H...A	d(D-H)	d(H...A)	d(D...A)	<(DHA)
N(1)-H(1A)...O(2)#1	0.91(2)	2.17(2)	3.0662(16)	169.3(17)
N(2)-H(2A)...O(1)#2	0.89(2)	2.20(2)	3.0787(16)	169.7(17)

Symmetry transformations used to generate equivalent atoms:
#1 -x,-y+1,-z #2 -x,-y,-z

Unit cell and structural representation for complex 5.22

Table 79 Crystal data and structure refinement for **5.22**.

Identification code	zg95
Empirical formula	C_{34} H_{35} Cl N_2 Pd • (CH_2Cl_2)
Formula weight	698.41
Temperature	133(2) K
Wavelength	0.71073 Å
Crystal system	Triclinic

Space group	$P\bar{1}$	
Unit cell dimensions	a = 12.2175(9) Å	α= 90.3288(9)°.
	b = 14.0837(11) Å	β= 94.4514(9)°.
	c = 20.3950(16) Å	γ = 95.4624(10)°.
Volume	3482.5(5) $Å^3$	
Z	4	
Density (calculated)	1.332 Mg/m^3	
Absorption coefficient	0.788 mm^{-1}	
F(000)	1432	
Crystal color	red	
Crystal size	0.698 x 0.477 x 0.404 mm^3	

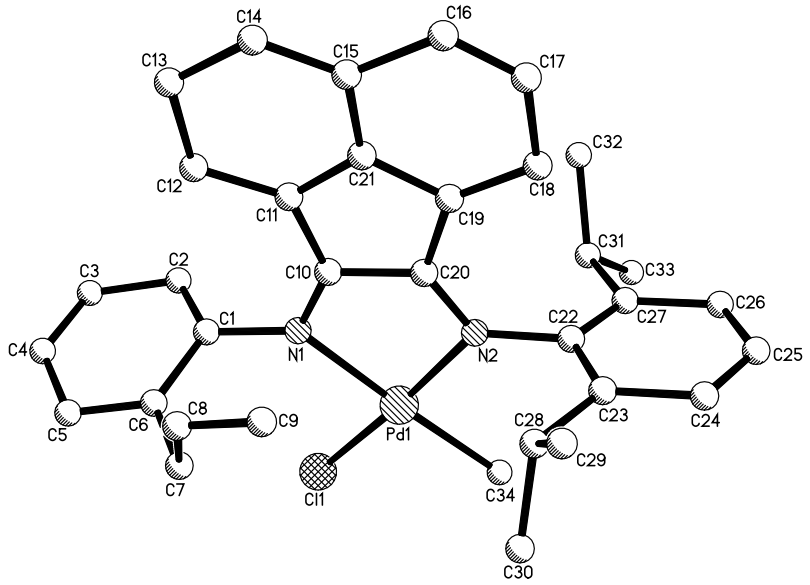

X-ray Data Collection, Structure Solution and Refinement for complex 5.27.

A bronze crystal of approximate dimensions 0.146 x 0.360 x 0.396 mm was mounted on a glass fiber and transferred to a Bruker SMART APEX II diffractometer. The APEX2[1] program package was used to determine the unit-cell parameters and for data collection (10 sec/frame scan time for a sphere of diffraction data). The raw frame data was processed using SAINT[2] and SADABS[3] to yield the reflection data file. Subsequent calculations were carried out using the SHELXTL[4] program. The diffraction symmetry was 2/*m* and the systematic absences were consistent with the monoclinic space group $P2_1/c$ that was later determined to be correct.

The structure was solved by direct methods and refined on F^2 by full-matrix least-squares techniques. The analytical scattering factors[5] for neutral atoms were used throughout the analysis. Hydrogen atoms were located from a difference-Fourier map and refined (x,y,z and U_{iso}). There was one molecule of dichloromethane solvent present. Cl(3) was disordered and included using multiple components, partial site-occupancy-factors and equivalent anisotropic thermal parameters.

At convergence, wR2 = 0.0782 and Goof = 1.033 for 522 variables refined against 8166 data (0.73Å), R1 = 0.0303 for those 7416 data with $I > 2.0\sigma(I)$.

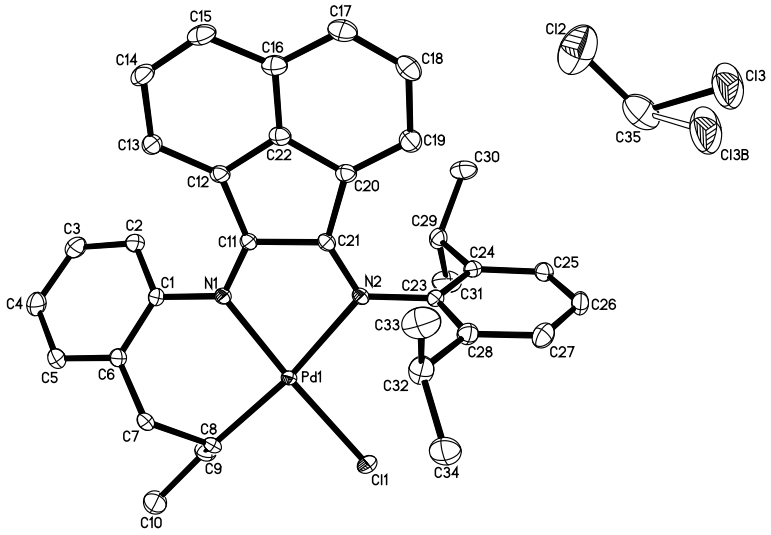

Table 80 Crystal data and structure refinement for **5.27**.

Identification code	zg94 (Tobias Friedberger)	
Empirical formula	C_{34} H_{35} Cl N_2 Pd • CH_2Cl_2	
Formula weight	698.41	
Temperature	88(2) K	
Wavelength	0.71073 Å	
Crystal system	Monoclinic	
Space group	$P2_1/c$	
Unit cell dimensions	a = 18.1381(12) Å	α= 90°.
	b = 11.2950(8) Å	β= 96.1599(8)°.
	c = 15.7258(11) Å	γ = 90°.
Volume	3203.1(4) $Å^3$	
Z	4	
Density (calculated)	1.448 Mg/m^3	
Absorption coefficient	0.857 mm^{-1}	
F(000)	1432	
Crystal color	bronze	
Crystal size	0.396 x 0.360 x 0.146 mm^3	
Theta range for data collection	2.128 to 29.201°	
Index ranges	$-24 \le h \le 24$, $-15 \le k \le 15$, $-21 \le l \le 20$	
Reflections collected	37790	
Independent reflections	8166 [R(int) = 0.0283]	
Completeness to theta = 25.500°	99.9 %	
Absorption correction	Numerical	
Max. and min. transmission	0.9643 and 0.7551	
Refinement method	Full-matrix least-squares on F^2	
Data / restraints / parameters	8166 / 0 / 522	
Goodness-of-fit on F^2	1.033	
Final R indices [I>2sigma(I) = 7416 data]	R1 = 0.0303, wR2 = 0.0754	
R indices (all data, 0.73Å)	R1 = 0.0342, wR2 = 0.0782	
Largest diff. peak and hole	1.215 and -1.327 $e.Å^{-3}$	

Table 81 Atomic coordinates (x 10^4) and equivalent isotropic displacement parameters ($Å^2$x 10^3) for **5.27**. U(eq) is defined as one third of the trace of the orthogonalized U^{ij} tensor.

	x	y	z	U(eq)
Pd(1)	3081(1)	4911(1)	4600(1)	11(1)
Cl(1)	2724(1)	6857(1)	4740(1)	21(1)
N(1)	3379(1)	3184(1)	4405(1)	12(1)
N(2)	2480(1)	4552(1)	3338(1)	12(1)
C(1)	3974(1)	2614(2)	4914(1)	13(1)
C(2)	4497(1)	1952(2)	4529(1)	17(1)
C(3)	5105(1)	1481(2)	5025(1)	21(1)
C(4)	5188(1)	1666(2)	5907(1)	24(1)
C(5)	4672(1)	2346(2)	6281(1)	20(1)
C(6)	4063(1)	2852(2)	5796(1)	15(1)
C(7)	3540(1)	3675(2)	6186(1)	15(1)
C(8)	3565(1)	4938(2)	5826(1)	14(1)
C(9)	4339(1)	5468(2)	5868(1)	19(1)
C(10)	4722(1)	5602(2)	6783(1)	26(1)
C(11)	2996(1)	2668(2)	3764(1)	13(1)
C(12)	2891(1)	1440(2)	3457(1)	14(1)
C(13)	3135(1)	340(2)	3754(1)	17(1)
C(14)	2842(1)	-684(2)	3313(1)	20(1)
C(15)	2343(1)	-617(2)	2591(1)	22(1)
C(16)	2084(1)	500(2)	2266(1)	18(1)
C(17)	1579(1)	711(2)	1528(1)	23(1)
C(18)	1367(1)	1852(2)	1300(1)	22(1)
C(19)	1625(1)	2854(2)	1789(1)	19(1)
C(20)	2123(1)	2672(2)	2505(1)	14(1)
C(21)	2497(1)	3441(2)	3175(1)	12(1)
C(22)	2357(1)	1504(2)	2725(1)	14(1)
C(23)	2028(1)	5326(2)	2776(1)	13(1)
C(24)	2321(1)	5786(2)	2055(1)	14(1)
C(25)	1869(1)	6542(2)	1524(1)	17(1)
C(26)	1158(1)	6825(2)	1709(1)	20(1)
C(27)	888(1)	6379(2)	2441(1)	21(1)
C(28)	1321(1)	5626(2)	2994(1)	17(1)
C(29)	3109(1)	5501(2)	1862(1)	17(1)
C(30)	3125(1)	5055(2)	948(1)	24(1)
C(31)	3609(1)	6587(2)	2024(2)	29(1)
C(32)	1032(1)	5113(2)	3794(1)	24(1)
C(33)	470(2)	4131(2)	3559(2)	35(1)
C(34)	710(1)	6064(2)	4334(2)	30(1)
C(35)	1064(2)	5422(3)	-545(2)	50(1)
Cl(2)	1253(1)	3898(1)	-503(1)	71(1)
Cl(3)	289(1)	5738(1)	-1264(1)	78(1)
Cl(3B)	218(4)	5850(6)	-612(6)	78(1)

Table 82 Bond lengths [Å] and angles [°] for **5.27**.

Pd(1)-C(8)	2.0316(18)
Pd(1)-N(1)	2.0563(14)
Pd(1)-N(2)	2.1969(14)

Pd(1)-Cl(1)	2.3087(5)
N(1)-C(11)	1.300(2)
N(1)-C(1)	1.426(2)
N(2)-C(21)	1.282(2)
N(2)-C(23)	1.436(2)
C(1)-C(2)	1.397(2)
C(1)-C(6)	1.405(2)
C(2)-C(3)	1.386(3)
C(3)-C(4)	1.395(3)
C(4)-C(5)	1.389(3)
C(5)-C(6)	1.395(3)
C(6)-C(7)	1.505(2)
C(7)-C(8)	1.538(2)
C(8)-C(9)	1.522(3)
C(9)-C(10)	1.537(3)
C(11)-C(12)	1.474(2)
C(11)-C(21)	1.503(2)
C(12)-C(13)	1.382(3)
C(12)-C(22)	1.424(2)
C(13)-C(14)	1.421(3)
C(14)-C(15)	1.376(3)
C(15)-C(16)	1.421(3)
C(16)-C(22)	1.406(2)
C(16)-C(17)	1.420(3)
C(17)-C(18)	1.381(3)
C(18)-C(19)	1.420(3)
C(19)-C(20)	1.381(3)
C(20)-C(22)	1.417(2)
C(20)-C(21)	1.474(2)
C(23)-C(28)	1.404(2)
C(23)-C(24)	1.404(2)
C(24)-C(25)	1.396(2)
C(24)-C(29)	1.525(2)
C(25)-C(26)	1.390(3)
C(26)-C(27)	1.393(3)
C(27)-C(28)	1.396(3)
C(28)-C(32)	1.528(3)
C(29)-C(30)	1.527(3)
C(29)-C(31)	1.531(3)
C(32)-C(34)	1.524(3)
C(32)-C(33)	1.524(3)
C(35)-Cl(3B)	1.602(8)
C(35)-Cl(3)	1.745(3)
C(35)-Cl(2)	1.754(4)

C(8)-Pd(1)-N(1)	93.56(6)
C(8)-Pd(1)-N(2)	169.19(6)
N(1)-Pd(1)-N(2)	78.64(6)
C(8)-Pd(1)-Cl(1)	89.53(5)
N(1)-Pd(1)-Cl(1)	176.88(4)
N(2)-Pd(1)-Cl(1)	98.35(4)
C(11)-N(1)-C(1)	122.89(15)
C(11)-N(1)-Pd(1)	114.44(12)
C(1)-N(1)-Pd(1)	122.63(11)
C(21)-N(2)-C(23)	119.84(15)

C(21)-N(2)-Pd(1)	109.96(12)
C(23)-N(2)-Pd(1)	129.65(11)
C(2)-C(1)-C(6)	121.27(16)
C(2)-C(1)-N(1)	120.42(15)
C(6)-C(1)-N(1)	117.92(15)
C(3)-C(2)-C(1)	119.85(17)
C(2)-C(3)-C(4)	119.73(18)
C(5)-C(4)-C(3)	119.90(18)
C(4)-C(5)-C(6)	121.68(18)
C(5)-C(6)-C(1)	117.47(17)
C(5)-C(6)-C(7)	121.83(16)
C(1)-C(6)-C(7)	120.62(16)
C(6)-C(7)-C(8)	112.20(15)
C(9)-C(8)-C(7)	114.36(16)
C(9)-C(8)-Pd(1)	110.49(12)
C(7)-C(8)-Pd(1)	107.98(11)
C(8)-C(9)-C(10)	113.64(17)
N(1)-C(11)-C(12)	135.64(16)
N(1)-C(11)-C(21)	117.01(15)
C(12)-C(11)-C(21)	107.30(14)
C(13)-C(12)-C(22)	118.93(16)
C(13)-C(12)-C(11)	135.21(17)
C(22)-C(12)-C(11)	105.58(15)
C(12)-C(13)-C(14)	118.52(18)
C(15)-C(14)-C(13)	122.39(18)
C(14)-C(15)-C(16)	120.53(18)
C(22)-C(16)-C(17)	116.44(18)
C(22)-C(16)-C(15)	116.51(18)
C(17)-C(16)-C(15)	127.05(18)
C(18)-C(17)-C(16)	120.45(18)
C(17)-C(18)-C(19)	122.48(18)
C(20)-C(19)-C(18)	118.09(18)
C(19)-C(20)-C(22)	119.45(16)
C(19)-C(20)-C(21)	134.86(17)
C(22)-C(20)-C(21)	105.67(15)
N(2)-C(21)-C(20)	134.51(16)
N(2)-C(21)-C(11)	118.11(15)
C(20)-C(21)-C(11)	107.38(14)
C(16)-C(22)-C(20)	123.02(17)
C(16)-C(22)-C(12)	123.05(17)
C(20)-C(22)-C(12)	113.94(16)
C(28)-C(23)-C(24)	122.95(16)
C(28)-C(23)-N(2)	118.28(15)
C(24)-C(23)-N(2)	118.72(15)
C(25)-C(24)-C(23)	117.33(16)
C(25)-C(24)-C(29)	120.86(16)
C(23)-C(24)-C(29)	121.80(16)
C(26)-C(25)-C(24)	120.99(17)
C(25)-C(26)-C(27)	120.39(17)
C(26)-C(27)-C(28)	120.74(18)
C(27)-C(28)-C(23)	117.53(17)
C(27)-C(28)-C(32)	121.61(17)
C(23)-C(28)-C(32)	120.83(16)
C(24)-C(29)-C(30)	111.68(16)
C(24)-C(29)-C(31)	110.47(16)

C(30)-C(29)-C(31)	110.46(16)
C(34)-C(32)-C(33)	111.21(18)
C(34)-C(32)-C(28)	112.15(17)
C(33)-C(32)-C(28)	110.83(19)
Cl(3B)-C(35)-Cl(2)	118.7(3)
Cl(3)-C(35)-Cl(2)	111.45(18)

Table 83 Anisotropic displacement parameters ($Å^2 x\ 10^3$) for **5.27**. The anisotropic displacement factor exponent takes the form: $-2\pi^2[\ h^2\ a^{*2}U^{11} + ...\ + 2\ h\ k\ a^*\ b^*\ U^{12}\ ]$

	U^{11}	U^{22}	U^{33}	U^{23}	U^{13}	U^{12}
Pd(1)	18(1)	9(1)	8(1)	0(1)	2(1)	1(1)
Cl(1)	34(1)	11(1)	18(1)	-2(1)	0(1)	5(1)
N(1)	16(1)	11(1)	9(1)	1(1)	3(1)	1(1)
N(2)	16(1)	13(1)	8(1)	1(1)	3(1)	1(1)
C(1)	18(1)	11(1)	12(1)	1(1)	1(1)	1(1)
C(2)	22(1)	14(1)	14(1)	-1(1)	3(1)	2(1)
C(3)	21(1)	18(1)	24(1)	-1(1)	2(1)	6(1)
C(4)	24(1)	22(1)	24(1)	1(1)	-6(1)	8(1)
C(5)	28(1)	18(1)	14(1)	0(1)	-3(1)	2(1)
C(6)	21(1)	12(1)	12(1)	1(1)	2(1)	0(1)
C(7)	22(1)	15(1)	9(1)	1(1)	2(1)	2(1)
C(8)	20(1)	15(1)	8(1)	-2(1)	1(1)	1(1)
C(9)	23(1)	18(1)	17(1)	-2(1)	0(1)	-3(1)
C(10)	29(1)	24(1)	24(1)	-4(1)	-7(1)	-1(1)
C(11)	18(1)	12(1)	9(1)	1(1)	4(1)	1(1)
C(12)	19(1)	13(1)	11(1)	-1(1)	5(1)	-1(1)
C(13)	23(1)	14(1)	14(1)	1(1)	5(1)	2(1)
C(14)	29(1)	11(1)	22(1)	0(1)	7(1)	0(1)
C(15)	27(1)	14(1)	25(1)	-5(1)	7(1)	-5(1)
C(16)	20(1)	16(1)	18(1)	-3(1)	4(1)	-4(1)
C(17)	23(1)	22(1)	23(1)	-6(1)	-1(1)	-7(1)
C(18)	19(1)	27(1)	19(1)	-2(1)	-4(1)	-4(1)
C(19)	19(1)	19(1)	18(1)	0(1)	1(1)	-1(1)
C(20)	16(1)	14(1)	12(1)	-1(1)	4(1)	-1(1)
C(21)	15(1)	14(1)	9(1)	1(1)	3(1)	1(1)
C(22)	18(1)	14(1)	12(1)	-1(1)	5(1)	-2(1)
C(23)	18(1)	10(1)	11(1)	0(1)	1(1)	1(1)
C(24)	18(1)	12(1)	12(1)	-1(1)	2(1)	1(1)
C(25)	23(1)	13(1)	13(1)	1(1)	0(1)	1(1)
C(26)	22(1)	15(1)	19(1)	2(1)	-5(1)	4(1)
C(27)	17(1)	20(1)	25(1)	1(1)	2(1)	4(1)
C(28)	18(1)	17(1)	16(1)	1(1)	4(1)	2(1)
C(29)	20(1)	17(1)	15(1)	4(1)	5(1)	4(1)
C(30)	29(1)	23(1)	21(1)	-6(1)	10(1)	-1(1)
C(31)	20(1)	34(1)	32(1)	-11(1)	4(1)	-4(1)
C(32)	22(1)	28(1)	23(1)	6(1)	11(1)	5(1)
C(33)	40(1)	30(1)	37(1)	0(1)	21(1)	-7(1)
C(34)	28(1)	37(1)	26(1)	-1(1)	11(1)	3(1)
C(35)	42(2)	65(2)	41(2)	-6(2)	-4(1)	-9(2)
Cl(2)	75(1)	71(1)	72(1)	24(1)	38(1)	27(1)
Cl(3)	78(1)	49(1)	93(1)	4(1)	-52(1)	-7(1)

Cl(3B)	78(1)	49(1)	93(1)	4(1)	-52(1)	-7(1)

Table 84 Hydrogen coordinates (x 10^4) and isotropic displacement parameters ($Å^2$x 10^3) for **5.27**.

	x	y	z	U(eq)
H(2A)	4446(13)	1850(20)	3946(16)	21(6)
H(3A)	5458(14)	1070(20)	4790(17)	28(7)
H(4A)	5602(15)	1350(30)	6221(18)	34(7)
H(5A)	4738(14)	2480(20)	6873(17)	31(7)
H(7A)	3684(13)	3700(20)	6794(15)	18(6)
H(7B)	3045(12)	3350(20)	6110(14)	13(5)
H(8A)	3224(13)	5450(20)	6140(16)	21(6)
H(9A)	4305(13)	6240(20)	5602(15)	22(6)
H(9B)	4640(15)	4980(20)	5551(18)	23(7)
H(10A)	5209(16)	5980(20)	6791(17)	33(7)
H(10B)	4834(17)	4870(30)	7050(19)	35(8)
H(10C)	4418(16)	6090(30)	7099(18)	36(7)
H(13A)	3489(13)	240(20)	4233(16)	16(6)
H(14A)	2995(14)	-1420(20)	3541(17)	29(7)
H(15A)	2164(14)	-1330(20)	2301(16)	25(6)
H(17A)	1410(18)	60(20)	1160(20)	41(9)
H(18A)	1027(14)	1980(20)	826(16)	26(6)
H(19A)	1450(13)	3640(20)	1612(16)	23(6)
H(25A)	2058(13)	6880(20)	1029(16)	22(6)
H(26A)	859(14)	7330(20)	1340(16)	23(6)
H(27A)	388(15)	6600(20)	2544(16)	28(7)
H(29A)	3313(14)	4870(20)	2254(16)	18(6)
H(30A)	3635(16)	4770(20)	898(18)	29(7)
H(30B)	2998(15)	5690(30)	507(18)	34(7)
H(30C)	2787(16)	4390(30)	841(19)	39(8)
H(31A)	4100(16)	6410(20)	1908(17)	33(7)
H(31B)	3619(16)	6820(30)	2590(20)	40(8)
H(31C)	3424(16)	7270(30)	1645(18)	37(7)
H(32A)	1469(15)	4760(20)	4141(18)	28(7)
H(33A)	670(16)	3510(30)	3210(19)	39(8)
H(33B)	62(14)	4410(20)	3192(16)	21(6)
H(33C)	296(16)	3770(30)	4058(19)	39(8)
H(34A)	1083(17)	6670(30)	4519(19)	41(8)
H(34B)	539(16)	5730(30)	4886(19)	40(8)
H(34C)	292(16)	6440(30)	4016(18)	33(7)
H(35A)	960(30)	5700(40)	40(30)	98(15)
H(35B)	1437(19)	5860(30)	-670(20)	50(9)

Table 85 Torsion angles [°] for **5.27**.

C(11)-N(1)-C(1)-C(2)	44.1(2)
Pd(1)-N(1)-C(1)-C(2)	-133.68(15)
C(11)-N(1)-C(1)-C(6)	-143.03(17)
Pd(1)-N(1)-C(1)-C(6)	39.2(2)

C(6)-C(1)-C(2)-C(3)	2.2(3)
N(1)-C(1)-C(2)-C(3)	174.89(17)
C(1)-C(2)-C(3)-C(4)	0.5(3)
C(2)-C(3)-C(4)-C(5)	-1.7(3)
C(3)-C(4)-C(5)-C(6)	0.3(3)
C(4)-C(5)-C(6)-C(1)	2.3(3)
C(4)-C(5)-C(6)-C(7)	-174.60(19)
C(2)-C(1)-C(6)-C(5)	-3.5(3)
N(1)-C(1)-C(6)-C(5)	-176.36(16)
C(2)-C(1)-C(6)-C(7)	173.35(17)
N(1)-C(1)-C(6)-C(7)	0.5(3)
C(5)-C(6)-C(7)-C(8)	114.74(19)
C(1)-C(6)-C(7)-C(8)	-62.0(2)
C(6)-C(7)-C(8)-C(9)	-52.3(2)
C(6)-C(7)-C(8)-Pd(1)	71.09(17)
C(7)-C(8)-C(9)-C(10)	-62.1(2)
Pd(1)-C(8)-C(9)-C(10)	175.82(14)
C(1)-N(1)-C(11)-C(12)	15.5(3)
Pd(1)-N(1)-C(11)-C(12)	-166.60(17)
C(1)-N(1)-C(11)-C(21)	-167.56(15)
Pd(1)-N(1)-C(11)-C(21)	10.37(19)
N(1)-C(11)-C(12)-C(13)	3.7(4)
C(21)-C(11)-C(12)-C(13)	-173.5(2)
N(1)-C(11)-C(12)-C(22)	177.21(19)
C(21)-C(11)-C(12)-C(22)	0.03(18)
C(22)-C(12)-C(13)-C(14)	0.1(3)
C(11)-C(12)-C(13)-C(14)	173.02(19)
C(12)-C(13)-C(14)-C(15)	1.8(3)
C(13)-C(14)-C(15)-C(16)	-1.4(3)
C(14)-C(15)-C(16)-C(22)	-0.9(3)
C(14)-C(15)-C(16)-C(17)	179.2(2)
C(22)-C(16)-C(17)-C(18)	-1.2(3)
C(15)-C(16)-C(17)-C(18)	178.6(2)
C(16)-C(17)-C(18)-C(19)	-1.3(3)
C(17)-C(18)-C(19)-C(20)	1.9(3)
C(18)-C(19)-C(20)-C(22)	0.0(3)
C(18)-C(19)-C(20)-C(21)	-178.12(19)
C(23)-N(2)-C(21)-C(20)	-1.8(3)
Pd(1)-N(2)-C(21)-C(20)	170.53(16)
C(23)-N(2)-C(21)-C(11)	178.14(14)
Pd(1)-N(2)-C(21)-C(11)	-9.56(18)
C(19)-C(20)-C(21)-N(2)	1.7(4)
C(22)-C(20)-C(21)-N(2)	-176.67(19)
C(19)-C(20)-C(21)-C(11)	-178.3(2)
C(22)-C(20)-C(21)-C(11)	3.41(18)
N(1)-C(11)-C(21)-N(2)	0.1(2)
C(12)-C(11)-C(21)-N(2)	177.91(15)
N(1)-C(11)-C(21)-C(20)	-179.94(15)
C(12)-C(11)-C(21)-C(20)	-2.15(18)
C(17)-C(16)-C(22)-C(20)	3.2(3)
C(15)-C(16)-C(22)-C(20)	-176.71(17)
C(17)-C(16)-C(22)-C(12)	-177.22(17)
C(15)-C(16)-C(22)-C(12)	2.9(3)
C(19)-C(20)-C(22)-C(16)	-2.6(3)
C(21)-C(20)-C(22)-C(16)	176.02(16)

C(19)-C(20)-C(22)-C(12)	177.74(16)
C(21)-C(20)-C(22)-C(12)	-3.6(2)
C(13)-C(12)-C(22)-C(16)	-2.6(3)
C(11)-C(12)-C(22)-C(16)	-177.37(16)
C(13)-C(12)-C(22)-C(20)	177.10(16)
C(11)-C(12)-C(22)-C(20)	2.3(2)
C(21)-N(2)-C(23)-C(28)	96.8(2)
Pd(1)-N(2)-C(23)-C(28)	-73.8(2)
C(21)-N(2)-C(23)-C(24)	-85.6(2)
Pd(1)-N(2)-C(23)-C(24)	103.77(17)
C(28)-C(23)-C(24)-C(25)	-2.2(3)
N(2)-C(23)-C(24)-C(25)	-179.64(15)
C(28)-C(23)-C(24)-C(29)	176.36(17)
N(2)-C(23)-C(24)-C(29)	-1.0(3)
C(23)-C(24)-C(25)-C(26)	0.2(3)
C(29)-C(24)-C(25)-C(26)	-178.44(17)
C(24)-C(25)-C(26)-C(27)	1.4(3)
C(25)-C(26)-C(27)-C(28)	-1.0(3)
C(26)-C(27)-C(28)-C(23)	-1.0(3)
C(26)-C(27)-C(28)-C(32)	-179.18(19)
C(24)-C(23)-C(28)-C(27)	2.6(3)
N(2)-C(23)-C(28)-C(27)	-179.96(17)
C(24)-C(23)-C(28)-C(32)	-179.14(18)
N(2)-C(23)-C(28)-C(32)	-1.7(3)
C(25)-C(24)-C(29)-C(30)	-53.0(2)
C(23)-C(24)-C(29)-C(30)	128.50(18)
C(25)-C(24)-C(29)-C(31)	70.4(2)
C(23)-C(24)-C(29)-C(31)	-108.1(2)
C(27)-C(28)-C(32)-C(34)	-50.3(3)
C(23)-C(28)-C(32)-C(34)	131.5(2)
C(27)-C(28)-C(32)-C(33)	74.6(2)
C(23)-C(28)-C(32)-C(33)	-103.5(2)

Definitions:

$wR2 = [\Sigma[w(F_o^2-F_c^2)^2] / \Sigma[w(F_o^2)^2]]^{1/2}$

$R1 = \Sigma||F_o|-|F_c|| / \Sigma|F_o|$

Goof = $S = [\Sigma[w(F_o^2-F_c^2)^2] / (n-p)]^{1/2}$ where n is the number of reflections and p is the total number of parameters refined.

References Appendix

(1) APEX2 Version 2011.4-1, Bruker AXS, Inc.; Madison, WI 2011.

(2) SAINT Version 7.68a, Bruker AXS, Inc.; Madison, WI 2009.

(3) Sheldrick, G. M. SADABS, Version 2008/1, Bruker AXS, Inc.; Madison, WI 2008.

(4) Sheldrick, G. M. SHELXTL, Version 2013/3, Bruker AXS, Inc.; Madison, WI 2013.

(5) International Tables for X-Ray Crystallography 1992, Vol. C., Dordrecht: Kluwer Academic Publishers.

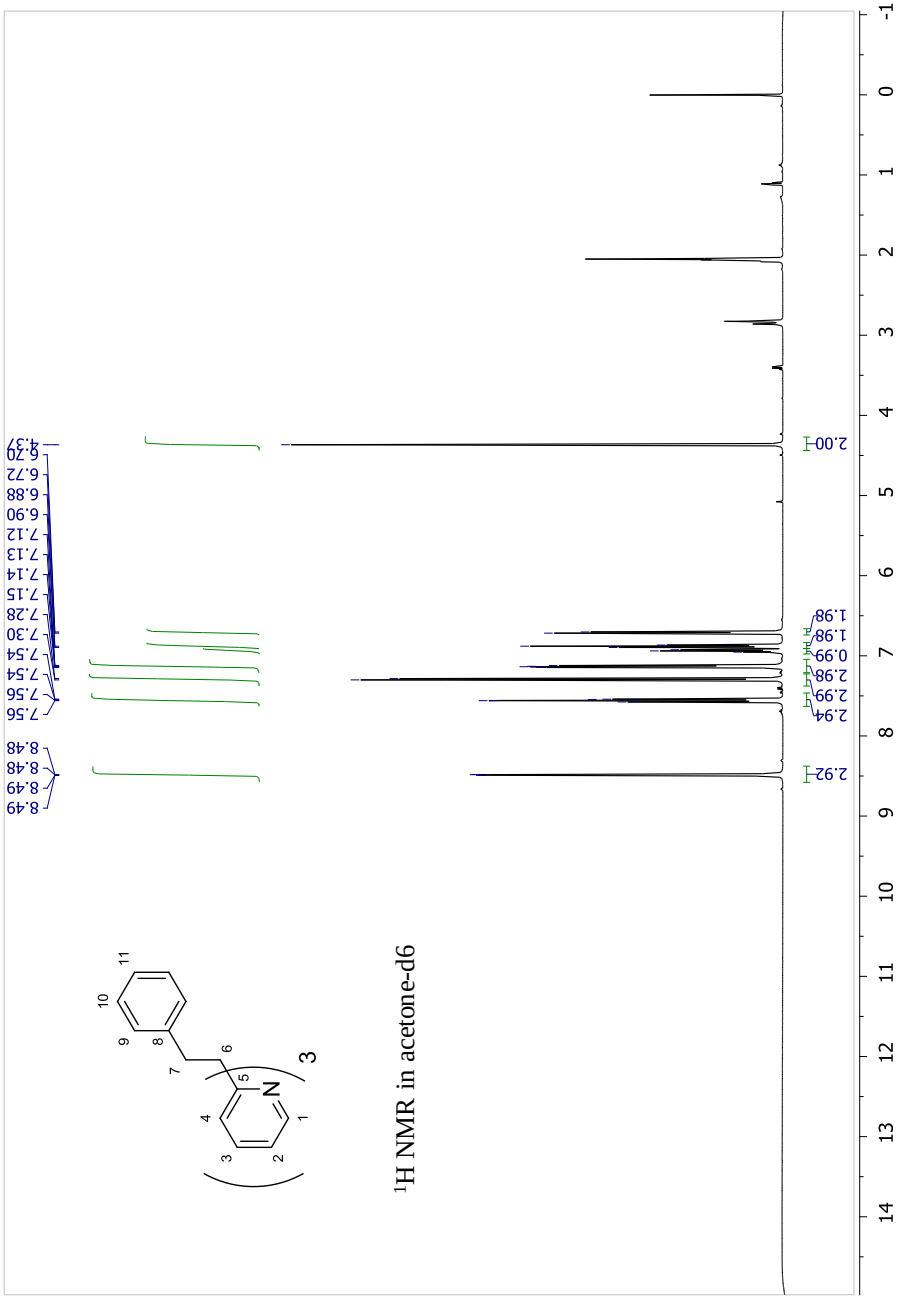
^{1}H NMR in acetone-d6
3
N
8.49
8.48
8.48
8.49
7.56
7.56
7.54
7.54
7.30
7.28
7.15
7.14
7.13
7.12
6.90
6.88
6.72
6.70
4.37
2.92
2.94
2.99
2.98
0.99
1.98
1.98
2.00

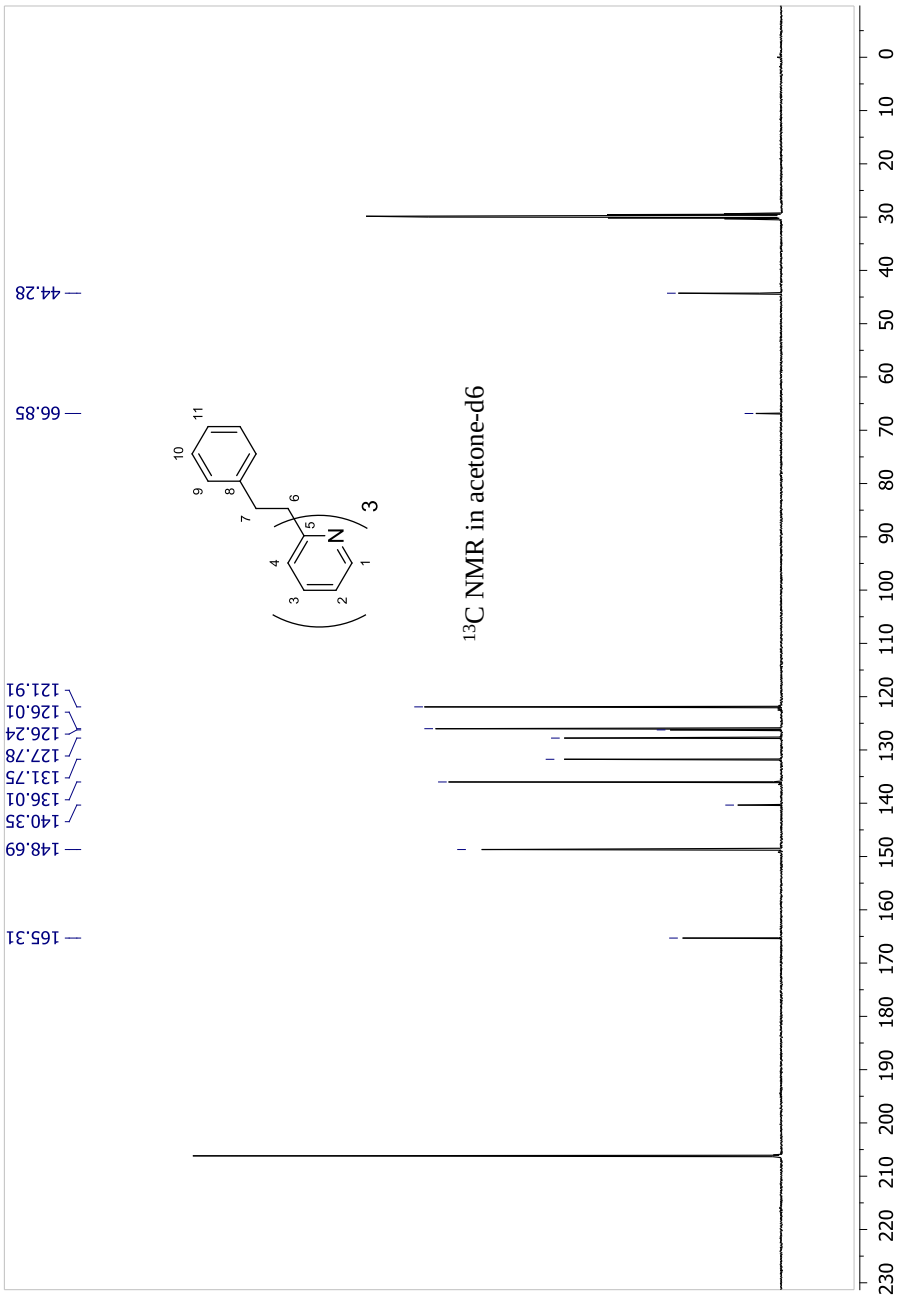
^{13}C NMR in acetone-d6
44.28
66.85
121.91
126.01
126.24
127.78
131.75
136.01
140.35
148.69
165.31
0
10
20
30
40
50
60
70
80
90
100
110
120
130
140
150
160
170
180
190
200
210
220
230

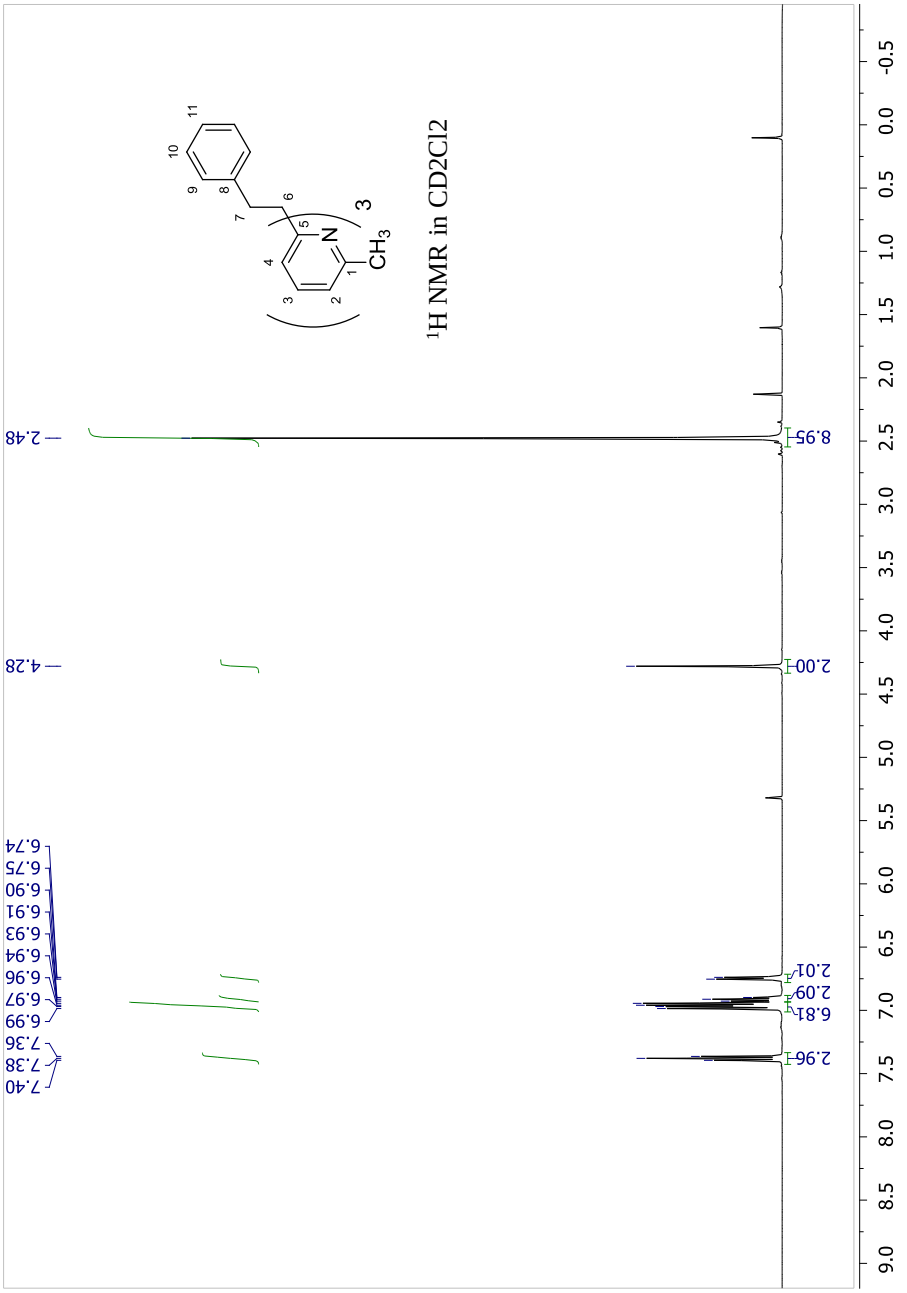
^{1}H NMR in CD2Cl2
CH3
N
7.40
7.38
7.36
6.99
6.97
6.96
6.94
6.93
6.91
6.90
6.75
6.74
4.28
2.48
2.96
6.81
2.09
2.01
2.00
8.95

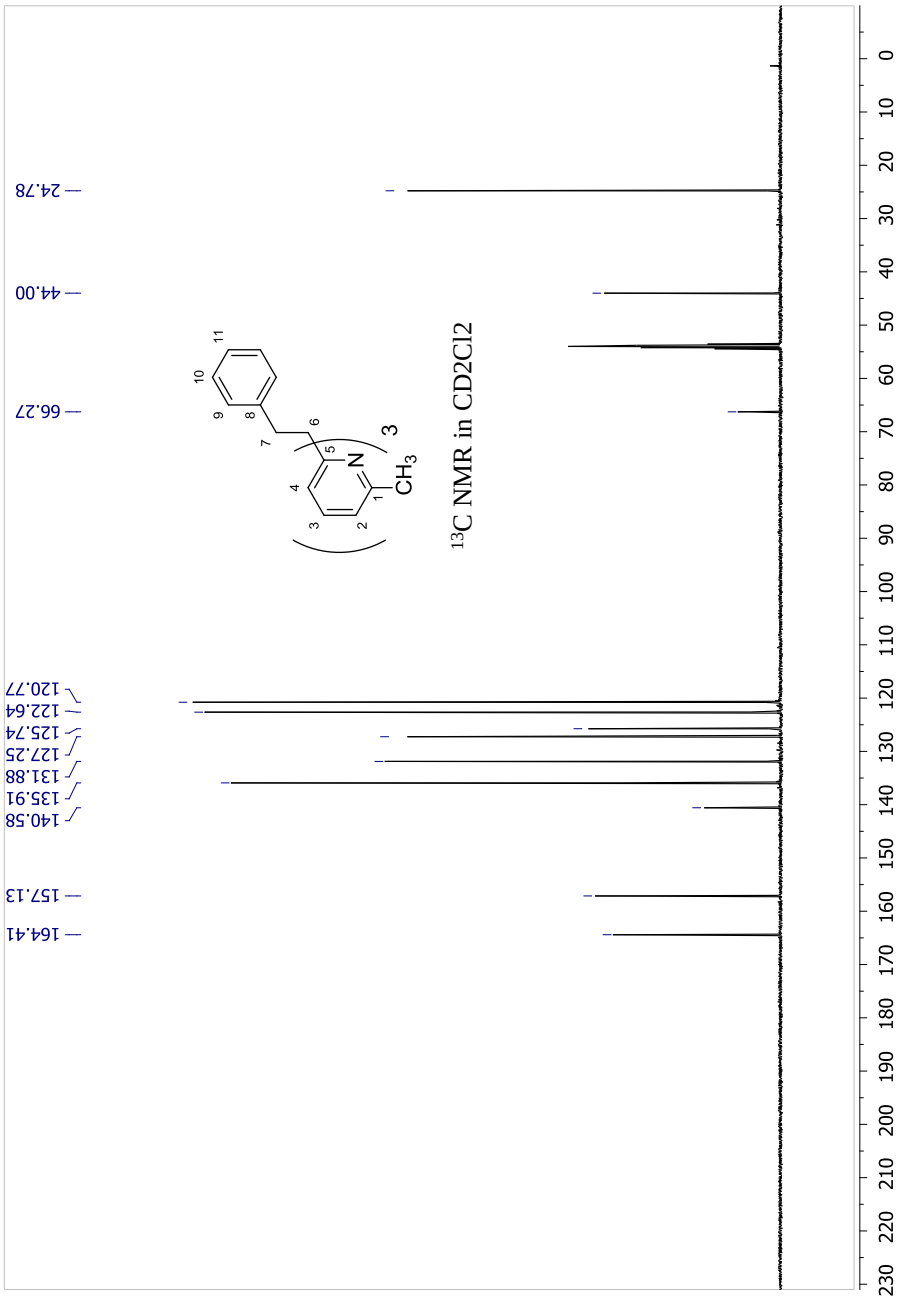
24.78
44.00
66.27
120.77
122.64
125.74
127.25
131.88
135.91
140.58
157.13
164.41
^{13}C NMR in CD2Cl2
N
CH3

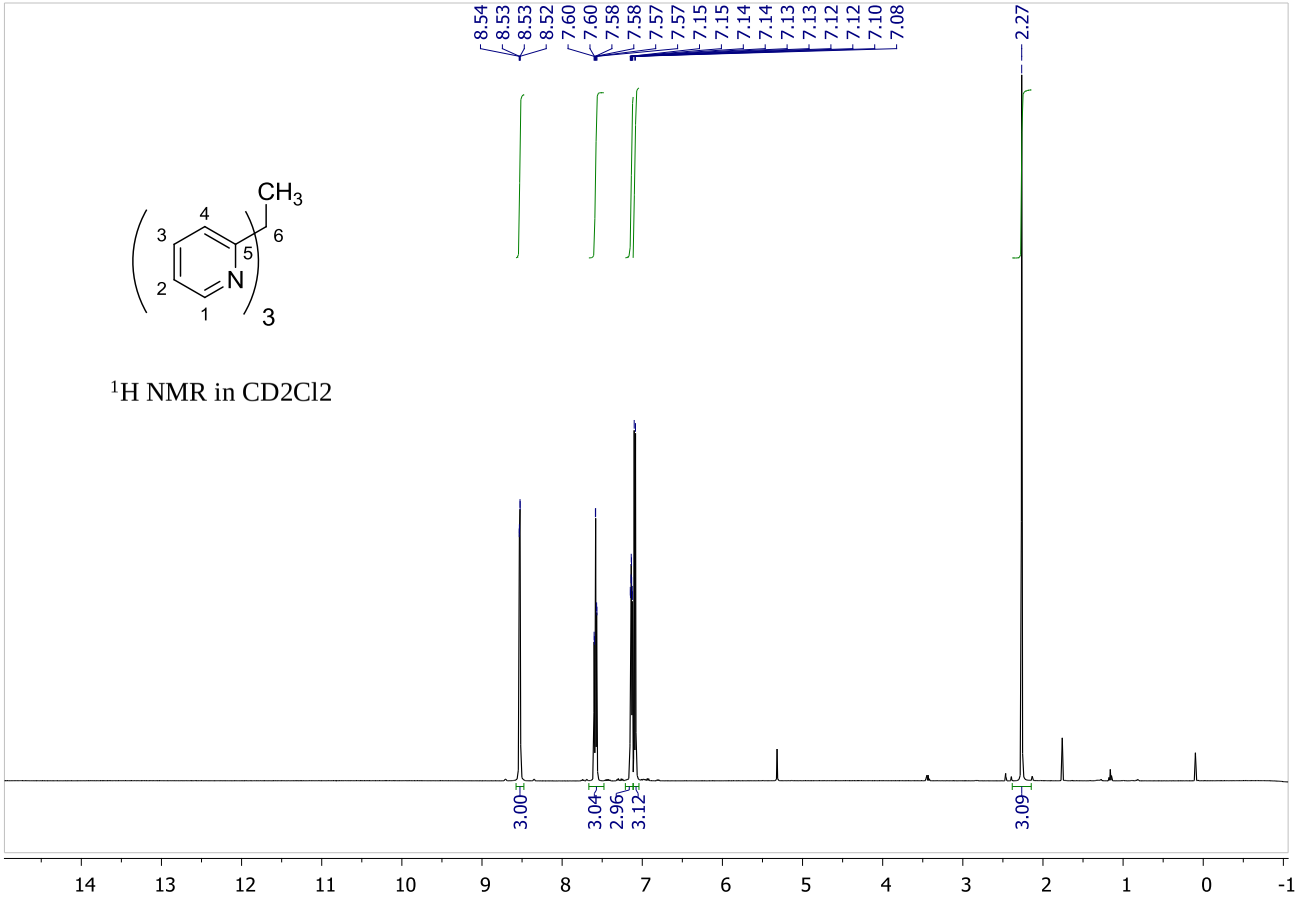
8.54
8.53
8.53
8.52
7.60
7.60
7.58
7.58
7.57
7.57
7.15
7.15
7.14
7.14
7.13
7.13
7.12
7.12
7.10
7.08
2.27
CH3
4
3
5
6
2
N
1
3
1H NMR in CD2Cl2
3.00
3.04
2.96
3.12
3.09
14
13
12
11
10
9
8
7
6
5
4
3
2
1
0
-1

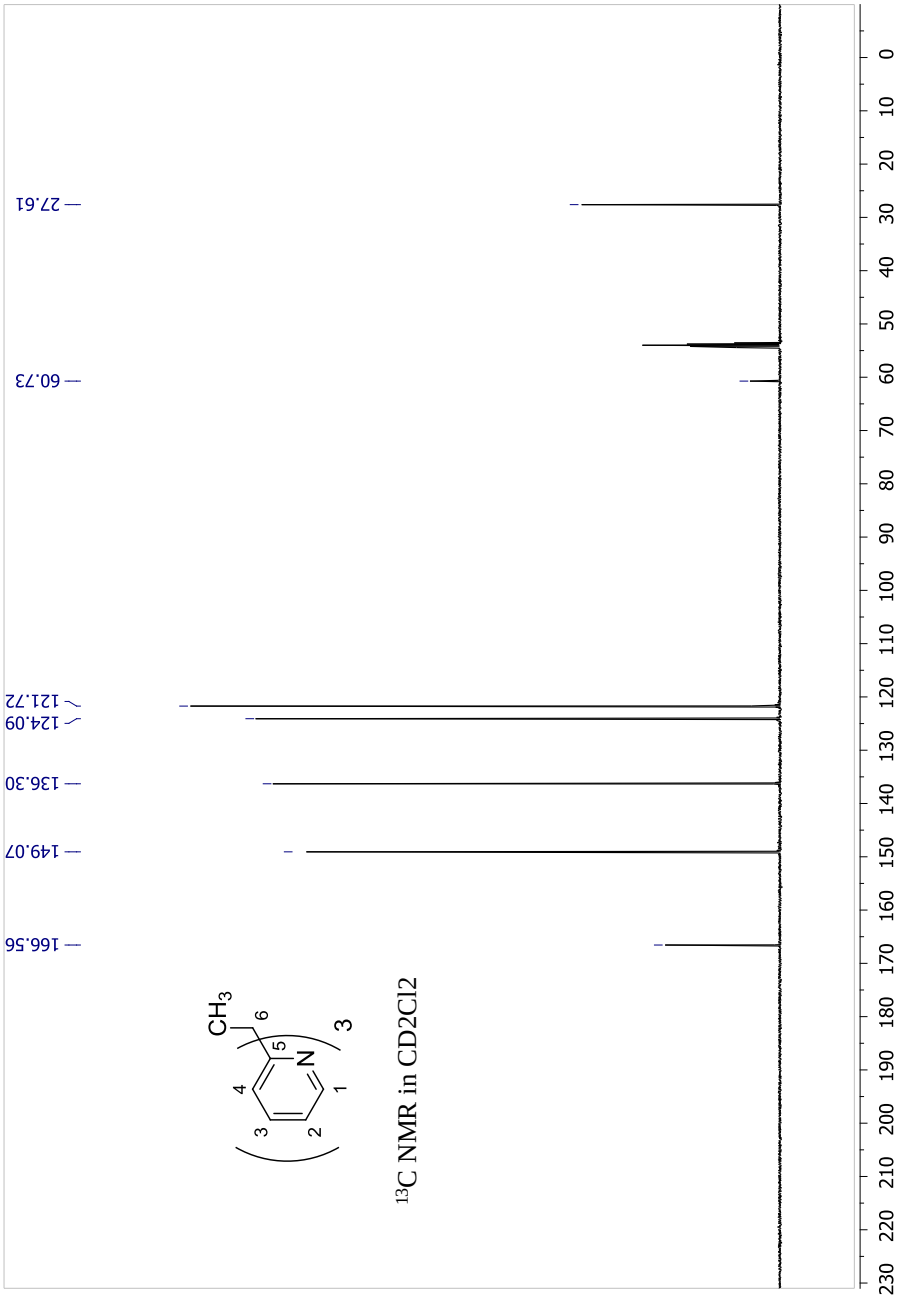
27.61
60.73
121.72
124.09
136.30
149.07
166.56
^{13}C NMR in CD2Cl2
CH3
N
0
10
20
30
40
50
60
70
80
90
100
110
120
130
140
150
160
170
180
190
200
210
220
230

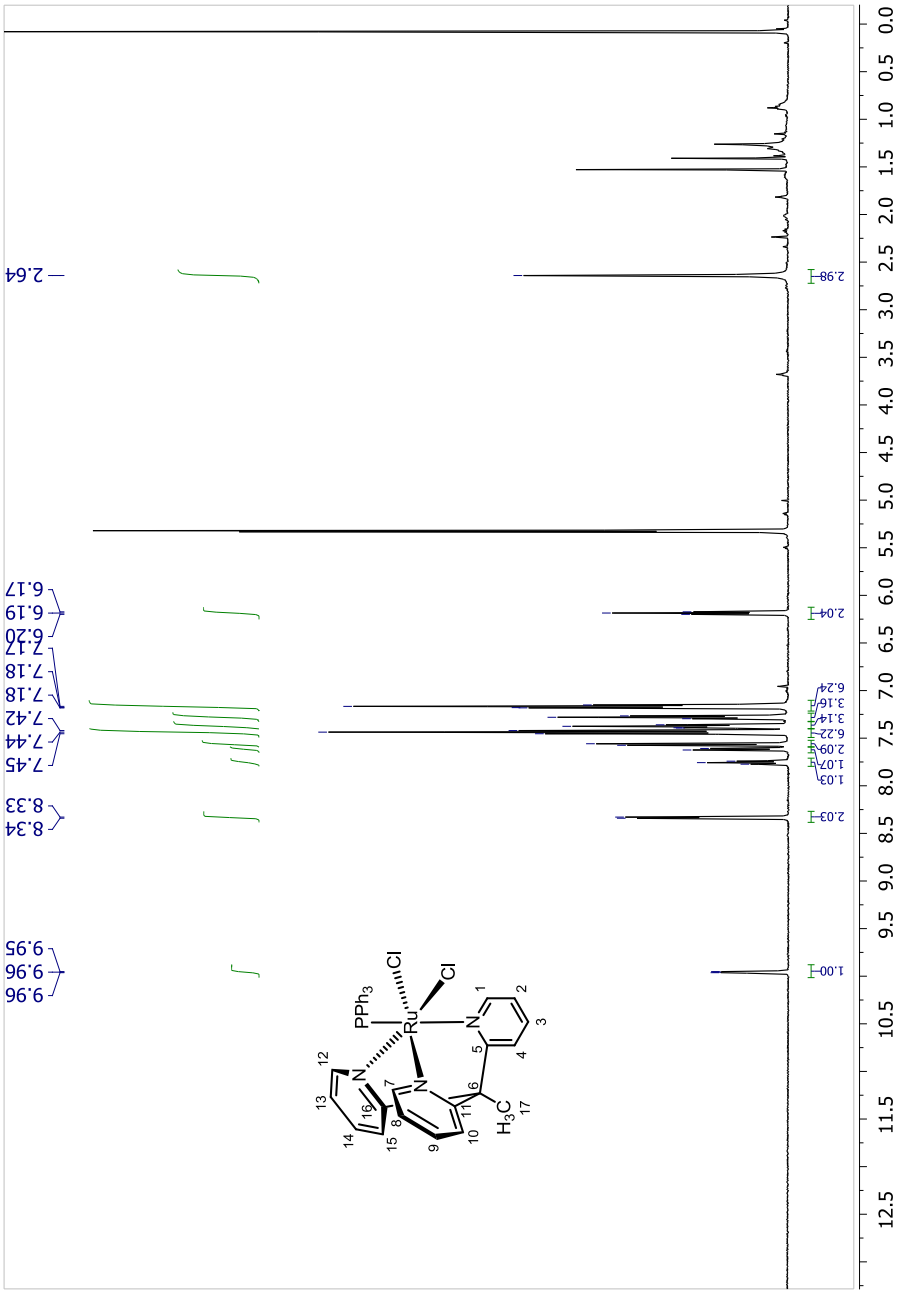
9.96
9.96
9.95
8.34
8.33
7.45
7.44
7.42
7.18
7.18
7.17
6.20
6.19
6.17
2.64
1.00
2.03
2.04
2.98
PPh3
Ru
Cl
Cl
N
N
N
H3C
1
2
3
4
5
6
7
8
9
10
11
12
13
14
15
16
17

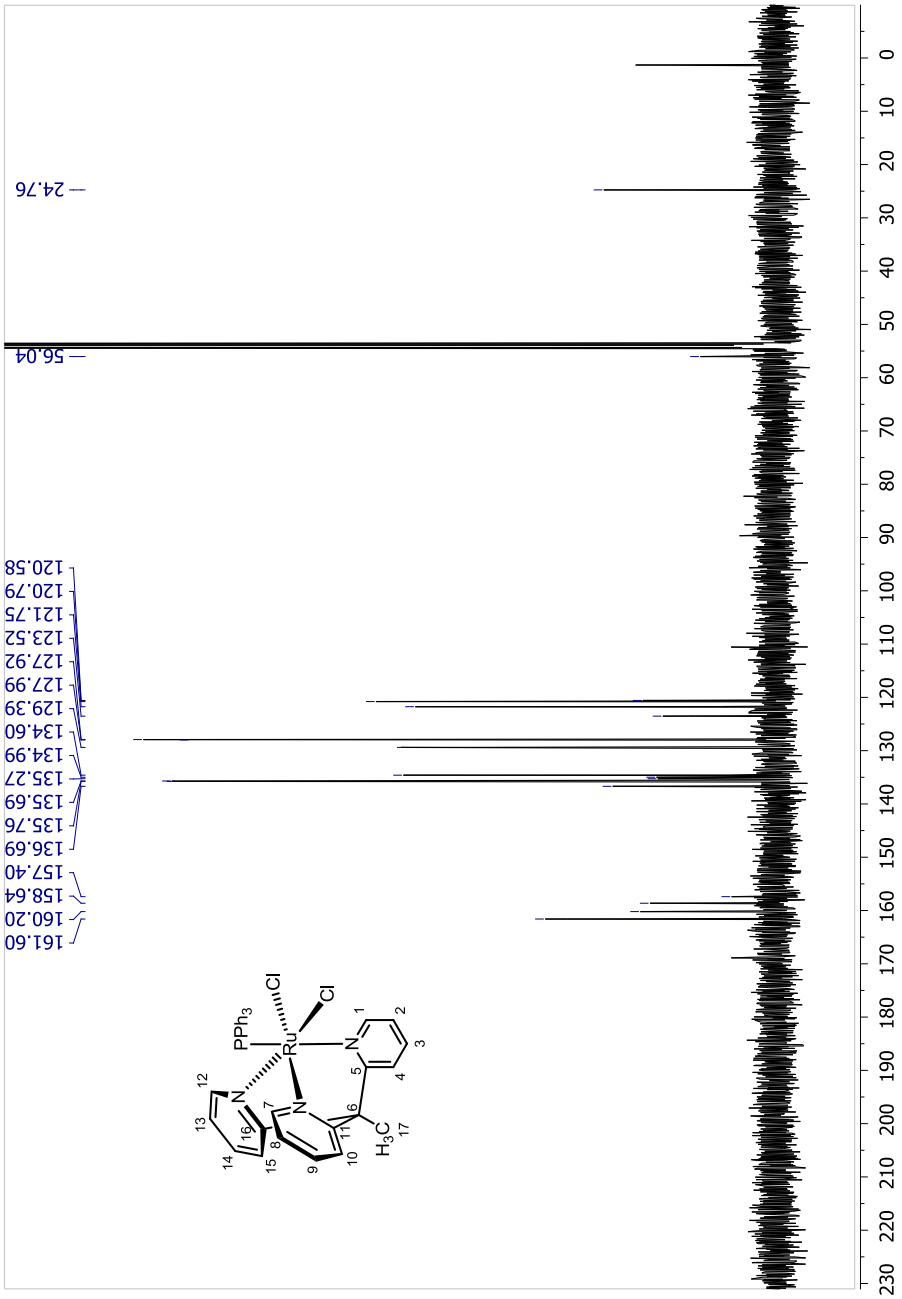
161.60
160.20
158.64
157.40
136.69
135.76
135.69
135.27
134.99
134.60
129.39
127.99
127.92
123.52
121.75
120.79
120.58
56.04
24.76
PPh3
Ru
Cl
Cl
N
N
N
H3C
0
10
20
30
40
50
60
70
80
90
100
110
120
130
140
150
160
170
180
190
200
210
220
230

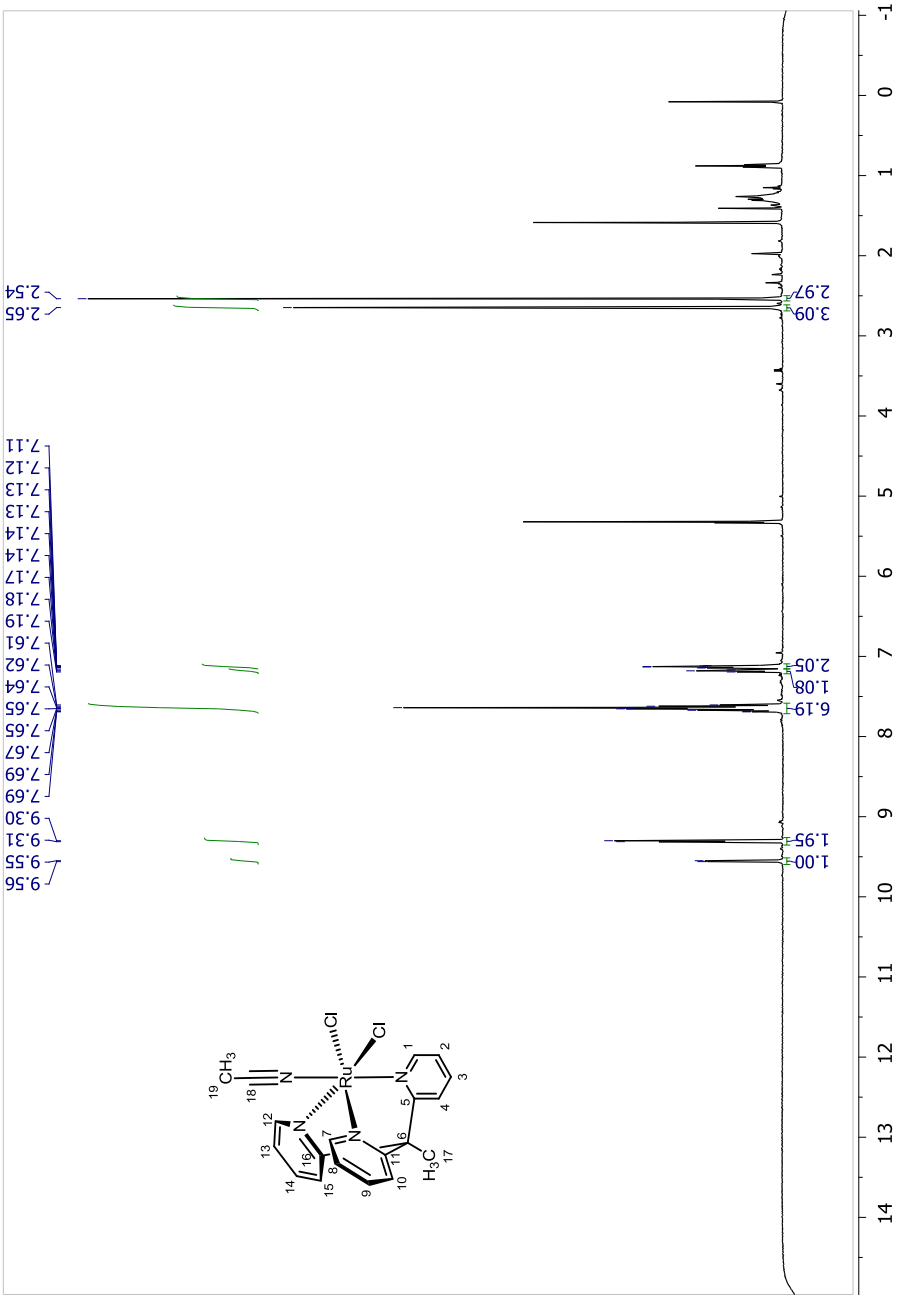
9.56
9.55
9.31
9.30
7.69
7.69
7.67
7.65
7.65
7.64
7.62
7.61
7.19
7.18
7.17
7.14
7.14
7.13
7.13
7.12
7.11
2.65
2.54
1.00
1.95
6.19
1.08
2.05
3.09
2.97
Cl
Cl
Ru
N
N
N
N
CH3
H3C

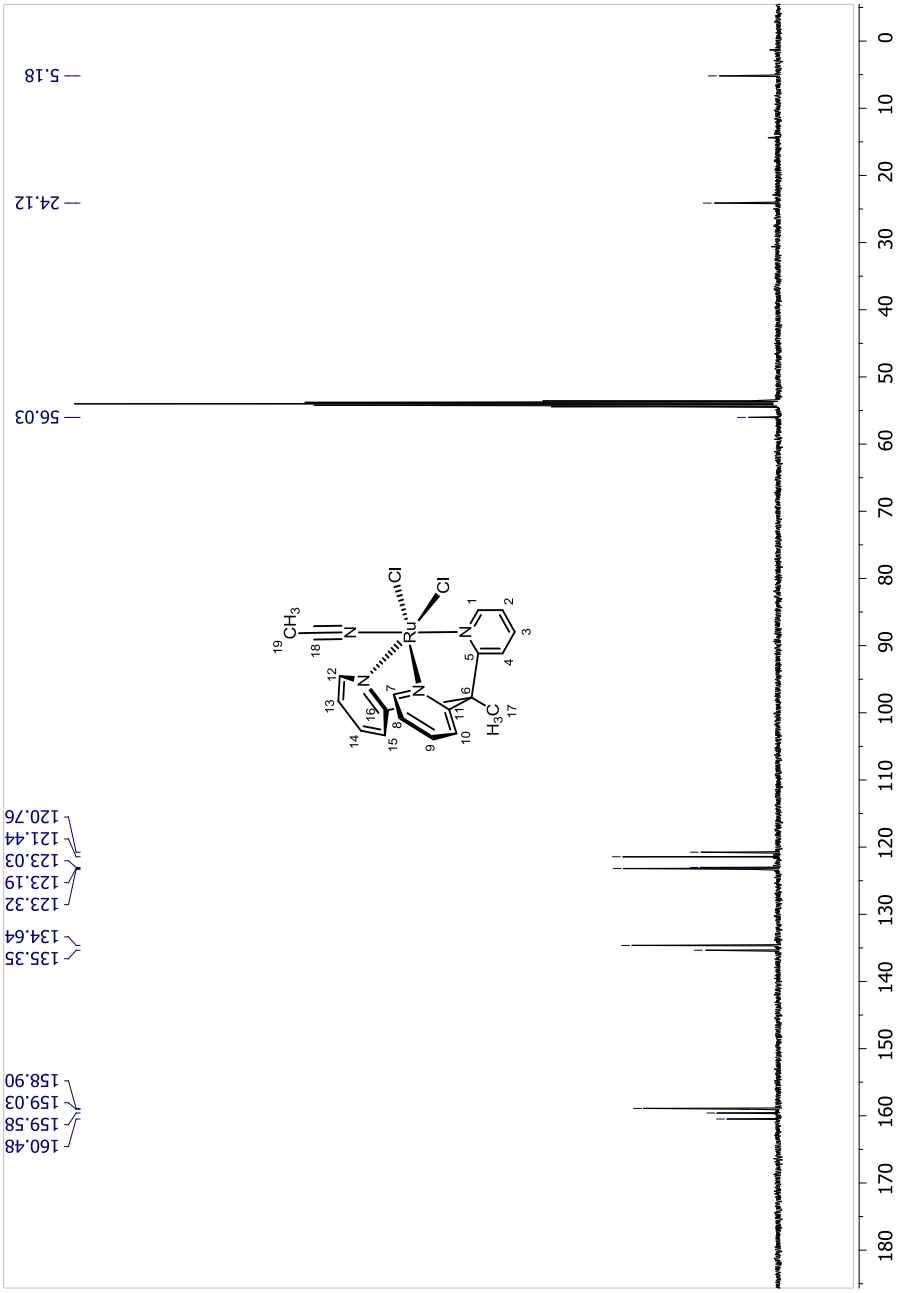
5.18
24.12
56.03
120.76
121.44
123.03
123.19
123.32
134.64
135.35
158.90
159.03
159.58
160.48
0
10
20
30
40
50
60
70
80
90
100
110
120
130
140
150
160
170
180

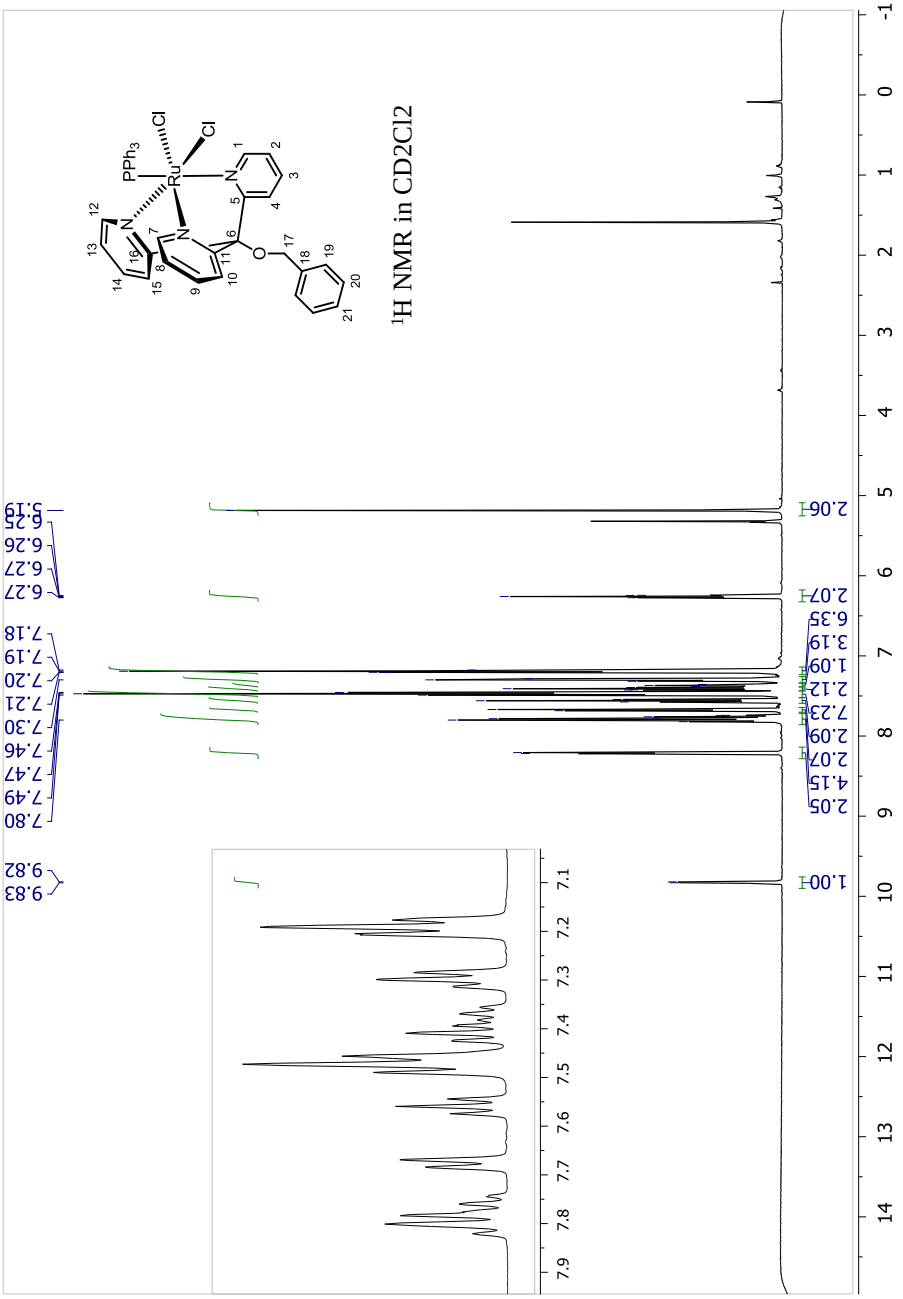
^{1}H NMR in CD2Cl2
PPh3
Ru
Cl
Cl
N
N
N
O
9.83
9.82
7.80
7.49
7.47
7.46
7.30
7.21
7.20
7.19
7.18
6.27
6.27
6.26
6.25
5.19
2.06
2.07
6.35
3.19
1.09
2.12
7.23
2.09
2.07
4.15
2.05
1.00

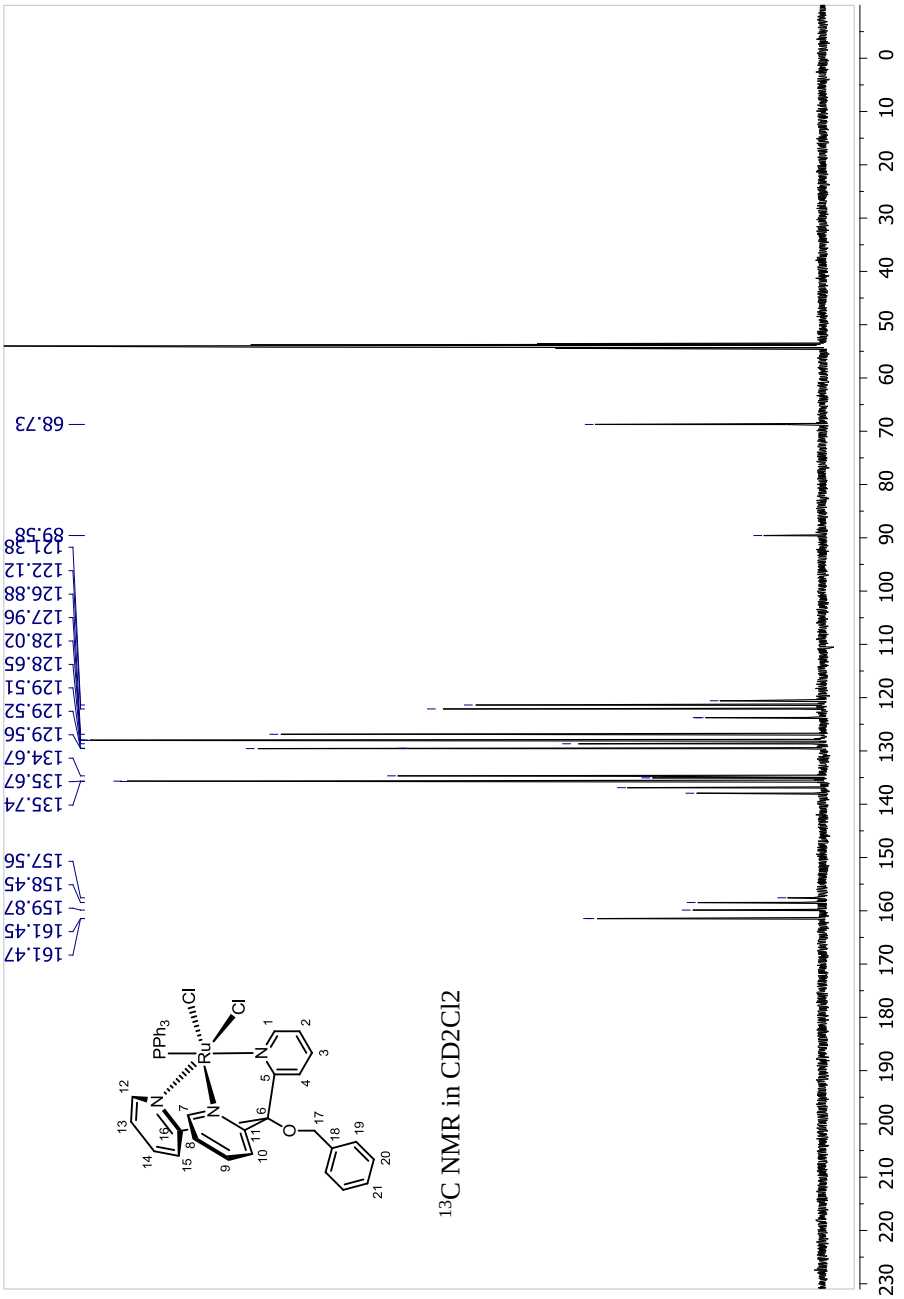
68.73
89.58
121.38
122.12
126.88
127.96
128.02
128.65
129.51
129.52
129.56
134.67
135.67
135.74
157.56
158.45
159.87
161.45
161.47
PPh3
Ru
Cl
Cl
N
O
13C NMR in CD2Cl2

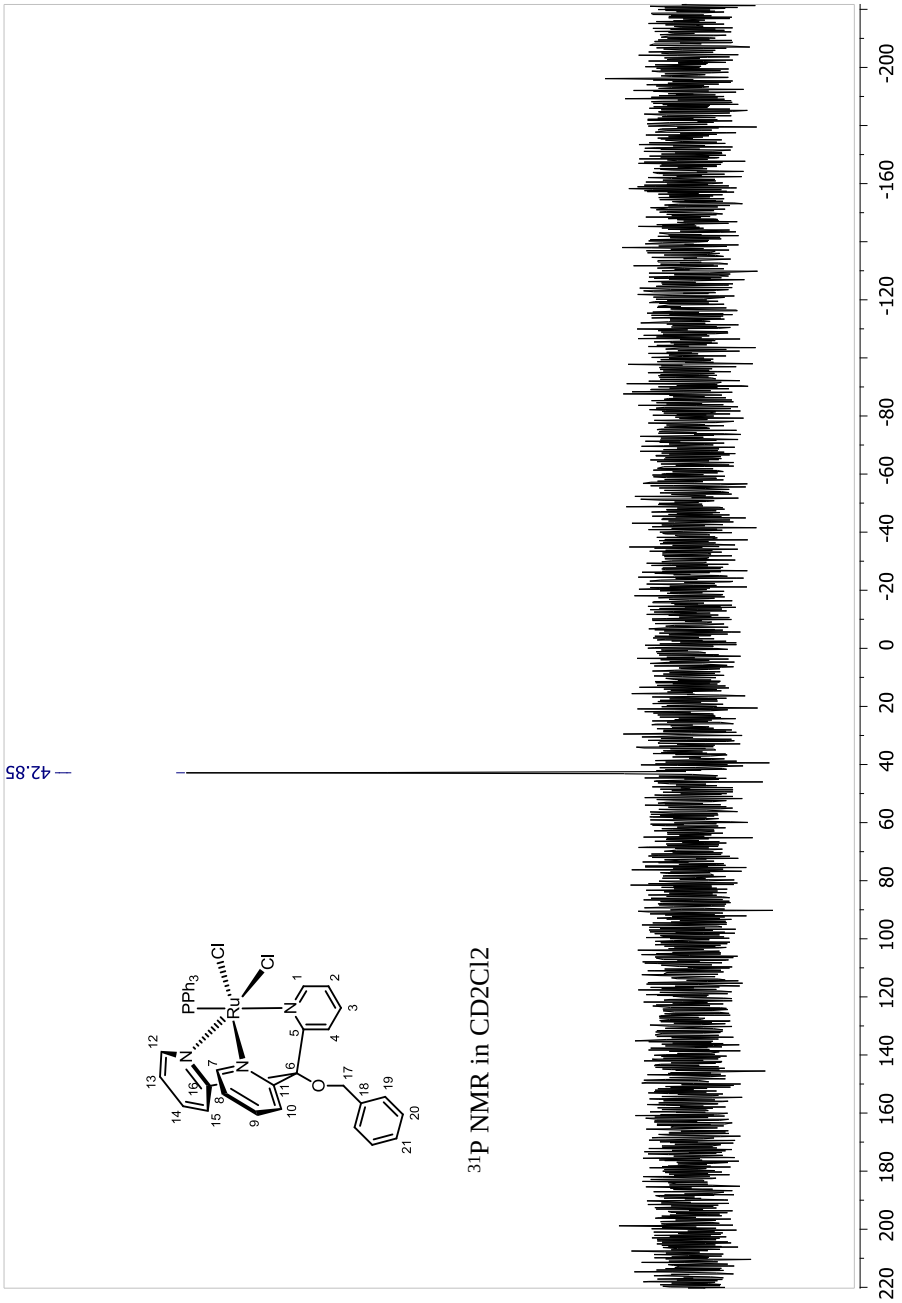
42.85
PPh3
Ru
Cl
Cl
N
O
^{31}P NMR in CD2Cl2
220
200
180
160
140
120
100
80
60
40
20
0
-20
-40
-60
-80
-120
-160
-200

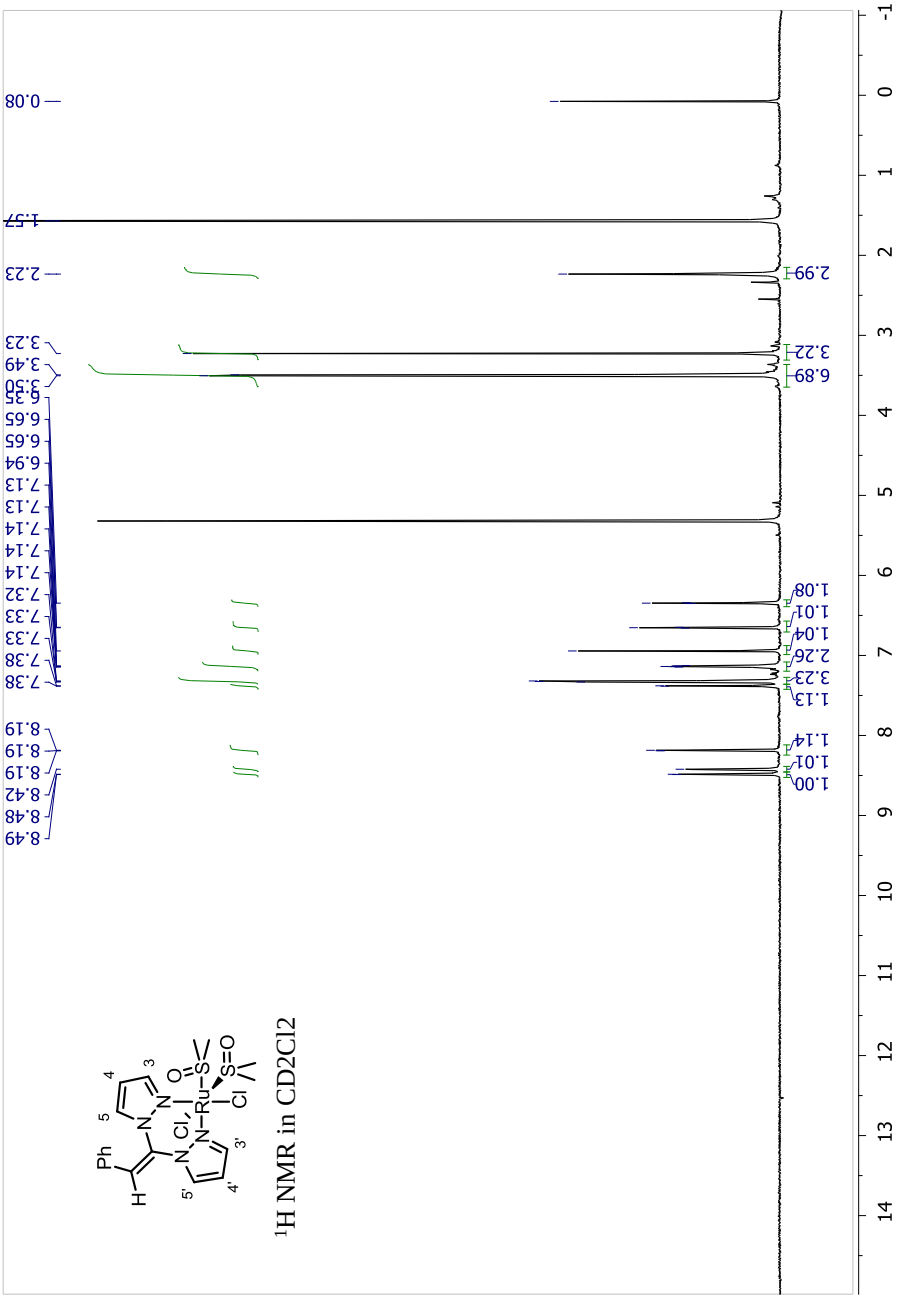

^{1}H NMR in CD2Cl2

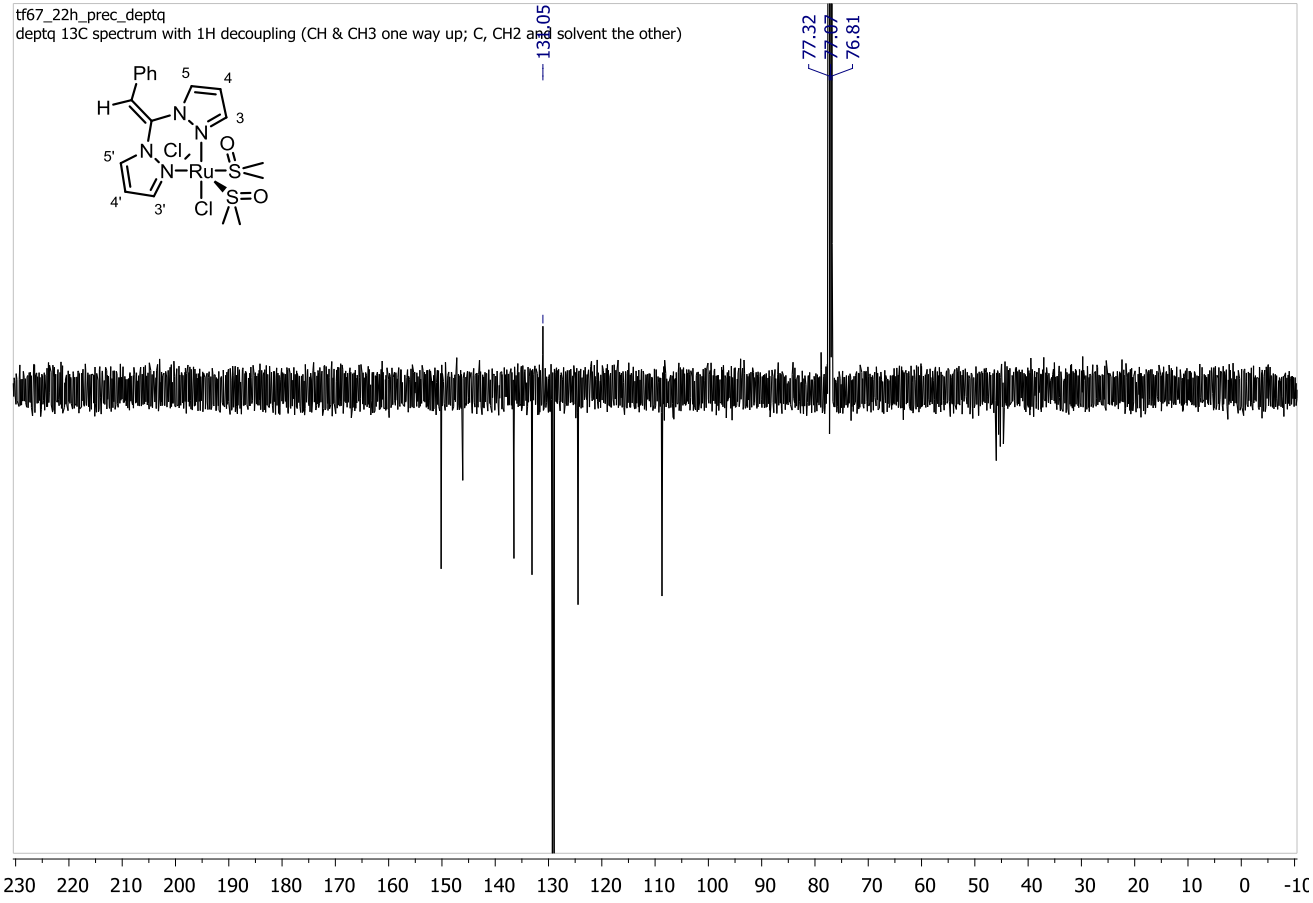
tf67_22h_prec_deptq
deptq 13C spectrum with 1H decoupling (CH & CH3 one way up; C, CH2 and solvent the other)
130.05
77.32
77.07
76.81
Ph
H
5
4
3
N
N
5'
N
Cl
O
N
Ru
S
4'
3'
Cl
S=O
230 220 210 200 190 180 170 160 150 140 130 120 110 100 90 80 70 60 50 40 30 20 10 0 -10

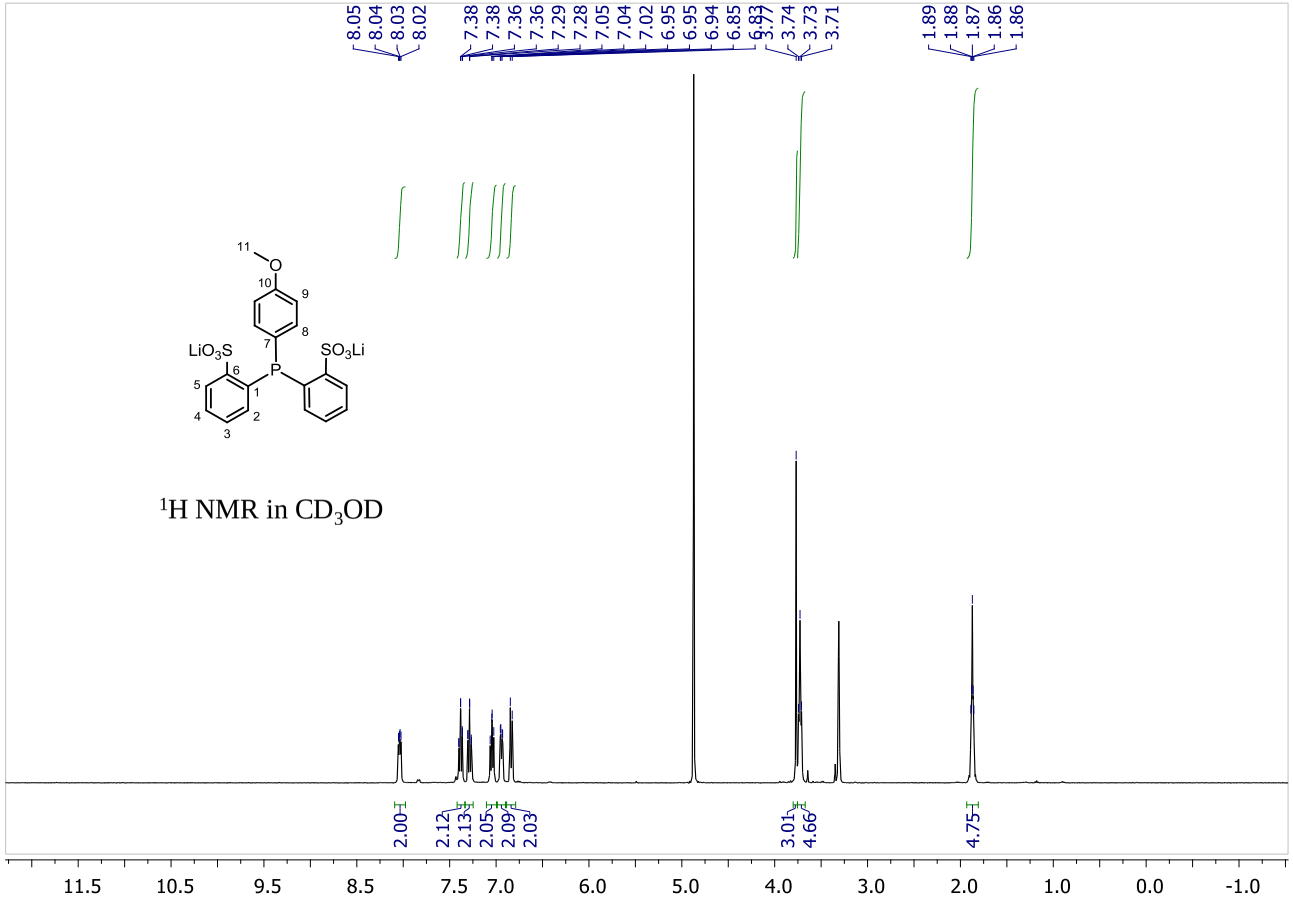
8.05
8.04
8.03
8.02
7.38
7.38
7.36
7.36
7.29
7.28
7.05
7.04
7.02
6.95
6.95
6.94
6.85
3.77
3.74
3.73
3.71
1.89
1.88
1.87
1.86
1.86
11
O
10
9
8
7
LiO3S
6
P
SO3Li
5
1
4
2
3
1H NMR in CD3OD
2.00
2.12
2.13
2.05
2.09
2.03
3.01
4.66
4.75
11.5
10.5
9.5
8.5
7.5
7.0
6.0
5.0
4.0
3.0
2.0
1.0
0.0
-1.0

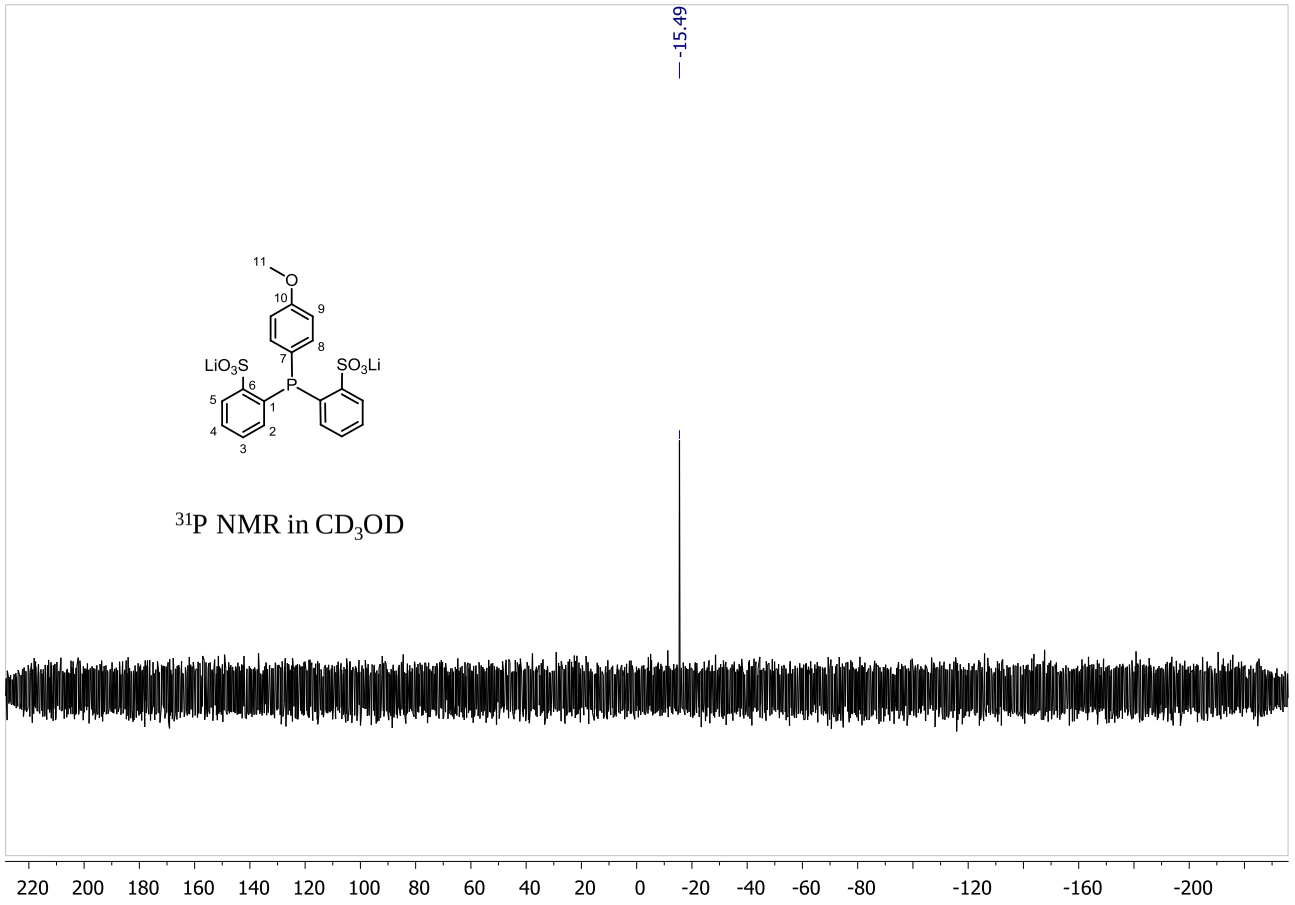
-15.49
11
O
10
9
8
7
LiO3S
SO3Li
P
6
5
1
4
2
3
31P NMR in CD3OD
220
200
180
160
140
120
100
80
60
40
20
0
-20
-40
-60
-80
-120
-160
-200

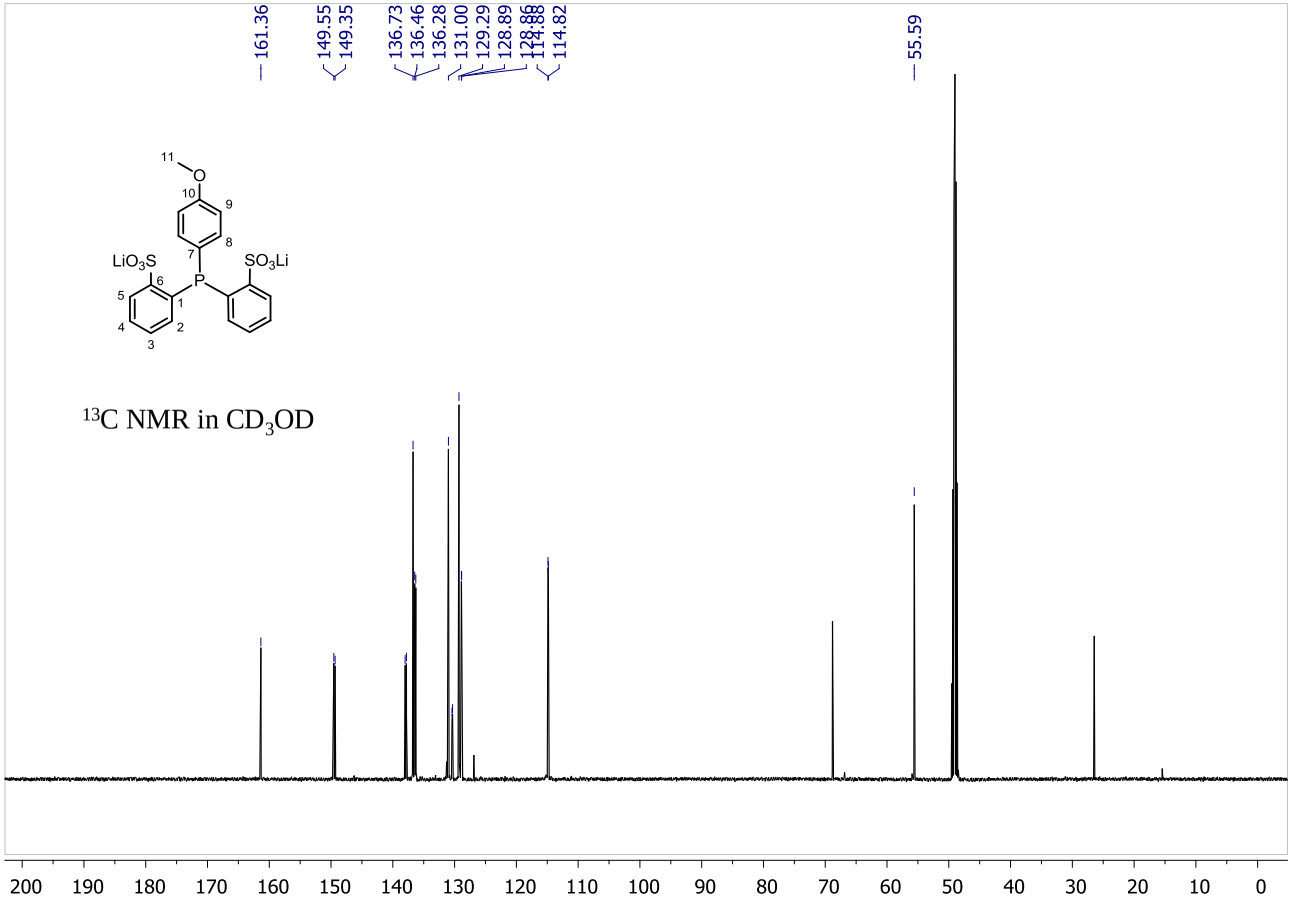
161.36
149.55
149.35
136.73
136.46
136.28
131.00
129.29
128.89
114.82
55.59
LiO3S
SO3Li
13C NMR in CD3OD
200 190 180 170 160 150 140 130 120 110 100 90 80 70 60 50 40 30 20 10 0

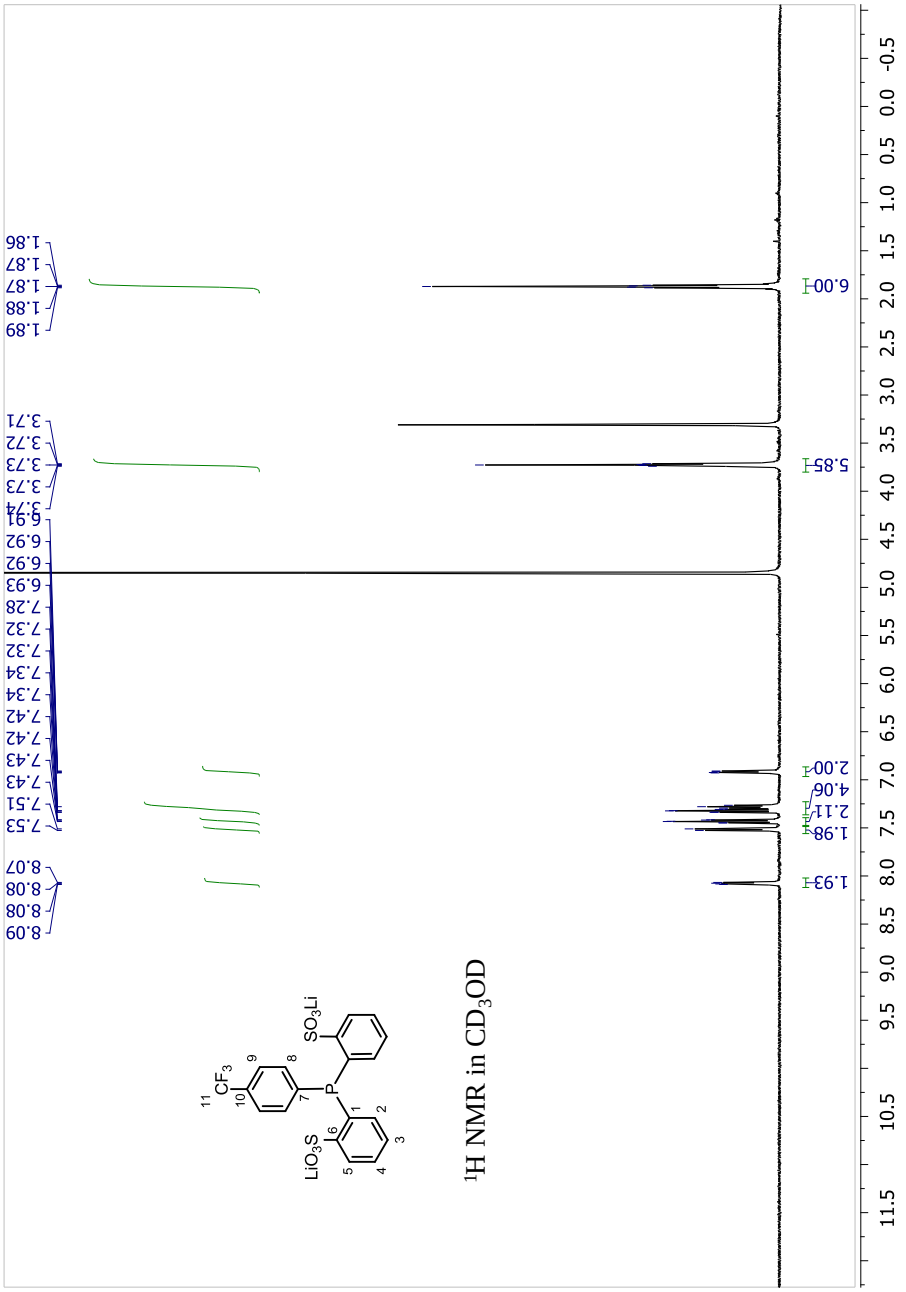
^{1}H NMR in CD_3OD
SO_3Li
CF_3
LiO_3S
P
1.89
1.88
1.87
1.87
1.86
3.74
3.73
3.73
3.72
3.71
6.91
6.92
6.92
6.93
7.28
7.32
7.32
7.34
7.34
7.42
7.42
7.43
7.43
7.51
7.53
8.07
8.08
8.08
8.09
6.00
5.85
2.00
4.06
2.11
1.98
1.93

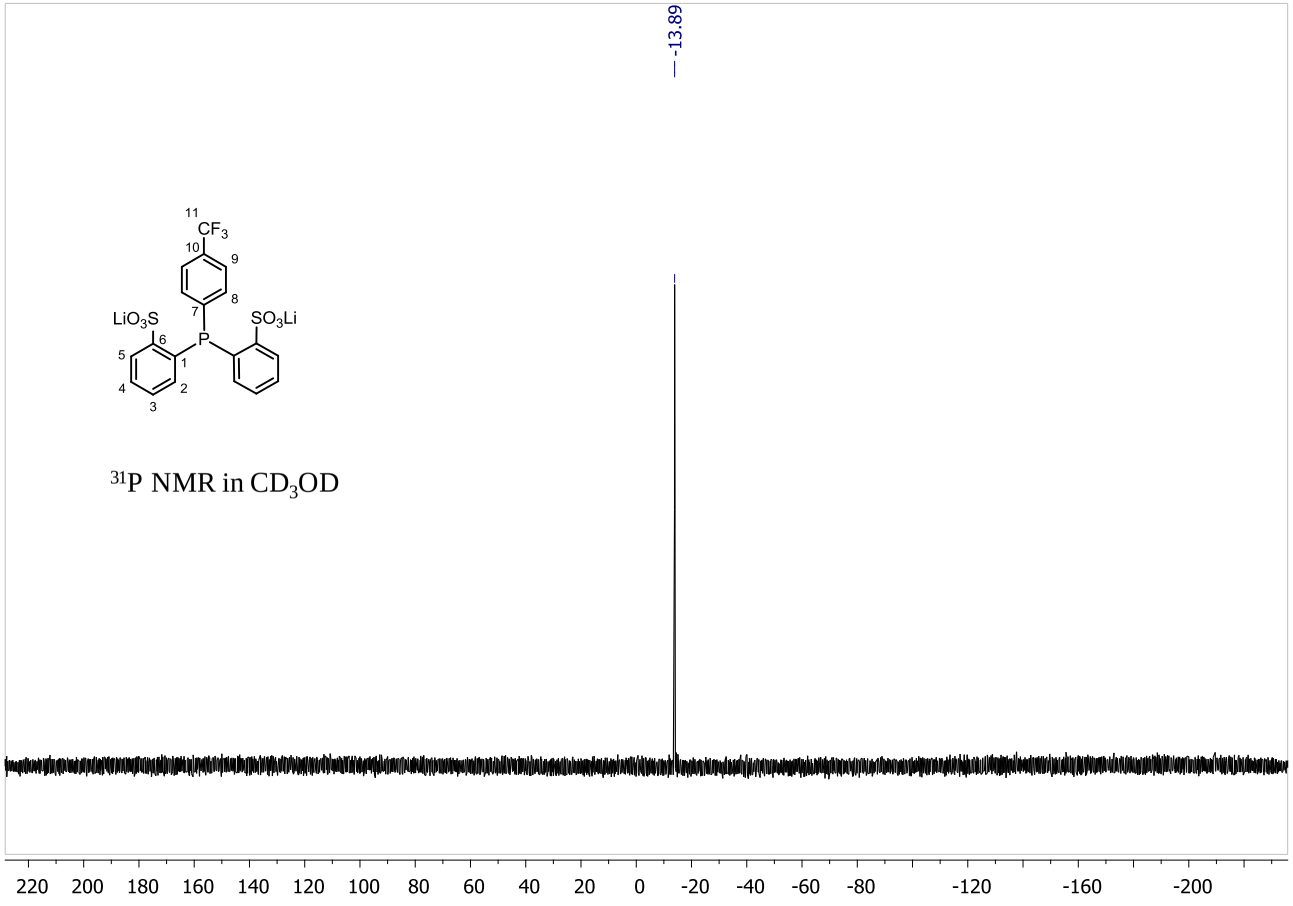
-13.89
11
CF3
10
9
8
7
LiO3S
6
P
SO3Li
5
1
4
2
3
31P NMR in CD3OD
220 200 180 160 140 120 100 80 60 40 20 0 -20 -40 -60 -80 -120 -160 -200

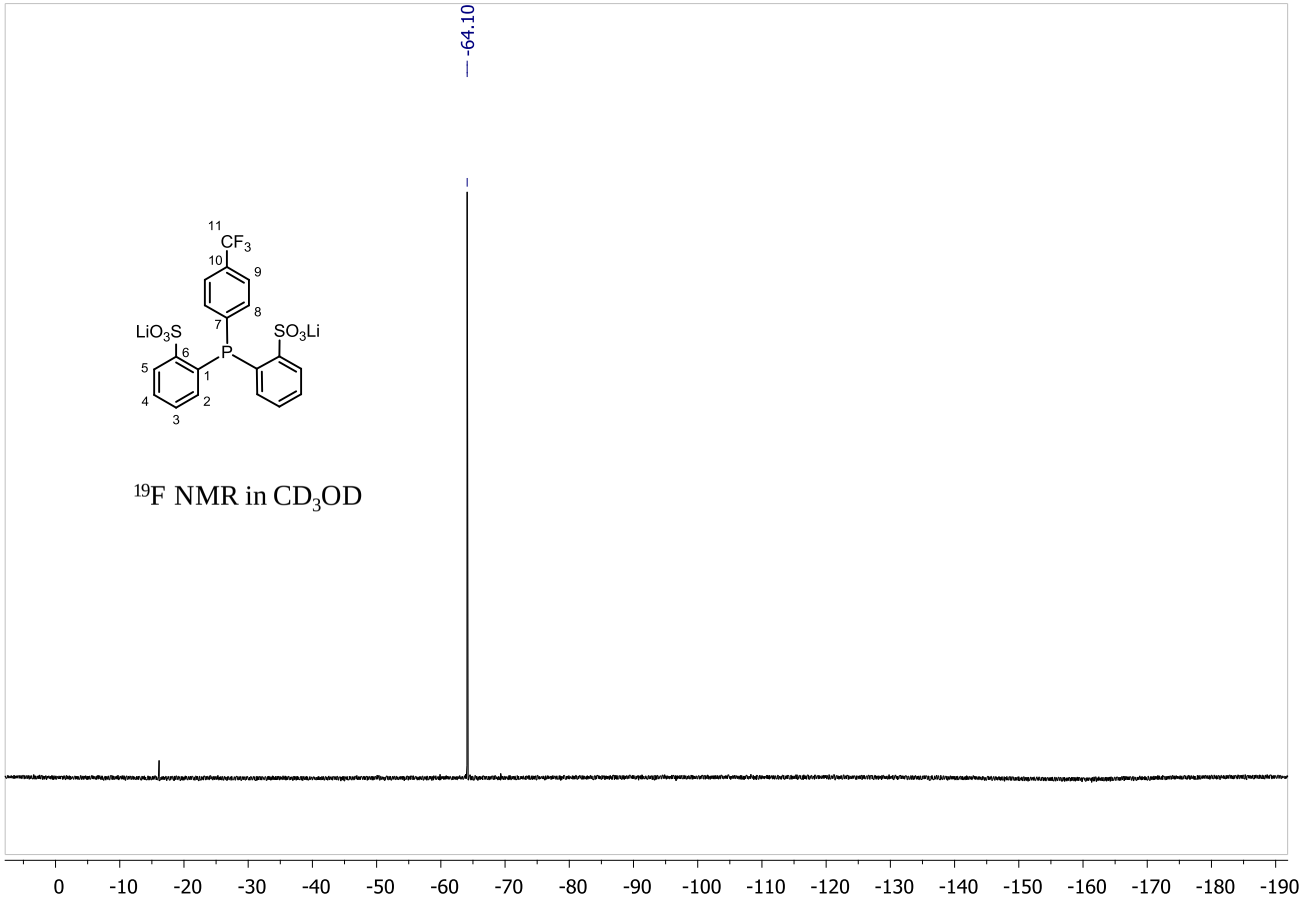
-64.10
11
CF3
10
9
8
7
LiO3S
6
P
SO3Li
5
1
4
2
3
19F NMR in CD3OD
0
-10
-20
-30
-40
-50
-60
-70
-80
-90
-100
-110
-120
-130
-140
-150
-160
-170
-180
-190

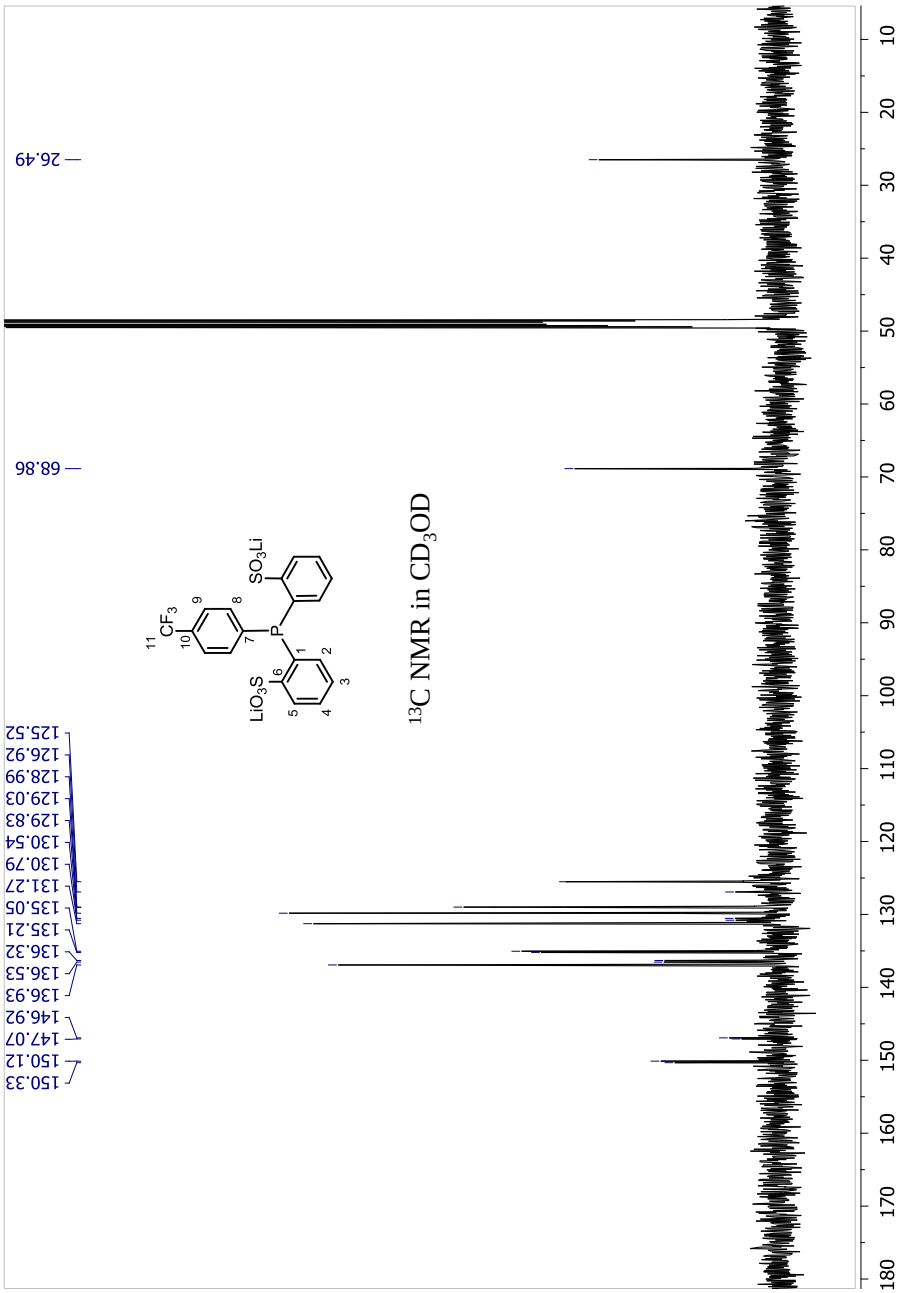
^{13}C NMR in CD_3OD
LiO_3S
SO_3Li
CF_3
P
26.49
68.86
125.52
126.92
128.99
129.03
129.83
130.54
130.79
131.27
135.05
135.21
136.32
136.53
136.93
146.92
147.07
150.12
150.33

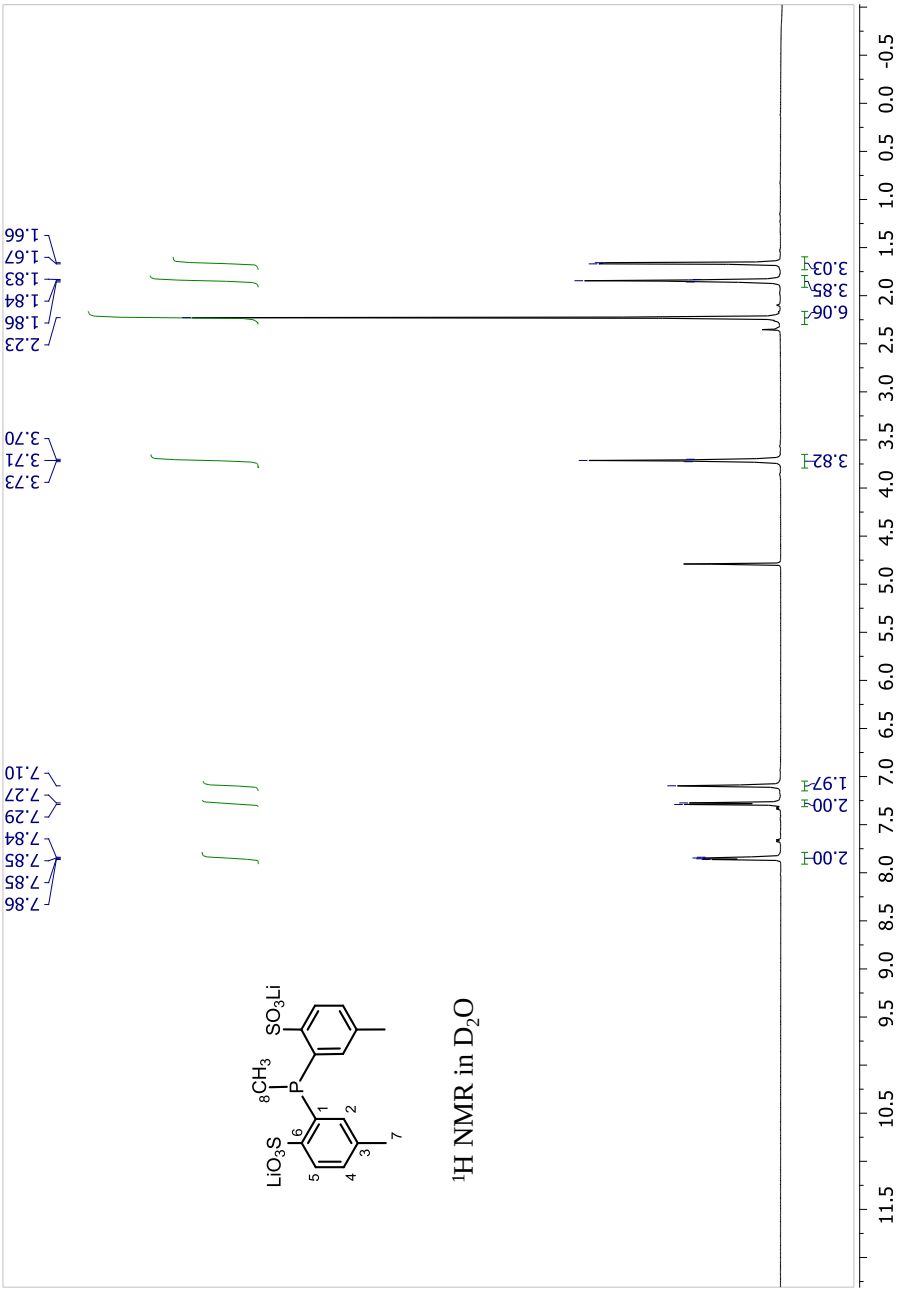
7.86
7.85
7.85
7.84
7.29
7.27
7.10
3.73
3.71
3.70
2.23
1.86
1.84
1.83
1.67
1.66
2.00
1.97
2.00
3.82
6.06
3.85
3.03
11.5
10.5
9.5
9.0
8.5
8.0
7.5
7.0
6.5
6.0
5.5
5.0
4.5
4.0
3.5
3.0
2.5
2.0
1.5
1.0
0.5
0.0
-0.5
LiO3S
SO3Li
8CH3
P
1
2
3
4
5
6
7

^{1}H NMR in D_2O

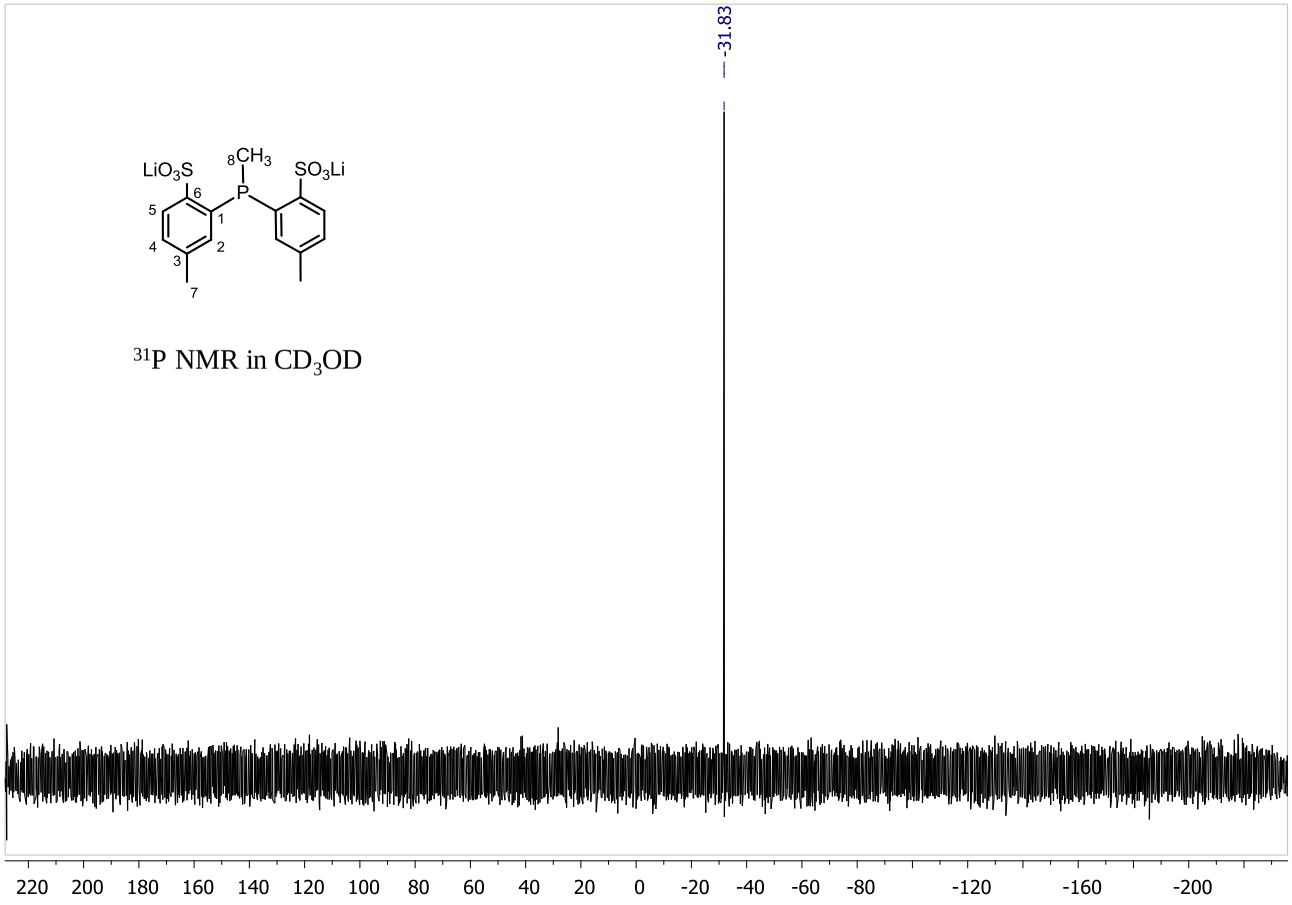
-31.83
LiO3S
8CH3
SO3Li
P
6
5
1
4
3
2
7
31P NMR in CD3OD
220 200 180 160 140 120 100 80 60 40 20 0 -20 -40 -60 -80 -120 -160 -200

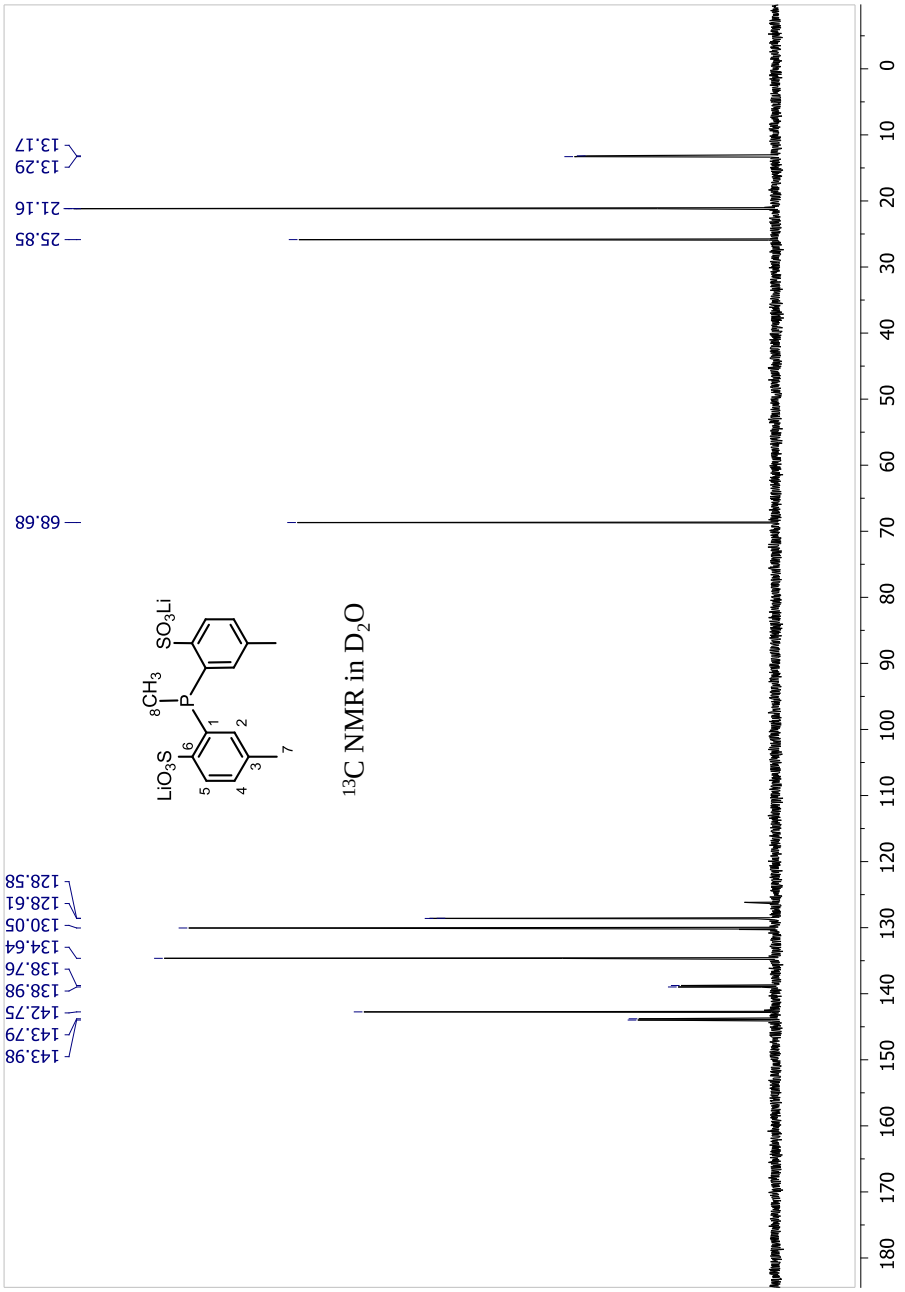
13.17
13.29
21.16
25.85
68.68
128.58
128.61
130.05
134.64
138.76
138.98
142.75
143.79
143.98
^{13}C NMR in D_2O
LiO_3S
SO_3Li
$^8CH_3$
P
1
2
3
4
5
6
7
0
10
20
30
40
50
60
70
80
90
100
110
120
130
140
150
160
170
180

^{1}H NMR in CD_3OD
SO_3Li
LiO_3S
P
1
2
3
4
5
6
7
8
9
8.00
7.99
7.98
7.97
7.70
7.23
7.21
3.74
3.73
3.71
2.35
1.28
1.25
1.97
2.00
1.86
1.56
1.63
5.87
8.59

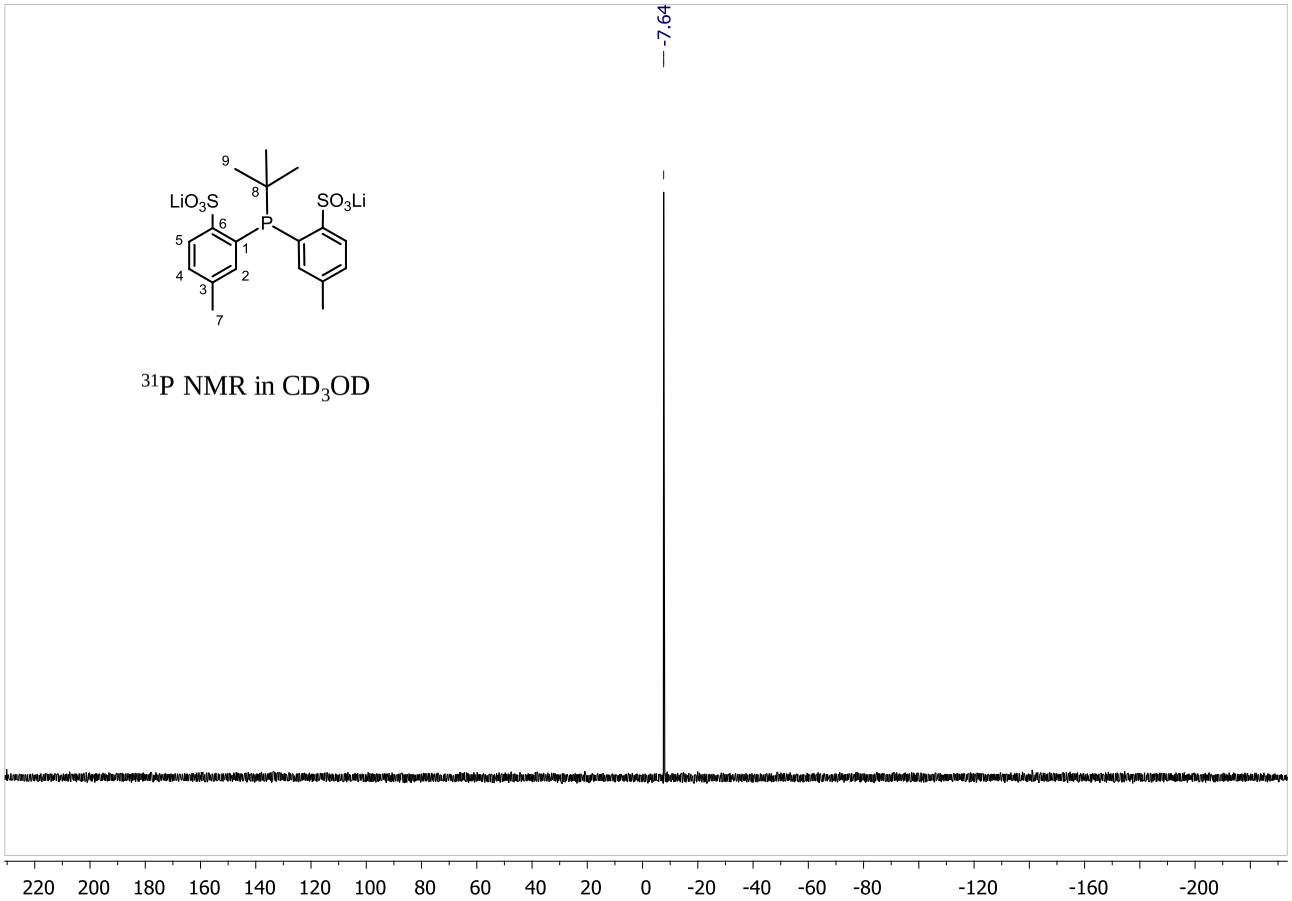

^{31}P NMR in CD_3OD

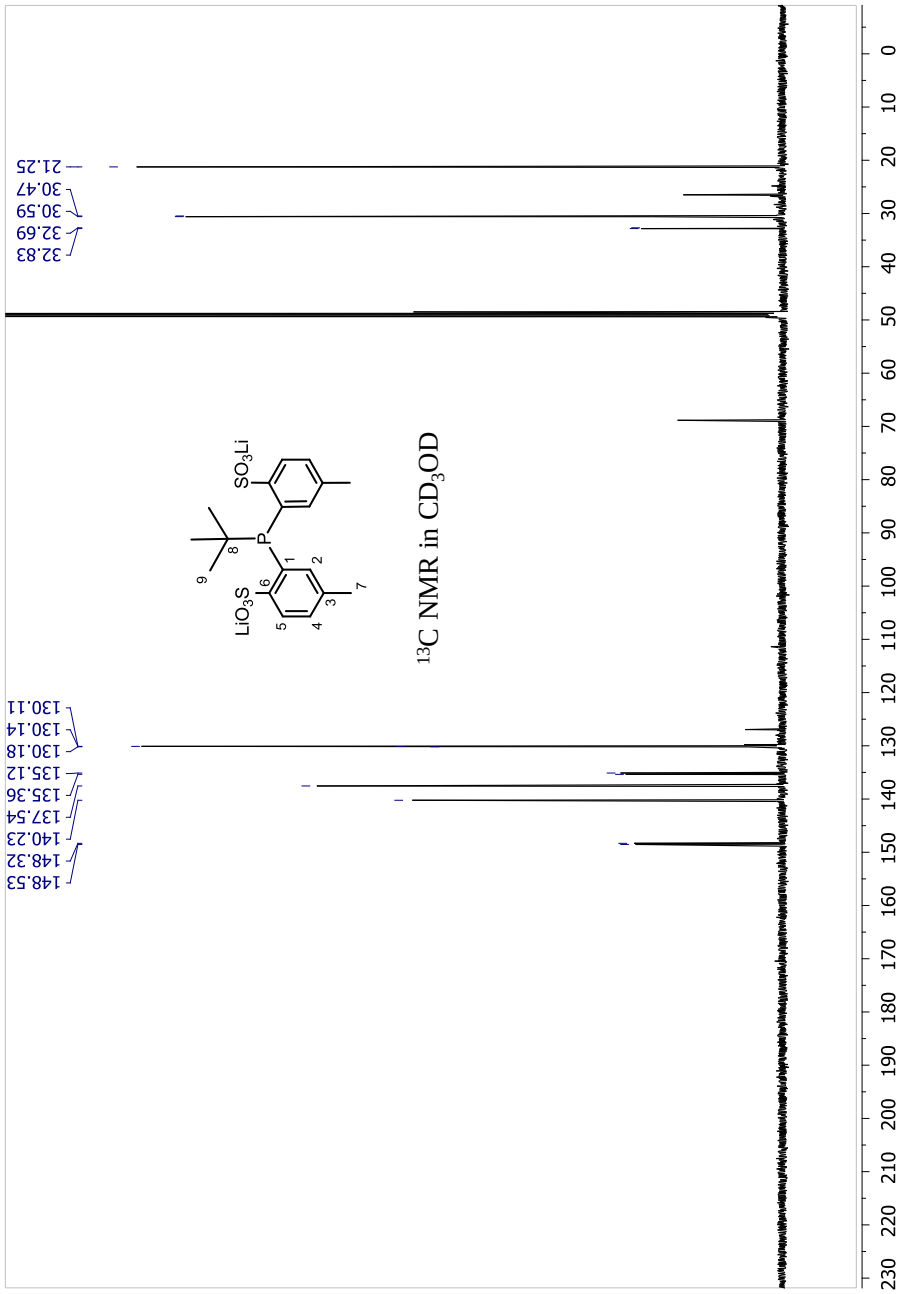
148.53
148.32
140.23
137.54
135.36
135.12
130.18
130.14
130.11
32.83
32.69
30.59
30.47
21.25
^{13}C NMR in CD_3OD
SO_3Li
LiO_3S
P
0 10 20 30 40 50 60 70 80 90 100 110 120 130 140 150 160 170 180 190 200 210 220 230

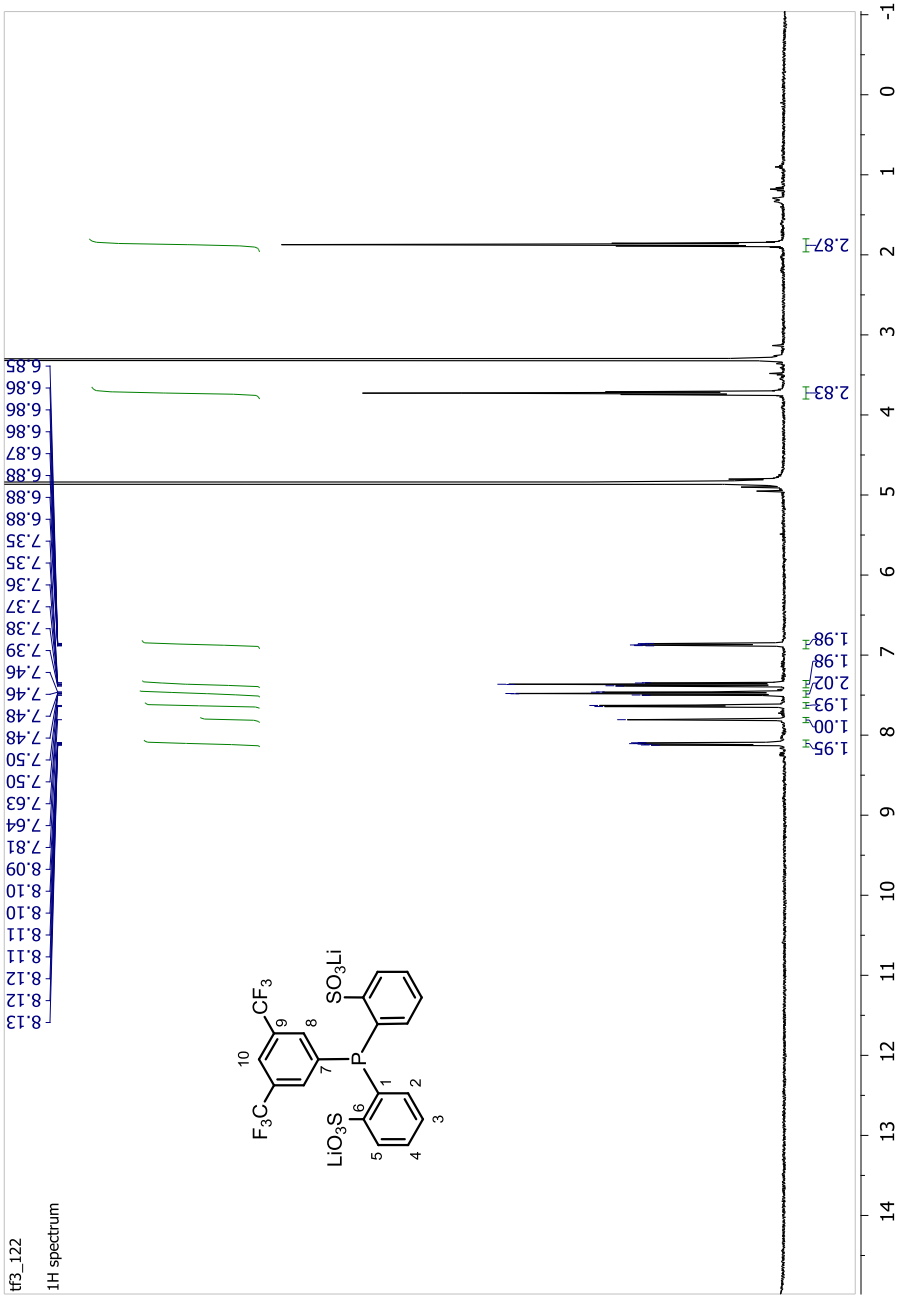
tf3_122
1H spectrum
2.87
2.83
1.98
1.98
2.02
1.93
1.00
1.95


tf3_122
19F spectrum
-64.41
F3C
CF3
LiO3S
SO3Li
P
10
9
8
7
6
5
4
3
2
1
10 0 -10 -20 -30 -40 -50 -60 -70 -80 -90 -100 -110 -120 -130 -140 -150 -160 -170 -180

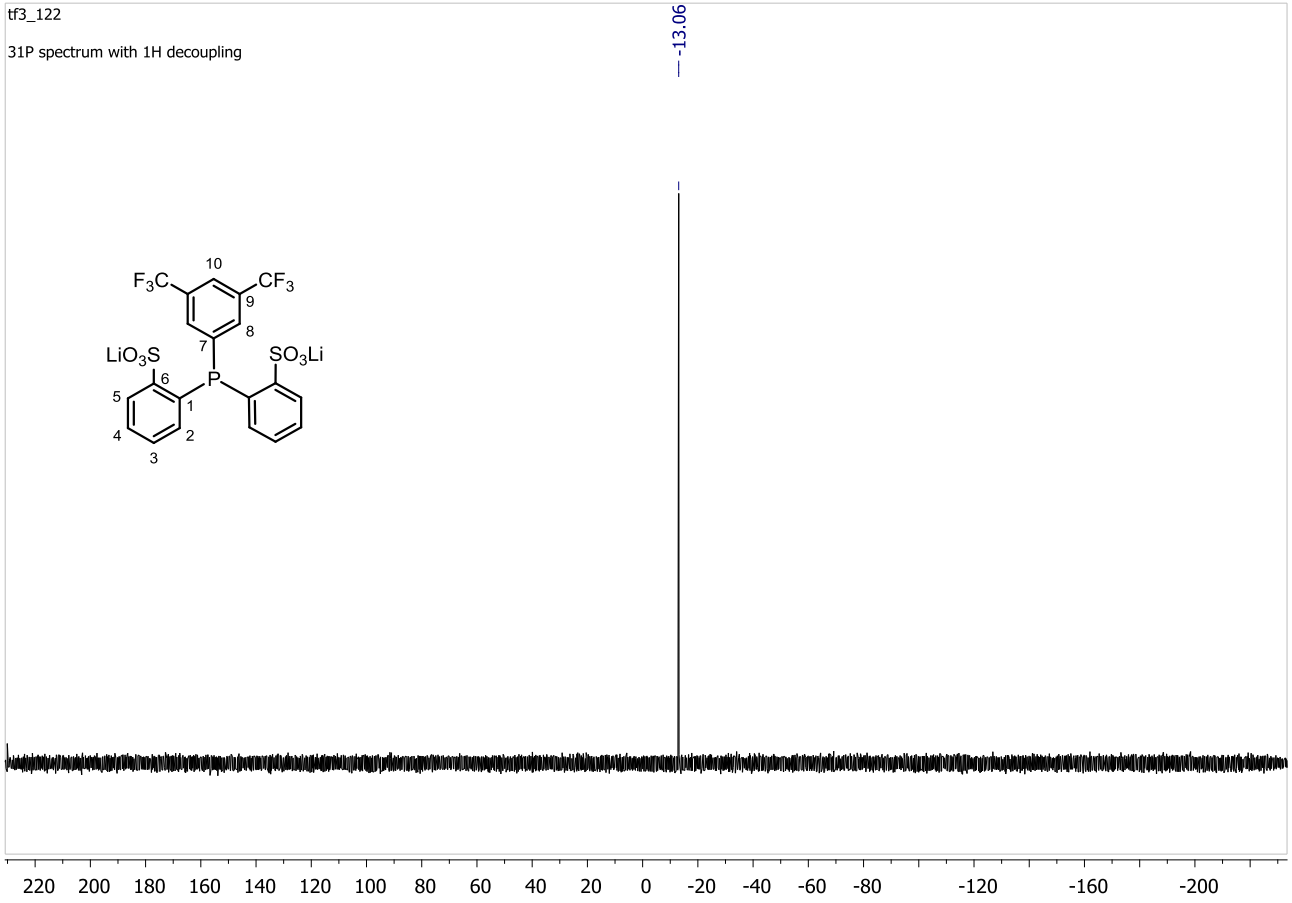
tf3_122
31P spectrum with 1H decoupling
-13.06
F3C
CF3
LiO3S
SO3Li
P
10
9
8
7
6
5
4
3
2
1
220 200 180 160 140 120 100 80 60 40 20 0 -20 -40 -60 -80 -120 -160 -200

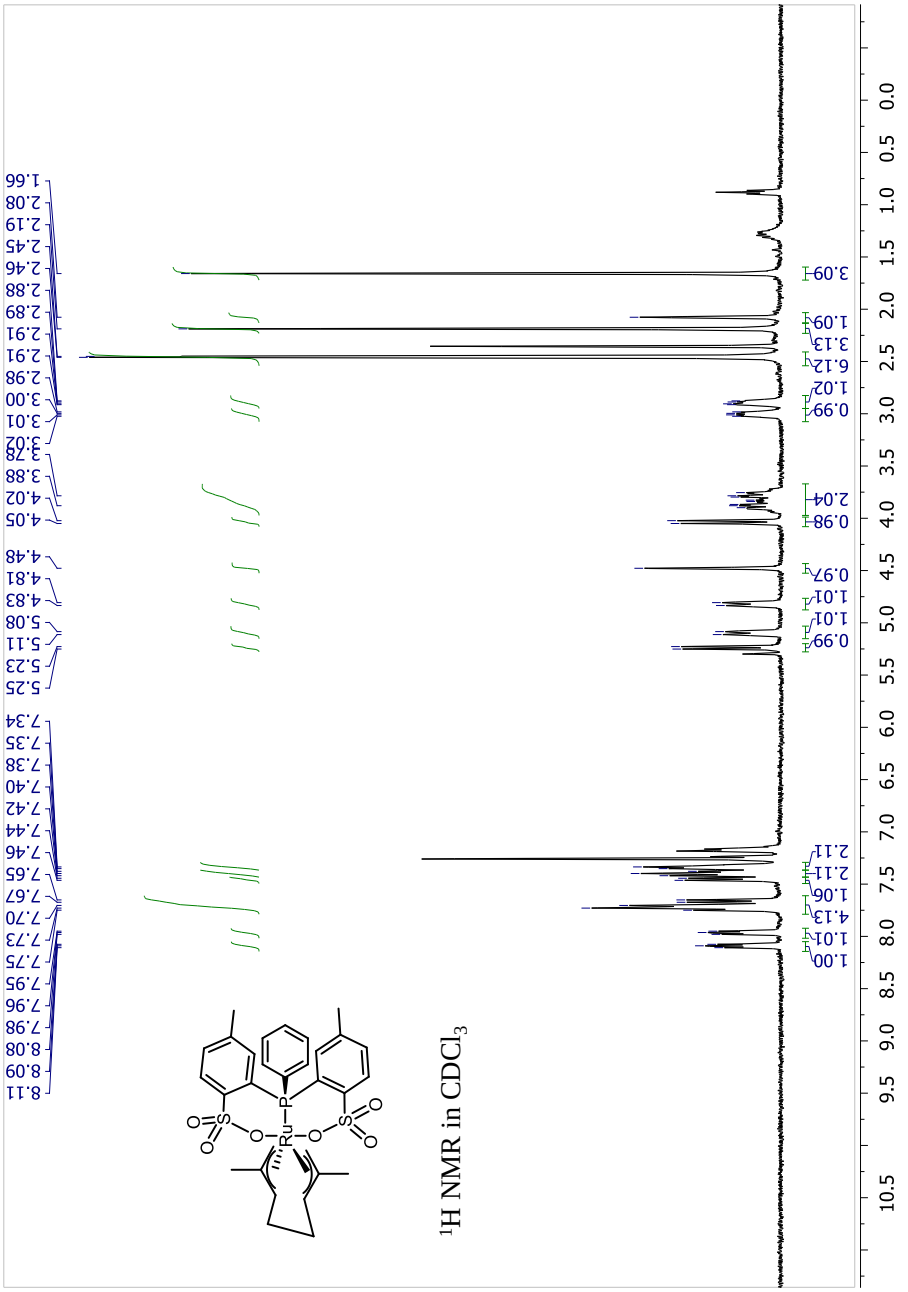
^{1}H NMR in $CDCl_3$

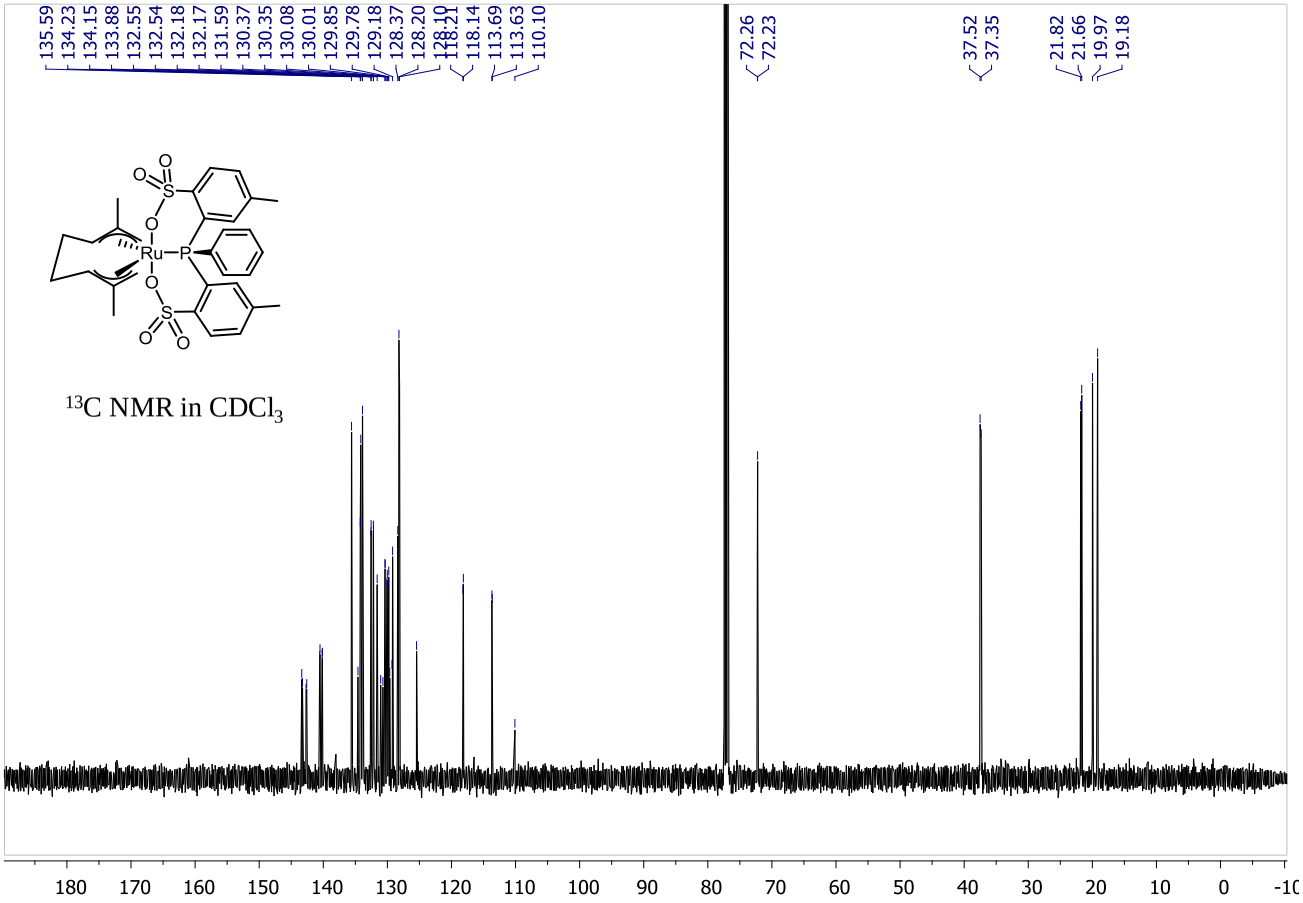
135.59
134.23
134.15
133.88
132.55
132.54
132.18
132.17
131.59
130.37
130.35
130.08
130.01
129.85
129.78
129.18
128.37
128.20
118.14
113.69
113.63
110.10
72.26
72.23
37.52
37.35
21.82
21.66
19.97
19.18
Ru
P
O
S
^{13}C NMR in $CDCl_3$
180
170
160
150
140
130
120
110
100
90
80
70
60
50
40
30
20
10
0

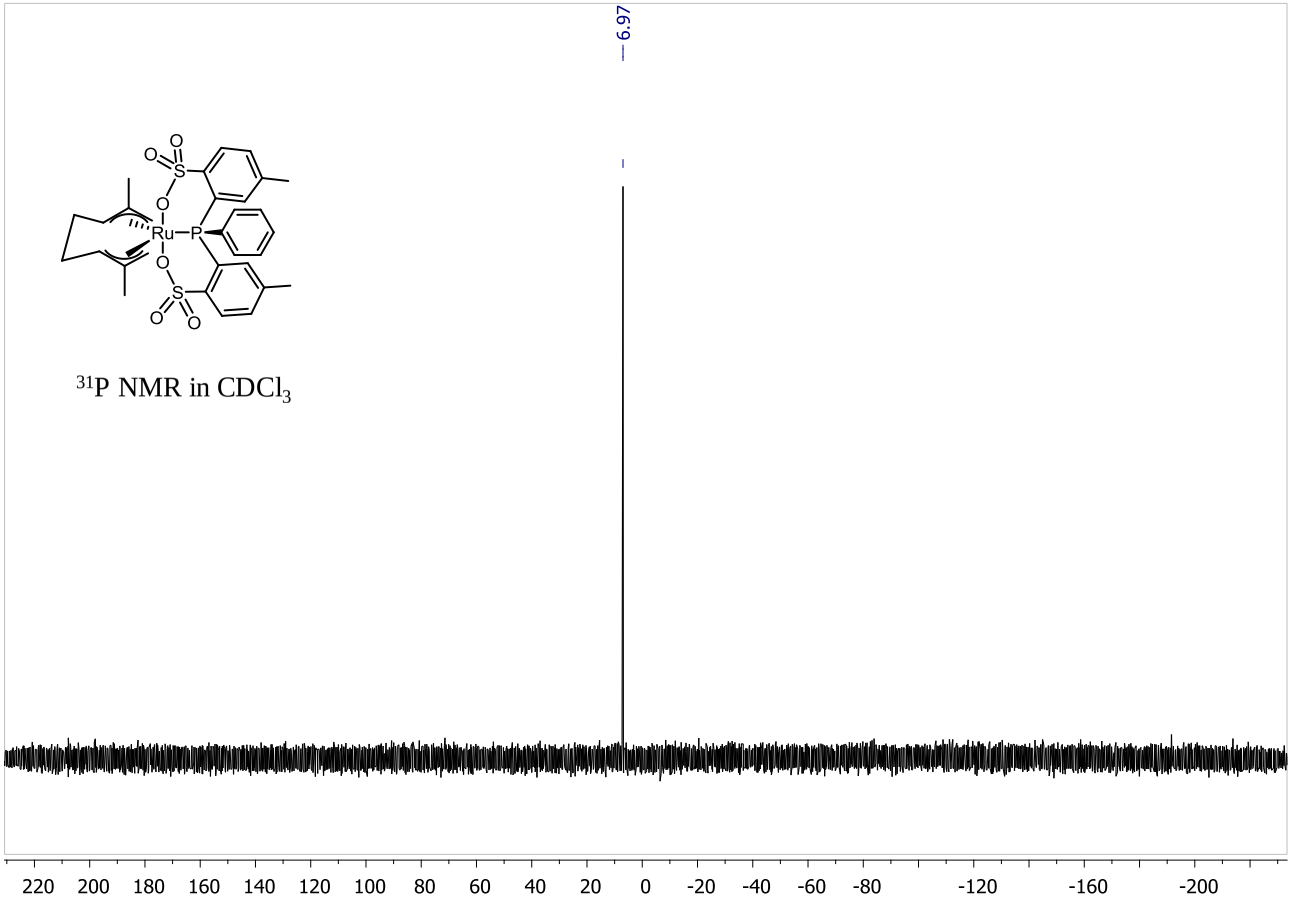

^{31}P NMR in $CDCl_3$

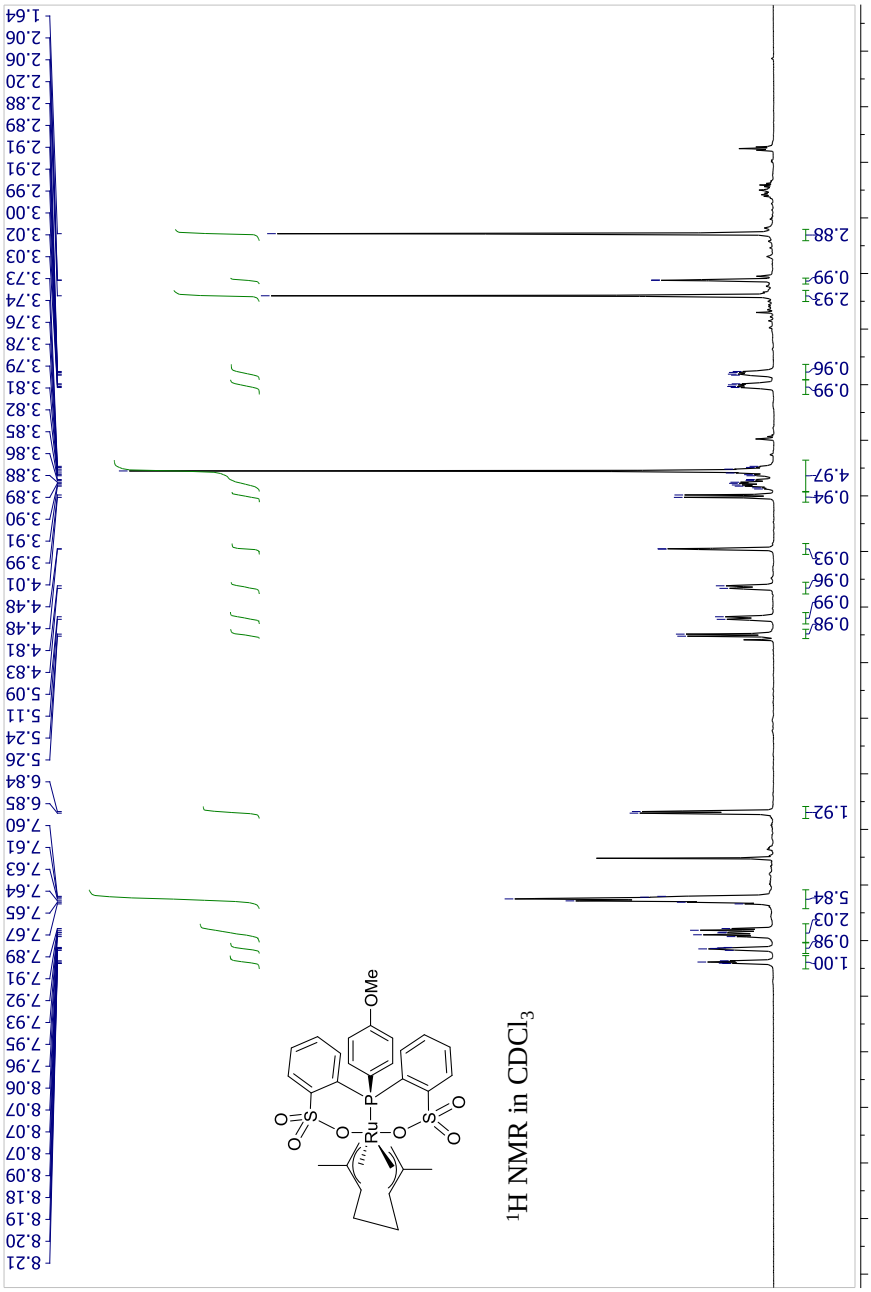
OMe
P
Ru
O
S
O
^{1}H NMR in $CDCl_3$

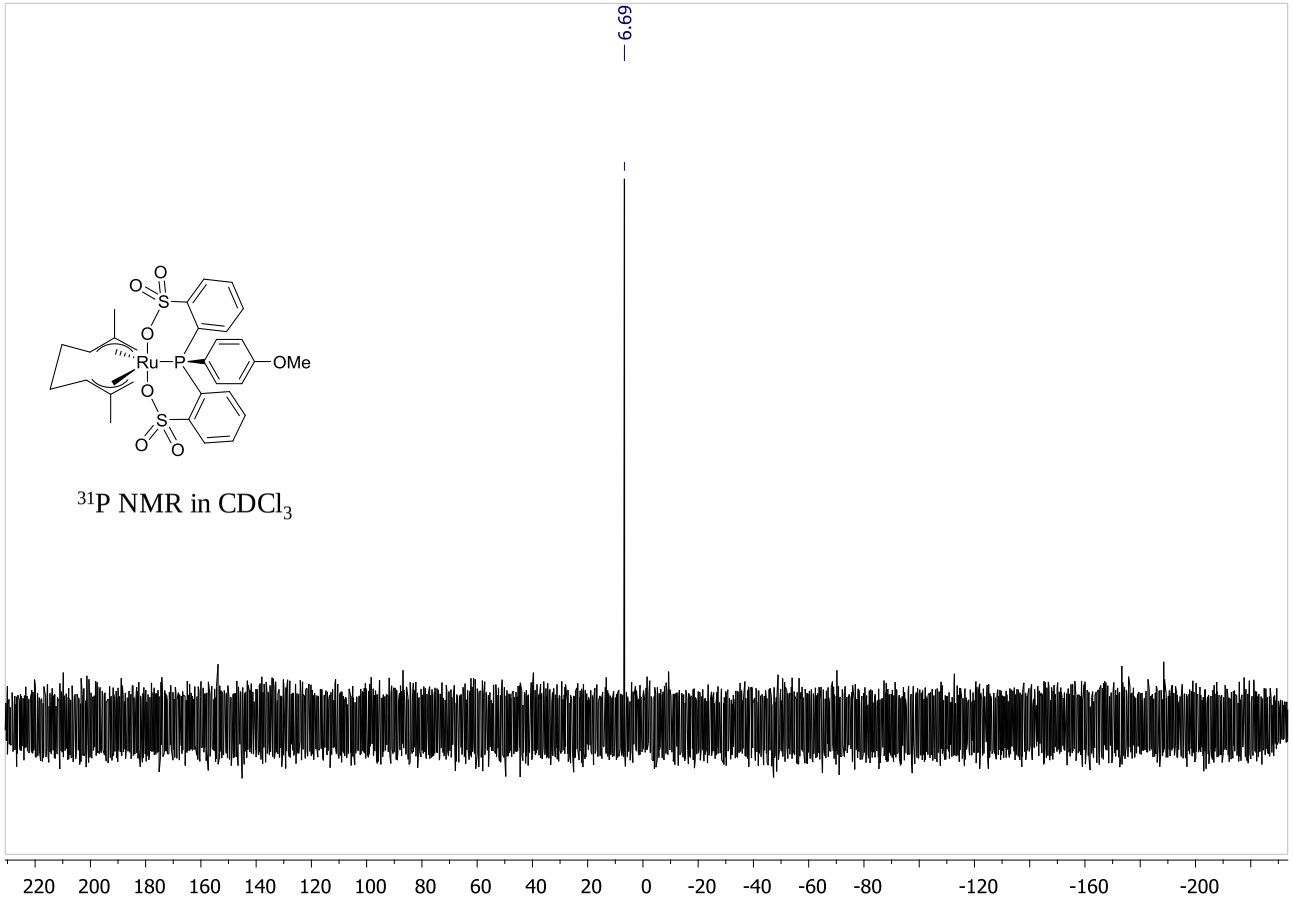

^{31}P NMR in $CDCl_3$

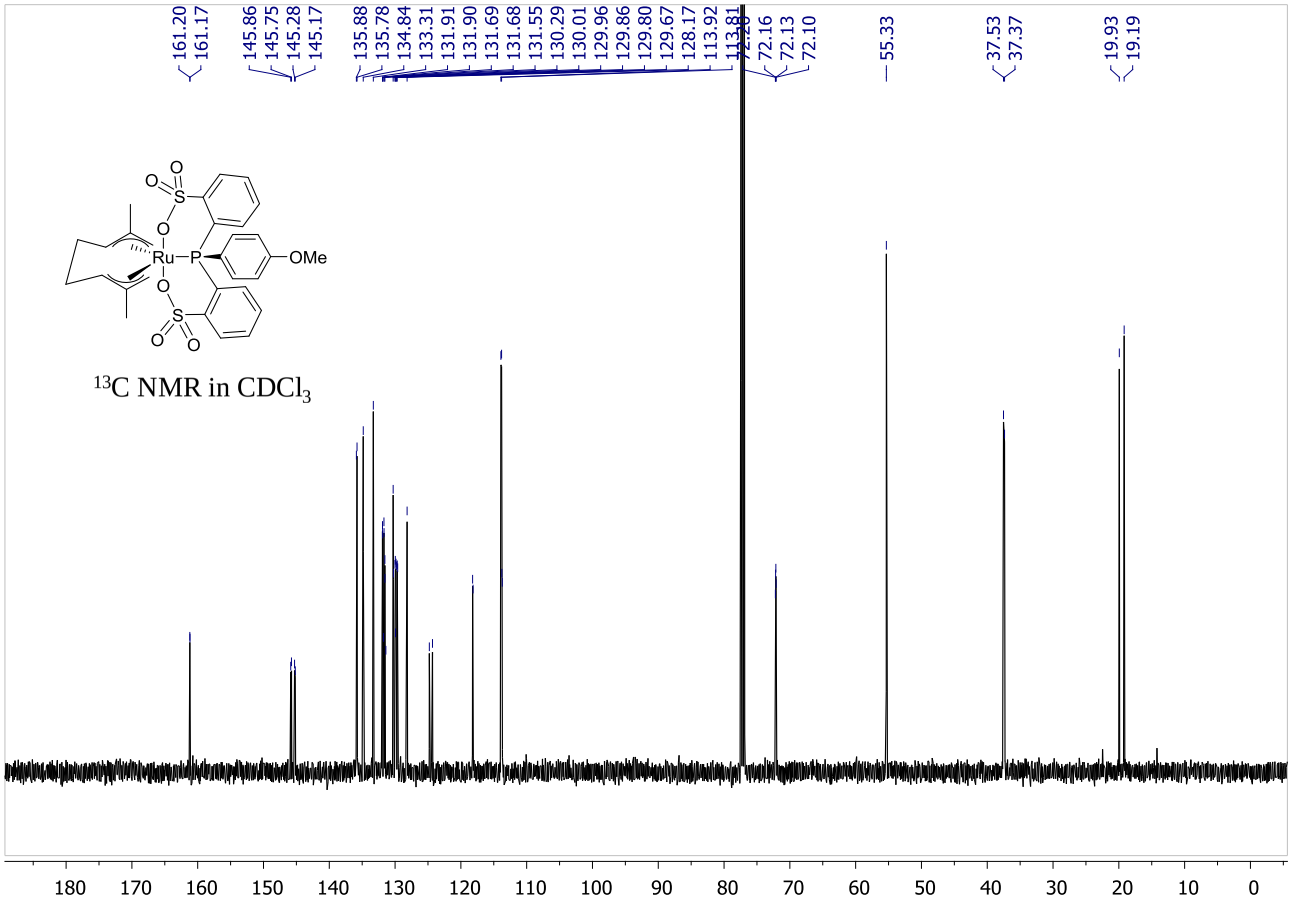

^{13}C NMR in $CDCl_3$

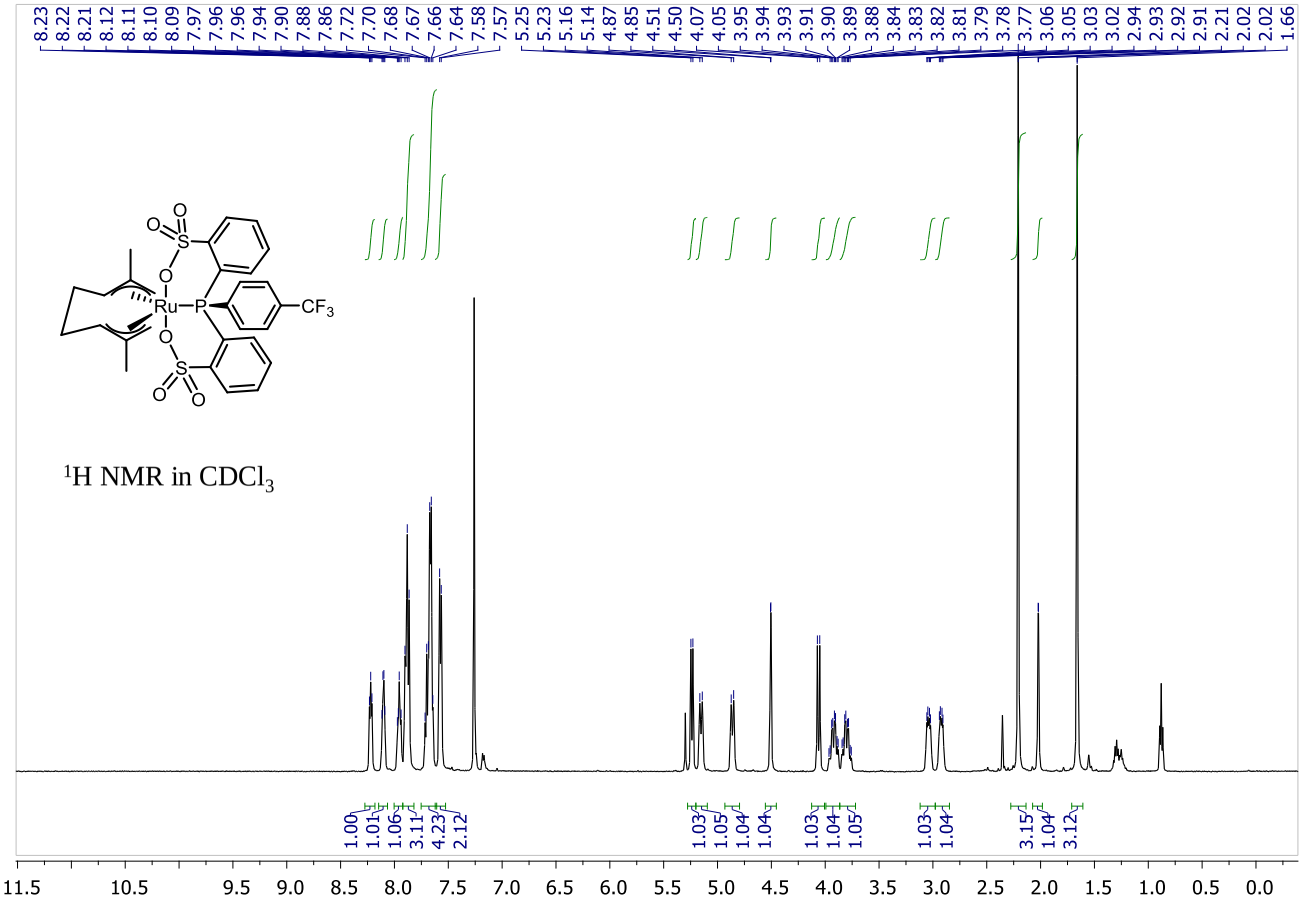
8.23 8.22 8.21 8.12 8.11 8.10 8.09 7.97 7.96 7.96 7.94 7.90 7.88 7.86 7.72 7.70 7.68 7.67 7.66 7.64 7.58 7.57
5.25 5.23 5.16 5.14 4.87 4.85 4.51 4.50 4.07 4.05 3.95 3.94 3.93 3.91 3.90 3.89 3.88 3.84 3.83 3.82 3.81 3.79 3.78 3.77 3.06 3.05 3.03 3.02 2.94 2.93 2.92 2.91 2.21 2.02 2.02 1.66
O
S
O
O
Ru
P
CF3
O
S
O
O
1H NMR in CDCl3
1.00 1.01 1.06 3.11 4.23 2.12
1.03 1.05 1.04 1.04
1.03 1.04 1.05
1.03 1.04
3.15 1.04 3.12
11.5 10.5 9.5 9.0 8.5 8.0 7.5 7.0 6.5 6.0 5.5 5.0 4.5 4.0 3.5 3.0 2.5 2.0 1.5 1.0 0.5 0.0

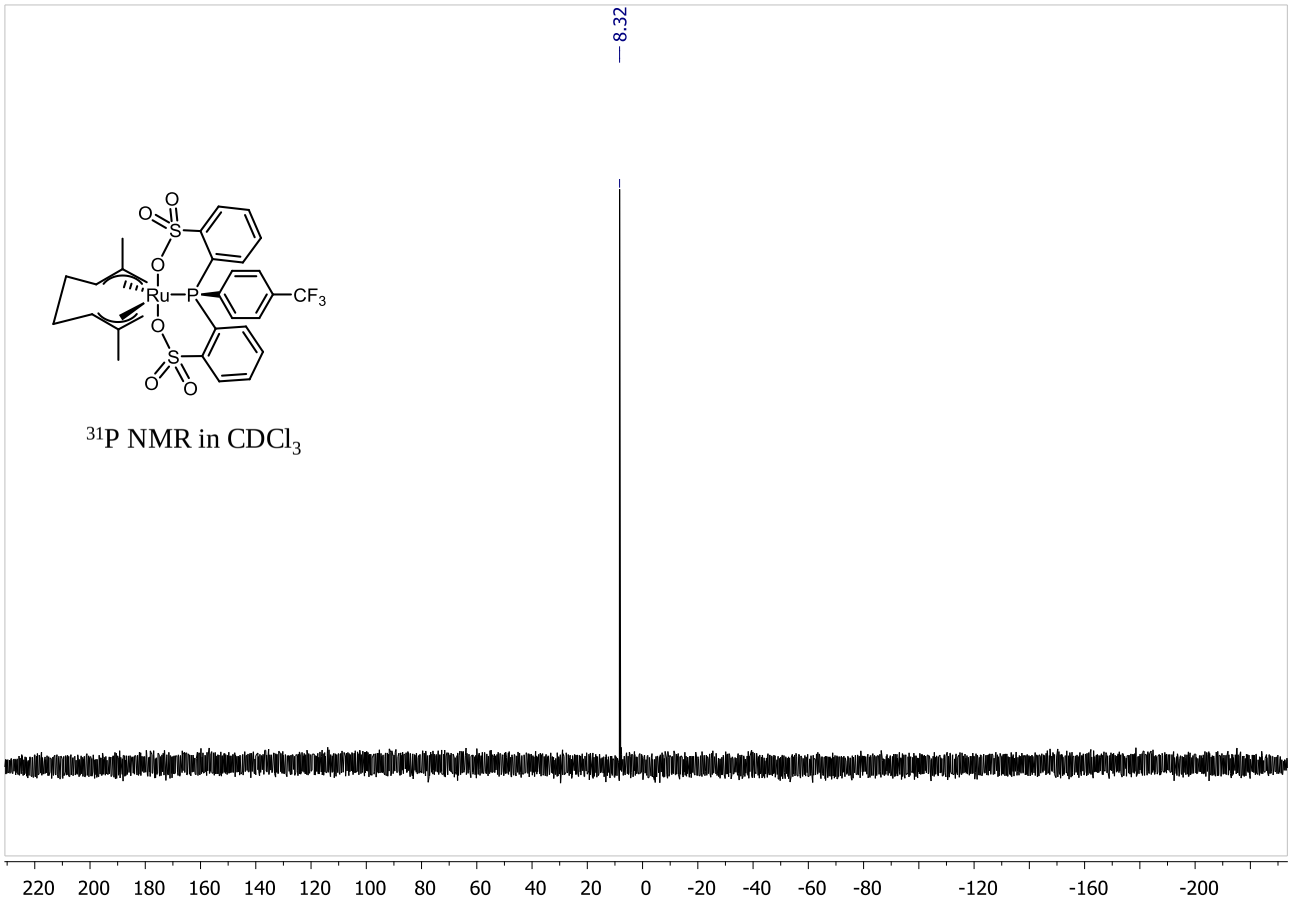

^{31}P NMR in $CDCl_3$

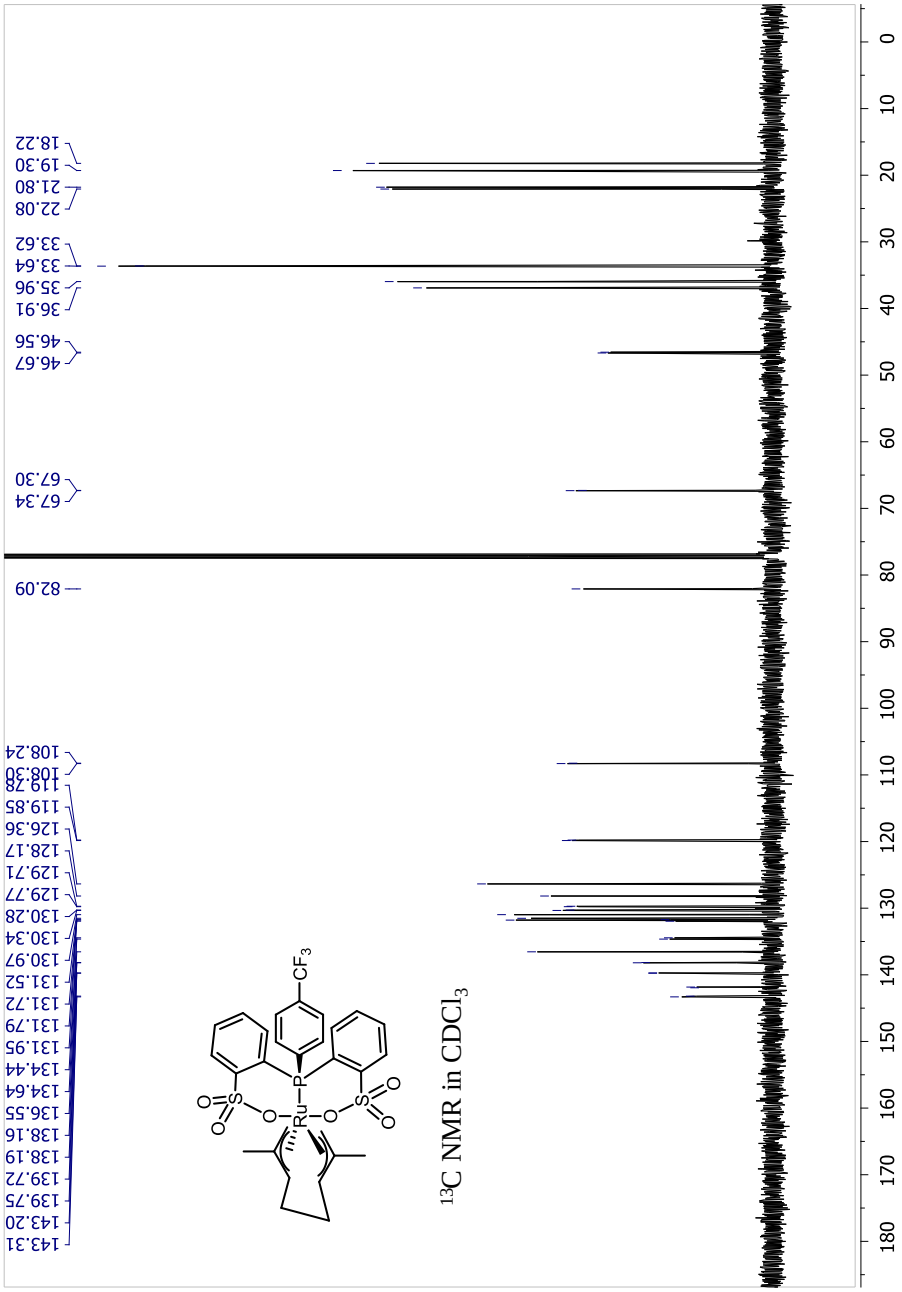
143.31
143.20
139.75
139.72
138.19
138.16
136.55
134.64
134.44
131.95
131.79
131.72
131.52
130.97
130.34
130.28
129.77
129.71
128.17
126.36
119.85
119.78
108.30
108.24
82.09
67.34
67.30
46.67
46.56
36.91
35.96
33.64
33.62
22.08
21.80
19.30
18.22
0
10
20
30
40
50
60
70
80
90
100
110
120
130
140
150
160
170
180
^{13}C NMR in $CDCl_3$
CF3
P
Ru
O
S

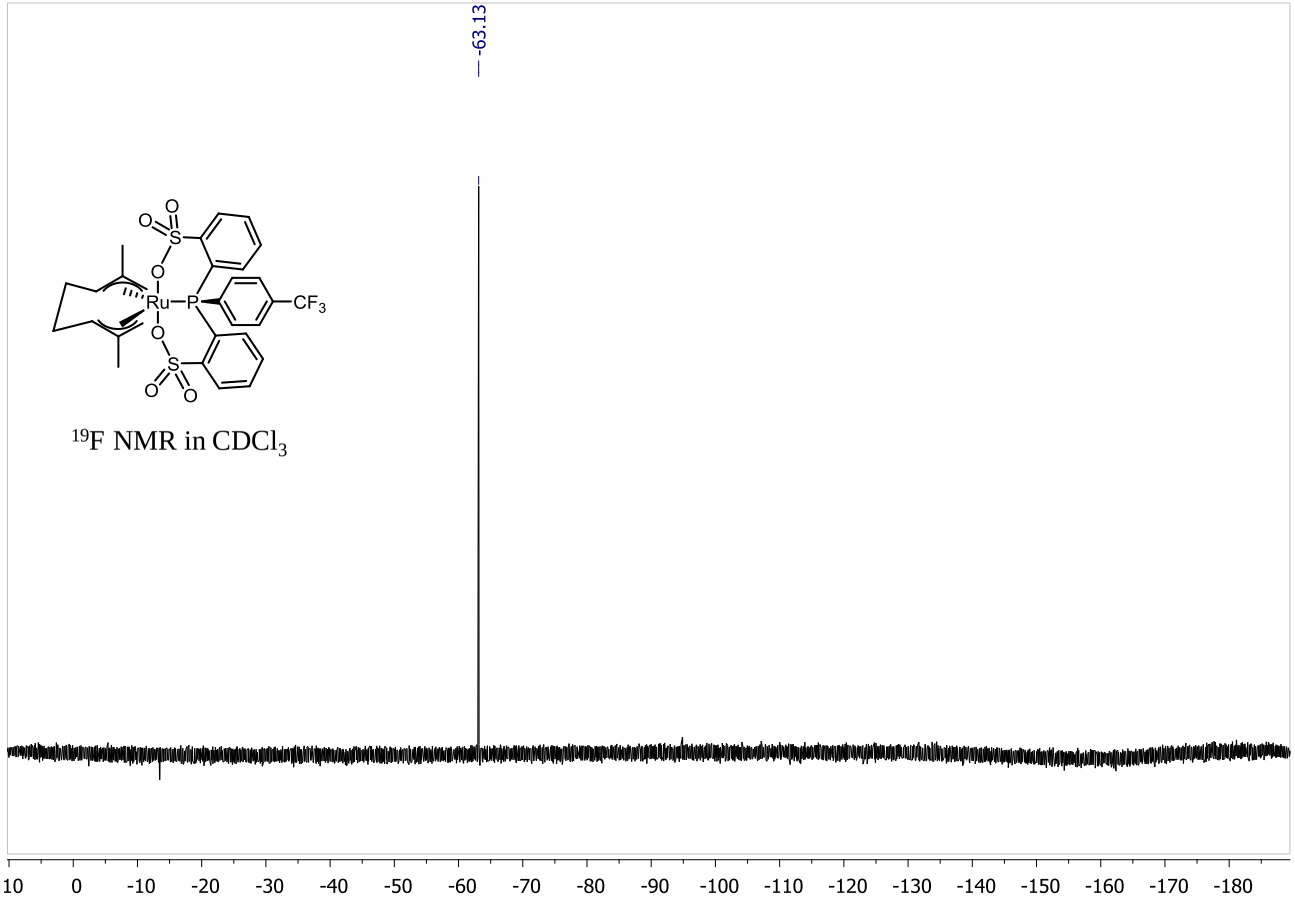

^{19}F NMR in $CDCl_3$

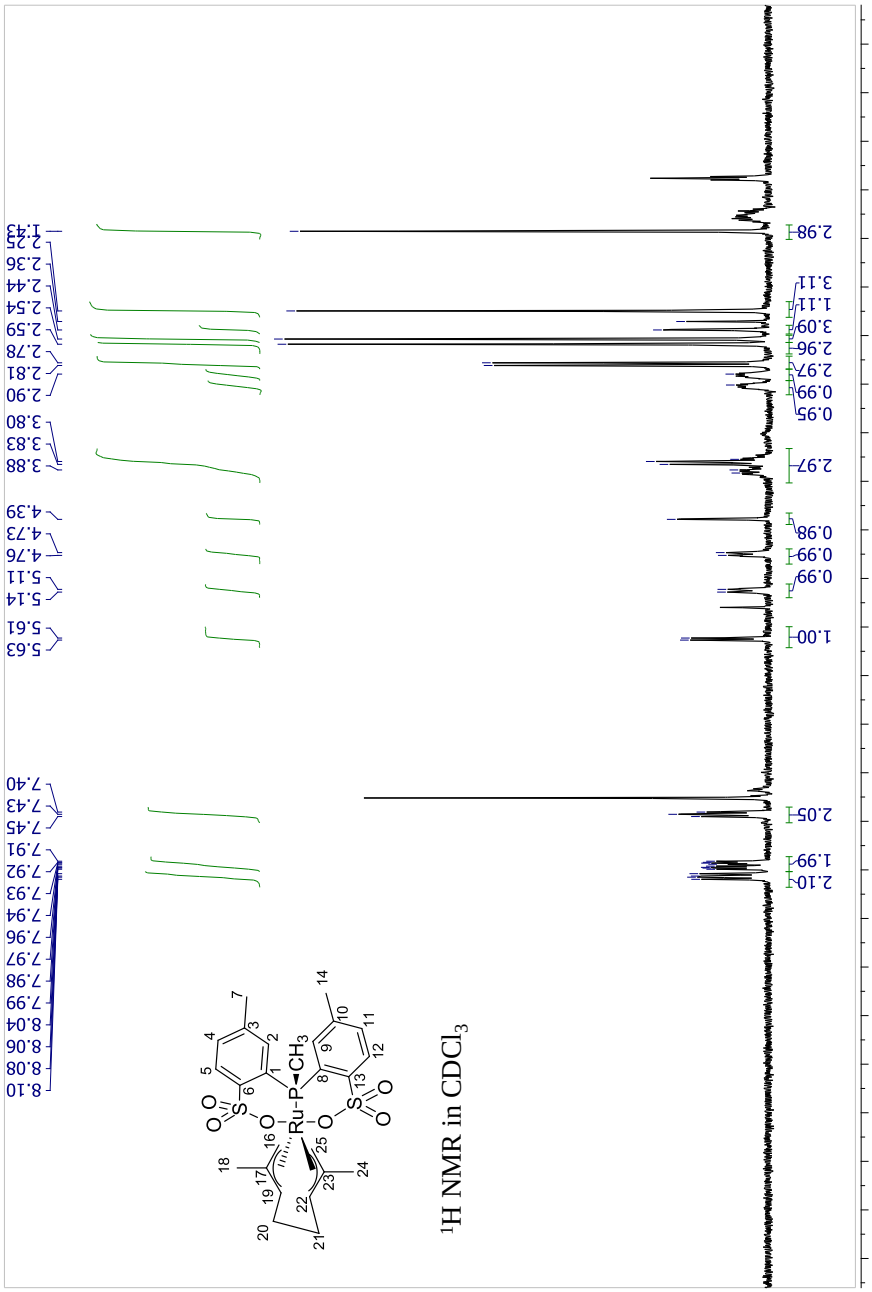
^{1}H NMR in $CDCl_3$

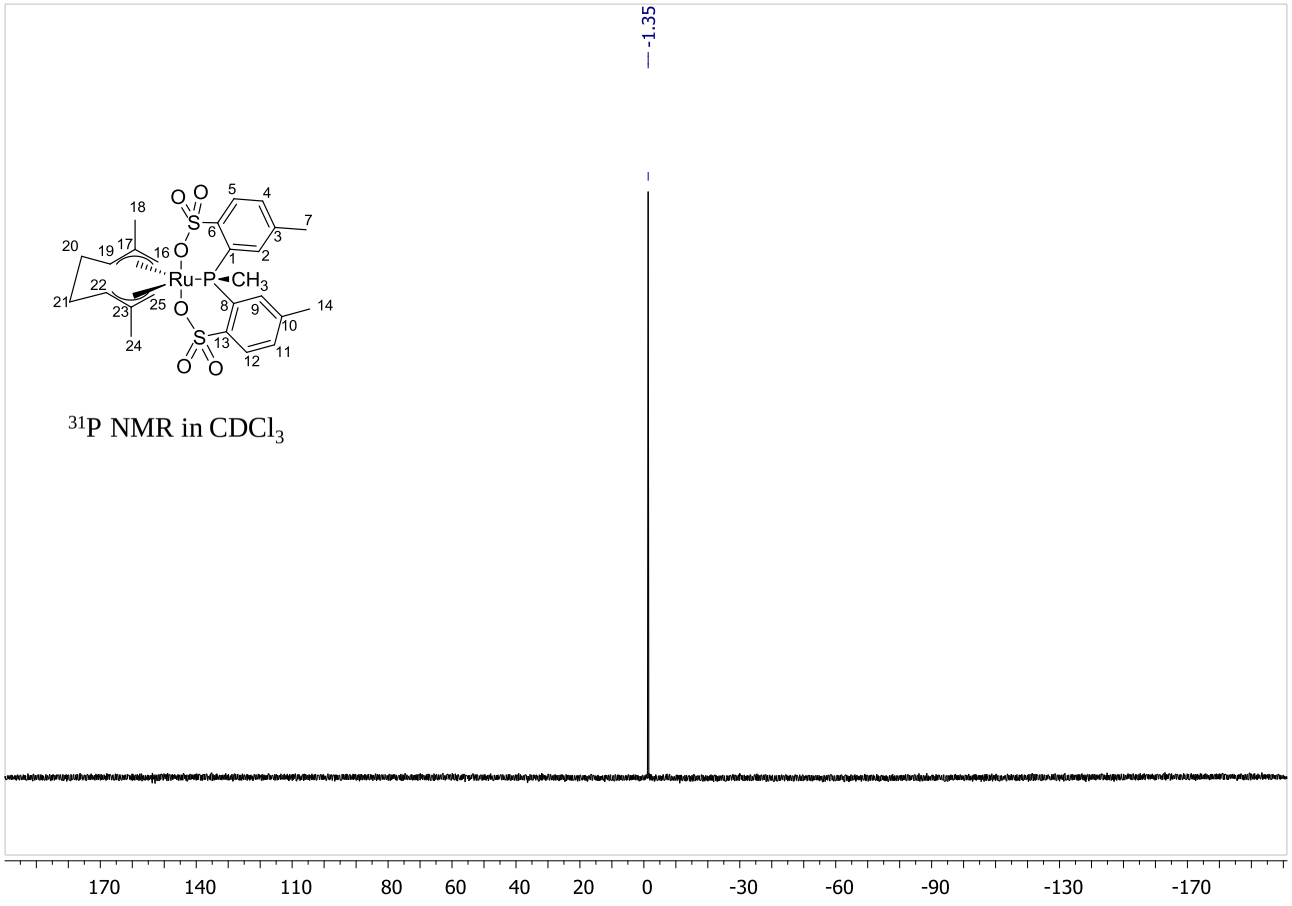

^{31}P NMR in $CDCl_3$

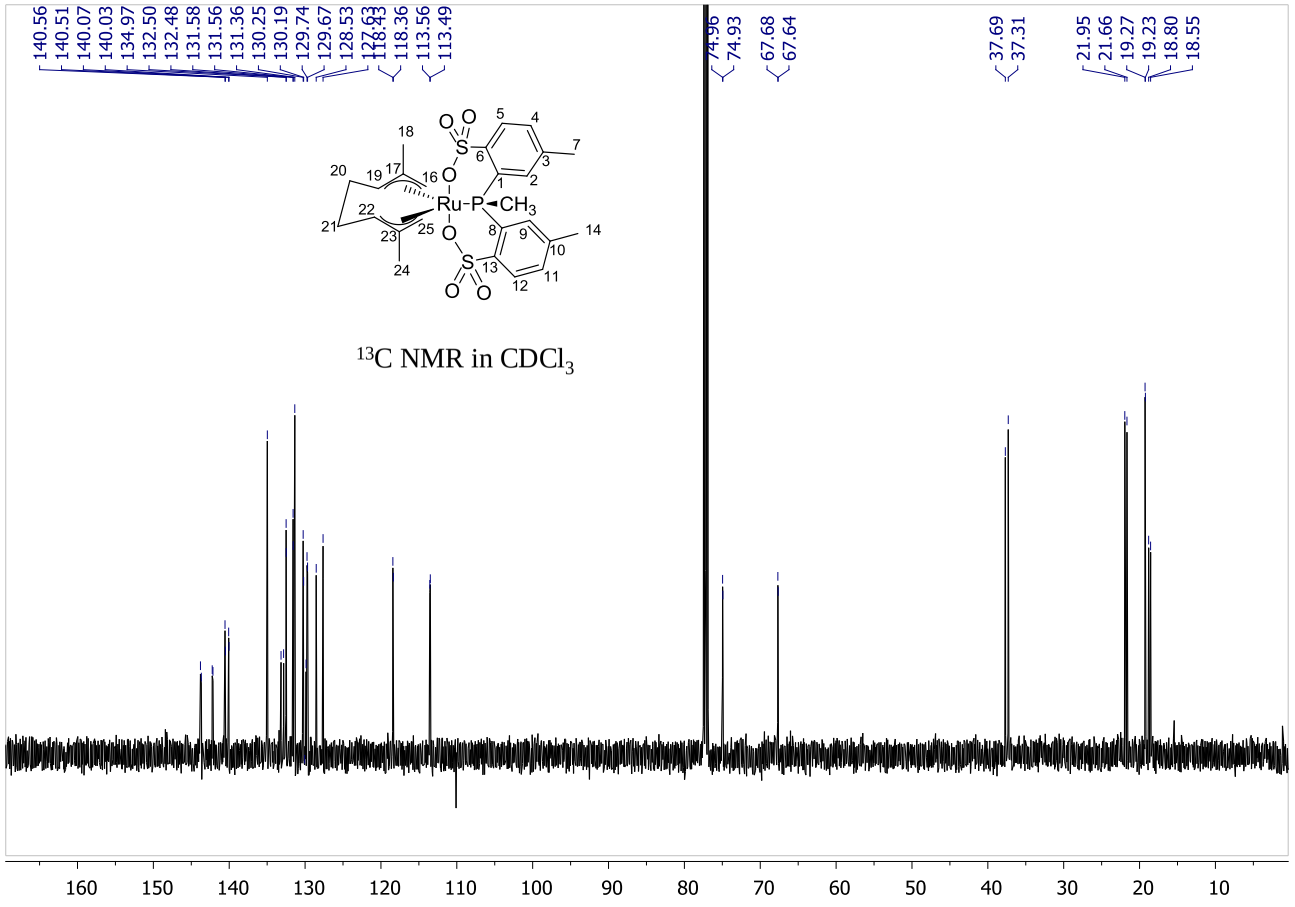
140.56
140.51
140.07
140.03
134.97
132.50
132.48
131.58
131.56
131.36
130.25
130.19
129.74
129.67
128.53
118.36
113.56
113.49
74.96
74.93
67.68
67.64
37.69
37.31
21.95
21.66
19.27
19.23
18.80
18.55
Ru-P-CH3
13C NMR in CDCl3
160
150
140
130
120
110
100
90
80
70
60
50
40
30
20
10

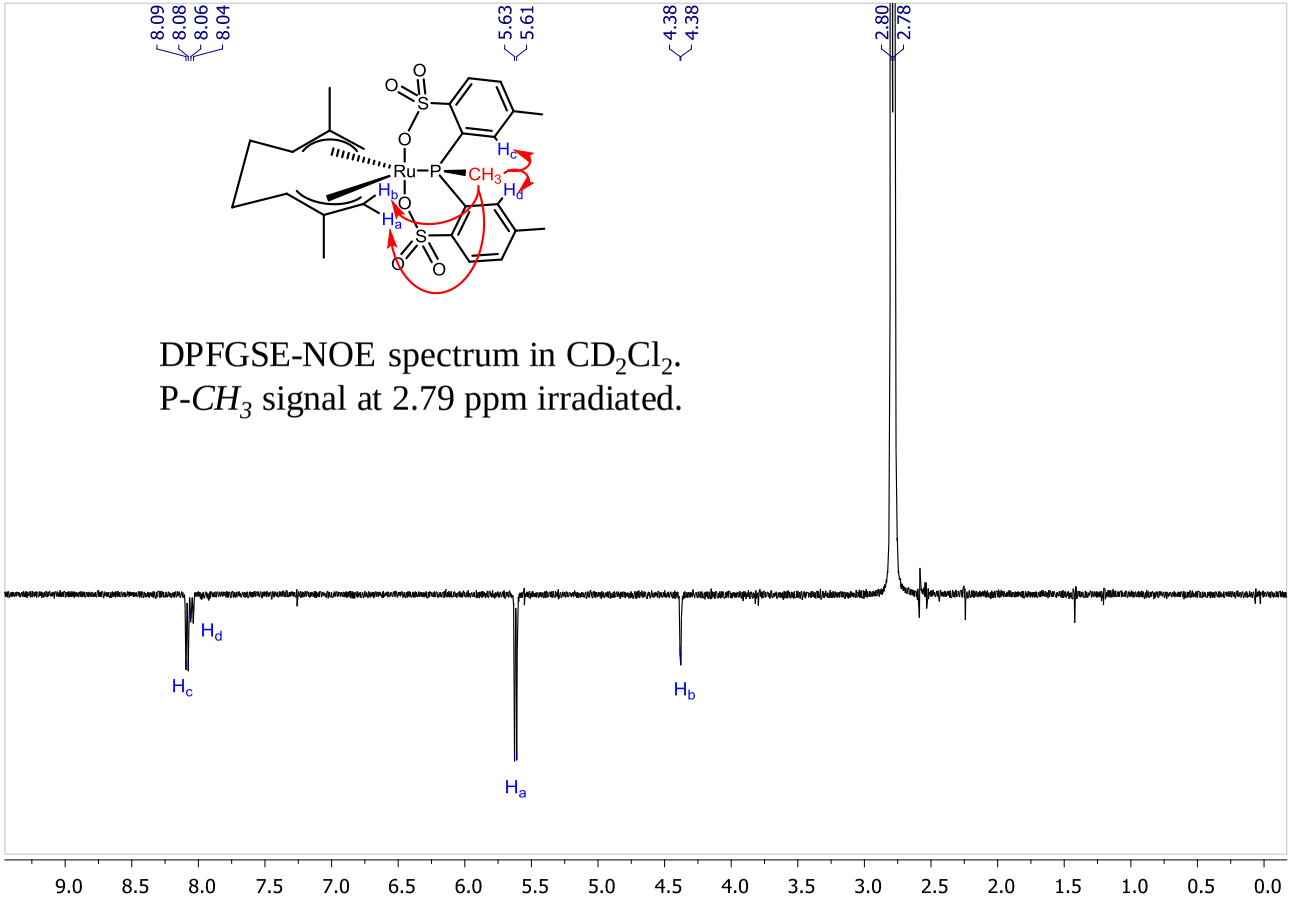

DPFGSE-NOE spectrum in CD_2Cl_2.
P-*CH_3* signal at 2.79 ppm irradiated.

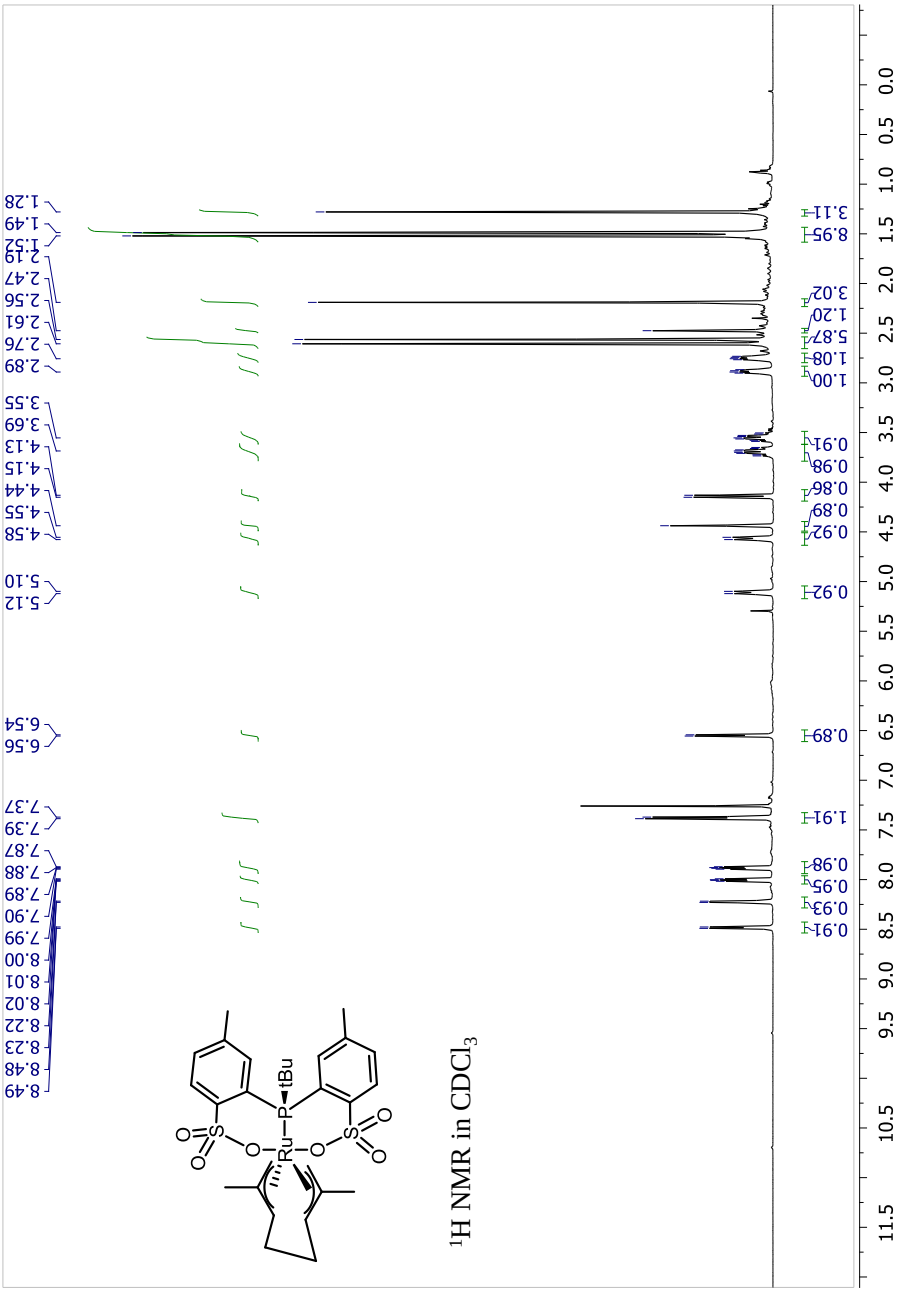
^{1}H NMR in $CDCl_3$

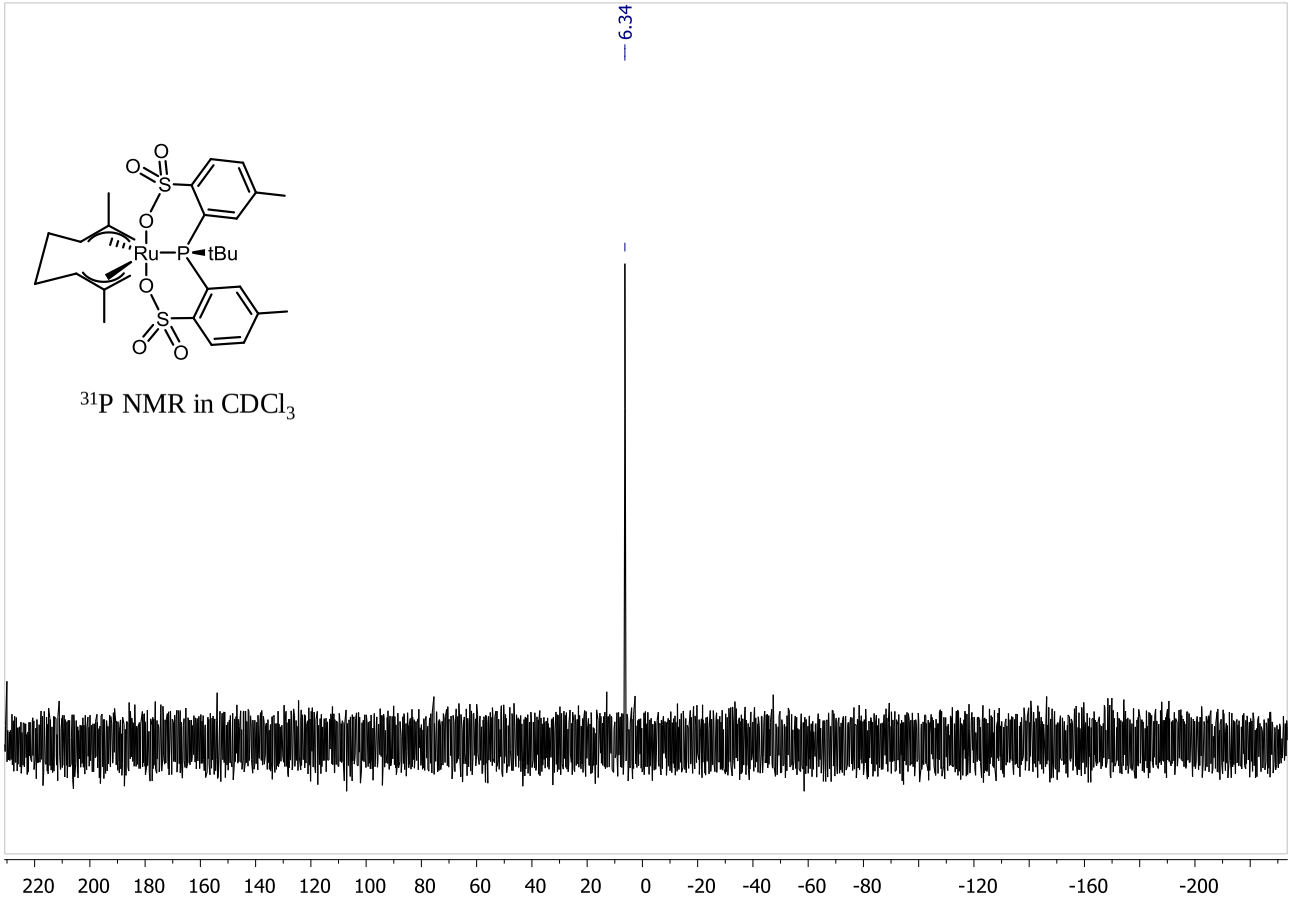

^{31}P NMR in $CDCl_3$

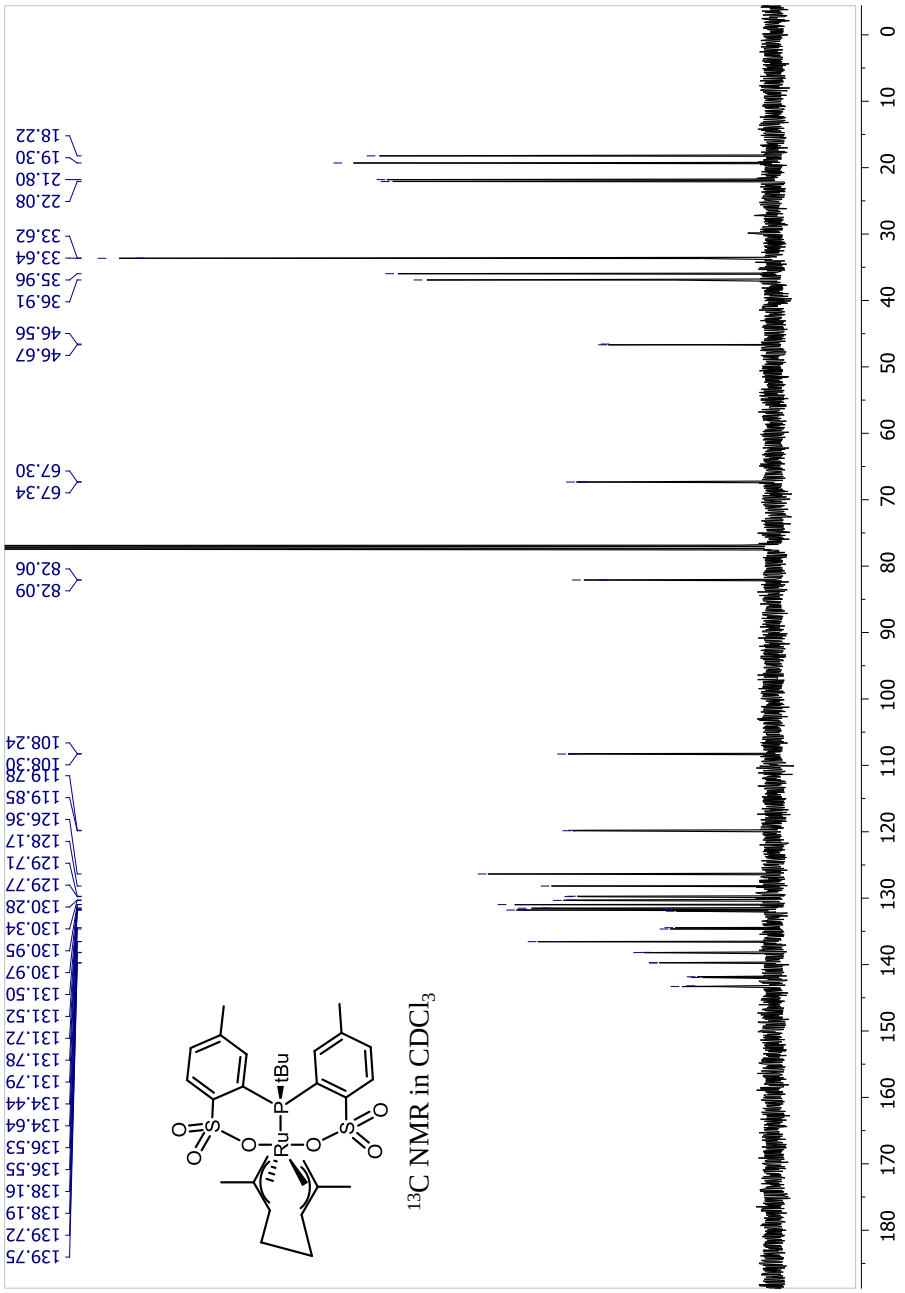
18.22
19.30
21.80
22.08
33.62
33.64
35.96
36.91
46.56
46.67
67.30
67.34
82.06
82.09
108.24
108.30
119.78
119.85
126.36
128.17
129.71
129.77
130.28
130.34
130.95
130.97
131.50
131.52
131.72
131.78
131.79
134.44
134.64
136.53
136.55
138.16
138.19
139.72
139.75
0
10
20
30
40
50
60
70
80
90
100
110
120
130
140
150
160
170
180
P
tBu
Ru
O
S
O
O
O
O
O
O
^{13}C NMR in $CDCl_3$

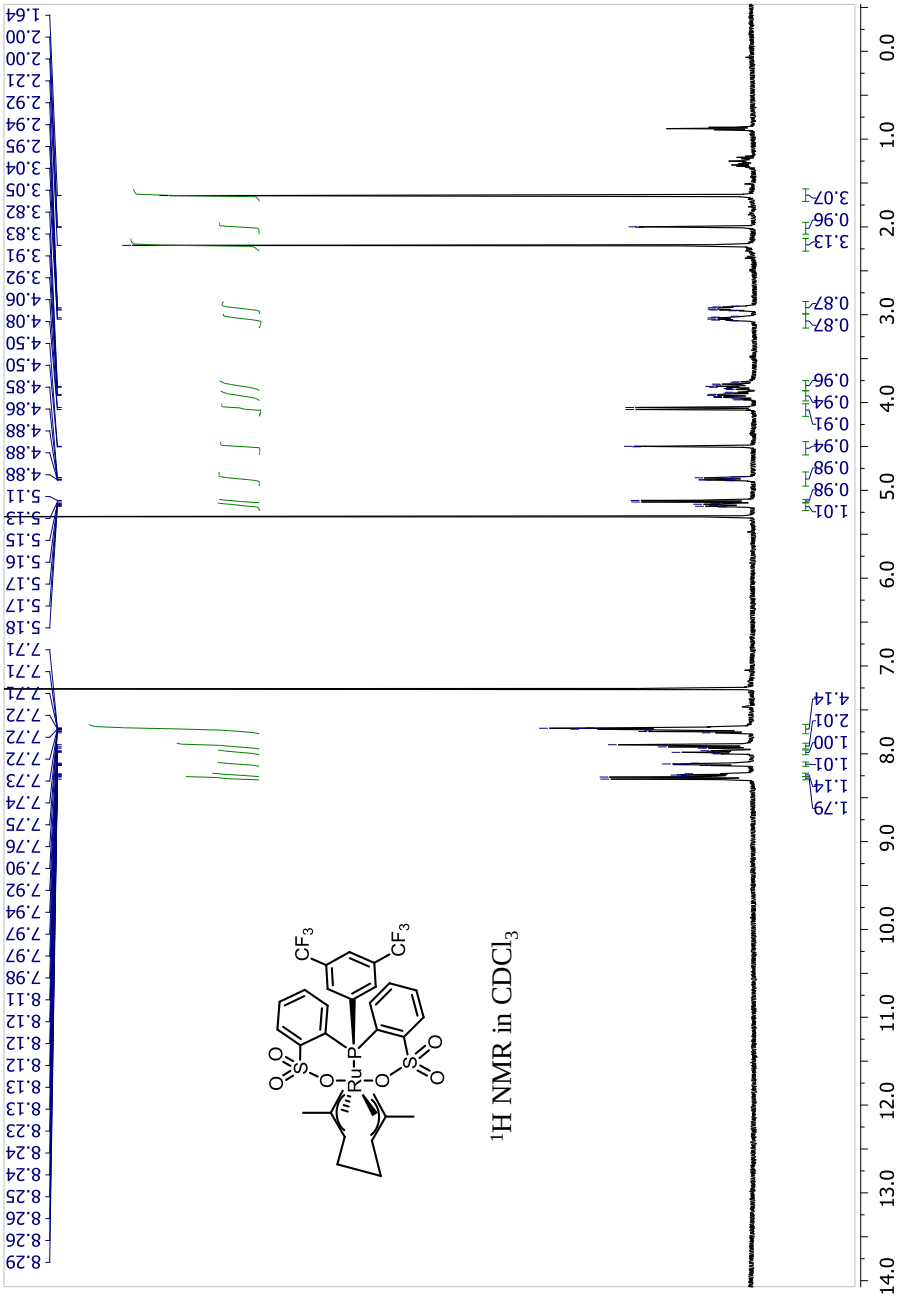
^{1}H NMR in $CDCl_3$
CF3
CF3
Ru
P
O
S

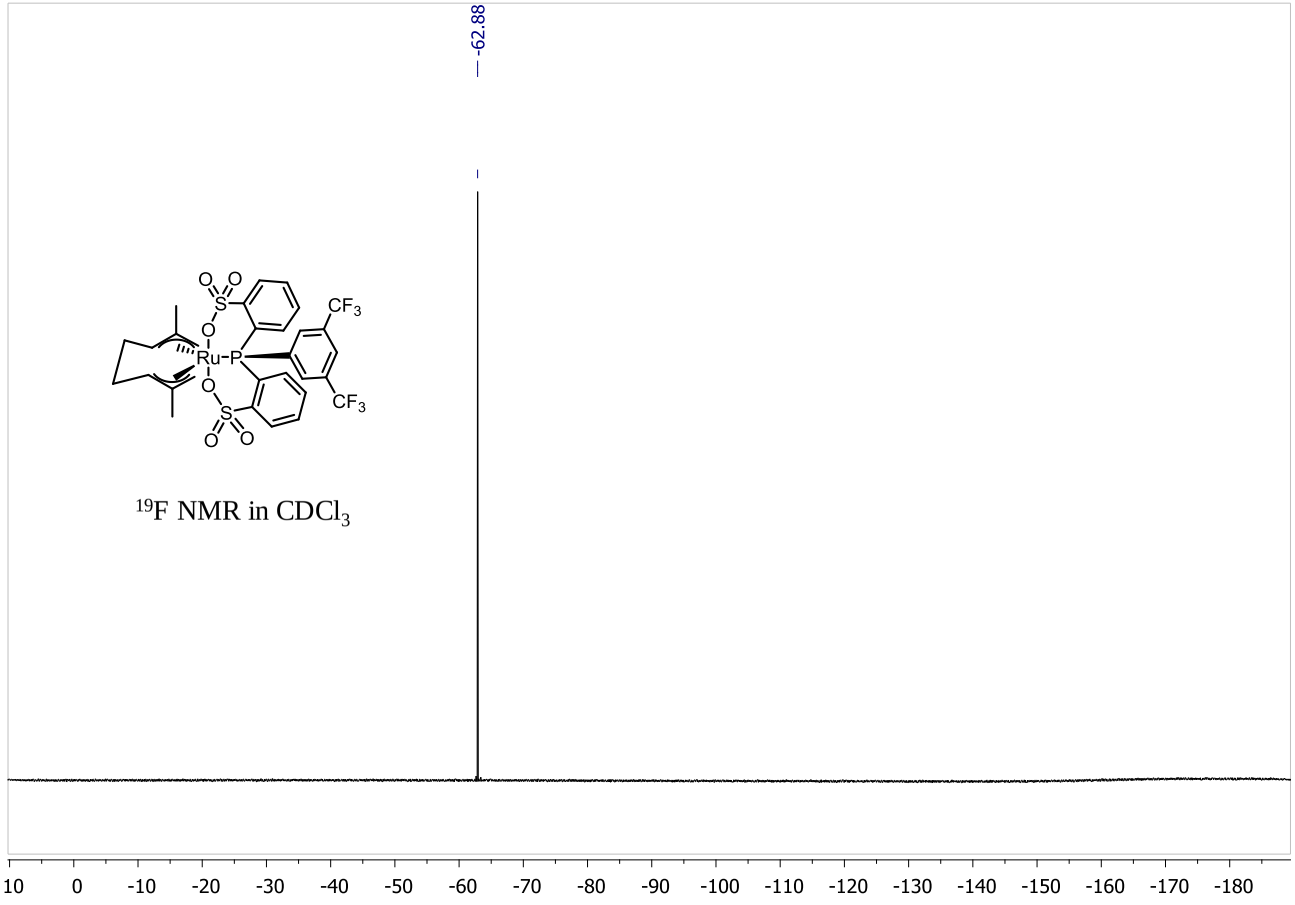

^{19}F NMR in $CDCl_3$

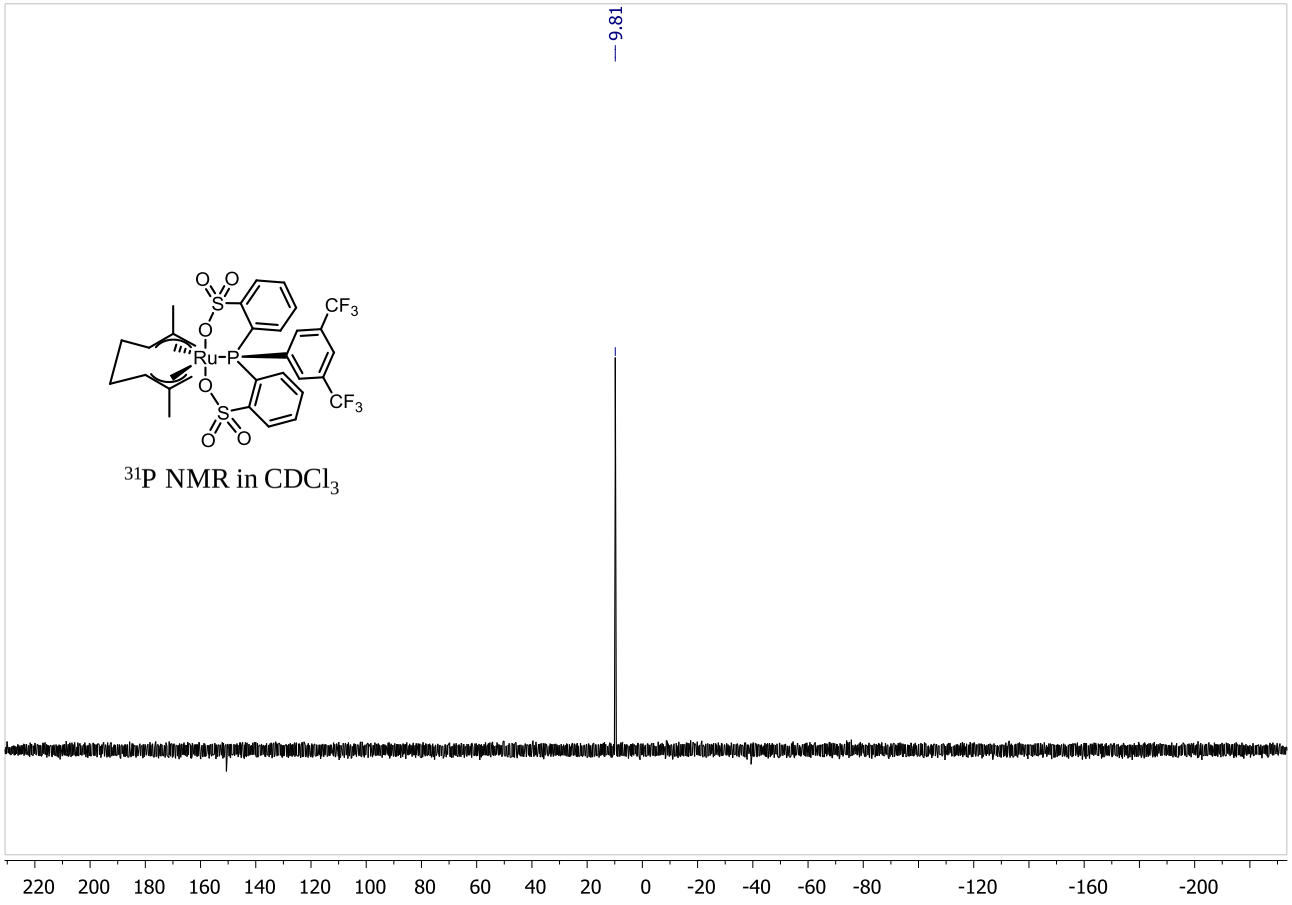

^{31}P NMR in $CDCl_3$

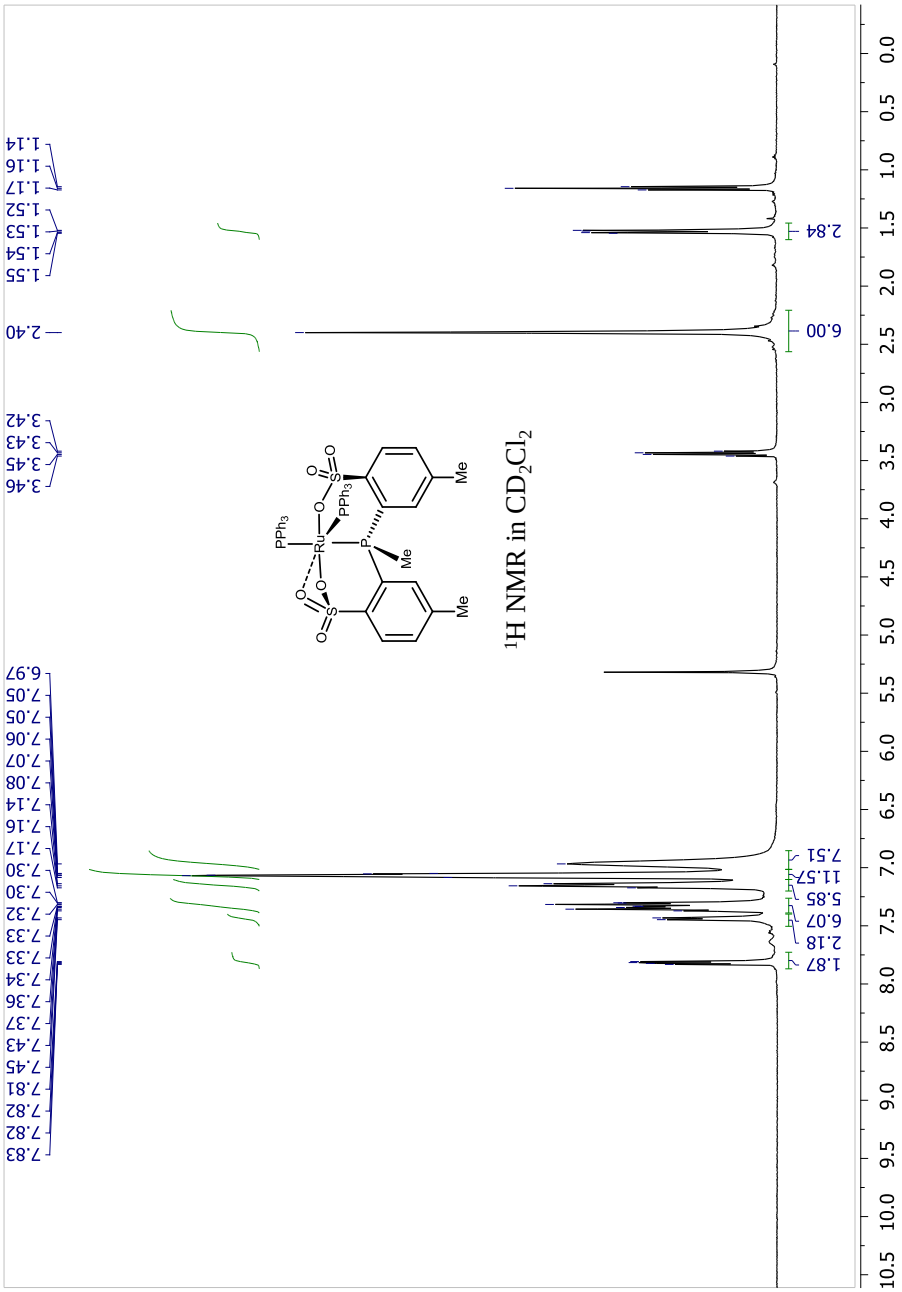
^{1}H NMR in CD_2Cl_2
PPh3
Ru
P
PPh3
Me
Me
Me
O
S
1.87
2.18
6.07
5.85
11.57
7.51
6.00
2.84
2.40
3.46
3.43
3.42
1.55
1.54
1.53
1.52
1.17
1.16
1.14
6.97
7.05
7.05
7.06
7.07
7.08
7.14
7.16
7.17
7.30
7.30
7.32
7.33
7.33
7.34
7.36
7.37
7.43
7.45
7.81
7.82
7.82
7.83
0.0
0.5
1.0
1.5
2.0
2.5
3.0
3.5
4.0
4.5
5.0
5.5
6.0
6.5
7.0
7.5
8.0
8.5
9.0
9.5
10.0
10.5

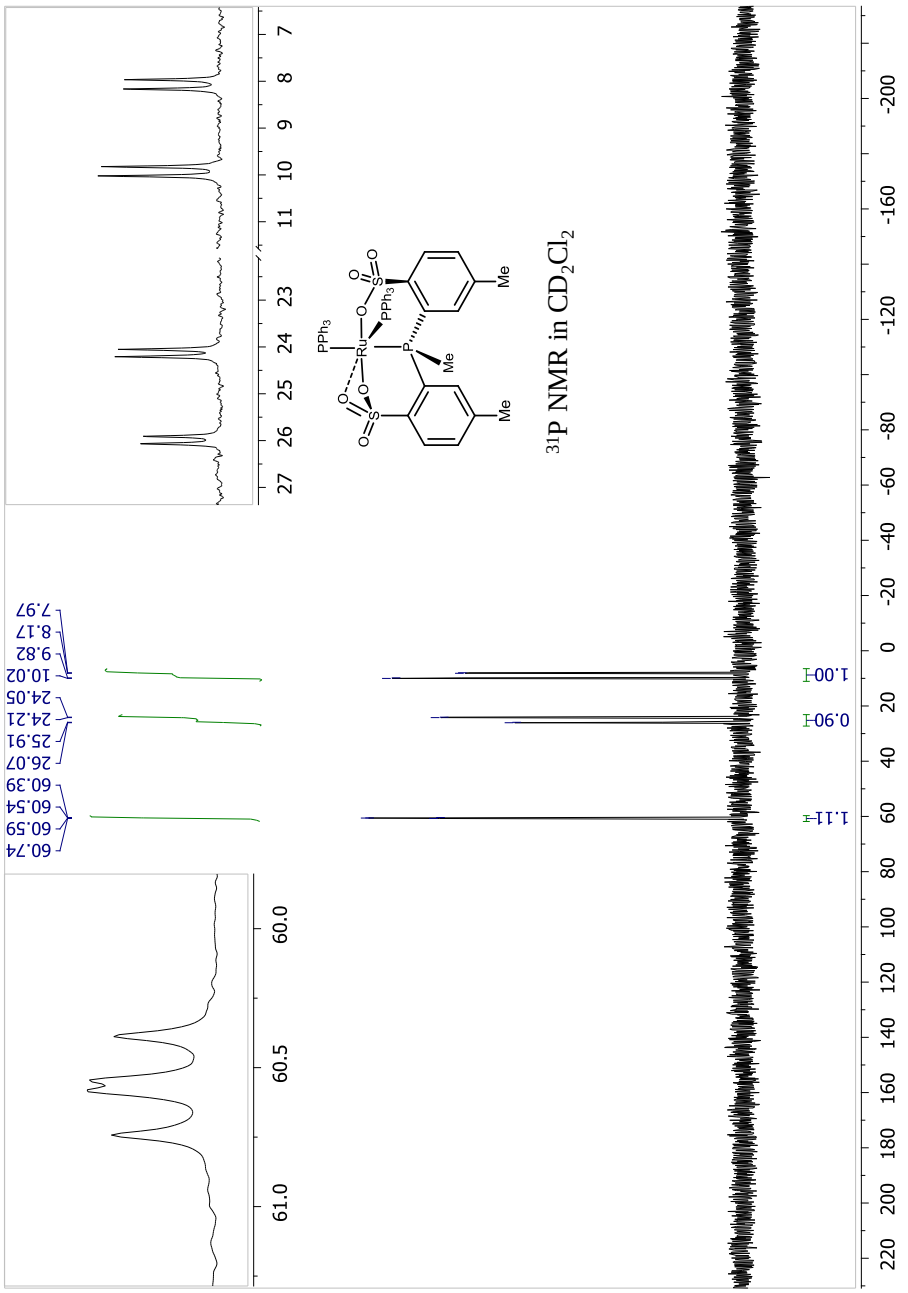
^{31}P NMR in CD_2Cl_2
PPh3
Ru
O
S
PPh3
P
Me
Me
Me
60.74
60.59
60.54
60.39
26.07
25.91
24.21
24.05
10.02
9.82
8.17
7.97
1.11
0.90
1.00

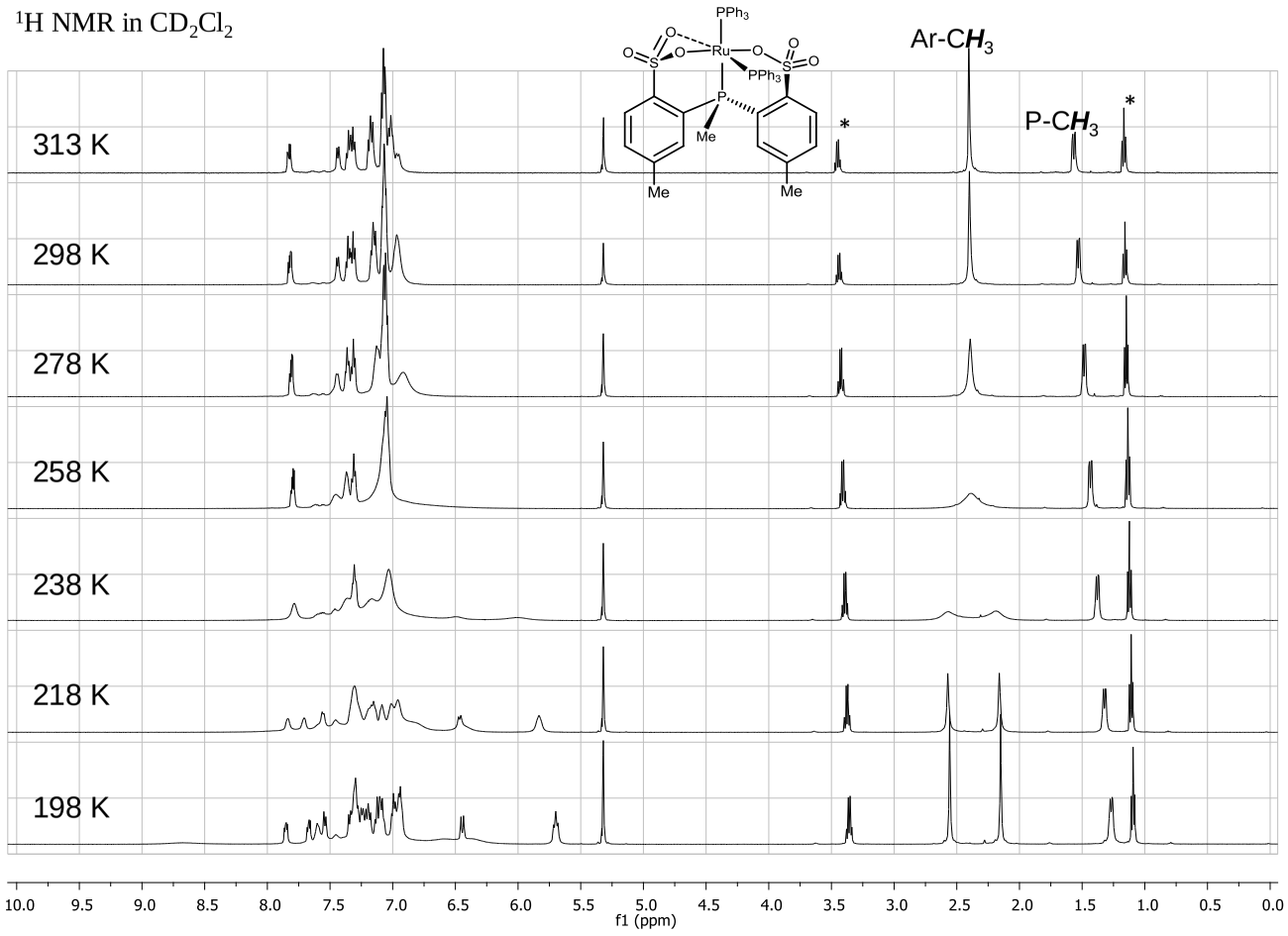
^{1}H NMR in CD_2Cl_2
313 K
298 K
278 K
258 K
238 K
218 K
198 K
Ar-CH_3
P-CH_3
*
*
PPh$_3$
Ru
P
Me
Me
Me
10.0 9.5 9.0 8.5 8.0 7.5 7.0 6.5 6.0 5.5 5.0 4.5 4.0 3.5 3.0 2.5 2.0 1.5 1.0 0.5 0.0
f1 (ppm)

^{31}P NMR in CD_2Cl_2

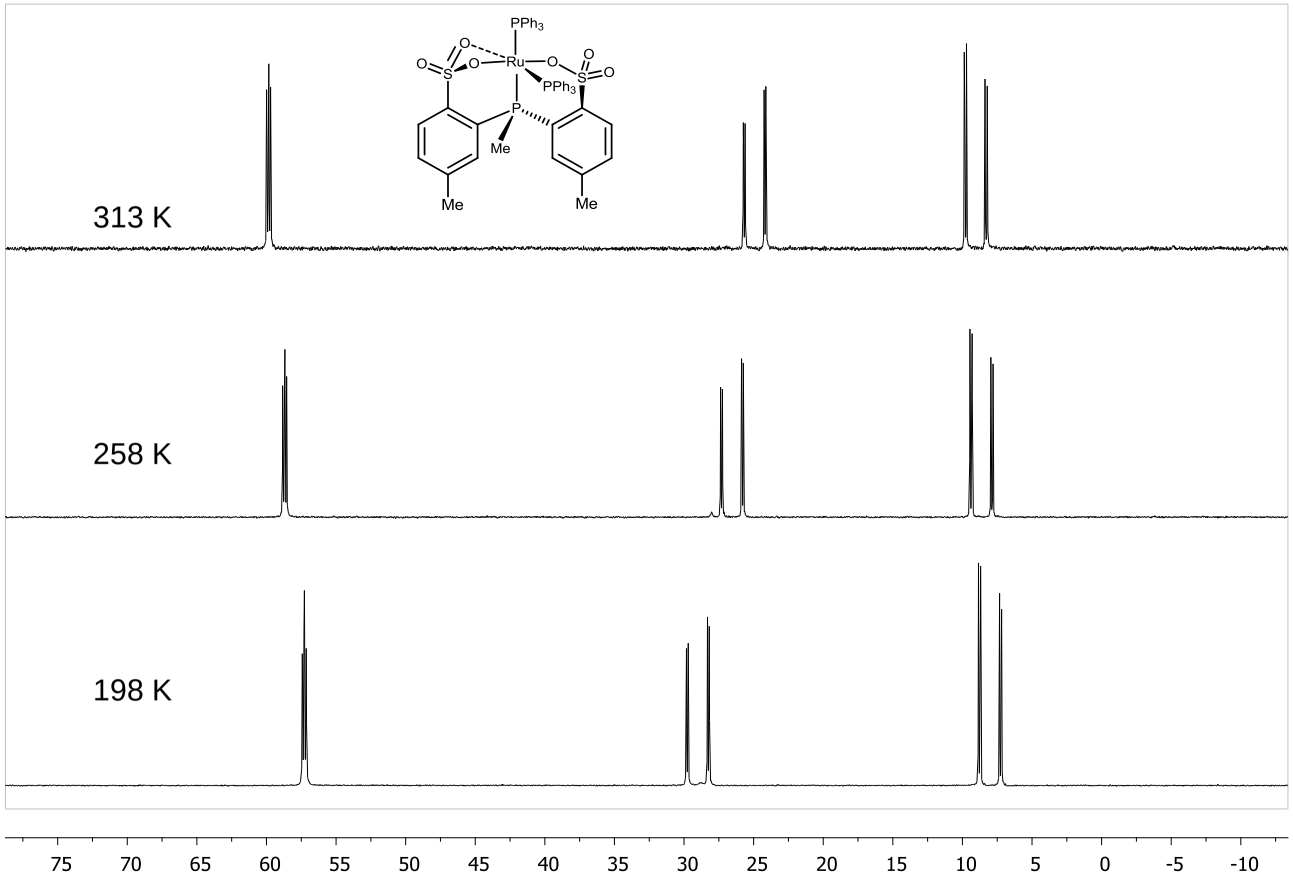

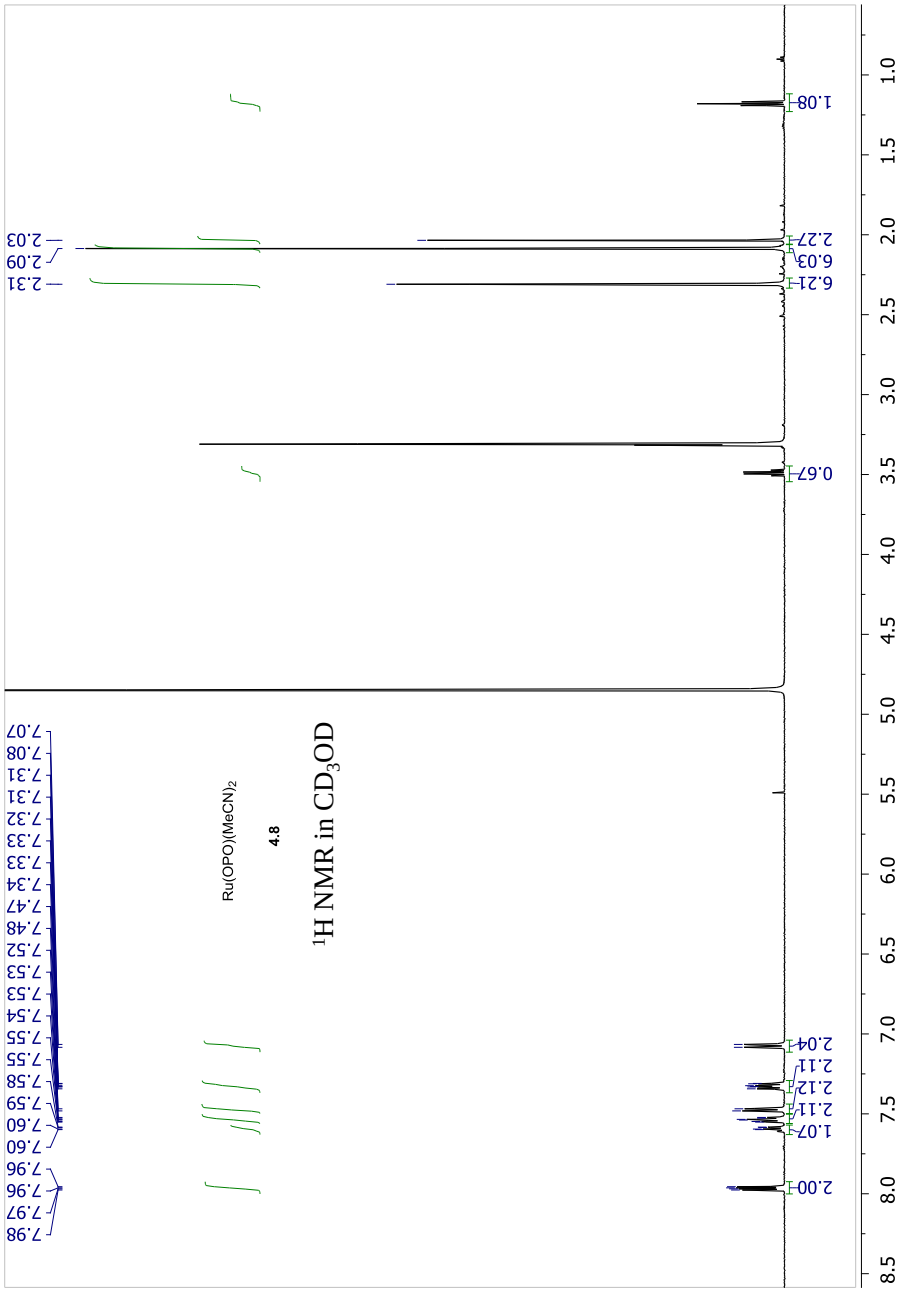
^{1}H NMR in CD_3OD
Ru(OPO)(MeCN)$_2$
4.8

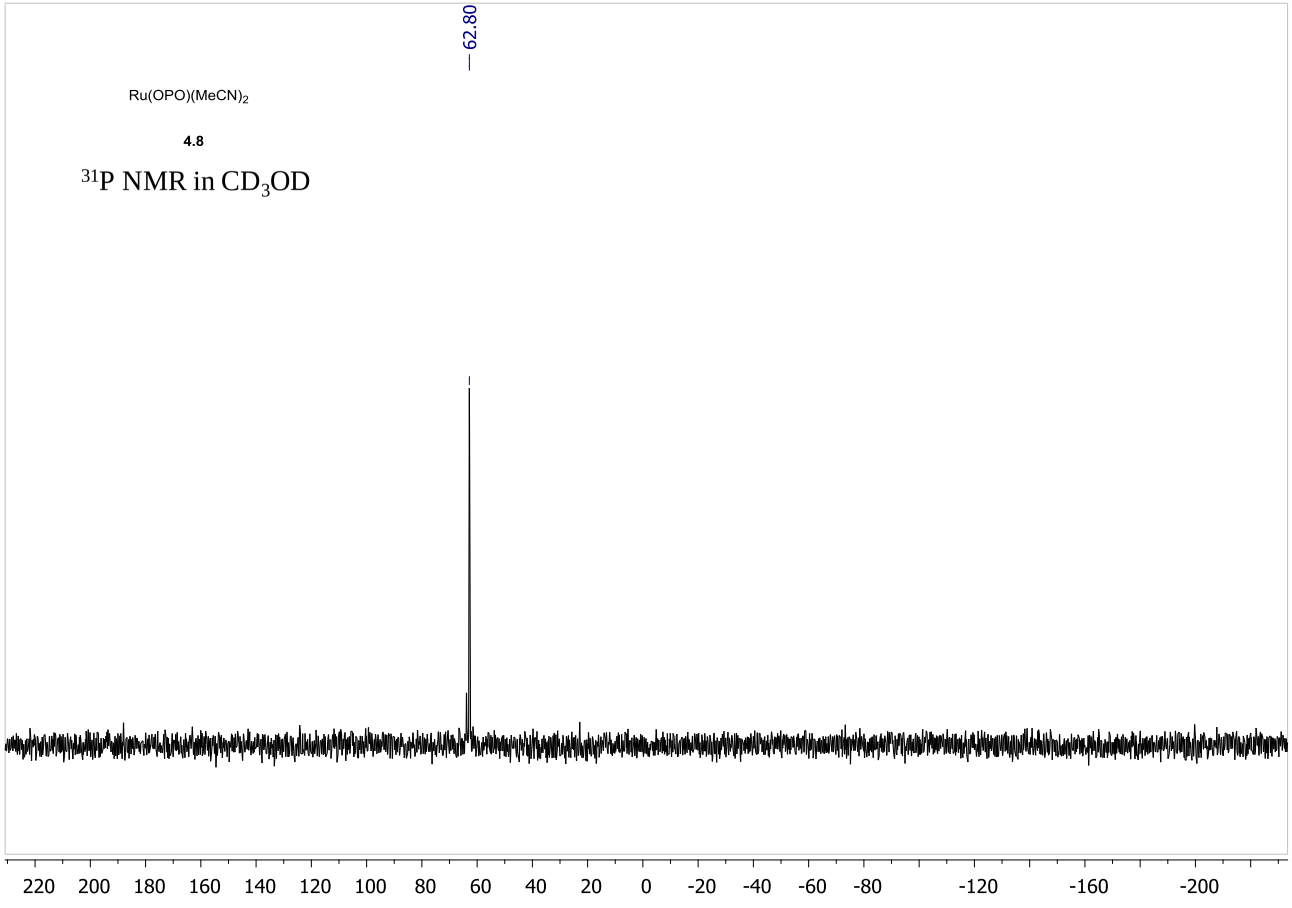
62.80
Ru(OPO)(MeCN)2
4.8
31P NMR in CD3OD
220
200
180
160
140
120
100
80
60
40
20
0
-20
-40
-60
-80
-120
-160
-200

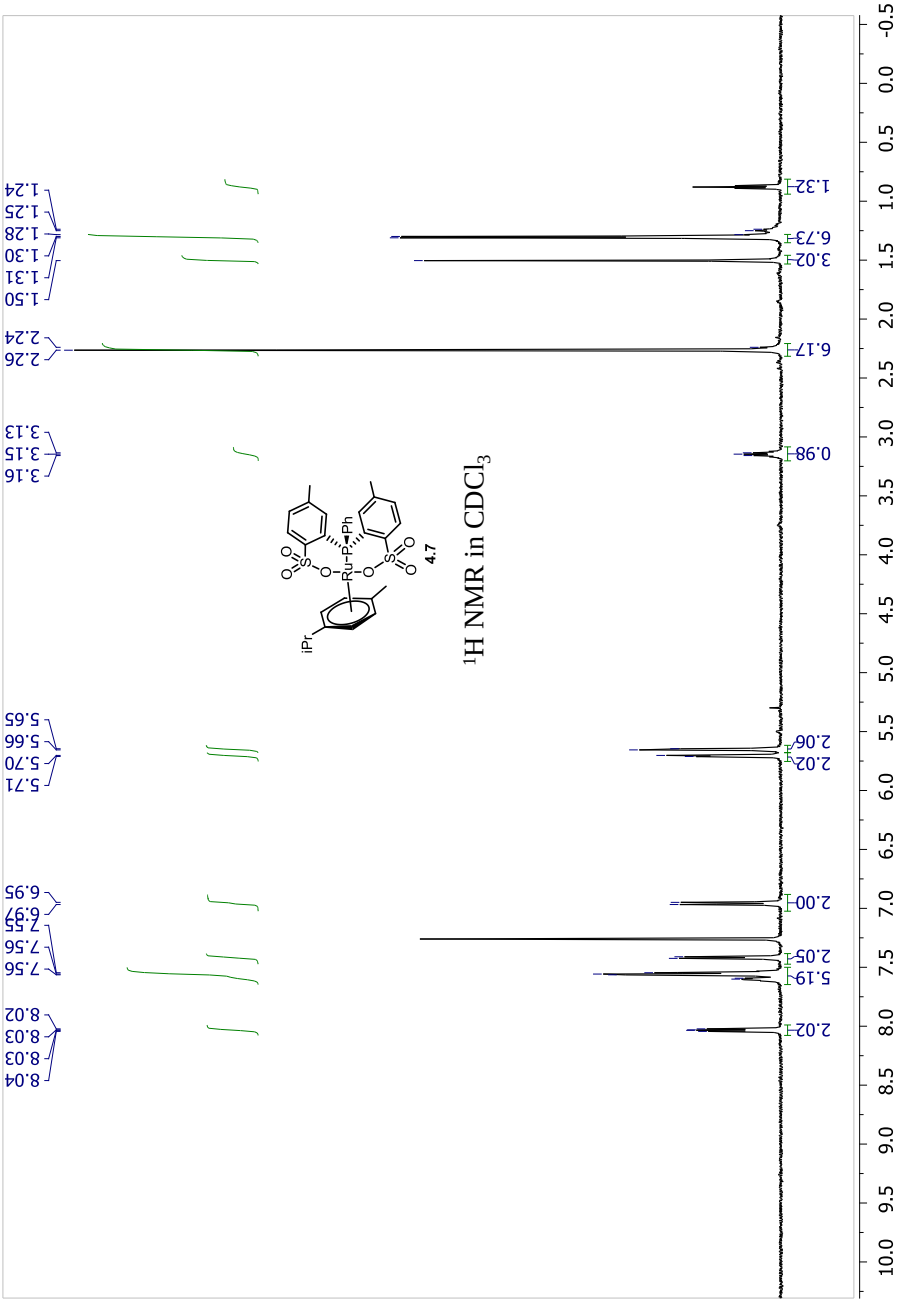
8.04
8.03
8.03
8.02
7.56
7.56
7.55
6.97
6.95
5.71
5.70
5.66
5.65
3.16
3.15
3.13
2.26
2.24
1.50
1.31
1.30
1.28
1.25
1.24
2.02
5.19
2.05
2.00
2.06
2.02
0.98
6.17
3.02
6.73
1.32
10.0
9.5
9.0
8.5
8.0
7.5
7.0
6.5
6.0
5.5
5.0
4.5
4.0
3.5
3.0
2.5
2.0
1.5
1.0
0.5
0.0
-0.5
iPr
Ru
P
Ph
O
S
4.7
^{1}H NMR in $CDCl_3$

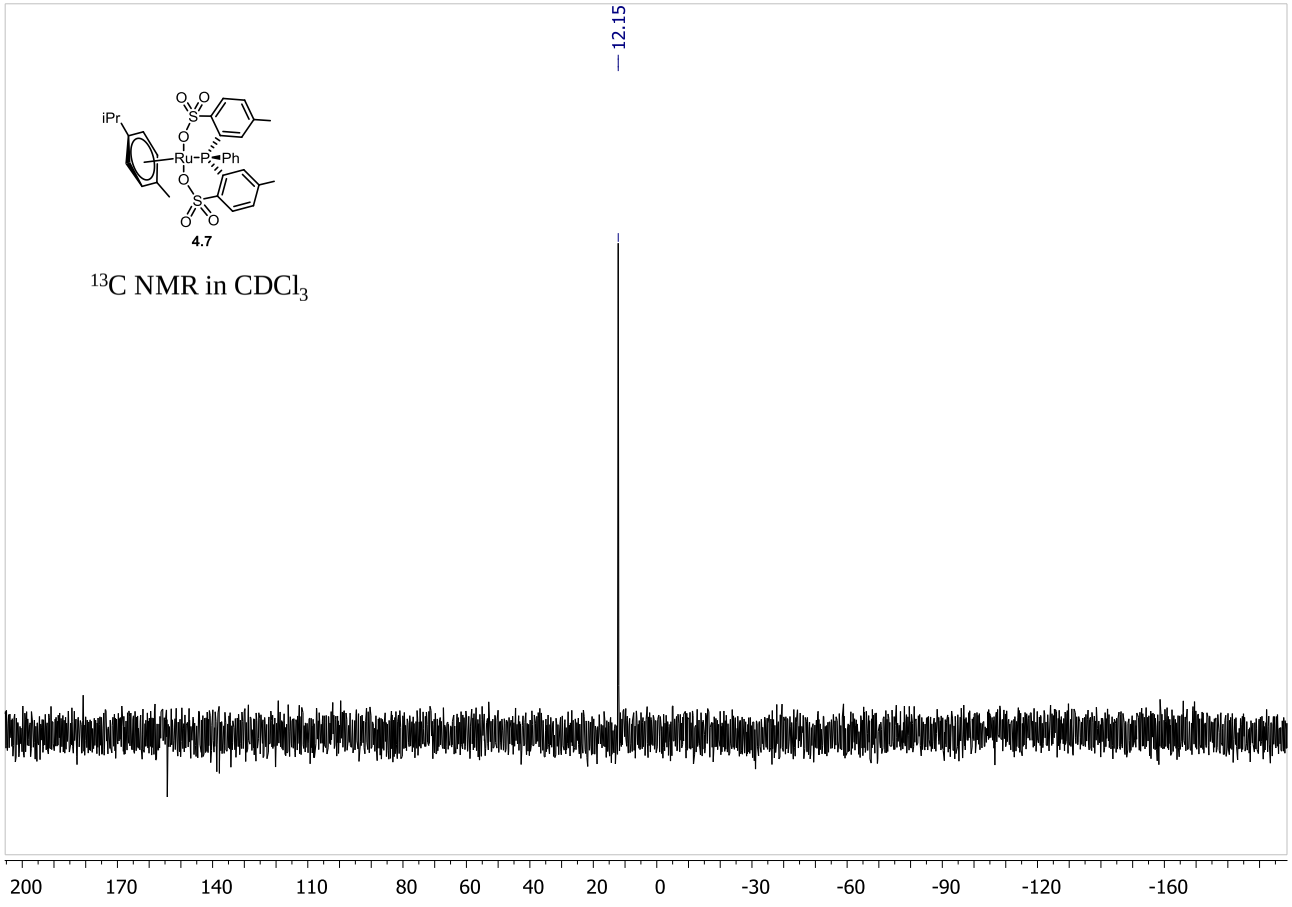
12.15
iPr
Ru
P
Ph
4.7
^{13}C NMR in CDCl$_3$
200
170
140
110
80
60
40
20
0
-30
-60
-90
-120
-160

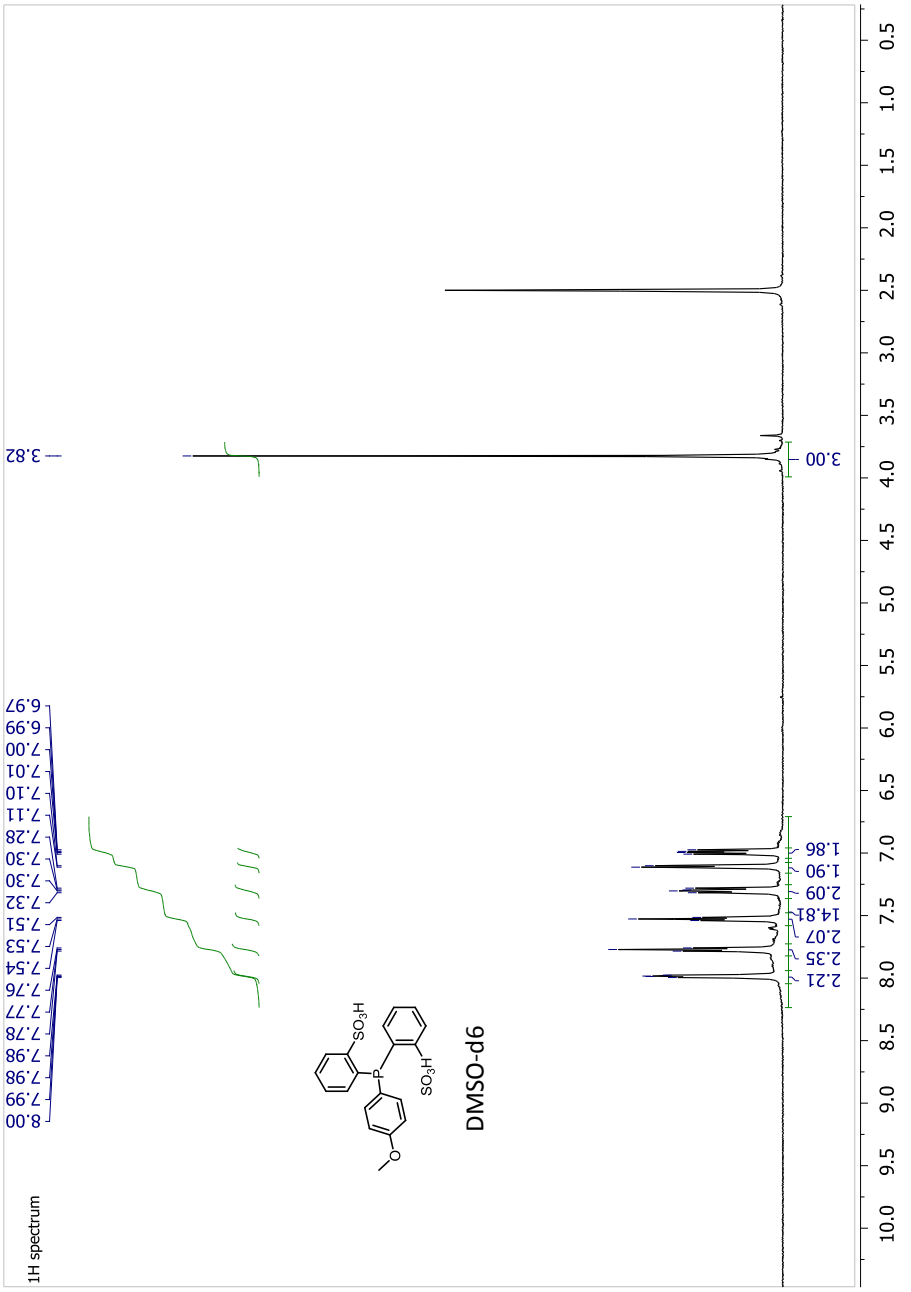
1H spectrum
DMSO-d6
SO3H
SO3H
O
P
8.00
7.99
7.98
7.98
7.78
7.77
7.76
7.54
7.53
7.51
7.32
7.30
7.30
7.28
7.11
7.10
7.01
7.00
6.99
6.97
3.82
3.00
2.21
2.35
2.07
14.81
2.09
1.90
1.86
10.0
9.5
9.0
8.5
8.0
7.5
7.0
6.5
6.0
5.5
5.0
4.5
4.0
3.5
3.0
2.5
2.0
1.5
1.0
0.5

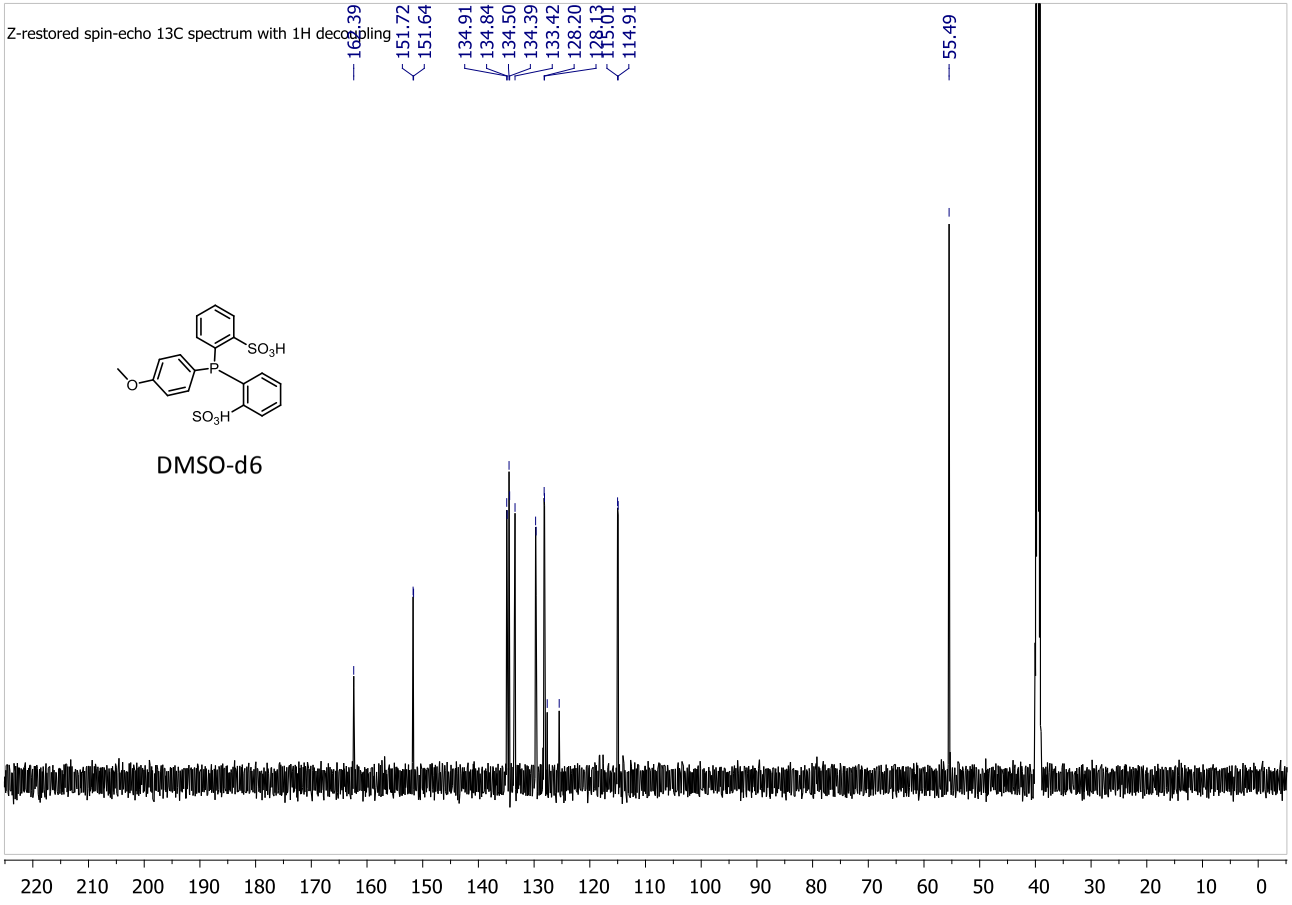
Z-restored spin-echo 13C spectrum with 1H decoupling
162.39
151.72
151.64
134.91
134.84
134.50
134.39
133.42
128.20
128.13
115.01
114.91
55.49
SO3H
SO3H
O
P
DMSO-d6
220 210 200 190 180 170 160 150 140 130 120 110 100 90 80 70 60 50 40 30 20 10 0

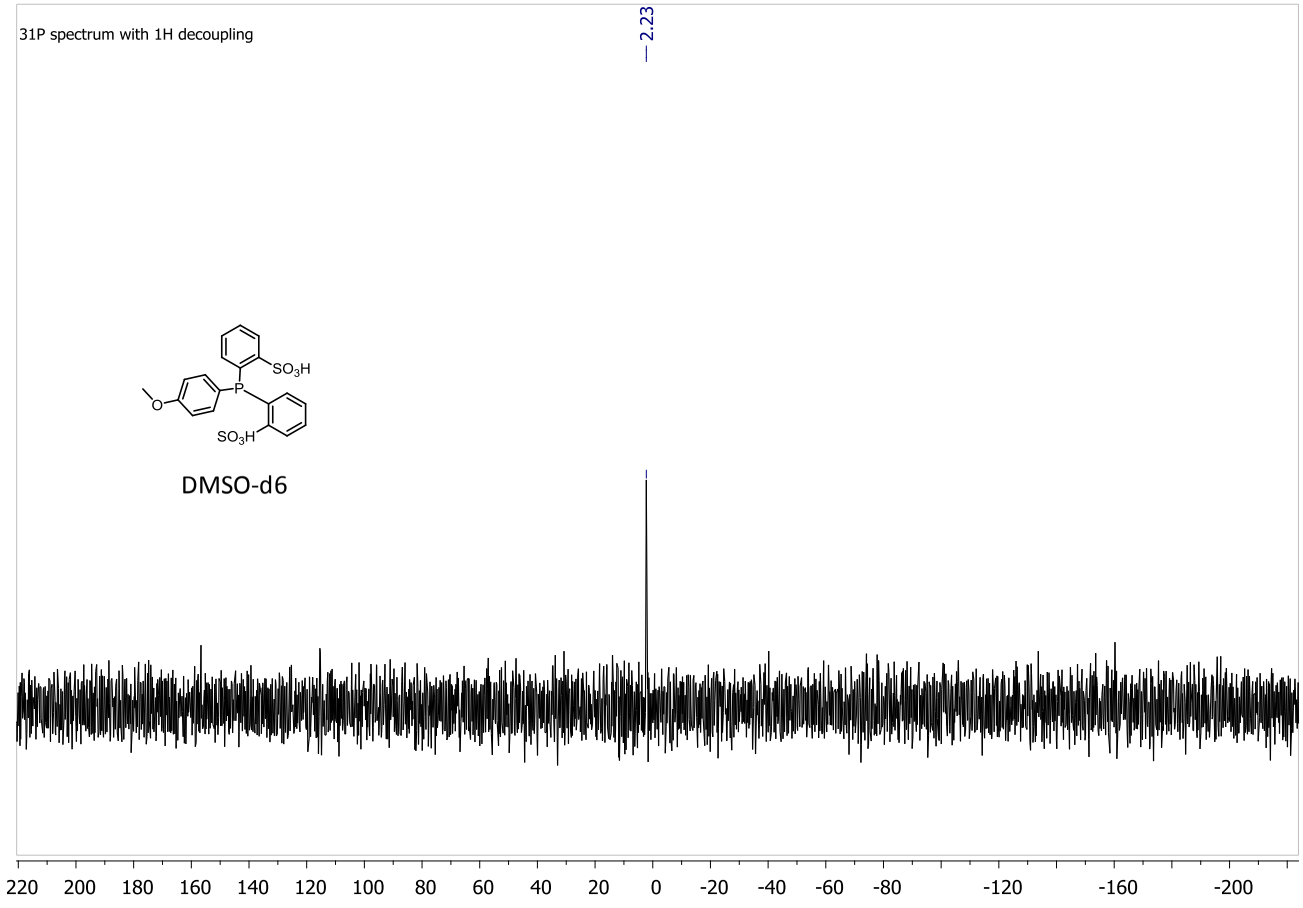
31P spectrum with 1H decoupling
2.23
SO3H
O
P
SO3H
DMSO-d6
220 200 180 160 140 120 100 80 60 40 20 0 -20 -40 -60 -80 -120 -160 -200

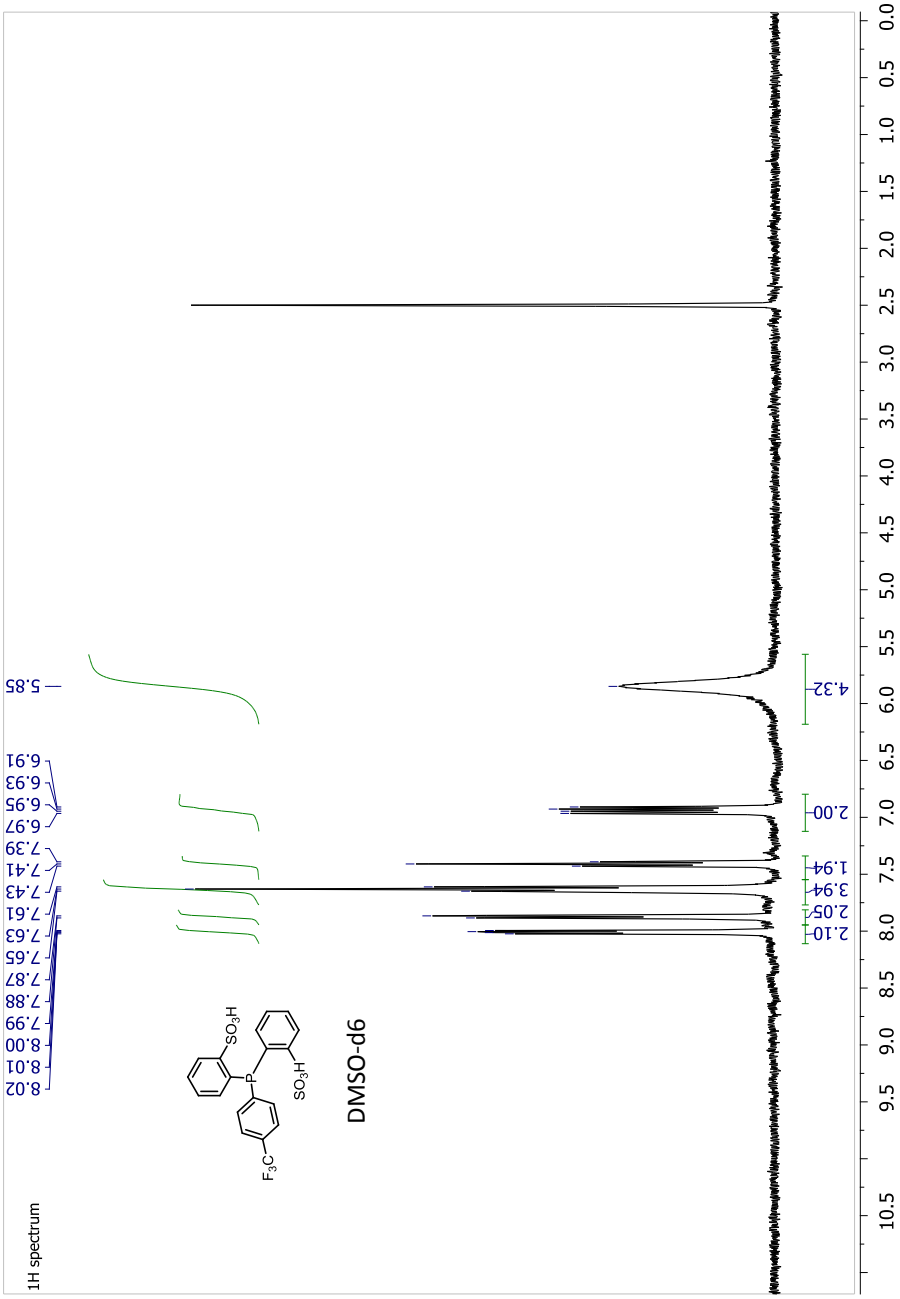
1H spectrum
DMSO-d6
SO3H
SO3H
F3C
P
8.02
8.01
8.00
7.99
7.88
7.87
7.65
7.63
7.61
7.43
7.41
7.39
6.97
6.95
6.93
6.91
5.85
4.32
2.00
1.94
3.94
2.05
2.10
10.5
9.5
9.0
8.5
8.0
7.5
7.0
6.5
6.0
5.5
5.0
4.5
4.0
3.5
3.0
2.5
2.0
1.5
1.0
0.5
0.0

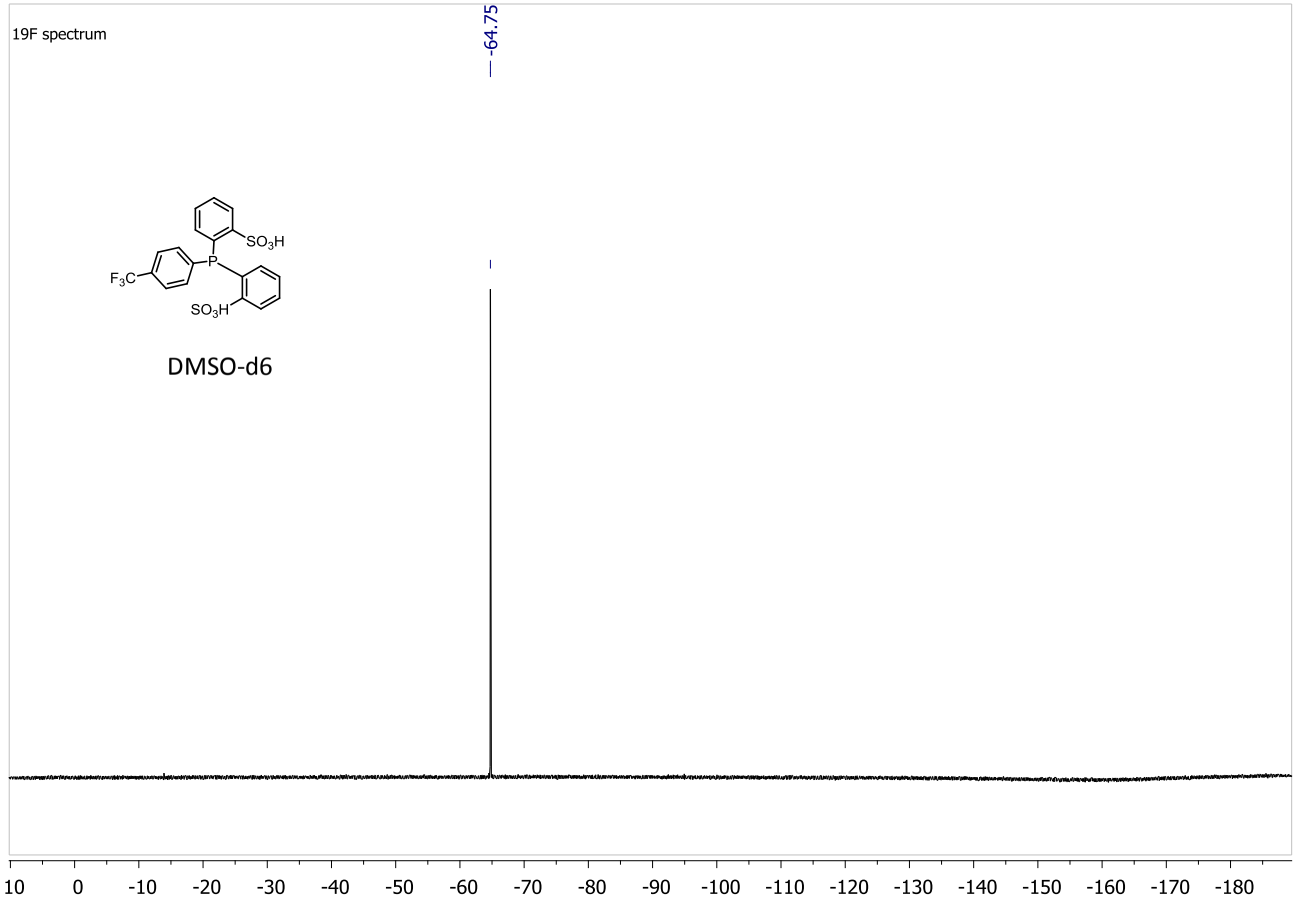
19F spectrum
-64.75
SO3H
F3C
P
SO3H
DMSO-d6
10
0
-10
-20
-30
-40
-50
-60
-70
-80
-90
-100
-110
-120
-130
-140
-150
-160
-170
-180

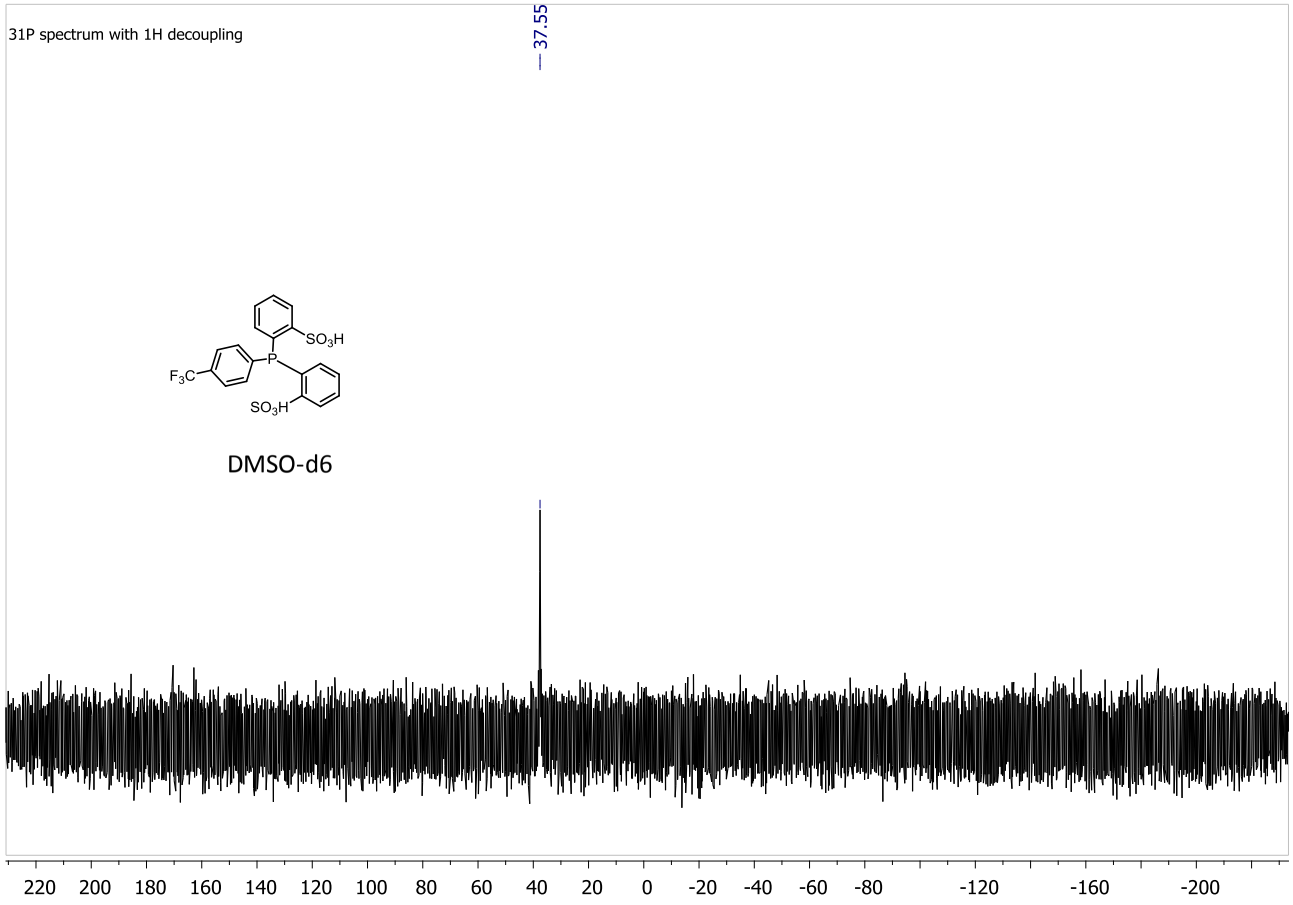
31P spectrum with 1H decoupling
37.55
SO3H
F3C
P
SO3H
DMSO-d6
220 200 180 160 140 120 100 80 60 40 20 0 -20 -40 -60 -80 -120 -160 -200

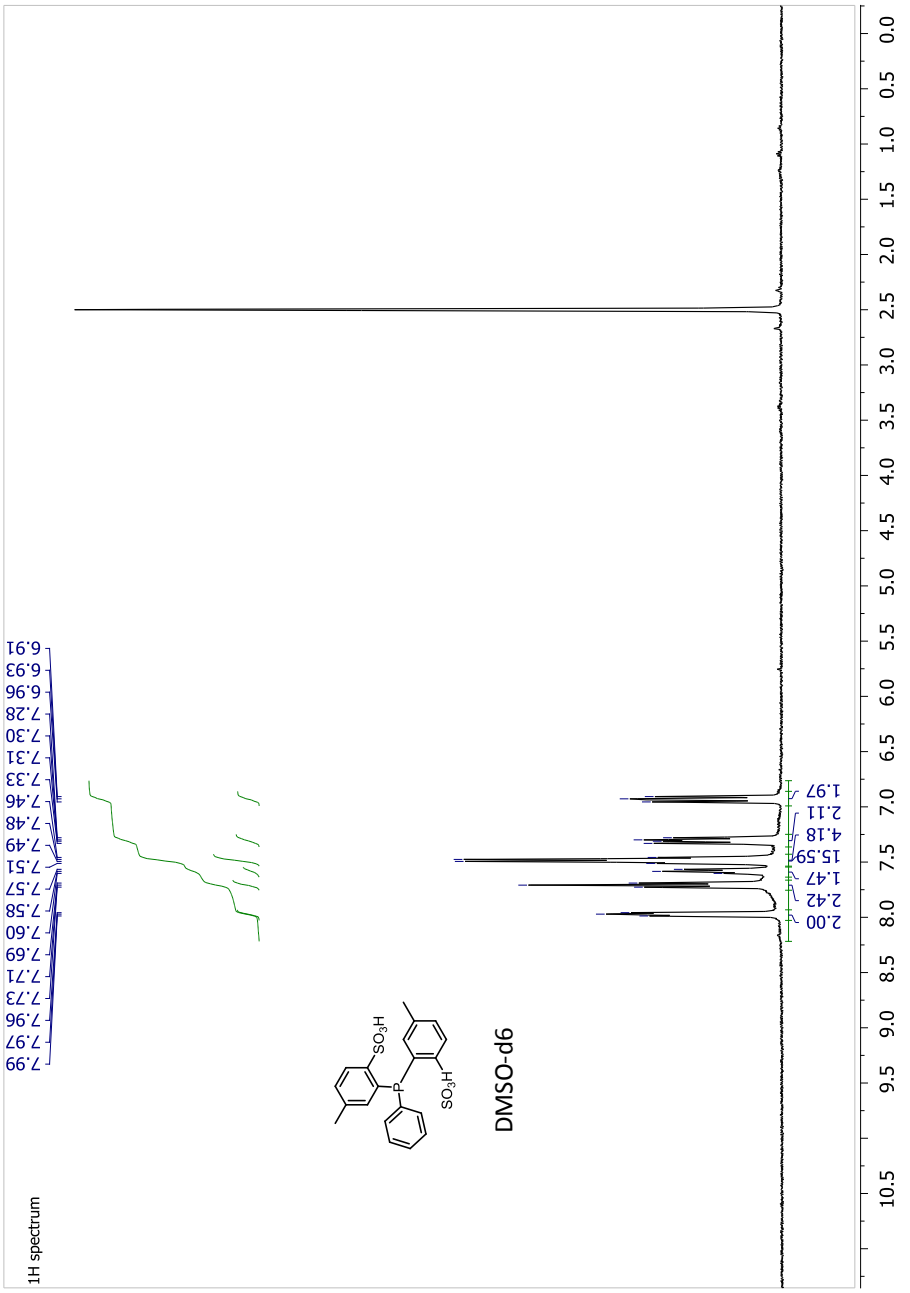
1H spectrum
DMSO-d6
SO3H
SO3H
P
7.99
7.97
7.96
7.73
7.71
7.69
7.60
7.58
7.57
7.51
7.49
7.48
7.46
7.33
7.31
7.30
7.28
6.96
6.93
6.91
2.00
2.42
1.47
15.59
4.18
2.11
1.97
10.5
9.5
9.0
8.5
8.0
7.5
7.0
6.5
6.0
5.5
5.0
4.5
4.0
3.5
3.0
2.5
2.0
1.5
1.0
0.5
0.0

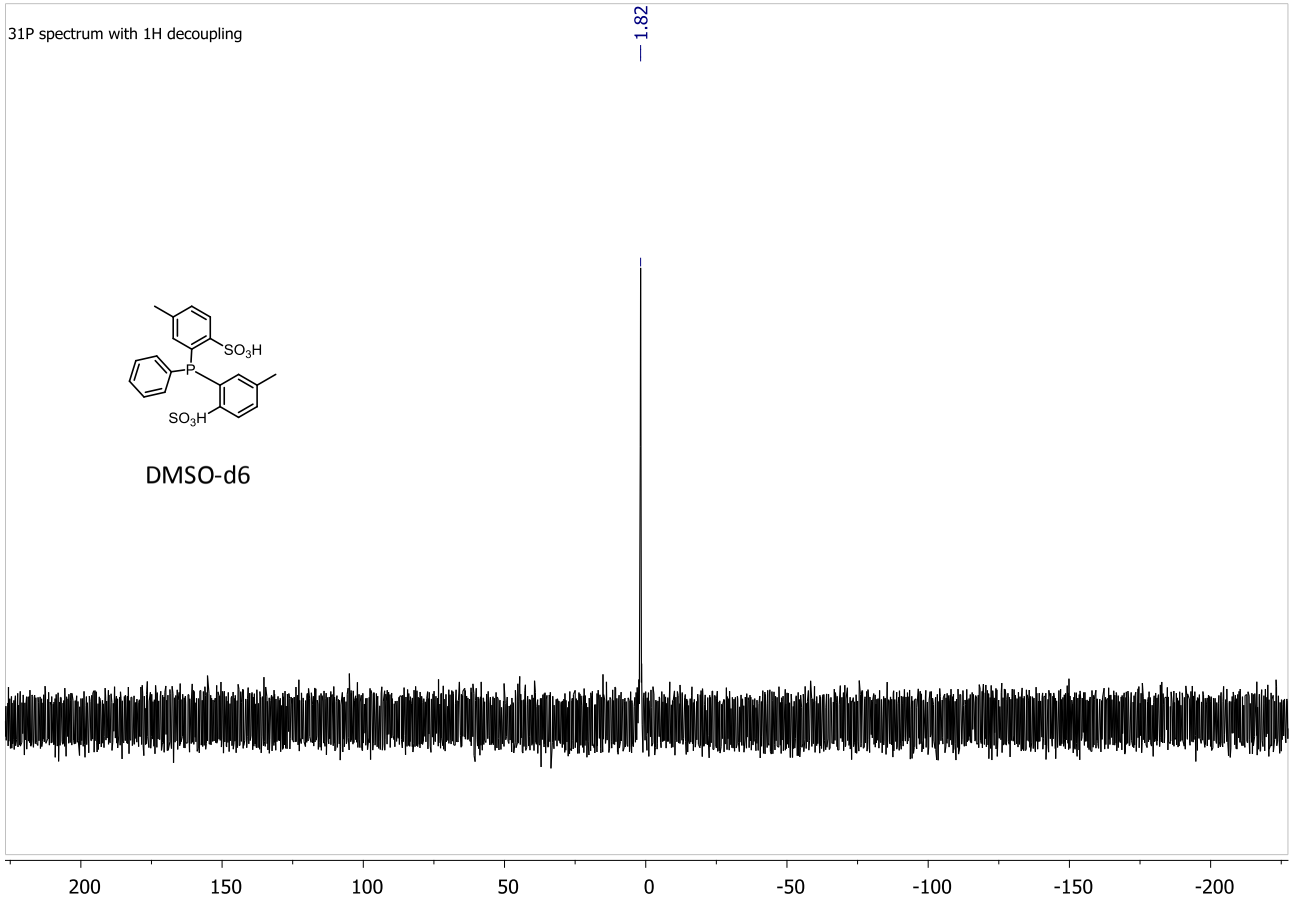
31P spectrum with 1H decoupling
1.82
SO3H
P
SO3H
DMSO-d6
200
150
100
50
0
-50
-100
-150
-200

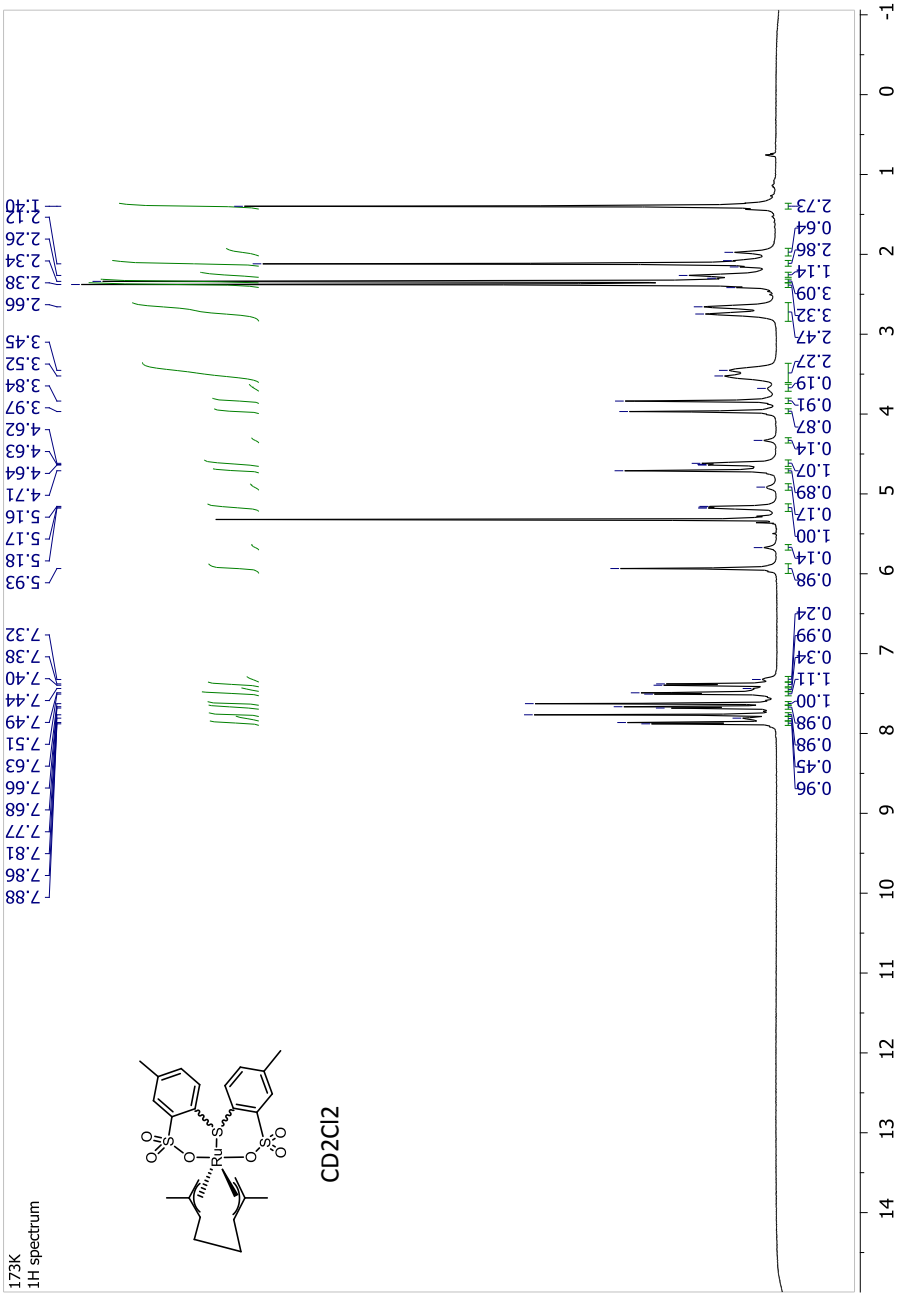
173K
1H spectrum
CD2Cl2
Ru
S
O
7.88
7.86
7.81
7.77
7.68
7.66
7.63
7.51
7.49
7.44
7.40
7.38
7.32
5.93
5.18
5.17
5.16
4.71
4.64
4.63
4.62
3.97
3.84
3.52
3.45
2.66
2.38
2.34
2.26
2.12
1.40
0.96
0.45
0.98
0.98
1.00
0.98
1.11
0.34
0.99
0.24
0.98
0.14
1.00
0.17
0.89
1.07
0.14
0.87
0.91
0.19
2.27
2.47
3.32
3.09
1.14
2.86
0.64
2.73

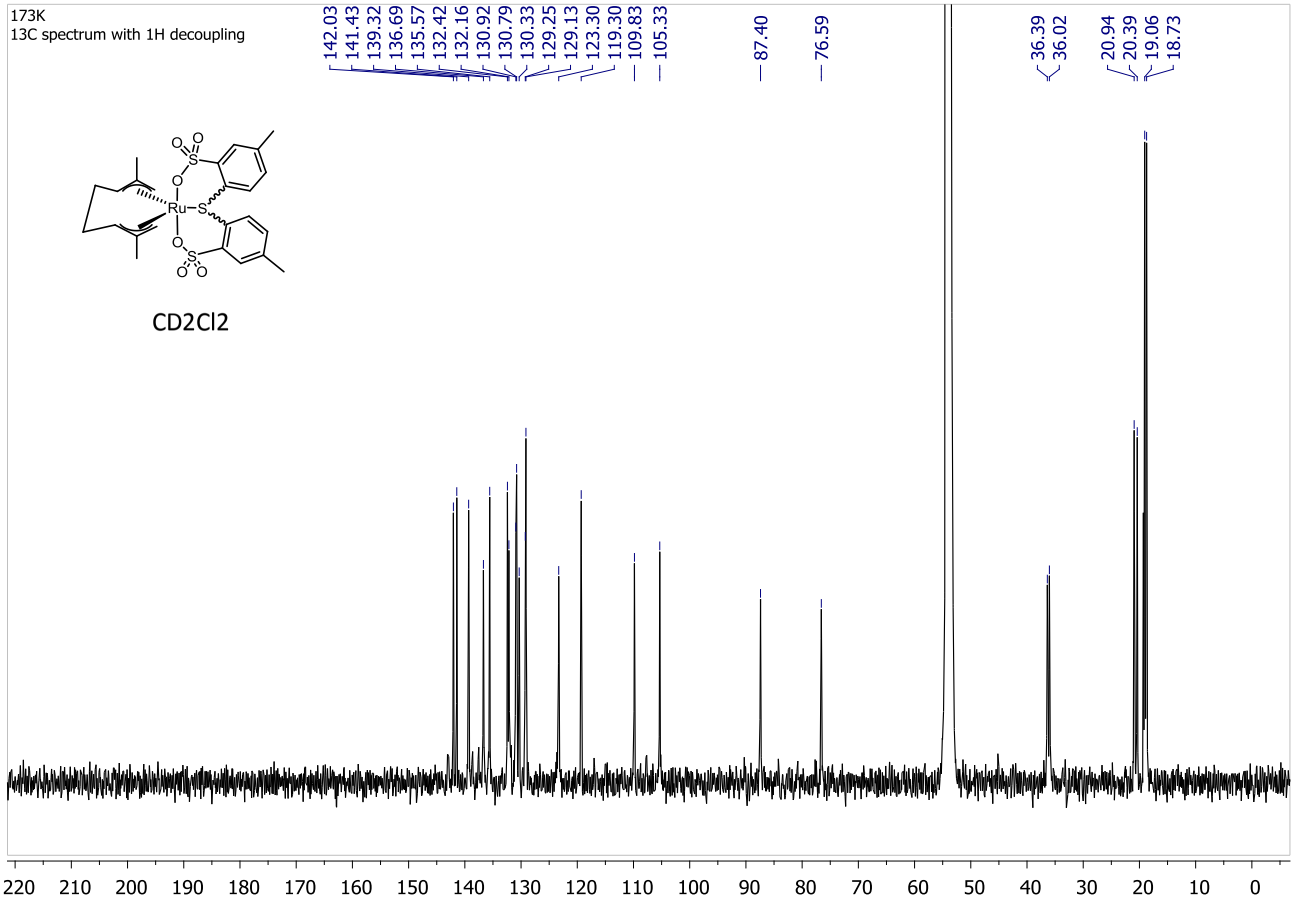
173K
13C spectrum with 1H decoupling
142.03
141.43
139.32
136.69
135.57
132.42
132.16
130.92
130.79
130.33
129.25
129.13
123.30
119.30
109.83
105.33
87.40
76.59
36.39
36.02
20.94
20.39
19.06
18.73
CD2Cl2
220
210
200
190
180
170
160
150
140
130
120
110
100
90
80
70
60
50
40
30
20
10
0

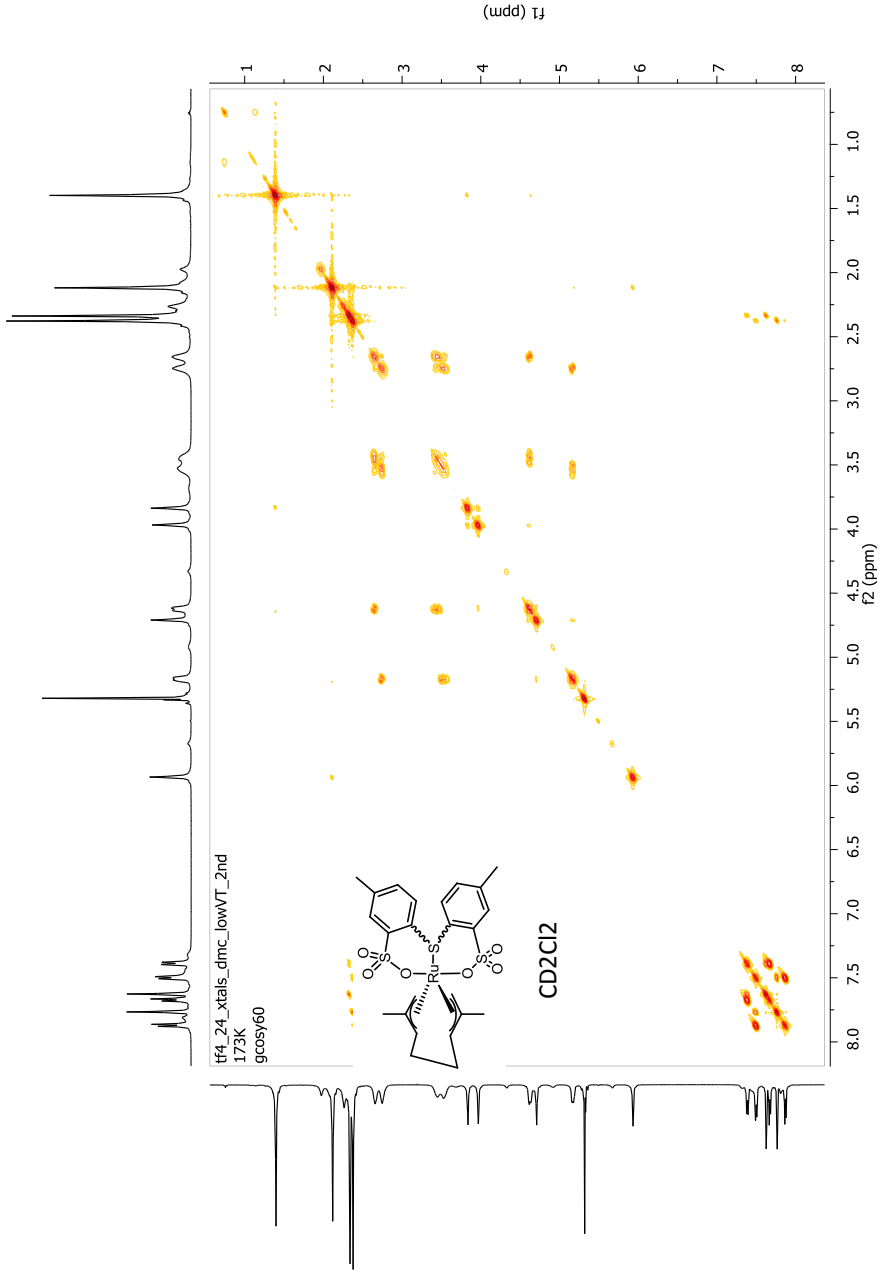
tf4_24_xtals_dmc_lowVT_2nd
173K
gcosy60
CD2Cl2
f2 (ppm)
f1 (ppm)

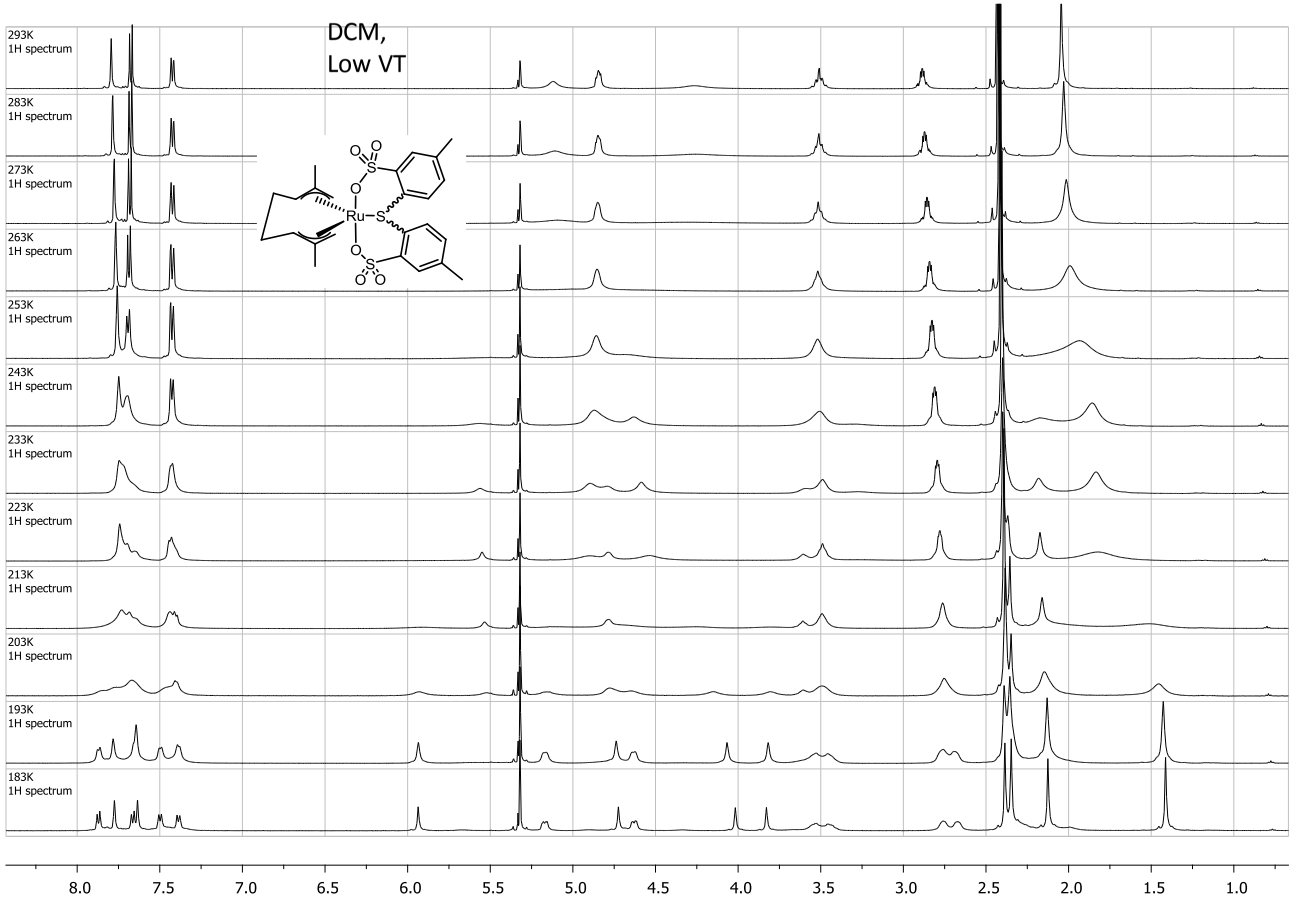
DCM,
Low VT
293K
1H spectrum
283K
1H spectrum
273K
1H spectrum
263K
1H spectrum
253K
1H spectrum
243K
1H spectrum
233K
1H spectrum
223K
1H spectrum
213K
1H spectrum
203K
1H spectrum
193K
1H spectrum
183K
1H spectrum
Ru
S
O
O
S
O
O
O
S
O
O
8.0
7.5
7.0
6.5
6.0
5.5
5.0
4.5
4.0
3.5
3.0
2.5
2.0
1.5
1.0

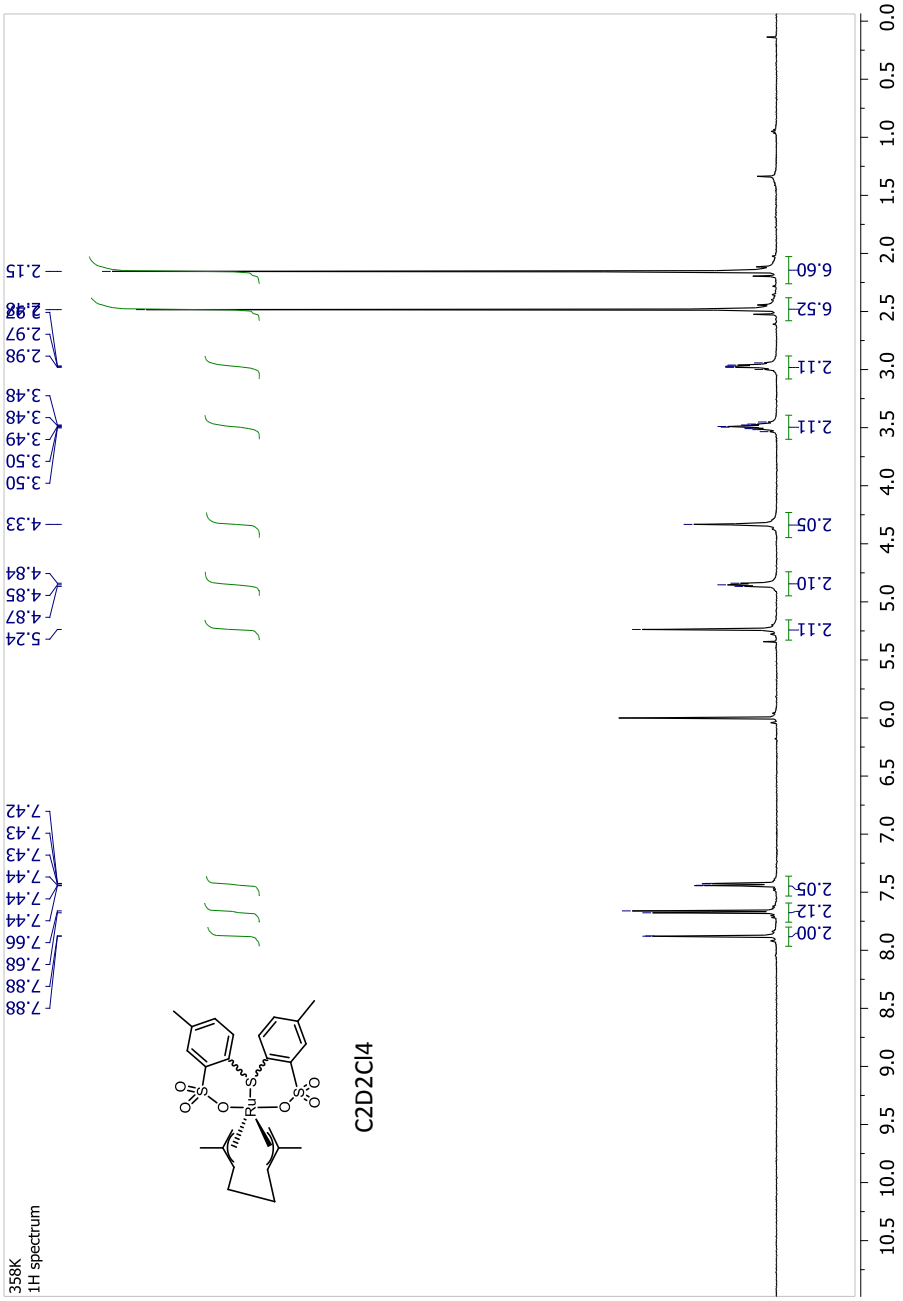
358K
1H spectrum
C2D2Cl4
6.60
6.52
2.11
2.11
2.05
2.10
2.11
2.05
2.12
2.00
2.15
4.33
5.24
4.87
4.85
4.84
3.50
3.50
3.49
3.48
3.48
2.98
2.97
7.88
7.88
7.68
7.66
7.44
7.44
7.44
7.43
7.43
7.42

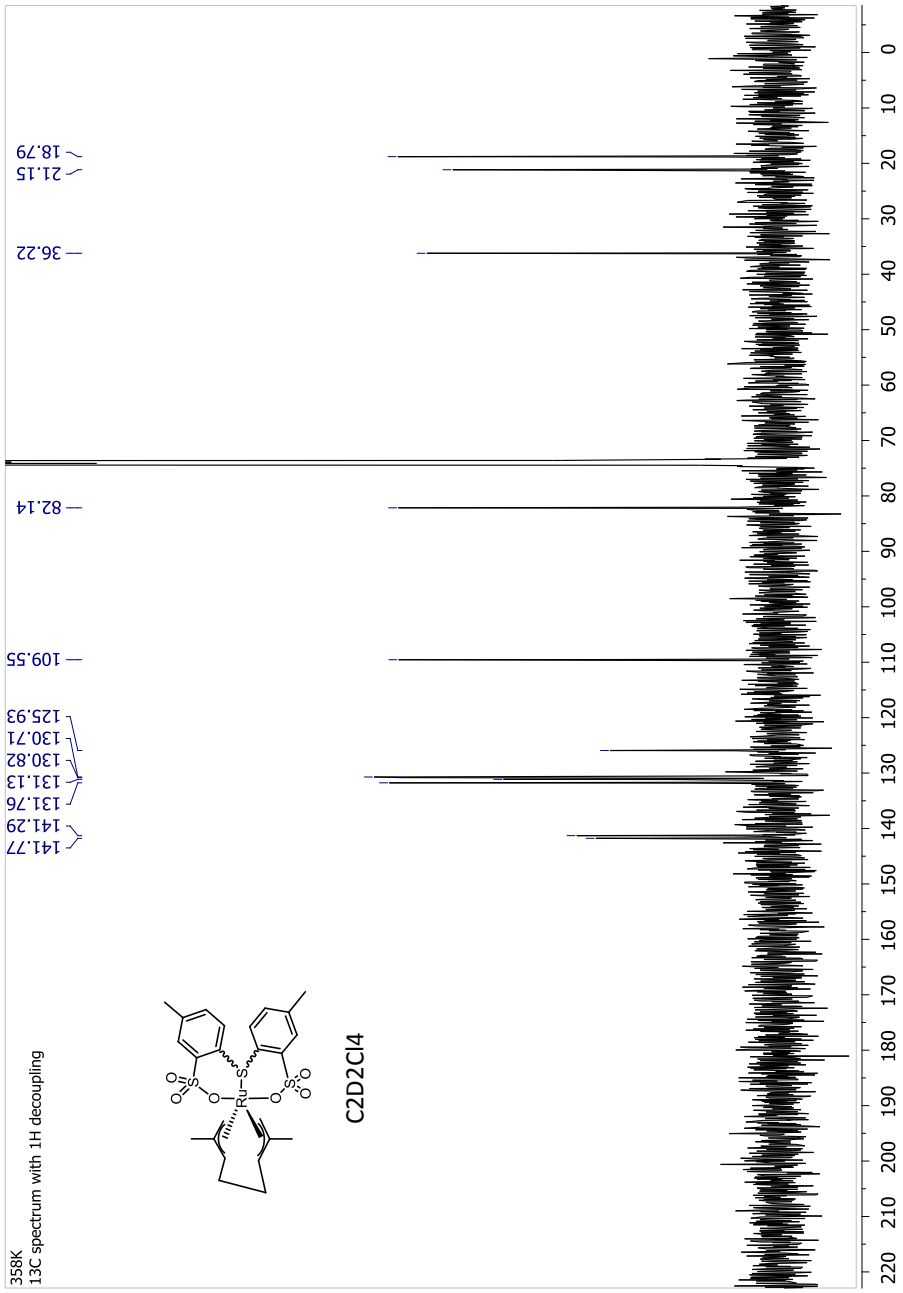
358K
13C spectrum with 1H decoupling
C2D2Cl4
141.77
141.29
131.76
131.13
130.82
130.71
125.93
109.55
82.14
36.22
21.15
18.79

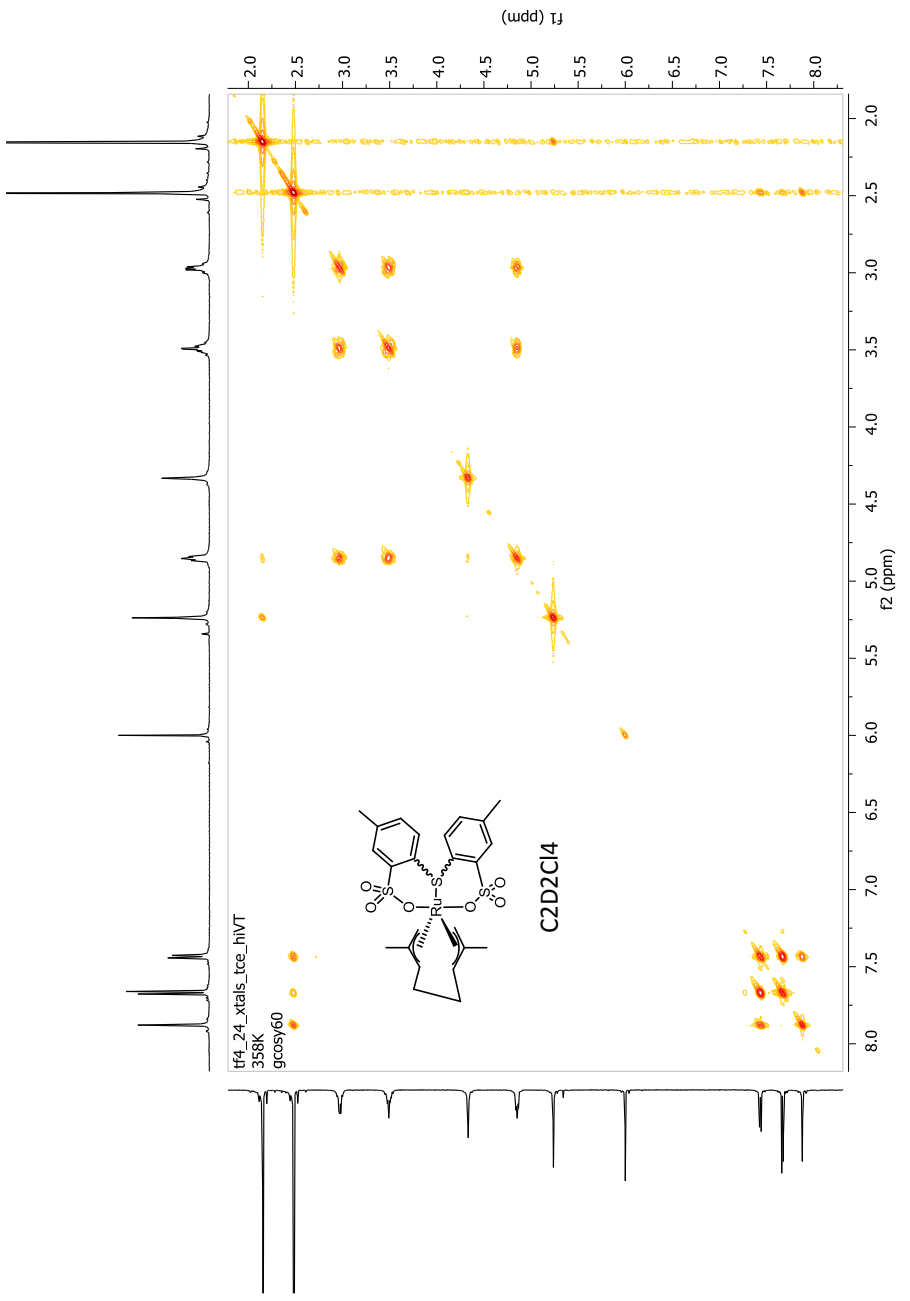
f1 (ppm)
2.0
2.5
3.0
3.5
4.0
4.5
5.0
5.5
6.0
6.5
7.0
7.5
8.0
f2 (ppm)
tf4_24_xtals_tce_hiVT
358K
gcosy60
C2D2Cl4
Ru
S
O

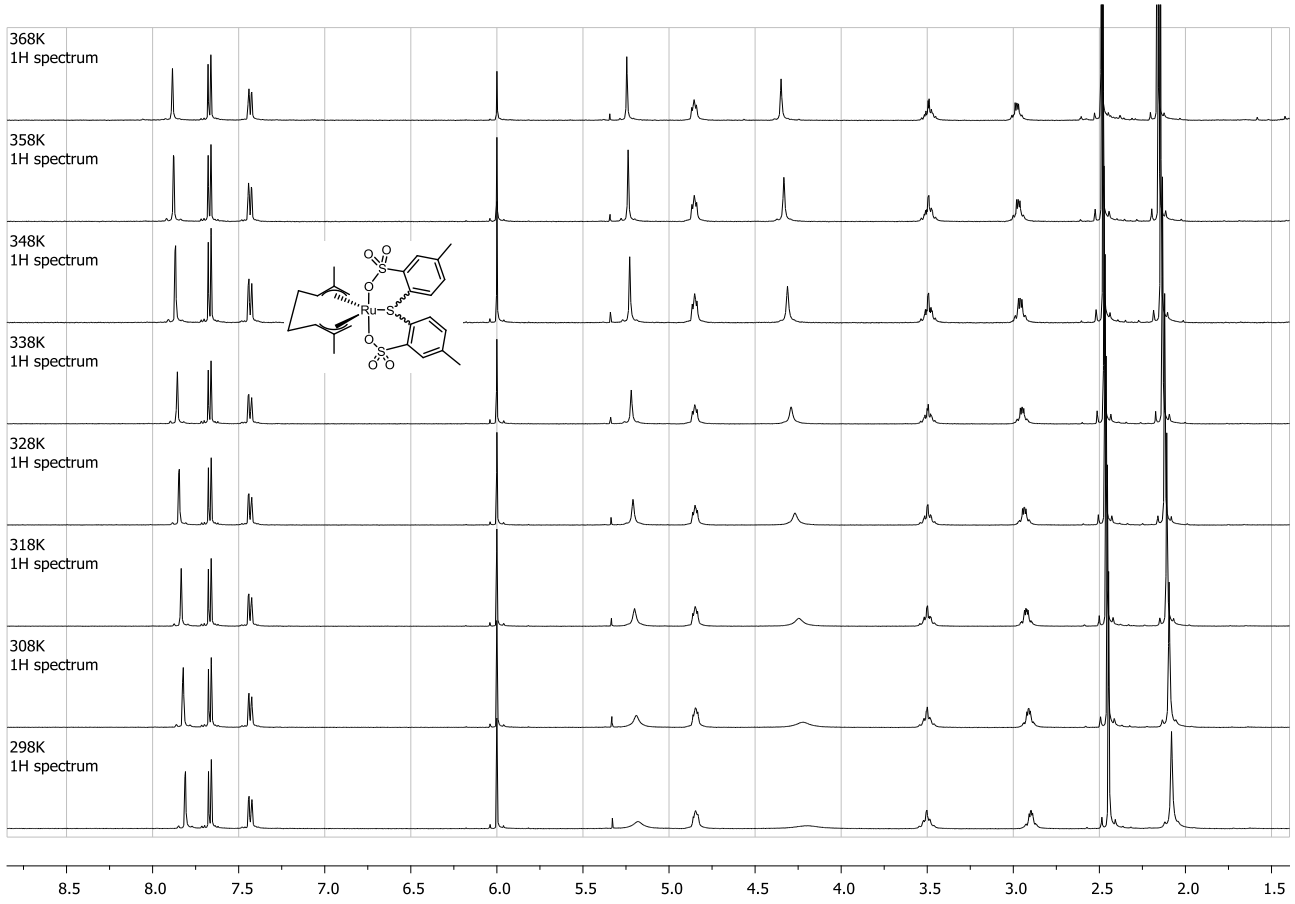
368K
1H spectrum
358K
1H spectrum
348K
1H spectrum
338K
1H spectrum
328K
1H spectrum
318K
1H spectrum
308K
1H spectrum
298K
1H spectrum
Ru
S
O
8.5
8.0
7.5
7.0
6.5
6.0
5.5
5.0
4.5
4.0
3.5
3.0
2.5
2.0
1.5

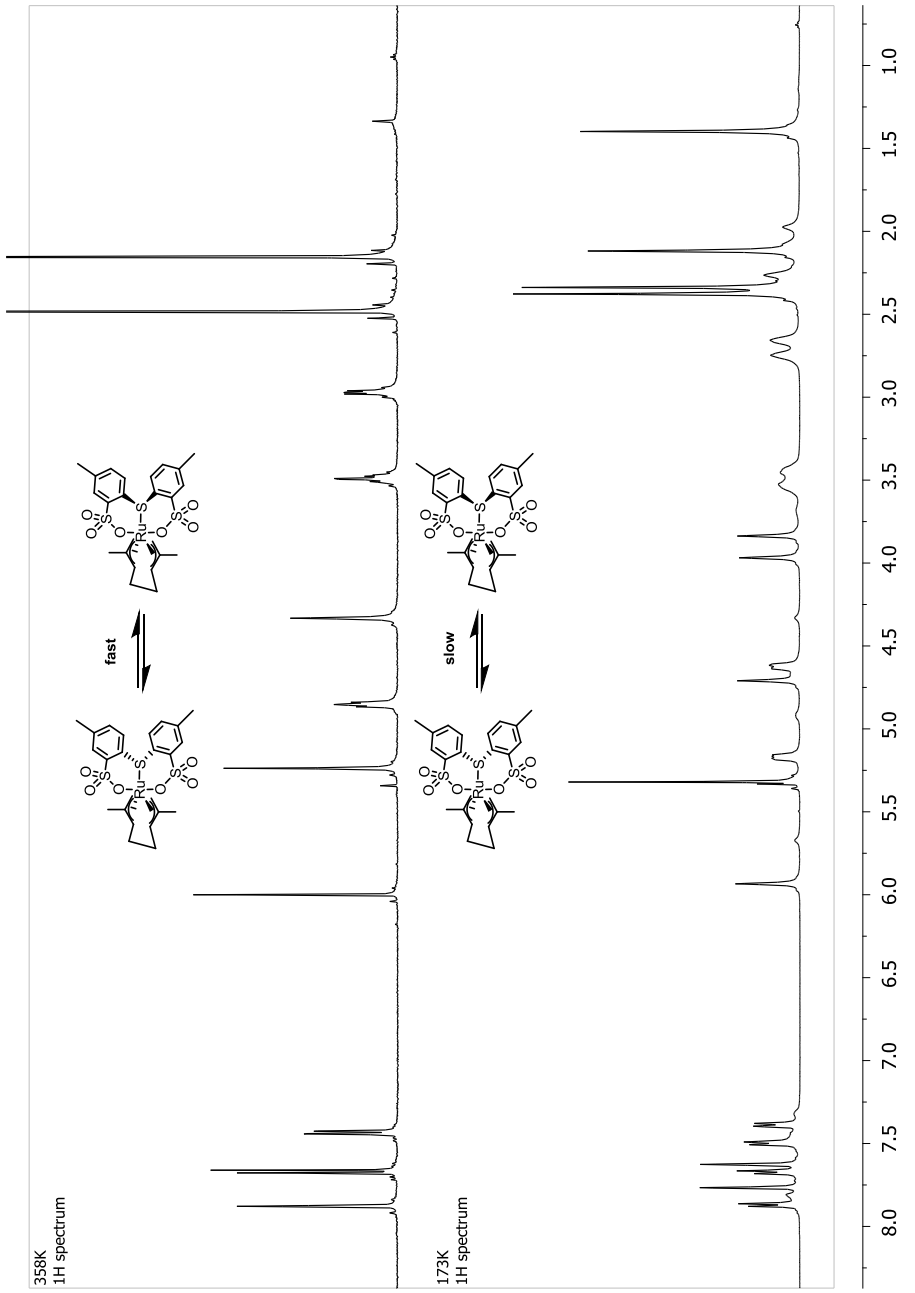
358K
1H spectrum
fast
173K
1H spectrum
slow
8.0
7.5
7.0
6.5
6.0
5.5
5.0
4.5
4.0
3.5
3.0
2.5
2.0
1.5
1.0

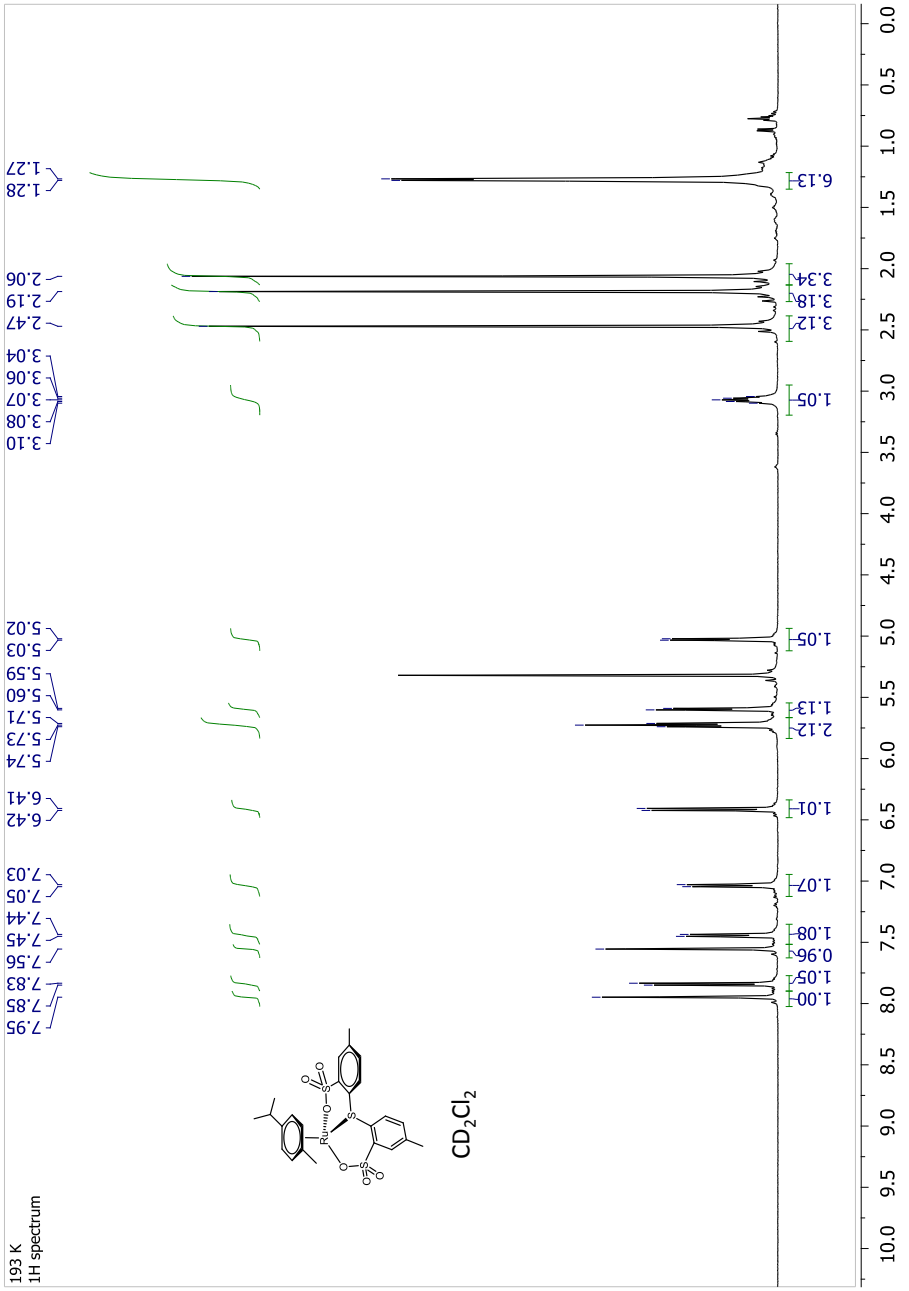
193 K
1H spectrum
CD2Cl2
7.95
7.85
7.83
7.56
7.45
7.44
7.05
7.03
6.42
6.41
5.74
5.73
5.71
5.60
5.59
5.03
5.02
3.10
3.08
3.07
3.06
3.04
2.47
2.19
2.06
1.28
1.27
6.13
3.34
3.18
3.12
1.05
1.05
1.13
2.12
1.01
1.07
1.08
0.96
1.05
1.00

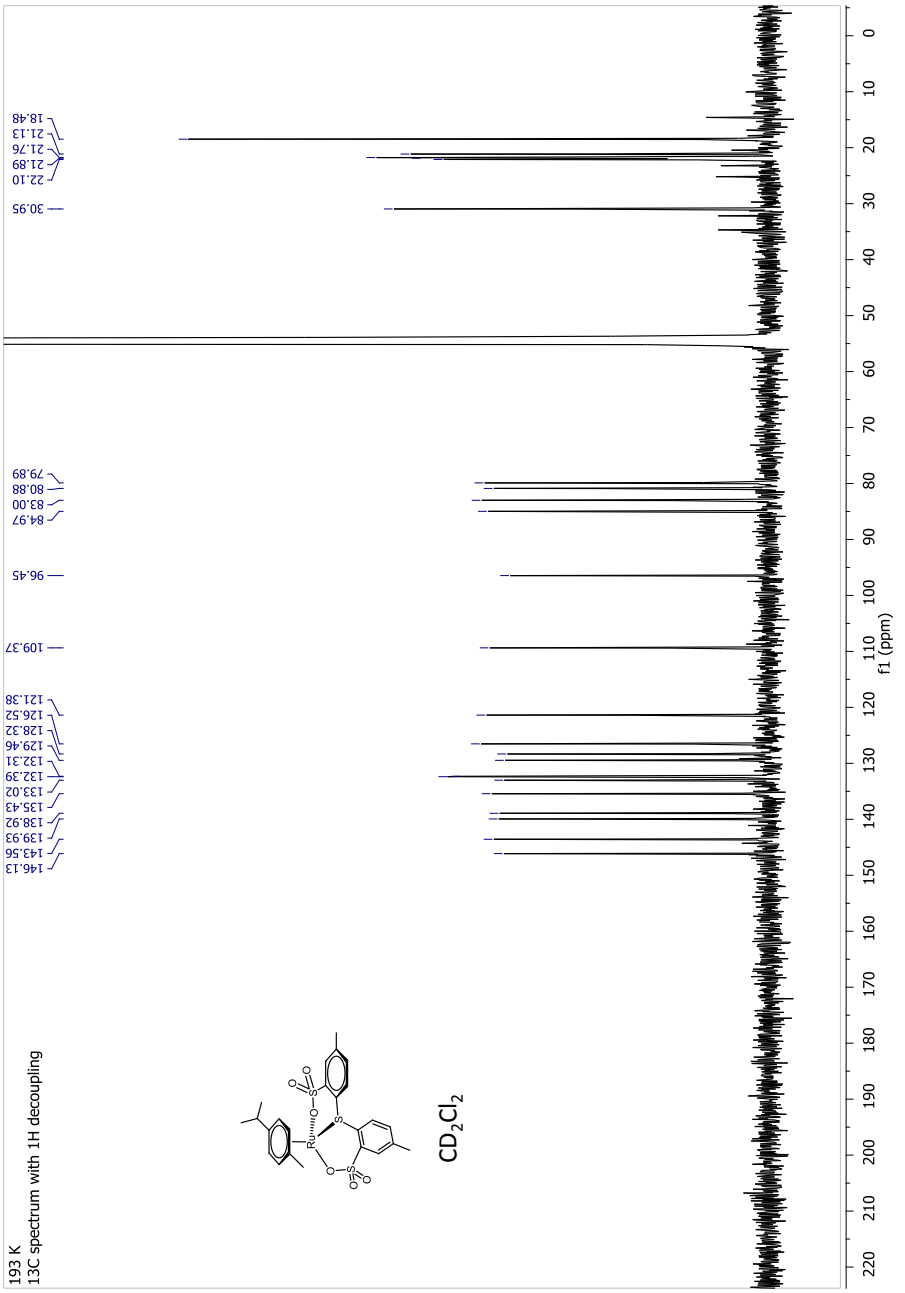
193 K
13C spectrum with 1H decoupling
18.48
21.13
21.76
21.89
22.10
30.95
79.89
80.88
83.00
84.97
96.45
109.37
121.38
126.52
128.32
129.46
132.31
132.39
133.02
135.43
138.92
139.93
143.56
146.13
CD2Cl2
f1 (ppm)

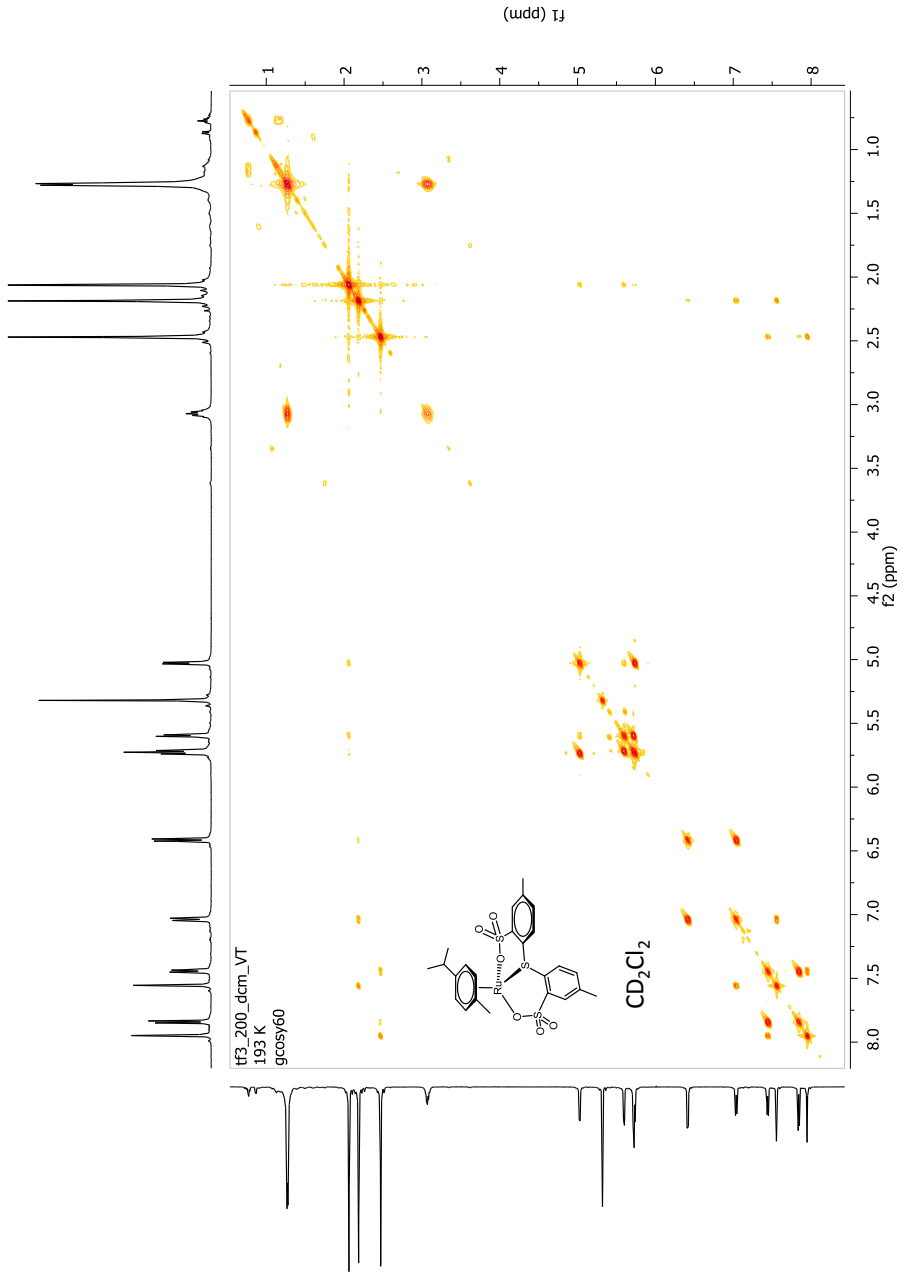
f1 (ppm)
1
2
3
4
5
6
7
8
f2 (ppm)
1.0
1.5
2.0
2.5
3.0
3.5
4.0
4.5
5.0
5.5
6.0
6.5
7.0
7.5
8.0
tf3_200_dcm_VT
193 K
gcosy60
CD2Cl2

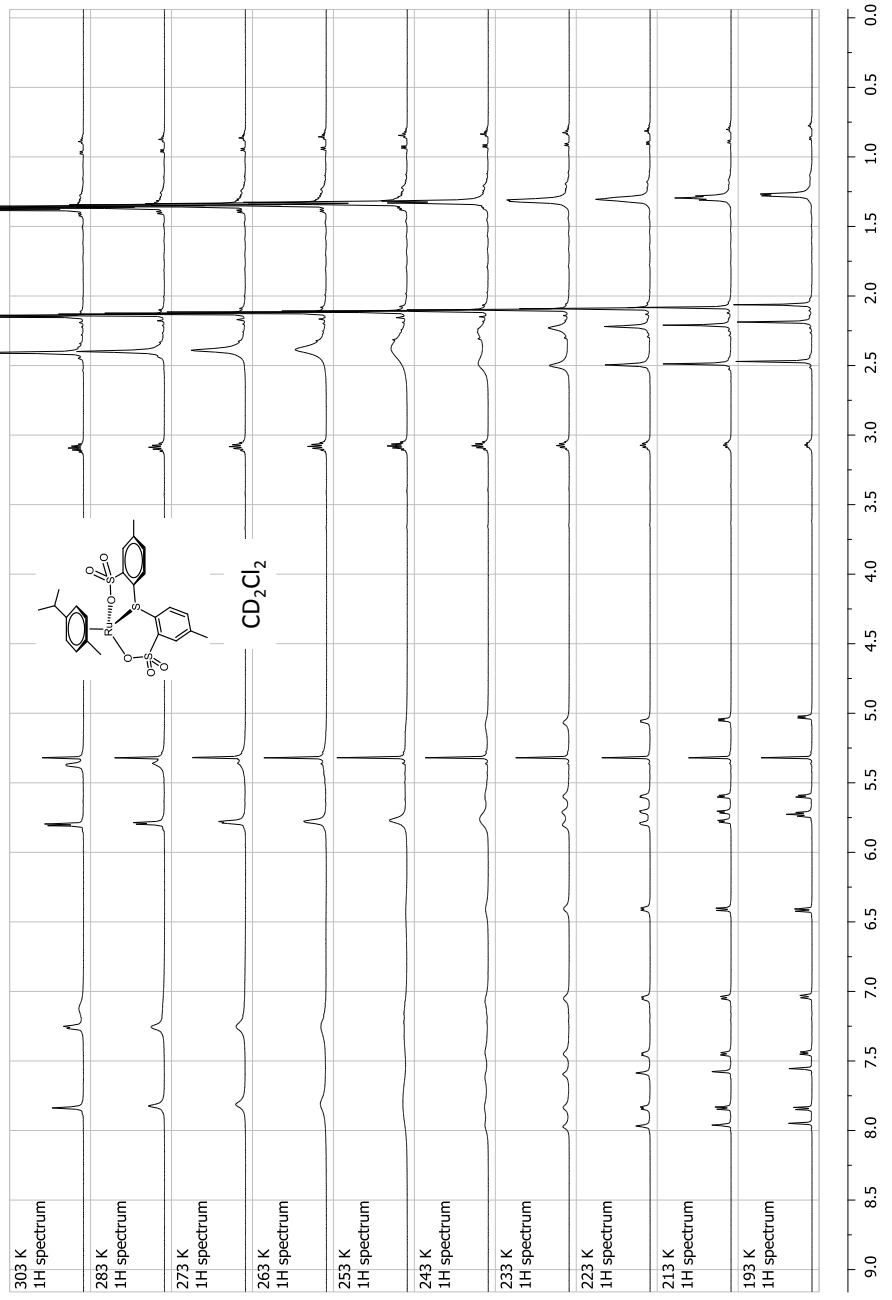
303 K
1H spectrum
283 K
1H spectrum
273 K
1H spectrum
263 K
1H spectrum
253 K
1H spectrum
243 K
1H spectrum
233 K
1H spectrum
223 K
1H spectrum
213 K
1H spectrum
193 K
1H spectrum
CD2Cl2
9.0
8.5
8.0
7.5
7.0
6.5
6.0
5.5
5.0
4.5
4.0
3.5
3.0
2.5
2.0
1.5
1.0
0.5
0.0

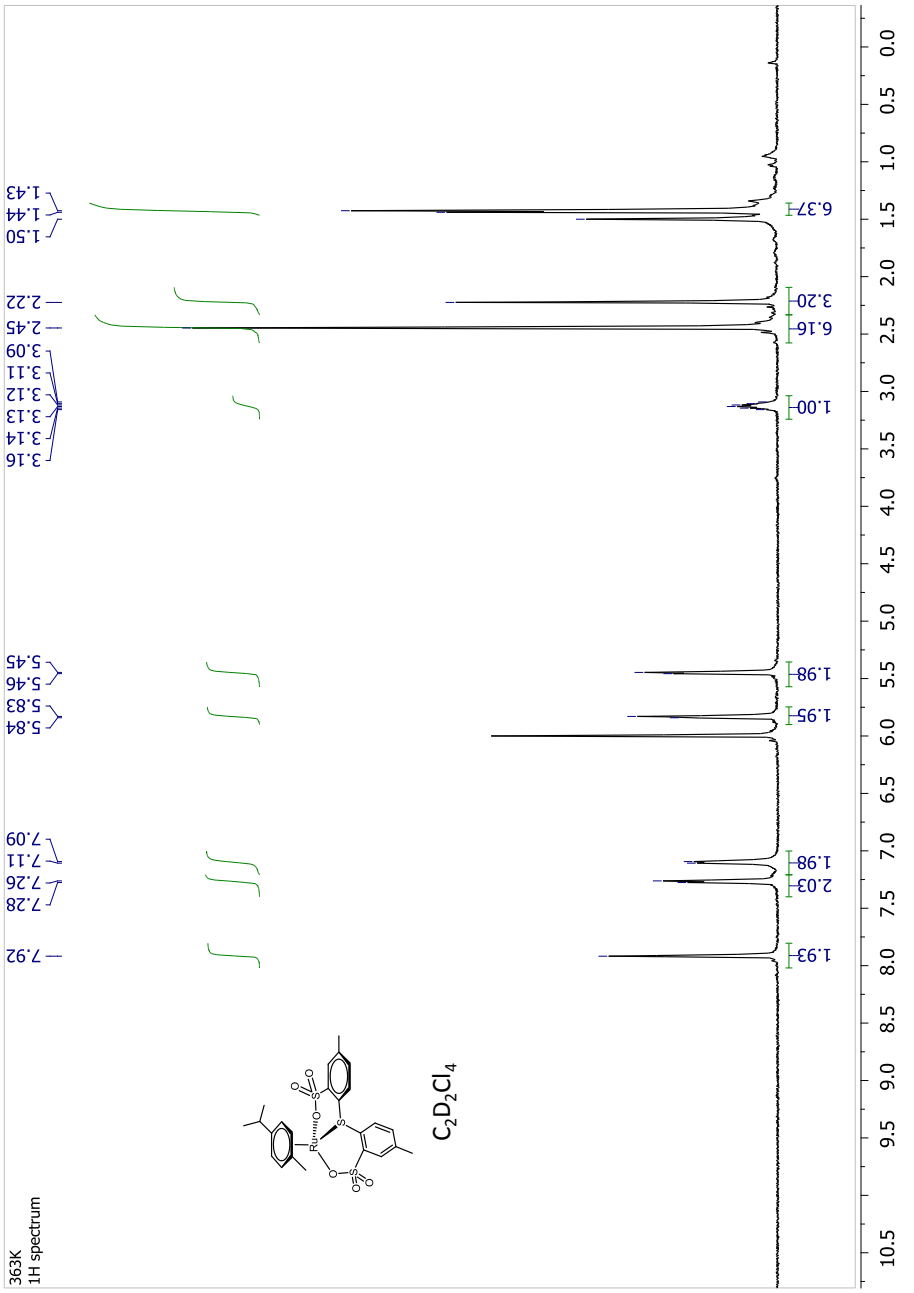
363K
1H spectrum
C2D2Cl4
1.43
1.44
1.50
2.22
2.45
3.09
3.11
3.12
3.13
3.14
3.16
5.45
5.46
5.83
5.84
7.09
7.11
7.26
7.28
7.92
6.37
3.20
6.16
1.00
1.98
1.95
1.98
2.03
1.93

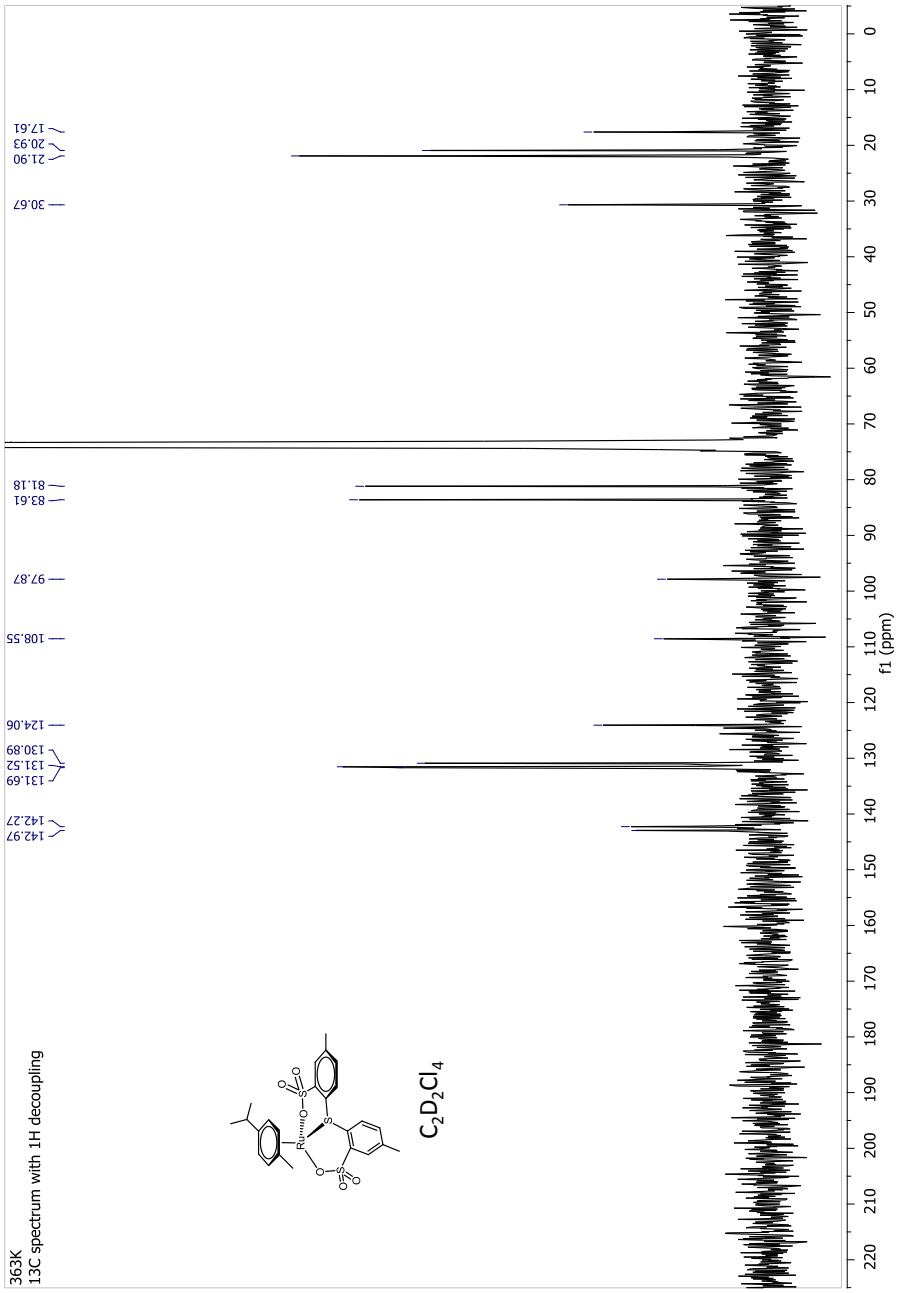
363K
13C spectrum with 1H decoupling
142.97
142.27
131.69
131.52
130.89
124.06
108.55
97.87
83.61
81.18
30.67
21.90
20.93
17.61
f1 (ppm)
C2D2Cl4

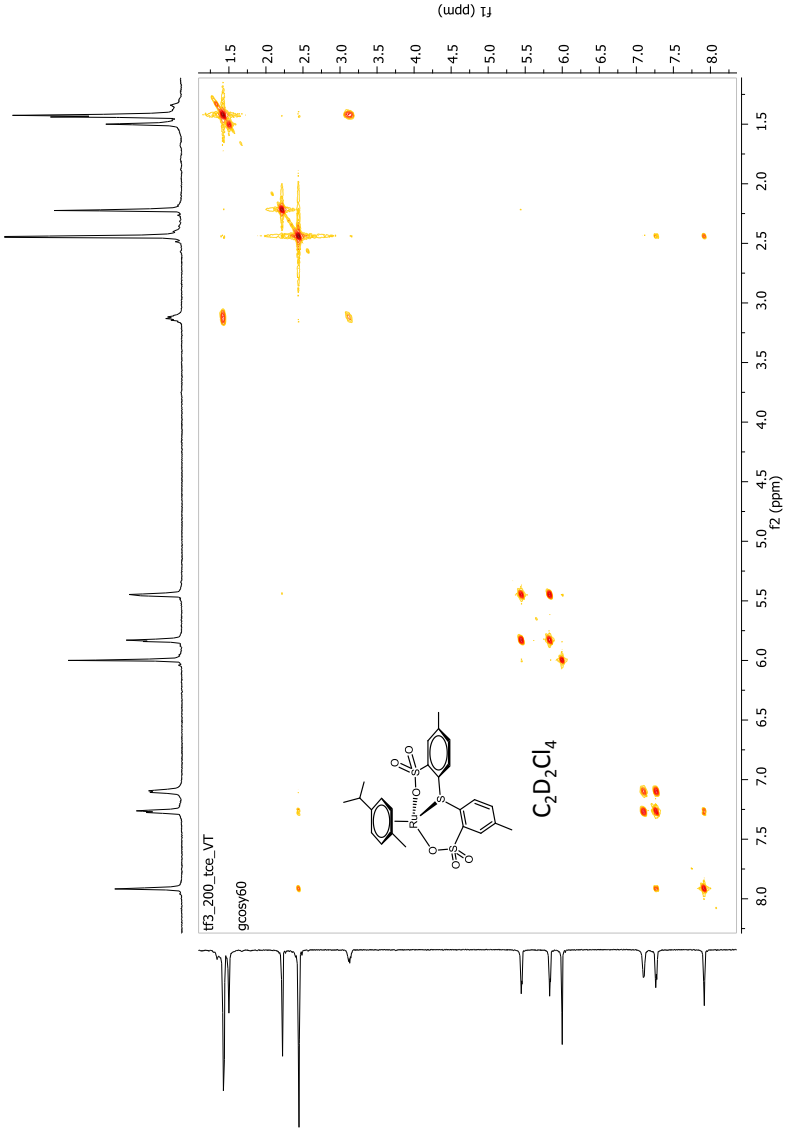
tf3_200_tce_VT
gcosy60
f1 (ppm)
f2 (ppm)
C2D2Cl4

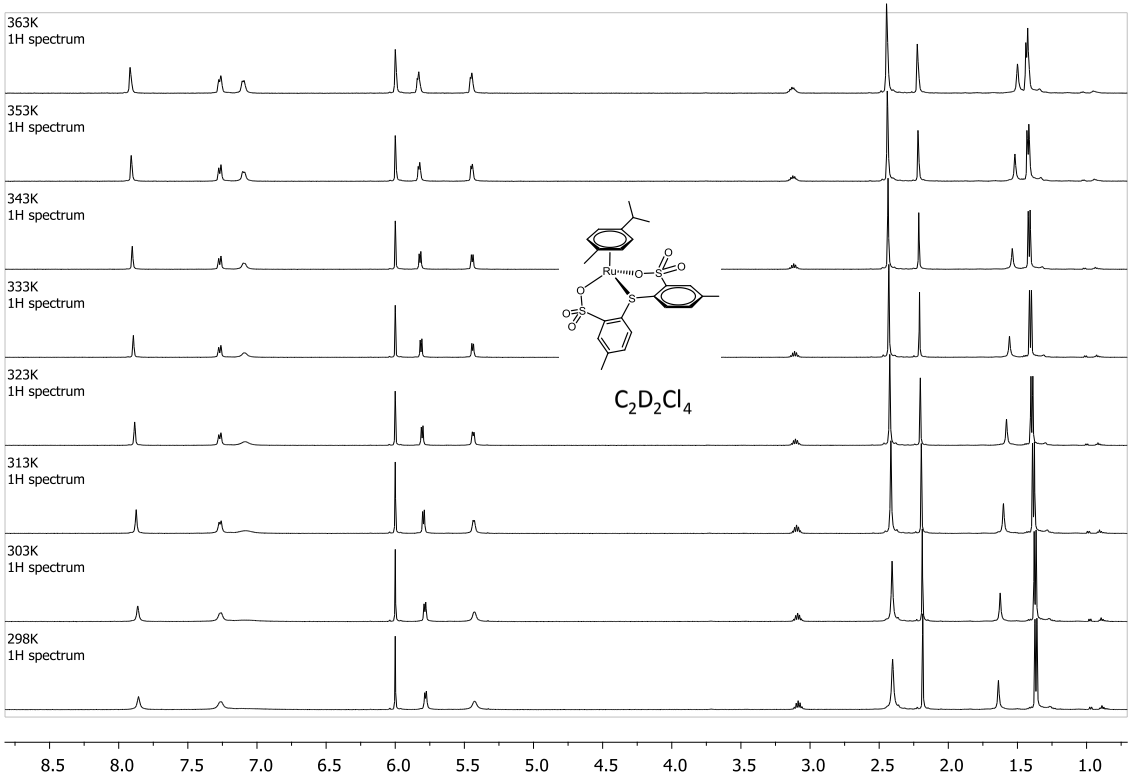
363K
1H spectrum
353K
1H spectrum
343K
1H spectrum
333K
1H spectrum
323K
1H spectrum
313K
1H spectrum
303K
1H spectrum
298K
1H spectrum
C2D2Cl4
8.5
8.0
7.5
7.0
6.5
6.0
5.5
5.0
4.5
4.0
3.5
3.0
2.5
2.0
1.5
1.0

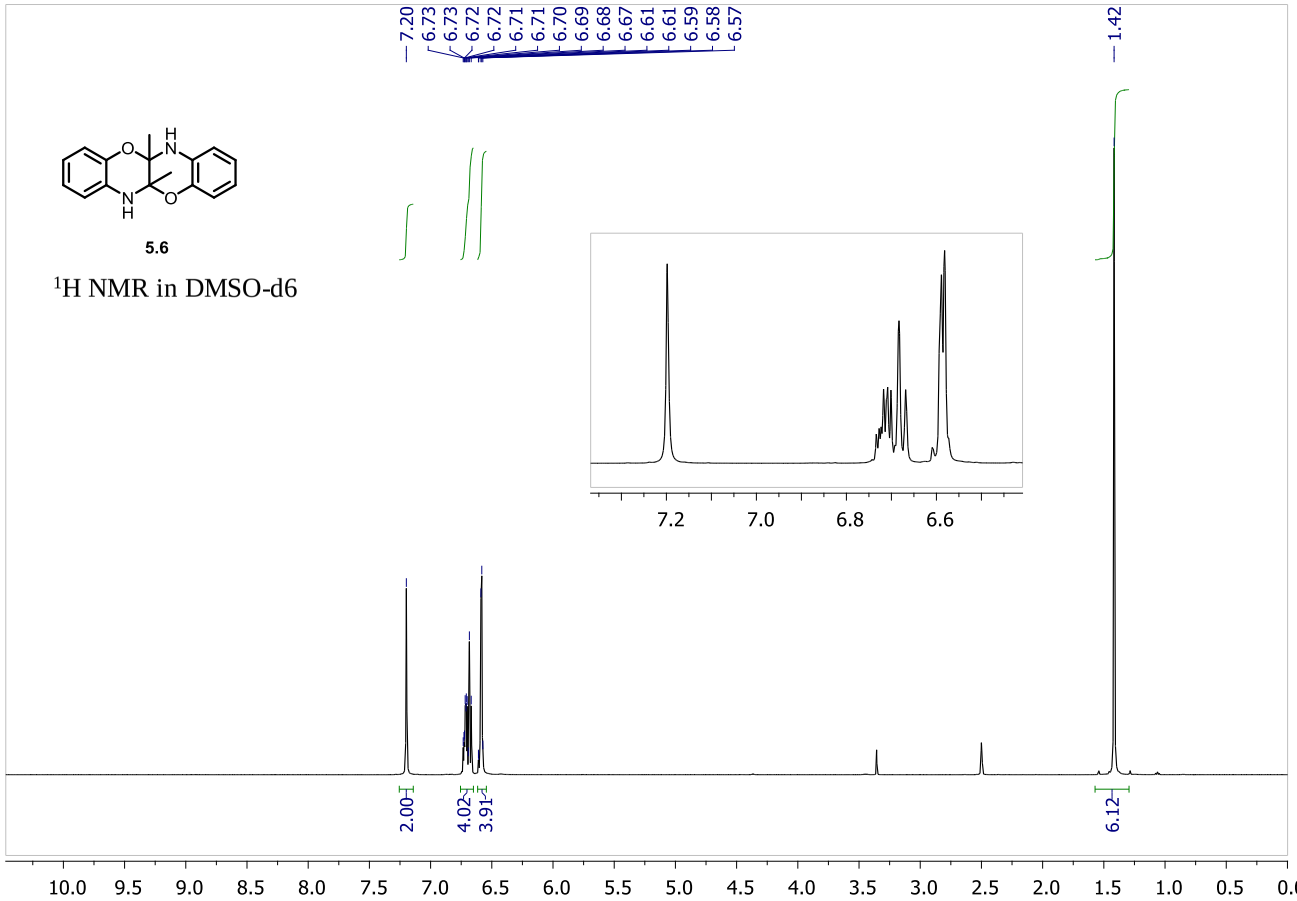
7.20
6.73
6.73
6.72
6.72
6.71
6.71
6.70
6.69
6.68
6.67
6.61
6.61
6.59
6.58
6.57
1.42
5.6
1H NMR in DMSO-d6
7.2
7.0
6.8
6.6
2.00
4.02
3.91
6.12
10.0
9.5
9.0
8.5
8.0
7.5
7.0
6.5
6.0
5.5
5.0
4.5
4.0
3.5
3.0
2.5
2.0
1.5
1.0
0.5

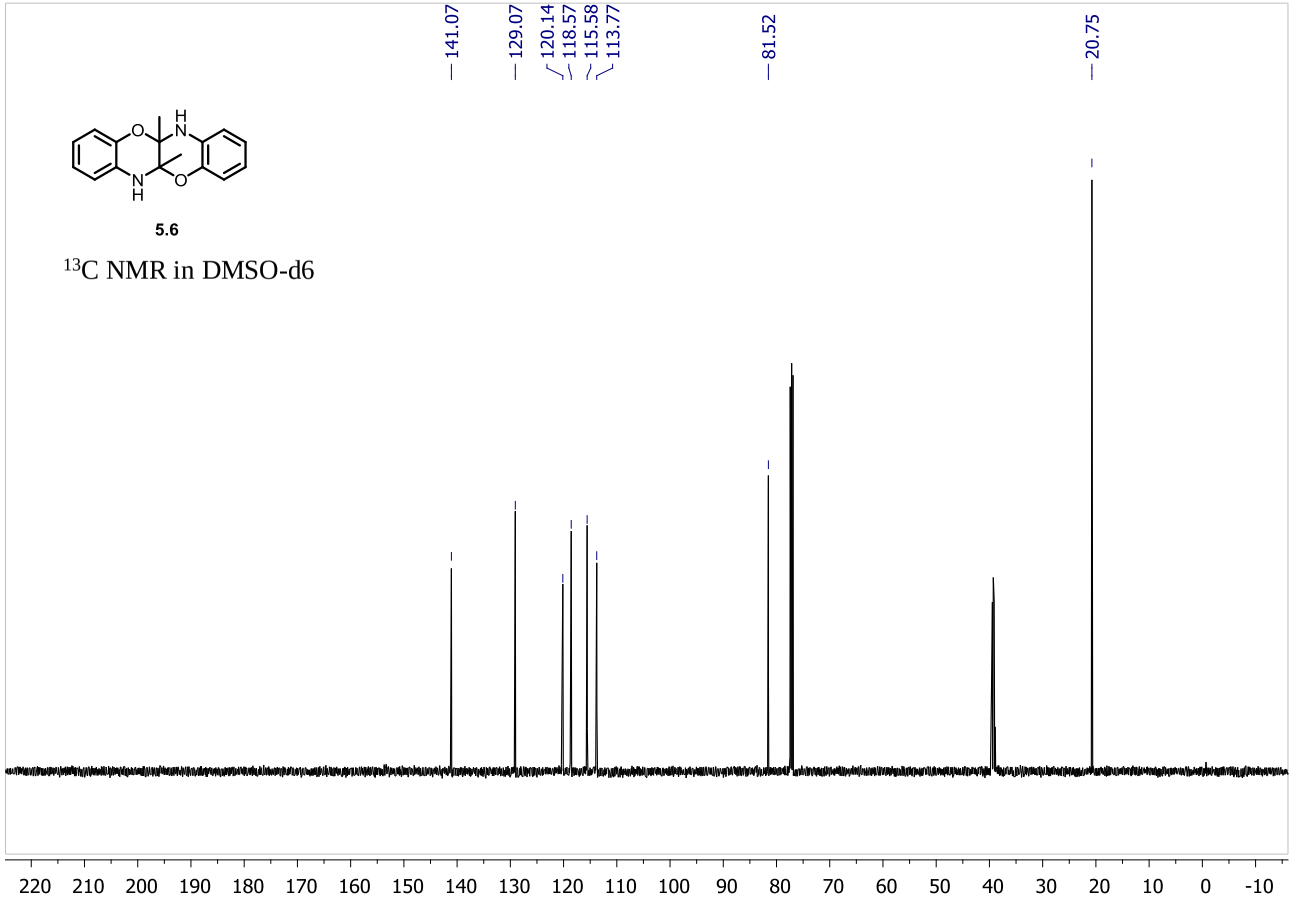
141.07
129.07
120.14
118.57
115.58
113.77
81.52
20.75
5.6
13C NMR in DMSO-d6
220 210 200 190 180 170 160 150 140 130 120 110 100 90 80 70 60 50 40 30 20 10 0 -10

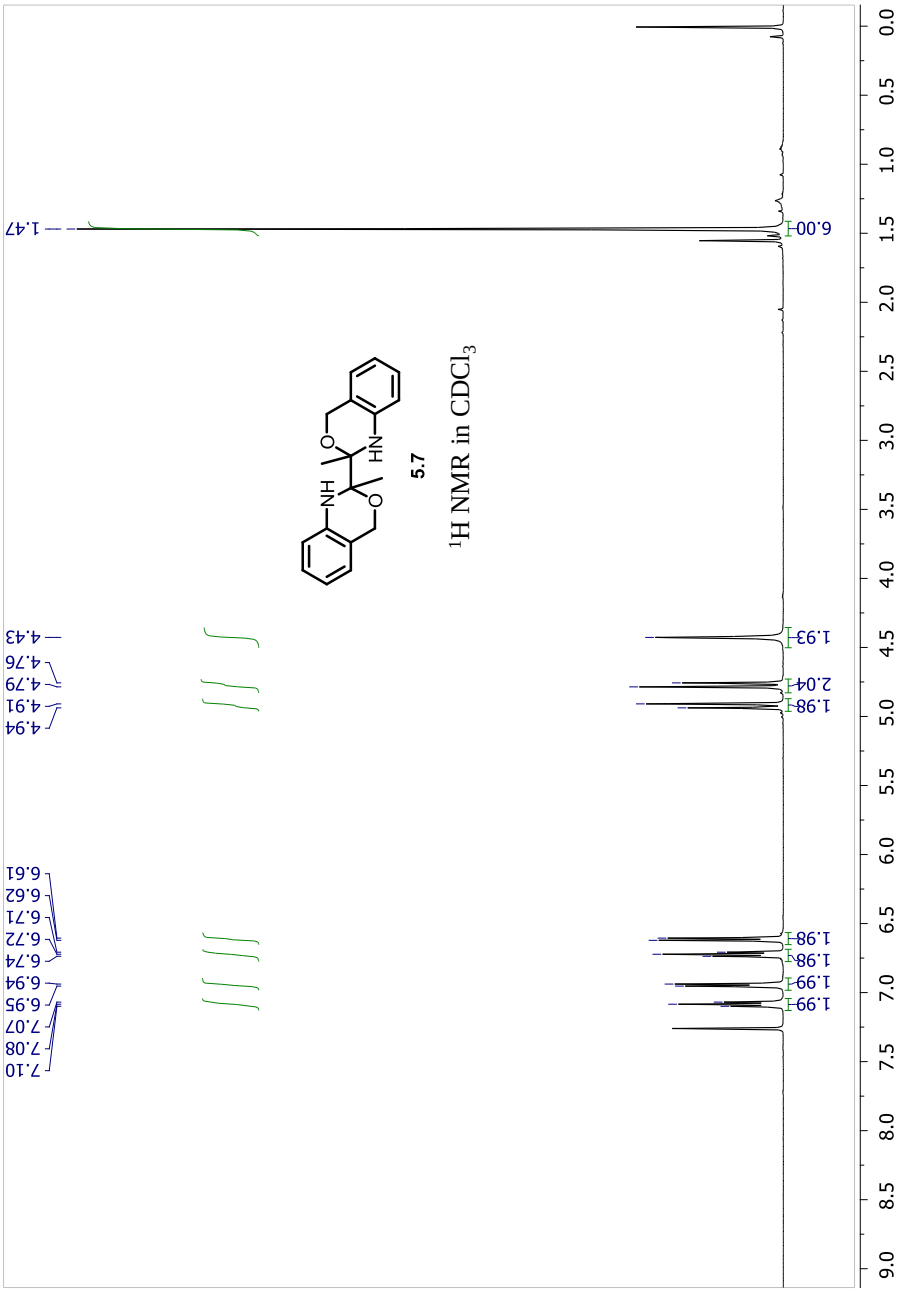
5.7
^{1}H NMR in $CDCl_3$
1.47
6.00
1.93
2.04
1.98
4.94
4.91
4.79
4.76
4.43
1.98
1.98
1.99
1.99
6.61
6.62
6.71
6.72
6.74
6.94
6.95
7.07
7.08
7.10
0.0
0.5
1.0
1.5
2.0
2.5
3.0
3.5
4.0
4.5
5.0
5.5
6.0
6.5
7.0
7.5
8.0
8.5
9.0

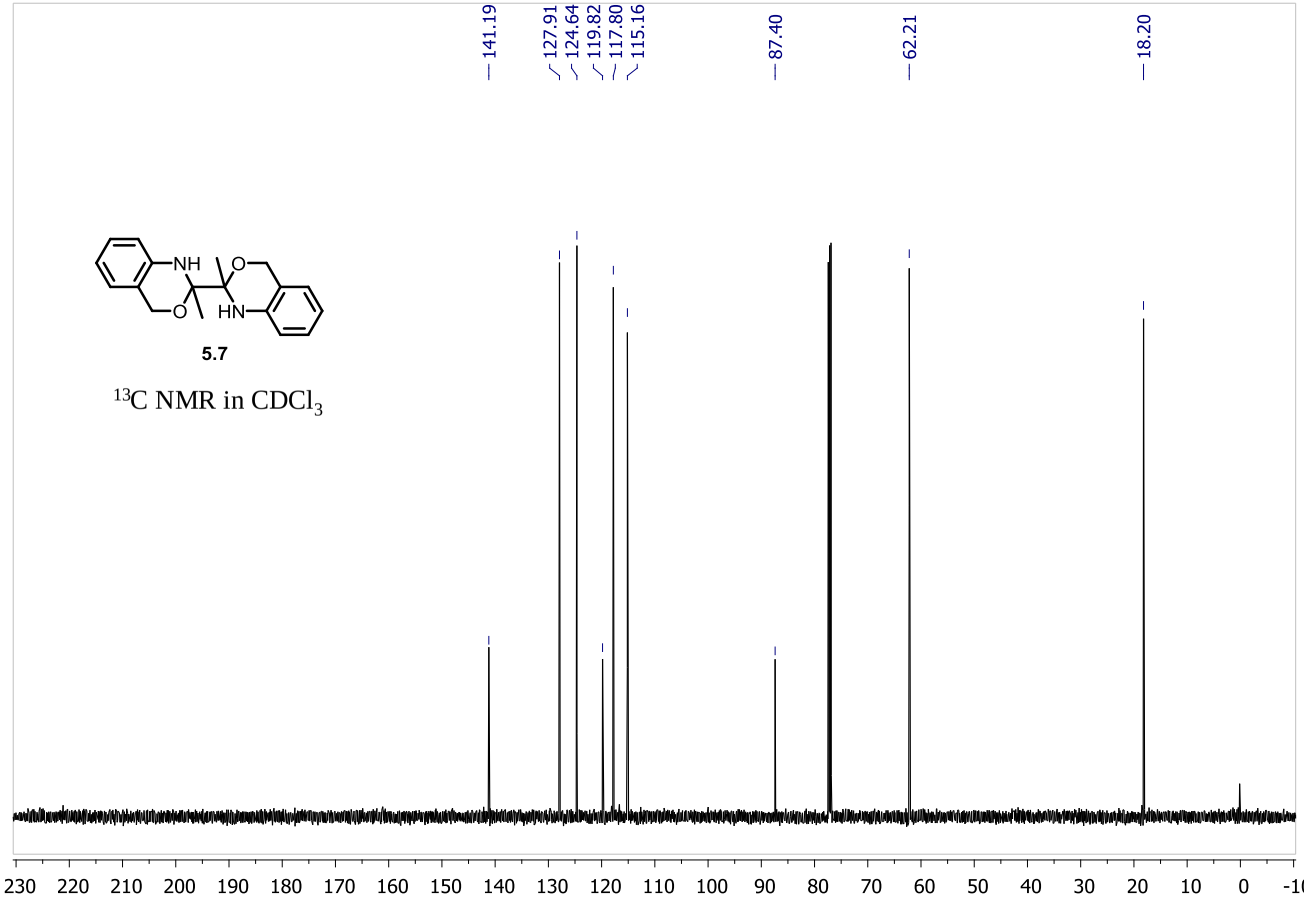
141.19
127.91
124.64
119.82
117.80
115.16
87.40
62.21
18.20
NH
O
O
HN
5.7
13C NMR in CDCl3
230 220 210 200 190 180 170 160 150 140 130 120 110 100 90 80 70 60 50 40 30 20 10 0 -10

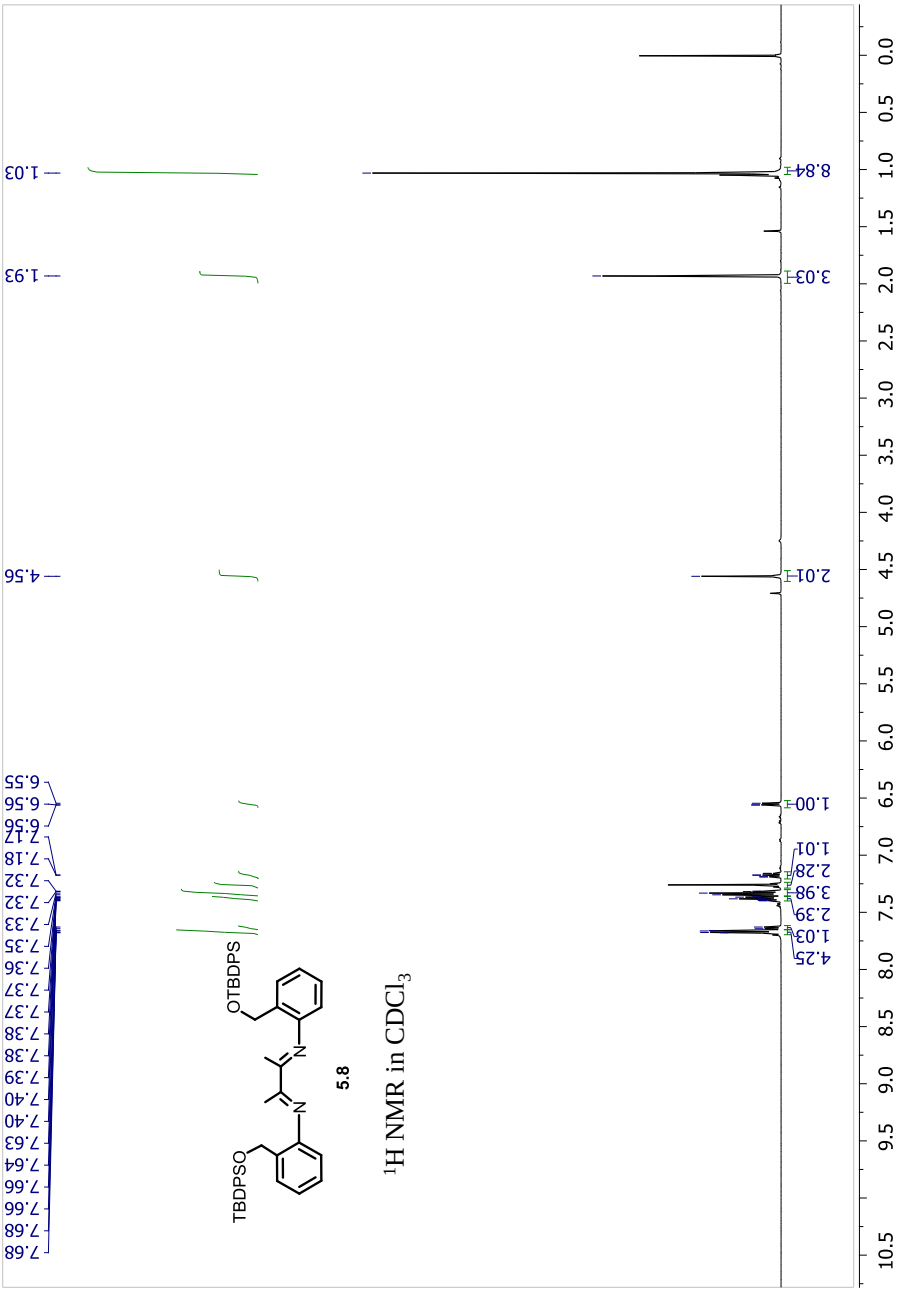
OTBDPS
TBDPSO
N
N
5.8
^{1}H NMR in $CDCl_3$

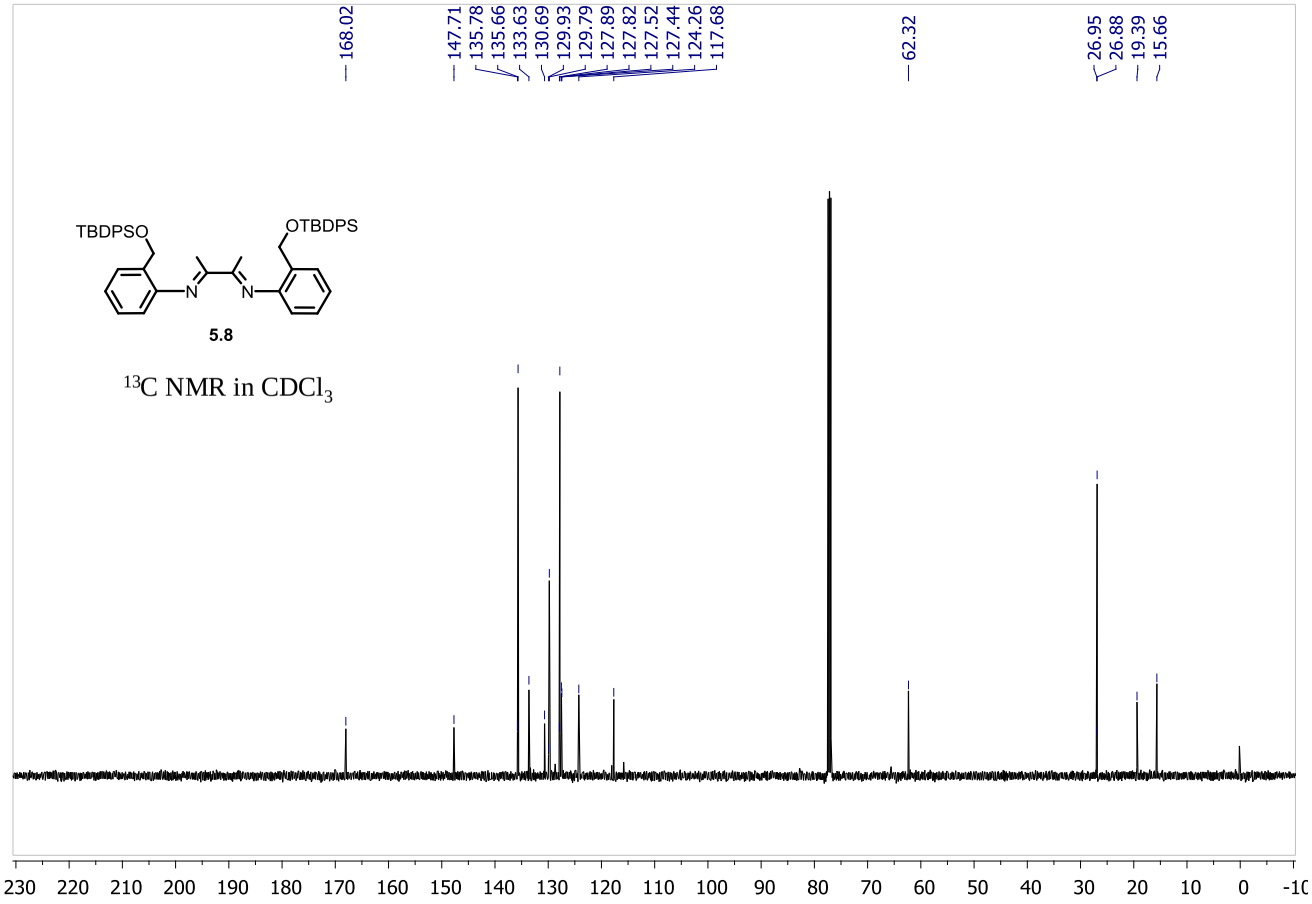
168.02
147.71
135.78
135.66
133.63
130.69
129.93
129.79
127.89
127.82
127.52
127.44
124.26
117.68
62.32
26.95
26.88
19.39
15.66
TBDPSO
OTBDPS
N
N
5.8
13C NMR in CDCl3
230 220 210 200 190 180 170 160 150 140 130 120 110 100 90 80 70 60 50 40 30 20 10 0 -10

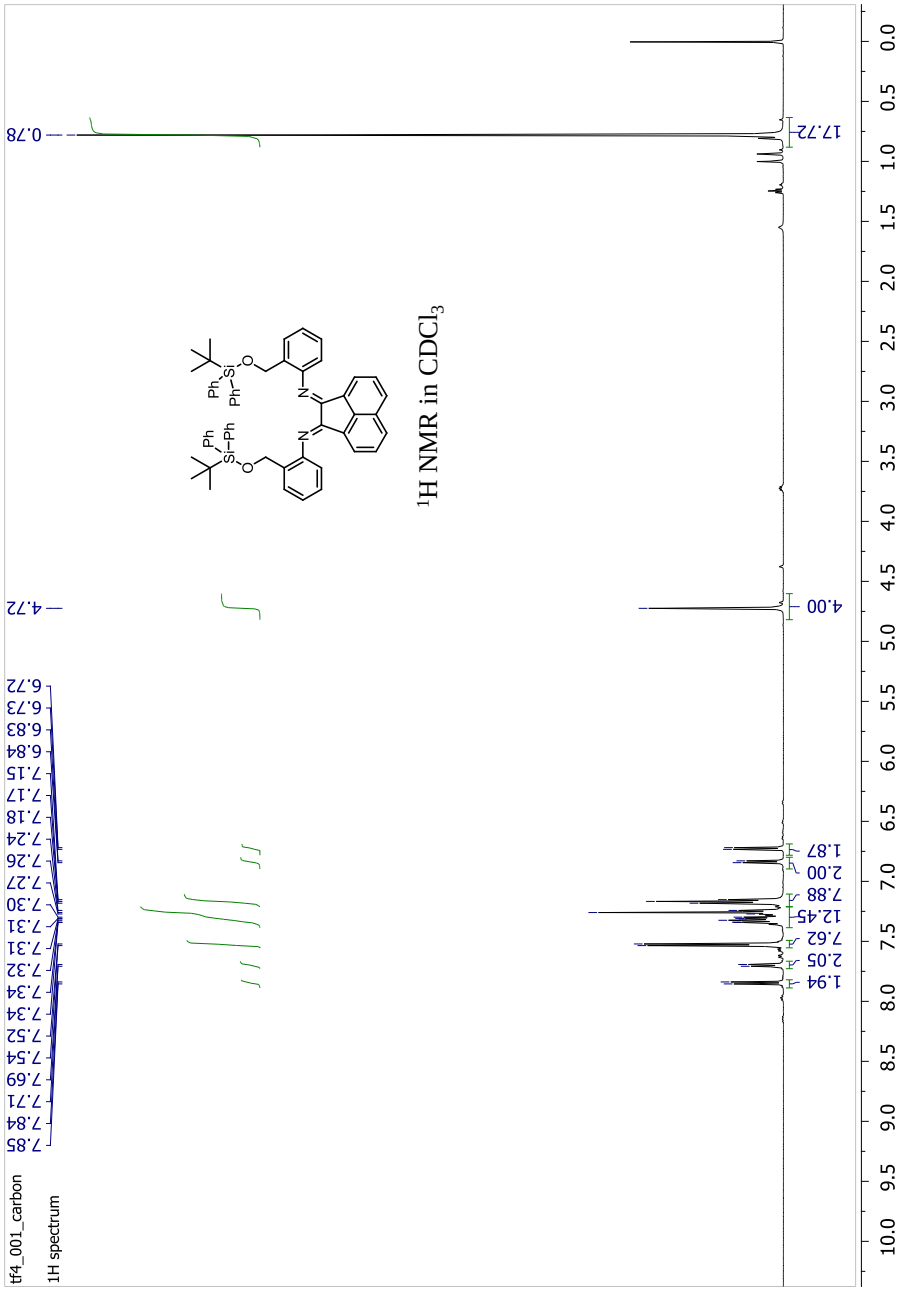
tf4_001_carbon
1H spectrum
7.85
7.84
7.71
7.69
7.54
7.52
7.34
7.34
7.32
7.31
7.31
7.30
7.27
7.26
7.24
7.18
7.17
7.15
6.84
6.83
6.73
6.72
4.72
0.78
17.72
4.00
1.87
2.00
7.88
12.45
7.62
2.05
1.94
0.0
0.5
1.0
1.5
2.0
2.5
3.0
3.5
4.0
4.5
5.0
5.5
6.0
6.5
7.0
7.5
8.0
8.5
9.0
9.5
10.0
Ph
Si
Ph
O
N
N
Ph
Si
Ph
O
^{1}H NMR in $CDCl_3$

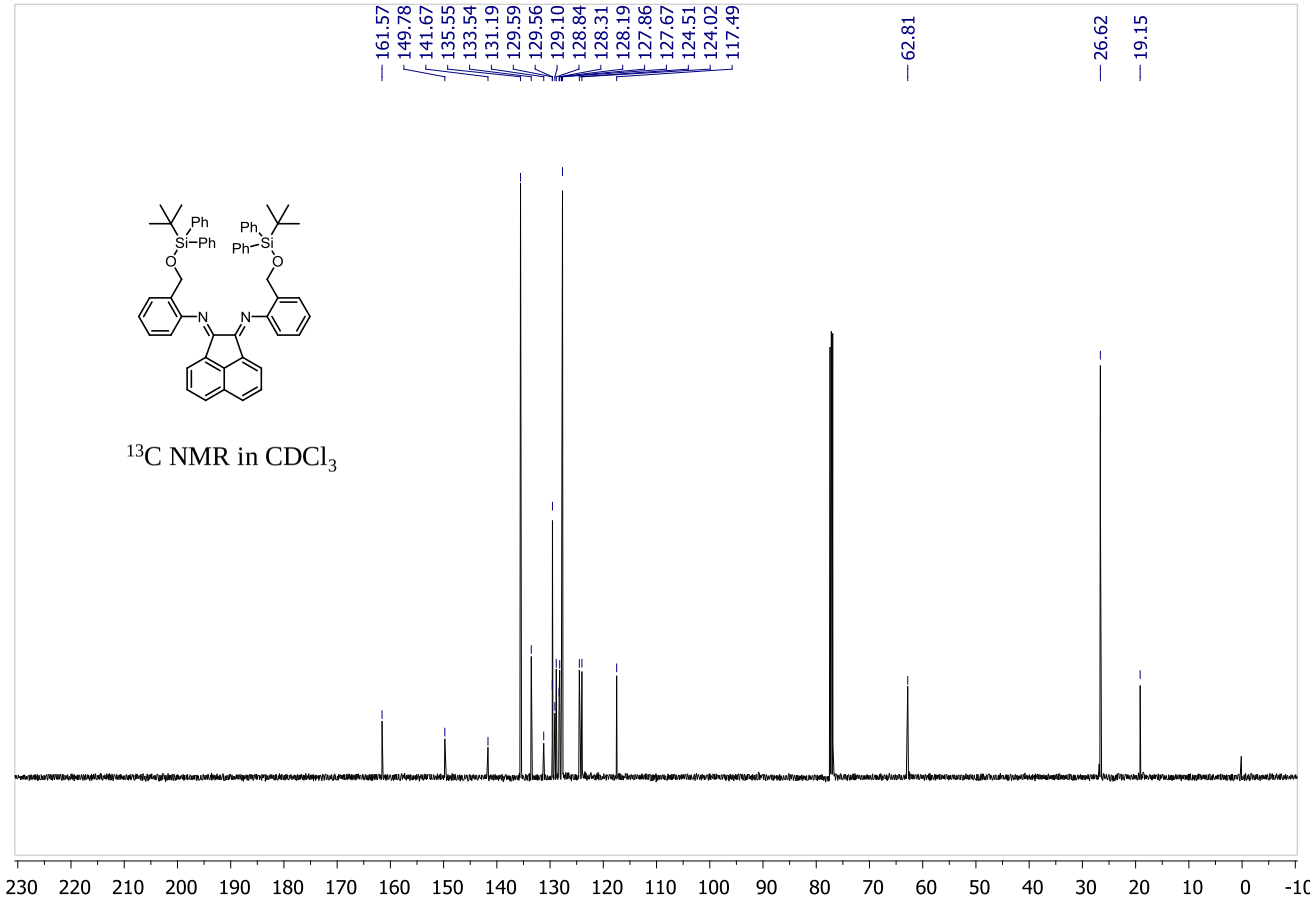

^{13}C NMR in $CDCl_3$

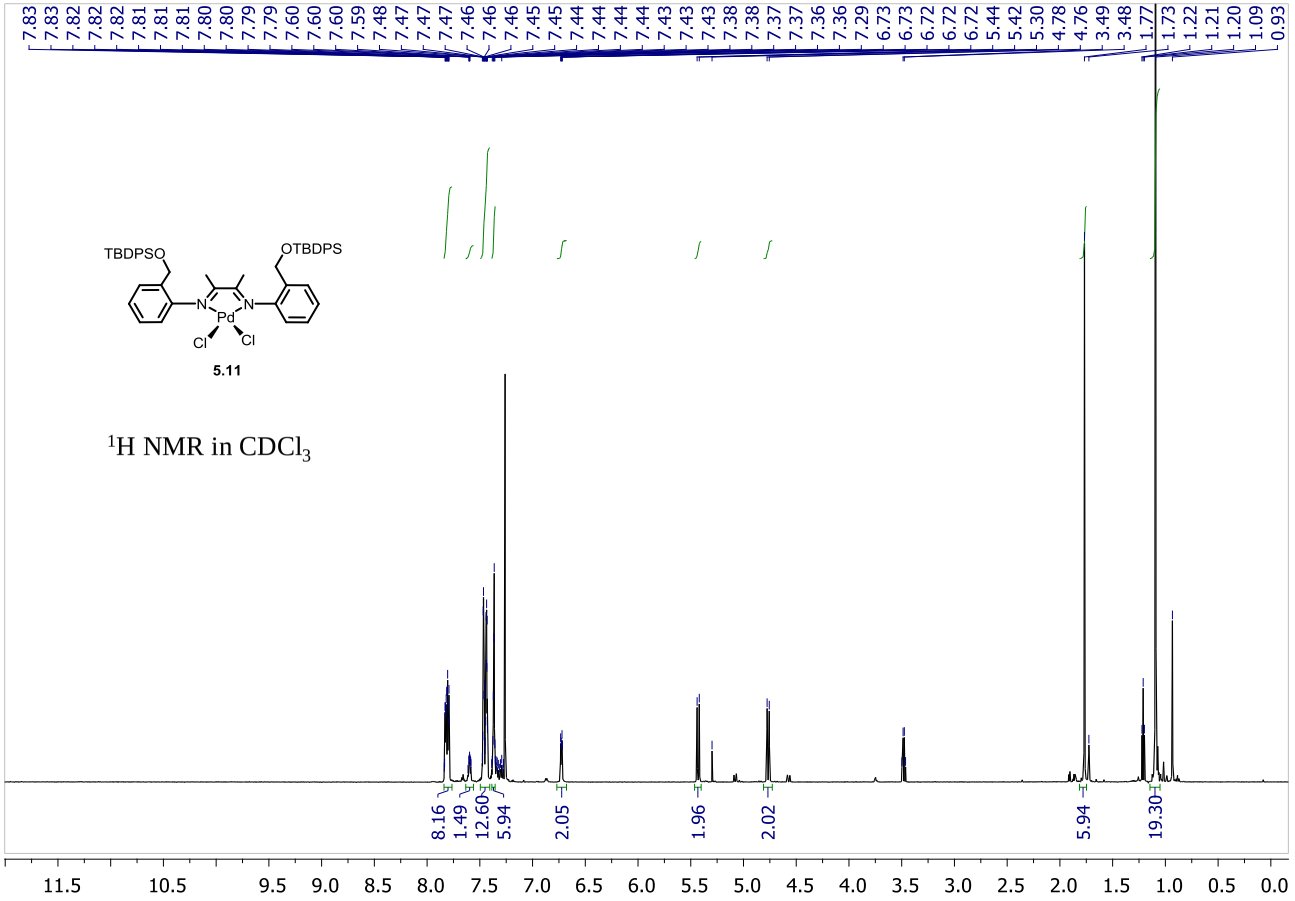
TBDPSO
OTBDPS
N
Pd
N
Cl
Cl
5.11
^{1}H NMR in $CDCl_3$
8.16
1.49
12.60
5.94
2.05
1.96
2.02
5.94
19.30

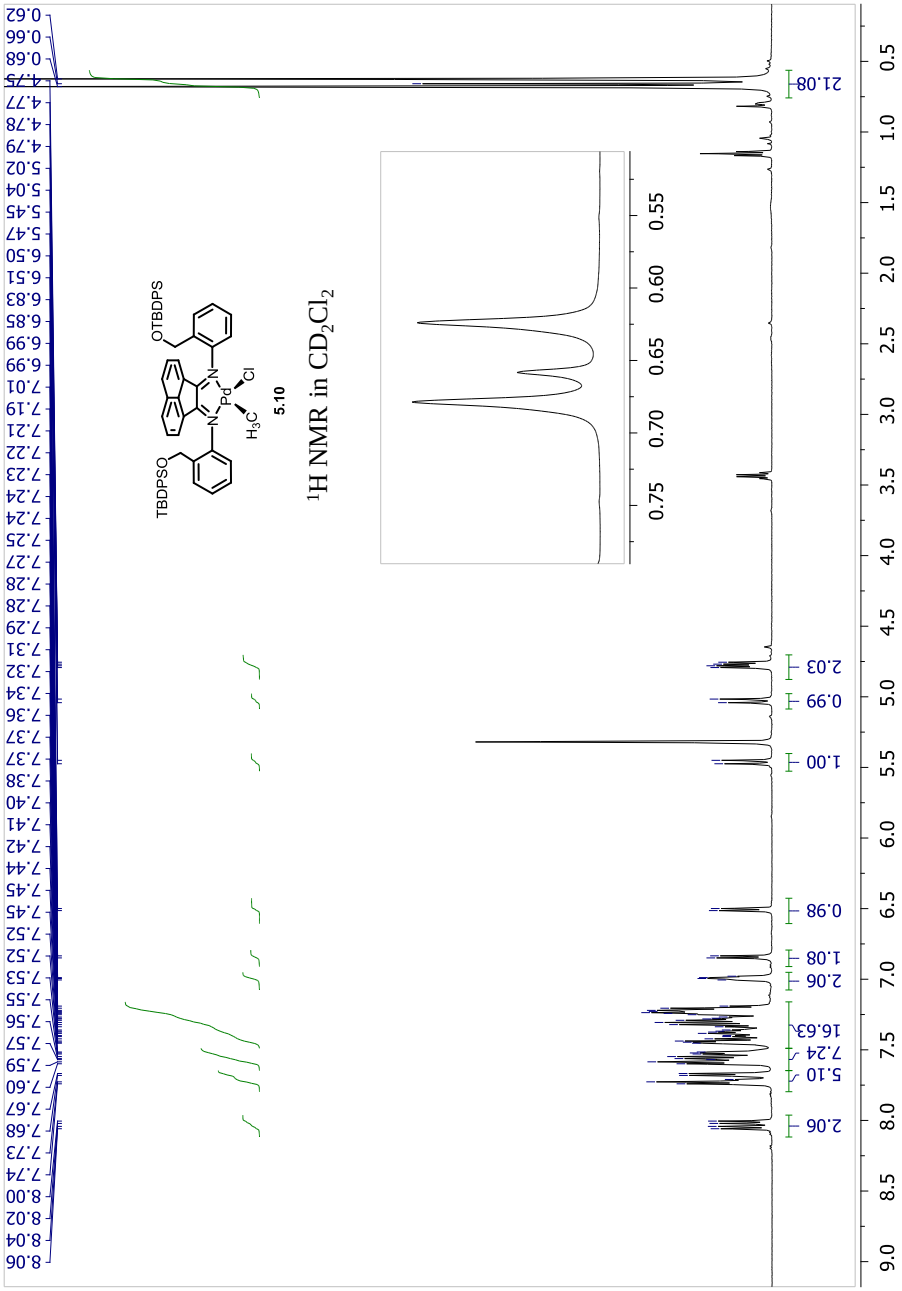
OTBDPS
TBDPSO
N
Pd
Cl
H_3C
5.10
^{1}H NMR in CD_2Cl_2
21.08
2.03
0.99
1.00
0.98
1.08
2.06
16.63
7.24
5.10
2.06

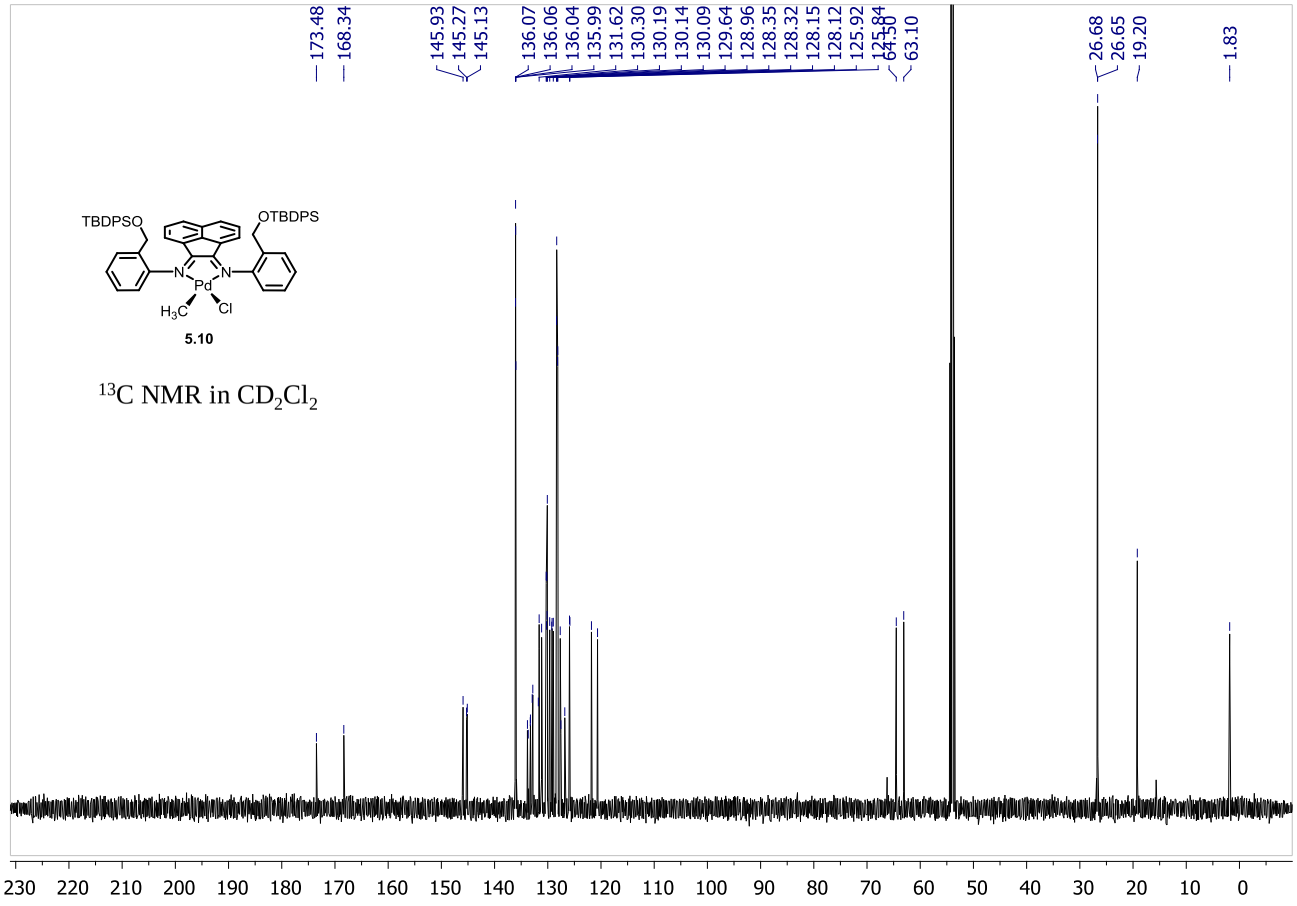
173.48
168.34
145.93
145.27
145.13
136.07
136.06
136.04
135.99
131.62
130.30
130.19
130.14
130.09
129.64
128.96
128.35
128.32
128.15
128.12
125.92
64.50
63.10
26.68
26.65
19.20
1.83
TBDPSO
OTBDPS
N
Pd
N
H3C
Cl
5.10
13C NMR in CD2Cl2
230 220 210 200 190 180 170 160 150 140 130 120 110 100 90 80 70 60 50 40 30 20 10 0

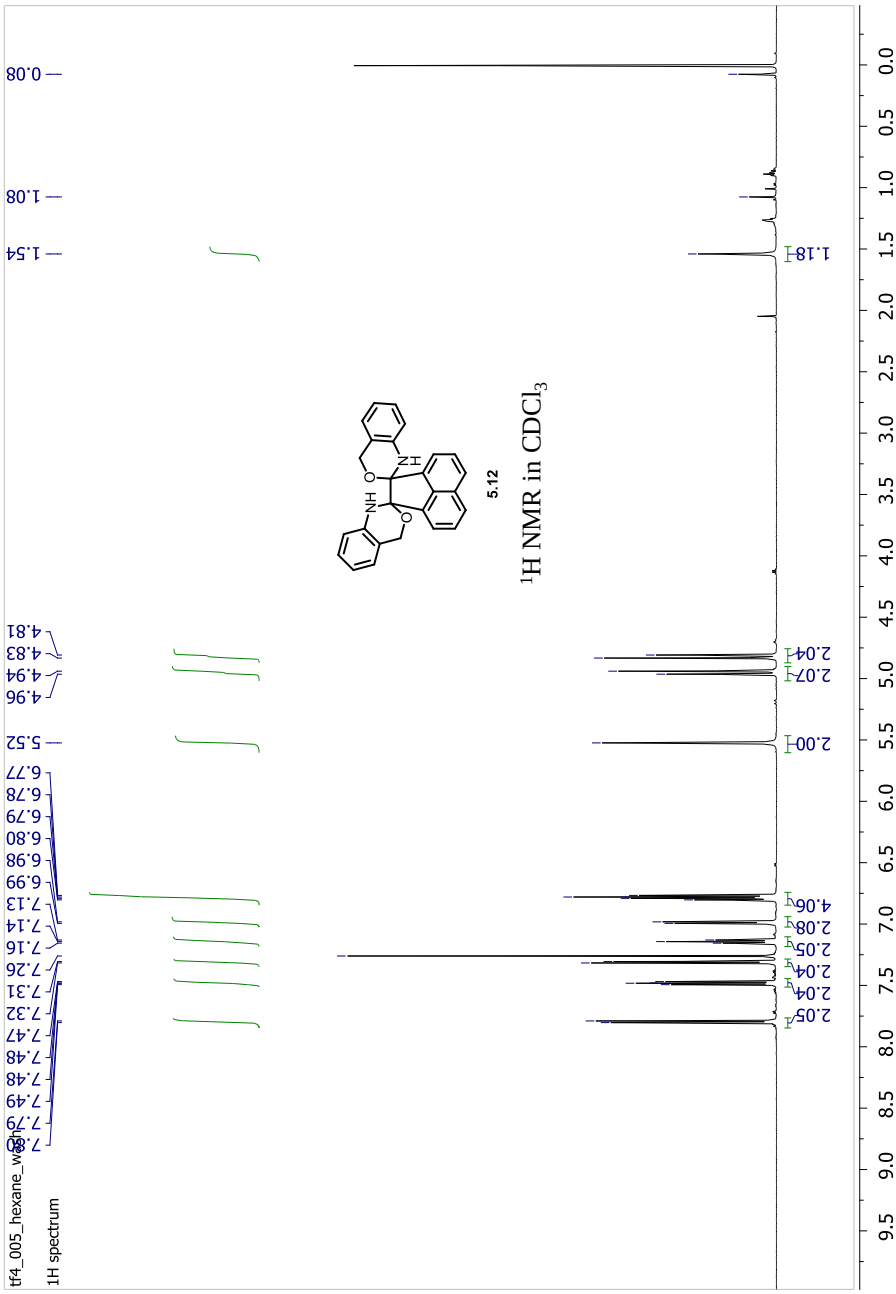
tf4_005_hexane_wash
1H spectrum
5.12
^{1}H NMR in $CDCl_3$

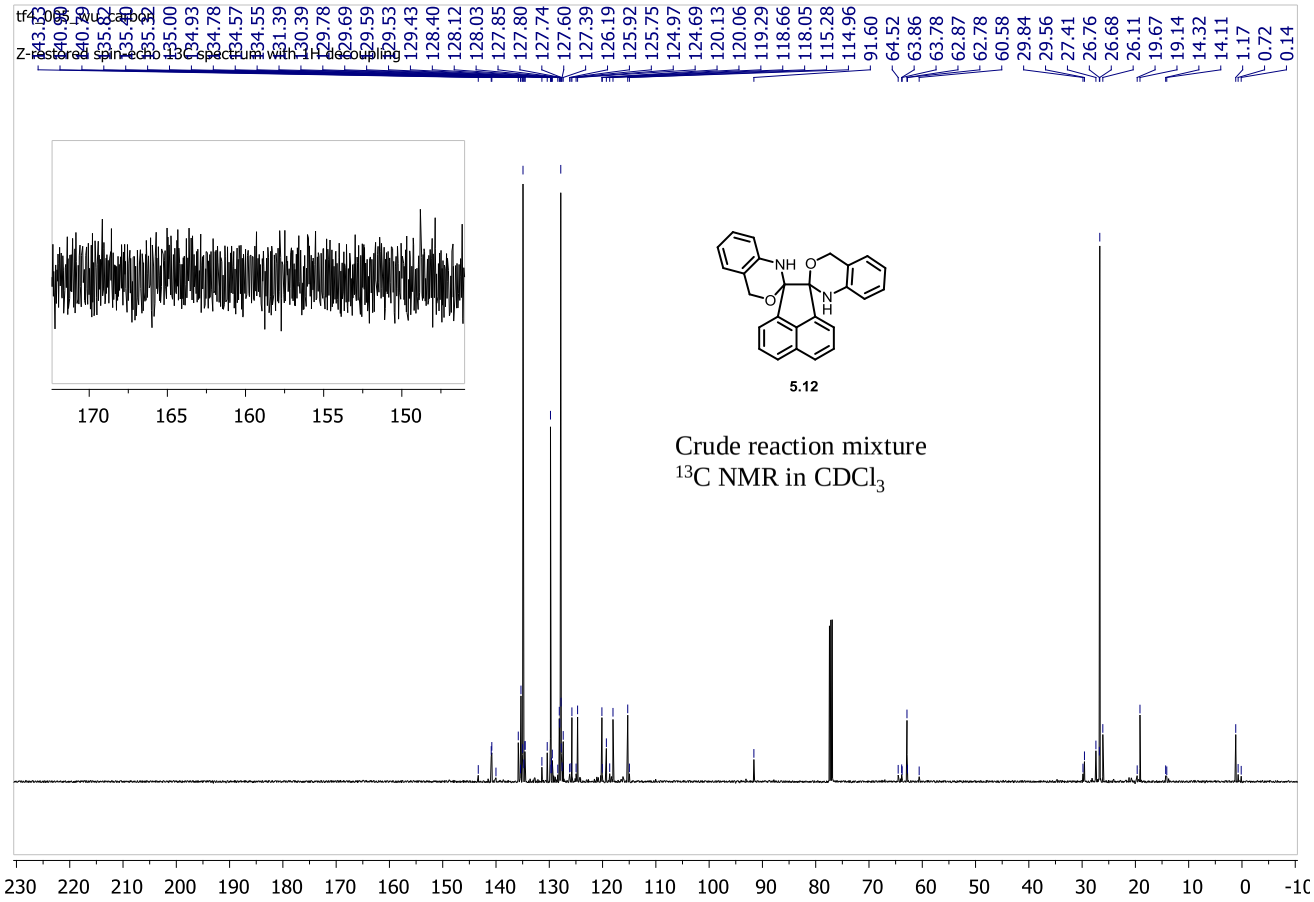
tf4-08_1_N_carbon
Z-restored spin-echo 13C spectrum with 1H decoupling
NH
O
O
N
H
5.12
Crude reaction mixture
13C NMR in CDCl3

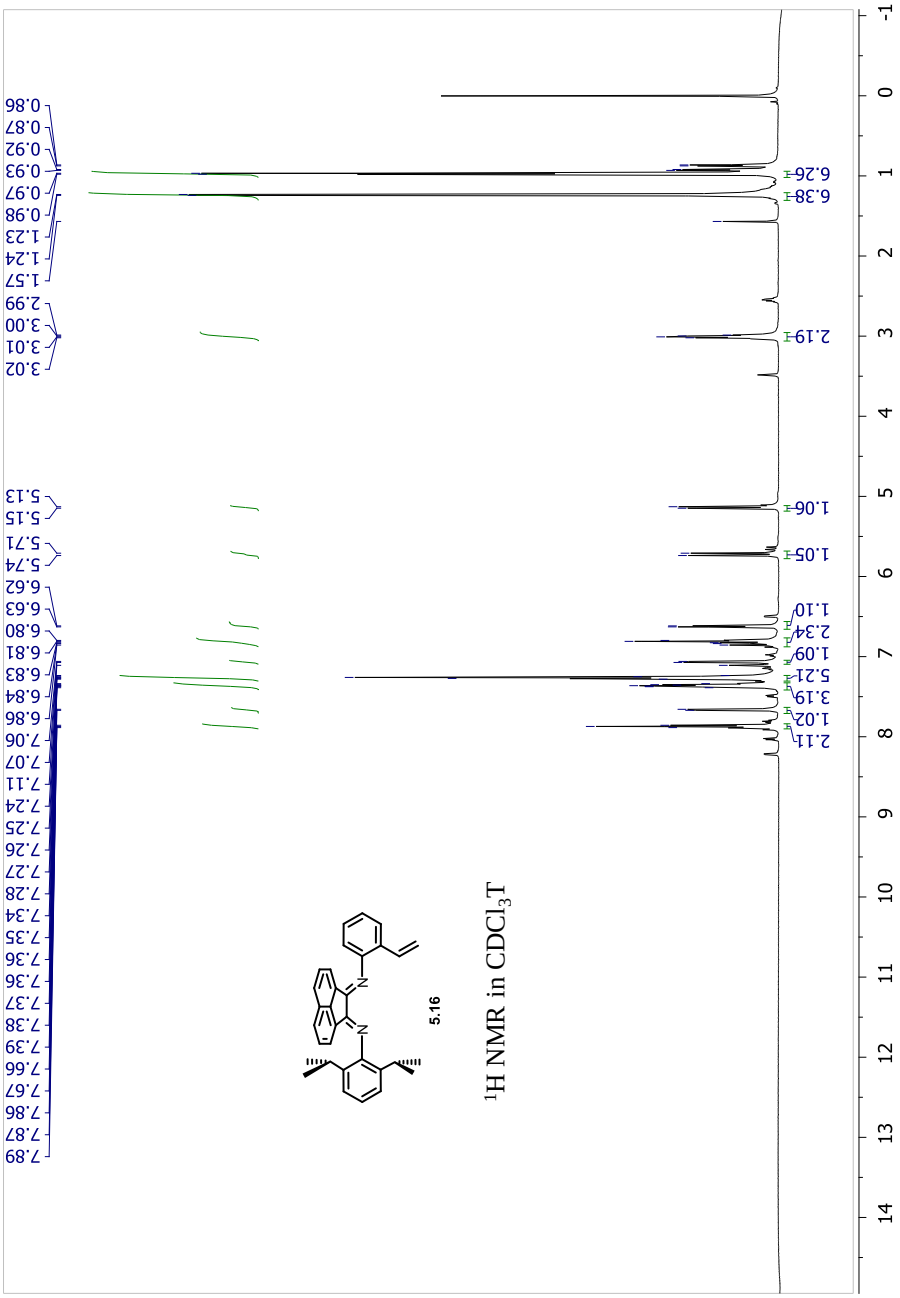
^{1}H NMR in $CDCl_3$T
5.16

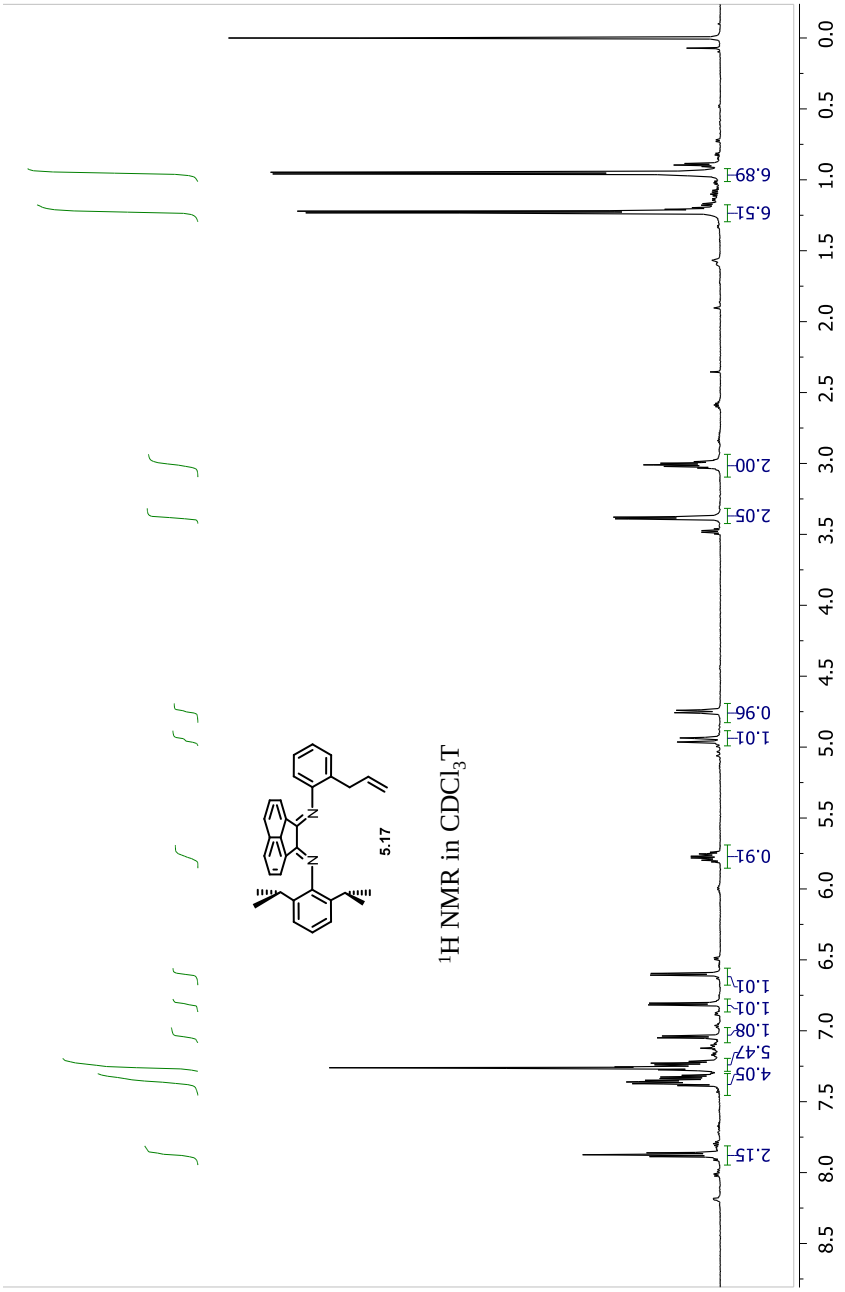
^{1}H NMR in $CDCl_3$T
5.17
6.89
6.51
2.00
2.05
0.96
1.01
0.91
1.01
1.01
1.08
5.47
4.05
2.15
0.0
0.5
1.0
1.5
2.0
2.5
3.0
3.5
4.0
4.5
5.0
5.5
6.0
6.5
7.0
7.5
8.0
8.5

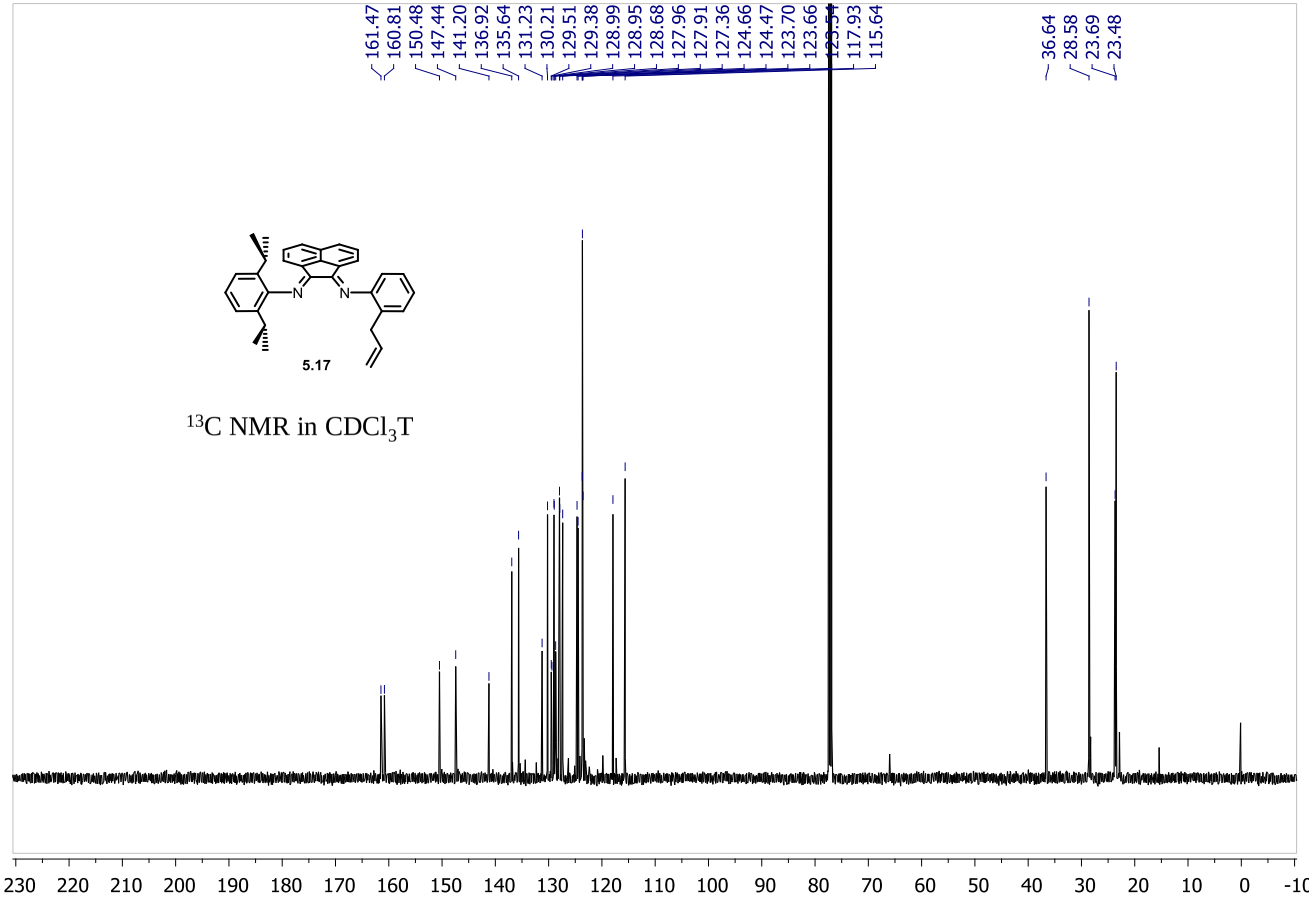
161.47
160.81
150.48
147.44
141.20
136.92
135.64
131.23
130.21
129.51
129.38
128.99
128.95
128.68
127.96
127.91
127.36
124.66
124.47
123.70
123.66
123.54
117.93
115.64
36.64
28.58
23.69
23.48
N
N
5.17
^{13}C NMR in $CDCl_3$T
230 220 210 200 190 180 170 160 150 140 130 120 110 100 90 80 70 60 50 40 30 20 10 0 -10

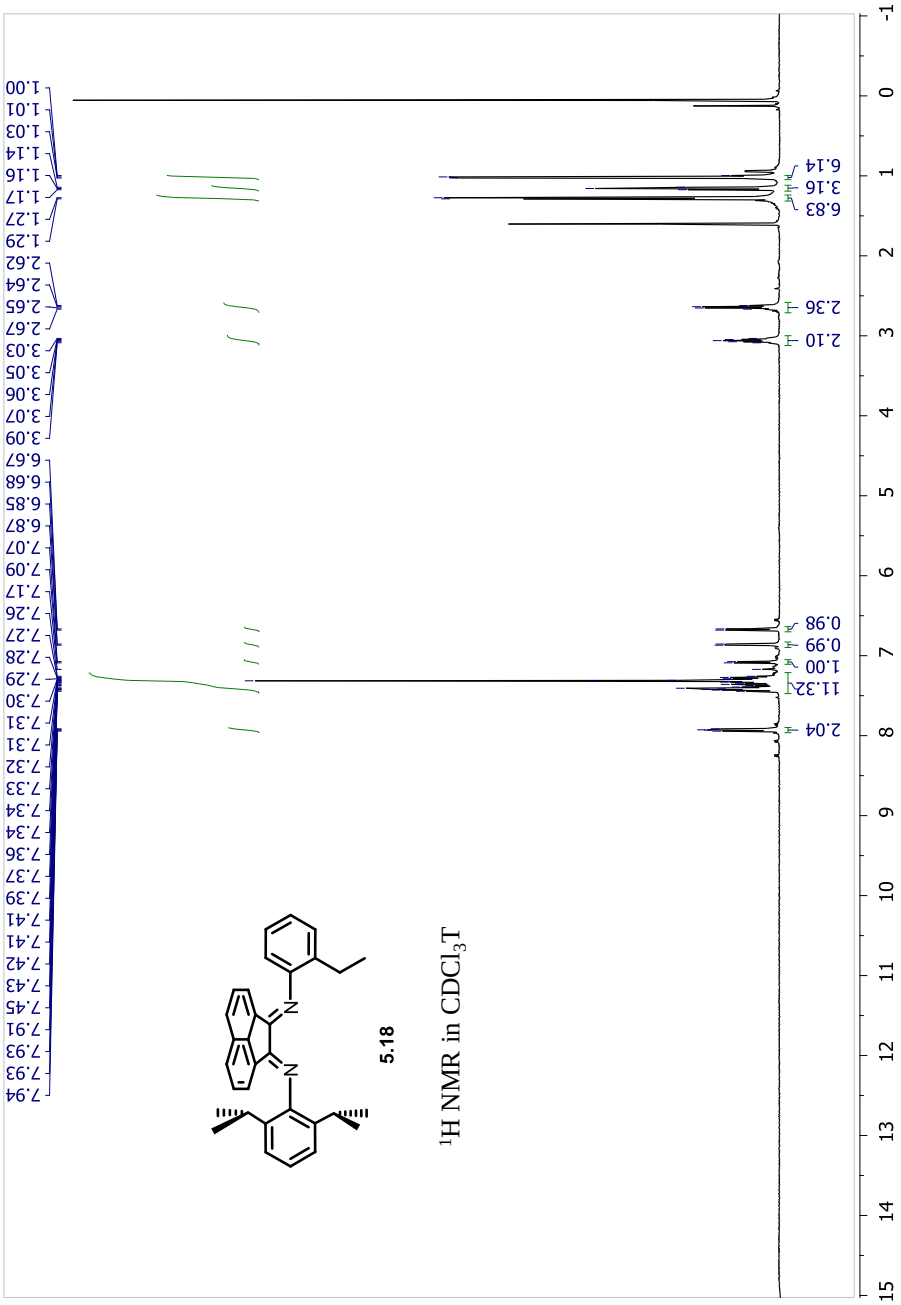
5.18
^{1}H NMR in $CDCl_3$T

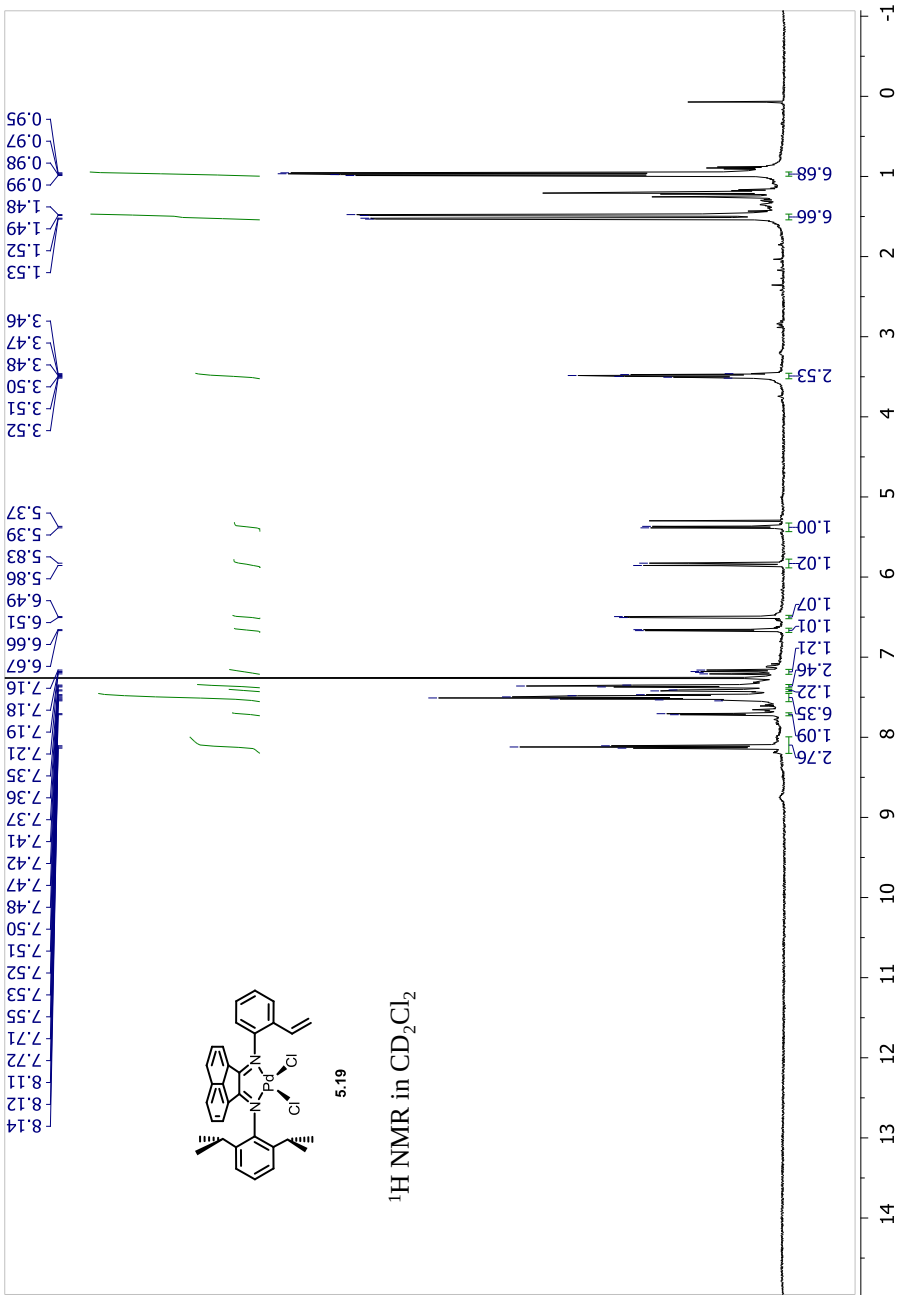
5.19
^{1}H NMR in CD_2Cl_2

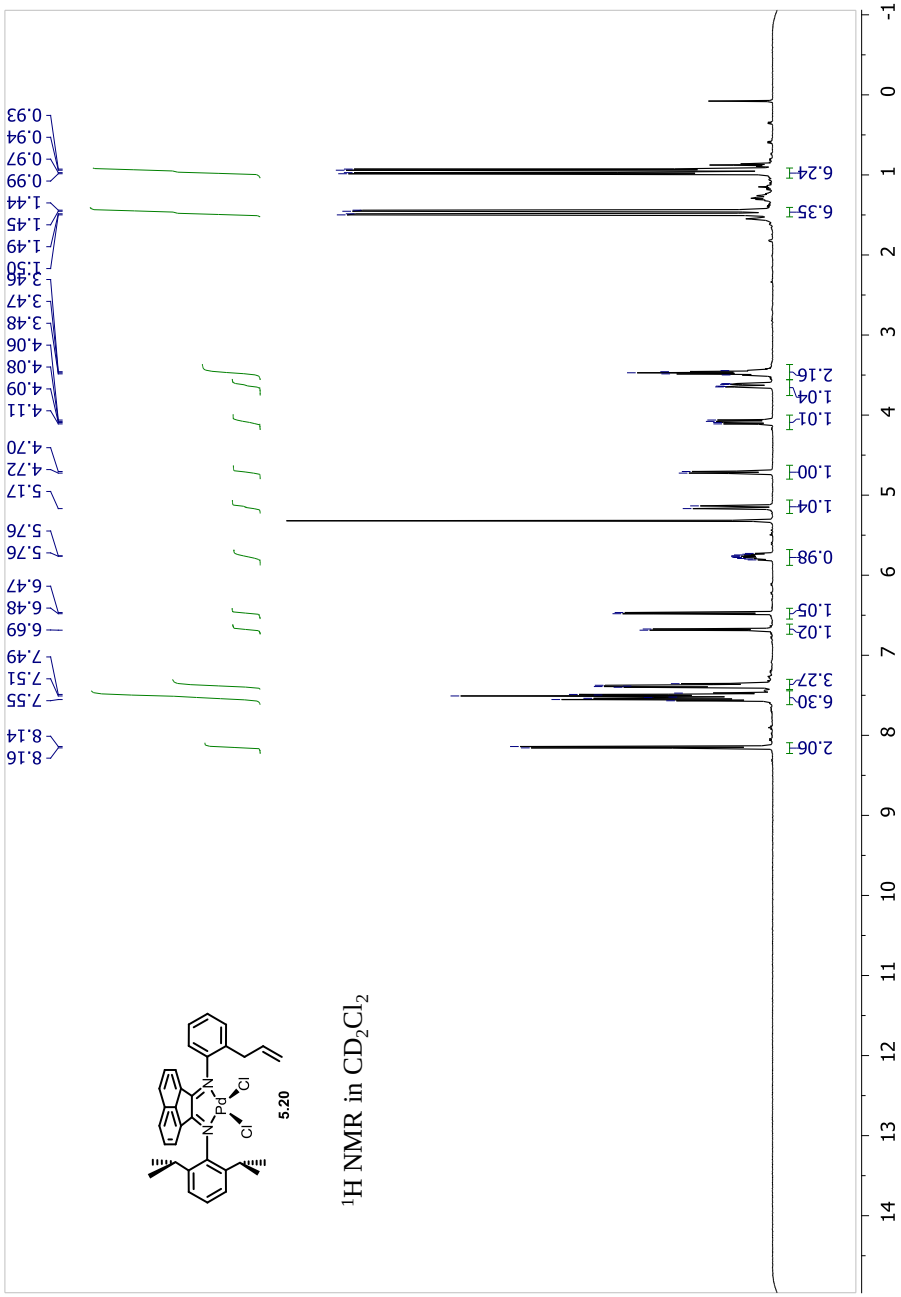
8.16
8.14
7.55
7.51
7.49
6.69
6.48
6.47
5.76
5.76
5.17
4.72
4.70
4.11
4.09
4.08
4.06
3.48
3.47
3.46
1.50
1.49
1.45
1.44
0.99
0.97
0.94
0.93
6.24
6.35
2.16
1.04
1.01
1.00
1.04
0.98
1.05
1.02
3.27
6.30
2.06
5.20
^{1}H NMR in CD_2Cl_2

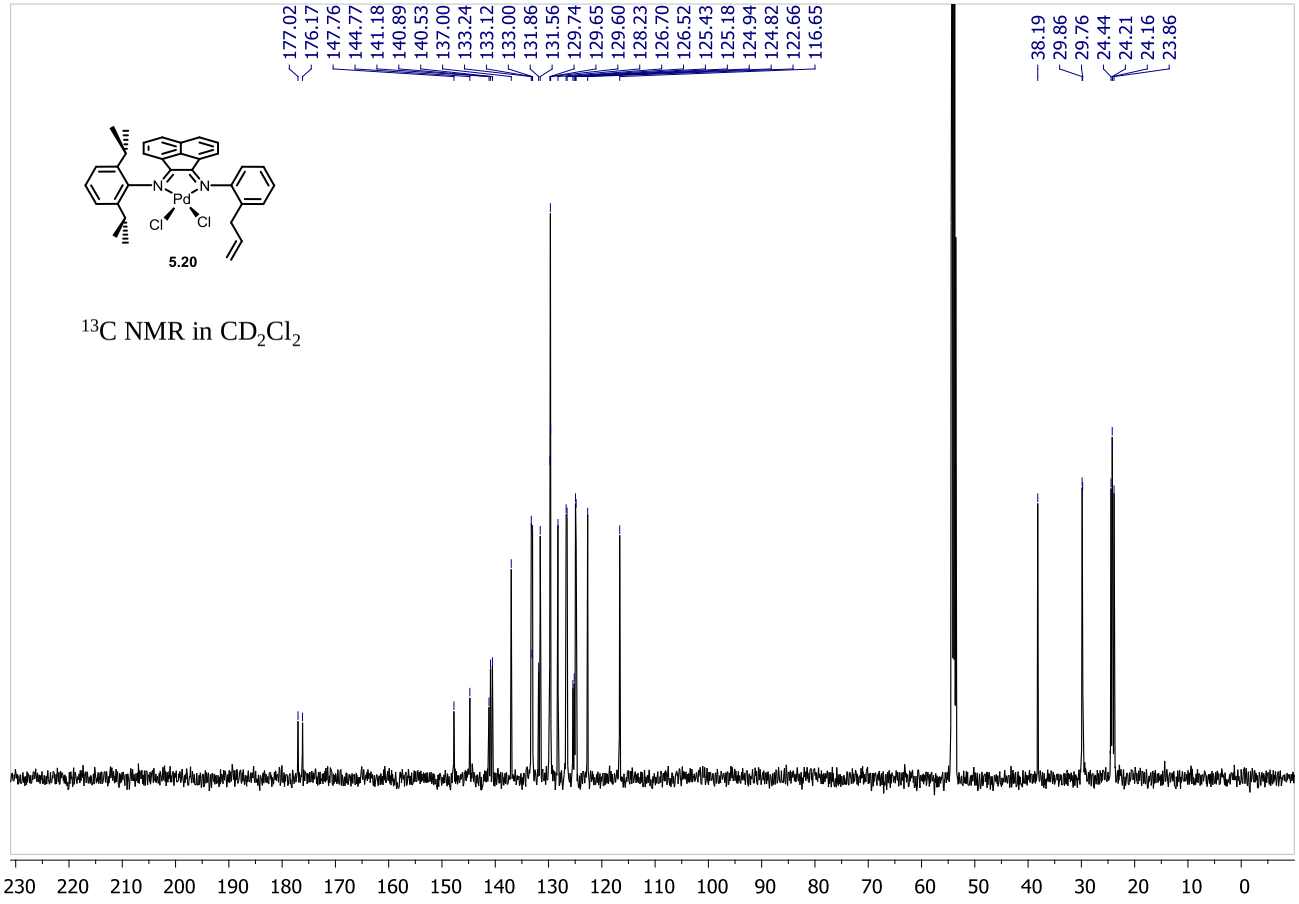
177.02
176.17
147.76
144.77
141.18
140.89
140.53
137.00
133.24
133.12
133.00
131.86
131.56
129.74
129.65
129.60
128.23
126.70
126.52
125.43
125.18
124.94
124.82
122.66
116.65
38.19
29.86
29.76
24.44
24.21
24.16
23.86
N
Pd
N
Cl
Cl
5.20
^{13}C NMR in CD_2Cl_2
230 220 210 200 190 180 170 160 150 140 130 120 110 100 90 80 70 60 50 40 30 20 10 0

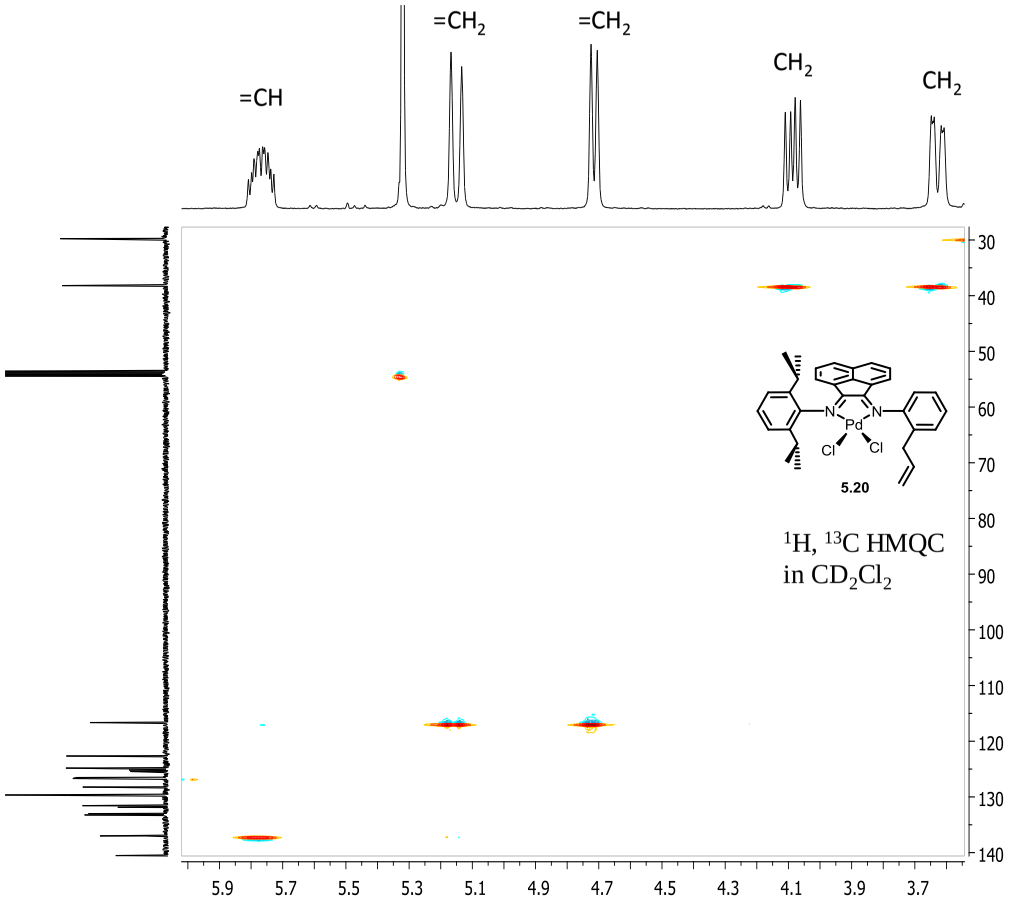
=CH
=CH2
=CH2
CH2
CH2
5.20
1H, 13C HMQC
in CD2Cl2
5.9
5.7
5.5
5.3
5.1
4.9
4.7
4.5
4.3
4.1
3.9
3.7
30
40
50
60
70
80
90
100
110
120
130
140

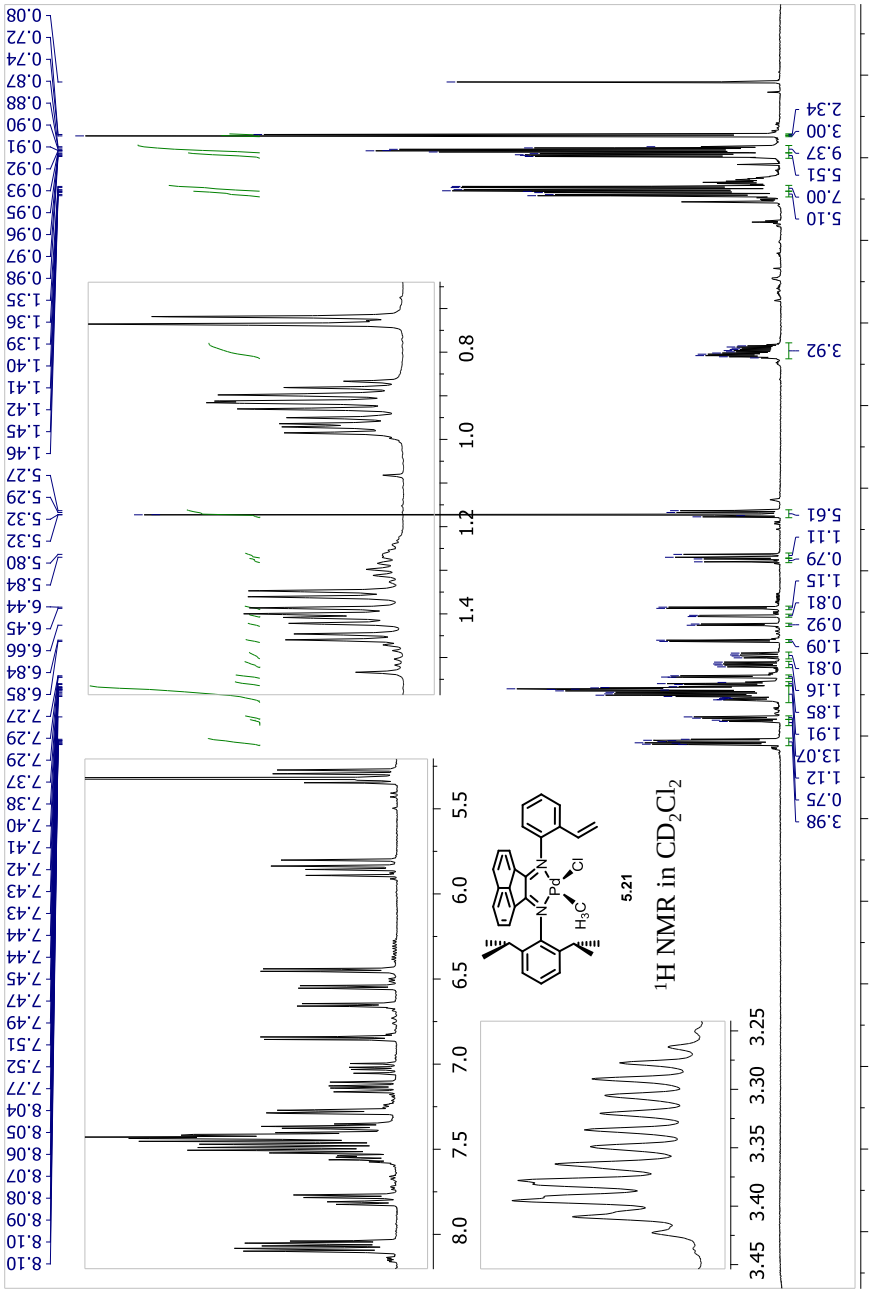
5.21
^{1}H NMR in CD_2Cl_2

5.21
^{13}C NMR in CD_2Cl_2
Pd
Cl
H_3C
N
N
1.31
2.16
2.88
14.38
22.89
23.66
23.69
23.90
24.04
24.17
24.22
24.40
24.72
28.98
29.13
29.43
29.51
116.74
118.01
121.52
122.44
124.27
124.34
125.11
125.14
125.26
125.40
125.48
125.62
126.71
127.03
127.55
127.61
127.75
127.83
128.48
128.82
129.13
129.29
129.36
129.44
129.74
130.07
130.37
131.41
131.47
131.50
131.81
131.83
131.88
132.91
138.86
139.26
139.94
140.19
141.71
144.68
144.93
0
10
20
30
40
50
60
70
80
90
100
110
120
130
140
150
160
170
180

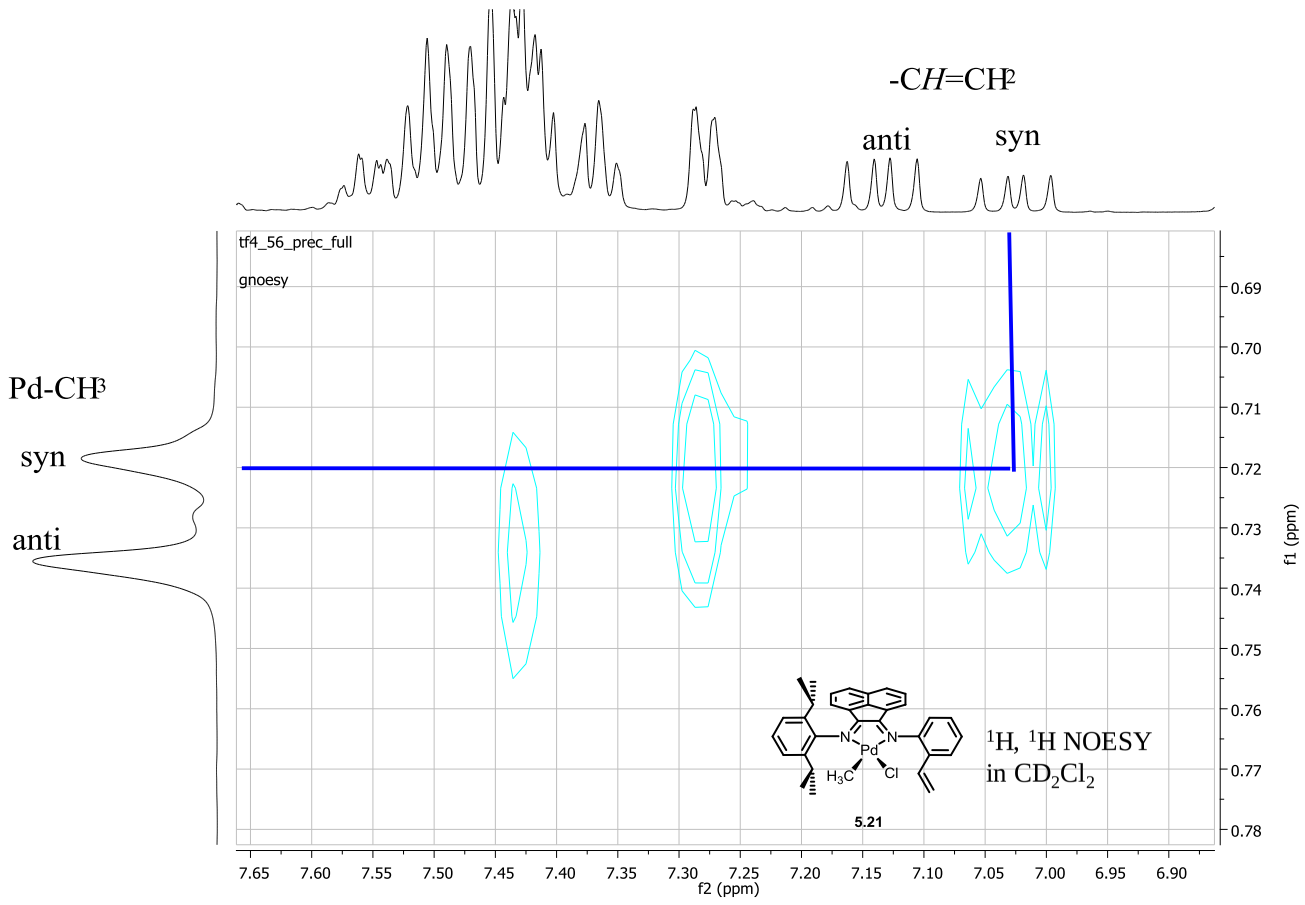
-CH=CH2
anti
syn
tf4_56_prec_full
gnoesy
Pd-CH3
syn
anti
5.21
1H, 1H NOESY
in CD2Cl2
f2 (ppm)
f1 (ppm)

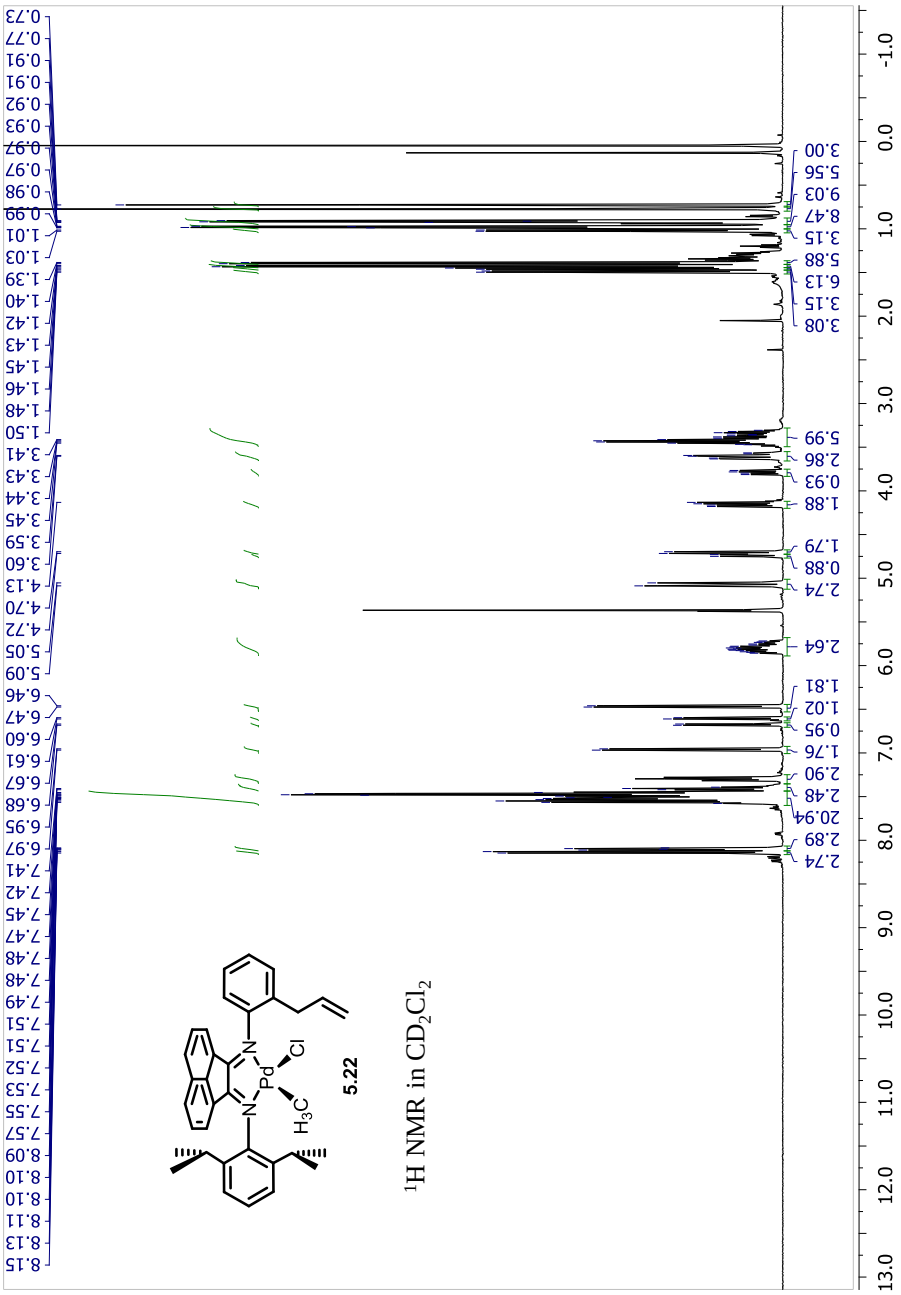
5.22
^{1}H NMR in CD_2Cl_2

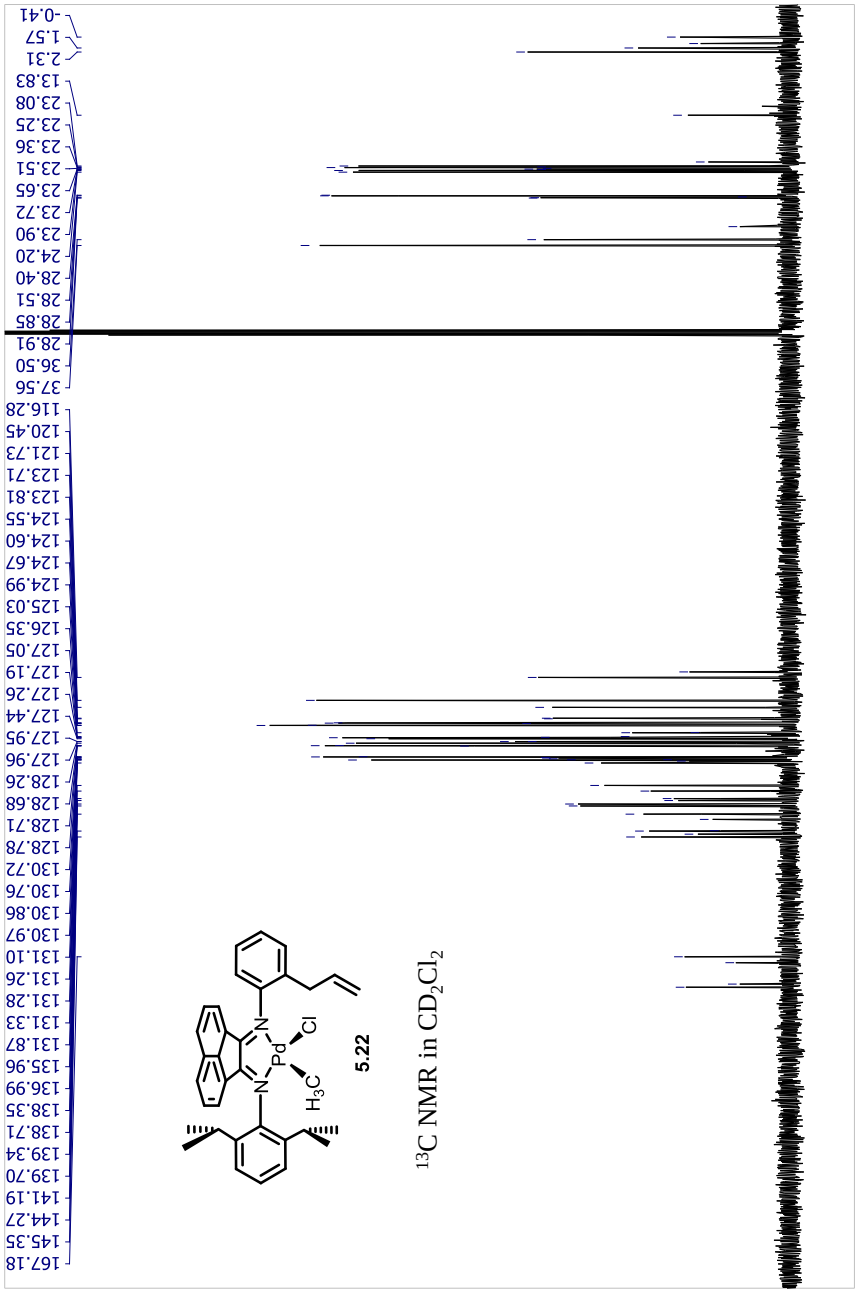
5.22
^{13}C NMR in CD_2Cl_2

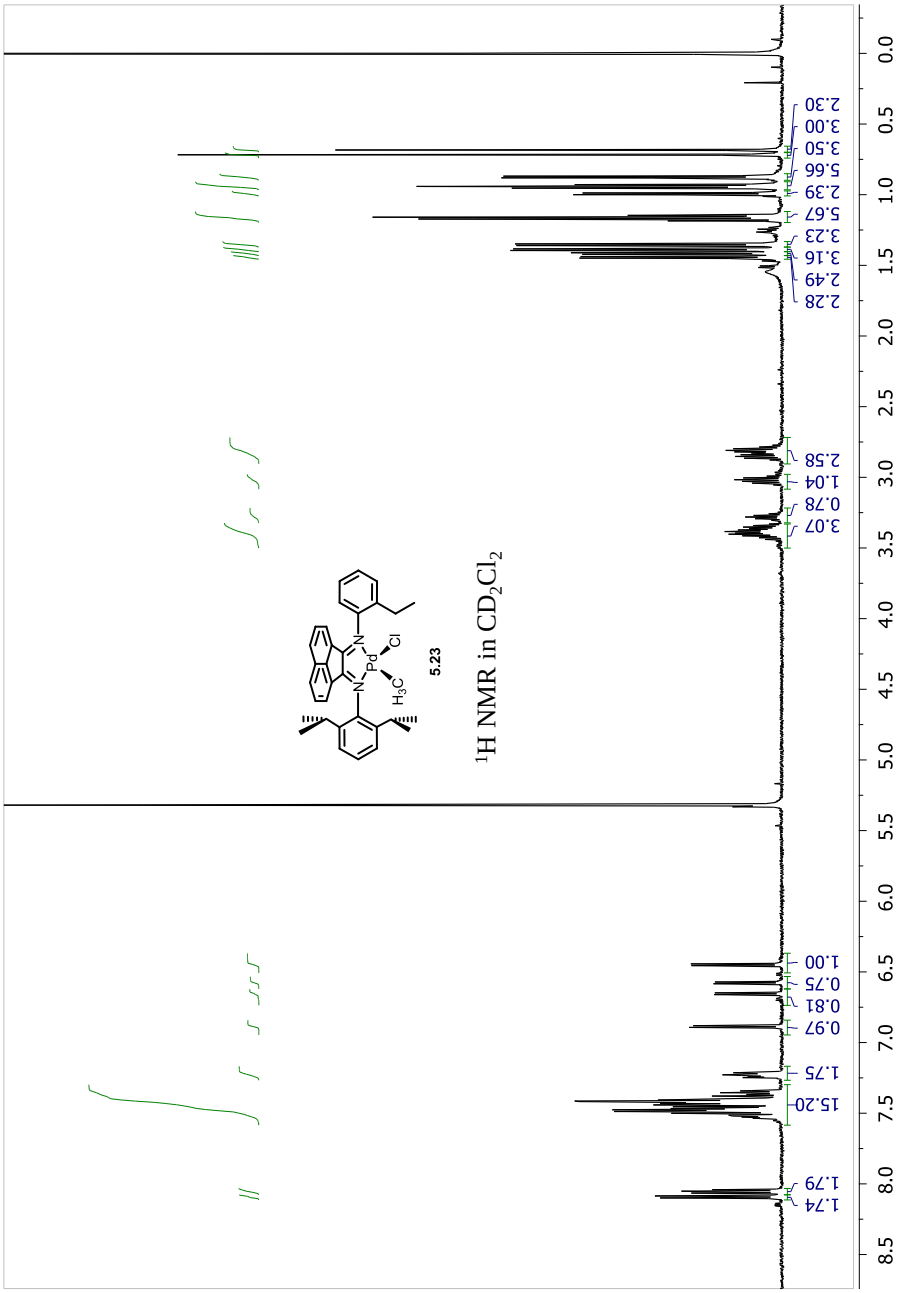
5.23
^{1}H NMR in CD_2Cl_2
1.74
1.79
15.20
1.75
0.97
0.81
0.75
1.00
3.07
0.78
1.04
2.58
2.28
2.49
3.16
3.23
5.67
2.39
5.66
3.50
3.00
2.30
8.5
8.0
7.5
7.0
6.5
6.0
5.5
5.0
4.5
4.0
3.5
3.0
2.5
2.0
1.5
1.0
0.5
0.0

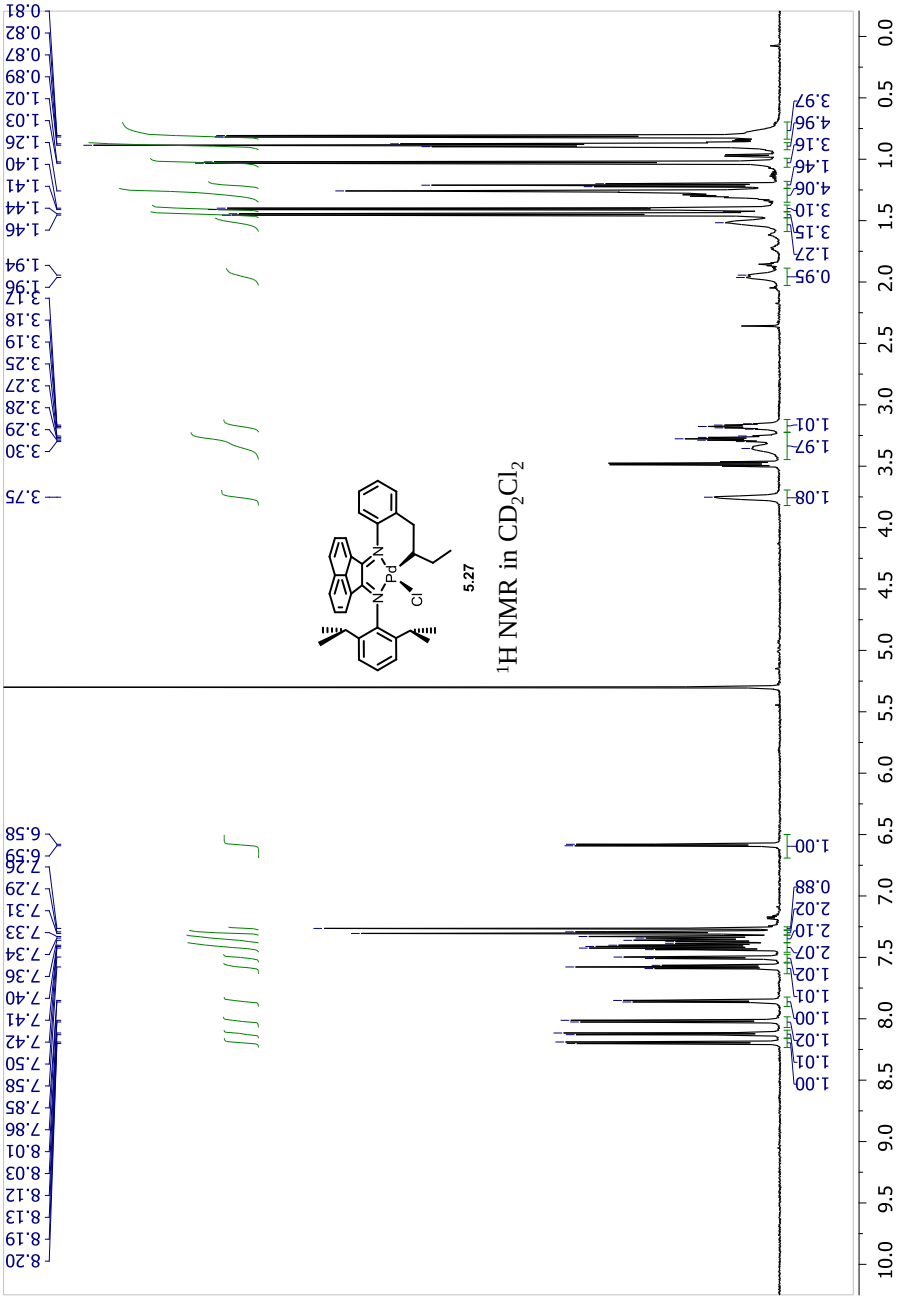
^{1}H NMR in CD_2Cl_2
5.27
Pd
Cl
N
N

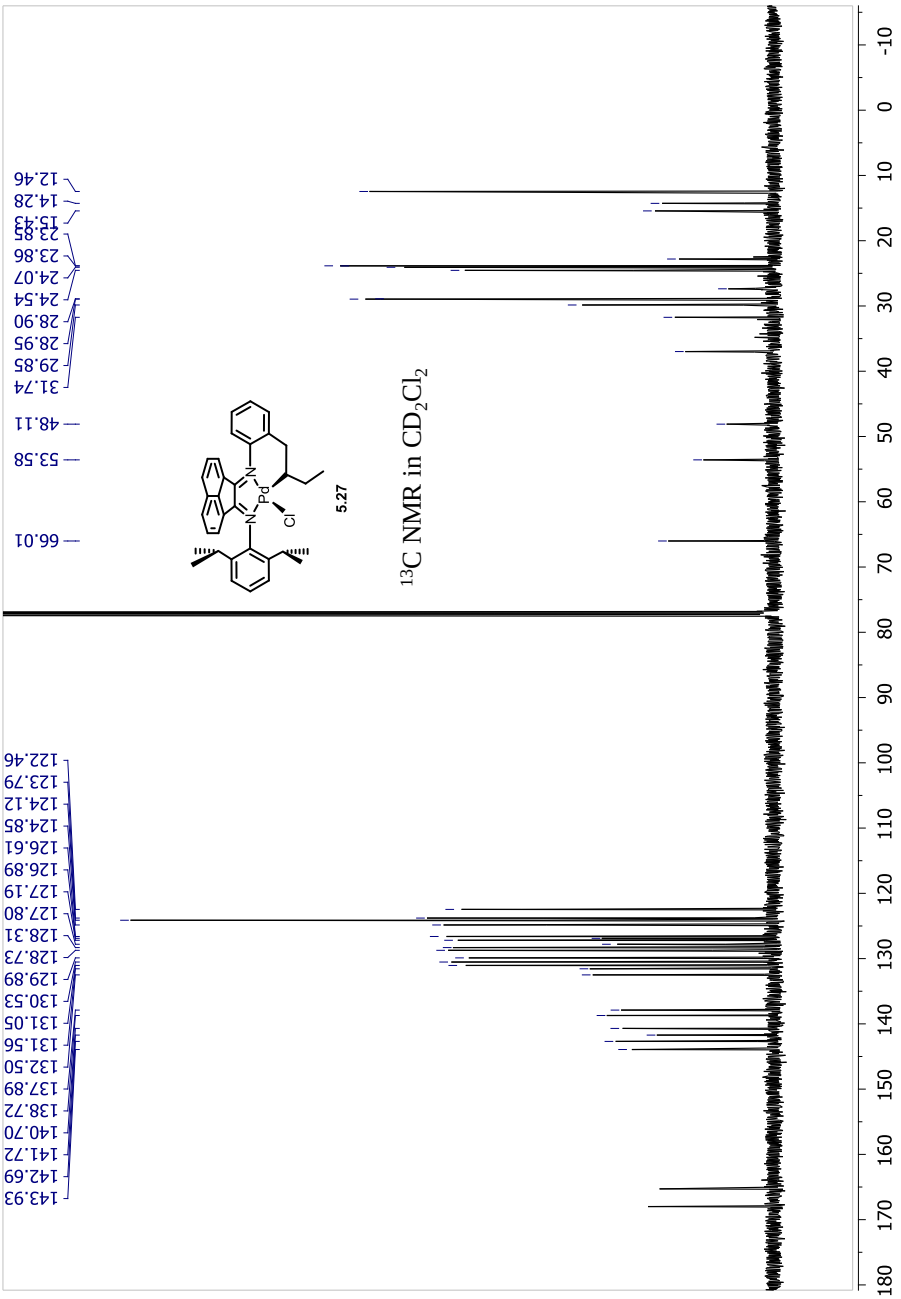
^{13}C NMR in CD_2Cl_2
5.27
Pd
Cl
N
N
12.46
14.28
15.43
23.85
23.86
24.07
24.54
28.90
28.95
29.85
31.74
48.11
53.58
66.01
122.46
123.79
124.12
124.85
126.61
126.89
127.19
127.80
128.31
128.73
129.89
130.53
131.05
131.56
132.50
137.89
138.72
140.70
141.72
142.69
143.93

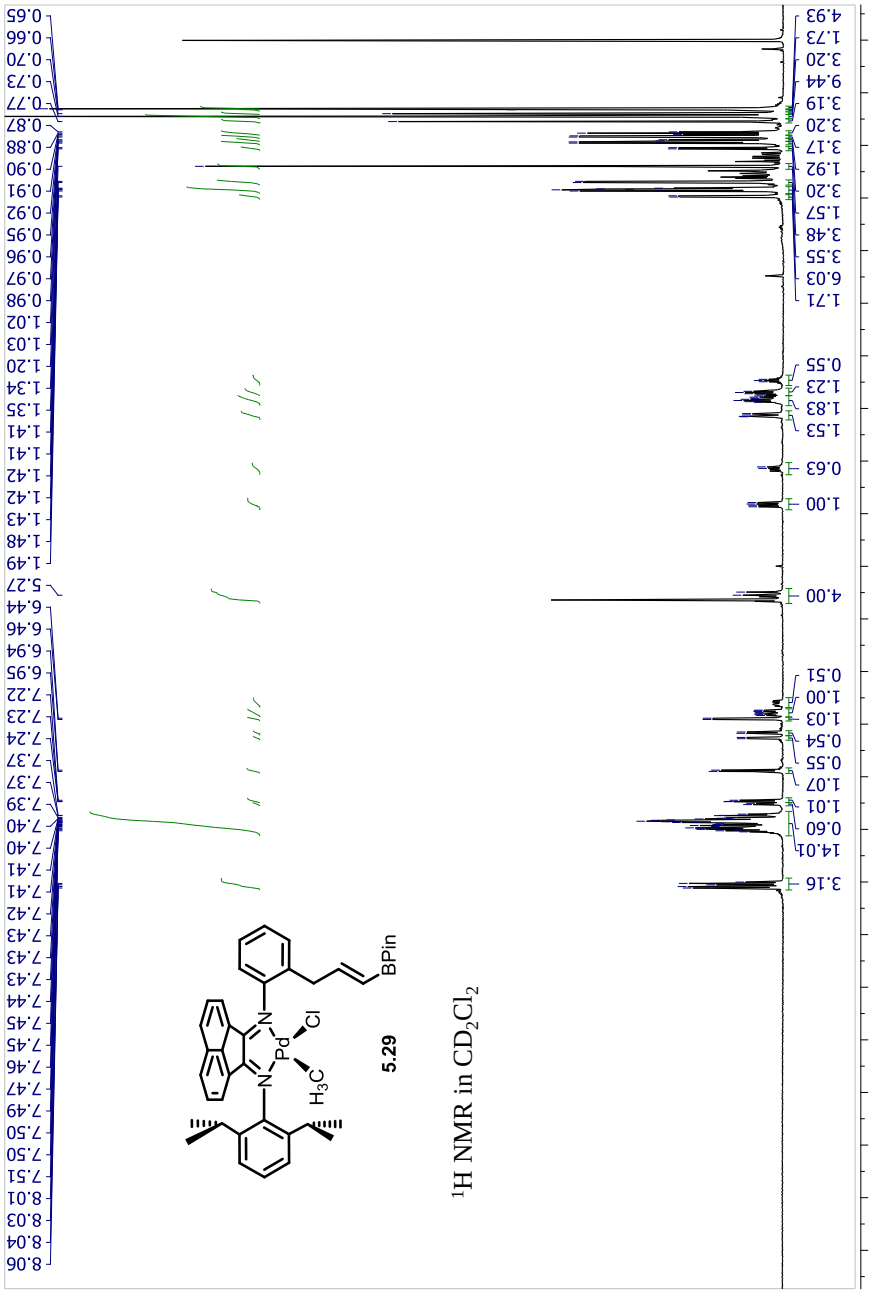
BPin
Cl
Pd
N
N
H3C
5.29
1H NMR in CD2Cl2

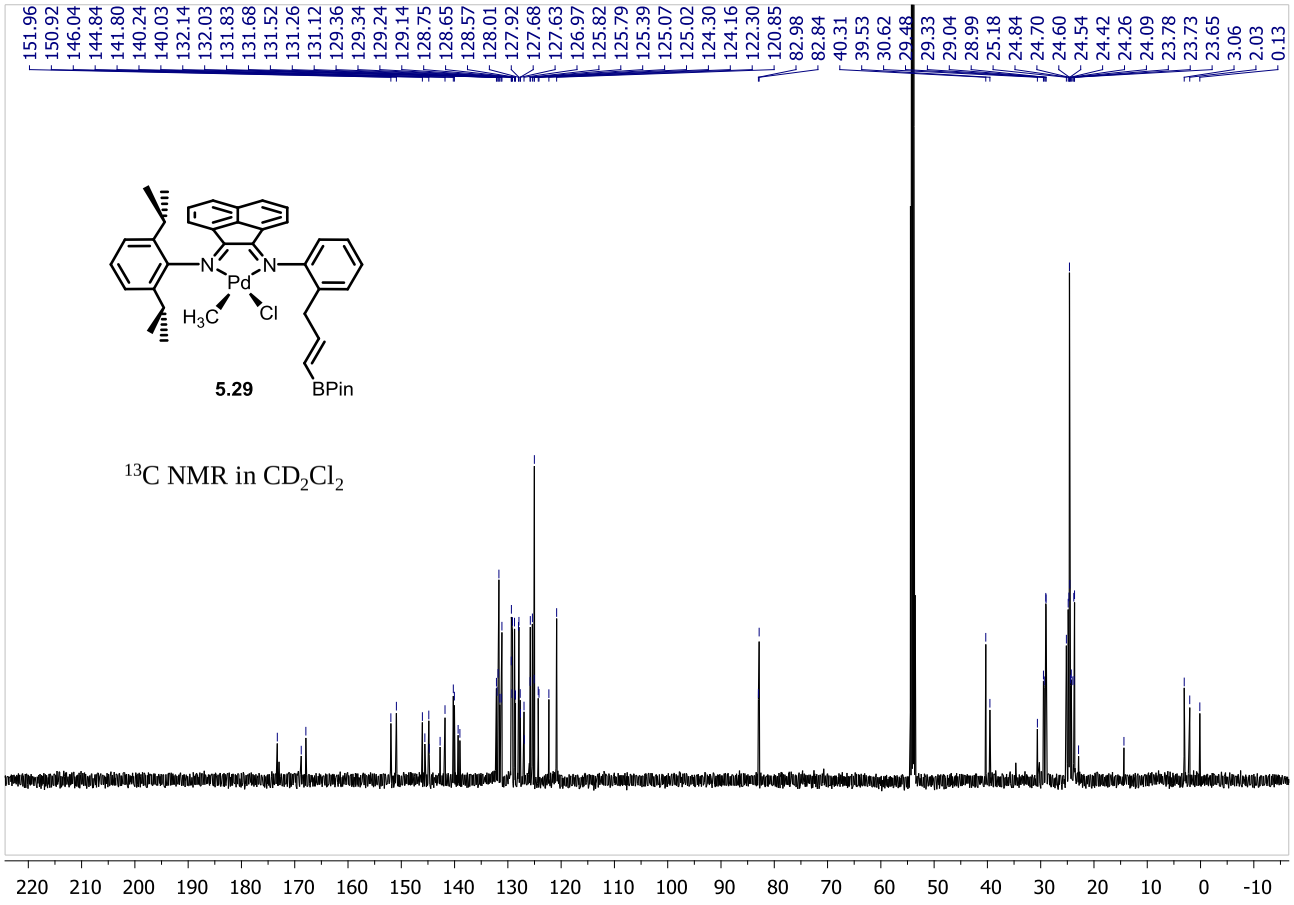
151.96
150.92
146.04
144.84
141.80
140.24
140.03
132.14
132.03
131.83
131.68
131.52
131.26
131.12
129.36
129.34
129.24
129.14
128.75
128.65
128.57
128.01
127.92
127.68
127.63
126.97
125.82
125.79
125.39
125.07
125.02
124.30
124.16
122.30
120.85
82.98
82.84
40.31
39.53
30.62
29.48
29.33
29.04
28.99
25.18
24.84
24.70
24.60
24.54
24.42
24.26
24.09
23.78
23.73
23.65
3.06
2.03
0.13
N
Pd
N
H3C
Cl
5.29
BPin
13C NMR in CD2Cl2
220
210
200
190
180
170
160
150
140
130
120
110
100
90
80
70
60
50
40
30
20
10
0
-10

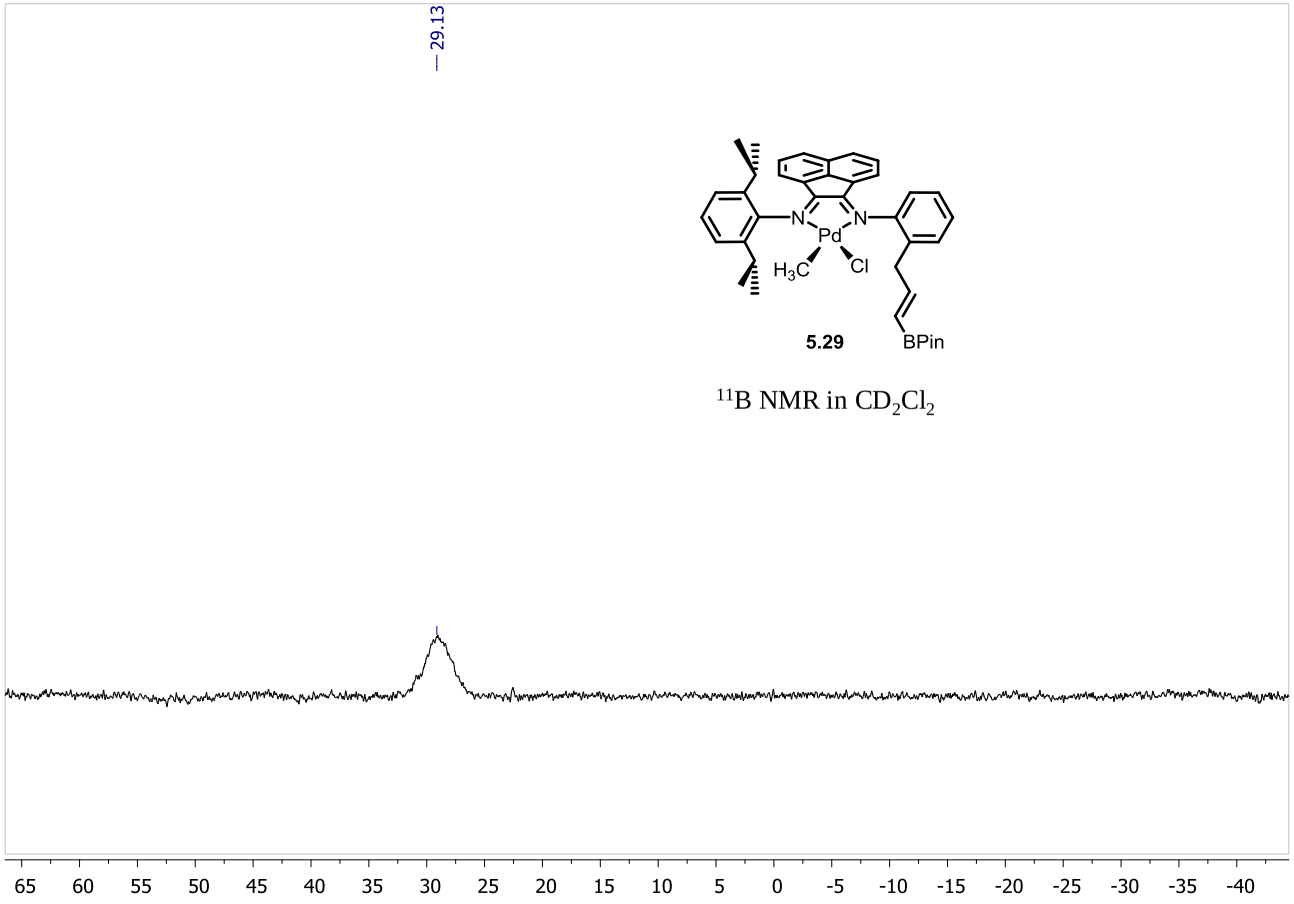

5.29

^{11}B NMR in CD_2Cl_2

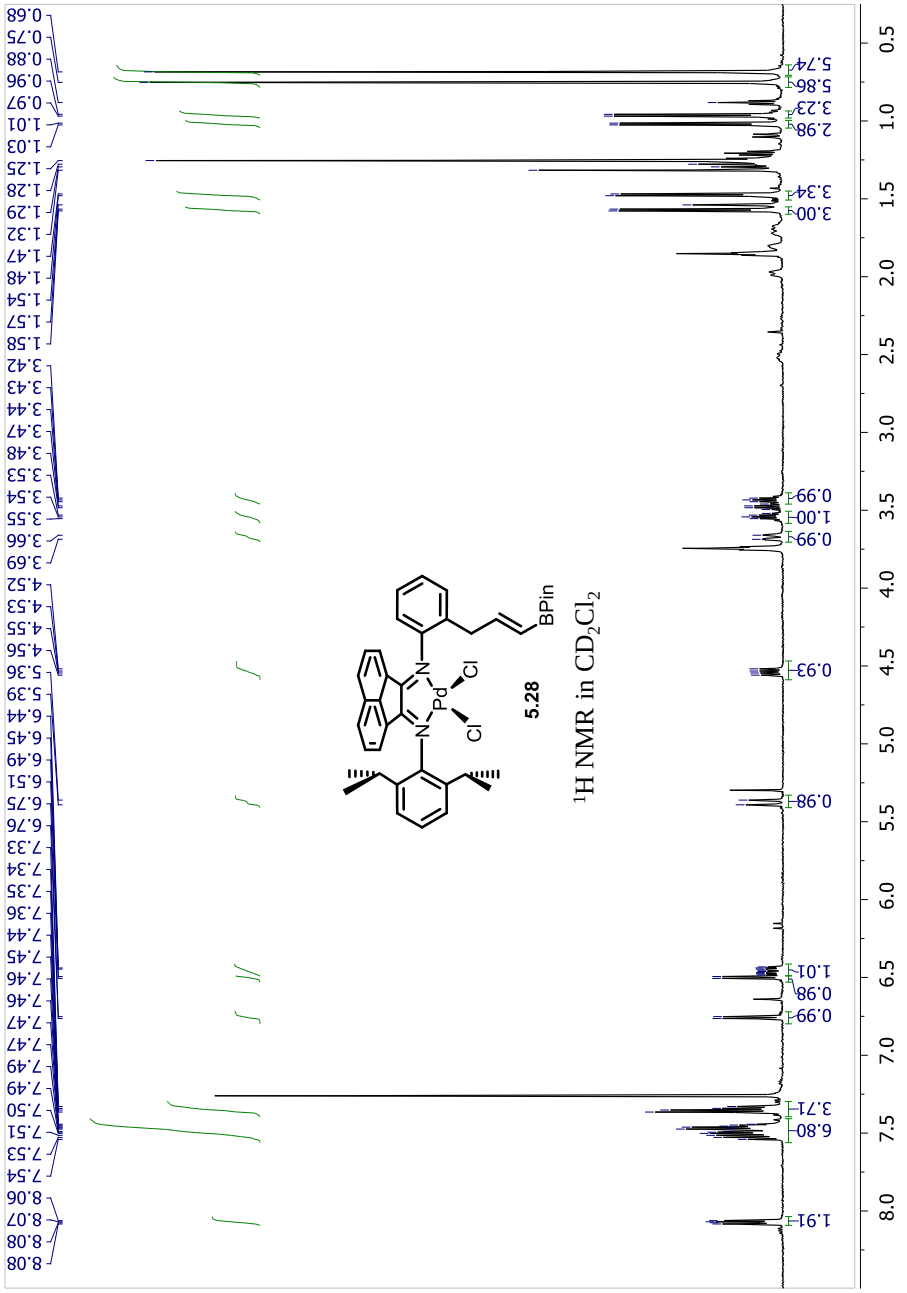
5.28
BPin
Cl
Cl
Pd
N
N
^{1}H NMR in CD_2Cl_2

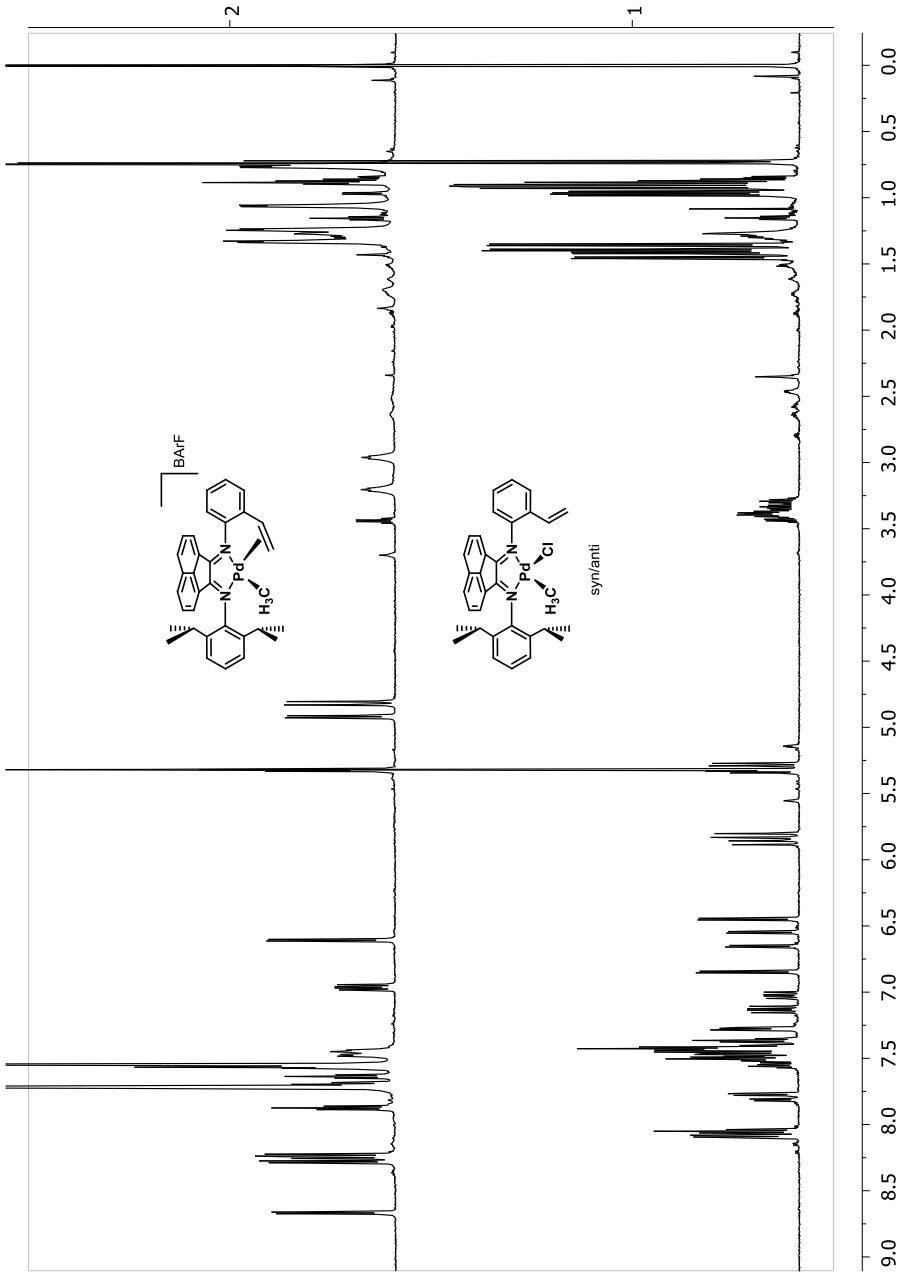
2
1
BArF
syn/anti
0.0
0.5
1.0
1.5
2.0
2.5
3.0
3.5
4.0
4.5
5.0
5.5
6.0
6.5
7.0
7.5
8.0
8.5
9.0

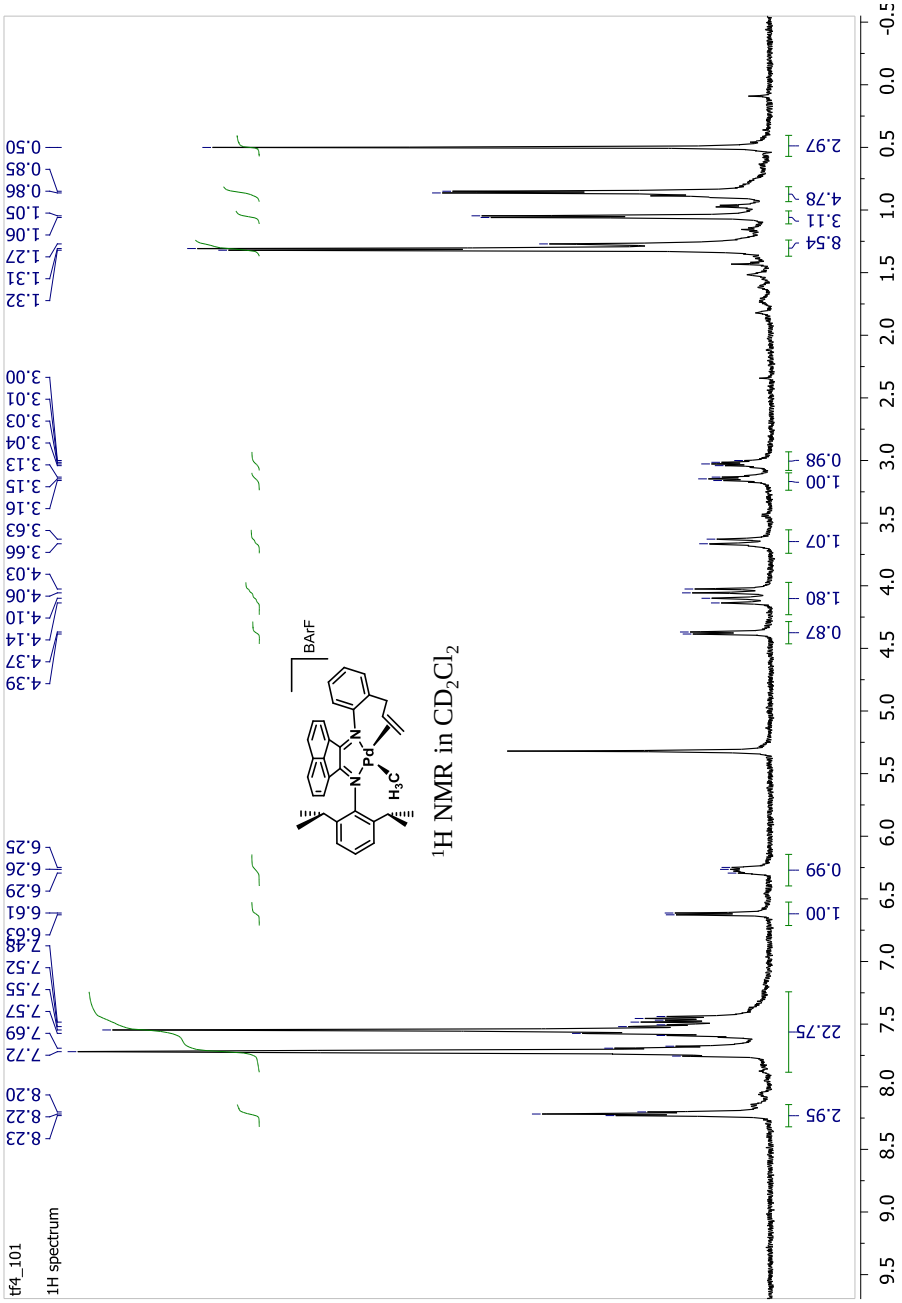
tf4_101
1H spectrum
^{1}H NMR in CD_2Cl_2
BArF
Pd
H_3C
N
8.23
8.22
8.20
7.72
7.69
7.57
7.55
7.52
7.48
6.63
6.61
6.29
6.26
6.25
4.39
4.37
4.14
4.10
4.06
4.03
3.66
3.63
3.16
3.15
3.13
3.04
3.03
3.01
3.00
1.32
1.31
1.27
1.06
1.05
0.86
0.85
0.50
2.95
22.75
1.00
0.99
0.87
1.80
1.07
1.00
0.98
8.54
3.11
4.78
2.97